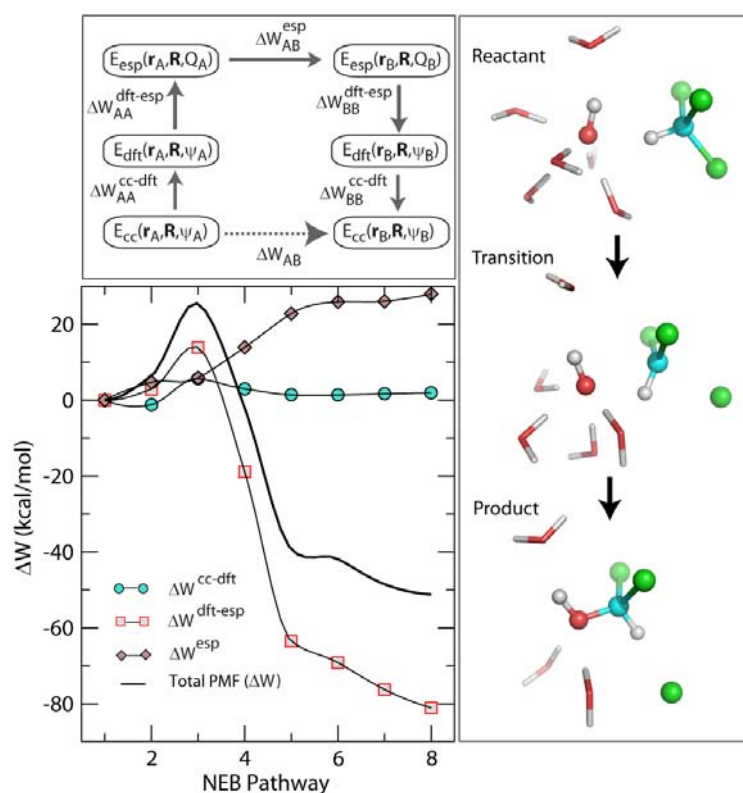


2007 Condensed Phase and Interfacial Molecular Science Research Meeting



Airlie Conference Center Warrenton,
Virginia October 21-24, 2007



Office of Basic Energy Sciences

Chemical Sciences, Geosciences & Biosciences Division

Cover

Thermodynamic cycle used to incorporate high-level electronic structure results in calculations of the free energy along a condensed-phase reaction path (top left), free energy profile (bottom left) and reactant, transition, and product states (right) for the reaction $\text{OH}^- + \text{CHCl}_3 \rightarrow \text{CHCl}_2\text{OH} + \text{Cl}^-$. Calculations were performed using NWChem. [J. Chem. Phys. **127**, 051102 (2007)]

*M. Valiev,^a B. C. Garrett,^b M.-K. Tsai,^b K. Kowalski,^b
S. M. Kathmann,^b G. K. Schenter,^b and M. Dupuis^b*
^a *Environmental Molecular Sciences Laboratory*
^b *Chemical & Materials Sciences Division
Pacific Northwest National Laboratory*

**This document was produced under contract number DE-AC05-06OR23100
between the U.S. Department of Energy and Oak Ridge Associated Universities.**

Foreword

This volume summarizes the scientific content of the 2007 Research Meeting on Condensed Phase and Interfacial Molecular Science (CPIMS) sponsored by the U. S. Department of Energy (DOE), Office of Basic Energy Sciences (BES). This marks the fourth meeting of CPIMS—the fourth of the regular Contractors' Meetings within the Fundamental Interactions Team.

Since its founding, the CPIMS Contractors' Meeting has fostered connections across BES research programs based on common topical interests. In keeping with that notion, we have invited four investigators who are funded under the BES Heavy Element Chemistry program to speak about their research: Corwin Booth (Lawrence Berkeley National Laboratory), Michael Heaven (Emory University), Asok Ray (University of Texas at Arlington), and Lynda Soderholm (Argonne National Laboratory). We hope that the blending of these external experts with the CPIMS principal investigators will provide an interesting and useful cross fertilization of ideas and concepts that benefits both groups.

This year's speakers are most gratefully acknowledged for their investment of time and for their willingness to share their ideas with the meeting participants. Thanks go to Lester Morss for consultations regarding the Heavy Element Chemistry program. Finally, this meeting would not be possible without the excellent logistical support it receives from Diane Marceau from our Division, Sophia Kitts from the Oak Ridge Institute of Science and Education, and the staff of the Airlie Conference Center.

Greg Fiechtner and Dick Hilderbrandt
Fundamental Interactions Team
Chemical Sciences, Geosciences and Biosciences Division
Office of Basic Energy Sciences
September 2007

Agenda

**U. S. Department of Energy
Office of Basic Energy Sciences
2007 Meeting on Condensed Phase and Interfacial Molecular Sciences**

Sunday, October 21

3:00-6:00 pm **** Check In ****
6:00 pm **** Reception at the Pub (No Host) ****
7:00 pm **** Dinner ****

Monday, October 22

7:00 am **** Breakfast ****

8:30 am *Introductory Remarks*
Gregory J. Fiechtner, DOE Basic Energy Sciences

Session I *Chair: Emily Carter, Princeton University*

8:45 am *Theory of Dynamics of Complex Systems*
David Chandler, Lawrence Berkeley National Laboratory

9:15 am *Algorithms for Nanostructures*
James R. Chelikowsky, University of Texas at Austin

9:45 am *Breakthrough Design and Implementation of Electronic and Vibrational
Many-Body Theories*
So Hirata, University of Florida

10:15 am **** Break ****

10:45 am *Correlated-electron effects in single molecules*
Corwin H. Booth, Lawrence Berkeley National Laboratory

11:15 am *A Fully Relativistic Density Functional Study of the Role of 5f Electrons in Chemical
Bonding in Transuranium Elements*
Asok K. Ray, University of Texas at Arlington

11:45 am *Structure and Properties of Pu-Oxide Nanoclusters*
Lynda Soderholm, Argonne National Laboratory

12:15 pm **** Lunch ****

5:00 pm **** Reception on the Rooftop Terrace (No Host) ****
6:00 pm **** Dinner ****

Session II Chair: **Caroline Chick Jarrold**, *Indiana University*

- 7:00 pm *Probing Actinide Electronic Structure using High-Resolution Photoelectron Spectroscopy*
Michael C. Heaven, *Emory University*
- 7:30 pm *Generation, Detection and Characterization of Gas-Phase Transition Metal Containing Molecules*
Timothy C. Steimle, *Arizona State University*
- 8:00 pm *Investigating the Mechanisms of Oxidation Reactions Occurring on Heterogeneous Catalysts*
A. W. Castleman, Jr., *Pennsylvania State University*
- 8:30 pm *Infrared Spectroscopy of Transition Metal-Molecular Interactions in the Gas Phase*
Michael A. Duncan, *University of Georgia*

Tuesday, October 23

7:00 am ***** Breakfast *****

Session III Chair: **Ward H. Thompson**, *University of Kansas*

- 8:00 am *Structural Dynamics in Complex Liquids Studied with Multidimensional Vibrational Spectroscopy*
Andrei Tokmakoff, *Massachusetts Institute of Technology*
- 8:30 am *Liquid and Chemical Dynamics in Nanoscopic Environments*
Michael D. Fayer, *Stanford University*
- 9:00 am *Molecular Theory & Modeling: The Structural-Spectral-Energetic Correspondence for Hydrogen Bonded Networks: Adding an Energy Component to Badger's Rule*
Sotiris S. Xantheas, *Pacific Northwest National Laboratory*
- 9:30 am *Chemical Kinetics and Dynamics at Interfaces: Structure and Reactivity of Ices, Oxides, and Amorphous Materials*
Bruce D. Kay, *Pacific Northwest National Laboratory*
- 10:00 am ***** Break *****
- 10:30 am *Understanding the Electron-water Interaction at the Molecular Level: Integrating Theory and Experiment in the Cluster Regime*
Mark A. Johnson, *Yale University*
- 11:00 am *Understanding the Electron-water Interaction at the Molecular Level: Integrating Theory and Experiment in the Cluster Regime*
Ken D. Jordan, *University of Pittsburgh*
- 11:30 am *Dynamics of Electrons at Interfaces on Ultrafast Timescales*
Charles B. Harris, *Lawrence Berkeley National Laboratory*
- 12:00 pm ***** Lunch *****

- Session IV** Chair: **Theresa Windus**, *Ames National Laboratory*
- 4:00 pm *Chemical Kinetics and Dynamics at Interfaces*
Greg A. Kimmel, *Pacific Northwest National Laboratory*
- 4:30 pm *Theory of the Reaction Dynamics of Small Molecules on Metal Surfaces*
Bret E. Jackson, *University of Massachusetts*
- 5:00 pm *Theoretical Studies of Surface Science and Intermolecular Interactions*
Mark S. Gordon, *Ames National Laboratory*
- 5:30 pm *Radiation Effects at the Solid-Aqueous Interface*
Dan Meisel, *Notre Dame Radiation Research Laboratory*
- 6:00 pm *Center for Radiation Chemistry Research: Excited States of Benzoquinone Radical Anion, New Ultrafast Single-Shot Detection at LEAF, and Non-Exponential Charge Capture*
Andrew R. Cook, *Brookhaven National Laboratory*
- 6:30 pm ***** Reception at the Pavilion (No Host) *****
- 7:00 pm ***** Banquet Dinner at the Pavilion *****

Wednesday, October 24

- 7:00 am ***** Breakfast *****
- Session V** Chair: **Carl Hayden**, *Sandia National Laboratories*
- 8:00 am *Optical Spectroscopy at the Spatial Limit*
Wilson Ho, *University of California, Irvine*
- 8:30 am *Experimental and Theoretical Studies of the Functional Relationship between Conformational Dynamics and Enzymatic Reactions*
Sunney Xie, *Harvard University*
- 9:00 am *Single-Molecule Dynamics in the Condensed Phase and at Interfaces: Time Resolved Single-Molecule Chemical Imaging Studies of Interfacial Electron Transfer*
H. Peter Lu, *Bowling Green State University*
- 9:30 am ***** Break *****
- 10:00 am *Ab Initio Approach to Interfacial Processes in Hydrogen Bonded Fluids*
Christopher J. Mundy, *Pacific Northwest National Laboratory*
- 10:30 am *Interfacial Oxidation of Complex Organic Molecules*
G. Barney Ellison, *University of Colorado*
- 11:00 am *Molecular Theory & Modeling Development of Statistical Mechanical Techniques for Complex Condensed-Phase Systems*
Gregory K. Schenter, *Pacific Northwest National Laboratory*
- 11:30 am *Closing Remarks*
Gregory J. Fiechtner, *DOE Basic Energy Sciences*
- 11:45 pm ***** Lunch *****
(Optional boxed lunches available)

Table of Contents

Invited Presentations (Ordered by Agenda)

Theory of Dynamics of Complex Systems
David Chandler1

Algorithms for Nanostructures
James R. Chelikowsky5

Breakthrough Design and Implementation of Electronic and Vibrational Many-Body Theories
So Hirata9

Correlated-Electron Effects in Single Molecules
Corwin H. Booth13

A Fully Relativistic Density Functional Study of the Role of 5f Electrons in Chemical Bonding in Transuranium Elements
Asok K. Ray14

Structure and Properties of Pu-Oxide Nanoclusters
Lynda Soderholm.....16

Probing Actinide Electronic Structure using High-Resolution Photoelectron Spectroscopy
Michael C. Heaven.....17

Generation, Detection and Characterization of Gas-Phase Transition Metal Containing Molecules
Timothy C. Steimle18

Investigating the Mechanisms of Oxidation Reactions Occurring on Heterogeneous Catalysts
A. W. Castleman, Jr......22

Infrared Spectroscopy of Transition Metal-Molecular Interactions in the Gas Phase
Michael A. Duncan.....26

Structural Dynamics in Complex Liquids Studied with Multidimensional Vibrational Spectroscopy
Andrei Tokmakoff30

Liquid and Chemical Dynamics in Nanoscopic Environments
Michael D. Fayer34

<i>Molecular Theory & Modeling- The Structural-Spectral-Energetic Correspondence for Hydrogen Bonded Networks: Adding an Energy Component to Badger's Rule</i> Sotiris S. Xantheas	38
<i>Chemical Kinetics and Dynamics at Interfaces: Structure and Reactivity of Ices, Oxides, and Amorphous Materials</i> Bruce D. Kay	42
<i>Understanding the Electron-water Interaction at the Molecular Level: Integrating Theory and Experiment in the Cluster Regime</i> Mark A. Johnson and Ken D. Jordan	46
<i>Dynamics of Electrons at Interfaces on Ultrafast Timescales</i> Charles B. Harris	50
<i>Chemical Kinetics and Dynamics at Interfaces: Non-Thermal Reactions at Surfaces and Interfaces</i> Greg A. Kimmel	54
<i>Theory of the Reaction Dynamics of Small Molecules on Metal Surfaces</i> Bret E. Jackson	58
<i>Theoretical Studies of Surface Science and Intermolecular Interactions</i> Mark S. Gordon	62
<i>Radiation Effects at the Solid-Aqueous Interface</i> Dan Meisel	66
<i>Center for Radiation Chemistry Research: Excited States of Benzoquinone Radical Anion, New Ultrafast Single-Shot Detection at LEAF, and Non-Exponential Charge Capture</i> Andrew R. Cook	70
<i>Optical Spectroscopy at the Spatial Limit</i> Wilson Ho	73
<i>Experimental and Theoretical Studies of the Functional Relationship between Conformational Dynamics and Enzymatic Reactions</i> Sunney Xie	77
<i>Single-Molecule Dynamics in the Condensed Phase and at Interfaces: Time Resolved Single-Molecule Chemical Imaging Studies of Interfacial Electron Transfer</i> H. Peter Lu	81
<i>Ab initio Approach to Interfacial Processes in Hydrogen Bonded Fluids</i> Christopher J. Mundy	87

<i>Interfacial Oxidation of Complex Organic Molecules</i> G. Barney Ellison	91
<i>Molecular Theory & Modeling Development of Statistical Mechanical Techniques for Complex Condensed-Phase Systems</i> Gregory K. Schenter	94
Research Summaries (Alphabetically by First PI)	
<i>Model Catalysis by Size-Selected Cluster Deposition</i> Scott Anderson	98
<i>Investigating Atoms to Aerosols with Vacuum Ultraviolet Radiation</i> Musahid Ahmed	102
<i>Thermochemistry and Reactivity of Transition Metal Clusters and Their Oxides</i> Peter B. Armentrout	106
<i>Electronic Structure of Transition Metal Clusters, and Actinide Complexes, and Their Reactivities</i> Krishnan Balasubramanian	110
<i>Influence of Medium on Radical Reactions</i> David M. Bartels	117
<i>Electron-Driven Processes in Condensed Phases</i> Ian Carmichael	121
<i>An Exploration of Catalytic Chemistry on Au/Ni(111)</i> Sylvia T. Ceyer	125
<i>Chemical Kinetics and Dynamics at Interfaces; Solvation / Fluidity on the Nanoscale And in the Environment</i> James P. Cowin	128
<i>Primary Processes of Radiation Chemistry: Solvent Mediated Charge Transfer Chemistry via Time-Resolved X-ray Spectroscopy</i> Robert A. Crowell	132

<i>Computational Studies of Liquid Interfaces</i> Liem X. Dang	136
<i>Molecular Theory & Modeling: Electronic Structure and Reactivity Studies in Aqueous Phase Chemistry Photochemistry at Interfaces</i> Michel Dupuis	141
<i>Photochemistry at Interfaces</i> Kenneth B. Eisenthal	144
<i>The Proton Pump in Bacteriorhodopsin, the other Photosynthetic System in Nature</i> Mostafa A. El-Sayed	148
<i>Statistical Mechanical and Multiscale Modeling of Surface Reaction Processes</i> Jim Evans	152
<i>Chemical Kinetics and Dynamics at Interfaces: Fundamentals of Solvation under Extreme Conditions</i> John L. Fulton	156
<i>Molecular Theory & Modeling: Reactions of Ions and Radicals in Aqueous Systems</i> Bruce C. Garrett	160
<i>Ion Solvation in Nonuniform Aqueous Environments</i> Phillip L. Geissler	164
<i>Computational Nanophotonics: Modeling Optical Interactions and Transport in Tailored Nanosystem Architectures</i> Stephen K. Gray	166
<i>Catalysis at Metal Surfaces Studied by Non-Equilibrium and STM Methods</i> Ian Harrison	173
<i>Fluctuations in Macromolecules Studied Using Time-Resolved, Multi-Spectral Single Molecule Imaging</i> Carl Hayden	175
<i>Electronic Structure and Optical Response of Nanostructures</i> Martin Head-Gordon	179

<i>Influence of Co-Solvents and Temperature on Nanoscale Self-Assembly of Biomaterials</i> Teresa Head-Gordon	183
<i>Chemical Kinetics and Dynamics at Interfaces – Laser Induced Reactions in Solids and at Surfaces</i> Wayne P. Hess	187
<i>Probing Catalytic Activity in Defect Sites in Transition Metal Oxides and Sulfides Using Cluster Models: A Combined Experimental and Theoretical Approach</i> Caroline Chick Jarrold	191
<i>Molecular Theory & Modeling: Nucleation: From Vapor Phase Clusters to Crystals in Solution</i> Shawn M. Kathmann	195
<i>Radiation Effects in Heterogeneous Systems and at Interfaces</i> Jay A. LaVerne	199
<i>Solvation, Reactivity of Nitrogen Oxides, Oxoacids, and Oxoanions</i> Sergei V. Lymar	203
<i>Spectroscopy of Organometallic Radicals</i> Michael D. Morse	207
<i>Laser Dynamic Studies of Photoreactions on Nanostructured Surfaces</i> Richard Osgood	211
<i>Optical Manipulation of Ultrafast Electron and Nuclear Motion on Metal Surfaces</i> Hrvoje Petek	215
<i>X-Ray Spectroscopy of Volatile Liquids and their Surfaces</i> Richard J. Saykally	219
<i>Computational Nanophotonics: Model Optical Interactions and Transport in Tailored Nanosystem Architectures</i> Mark Stockman	223
<i>Understanding Nanoscale Confinement Effects in Solvent-Driven Chemical Reactions</i> Ward H. Thompson	227
<i>The Role of Electronic Excitations on Chemical Reaction Dynamics at Metal, Semiconductor and Nanoparticle Surfaces</i> John C. Tully	231

Chemical Kinetics and Dynamics at Interfaces: Gas Phase Investigation of Condensed Phase Phenomena

Lai-Sheng Wang.....235

Surface Chemical Dynamics

Michael G. White239

Ionic Liquids: Radiation Chemistry, Solvation Dynamics and Reactivity Patterns

James F. Wishart243

Electronically non-adiabatic interactions in molecule metal-surface scattering:

Can we trust the Born-Oppenheimer approximation in surface chemistry?

Alec M. Wodtke.....247

Invited Presentations
(ordered by agenda)

Theory of Dynamics of Complex Systems

David Chandler

*Chemical Sciences Division, Lawrence Berkeley National Laboratory
and
Department of Chemistry, University of California, Berkeley CA 94720*

DOE funded research in our group concerns the theory of dynamics in systems involving large numbers of correlated particles. Glassy dynamics is a quintessential example. Here, dense molecular packing severely constrains the allowed pathways by which a system can rearrange and relax. The majority of molecular motions that exist in a structural glass former are trivial small amplitude vibrations that couple only weakly to surrounding degrees of freedom. In contrast, motions that produce significant structural relaxation take place in concerted steps involving many particles. In our recent work, we have related this hierarchical dynamics to dynamical heterogeneity [12],¹ shown how it is manifested in transport de-couplings [1-3,7,8,16], and finally, shown how it results in a first-order phase transition in trajectory space [5,11]. This first-order transition is the glass transition. It is a non-equilibrium phenomenon that is distinct from traditional equilibrium phase transitions. This finding is consistent with there being no thermodynamic signatures of the glass transition [6].

The kinetics or nucleation of equilibrium phase transitions is another example of correlated many-particle dynamics. On this topic, we have carried out trajectory studies and compared theory to experiments [9]. We have also studied the dynamics of hydrophobic assembly [14,17]. This process is closely related to nucleation of vapor in water and the formation of a water-vapor interface [4,15]. Figure 1 illustrates a transition state for the hydrophobic collapse of two hydrated nano-scale hydrophobic spheres. This dynamics is not of the hierarchical sort encountered in the formation of structural glass, and it is also not of the hierarchical sort encountered in the self-assembly of hard matter. We have studied the latter in the example of virus-capsid assembly [10]. In this case, the requisite conditions for successful assembly are not only thermodynamic meta-stability, but also the ability to self-anneal. Clusters that gather too quickly cannot self-anneal, and clusters that cannot self-anneal are malformed with frozen defects.

For the future, we plan DOE funded research on electron transfer, chemical dynamics and inhomogeneous fluids. We aim to develop techniques and concepts that will ultimately prove useful in the specific context of combining sunlight and renewable resources to produce transportation fuels. That specific effort will be part of the LBNL Helios Program. To reach the point where we can contribute to Helios, we plan to use our DOE support in this program to address basic underlying issues. Applications can then be done with Helios support. The first of these basic issues is the nature of ionic solutions

¹ Numbers in square brackets refer to papers cited in **Recent DOE Supported Research Publications**

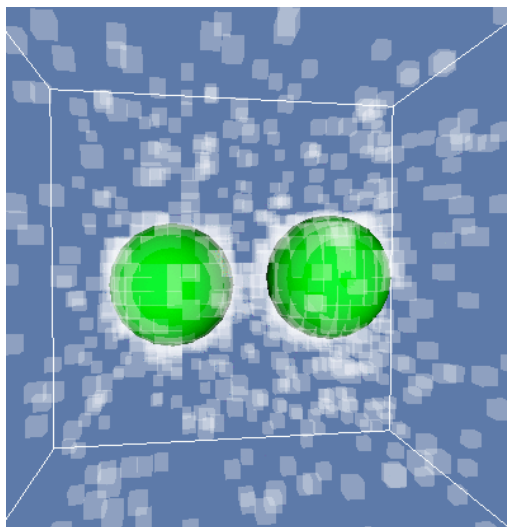


Figure 1. Two nano-scale hydrophobic spheres in water at a transition state configuration leading to the association of their associated dimmer. Water is rendered with a coarse graining over space and time, projecting water density onto a $(0.2\text{nm})^3 \times (10\text{ps})$ grid. Shading indicates density on this grid ranging from 1 g/cc (darkest), to zero (white).

at metal and semiconductor surfaces. The second is the development of ways to carry out numerical simulations of electronically non-adiabatic transitions. We have already made substantial progress in the first of these areas. Figure 2 shows a snapshot from a simulation we are currently carrying out of an ionic solution confined by metal-electrodes. To do it, we have adopted a model of Siepmann and Sprik [*J.Chem.Phys.* **102**, 511 (1995)] to successfully capture the electronic polarization effects of a metal. The results of this simulation reveal fluctuation effects that are large and significant to

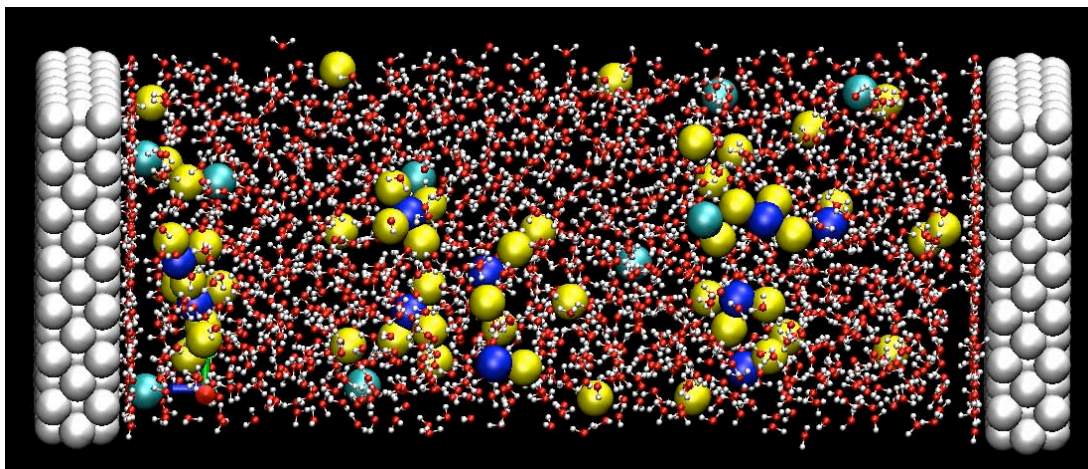


Figure 2. A view of simulated room-temperature aqueous ionic solution confined by metal-electrode surfaces. Potentials of interaction are chosen so that the metal is a model of Pt, and the ions are Cl^- , Ru^{2+} and Ru^{3+} .

electron transfer. Notice in Figure 2, for example, the layering induced by water molecules that are highly ordered at the water-metal interface. Also notice the clustering of ions, and how the ions are repelled from the metal surfaces due to ordered water layer. These effects are distinct from continuum and mean field approximations traditionally applied to electrochemistry.

Recent DOE Supported Research Publications

1. Jung, Y., J.P. Garrahan and D. Chandler. "Excitation lines and the breakdown of Stokes-Einstein relations in super-cooled liquids," *Phys. Rev. E* **69**, 061205.1-7 (2004).
2. Pan, A.C, J.P. Garrahan and D. Chandler. " Heterogeneity and growing lengthscales in the dynamics of kinetically constrained lattice gases in two dimensions," *Phys. Rev. E* **72**, 041106 (2005).
3. Pan, A.C, J.P. Garrahan and D. Chandler, "Decoupling of self-diffusion and structural relaxation during a fragile-to-strong cross-over in a kinetically constrained lattice gas," *ChemPhysChem* **6**, 1783-85 (2005).
4. Chandler, D., "Insight Review: Interfaces and the driving force of hydrophobic assembly", *Nature* **437**, 640-47 (2005).
5. Merolle, M., J.P. Garrahan and D. Chandler. " Space-time thermodynamics of the glass transition," *Proc. Natl Acad. Sci. USA* **102**,10837-40, (2005).
6. Chandler, D., and J.P. Garrahan, " Thermodynamics of coarse grained models of super-cooled liquids," *J. Chem. Phys* **123**, 044511.1-5, (2005).
7. Jung, Y.J., J.P. Garrahan and D. Chandler, "Dynamical exchanges in facilitated models of supercooled liquids," *J.Chem. Phys.* **123**, 084509.1-10, (2005).
8. Pan, A.C., " Rotational correlation and dynamic heterogeneity in a kinetically constrained lattice gas," *J. Chem. Phys.* **123**, 164501 (2005).
9. Pan, A.C, T.J. Rappl, D. Chandler, and N.P. Balsara, "Neutron scattering and Monte Carlo determination of the variation of the critical nucleus size with quench depth," *J. Phys. Chem. B* **110**, 3692-96 (2006).
10. Hagan, M.F. and D. Chandler, "Dynamic pathways for viral capsid assembly," *Biophys. J.* **91**, 42-54 (2006).
11. Jack, R.L., J.P. Garrahan and D. Chandler, "Spacetime thermodynamics and subsystem observables in a kinetically constrained model of glassy systems," *J. Chem. Phys.* **125**, 184509 (2006).

12. Chandler, D., J.P. Garrahan, R.L. Jack, L. Maibaum and A.C. Pan, "Lengthscale dependence of dynamic four-point susceptibilities in glass formers," *Phys. Rev. E* **74**, 051501 (2006).
13. Miller, T.F. and C. Predescu, "Sampling diffusive transition paths," *J. Chem. Phys.* **126**, 144102 (2007) .
14. Miller, T.F., E. Vanden-Eijnden and D. Chandler, "Solvent coarse-graining and the string method applied to the hydrophobic collapse of a hydrated chain," *Proc. Natl Acad. Sci. USA* **104**, 14559-64, (2007).
15. Maibaum, L. and D. Chandler, "Segue between favorable and unfavorable solvation," *J. Phys. Chem. B* **111**, 9025 (2007).
16. Hedges, L.O., L. Maibaum, D. Chandler and J.P.Garrahan "De-coupling of Exchange and Persistence Times in Atomistic Models of Glass Formers," arXiv:0708.0760v1, (2007).
17. Willard, A. P., D. Chandler "The Role of Solvent Fluctuations in Hydrophobic Assembly," arXiv:0709.1133, (2007).

Algorithms for Nanostructures

James R. Chelikowsky (jrc@ices.utexas.edu)

*Center for Computational Materials, Institute for Computational Engineering and Sciences
Departments of Physics and Chemical Engineering, 1 University Station C0200,
University of Texas, Austin, TX 78712*

1. Scope of Project.

Work in nanoscience has increased substantially in recent years owing to its potential technological applications and to fundamental scientific interest. In particular, new phenomena occur at the nanoscale such as quantum confinement, which can dramatically alter the electronic and optical properties of matter. Our work over the past several years has focused on developing new scalable algorithms for describing the electronic and optical properties of matter, and the application of previously developed algorithms to problems of interest at the nanoscale

Since nanostructures are neither at the molecular nor the bulk limits, calculations of their electronic and optical properties can be computationally intensive owing to the large number of both atomic and electronic degrees of freedom. A central activity of our current research is to develop new methods and algorithms to handle such systems. Current methods often allow one to consider systems of hundreds of atoms, whereas the size regimes of interest here can often extend to thousands of atoms. The creation of algorithms capable of addressing these large systems will allow us to predict properties across the entire nano space, *i.e.*, from the atom to the bulk limit.

We are especially interested in role of quantum confinement on the optical and electronic properties of confined systems such as nanocrystals and nanowires, both doped and intrinsic systems. For example, we explored the optical spectra of nanocrystals such as CdSe with several methodologies such as Green function methods (GW and Bethe-Salpeter equations) and time dependent density functional theory. We also wish to understand the evolution of doping properties in silicon nanocrystals, e.g., the evolution of shallow donors such as phosphorous from small nanocrystals to the bulk limit. In addition to non-magnetic dopants such as boron and phosphorous, we have also targeted the properties of magnetic dopants such as Mn in semiconductors to predict the role of quantum confinement on the magnetic properties of “spintronic materials.” Moreover, we examined the evolution of elemental magnetic materials such as iron from an atom to a nanocrystal representing the bulk limit.

2. Summary of Recent Progress.

High Performance algorithms for nano-scale systems.

One of the most significant goals in computational materials science is the development of new algorithms and physical concepts for describing matter at all length scales, especially at the nano-scale. Achieving an efficacious algorithm for predicting the role of quantum confinement and its role in determining the properties of nanocrystals is a difficult task owing to the complexity of nanocrystals. However, we have made notable progress by implementing new algorithms designed for highly parallel platforms. Our goal is to solve the electronic structure for large systems using pseudopotentials and density functional theory. The spatial and energetic distributions of electrons can be described by a solution of the Kohn-Sham equation:

$$\left(\frac{-\hbar^2 \nabla^2}{2m} + V_{ion}^p + V_H + V_{xc} \right) \psi_n = E_n \psi_n$$

where V_{ion}^p is an ionic pseudopotential, V_H is the Coulomb potential, and V_{xc} is the exchange correlation potential. The Hartree and exchange-correlation potentials can be determined from the electronic charge density. The density is given by

$$\rho = e \sum_{n, \text{occup}} |\psi_n|^2$$

The summation is over all occupied states. The Hartree potential is then determined by

$$\nabla^2 V_H = -4\pi e \rho$$

This term can be interpreted as the electrostatic interaction of an electron with the charge density of the system. The exchange-correlation potential, V_{xc} , is more problematic. This potential can be evaluated using the local density approximation. A traditional procedure for solving this equation is to approximate an input potential and then iterate the equation until the charge density and potential are self-consistent. This method is often used with a full diagonalization step at each iteration. The diagonalization step is very costly and can be replaced with a “filtering operation.” For example, if we consider a simple function that is large over the eigenvalue space of interest, we can filter the wave functions using a polynomial, $C_m(H)$, which has a small amplitude energy regime of interest:

$$\{\hat{\psi}_n\} = C_m(H)\{\psi_n\}$$

The set of wave functions, $\{\hat{\psi}_n\}$, is a better approximation to a solution to the Kohn-Sham equation than is the original set of wave function. The iterative cycle can now be summarized in Figure 1. By eliminating the explicit diagonalization step from the self-consistency loop, one can speed up the solution process by one to two orders of magnitude. This allows us to examine much larger systems than what we could otherwise examine.

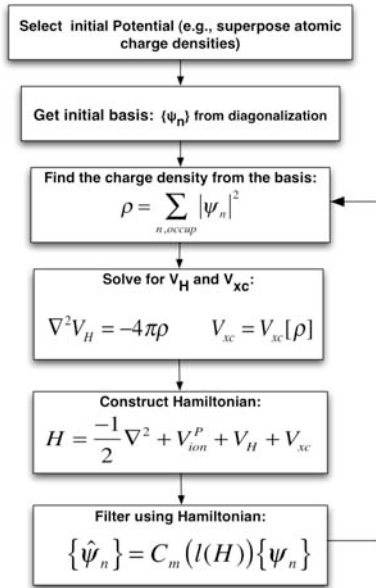


Figure 1. Block diagram illustrating the filtering process to achieve a self-consistent solution.

Doping Nanocrystal Systems. Doping a small percentage of foreign atoms in bulk semiconductors can profoundly change their electronic properties and makes possible the creation of modern electronic devices. Phosphorus doped into Si will introduce defect energy states close to the conduction band of Si. For such shallow donors, electrons can be easily thermally excited, greatly enhancing the conductivity of the original pure semiconductor by orders of magnitude. A major trend of semiconductor devices is their inexorable size reduction. This device miniaturization will ultimately approach nano-scale. As such, it is of the utmost importance to understand how doping and impurities operate at this length scale. Quantum confinement in this size regime is expected to alter the electronic properties of doped Si nano-crystals and important questions arise as to whether the defect energy levels are shallow or not, e.g., at what length scale will device construction based on macroscopic laws fail? Phosphorus-doped silicon nanocrystals represents the classical system for studying impurities in quantum dots.

We examined the electronic properties of phosphorus-doped silicon nanocrystals using real-space first-principles pseudopotential method. Nanocrystals with diameter up to 6 nm (containing over 5,000 atoms) were simulated and direct comparison with experimental measurement were made for *the first time* for this system.

Our calculated size dependence of hyperfine splitting is in excellent agreement with experimental data. Strong effects due to quantum confinement manifest itself not only in hyperfine splitting, but also in the higher binding energy of the dopant electron. We estimate that phosphorus in silicon nanocrystals of less than 20 nm in diameter will not be a shallow donor and we find a critical nanocrystal size below which the dopant will be ejected to the surface. In addition, we find that a hydrogen-like quantum model can characterize the electronic properties of the defect electron, which will be useful for modeling impurities in semiconductor nano-structures.

Evolution of Magnetism from an Atom to a Crystal. The existence of spontaneous magnetization in metallic systems is an intriguing problem, both because of the extensive technological applications of magnetic phenomena and the incomplete understanding of its fundamental mechanism at the level of basic science. In this scenario, clusters of metallic atoms are ideal systems of study because they provide a bridge between macroscopic samples and isolated atoms, which have much simpler behavior. Several phenomena such as ferromagnetism, metallic behavior, and ferroelectricity have been intensely explored in bulk metals, but the way they manifest themselves in clusters is an open topic of debate. In particular, ferromagnetism in the bulk has been understood in term of the itinerant electron model, which assumes partial delocalization of the 3d orbitals. In a cluster, delocalization is weaker due to the presence of a surface, whose shape affects the magnetic properties of the cluster.

To assess such issues, we examined the evolution of the magnetic moment in iron clusters containing 50 to 400 atoms using the local spin density approximation and a real space pseudopotentials. We examined three families of clusters that could be broadly characterized as icosahedral, body-centered cubic centered on an atom site, and body-centered cubic centered on the bridge between two neighboring atoms. We found an overall decrease of magnetic moment as the clusters grow in size, as well as suppression of magnetic moment in clusters with faceted surfaces. We also studied their structural stability and compared the calculated results for the moments to experiment with generally good agreement.

3. Future Research Plans.

We plan to focus future research projects on optimizing algorithms and extending our computational work to complex nanoscale systems. In terms of algorithm development, we will implement “mixed boundary” conditions so that we can examine materials confined in certain directions and periodic in other directions, e.g., we might consider nanowires with periodicity along the axial direction, but confined in directions perpendicular to the axis. We will also consider developing numerical methods to avoid the most time consuming operations, i.e., the initial diagonalization step and more efficient parallelization methods such as windowing the eigenvalue spectrum.

In terms of materials systems, we would like to examine magnetic dopants in both nanocrystals and nanowires. These systems provide an interesting example of “spins” in a box. We will be able to examine magnetic in both isotropic and anisotropic environments. We will also continue our research program on the optical properties of these systems.

4. Publications from DOE Sponsored Work, 2004-present.

[1] D.V. Melnikov and J.R. Chelikowsky: “Electron affinities and ionization energies of semiconductor nanocrystals,” *Phys. Rev. B* **69**, 113305 (2004).

[2] D.V. Melnikov and J.R. Chelikowsky: “Quantum confinement in phosphorus-doped silicon nanocrystals,” *Phys. Rev. Lett.* **92**, 046802 (2004).

[3] M.M.G. Alemany, M. Jain, J.R. Chelikowsky and L. Kronik: “A real space pseudopotential method for computing the electronic properties of periodic systems,” *Phys. Rev. B* **69**, 075101 (2004).

[4] F.-C. Chuang, C.Z. Wang, S. Ogut, J.R. Chelikowsky and K.M. Ho: “Melting of small Sn clusters by ab initio molecular dynamics simulations,” *Phys. Rev. B* **69**, 165408 (2004).

[5] E. L. de la Grandmaison, S.B. Gowda, Y. Saad, M. Tiago, and J.R. Chelikowsky: “An Efficient Computation of the Coupling Matrix in Time Dependent Density Functional Theory,” *Comp. Phys. Comm.* **167**, 7 (2005).

[6] S. Li, M.M.G. Alemany and J.R. Chelikowsky: “Ab initio calculations for the photoelectron spectra of vanadium clusters,” *J. Chem. Phys.* **121**, 5893 (2004).

[7] L. Kronik, M. Jain, and J.R. Chelikowsky: “Electronic structure and spin-polarization of MnGaP,” *Applied Phys. Lett.* **85**, 2014 (2004).

[8] G. Neshler, L. Kronik and J.R. Chelikowsky: “Ab initio absorption spectra of Ge nanocrystals,” *Phys. Rev. B* **71**, 035344 (2005).

[9] X. Huang, E. Lindgren and J.R. Chelikowsky: “Surface passivation method for semiconductor nanostructures,” *Phys. Rev. B* **71**, 165328 (2005).

[10] S. Li, M.M.G. Alemany, and J.R. Chelikowsky: “Ab initio calculations of the photoelectron spectra of transition metal clusters,” *Phys. Rev. B* **71**, 165433 (2005).

[11] M.L. Tiago and J.R. Chelikowsky: “First-principles GW-BSE excitations in organic molecules,” *Solid State Comm.* **136**, 333 (2005).

- [12] X. Huang, A. Makmal, J. R. Chelikowsky and L. Kronik: “Size dependent spintronic properties of dilute magnetic semiconductor nanocrystals,” *Phys. Rev. Lett.* **94**, 236801 (2005).
- [13] K.S. Nakayama, M.M.G. Alemany, H. Kwak, T. Sugano, K. Ohmori, J.R. Chelikowsky and J.H. Weaver: “Electronic structure of Si(001)-c(4 \times 2) analyzed by scanning tunneling spectroscopy and ab initio simulations,” *Phys. Rev. B* **73**, 035330 (2006).
- [14] C. Bekas, Y. Saad, M.L. Tiago and J.R. Chelikowsky: “Computing charge densities with partially reorthogonalized Lanczos,” *Comp. Phys. Comm.* **171**, 175 (2005).
- [15] M. Lopez del Puerto, M.L. Tiago, I. Vasiliev and J.R. Chelikowsky: “Real space pseudopotential calculations of the ground state and excited state properties of the water molecule,” *Phys. Rev. A* **72**, 052504 (2005).
- [16] M.M.G. Alemany and J.R. Chelikowsky: “Ab initio calculations for the interconversion of optically active defects in amorphous silica,” *Phys. Rev. B* **73**, 235211 (2006).
- [17] Y. Zhou, Y. Saad, M. L. Tiago and J. R. Chelikowsky: “Self-consistent-field calculations using Chebyshev-filtered subspace iteration,” *J. Comp. Phys.* **219**, 172 (2006).
- [18] M.L. Tiago and J.R. Chelikowsky: “Optical excitations in organic molecules, clusters and defects from first principles Green's function methods,” *Phys. Rev. B* **73**, 205334 (2006).
- [19] L. Kronik, A. Makmal, M.L. Tiago, M.M.G. Alemany, M. Jain, X. Huang, Y. Saad and J.R. Chelikowsky: “PARSEC-the pseudopotential algorithm for real space electronic structure calculations: recent advances and novel applications to nano-structures,” *phys. stat. sol. (b)* **243**, 1063 (2006).
- [20] G. Dalpian, M.L. Tiago, M. Lopez del Puerto and J.R. Chelikowsky: “Symmetry considerations for semiconductor nanocrystals,” *Nano Letters* **6**, 501 (2006).
- [21] L. Kong, M. L. Tiago and J. R. Chelikowsky: “Real-space pseudopotential method for electron transport properties of nano-scale junctions,” *Phys. Rev. B* **73**, 195118 (2006).
- [22] G. Dalpian and J.R. Chelikowsky: “Self-Purification in Semiconductor Nanocrystals,” *Phys. Rev. Lett.* **96**, 226802 (2006).
- [23] S. Li, M.M.G. Alemany and J. R. Chelikowsky: “Real-space Ab initio pseudopotential calculations for anion clusters: Fe $_n^+$ (n=3-6),” *Phys. Rev. B* **73**, 233404 (2006).
- [24] S. Li, M.M.G. Alemany and J. R. Chelikowsky: “Real space pseudopotential calculations for copper clusters,” *J. Chem. Phys.* **125**, 034311(2006).
- [25] Y. Saad, Y. Zhou, C. Bekas and J.R. Chelikowsky: “Diagonalization Methods in PARSEC,” *phys. stat. sol. (b)* **243**, 2188 (2006).
- [26] J.R. Chelikowsky, E. Kaxiras and R.M. Wentzcovitch: “Theory of Spintronic Materials,” *phys. stat. sol. (b)* **243**, 2133 (2006).
- [27] M. Lopez del Puerto, M.L. Tiago, and J.R. Chelikowsky: “Excitonic effects and optical properties of passivated CdSe clusters,” *Phys. Rev. Lett.* **97**, 096401 (2006).
- [28] M.L. Tiago and J.R. Chelikowsky: “Confinement effects in the optical properties of semiconductor nanocrystals,” *phys. stat. sol. (b)* **243**, 2151 (2006).
- [29] S. Beckman, J. Han, and J.R. Chelikowsky: “Role of Quantum Confinement in Ge Nanowires,” *Phys. Rev. B* **74**, 165314 (2006).
- [30] M.L. Tiago, Y. Zhou, M.M.G. Alemany, Y. Saad, J.R. Chelikowsky: “The Evolution of Magnetism in Iron from the Atom to the Bulk,” *Phys. Rev. Lett.* **97**, 147201 (2006).
- [31] N.S. Norberg, G.M. Dalpian, J.R. Chelikowsky, and D.R. Gamelin: “Vacuum Pinning of Magnetic Impurity Levels in Quantum Confined Semiconductors,” *Nano Letters* **6**, 2887 (2006).
- [32] J.R. Chelikowsky: “The Role of Self-Purification and the Electronic Structure of Magnetically Doped Semiconductor Nanocrystals,” *Phase Transitions* **79**, 739 (2006).
- [33] Y. Zhou, Y. Saad, M.L. Tiago, and J.R. Chelikowsky: “Parallel Self-Consistent-Field Calculations via Chebyshev-Filtered Subspace Acceleration,” *Phys. Rev. E* **74**, 066704 (2006).
- [34] M.M.G. Alemany, X. Huang, M.L. Tiago, and J.R. Chelikowsky: “p-type Doping in Indium Phosphide Nanowires: the Role of Dimensionality and Quantum Confinement in the Acceptor Impurity States,” *Nano Lett.* **7**, 1878 (2007).
- [35] J.R. Chelikowsky, M.L. Tiago, Y. Saad, and Y. Zhou: “Algorithms for the Evolution of Electronic Properties in Nanocrystals,” *Comp. Phys. Comm.* **177**, 1 (2007).
- [36] M.M.G. Alemany, M. Jain, M. L. Tiago, Y. Zhou, Y. Saad and J.R. Chelikowsky: “Efficient first principles calculations of the electronic structure of periodic systems,” *Comp. Phys. Comm.* **177**, 339 (2007).
- [37] G. Rollmann, M.E. Gruner, A. Hucht, P. Entel, M.L. Tiago and J.R. Chelikowsky: “Shell-wise Mackay transformation in iron nano-clusters,” *Phys. Rev. Lett.* **99**, 083402 (2007).

Breakthrough Design and Implementation of Electronic and Vibrational Many-Body Theories

So Hirata (principal investigator: DE-FG02-04ER15621)
Quantum Theory Project, Department of Chemistry
University of Florida, Gainesville, FL 32611-8435
hirata@qtp.ufl.edu

Program Scope

Predictive chemical computing requires hierarchical methods of increasing accuracy for both electronic and vibrational many-body problems. Such hierarchies are established, at least conceptually, as configuration-interaction (CI), many-body perturbation (PT), and coupled-cluster (CC) methods for electrons and for vibrations, which all converge at the exact limit with increasing rank of a hierarchical series. The series can generate results of which the convergence with respect to various parameters of calculations can be demonstrated and which can be predictive in the absence of experimental information.

The progress in these methods and their wide use are, however, hindered by (1) the immense complexity and cost of designing and implementing some of the high-rank members of the hierarchical methods and the difficulty in code verification and optimization (including parallelization) and by (2) the extremely slow convergence of electronic energies and wave functions with respect to one-electron basis set sizes, which is compounded with the high-rank polynomial or even factorial molecular size dependence of the computational cost of these methods. These two difficulties are furthermore aggravated by the diversity of chemical species and interactions that chemists must deal with.

The overarching goal of our research is to address both difficulties for electrons and vibrations. We will eradicate the first difficulty for electrons by developing a computerized symbolic algebra system which completely automates the mathematical derivations of electron-correlation methods and their implementation into massively-parallel executions programs, while also incorporating domain-specific optimizations. We will perform the code verification with the aid of the determinant-based algorithms that implement general-order CI, PT, and CC and their various combinations. Once this research infrastructure is in place, we will explore various combinations of CC, CI, and PT expansions to design and assess a new class of electron-correlation methods. For vibrations, the vibrational SCF (VSCF) and CI (VCI) codes will be developed in the general-order product-based algorithm (akin to the determinant-based algorithm) that are applicable to polyatomic molecules and allow us to include anharmonicity and vibrational mode-mode couplings to any desired extent.

We address the second difficulty by radically departing from the conventional Gaussian-basis-set LCAO framework and introduce a new hierarchy of converging electron-correlation methods with completely flexible but rational (e.g., satisfying asymptotic decay and cusp conditions) basis functions on interlocking multicenter quadrature grids that are not only of one-electron type but also of two-electron and possibly higher-order types. These methods can, therefore, reach the solutions free from the basis-set errors and, when the order of hierarchical electron-correlation methods is raised, they can achieve the exact or nearly exact solutions of the Schrödinger equation. The rank of polynomial size dependence of the computational cost will be lowered by the use of highly localized grid representations. The software products that will result from this project are the grid-based HF, MP2, and higher-order correlation codes and the automatic symbolic algebra that assists in synthesizing the higher-order methods.

Recent Progress

We have developed the TENSOR CONTRACTION ENGINE (TCE),¹ which has synthesized the parallel execution programs (many for the first time) of the CI through quadruples (CISDTQ), Møller-Plesset PT through fourth order, and CC through quadruples (CCSDTQ),¹ CC for ground-state molecular properties,² equation-of-motion coupled-cluster (EOM-CC) through EOM-CCSDTQ for excitation energies and excited-state properties,² for ionization,³ and for electron-attachment⁴ energies. It has also auto-

mated the development of new classes of methods such as combined CC and PT methods,⁵ combined CI and PT methods,⁶ active-space methods,^{7,8} relativistic methods,^{9,10} and combined CC, CI, and PT methods.²⁴ We have tested all of our automatically synthesized programs against independent determinant-based implementations also developed by us. The scalability of the massively-parallel execution speed is reasonable for all the methods tested including CCSD(T).⁵ The synthesized programs make use of sparsity and data dependency caused by spin symmetry (within the spin-orbital formalisms), point-group symmetry, and index permutation symmetry. These computerized implementations have enabled highly accurate predictions of spectroscopic properties of small molecules, some containing heavy elements.^{9,10}

We have written the VSCF and general-order VCI codes for polyatomic molecules using harmonic oscillator wave functions as the basis set, which have been integrated with electronic structure programs that are used to scan a small part of a potential energy surface (PES) in either the direct fashion (the energies are computed on the fly and discarded after their use) or in a quartic force field representation with or without the so-called n -mode coupling approximation. Various combinations of these different PES representations, grid sizes, electronic structure theories, etc. have been explored to achieve optimal efficiency and quality of PES.¹¹ The PES scan module has a built-in capability of fault recovery for cases in which the electronic structure program fails to supply the energies in highly strained geometries: The missing entries will be inter/extrapolated. These methods have been applied to Franck–Condon integrals over anharmonic vibrational wave functions¹² and accurate predictions of Fermi polyad frequencies.^{13,14} A new vibrational quasi-degenerate perturbation theory has been proposed, implemented, and assessed.¹⁴

We have also developed a grid-based numerical solver¹⁵ of the Hartree–Fock (HF) equation for polyatomic molecules and also a prototype grid-based second-order Møller–Plesset perturbation (MP2) code for atoms with some provision to applications for polyatomic molecules. Exact numerical HF energies of diatomic and triatomic molecules have been obtained within $10^{-5} E_h$ accuracy without any extrapolation. A finite-difference method has been used to solve Poisson’s equation for the Coulomb and exchange potentials and to evaluate the action of the Laplace operator on numerical orbitals expanded on an interlocking multicenter quadrature grid of Becke.

Twenty-two (22) published or accepted papers,^{3-9,11-13,16-27} three (3) submitted papers,^{14,15,28} and an invited book chapter²⁹ have originated from the work performed by the PI at University of Florida which was supported by this DOE award (DE-FG02-04ER15621) during the last funding period (September 1, 2004 through October 31, 2007). NWChem 5.0 has been released in September 2006, containing the computer codes and new capabilities developed in the PI’s group and is being used by applications chemists to solve chemical problems on massively parallel supercomputers worldwide. Furthermore, the PI has launched an online database of working equations and benchmark results of high-end electron-correlation methods (<http://www.qtp.ufl.edu/~hirata/Database.html>).

Owing to the space limitation, we summarize only some of the research highlights in more detail:

Combined Coupled-Cluster and Many-Body Perturbation Theories.⁵ Various approximations combining CC and PT have been derived and implemented into the parallel execution programs. The implemented models range from the CCSD(T), CCSD(2)_T, CCSD(2)_{TQ}, and CCSDT(2)_Q methods to the CR-CCSD(T) approach. The perturbative correction part of the CCSD(T)/cc-pVDZ calculations for azulene exhibited a 45-fold speedup upon a 64-fold increase in the number of processors from 8 to 512.

Third- and Fourth-Order Perturbation Corrections to Excitation Energies from Configuration Interaction Singles.⁶ Complete third-order and partial fourth-order Rayleigh–Schrödinger perturbation corrections to excitation energies from CIS have been derived and implemented by TCE as CIS(3) and CIS(4)_P. The consistent use of factorization, first introduced by Head-Gordon *et al.* in the second-order correction to CIS denoted CIS(D), has reduced the computational cost of CIS(3) and CIS(4)_P from $O(n^8)$ and $O(n^6)$ to $O(n^6)$ and $O(n^5)$, respectively, with n being the number of orbitals. It has also guaranteed the size intensity of excited-state energies of these methods.

Symbolic Algebra in Quantum Chemistry.²⁴ The PI has been invited to contribute an article to a special issue entitled *New Perspectives in Theoretical Chemistry* by C. J. Cramer and D. G. Truhlar, editors of *Theor. Chem. Acc.* In the article, the PI summarizes the computerization of complex symbolic

algebra in the context of electron-correlation theories such as the manipulation of second-quantized operators, Slater determinants, and Feynman diagrams.

High-Order Electron-Correlation Methods with Scalar Relativistic and Spin-Orbit Corrections.⁹ The TCE-synthesized high-order electron-correlation programs have been fitted with the ability to use relativistic reference wave functions on the basis of scalar relativistic and spin-orbit effective potentials and by allowing the computer-generated programs to handle complex-valued, spinless orbitals determined by these potentials. We demonstrate the utility of the implemented methods in chemical simulation wherein the consideration of spin-orbit effects is essential: Ionization energies of rare gases, spectroscopic constants of protonated rare gases, and photoelectron spectra of hydrogen halides.



Fig.1. A large formaldehyde-water cluster for which an excited-state coupled-cluster calculation with an aug-cc-pVDZ basis was performed by us.

Fast Electron Correlation Methods for Molecular Clusters in the Ground and Excited States.¹⁷ An efficient (linear and sublinear scaling) and accurate electronic structure method for clusters of weakly interacting molecules has been proposed and combined with a variety of methods. It retains the one- and two-body (and three-body) Coulomb, exchange, and correlation energies exactly and higher-order Coulomb energies in the dipole approximation (hence the induction). The record largest EOM-CCSD calculation was performed with the aug-cc-pVDZ basis set for a formaldehyde-(H₂O)₈₁ cluster containing 247 atoms (**Fig.1**). Two extensions to this scheme (a basis set superposition error correction and the use of self-consistent atom-centered partial charges for higher-order Coulomb energies) have also been made recently.²⁸

Franck-Condon Factors Based on Anharmonic Vibrational Wave Functions of Polyatomic Molecules.¹² Franck-Condon (FC) integrals of polyatomic molecules have been computed on the basis of the VSCF or VCI calculations capable of including vibrational anharmonicity to any desired extent, also taking account of the Duschinsky rotations, geometry displacements, and frequency changes. This method in conjunction with the VCI and CCSD(T) method has predicted the peak positions and intensities of the vibrational manifold in a photoelectron band of H₂O with quantitative accuracy, revealing the importance of intensity borrowing in reproducing some small peaks.

Fermi Resonance in CO₂: A Combined Electronic Coupled-Cluster and Vibrational Configuration-Interaction Prediction.¹³ We have presented a first-principles prediction of the energies of the eight lowest-lying anharmonic vibrational states of CO₂, including the fundamental symmetric stretching mode and the first overtone of the fundamental bending mode, which undergo a strong coupling known as Fermi resonance. We have employed CCSD(T) and CCSDT in conjunction with a range of Gaussian basis sets to calculate the PES of the molecule, with the errors arising from the finite basis-set sizes eliminated by extrapolation. With the VCI, the best theoretical estimates of the anharmonic energy levels agree excellently with experimental values within 3.5 cm⁻¹.

Future Plans

We will continue the ongoing effort in our laboratory to develop grid-based HF and MP2 methods for polyatomic molecules. The $1/r_{12}$ type singularity will be removed analytically from the Sinanoğlu equation and this singularity-free equation will be solved on a grid. Once these are completed, we will extend these methods to higher-order correlation treatments beginning with the development of grid-based LCCD, CCD, LCCSD, CCSD, and MP3.

We also propose to complement the vibrational many-body methods developed with a capability to evaluate the transition integrals of dipole and polarizability operators with VSCF or VCI wave functions. The ultimate purpose is to deliver a predictive theory and quantitative computational method to simulate the multidimensional nonlinear spectroscopies such as the two-dimensional (2D) IR and Raman spectroscopies that directly measure anharmonicity and vibrational mode-mode couplings and have exceptional promise as a technique providing time-resolved information in structural biology.

References to Related Publications or Submitted Manuscripts

- ¹ S. Hirata, "Tensor Contraction Engine: Abstraction and Automated Parallel Implementation of Configuration-Interaction, Coupled-Cluster, and Many-Body Perturbation Theories", *J. Phys. Chem. A* **107**, 9887 (2003).
- ¹⁴ K. Yagi, S. Hirata, and K. Hirao, "Vibrational Quasi-Degenerate Perturbation Theory: Application to Fermi Resonances in CO₂, H₂CO, and C₆H₆", submitted (2007).
- ¹⁵ T. Shiozaki and S. Hirata, "Exact Grid-Based Hartree-Fock Solutions of Polyatomic Molecules", submitted (2007).
- ²⁸ M. Kamiya, S. Hirata, and M. Valiev, "Fast Electron Correlation Methods for Molecular Clusters without Basis Set Superposition Errors", submitted (2007).

References to Publications of DOE Sponsored Research (2004–Present)

- ² S. Hirata, "Higher-Order Equation-of-Motion Coupled-Cluster Methods", *J. Chem. Phys.* **121**, 51 (2004).
- ³ M. Kamiya and S. Hirata, "Higher-Order Equation-of-Motion Coupled-Cluster Methods for Ionization Processes", *J. Chem. Phys.* **125**, 074111 (2006).
- ⁴ M. Kamiya and S. Hirata, "Higher-Order Equation-of-Motion Coupled-Cluster Methods for Electron Attachment", *J. Chem. Phys.* **126**, 134112 (2007).
- ⁵ S. Hirata, P.-D. Fan, A. A. Auer, M. Nooijen, and P. Piecuch, "Combined Coupled-Cluster and Many-Body Perturbation Theories", *J. Chem. Phys.* **121**, 12197 (2004).
- ⁶ S. Hirata, "Third- and Fourth-Order Perturbation Corrections to Excitation Energies from Configuration Interaction Singles", *J. Chem. Phys.* **122**, 094105 (2005).
- ⁷ P.-D. Fan and S. Hirata, "Active-Space Coupled-Cluster Methods through Connected Quadruple Excitations", *J. Chem. Phys.* **124**, 104108 (2006).
- ⁸ P.-D. Fan, M. Kamiya, and S. Hirata, "Active-Space Equation-of-Motion Coupled-Cluster Methods through Quadruples for Excited, Ionized, and Electron-Attached States", *J. Chem. Theo. Comp.* **3**, 1036 (2007).
- ⁹ S. Hirata, T. Yanai, R. J. Harrison, M. Kamiya, and P. D. Fan, "High-Order Electron-Correlation Methods with Scalar Relativistic and Spin-Orbit Corrections", *J. Chem. Phys.* **126**, 024104 (2007).
- ¹⁰ S. Hirata, T. Yanai, W. A. de Jong, T. Nakajima, and K. Hirao, "Third-Order Douglas-Kroll Relativistic Coupled-Cluster Theory through Connected Single, Double, Triple, and Quadruple Substitutions: Applications to Diatomic and Triatomic Hydrides", *J. Chem. Phys.* **120**, 3297 (2004).
- ¹¹ K. Yagi, S. Hirata, and K. Hirao, "Multiresolution Potential Energy Surfaces for Vibrational State Calculations", *Theor. Chem. Acc.*, in press (2007).
- ¹² V. Rodriguez-Garcia, K. Yagi, K. Hirao, S. Iwata, and S. Hirata, "Franck-Condon Factors Based on Anharmonic Vibrational Wave Functions of Polyatomic Molecules", *J. Chem. Phys.* **125**, 014109 (2006).
- ¹³ V. Rodriguez-Garcia, S. Hirata, K. Yagi, K. Hirao, T. Taketsugu, I. Schweigert, and M. Tasumi, "CO₂ Fermi Resonance: A Combined Electronic Coupled-Cluster and Vibrational Configuration-Interaction Prediction", *J. Chem. Phys.* **126**, 124303 (2007).
- ¹⁶ S. Hirata, S. Ivanov, R. J. Bartlett, and I. Grabowski, "Exact-Exchange Time-Dependent Density-Functional Theory for Static and Dynamic Polarizabilities", *Phys. Rev. A* **71**, 032507 (2005).
- ¹⁷ S. Hirata, M. Valiev, M. Dupuis, S. S. Xantheas, S. Sugiki, and H. Sekino, "Fast Electron Correlation Methods for Molecular Clusters in the Ground and Excited States", *Mol. Phys.* **103**, 2255 (2005).
- ¹⁸ S. A. Perera, P. B. Rozyczko, R. J. Bartlett, and S. Hirata, "Improving the Performance of Direct Coupled Cluster Analytical Gradients Algorithms", *Mol. Phys.* **103**, 2081 (2005).
- ¹⁹ S. Hirata, "Time-Dependent Density Functional Theory Based on Optimized Effective Potentials for Van Der Waals Forces", *J. Chem. Phys.* **123**, 026101 (2005).
- ²⁰ H. Wang, J. Szczepanski, S. Hirata, and M. Vala, "Vibrational and Electronic Absorption Spectroscopy of Dibenzo[b,def]Chrysene and Its Ions", *J. Phys. Chem. A* **109**, 9737 (2005).
- ²¹ P. Piecuch, S. Hirata, K. Kowalski, P.-D. Fan, and T. L. Windus, "Automated Derivation and Parallel Computer Implementation of Renormalized and Active-Space Coupled-Cluster Methods", *Int. J. Quantum Chem.* **106**, 79 (2006).
- ²² Y. Shigeta, K. Hirao, and S. Hirata, "Exact-Exchange Time-Dependent Density-Functional Theory with the Frequency-Dependent Kernel", *Phys. Rev. A* **73**, 010502(R) (2006).
- ²³ **Invited article:** Y. Shao, *et al.*, "Advances in Methods and Algorithms in a Modern Quantum Chemistry Program Package", *Phys. Chem. Chem. Phys.* **8**, 3172 (2006).
- ²⁴ **Invited article:** S. Hirata, "Symbolic Algebra in Quantum Chemistry", *Theor. Chem. Acc.* **116**, 2 (2006).
- ²⁵ **Invited article:** S. Hirata, "Automated Symbolic Algebra for Quantum Chemistry", *J. Phys. Conf. Ser.* **46**, 249 (2006).
- ²⁶ T. Shiozaki, K. Hirao, and S. Hirata, "Second- and Third-Order Triples and Quadruples Corrections to Coupled-Cluster Singles and Doubles in the Ground and Excited States", *J. Chem. Phys.* **126**, 244106 (2007).
- ²⁷ K. Yagi, S. Hirata, and K. Hirao, "Efficient Configuration Selection Scheme for Vibrational Second-Order Perturbation Theory", *J. Chem. Phys.* **127**, 034111 (2007).
- ²⁹ **Invited book chapter:** S. Hirata, P.-D. Fan, T. Shiozaki, and Y. Shigeta, "Single-Reference Methods for Excited States in Molecules and Polymers", in *Radiation Induced Molecular Phenomena in Nucleic Acid: A Comprehensive Theoretical and Experimental Analysis*, edited by J. Leszczynski and M. Shukla (Springer), in press (2007)

Correlated-electron effects in single molecules*

Corwin H. Booth
Chemical Sciences Division
Lawrence Berkeley National Laboratory
Berkeley, CA 94720
chbooth@lbl.gov

Pauling first viewed the single/double bond pairs in the conjugated benzene ring as hybrid orbitals with delocalized electrons [1], analogous to orbital behavior in metals. In particular, the delocalized electrons are diamagnetic, as in a metal. The main difference with actual metallic behavior is the presence of discrete, atomic-like energy states in aromatic molecules, whereas relatively broad bands exist in metallic systems. This situation in aromatic molecules is the same as in metallic nanoparticles, making such molecules an attractive arena for studying quantum confinement effects on the nanoscale. Here, we consider the role of magnetic interactions between local *f*-electrons and orbitals on aromatic rings. Early calculations that considered this effect on cerocene [2-4], $\text{Ce}(\text{C}_8\text{H}_8)_2$, found that an intermediate valent, multiconfigurational ground state can develop in analogy to the Kondo effect in metallic systems with small magnetic impurities. Past and present evidence for this state will be present for cerocene [5,6], as well as a collection of related molecules, including the cerium pentalene complex, $\text{Ce}(\text{C}_8\text{H}_6)_2$ [7], and a collection of cyclopentadienyl-based ytterbium adducts [5,8,9]. The ytterbocenes yield an astonishing array of intermediate valent behavior, including valence/structural phase transitions.

References:

- [1] L. Pauling, *J. Chem. Phys.* **4**, 673 (1936).
- [2] C.-S. Neumann and P. Fulde, *Z. Phys. B* **74**, 277 (1989).
- [3] M. Dolg et al., *J. Chem. Phys.* **94**, 3011 (1991).
- [4] M. Dolg et al., *Chem. Phys.* **195**, 71 (1995).
- [5] C. H. Booth et al., *Phys. Rev. Lett.* **95**, 267202 (2005).
- [6] N. M. Edelstein et al., *J. Am. Chem. Soc.* **118**, 13115 (1996).
- [7] A. Ashley et al., *Chem. Comm.*, 1515 (2007).
- [8] M. Schultz et al., *Organometallics* **21**, 460 (2002).
- [9] M. D. Walter et al., *Organometallics* **26**, 2296 (2007).

*This work was supported by the Chemical Sciences Research Program, Office of Basic Energy Sciences, Office of Science, Department of Energy, by Contract No. DE-AC02-05CH11231.

Program: Heavy Element Chemistry

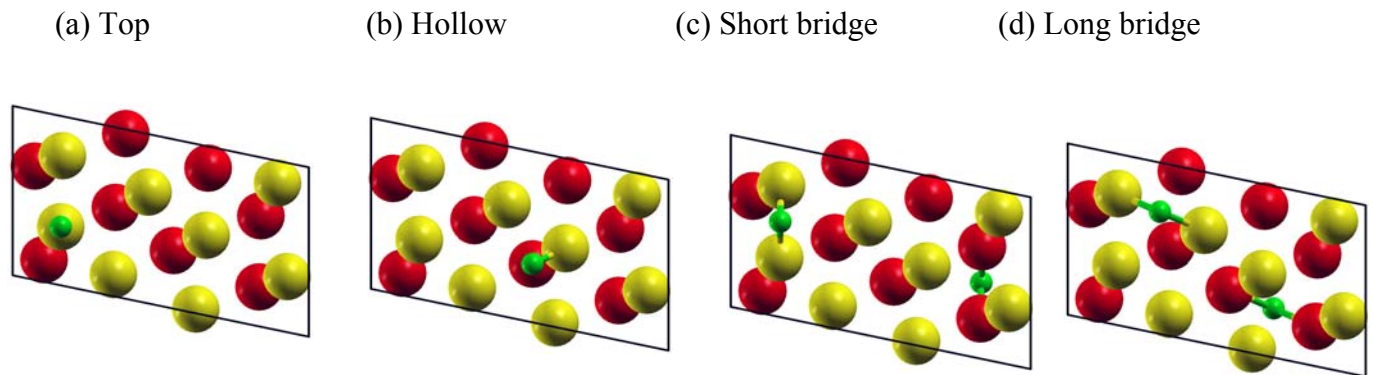
Program Title: A Fully Relativistic Density Functional Study of the Role of 5f Electrons in Chemical Bonding in Transuranium Elements

Principal Investigator: Dr. Asok K. Ray, Professor of Physics, University of Texas at Arlington, Arlington, Texas 76019

Our work is primarily concerned with actinide surfaces and adsorptions of atomic and molecular systems on such surfaces. In this abstract, we outline the results from two most recently completed projects, namely adsorptions of atomic carbon, nitrogen, and oxygen on the (111) surface of δ -Pu and on the (020) surface of α -Pu. For both cases, first principles total energy calculations within the framework of generalized gradient approximation to density functional theory with the Perdew-Burke-Ernzerhof (PBE) exchange-correlation functional have been performed. The computational formalism is the full potential all electron linearized augmented plane wave plus local orbitals (FP-LAPW+lo) method as implemented in the Wien2k suite of software. This method makes no shape approximation to the potential or the electron density. Within the FP-LAPW+lo method, the unit cell is divided into non-overlapping muffin-tin spheres and an interstitial region. The δ -Pu (111) surface is modeled by a supercell consisting of periodic 3-layer slabs with two atoms per surface unit cell, where periodic slabs are separated in the z-direction by vacuum regions of 60 Bohr thick. Chemisorption energies have been optimized with respect to the distance of the adatom from the Pu surface for four adsorption sites, namely the top site (adatom is directly on top of a Pu atom), bridge site (adatom is placed in the middle of two nearest neighbor Pu atoms), hcp hollow site (adatom sees a Pu atom located on the layer directly below the surface); and fcc hollow site (adatom sees a Pu atom two layers below the surface). The adlayer structure corresponds to a coverage of 0.50 of a monolayer in all cases. Computations were carried out at two theoretical levels, one without spin-orbit coupling (NSOC) and one with spin-orbit coupling (SOC). For NSOC calculations, the hollow fcc adsorption site was found to be the most stable site for C and N with chemisorption energies of 6.272 eV and 6.504 eV respectively, while the hollow hcp adsorption site was found to be the most stable site for O with chemisorption energy of 8.025 eV. For SOC calculations, the hollow fcc adsorption site was found to be the most stable site in all cases with chemisorption energies for C, N, and O being 6.539 eV, 6.714 eV, and 8.2 eV respectively. The respective distances of the C, N, and O adatoms from the surface were found to be 1.16 Å, 1.08 Å, and 1.25 Å. Our calculations indicate that SOC has negligible effect on the chemisorption geometries but energies with SOC are more stable than the cases with NSOC within a range of 0.05 to 0.27 eV. The work function and net magnetic moments respectively increased and decreased in all cases upon chemisorption compared with the bare δ -Pu (111) surface.

The α -Pu (020) surface was modeled by a 4-layer periodic slab consisting of a total of 32 Pu atoms. Adsorption energies were optimized with respect to the distance of the adatom from the Pu surface for four adsorption sites (see figure below). The sites are the one-fold top site, one-fold hollow site, two-fold short bridge and two-fold long bridge. At the top site the adatom sits directly on top of a Pu atom. At the hollow site the

adatom sits a site that is on top of a Pu atom on the second layer. At the short bridge site, the adatom sits between two Pu atoms having a short bond, whereas at the long bridge site, the adatom sits between two Pu atoms with a long bond. The short bridge site was the most stable adsorption site for C with chemisorption energies of 5.880 eV and 6.038 eV at the NSOC and SOC levels of theory respectively. The long bridge site was the most stable adsorption site for N and O with chemisorption energies at the NSOC and SOC levels of theory respectively being 5.806 eV and 6.067 eV for N and 7.155 eV and 7.362 eV for O. The respective distances of the C, N, and O adatoms from the surface for the most stable adsorption sites were found to be 1.32 Å, 1.26 Å, and 1.35 Å. Our results show that SOC adsorption energies are more stable than NSOC adsorption energies in the 0.14-0.32 eV range. Here also, the work function and net spin magnetic moments respectively increased and decreased in all cases upon chemisorption compared to the bare surface. The local density of states and difference charge densities has been used to analyze the interaction between the adatoms and the substrate.



Some recent publications

1. D. Gao and A. K. Ray, Actinides 2005 – Basic Science, Applications and Technology, MRS Symposium Proceedings, **803**, 39-44 (2006).
2. H. R. Gong and A. K. Ray, Actinides 2005 – Basic Science, Applications and Technology, MRS Symposium Proceedings, **803**, 44-50 (2006).
3. D. Gao and A. K. Ray, European Physical Journal B, **50**, 497-503 (2006).
4. H. R. Gong and A. K. Ray, Surface Science, **600**, 2231-2241 (2006).
5. D. Gao and A. K. Ray, Surface Science, **600**, 4941-4952 (2006).
6. R. Atta-Fynn and A. K. Ray, Physica B, **392**, 112 - 126(2007).
7. P. Dholabhai and A. K. Ray, Physica Scripta, **75**, 506-514 (2007).
8. D. Gao and A. K. Ray, European Physical Journal B, **55**, 13-22 (2007).
9. R. Atta-Fynn and A. K. Ray, Physical Review B, **75**, 195112-1-13 (2007).
10. D. Gao and A. K. Ray, Journal of Alloys and Compounds, **444-445**, 184-190 (2007).
11. P. Dholabhai and A. K. Ray, Journal of Alloys and Compounds, **444-445**, 356-362 (2007).
12. R. Atta-Fynn and A. K. Ray, Physical Review B, **76**, 115101-1-12 (2007).

Structure and Properties of Pu-Oxide Nanoclusters

Lynda Soderholm, S. Skanthakumar, Richard E. Wilson
Chemistry Division, Argonne National Laboratory, Argonne IL 60439
LS@anl.gov

A metrical description of actinide aggregates that form following hydrolysis has remained elusive, despite their impact on chemical reactivity and physical properties. Tetravalent Pu hydrolysis has received specific attention because the aggregates, known as “Pu polymer”, remain soluble and once formed have proven difficult to remove or destroy. Their presence in solution prohibits effective metal separations and impacts the prediction of Pu transport and mobility in the environment. Long thought to be amorphous, ill-defined oxyhydroxides formed by oxolation reactions, they are known to form PuO₂-like metal clusters upon aging. Our recent studies point to a very different chemistry. Single-crystal structural studies of polymer reveal well-formed, Pu-oxide crystallites and high-energy x-ray scattering (HEXS) results confirm monodisperse complexes with correlations that extend out to 12 Å or longer in solution. For example, the cluster [Pu₃₈O₅₆]⁴⁰⁺ has been isolated in several different structures and seems to be particularly stable. The packing in this moiety is slightly distorted from the classic fluorite (Fm3m) symmetry found for PuO₂. The clusters themselves are decorated with anions in the solid state, for example to form the anion [Pu₃₈O₅₆Cl₅₄(H₂O)₈]¹⁴⁻. The Fourier transform of HEXS data obtained from solution is well modeled by the Pu-38 cluster but does not conclusively confirm the full chloride coordination. Optical data, also obtained from solution samples, indicate the decorating anion’s lability, a result supported by structural studies. Overall, our work suggests cluster formation via oxolation, a chemistry seen with higher-valent transition metals such as Mo⁶⁺ and W⁶⁺, which form a wide variety of stable polyoxometalates. Structural studies have isolated samples with several monodisperse cluster sizes, suggesting magic-numbers may be stabilized, a possible effect of anion species, pH and/or concentration. These factors will be discussed in context of their impact on electronic properties.

This work is supported by the Heavy Elements Chemistry and Separation Sciences Programs, Office of Basic Energy Sciences, Office of Science, Department of Energy, at Argonne National Laboratory under contract DE-AC02-06CH11357.

Probing Actinide Electronic Structure using High-Resolution Photoelectron Spectroscopy*

Michael C. Heaven
Department of Chemistry
Emory University
Atlanta, GA 30322

High-level theoretical models of the electronic structures and properties of actinide compounds are being developed by several research groups. This is a challenging problem due to the need for explicit treatment of relativistic effects, and the circumstance that many of these molecules exist in states where the f and/or d orbitals are partially filled. Current theoretical models are being evaluated through comparisons with experimental results. Gas phase data are most suitable for this purpose, but there have been very few gas phase studies of actinide compounds. We are addressing this problem by carrying out spectroscopic studies of simple uranium and thorium compounds (oxides and halides). Multiple resonance spectroscopy and jet cooling techniques are being used to unravel the complex electronic spectra of these compounds. Recent results for the oxides will be discussed. Systematic errors in the accepted values for the ionization energies have been discovered, and the patterns of electronic states for these molecules provide information concerning the occupation of the $5f$ orbitals and their participation in bond formation.

*This work was supported by a grant from the Heavy Elements Chemistry Branch, Division of Chemical Sciences, Office of Basic Energy Sciences, Department of Energy (DE-FG02-01ER15153-A003)

Generation, Detection and Characterization of Gas-Phase Transition Metal
Containing Molecules

Timothy C. Steimle

Department of Chemistry and Biochemistry

Arizona State University

Tempe, Arizona 85287-1604

E-mail: tsteimle@asu.edu

I. Program Scope

The objective is to identify transient, transition metal containing, molecules and produce highly quantitative information that elucidates bonding mechanisms and can be used to evaluate the predictability of electronic structure calculations. Studies of late *4d* and *5d* metal elements (e.g. Rh, Pd, Ir and Pt) are emphasized due to their role in efficient activation of C-H or C-halogen bonds. The need for highly quantifiable data to gauge the quality of electronic structure predictions has significantly increased as computational approaches have evolved from traditional high level *ab initio* approaches to the current extensively implemented density functional theory (DFT) approaches because the results of DFT predictions depend radically on the nature of both the functional and basis set employed. Experimental determination of permanent electric dipole moments, μ_e , magnetic dipole moments, μ_m , and magnetic hyperfine interactions (Fermi-contact, b_F etc.) are performed because μ_m , μ_e and b_F are highly sensitive to the nature of the chemically relevant valence electrons and are routinely predicted. Furthermore, unlike other routinely theoretically predicted properties such as bond lengths, R , and harmonic vibrational frequencies, ω_e , these properties vary radically across the Rh, Pd, Ir and Pt series (e.g. PtS ($X[\Omega=0^+]$): $\mu_e = 1.78(2)$ D vs. RhS ($X^4\Sigma_{3/2}^-$) $3.40(2)$ D).

Two classes of gas-phase spectroscopic studies are implemented: a) visible and near infrared electronic spectroscopy using laser induced fluorescence (LIF) detection, b) mid-infrared vibrational spectroscopy in the OH, CH and NH fundamental stretching region (2.8 μ m-3.6 μ m). Small magnetic (Zeeman) and electric (Stark) field induced shifts in the very high resolution spectra are analyzed to produce experimental values for μ_m and μ_e . Molecular beams of the transition metal containing radical molecules are produced by skimming the output of a laser ablated/reagent supersonic expanding gas. The molecules are produced with an internal temperature of typically 10 K to minimize spectral congestion and recorded at near the natural linewidth limit (typically 30 MHz).

II. Recent Progress

A. RhH, RhC, RhF, RhN (Publ. #7), RhO (Publ. #6), RhS(Publ. #8),

Recently we recorded and analyzed the optical Stark spectra of RhO, RhN and RhS. The determined ground state values for μ_e were (RhN:2.43(9)D) < (RhO:3.81(4)D) \approx μ_e (RhS:3.40(2)D). More insightful than μ_e is a comparison of the reduced dipole moment ($\equiv \mu_e/R_v$) amongst the series where the observed ordering is RhN (1.48 D/Å) < RhS (1.65 D/Å) < RhO (2.22 D/Å). A major finding of these studies is how well a relatively simple molecular orbital correlation diagram can qualitatively predict the observed relative values of μ_e/R_v . This correlation diagram predicts that the primary configurations are $1\sigma^2 1\pi^4 1\delta^4 2\sigma^2$ for RhN($X^1\Sigma^+$) and $1\sigma^2 1\pi^4 1\delta^4 2\sigma^1 2\pi^2$ for RhO and RhS ($X^4\Sigma^-$). Here only the valence electrons are used in numbering the molecular orbitals. The 1σ and 1π are the $4d(\text{Rh})+p(\text{O,N,S})$ bonding combinations, the 1δ a non-bonding $4d_{\pm 2}$, the 2σ a non-bonding

5s/5p hybrid orbital polarized away from the bond, and the 2π the 4d(Rh)-p(O,N,S) anti-bonding combination. The three major contributions responsible for the observed ordering of μ_e/R_v are: 1) the changes in the polarity of the bonding σ and π orbitals; 2) the occupation of the non-bonding 2σ; 3) the occupation of the anti-bonding 2π orbital. The polarity of the bonding 1σ and 1π orbitals, which are fully occupied in this series, should be RhS < RhN < RhO, mimicking the trend in electronegativities. This alone would predict an order for μ_e/R_v of RhS < RhN < RhO. Occupation of the 2σ orbital greatly reduces μ_e/R_v because it moves electron density away from N, O and S. The 2σ orbital is doubly occupied for RhN and singly occupied for RhO and RhS, thus the order for μ_e/R_v becomes RhN < RhS < RhO. Occupation of the 2π anti-bonding orbital increases μ_e/R_v because it places partial charge on the N, O or S atom. The lack of occupation of the 2π orbital in RhN and double occupation for RhO and RhS contributes to reducing μ_e/R_v .

The results of a recent DFT calculation for RhN and RhO and a high level *ab initio* prediction for RhN are compared in Table I. The DFT value of 4.107 D for RhN predicted utilizing the hybrid functional B3LYP with a LanL2DZ basis set was closest to the observed value of 3.81(2) D. The four other functionals used (SVWN, BP86, Meta-BP86, and Lb94) produced values of μ_e in the range of 3.041D to 3.235D. Unfortunately, the B3LYP/LanL2DZ calculation, which gives the best agreement for μ_e , gives the poorest prediction for *R*. Similarly, the hybrid functional B3LYP with a LanL2DZ basis set gives a prediction of μ_e for RhO (=2.466 D) closest to the true value (= 2.43(5) D) with the four other functionals (SVWN, BP86, Meta-BP86, and Lb94) producing values that range from 1.486 D to 3.372 D. The *ab initio* value is approximately 20% below observation.

Table I. Ground state electric dipole moments, μ_e , of RhN, RhO and RhS (in Debye)

	RhN($X^1\Sigma^+$)	RhO($X^4\Sigma_{3/2}^-$)	RhS($X^4\Sigma_{3/2}^-$)
Exp.	2.43(5)	3.81(2)	3.40(2)
DFT	3.27 ^a , 3.37 ^b , 1.49 ^c , 2.47 ^d , 1.56 ^e	3.04 ^a , 3.24 ^b , 3.09 ^c , 4.11 ^d , 3.13 ^e	-
<i>Ab initio</i>	2.08 ^a	-	-

DFT: (CPL,**421**, 281,2006) Various functionals: ^aSVWN; ^bBp86; ^cmeta-Bp86; ^dB3LYP; ^eLb94; *Ab initio*: (THEOCHEM, **393**, 127 (1997)) CASSCF/MRCI

We recently recorded the low-resolution, near uv, LIF spectra of RhF, RhH and RhC produced in the reaction of ablated rhodium with SF₆, H₂ and CH₄, respectively (see Figure 1). Numerous other spectral features were also observed.

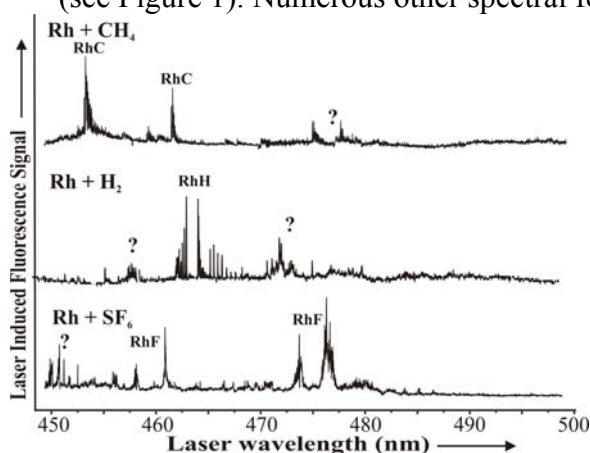


Figure 1. Low-resolution, near uv, LIF spectra of the reaction products of ablated rhodium and a supersonic expansion of SF₆/Ar, (lower), H₂ (middle), and CH₄ (upper). Bands associate with electronic transitions of RhF, RhH and RhC are readily identified using existing information. Numerous other bands are also evident. Optical Stark measurements of RhC, RhF and RhH are in progress.

B. Molybdenum monocarbide, MoC(Publ. # 9)

Understanding the nature of the transition metal/carbon bond is fundamental to many areas of organometallic chemistry and μ_e is the best gauge of the direction and magnitude of the polarity of this bond. We recently recorded and analyzed the optical Stark effect in the $R_e(0)$ and $Q_{fe}(1)$ branch features of the $[18.6]^3\Pi_1 - X^3\Sigma^-(0,0)$ band of ^{98}MoC to determine μ_e values of 2.68(2) D and 6.07(18) D for the $[18.6]^3\Pi_1(v=0)$ and $X^3\Sigma^-(v=0)$ states, respectively. The only previously determined μ_e values for transition metal monocarbides are those for FeC, RuC, IrC and PtC, which were all measured in our laboratory. μ_e for MoC has been predicted by various DFT and *ab initio* theoretical methods the results of which are collected in Table II. The DFT values vary from 3.145 D to 5.50D depending upon basis set and functional. The all electron, *ab initio*, CASSCF/MRCI calculation performed better than the relativistic effective core potential (ECP) approach. A molecular orbital correlation diagrams for the early (Y, Zr, Nb, Mo and Ru) monocarbides was developed that qualitatively predicts the trend in μ_e .

Table II. Permanent electric dipole moments of MoC (Debye) $X^3\Sigma^-$

Exp.	<i>Ab initio</i>				DFT			
	All-elec. MRCI	ECP. MRCI	SVWN	Bp86	Meta- Bp86	Lb94	B3LYP	B3LYP
6.07(2)	6.15 ^a	5.87 ^b	5.218 ^c	5.209 ^c	5.200 ^c	5.080 ^c	5.50 ^d	3.145 ^c

(a) I. Shim and Karl A. Gingerich, J. Chem. Phys., **106(19)**, 8093 (1997), (b) P. A. Denis and K. Balasubramanian, J. Chem. Phys., **125**, 024306 (2006)., (c) J. Wang, X. Sun, and Z. Wu, Chem. Phys. Lett., **141**, 426(1-3)(2006). (d) F. Stevens, V. Van Speybroeck, I. Carmichael, F. Callens, M. Waroquier, Chem. Phys. Lett., **281**, 421(2006)

C. Mid-infrared spectroscopy using Stark Modulation

A very sensitive and selective mid-infrared spectroscopic spectrometer has been successfully developed (Figure 2) and is being used in the search for polyatomic metal containing radicals. It employs a difference frequency generation (DFG) scheme using a periodically poled lithium niobate (PPLN) crystal similar to that previously used by Curl's group (Rice) and currently used by Nesbitt's group (NIST). Like those spectrometers, dual balance beam detection and high-pass filtering is used to enhance S/N. Unlike the Rice and NIST spectrometers, Stark modulation is also implemented. Our first Stark modulation spectra (CH_3OH seeded in Argon) were recently recorded.

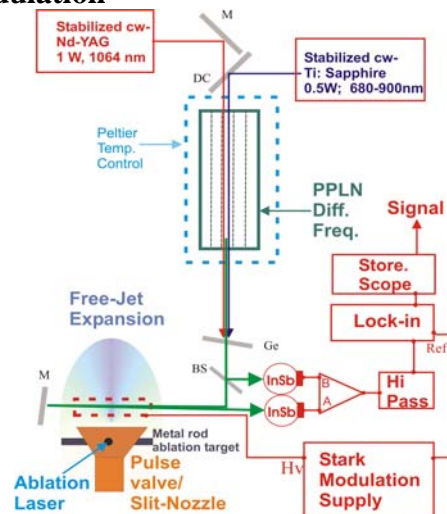


Fig. 2 The high-resolution, mid-IR, spectrometer developed for the study of polyatomic metal containing radicals.

III. Future Plans

A. Near uv ultrahigh resolution LIF of metal systems.

Many of the transition metal containing radicals of interest (see Fig. 1) have intense electronic transitions in the near uv (370-460 nm) spectral region where we previously did not have tunable monochromatic radiation sources. We recently purchase an external cavity doubler to be used with our cw-dye and Ti:Sapphire lasers that will extend our wavelength coverage to down 420 nm. In addition to the RhC, RhH and RhF molecules, studies of PdX series (X=C,N,O,H,F) will be initiated. Information on gas-phase Pd containing molecules is very limited.

B. Mid-IR spectrometer: Pulsed discharge source for radical generation

The 50 kHz Stark modulation scheme that we have recently implemented has resulted in an approximate 10^2 enhancement in the S/N. In those preliminary experiments involving CH₃OH seeded in argon the pulsed molecular beam had a temporal distribution long enough ($\cong 500 \mu\text{s}$) for sufficient modulation. The laser ablation scheme we have traditionally used has a temporal distribution too short ($\cong 50 \mu\text{s}$) for implementation. An alternative dc discharge source is being constructed for molecular production.

Publications of DOE sponsored research - 2004-present:

1. "The permanent electric dipole moments of Ruthenium Monocarbide in the $^3\Pi$ and $^3\Delta$ states" Wilton L. Virgo, Timothy C. Steimle, Laura E. Aucoin and J.M. Brown, Chem. Phys. Lett. **391**, 75-80, (2004).
2. "The permanent electric dipole moments of WN and ReN and nuclear quadrupole interaction in ReN" Timothy C. Steimle and Wilton Virgo, J. Chem. Phys. **121** 12411 (2004).
3. "The permanent electric dipole moment and hyperfine interaction in Ruthenium Monofluoride, RuF." Timothy C. Steimle, Wilton L. Virgo and Tongmei Ma, J. Chem. Phys. **124**, 024309-7 (2006).
4. "High Resolution Laser Induced Fluorescence Spectroscopy of the [18.8] $^3\Phi_i - X^3\Phi_i$ (0,0) Band of Cobalt Monofluoride" Timothy C. Steimle, Tongmei Ma, Allan G. Adam, William D. Hamilton and Anthony J. Merer, J. Chem. Phys. **125**, 6 064302-1-064302-9 (2006).
5. "The permanent electric dipole moment and magnetic g-factors of uranium monoxide, UO" Michael. C. Heaven, Vasilij Goncharon, Timothy C. Steimle, Tongmei Ma, Colan Linton J. Chem Phys. **125** 204314/1-20431/11 (2006).
6. "A Molecular Beam Optical Stark Study of the [15.8] and [16.0] $^2\Pi_{1/2} - X^2\Sigma^+$ (0,0) Band Systems of Rhodium Monoxide, RhO." Jamie Gengler, Tongmei M, Allan G. Adam, and Timothy C. Steimle, J. Chem. Phys. **126** 134304-11 (2007)
7. "A Molecular Beam Optical Stark Study of Rhodium Mononitride, RhN" Tongmei Ma, Jamie Gengler, Zhong Wang, Hailing Wang and T.C. Steimle, J. Chem. Phys. J.Chem. Phys. J. Chem. Phys. **126** 244312-8 (2007).
8. "A Molecular Beam Optical Stark Study of the [18.1] $^2\Pi_{1/2} - X^4\Sigma_{1/2}^-$, RhS" Tongmei Ma, Hailing Wang and T.C. Steimle, J. Chem. Phys. (Accepted August (2007).
9. "Optical Stark spectroscopy of molybdenum carbide, MoC" Wilton L. Virgo and Timothy C. Steimle, J. Chem. Phys. (Accepted Aug 2007).

Investigating the Mechanisms of Oxidation Reactions Occurring on Heterogeneous Catalysts

A. W. Castleman, Jr.
Pennsylvania State University
Departments of Chemistry and Physics
104 Chemistry Building
University Park, PA 16802
awc@psu.edu

Program Scope:

Increased consumption of energy worldwide has induced major expansions in research efforts devoted to discovering more efficient processes. Catalysts have the capability to considerably reduce the energy requirements of chemical reactions and to selectively promote the creation of desired products. Moreover, catalysts are widely employed in the production and storage of both conventional as well as alternative forms of energy and find particular value in reactions designed to effect pollution abatement. To sensibly improve the performance of existing catalysts and develop new ones, an elementary molecular level understanding of catalytic reactions is crucial. The current approach to designing heterogeneous catalysts involves mainly the combinatorial preparation and testing of different catalytic materials. From a conceptual point of view, unfortunately, such methods yield little insight into why one particular catalyst loading is more active than another. Analytical approaches, employing surface science techniques, have made significant contributions to the understanding of heterogeneous catalysis. Regrettably, even such sophisticated methods are not always able to determine the exact nature of the active sites responsible for catalytic activity.

Our experimental approach, employing gas phase metal oxide clusters, is designed to provide molecular level insight into the mechanisms of oxidation reactions occurring in the presence of transition metal oxide catalysts. Through a multistage mass spectrometry technique we are able to investigate, with atomic level precision, how the physical and chemical characteristics of different materials influence their ability to facilitate catalytic reactions.

The study of gas phase clusters has been demonstrated to be an effective method of investigating the chemical and physical properties of catalytically active bulk materials. The surface of a metal oxide catalyst may be viewed as a collection of clusters, as proposed by Muetterties. Somorjai, furthermore, has established that surface chemical bonds have properties similar to those of clusters. Additionally, investigations of cluster reactivity have demonstrated correlations between reactions occurring on gas phase clusters and those taking place on the corresponding bulk phase catalysts. The study of gas phase clusters, therefore, offers the advantage of investigating isolated potential catalytic active sites in the absence of solvent effects and surface inhomogeneities that complicate research in the condensed phase. Gas phase experiments, additionally, allow the effects of cluster size and composition to be studied on an atom by atom basis. This is particularly relevant in nanocatalysis where the properties of catalytic nanoparticles have been found to change over orders of magnitude by the incorporation or removal of a single atom. Cationic or anionic clusters may also better emulate charged active sites on bulk surfaces that result from electron transfer between the support material and the catalyst. Finally, clusters are small systems that can be accurately described using high level theoretical calculations. Our cluster based approach, therefore, has significant advantages and provides detailed insight into the molecular level mechanisms of catalytic oxidation reactions. Information gained from these studies may aid in the directed design of future catalysts with improved activity and selectivity.

Recent Progress:

During the current grant period, we continued investigating the molecular level details of heterogeneous oxidation reactions. In particular, we completed a systematic study of the reactivity of several 3d transition metal oxides with CO. These experiments were conducted to gain understanding of the fundamental steps of CO oxidation, a reaction of substantial importance to environmental pollution abatement. To acquire more detailed insight into the mechanisms and energetics of these reactions we collaborated with the theoretical physics group of Professor Shiv N. Khanna at the Virginia Commonwealth University.

Our experiments involving iron oxides were motivated by theoretical calculations suggesting an energetically favorable oxidation reaction with CO. Through a joint experimental and theoretical effort we determined the

effect of ionic charge state on the reactivity of $\text{FeO}_3^{+/-}$ clusters with CO. Studies of both the cationic and anionic FeO_3 clusters demonstrated that charge state has a dramatic effect on the oxidation behavior. Similar to gold oxide clusters, which we have also studied in this context, FeO_3^+ cations were determined to be far more active than the corresponding anions. Theoretical calculations predicted that it is energetically favorable for the reaction of FeO_3^+ with CO to proceed to a final stage forming FeO_2^+ , FeO^+ , and Fe^+ as the products. Indeed, each of these products were observed experimentally for the reaction of FeO_3^+ with CO. In contrast, for anionic FeO_3^- , only the product FeO_2^- was observed experimentally. A theoretical analysis of the reaction pathways provides evidence that the observed dependence of reactivity on ionic charge state is in part caused by the binding energy of oxygen to the metal atom. More energy is required to remove oxygen from the anionic clusters than from the cationic clusters. For cations, a charge deficiency localized on the iron atom weakens the Fe-O bonds and enables higher reactivity with CO. The relative reactivity of iron oxide and gold oxide clusters with CO was revealed to be very similar. Iron, however, being cheap and abundant, may be much more practical for application in commercial pollution abatement processes.

Systematic studies of the reactivity of anionic iron oxide clusters with CO were conducted to determine the influence of stoichiometry on oxidation efficiency. CO oxidation was determined to be the dominant reaction channel for most anionic iron oxide clusters. A theoretical analysis of the molecular level mechanisms was carried out to establish the energy profiles of the reactions and the influence of the spin states of the intermediates on the oxidation efficiency. The most active and selective iron oxide anions for CO oxidation were composed of one more oxygen atom than iron atom. The increased reactivity of this stoichiometry is attributed to two factors: (1) The energy required to remove an O atom from these clusters is less than the energy gained from forming CO_2 , thereby making the oxidation energetically favorable. (2) The small size of the clusters, compared to bulk iron oxide, allows structural rearrangements that eliminate or reduce the energy barriers making oxidation kinetically feasible.

Comprehensive investigation of the reactivity of cationic iron oxide clusters with CO revealed that the FeO^+ , Fe_2O^+ , and Fe_2O_3^+ stoichiometries were particularly active for CO oxidation. The reaction of Fe_2O_3^+ with CO yielded a particularly intense oxygen atom transfer product. The oxidation reaction was calculated to be exothermic by 2.12 eV and found to involve CO binding to a weakly bound oxygen atom followed by CO_2 loss. Our experiments show that Fe_2O_3^+ promotes CO oxidation, in agreement with studies by others involving neutral Fe_2O_3 nanoparticles. Theoretical structural calculations predict that the weakly bound oxygen atom outside of the Fe_2O_2^+ ring of Fe_2O_3^+ exhibits increased activity for O atom transfer to CO. Indeed, collision induced dissociation (CID) experiments with inert xenon gas also produced a small atomic oxygen loss product at near thermal energies, verifying this important theoretical prediction.

To complement our investigation of iron oxide clusters, experiments were undertaken in our laboratory to determine the structural characteristics of cobalt oxide and nickel oxide clusters as well as their reactivity with CO. CID experiments were conducted employing Xe gas to elucidate the structural building blocks of the larger clusters. These studies provided insight into how different d-electron configurations impact the dissociation pathways and bonding motifs of 3d transition metal oxide clusters. Reactivity studies with CO were also carried out and revealed that metal oxide clusters composed of various 3d metals have different stoichiometries which are the most active for CO oxidation.

The anionic cobalt oxide clusters studied, CoO_{2-3}^- , $\text{Co}_2\text{O}_{3-5}^-$, and $\text{Co}_3\text{O}_{3-6}^-$, exhibited oxygen atom loss as the most common CID fragment. This indicates the presence of atomically bound oxygen on the majority of anionic cobalt oxide clusters. The more oxygen rich cobalt oxide cluster anions, however, also fragmented through loss of molecular oxygen, sometimes at very low collision energies. These oxygen rich species, therefore, contain weakly bound molecular O_2 subunits which are not highly activated. Loss of neutral metal oxide fragments was also observed for anionic cobalt dimer and trimer oxide clusters. The more oxygen deficient dimer species, however, showed loss of a metal oxide fragment at lower energy than O atom dissociation. The anionic trimer oxide clusters exhibited a Co_2O_3^- product as the most stable structural subunit. In order to determine the influence of charge state on the structure of cobalt oxide clusters, cationic CoO_{1-4}^+ and $\text{Co}_2\text{O}_{2,4,6}^+$, were also studied. Both CoO^+ and Co_2O_2^+ fragmented revealing an oxygen atom product at slightly elevated collision energies and indicating the presence of atomically bound oxygen. The oxygen rich cationic monomer clusters exhibited loss of an O_2 first, followed by an O atom, demonstrating the presence of loosely bound molecular O_2 subunits. The CID results for the cationic cobalt oxides were somewhat different from the anionic clusters in that the fragmentation

of molecular O₂ units was far more common for cations. Furthermore, these fragments were often produced at very low collisional energies indicating that O₂ units are weakly bound and, therefore, not significantly activated.

Reactivity experiments with CO revealed oxygen atom transfer products for all anionic monomer through trimer cobalt oxide clusters. It is interesting that Co₃O₅⁻ and Co₃O₆⁻, which are oxygen rich species exhibiting O₂ fragmentation in CID experiments, underwent oxygen atom transfer as the major reaction channel with CO. This may indicate the presence of highly activated O₂ species. For the cationic cobalt oxide clusters, dissociation of O₂ followed by association of CO was the major reaction channel observed. Association of multiple CO molecules following dissociation of O₂ subunits was also observed for several cluster species.

The nickel oxide anion clusters studied were NiO_{2,3}⁻, Ni₂O_{3,4}⁻, Ni₃O_{3,5}⁻ and Ni₄O_{4,5}⁻. The general trends in the CID fragmentation of these clusters are consistent with those observed for cobalt oxide anions. The more oxygen deficient species dissociate O atoms and more oxygen rich clusters fragment intact O₂ units. Upon careful inspection, however, certain differences between cobalt oxides and nickel oxides become apparent. For the MO₃⁻ species, cobalt dissociates an atomic oxygen atom, while nickel fragments an intact O₂ unit. The additional d electron in nickel, therefore, seems to favor the binding of molecular rather than atomic oxygen. Furthermore, for M₃O₅⁻ clusters, dissociation of an O₂ unit requires significant energy for cobalt, while nickel fragments an O₂ unit at thermal energy. Nickel, therefore, seems to bind oxygen more loosely than cobalt. To determine the effect of charge state on nickel oxide clusters NiO₁₋₄⁺ and Ni₂O₂₋₃⁺ cations were studied. For all of the cation clusters except NiO⁺, O₂ was the first fragment observed indicating that cationic nickel centers bind oxygen preferentially in the molecular form. The dimer clusters, furthermore, fragmented O₂ at near thermal collision energies, demonstrating that this unit is only weakly bound to the nickel cations. Nickel oxide anions, when reacted with CO, exhibited atomic oxygen loss products. For larger clusters, only Ni₃O₄⁻ and Ni₄O₅⁻ showed oxygen atom transfer products, which is evidence that clusters with one more oxygen atom than nickel atom have a particularly active stoichiometry for the oxidation of CO. Furthermore, no products were observed with clusters containing the same number of metal and oxygen atoms, Ni₃O₃⁻ and Ni₄O₄⁻. For cationic nickel oxides reacted with CO, oxygen atom transfer was observed only for NiO⁺, NiO₂⁺, and Ni₂O₃⁺, however, only for NiO⁺ was it the major reaction channel. The most prominent product channel detected for cationic clusters was the dissociation of an O₂ followed by association of a CO molecule. The dimer nickel oxide cation species also exhibited products of the fragmentation of Ni, NiO, and NiO₂ units. The adsorption energy of CO onto these clusters, therefore, is sufficiently exothermic to break the Ni-O bonds of the nascent cluster. These recent experiments, therefore, reveal that metal oxide clusters composed of various 3d metals bind oxygen in specific configurations and have distinct stoichiometries which are ideal for CO oxidation.

Future Studies:

Catalyst support materials can have a significant influence on the activity of metal catalyst particles. Primarily, the binding mode of the catalyst particles to the support material can dramatically affect the size distribution of the active phase. Additionally, the metal-metal bonds of catalyst particles can become strained upon adsorption onto the support. This in turn creates regions of charge accumulation and deficiency that are critical to catalytic activity. Differences in the electronegativity of the elements comprising the support and catalyst may also lead to charged active sites. Finally, the interface between the support and catalyst material can serve as a unique bifunctional site where reactants may bind in configurations which are favorable for reaction. To gain further understanding of the molecular level mechanisms involved in heterogeneous oxidation catalysis, we plan to investigate the influence of elements used as support materials on the activity of commercial catalysts. We intend to focus specifically on the oxidation of CO, SO₂ and simple chemical feedstocks such as methanol, methane and propylene. Preliminary results on aluminum and zirconium oxide clusters have revealed certain stoichiometries that are particularly active for the oxidation of CO and methanol, respectively. After characterizing the behavior of the pure support materials we plan to investigate the influence of catalyst-support interactions through reactivity studies of bimetallic oxide clusters. Mass selected reactivity studies will provide insight into how systematically doping single metal oxide clusters with a second metal influences reactivity. CID experiments will aid in determining bond energetics and structural configurations. Our forthcoming bimetallic studies will build upon our previous work with gold and iron and our preliminary studies of zirconium. We plan to study the reactivity of mixed iron/gold and copper/zirconium oxide clusters with CO and methanol, respectively. We also intend to continue our valuable collaboration with the theoretical groups of Professor

Vlasta Bonačić-Koutecký at the Humboldt University in Berlin and Professor Shiv N. Khanna at the Virginia Commonwealth University. The insight provided by their computational work allows us to develop a much more complete and detailed understanding of the mechanisms involved in catalytic oxidation reactions.

Publications Resulting from this Grant (2004 to Present):

559. "Photodissociation of Sulfur Dioxide: The \tilde{E} State Revisited," K. L. Knappenberger and A. W. Castleman, Jr., *J. Phys. Chem. A*, 108, 9-14 (2004).
560. "Probing the Dynamics of Ionization Processes in Clusters", A. W. Castleman, Jr. and T. E. Dermota, *Latest Advances in Atomic Cluster Collisions* (A. Solov'yov and J.-P. Connerade, Eds.) World Scientific: Singapore, New Jersey, London, 253-269 (2004).
561. "Ultrafast dynamics in cluster systems", T. E. Dermota, Q. Zhong, and A. W. Castleman, Jr., *Chemical Reviews*, 104, 1861-1886 (2004)
563. "Reactivity of Atomic Gold Anions Toward Oxygen and the Oxidation of CO: Experiment and Theory," M. L. Kimble, A. W. Castleman, Jr., R. Mitrić, C. Bürgel, and V. Bonačić-Koutecký, *J. Am. Chem. Soc.*, 126, 2526-2535 (2004).
564. "Probing the Oxidation of Carbon Monoxide Utilizing Au_n^- ," M. L. Kimble and A. W. Castleman, Jr., *Proceedings of Gold 2003: New Industrial Applications for Gold Conference Vancouver, Canada, September 28 – October 1, 2003*.
565. "Gas phase Studies of Au_n^+ for the Oxidation of Carbon Monoxide," M. L. Kimble and A. W. Castleman, Jr., *Special Issue of the Int. J. Mass Spectrom.*, in Honor of Professor Tilmann D. Märk. 233, 99-101 (2004).
568. "Reactions of Vanadium and Niobium Oxides with Methanol," D. R. Justes, N. A. Moore, and A.W. Castleman, Jr., *J. Phys. Chem. B*, 108, 3855-3862 (2004).
570. "Elucidating Mechanistic Details of Catalytic Reactions Utilizing Gas Phase Clusters," M. L. Kimble, D. R. Justes, N. A. Moore, and A. W. Castleman, Jr., *Clusters and Nano-Assemblies: Physical and Biological Systems* (P. Jena, S. N. Khanna, B. K. Rao, Eds.) World Scientific: Singapore, New Jersey, London, 127-134 (2005).
572. "The Influence of Cluster Formation on the Photodissociation of Sulfur Dioxide: Excitation to the E State", K. L. Knappenberger, Jr., and A. W. Castleman, Jr., *J. Chem. Phys.*, 121, 3540-3549 (2004).
573. "A Kinetic Analysis of the Reaction between $(V_2O_5)_{n=1,2}^+$ and Ethylene," N. A. Moore, R. Mitrić, D. R. Justes, V. Bonačić-Koutecký, and A. W. Castleman, Jr., *J. Phys. Chem. B*, 110, 3015 (2006)
586. "Clusters: A bridge between disciplines," A. W. Castleman, Jr., *Puru Jena, Proc. Nat. Acad. Sci.* 103, 10552 (2006)
588. "Interactions of CO with $Au_nO_m^-$ ($n \geq 4$)", M. L. Kimble, A. W. Castleman, Jr., C. Bürgel, R. Mitrić, and V. Bonačić-Koutecký, *Int. J. Mass. Spec.* 254, 163 (2006).
592. "Clusters: A bridge across the disciplines of physics and chemistry," *Puru Jena, A. W. Castleman, Jr., Proc. Nat. Acad. Sci.* 103, 10560 (2006)
593. "Clusters: A bridge across the disciplines of environment, materials science, and biology," A. W. Castleman, Jr., *Puru Jena, Proc. Nat. Acad. Sci.* 103, 10554 (2006)
595. "Joint Experimental and Theoretical Investigations of the Reactivity of $Au_2O_n^-$ and $Au_3O_n^-$ ($n=1-5$) with Carbon Monoxide," M. L. Kimble, N. A. Moore, G. E. Johnson, A. W. Castleman, Jr., C. Bürgel, R. Mitrić, and V. Bonačić-Koutecký, *J. Chem. Phys.* 125, 204311 (2006)
599. "Reactivity of Anionic Gold Oxide Clusters Towards CO: Experiment and Theory," M. L. Kimble, N. A. Moore, A. W. Castleman, Jr., C. Bürgel, R. Mitrić, and V. Bonačić-Koutecký, *EPJ-ISSPIC*
600. "Influence of Charge State on the Reaction of $FeO_3^{+/-}$ with Carbon Monoxide," N. M. Reilly, J. U. Reveles, G. E. Johnson, S. N. Khanna, and A. W. Castleman, Jr., *Chem. Phys. Lett.* 435, 295 (2007)
601. "Recent Advances in Cluster Science," A. W. Castleman, Jr., *Proceedings for the Advances in Mass Spectrometry for the 17th IMSC*, in press
603. "Femtochemistry VII: Fundamental Ultrafast Processes in Chemistry, Physics, and Biology," A. W. Castleman, Jr., and M. L. Kimble, Elsevier, ISBN 0 444 52821 0
606. "Multi-component fitting of cluster dynamics," K. L. Knappenberger, Jr., and A. W. Castleman, Jr., *Femtochemistry VII: Fundamental Ultrafast Processes in Chemistry, Physics, and Biology*, Elsevier, ISBN 0 444 52821 0
610. "Experimental and Theoretical Study of the Structure and Reactivity of $Fe_{1,2}O_{\leq 6}^-$ Clusters with CO," N. M. Reilly, J. U. Reveles, G. E. Johnson, S. N. Khanna, and A. W. Castleman, Jr., *J. Phys. Chem. A*, 111, 4158 (2007)

Infrared Spectroscopy of Transition Metal-Molecular Interactions in the Gas Phase

DE-FG02-96ER14658

Michael A. Duncan

Department of Chemistry, University of Georgia, Athens, GA 30602-2556

maduncan@uga.edu

Program Scope

The focus of our research program is the study of gas phase metal clusters and metal ion-molecular complexes as models for the fundamental interactions present in heterogeneous catalysis and metal ion solvation. The clusters studied are molecular sized aggregates of metal or metal compounds (oxides, carbides). We focus specifically on the bonding exhibited by "physisorption" versus "chemisorption" on cluster surfaces, where the distinction is one of the cluster-adsorbate bond energy, and on solvation interactions in which the ligand is a solvent molecule such as water. Complexes containing a metal center with one or more atoms and one or more attached small molecules provide the models for adsorption and solvation. These studies investigate the nature of the metal-molecular interactions and how they vary with metal composition and cluster size. To obtain size-specific information, we focus on ionized complexes that can be mass-selected. Infrared photodissociation spectroscopy is employed to measure the vibrational spectroscopy of these ionized complexes. The vibrational frequencies measured are compared to those for the corresponding free-molecular resonances and with the predictions of theory to reveal the electronic state and geometric structure of the system. Experimental measurements are supplemented with calculations using density functional theory (DFT) with standard functionals such as B3LYP.

Recent Progress

The main focus of our work over the last two years has been infrared spectroscopy of mass-selected cation-molecular complexes, e.g., $\text{Ni}^+(\text{C}_2\text{H}_2)_n$, $\text{Ni}^+(\text{H}_2\text{O})_n$, $\text{Nb}^+(\text{N}_2)_n$ and $\text{M}^+(\text{CO})_n$. These species are produced by laser vaporization in a pulsed-nozzle cluster source, size-selected with a specially designed reflectron time-of-flight mass spectrometer and studied with infrared photodissociation spectroscopy using an IR optical parametric oscillator laser system (OPO). We have studied the infrared spectroscopy of various transition metal ions in complexes with the ligands indicated. In each system, we examine the shift in the frequency for selected vibrational modes in the adsorbate molecule that occur upon binding to the metal. The number and frequencies of IR-active modes in multi-ligand complexes reveal the structures of these systems, while sudden changes in vibrational spectra or IR dissociation yields are used to determine the coordination number for the metal ion in these complexes. In some systems, new vibrational bands are found at a certain complex size that correspond to intra-cluster reaction products. In small complexes with strong bonding, we use the method of "rare gas tagging" with argon or neon to enhance dissociation yields. In all of these systems, we employ a close interaction with theory to investigate the details

of the metal-molecular interactions that best explain the spectroscopy data obtained. We perform our own density functional theory (DFT) or MP2 calculations (using Gaussian 03W or GAMESS) and when higher level methods are required (e.g., CCSD), we collaborate with local theorists (Profs. P.v.R. Schleyer, H.F. Schaefer) or those at other universities (Prof. Mark Gordon, Iowa State). Our infrared data on these transition metal ion-molecule complexes are the first available, and they provides many examples of unanticipated structural and dynamical information.

One technical improvement implemented this year has been the extension of our infrared lasers to longer wavelengths. With the original configuration of our OPO system, the wavelength coverage was 2000-4500 cm^{-1} . Now we have added AgGaSe₂ and LiInS₂ crystals to this system, which extend the coverage to the region of 700-2000 cm^{-1} . In particular, this allows investigation of the carbonyl stretching region, the bending mode of water, the carbon skeletal modes of benzene, etc. New infrared spectra have been obtained in the 700-2000 cm^{-1} region for several new cation-molecular complexes.

$M^+(\text{H}_2\text{O})_n$ complexes and those tagged with argon have been studied previously in our lab for the metals iron, nickel, cobalt and vanadium. In the past year, we extended these studies to titanium, chromium, scandium, copper, silver, gold and zinc complexes. We have studied the noble metal ions copper, silver and gold with one and two water molecules. The gold system prefers a coordination of two ligands, and red-shifts its O-H stretches much more than those of copper and silver. In the vanadium system, we have studied multiple water complexes. Hydrogen bonding bands appear for the first time for the complex with five water molecules, establishing that four water molecules is the coordination for V^+ . Copper and zinc complexes with a single attached water have unexpected vibrational bands at high frequency above the normal region of the symmetric and asymmetric O-H stretches. With the help of theory by Prof. Anne McKoy (Ohio State), we are able to assign these features to combination bands involving the twisting motion of the water. Silver and chromium complexes were rotationally resolved, providing the H-O-H bond angle in these systems. In very new work, we have been able for the first time to produce multiply charged transition metal cation-water complexes for chromium and scandium systems tagged with multiple argons. IR spectra of these systems have very different intensity patterns and O-H shifts than those for the singly charged systems.

$M^+(\text{N}_2)_n$ complexes have been studied in the N-N stretch region for Fe^+ , V^+ and Nb^+ complexes. Binding to metal makes the N-N stretch IR active even though it is forbidden in the isolated molecule. Theory shows that most metals prefer end-on binding configurations, but some (e.g., cobalt) prefer to bind side-on as in a π -complex. The N-N stretch is red shifted for these metals compared to this frequency for the free nitrogen molecule, in much the same way that carbonyl stretches also shift to the red. $M^+(\text{N}_2)_4$ complexes for both of these metals are found to have a square-planar structure. However, the most stable coordination for both metals occurs in a complex with six ligands. In Nb^+ , addition of the fifth ligand induces a spin change on the metal ion from quintet to triplet, and this spin state persists in the larger complexes.

$M^+(\text{CO})_n$ complexes are analogous to well-known species in conventional inorganic chemistry. However, we are able to make these systems without the complicating influences of solvent or counter ions. The C-O stretch in most transition metal complexes shifts strongly to the red from free CO, and this vibration falls below 2000 cm^{-1} . This lies outside the tuning range of our OPO lasers in their former configuration, but this region is now accessible with our new crystals. We have examined so-called non-classical carbonyl complexes of gold, silver and platinum.

$M^+(\text{CO})_n$ complexes for these systems have been studied, and they exhibit the expected blue-shift of the carbonyl stretch relative to free CO. The size dependence of these resonances provides insight into the structures of these complexes. We collaborated on the gold system with Prof. Mark Gordon (Iowa State) who was able to do relativistic calculations to compare to our spectra.

In a new venture, we have collaborated with Prof. Stephen Leone (UC-Berkeley) on a project using the Advanced Light Source at Lawrence Berkeley National Lab. In this work, a cluster beam machine with a pulsed laser vaporization source has been upgraded and optimized to interface with the quasi-continuous VUV output of the ALS. In initial experiments, threshold ionization measurements were conducted on carbon clusters containing up to 15 atoms. We collaborated with Prof. Fritz Schaefer and Dr. Wesley Allen at Georgia on new high level calculations on the carbon clusters in the size range of 4-10 atoms. Ionization energies were computed for linear and cyclic isomers for comparison to the ionization thresholds measured. In many cases, evidence was strong for the presence of a single isomeric species (e.g., linear C_9 and cyclic C_{10}) in the neutral cluster distribution.

Future Plans

Future plans for this work include the extension of these IR spectroscopy studies to more ligands and to complexes with multiple metal atoms. We want to study more reactive metals with hydrocarbons such as ethylene or methane that might produce carbenes, vinylidene or ethylidyne species. These systems should exhibit characteristic IR spectra, and will allow us to make better contact with IR spectroscopy on metal surfaces. Studies of carbon monoxide have been limited so far because the tuning range of our present laser system only extends down to 2000 cm^{-1} . However, the new crystals that we now have extend the range of OPO systems like ours down to the $1000\text{-}2000\text{ cm}^{-1}$ range, where many new metal carbonyls can be studied. We are continuing to redesign and improve the cluster beam machine at the ALS, and will employ it in the future for ionization threshold measurements on a number of metal oxide clusters.

In all of these studies, we have focused on the qualitative effects of metal-adsorbate interactions and trends for different transition metals interacting with the same ligand. Our theoretical work has revealed that density functional theory has some serious limitations for small metal systems that were not previously recognized. This is particularly evident in metals such as vanadium and iron, where two spin states of the metal lie at low energy. DFT has difficulty identifying the correct relative energies of these spin states. Further examinations of this issue are planned, as it has significant consequences for the applications of DFT.

Publications (2004-2007) for this Project

1. N.R. Walker, R.S. Walters and M.A. Duncan, "Infrared Photodissociation Spectroscopy of $V^+(\text{CO}_2)_n$ and $V^+(\text{CO}_2)_n\text{Ar}$ Complexes," *J. Chem. Phys.* **120**, 10037 (2004).
2. T.D. Jaeger, A. Fielicke, G. von Helden, G. Meijer and M.A. Duncan, "Infrared Spectroscopy of Water Adsorption on Vanadium Cluster Cations (V_x^+ ; $x=3\text{-}15$)," *Chem. Phys. Lett.* **392**, 409 (2004).

3. R.S. Walters and M.A. Duncan, "Infrared Spectroscopy of Solvation and Isomers in $\text{Fe}^+(\text{H}_2\text{O})_{1,2}\text{Ar}_m$ Complexes," *Austr. J. Chem.* **57**, 1145 (2004).
4. N.R. Walker, G.A. Grieves, R.S. Walters and M.A. Duncan, "Growth Dynamics and Intracluster Reactions in $\text{Ni}^+(\text{CO}_2)_n$ Complexes via Infrared Spectroscopy," *J. Chem. Phys.* **121**, 10498 (2004).
5. R.S. Walters, P.v.R. Schleyer, C. Corminboeuf and M.A. Duncan, "Structural Trends in Transition Metal Cation-Acetylene Complexes Revealed Through the C-H Stretch Fundamentals," *J. Am. Chem. Soc.* **127**, 1100 (2005).
6. T.D. Jaeger and M.A. Duncan, "Infrared Photodissociation Spectroscopy of $\text{Ni}^+(\text{benzene})_x$ Complexes," *J. Phys. Chem. A* **109**, 3311 (2005).
7. E.D. Pillai, T.D. Jaeger and M.A. Duncan, "Infrared spectroscopy and density functional theory of small $\text{V}^+(\text{N}_2)_n$ clusters," *J. Phys. Chem. A* **109**, 3521 (2005).
8. R.S. Walters, E.D. Pillai and M.A. Duncan, "Solvation Processes in $\text{Ni}^+(\text{H}_2\text{O})_n$ Complexes Revealed by Infrared Photodissociation Spectroscopy," *J. Am. Chem. Soc.* **127**, 16599 (2005).
9. R.S. Walters, E.D. Pillai, P.v.R. Schleyer and M.A. Duncan, "Vibrational spectroscopy of $\text{Ni}^+(\text{C}_2\text{H}_2)_n$ ($n=1-4$) complexes," *J. Am. Chem. Soc.* **127**, 17030 (2005).
10. N.R. Walker, R.S. Walters and M.A. Duncan, "Frontiers in the Infrared Spectroscopy of Gas Phase Metal Ion Complexes," *New J. Chem.* **29**, 1495 (2005).
11. E.D. Pillai, T.D. Jaeger and M.A. Duncan, "Infrared Spectroscopy of $\text{Nb}^+(\text{N}_2)_n$ Complexes: Coordination, Structures and Spin States," *J. Am. Chem. Soc.* **129**, 2297 (2007).
12. A.C. Scott, N.R. Foster, G.A. Grieves and M.A. Duncan, "Photodissociation of lanthanide metal cation complexes with cyclooctatetraene," *Int. J. Mass Spectrom.* **263**, 171 (2007).
13. V. Kasalova, W.D. Allen, H.F. Schaefer, E.D. Pillai and M.A. Duncan, "Model systems for probing metal cation hydration: The $\text{V}^+(\text{H}_2\text{O})$ and $\text{V}^+(\text{H}_2\text{O})\text{Ar}$ complexes," *J. Phys. Chem. A* **111**, 7599 (2007).
14. L. Belau, S.E. Wheeler, B.W. Ticknor, M. Ahmed, S.R. Leone, W.D. Allen, H.F. Schaefer, and M.A. Duncan, "Ionization Thresholds of Small Carbon Clusters: Tunable VUV Experiments and Theory," *J. Am. Chem. Soc.* **129**, 10229 (2007).
15. J. Velasquez, III, B. Njagic, M. S. Gordon and M. A. Duncan, "IR photodissociation spectroscopy and theory of $\text{Au}^+(\text{CO})_n$ complexes: Nonclassical carbonyls in the gas phase," *J. Phys. Chem. A*, to be submitted.

Structural Dynamics in Complex Liquids Studied with Multidimensional Vibrational Spectroscopy

Andrei Tokmakoff

Department of Chemistry, Massachusetts Institute of Technology, Cambridge, MA 02139

E-mail: tokmakof@MIT.edu

Water's complexity as a liquid and solvent originates in the hydrogen bonding interactions, which result in a locally structured hydrogen bond network that reorganizes on femtosecond and picosecond time scales. Aqueous reactivity and charge transport is largely dictated by the fluctuations and distortions of this network. The goal of our research is to develop ultrafast spectroscopies that can be used to characterize the molecular dynamics of hydrogen bonding in water and aqueous solutions, and reveal how these dynamics influence aqueous charge transport and reactivity. Our work can be divided into three areas: (1) studies of hydrogen bonding dynamics in water; (2) studies of proton transfer in aqueous acid and base solutions; and (3) development of new optical and spectroscopic technology used in these studies.

Hydrogen Bond Dynamics in Water

In order to monitor water's evolving structure, we employ ultrafast, infrared spectroscopy of the OH stretch of a solution of dilute HOD in D₂O. The OH absorption lineshape is broad due to the large distribution of hydrogen bonding environments present in the liquid, with molecules involved in strong hydrogen bonds absorbing low frequency side of the lineshape and molecules in strained or broken hydrogen bonds absorbing at the high frequency side. Our experiments observe the fluctuations of water's hydrogen bonding network by tagging molecules at a particular initial frequency and watching how this frequency varies in time. In previous experiments we characterized the global hydrogen-bonding and orientational fluctuations of the liquid. Vibrational echo peak shift measurements were used to characterize the OH frequency correlation function, which shows an initial 60 fs decay, a 200 fs beat due to hydrogen bond stretching motion, and a 1.4 ps decay corresponding to hydrogen bonding reorganization. A pump-probe anisotropy measurement, which describes HOD reorientation, showed a fast 50 fs decay due to intermolecular librations (hindered rotations) followed by diffusive reorientation on a 3 ps timescale. Unfortunately, both of these measurements average over all hydrogen bonding configurations and, while able to determine the timescales of the rearrangement of the liquid, are unable to shed light on the mechanism by which this reorganization occurs.

2D IR spectroscopy provides us with the ability to track how different hydrogen bonding environments interconvert over time. A 2D spectrum correlates how a molecule excited at an initial frequency evolves to a final frequency after a given waiting time. By varying the waiting time, we can follow how molecules initially in strong or weak hydrogen bonds exchange. For waiting times up to the vibrational lifetime of 700 fs, the overall changes to the 2D lineshape describe the loss of frequency correlation of HOD molecules. We have developed a number of metrics that quantify this loss of frequency memory in 2D lineshapes.

More interesting are the frequency dependent changes to the lineshape. If we apply our lineshape metrics to the high and low frequency sections of the 2D spectra, they show very different results indicating that molecules in strong hydrogen bonds experience different fluctuations than molecules in weak hydrogen bonds. Moreover, the 2D spectra indicate that molecules in strained or broken hydrogen bonding configurations relax to band center on the timescale of librational motions, which strongly suggests broken hydrogen bond states do not exist as stable minima on water's free energy surface. This argues that hydrogen bond switching is a concerted process in which broken hydrogen bonds are a configuration visited fleetingly as a water molecule reorients from one hydrogen-bonding partner to another. MD simulations of the switching event indicate that the free energy surface probed by our experiments projects well onto a bifurcation coordinate that describes distance and angular changes between the hydrogen bond donor and the initial and final acceptor molecules.

The fact that hydrogen bond switching is a concerted motion implies that an appropriate reaction coordinate for describing the exchange of hydrogen bonding partners must involve the collective motion of no less than three water molecules. To experimentally study this mechanism another frequency marker must be introduced to directly map the relative motion between multiple water molecules. Our plans are to attempt this by introducing a second isotope label, tritium, and probing the OD and OT stretches of a dilute mixture of HOD and HOT in H₂O.

As a first step in this direction, we have characterized the OT stretch of HOT in H₂O by measuring the infrared spectrum of this isotopic solution. Comparison of the line shape parameters to the OD stretch (HOD in H₂O) and OH stretch (HOD in D₂O) shows an inverse scaling of the linewidth with the square root of the reduced mass. This supports our previous findings that electric field fluctuations properly describe line broadening. We have also performed preliminary pump-probe measurements on the OT stretch and found that its vibrational relaxation timescale is 850 fs. This lies between the T₁ measured for the other isotopologues, and is in agreement with the proposal that the OT stretch relaxes via the intramolecular HOT bend.

In addition, the 2D IR and 3PEPS experiments described above have served as new experimental benchmarks that have been used to test the validity of classical models of water commonly employed in molecular dynamics simulations. Together with the Skinner and Fayer groups, we have compared experimental IR observables to those calculated from classical simulation models. The best agreement is given by SPC/E water. In a separate collaborative study with the Berne group, we investigated the role of polarizability in water models and found that there is great variability, but polarizability appears to be an important component for dynamical agreement. The best agreement was found for the Pol5 water model that includes an out of plane polarizable dipole.

Recent results from the Skinner group indicate that the OH transition dipole moment varies greatly with the local environment, increasing with the strength of the hydrogen bond to the proton. This breakdown of the Condon approximation calls into question the conclusions drawn from our 2D IR experiments since they depend on transition dipole to the fourth power. Since the Raman polarizability is relatively independent of the local environment of the OH bond, we have used the ratio of the IR and Raman lineshapes to estimate the frequency variation of the transition dipole moment. Using a static model we can reproduce the intensity variation of third order

echo signals with temperature. We have also included non-Condon effects in our simulation model for water and found that the inclusion of dynamics weakens the effect of the variation of the transition dipole moment and does not change the conclusions that we have drawn regarding the mechanism of hydrogen bond rearrangements in water.

Proton Transport in Water

Recently, we have worked to understand how water dynamics influences the transport of hydronium and hydroxide ions. These ions show anomalously fast diffusion in water due to their ability to transfer protons from one water molecule to another. However, the exact mechanism by which this occurs is not well understood and the solvation structure adopted by these species solution is contested.

We have made preliminary measurements on solutions of dilute HOD in concentrated NaOD:D₂O solution. New spectral features indicative of the protonated species appear in the vicinity of the OH stretching transition, including a new peak at high frequency due to the OH⁻ stretch and a broad shoulder that extends to low frequency due to HOD molecules hydrogen bonded to OD⁻ ions. Transient grating measurements find that as the NaOD concentration increases, a second vibrational relaxation component appears with an extremely fast timescale of ~160 fs. Peak shift experiments show a picosecond offset that grows with NaOD concentration indicating long lived static inhomogeneity. Most interestingly though, is the presence of large off-diagonal intensity in the 2D IR lineshape that disappears on the ~160 fs timescale. A tentative explanation for the off-diagonal intensity is that it results from molecules in the process of transferring a proton from a HOD molecule to an OD⁻ ion.

Spectroscopic Methods

The ability to interpret 2D IR experiments depends critically on a number of technical advances that we have implemented over the course of the last year. For time-domain detection methods, we have implemented a new method of quickly acquiring 2D data by sweeping the stage that sets one of the experimental time delays at constant velocity. The instantaneous stage position is determined via quadrature detection that determines the phase of a HeNe beam that co-propagates with the infrared excitation pulses. In a different approach that uses frequency domain detection, we have also demonstrated a new method that greatly simplifies the acquisition of 2D data by using a pump-probe geometry wherein the pump is a collinear pulse pair. Simultaneous collection of the third order response and the interferometric autocorrelation of the pulse pair allows for automated phasing of the data as well as rapid acquisition since only a single delay stage needs to be scanned.

DOE Supported Publications (2005-2007)

1. "Local hydrogen bonding dynamics and collective reorganization in water: Ultrafast IR spectroscopy of HOD/D₂O," C. J. Fecko, J. J. Loparo, S. T. Roberts and A. Tokmakoff, *Journal of Chemical Physics*, **122** (2005) 054506.
2. "Amide I vibrational dynamics of N-methylacetamide in polar solvents: The role of electrostatic interactions," M. F. DeCamp, L. P. DeFlores, J. M. McCracken, A. Tokmakoff, K. Kwac, and M. Cho, *J. Phys. Chem. B*, **109** (2005) 11016.
3. "Upconversion multichannel infrared spectrometer," M. F. DeCamp and A. Tokmakoff, *Optics Letters*, **30** (2005) 1818.

4. "Electric field fluctuations drive vibrational dephasing in water," J. D. Eaves, A. Tokmakoff, and P. L. Geissler, *Journal of Physical Chemistry A*, **109** (2005) 9424.
5. "Hydrogen bonds in liquid water are broken only fleetingly," J. D. Eaves, J. J. Loparo, C. J. Fecko, S. T. Roberts, A. Tokmakoff and P. L. Geissler, *Proceedings of the National Academy of Sciences, USA*, **102** (2005) 13019.
6. "Polarizable molecules in the vibrational spectroscopy of water," E. Harder, J. D. Eaves, A. Tokmakoff and B. J. Berne, *PNAS*, **102** (2005) 11611.
7. "A study of phonon-assisted exciton relaxation dynamics for a (6,5) enriched DNA-wrapped single walled carbon nanotubes sample," S. G. Chou, M. F. DeCamp, J. Jiang, Ge. G. Samsonidze, E. B. Barros, F. Plentz, A. Jorio, M. Zheng, G. B. Onoa, E. D. Semke, A. Tokmakoff, R. Saito, G. Dresselhaus, M. S. Dresselhaus, *Physical Review B*, **72** (2005) 195415.
8. "Single-shot two-dimensional spectrometer," M. F. DeCamp and A. Tokmakoff, *Optics Letters*, **31** (2006) 113.
9. "Spectral signatures of heterogeneous protein ensembles revealed by MD simulations of 2DIR spectra," Z. Ganim and A. Tokmakoff, *Biophysical Journal*, **91** (2006) 2636.
10. "Multidimensional infrared spectroscopy of water. I. Vibrational dynamics in 2D IR lineshapes," J. J. Loparo, S. T. Roberts, and A. Tokmakoff, *J. Chem. Phys.*, **125** (2006) 194521.
11. "Multidimensional infrared spectroscopy of water. II. Hydrogen bond switching dynamics," J. J. Loparo, S. T. Roberts, and A. Tokmakoff, *J. Chem. Phys.*, **125** (2006) 194522.
12. "Characterization of spectral diffusion from two-dimensional lineshapes," S. T. Roberts, J. J. Loparo, and A. Tokmakoff, *J. Chem. Phys.*, **125** (2006) 084502.
13. "2D IR spectroscopy of hydrogen bond switching in liquid water," J. J. Loparo, S. T. Roberts, and A. Tokmakoff, in *Ultrafast Phenomena XV*, ed. by P. Corkum, D. Jonas, R. J. D. Miller, and A.M. Weiner (Springer, Berlin, 2007), p. 341.
14. "Single-shot two-dimensional infrared spectroscopy," M. F. DeCamp, L. P. DeFlores, K. C. Jones, and A. Tokmakoff, *Optics Express*, **15** (2007) 233.
15. "Are water simulation models consistent with steady-state and ultrafast vibrational spectroscopy experiments?" J. R. Schmidt, S. T. Roberts, J. J. Loparo, A. Tokmakoff, M. D. Fayer, and J. L. Skinner, *Chemical Physics*, in press.
16. "Variation of the transition dipole moment across the OH stretching band of water," J. J. Loparo, S. T. Roberts, R. A. Nicodemus and A. Tokmakoff, *Chem. Phys.*, in press.
17. "Shining light onto water's rapidly evolving structure," A. Tokmakoff, *Science*, **317** (2007) 54.
18. "Two-dimensional Fourier transform spectroscopy in the pump-probe geometry," L. P. DeFlores, R. A. Nicodemus, and A. Tokmakoff, *Optics Letters*, in press.

Liquid and Chemical Dynamics in Nanoscopic Environments (DE-FG03-84ER13251)

Michael D. Fayer
Department of Chemistry, Stanford University, Stanford, CA 94305
fayer@stanford.edu

The Fayer group is addressing an interrelated set of research topics directed toward understanding how nanoconfinement, interfaces, and nanoscopic size influence dynamics of water and processes, particular proton dynamics, that occur in water. Nanoscopic water is the focus because of its importance in a wide range of chemical and biological processes and technological devices relevant to energy applications. In many systems, water is not found in its bulk form. Our recent work was the first to use ultrafast infrared methods to directly examine the dynamics of nanoscopic water, that is, water confined on a length scale of a few nanometers.¹⁻⁴

Water can make four hydrogen bonds and forms an extended hydrogen bonding network. The network structure is constantly undergoing global changes on timescales ranging from tens of femtoseconds to picoseconds. Water's ability to reorganize its hydrogen bonding network and thereby solvate charges and other chemical species gives it its unique importance. When water is confined on nanoscopic distance scales, its hydrogen bond network dynamics change, and these changes influence processes, such as proton transport, that occur in nanoscopic water. To understand the role of nanoconfinement and interfaces on the dynamics and properties of water, a variety of materials are being investigated. These include ionic and non-ionic reverse micelles, Nafion a polyelectrolyte fuel cell membrane, and concentrated salt solutions. The research addresses how such physical constraints on systems influence chemical and physical processes. Proton transport is an important focus particularly in fuel cell membranes.

The experimental methods that are being employed are able to focus directly on the dynamics of water and proton (hydronium ion) dynamics. The IR experiments include ultrafast 2D-IR vibrational echo spectroscopy and polarization selective IR pump-probe experiments. These experiments make measurements on the hydroxyl stretching mode of water. The 2D-IR vibrational echo experiments measure spectral diffusion through the time dependence of the 2D-IR lineshapes. Spectral diffusion measures the time evolution of the hydroxyl stretch frequencies that evolve as the hydrogen bond network structure changes with time. The polarization selective pump-probe experiments measure the orientational relaxation of water and the vibrational population relaxation. The orientational relaxation provides information on the concerted rearrangement of hydrogen bonds, and the population relaxation provides information on different local water environments. UV/Vis experiments including ultrafast pump – broadband probe transient absorption and stimulated emission spectroscopy, and time dependent fluorescence using time correlated single photon counting, are used to study proton dynamics. In these experiments, a photoacid is electronically excited and injects a proton into the systems. Proton transfer, solvation, solvent separation of contact ion pairs, and proton transport are then followed by the associated spectroscopic changes.

Nafion (a product of Du Pont) is the most common membrane separator used in polymer electrolyte membrane fuel cells due to its chemical and thermal stability and its high proton conductivity. It is a polymer, consisting of a long chain fluorocarbon backbone with pendant, sulfonic acid terminated, polyether side chains. For the first time, we have studied the complex environments experienced by water molecules in the hydrophilic channels of Nafion membranes using ultrafast infrared pump-probe spectroscopy.^{7,8} Fig. 1 shows population relaxation decays of the OD hydroxyl stretch of HOD in H₂O in Nafion nanochannels for three wavelengths taken on a $\lambda = 3$ sample, that is, 3 water molecules per sulfonate head group.⁸ The wavelengths are on the red edge of the spectrum, on the red side but near the center, and far on the blue side.

The solid lines are biexponential fits to the data at each frequency with the time constants fixed at $\tau_1 = 3.2$ ps and $\tau_2 = 8.6$ ps. Only the relative amplitude of the two components is varied.

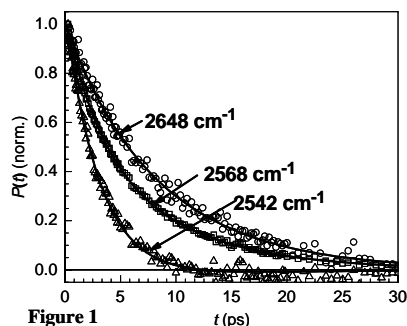


Figure 1

Decays at many other wavelengths were recorded. All of the decays are fit with the same biexponential decay constants but have a systematic variation in the amplitudes with the fast component approaching an amplitude of 1 on the red side of the line and the slow component approaching an amplitude of 1 on the blue side of the line. By way of comparison, the OD hydroxyl stretch population decay in bulk water is single exponential with a decay constant of 1.7 ps. These results demonstrate that water resides in two distinct environments. The results suggest that the blue side of the line corresponds to the hydroxyl associated with the sulfonate head group while the red side of the line has the hydroxyl hydrogen bonded to another water molecule. Similar results were obtained at other λ values.

Fig. 2 shows the results of orientational relaxation measurements as a function of λ at the center wavelength of each sample with bulk water for comparison.⁸ The decays in Nafion are biexponential with the longest component caused by complete orientational randomization.

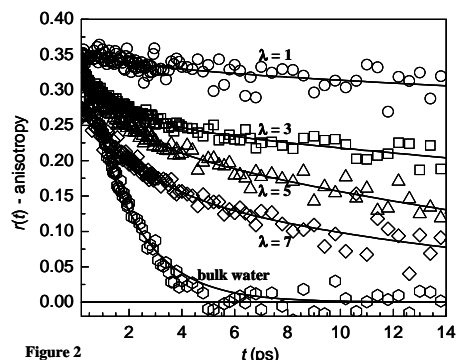


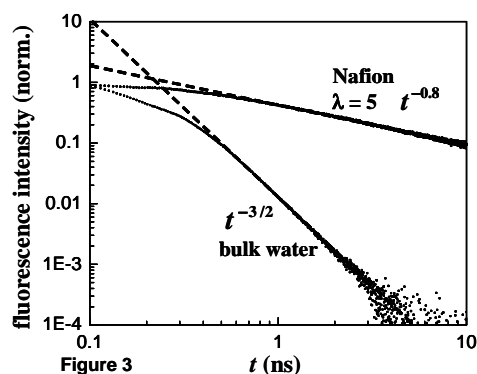
Figure 2

The fast component is the result of restricted orientational relaxation that occurs on a time scale fast compared to global hydrogen bond network rearrangement.^{1-4,8} As the amount of water in the channels is reduced, the rate of orientational relaxation decreases substantially. Proton transfer (see below) is related to the rate of hydrogen bond rearrangement. Proton transfer through Nafion ceases below $\lambda = 5$.

As shown in figs. 1 and 2 and in our studies of reverse micelles¹⁻⁴, nanoconfinement has a profound effect on the dynamics of water. We have begun to investigate the influence of nanoconfinement on the very important process of proton transport in Nafion and in reverse micelles by directly observing proton transfer in nanoenvironments.¹⁴ The basic approach for the study of proton transfer and transport dynamics in polyelectrolyte fuel cell membranes is the use of photoacids such as 8-hydroxypyrene-1,3,6-trisulfonate (HPTS) and related compounds. The proton dynamics in Nafion are compared to those in AOT reverse micelles and bulk water. HPTS undergoes a dramatic change in its acidity upon electronic excitation. The ground state pKa of HPTS is 7.7, which results in it being primarily protonated in neutral water. Upon photoexcitation the pKa drops approximately 7 units and HPTS rapidly transfers a proton to the surrounding water. The dynamics of proton transfer are dramatically affected by the ability of the solvent to reorganize and solvate the ion pair formed in the reaction. Since the reaction is reversible, the observed dynamics also depend on the proton mobility, that is, ability of the hydronium ion to move away from the resulting anion. These properties make excited state proton transfer a convenient probe for the local water environment and proton transport in nanoporous materials. For Nafion, proton transfer is particularly important because it is Nafion's primary function in fuel cells.

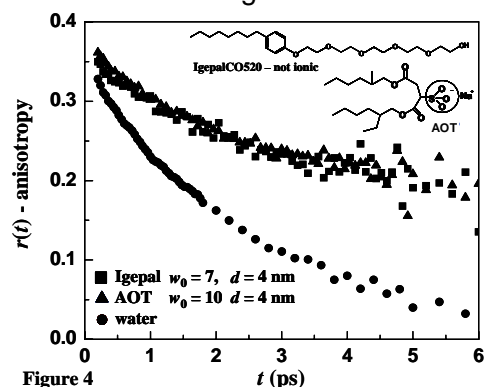
Fig. 3 shows the proton transport dynamics in Nafion nanochannels for $\lambda = 5$ and bulk water. The fluorescence decays (log plot) are for the protonated state of HPTS. The short time portion of the curve is related to the initial proton transfer and solvent separation following optical excitation of the photoacid.¹³ The long time portion of the decay is determined by proton transport, which is diffusive in bulk water. It is known that in bulk water the decay is a $t^{-3/2}$ power law (see fig. 3). In contrast to proton transfer in bulk water, the decay in the Nafion

sample is a $t^{-0.8}$ power law (see fig.3). We have made these measurements on Nafion samples



with a range of λ s. Changing λ changes the amount of water in the channels and their size. We have made the same measurements on a range of sizes of AOT reverse micelle water nanopools. In both types of samples, except at exceeding low water content, a $t^{-0.8}$ power law is observed. The important result is that the long time behavior for a range of sizes of both AOT and Nafion show the $t^{-0.8}$ power law. These results are the first measurements of the nanoscopic proton dynamics in Nafion fuel cell membranes. These observations are very new. To date, the seemingly ubiquitous $t^{-0.8}$ power law found as the signature of proton transport in nanoconfined systems does not have a theoretical explanation.

A central question concerning reverse micelles, Nafion fuel cell membranes, and other nanoconfined systems is the role of charged groups at the interface. Are the changes in water dynamics caused by nanoconfinement or the presence of charges? We have an initial result that will be investigated further that suggests that confinement is important rather than charges at the interface. Figure 4 displays orientational relaxation data for AOT and the non-ionic surfactant IgepalCO520 reverse micelles as well as bulk water for comparison.



The structures of the surfactants are shown in fig. 4. Igepal has an alcohol with polyether chain head group. These Igepal reverse micelles are essentially the only non-ionic reference micelles that have been well characterized using neutron scattering in terms of size, shape, and a phase diagram. The AOT and Igepal reverse micelles used in the experiments both have spherical water nanopools 4 nm in diameter. As can be seen from the figure, the orientational relaxation decays are almost the same. They are biexponential with both short time components 0.6 ± 0.2 ps, and the long time components are 9.6 ± 0.8 and 11.6 ± 1 for AOT and Igepal, respectively. These results strongly suggest that confining the water to 4 nm causes the substantial change in the dynamics in spite of the differences in the nature of the interfaces.

Understanding the influence of nanoscopic water on proton transfer, particularly in polyelectrolyte fuel cell membranes can have direct impact on fuel cell materials. We are continuing and extending our work to other polymer electrolyte fuel cell membranes to examine both water dynamics and proton dynamics. We are expanding our efforts on the investigation of water in reverse micelles and other structures such as 2 dimensional confinement. We are also beginning investigations of the influence of ions on water dynamics to understand the role of charges at interfaces. In addition to the experimental methods used to obtain the data presented here, we are employing ultrafast 2D-IR vibrational echo spectroscopy that provides very detailed observables for the investigation of water dynamics. The net result of our research is a greatly increased understanding of the dynamics and properties of nanoscopic water and processes in nanoscopic water, which are important for both fundamental and technological reasons.

Publication from DOE Sponsored Research 2005 – present

- (1) Tan, H.-S.; Piletic, I. R.; Riter, R. E.; Levinger, N. E.; Fayer, M. D. Dynamics of Water Confined on a Nanometer Length Scale in Reverse Micelles: Ultrafast Infrared Vibrational Echo Spectroscopy. *Phys. Rev. Lett.* **2005**, *94*, 057405.
- (2) Tan, H.-S.; Piletic, I. R.; Fayer, M. D. Orientational Dynamics of Nanoscopic Water in Reverse Micelles: Ultrafast Infrared Frequency Selective Transient Absorption Experiments. *J. Chem. Phys.* **2005**, *122*, 174501(174509).
- (3) Piletic, I.; Moilanen, D. E.; Spry, D. B.; Levinger, N. E.; Fayer, M. D. Testing the Core/Shell Model of Nanoconfined Water in Reverse Micelles Using Linear and Nonlinear Ir Spectroscopy. *J. Phys. Chem. A* **2006**, *110*, 4985-4999.
- (4) Piletic, I. R.; Tan, H.-S.; Fayer, M. D. Dynamics of Nanoscopic Water: Vibrational Echo and Infrared Pump-Probe Studies of Reverse Micelles. *J. Phys. Chem. B.* **2005**, *109*, 21273-21284.
- (5) Piletic, I.; Tan, H.-S.; Moilanen, D. E.; Spry, D. B.; Fayer, M. D. Vibrational Echo and Pump-Probe Spectroscopic Studies of the Dynamics of Water Molecules Confined to Nanoscopic Dimensions. In *Femtochemistry VII: Fundamental Ultrafast Processes in Chemistry, Physics, and Biology*; Castleman, A. W., Kimble, M. L., Eds.; Elsevier: Amsterdam, 2006; pp 195-203.
- (6) Piletic, I. R.; Moilanen, D. E.; Levinger, N. E.; Fayer, M. D. What Nonlinear-Ir Experiments Can Tell You About Water That the Ir Spectrum Cannot. *J. Am. Chem. Soc.* **2006**, *128*, 10366-10367.
- (7) Moilanen, D. E.; Piletic, I. R.; Fayer, M. D. Tracking Water'S Response to Structural Changes in Nafion Membranes. *J. Phys. Chem. A.* **2006**, *110*, 9084-9088.
- (8) Moilanen, D. E.; Piletic, I. R.; Fayer, M. D. Water Dynamics in Nafion Fuel Cell Membranes: The Effects of Confinement and Structural Changes on the Hydrogen Bonding Network. *J. Phys. Chem. C* **2007**, *111*, 8884-8891.
- (9) Tan, H.-S.; Piletic, I. R.; Fayer, M. D. Polarization Selective Spectroscopy Experiments: Methodology and Pitfalls," Howe-Siang Tan, Ivan R. Piletic and M. D. Fayer. *J.O.S.A. B* **2005**, *22*, 2009-2017.
- (10) Park, S.; Kwak, K.; Fayer, M. D. Ultrafast 2D-IR Vibrational Echo Spectroscopy: A Probe of Molecular Dynamics. *Laser Phys. Lett.* **2007**, *4*, 704-718.
- (11) Spry, D. B.; Fayer, M. D. Observation of Slow Charge Redistribution Preceding Excited State Proton Transfer. *submitted* **2007**.
- (12) Spry, D. B.; Goun, A.; Fayer, M. D. Identification and Properties of the 1Ia and 1Ib States of Pyranine (Hpts). *J. Chem. Phys.* **2006**, *125*, 144514.
- (13) Spry, D. B.; Goun, A.; Fayer, M. D. Deprotonation Dynamics and Stokes Shift of Pyranine (Hpts). *J. Phys. Chem. A* **2007**, *111*, 230-237.
- (14) D. B. Spry, A. G., K. Glusac, David E. Moilanen, W. Childs, and M. D. Fayer. Proton Transport and the Water Environment in Nafion Fuel Cell Membranes and Aot Reverse Micelles. *J. Am. Chem. Soc.* **2007**, *129*, 8122-8130.
- (15) Goun, A.; Glusac, K.; Fayer, M. D. Photoinduced Electron Transfer and Geminate Recombination in Liquids on Short Time Scales: Experiments and Theory. *J. Chem. Phys.* **2006**, *124*, 084504.
- (16) Nanda, J.; Behera, P. K.; Tavernier, H. L.; Fayer, M. D. Photoinduced Electron Transfer in the Head Group Region of Sodium Dodecyl Sulfate Micelles. *J. Lumin.* **2005**, *115*, 138-146.
- (17) Glusac, K.; Goun, A.; Fayer, M. D. Photoinduced Electron Transfer and Geminate Recombination in the Head Group Region of Micelles. *J. Chem. Phys.* **2006**, *125*, 054712(054712 pages).

Molecular Theory & Modeling
The Structural-Spectral-Energetic Correspondence for hydrogen bonded networks:
Adding an Energy component to *Badger's rule*

Sotiris S. Xantheas
Chemical & Materials Sciences Division
Pacific Northwest National Laboratory
902 Battelle Blvd.
Mail Stop K1-83
Richland, WA 99352
sotiris.xantheas@pnl.gov

The objective of this research effort is to develop a comprehensive understanding of the collective phenomena associated with aqueous solvation. The molecular level details of aqueous environments are central in the understanding of important processes such as reaction and solvation in a variety of homogeneous and heterogeneous systems. The fundamental understanding of the structural, thermodynamic and spectral properties of these systems is relevant to the solvation in aqueous solutions, the structure, reactivity and transport properties of clathrate hydrates, in homogeneous catalysis and in atmospheric processes.

Of particular importance is the ability to account for and understand the origin of the energetic stabilization of various hydrogen bonded networks in conjunction with their corresponding experimental signatures. It is therefore desirable to be able to identify the energetically most stable networks and relate the underlying molecular structure to experimental results, such as the ones obtained from infrared (IR) vibrational spectroscopy. It has long been established that the IR spectra of hydrogen bonded clusters in the 3,000-4,000 cm^{-1} represent a fingerprint of the underlying hydrogen bonding network. Badger's rule already provides a relationship between intermolecular distances and bond force constants.¹ Its application to hydrogen bonded systems since its introduction² has paved the path for establishing the *structural-spectral correspondence*, i.e. the correlation between molecular structure and vibrational spectra. This principle has been previously successfully used for the assignment of cluster structures (hydrogen bonding topology) from the experimentally measured IR spectra in the intramolecular region of the spectra (3,000-4000 cm^{-1}) with the realization that different cluster isomers (and in turn different hydrogen bonding networks) have dissimilar spectral signatures.³

The existing relation between structure and spectra can be extended in order to include an additional component that accounts for the energetic stabilization of the underlying network. This extension is based upon the observation that the most red-shifted, IR active hydrogen bonded OH stretching vibrations for $(\text{H}_2\text{O})_n$ in the cluster regime $2 \leq n \leq 21$ correspond to localized vibrations of donor OH stretches that are connected to neighbors via "strong" (water dimer-like)

¹ R. M. Badger, *J. Chem. Phys.* **2**, 128 (1934); R. M. Badger, *J. Chem. Phys.* **3**, 710 (1935).

² R. M. Badger and S. H. Bauer, *J. Chem. Phys.* **5**, 839 (1937).

³ O. M. Cabarcos, C. J. Weinheimer, and J. M. Lisy, S. S. Xantheas, *J. Chem. Phys.* **110**, 5 (1999); H. E. Dorsett and R. O. Watts, S. S. Xantheas, *J. Phys. Chem.* **103**, 3351 (1999); J. M. Weber, J. A. Kelley, S. B. Nielsen, P. Ayotte, M. A. Johnson, *Science* **287**, 2461 (2000); K. Nauta and R. E. Miller, *Science* **287**, 293 (2000).

arrangements of adjacent water molecules and belong to a water molecule that has a “free” (non-hydrogen bonded) OH stretch.⁴ This orientational dependence of the nearest neighbor molecules that is associated with the most IR active vibrations is the basis of a discrete model that is used

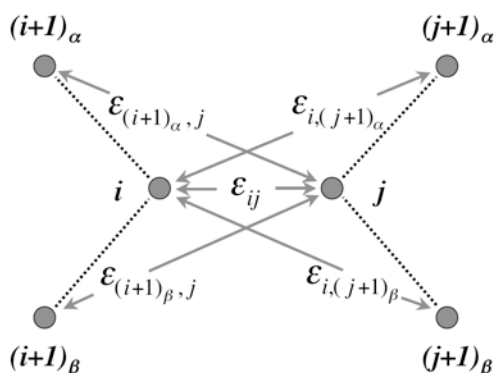


Figure 1. Definition of the *effective* pair interaction hydrogen bond energy, U_{ij}^{eff} , between fragments i and j on the surface of a PWC.

for the fast screening of hydrogen bonded networks.

The discrete model that is used to screen the various networks is based on the definition of an *effective* pair interaction energy that incorporates pair interactions between nearest-, second-, and third-neighbors as shown in Figure 1. Assuming that ϵ_{ij} is the pair interaction of nearest-neighbor (n - n) molecules i and j , $\epsilon_{i,j+1}$ is the pair interaction between i and the first neighbor of j ($\neq i$) and $\epsilon_{i+1,j+1}$ the pair interaction between the first neighbors of i ($\neq j$) and j ($\neq i$), we define the *effective* energy, U_{ij}^{eff} , of the (n - n) hydrogen bond between molecules i and j as:

$$U_{ij}^{eff} = \epsilon_{ij} + \frac{1}{2} \left(\epsilon_{i,(j+1)_\alpha} + \epsilon_{(i+1)_\alpha,j} + \epsilon_{i,(j+1)_\beta} + \epsilon_{(i+1)_\beta,j} \right) + \left(\epsilon_{(i+1)_\alpha,(j+1)_\beta} + \epsilon_{(i+1)_\beta,(j+1)_\alpha} \right) \quad (1)$$

We applied this discrete model to the screening of the various networks of the 5^{12} pentagonal dodecahedron $(\text{H}_2\text{O})_{20}$ polyhedral water cluster (PWC). PWCs exhibit a variety of features that make them attractive for the theoretical analysis of the properties of hydrogen bonds such as the orientational dependence of their relative strength, the dependence of the stability of the underlying hydrogen bonding network upon the local structure and the interplay between structure and accompanying spectroscopic signatures. One important feature of PWCs is the essential dependence of their properties on the underlying proton orientation pattern. This determines the number of symmetry distinct isomers within a family of PWCs according to the Bernal-Fowler ice rules. The number of accessible configurations that obey the Bernal-Fowler rules for a fixed O-O lattice grows as $(3/\sqrt{2})^N$. For the 5^{12} PWC the number of non-isomorphic (symmetry distinct) configurations in this cluster (again for fixed oxygen positions) is⁵ 30,026.

The analysis of the effective pair energies of all 30,026 networks of the 5^{12} PWC suggests the preferential energetic stabilization of a class of isomers that have the maximum number of a hydrogen bond type with the following characteristics: it corresponds to a *trans* nearest-neighbor orientation and has 1 dangling bond which resides on the donor molecule. For the pentagonal dodecahedron cluster there are 64 isomers of this type. Further quantitative refinement using electronic structure DFT and MP2 calculations of candidates within the lowest class of 64 isomers, predicted with the discrete model, identifies a new global minimum for the dodecahedron family of $(\text{H}_2\text{O})_{20}$, which has been previously missed using other sampling methods such as basin-hopping Monte Carlo methods.

⁴ A Lagutschenkov, GS Fanourgakis, G Niedner-Schatteburg and SS Xantheas, *J. Chem. Phys.* **122**, 194310 (2005).

⁵ S McDonald, L Ojamäe, and SJ Singer, *J. Phys. Chem.* **102**, 2824 (1998); J-L Kuo, JV Coe, and SJ Singer, *J. Chem. Phys.* **114**, 2527 (2001).

The implications of this scheme for the analysis of the structural patterns in other PWCs such as $\text{H}_3\text{O}^+(\text{H}_2\text{O})_{20}$ as well as in liquid water in conjunction with recent IR spectra will be also discussed.

Acknowledgements: This research was performed in part using the computational resources in the National Energy Research Supercomputing Center (NERSC) at Lawrence Livermore National Laboratory. Battelle operates Pacific Northwest National Laboratory for the US Department of Energy.

References to publications of DOE sponsored research (2005-present)

1. B. C. Garrett, D. A. Dixon, *et al* "The Role of Water on Electron-Initiated Processes and Radical Chemistry: Issues and Scientific Advances", *Chemical Reviews* **106**, 355 (2005)
2. G. S. Fanourgakis, E. Aprà, W. A. de Jong, and S. S. Xantheas, "High-level *ab-initio* calculations for the four low-lying families of minima of $(\text{H}_2\text{O})_{20}$: II. Spectroscopic signatures of the dodecahedron, fused cubes, face-sharing and edge-sharing pentagonal prisms hydrogen bonding networks", *Journal of Chemical Physics* **122**, 134304 (2005)
3. A. Lagutschenkov, G. S. Fanourgakis, G. Niedner-Schatteburg and S. S. Xantheas, "The spectroscopic signature of the "all-surface" to "internally solvated" structural transition in water clusters in the $n=17-21$ size regime", *Journal of Chemical Physics* **122**, 194310 (2005). Featured in the *Virtual Journal of Biological Physics Research*.
4. S. Hirata, M. Valiev, M. Dupuis and S. S. Xantheas, S. Sugiki and H. Sekino, "Fast electron correlation methods for molecular clusters in the ground and excited states", *Molecular Physics* (R. J. Bartlett special issue) **103**, 2255 (2005)
5. S. S. Xantheas, "Interaction potentials for water from accurate cluster calculations" in *Structure and Bonding: Intermolecular Forces and Clusters II*, Springer-Verlag Berlin Heidelberg, D. J. Wales (Editor), vol. **116**, pp. 119-148 (2005)
6. S. S. Xantheas, W. Roth, I. Fischer, "Competition between van der Waals and Hydrogen Bonding Interactions: The structure of the trans-1-Naphthol/ N_2 cluster", *Journal of Physical Chemistry A* **109**, 9584 (2005)
7. G. S. Fanourgakis and S. S. Xantheas, "The flexible, polarizable, Thole-type interaction potential for water (TTM2-F) revisited" *Journal of Physical Chemistry A* **110**, 4100 (2006)
8. G. S. Fanourgakis and S. S. Xantheas, "The bend angle of water in ice Ih and liquid water: The significance of implementing the non-linear monomer dipole moment surface in classical interaction potentials" *Journal of Chemical Physics* **124**, 174504 (2006). Featured in the *Virtual Journal of Biological Physics Research*.
9. K. A. Ramazan, L. M. Wingen, Y. Miller, G. M. Chaban, R. B. Gerber, S. S. Xantheas and B. J. Finlayson-Pitts, "New Experimental and Theoretical Approach to the Heterogeneous Hydrolysis of NO_2 : Key Role of Molecular Nitric Acid and Its Complexes", *Journal of Physical Chemistry A* **110**, 6886 (2006)
10. T. A. Blake, S. S. Xantheas, "The Structure, Anharmonic Spectra and Puckering Barrier of Cyclobutane: A Theoretical Study", *Journal of Physical Chemistry A* **110**, 10487 (2006)

11. S. S. Xantheas, "Anharmonic vibrational spectra of hydrogen bonded clusters: Comparison between higher energy derivative and mean-field grid based methods", Roger E. Miller memorial issue (invited), *International Reviews in Physical Chemistry* **25**, 719 (2006)
12. G. S. Fanourgakis, G. K. Schenter and S. S. Xantheas, "A quantitative account of quantum effects in liquid water", *Journal of Chemical Physics* **125**, 141102 (2006). Featured in the *Virtual Journal of Ultrafast Science*, November 2006
13. S. Bulusu, S. Yoo, E. Aprà, S. S. Xantheas, X. C. Zeng, "The lowest energy structures of water clusters (H₂O)₁₁ and (H₂O)₁₃", *Journal of Physical Chemistry A* **110**, 11781 (2006)
14. G. S. Fanourgakis, V. Tipparaju, J. Nieplocha and S. S. Xantheas, "An efficient parallelization scheme for molecular dynamics simulations with many-body, flexible, polarizable empirical potentials: Application to water", *Theoretical Chemistry Accounts* **117**, 73 (2007)
15. T. Pankewitz, A. Lagutschenkov, G. Niedner-Schatteburg, S. S. Xantheas, Y.-T. Lee, "The Infrared Spectrum of NH₄⁺(H₂O): Evidence for mode specific fragmentation", *Journal of Chemical Physics* **126**, 074307 (2007)
16. M. N. Slipchenko, B. G. Sartakov and A. F. Vilesov, S. S. Xantheas, "A study of NH stretching vibrations in small ammonia clusters by infrared spectroscopy in He droplets and *ab-initio* calculations", Roger E. Miller memorial issue (invited), *Journal of Physical Chemistry A* **111**, 7460 (2007)
17. L. Rubio-Lago, D. Zaouris, Y. Sakellariou, D. Sofikits and T. N. Kitsopoulos, F. Wang and X. Yang, B. Cronin and M. N. R. Ashfold, S. S. Xantheas, "Photofragment slice imaging studies of pyrrole and the Xe-pyrrole cluster", *Journal of Chemical Physics* **127**, 064306 (2007)
18. T. A. Blake, E. D. Glendening, R. L. Sams, S. W. Sharpe and S. S. Xantheas, "High Resolution Infrared Spectroscopy in the 1200 to 1300 cm⁻¹ Region and Accurate Theoretical Estimates for the Structure and Ring Puckering Barrier of Perfluorocyclobutane", Thom H. Dunning Jr. Festschrift (invited), *Journal Physical Chemistry A* (in press, web release date: 06-Jul-2007, DOI:10.1021/jp072521f)

Chemical Kinetics and Dynamics at Interfaces

Structure and Reactivity of Ices, Oxides, and Amorphous Materials

Bruce D. Kay (PI), R. Scott Smith, and Zdenek Dohnalek

Chemical Sciences Division
Pacific Northwest National Laboratory
P.O. Box 999, Mail Stop K8-88
Richland, Washington 99352
bruce.kay@pnl.gov

Additional collaborators include P. Ayotte, C. T. Campbell, J. L. Daschbach, H. Jonsson, J. Kim, G. A. Kimmel, C. B. Mullins, N. G. Petrik, G. K. Schenter, J. M. White, and T. Zubkov

Program Scope

The objective of this program is to examine physiochemical phenomena occurring at the surface and within the bulk of ices, oxides, and amorphous materials. The microscopic details of physisorption, chemisorption, and reactivity of these materials are important to unravel the kinetics and dynamic mechanisms involved in heterogeneous (i.e., gas/liquid) processes. This fundamental research is relevant to solvation and liquid solutions, glasses and deeply supercooled liquids, heterogeneous catalysis, environmental chemistry, and astrochemistry. Our research provides a quantitative understanding of elementary kinetic processes in these complex systems. For example, the reactivity and solvation of polar molecules on ice surfaces play an important role in complicated reaction processes that occur in the environment. These same molecular processes are germane to understanding dissolution, precipitation, and crystallization kinetics in multiphase, multicomponent, complex systems. Amorphous solid water (ASW) is of special importance for many reasons, including the open question over its applicability as a model for liquid water, and fundamental interest in the properties of glassy materials. In addition to the properties of ASW itself, understanding the intermolecular interactions between ASW and an adsorbate is important in such diverse areas as solvation in aqueous solutions, cryobiology, and desorption phenomena in cometary and interstellar ices. Metal oxides are often used as catalysts or as supports for catalysts, making the interaction of adsorbates with their surfaces of much interest. Additionally, oxide interfaces are important in the subsurface environment; specifically, molecular-level interactions at mineral surfaces are responsible for the transport and reactivity of subsurface contaminants. Thus, detailed molecular-level studies are germane to DOE programs in environmental restoration, waste processing, and contaminant fate and transport.

Our approach is to use molecular beams to synthesize “chemically tailored” nanoscale films as model systems to study ices, amorphous materials, supercooled liquids, and metal oxides. In addition to their utility as a synthetic tool, molecular beams are ideally suited for investigating the heterogeneous chemical properties of these novel films. Modulated molecular beam techniques enable us to determine the adsorption, diffusion, sequestration, reaction, and desorption kinetics in real-time. In support of the experimental studies, kinetic modeling and Monte Carlo simulation techniques are used to analyze and interpret the experimental data.

Recent Progress and Future Directions

Deeply Supercooled Binary Liquid Solutions from Nanoscale Amorphous Films Supercooled liquids are thermodynamically metastable which makes studies of this fundamentally important regime difficult. One challenge in the study of the physiochemical properties of liquid in a supercooled state is the difficulty in preventing crystallization. We have recently demonstrated an alternate approach to create and study these elusive liquids which we call “beakers without walls.” Through the use of use of molecular beams and nanoscale amorphous solid films we are able to produce deeply supercooled liquid solutions and study their transport properties. Our approach is to heat an amorphous solid above its glass transition temperature, T_g , where upon it transforms into a supercooled liquid prior to crystallization.

For pure substances these supercooled liquids rapidly freeze into the thermodynamically stable crystalline solids. The FTIR spectra show that pure species rapidly crystallize whereas crystallization is inhibited in the mixtures. However, a compositionally tailored nanoscale film (20 nm thick) comprised of methanol deposited on top of ethanol undergoes extensive diffusive intermixing upon heating above the glass transition. This intermixing produces a deeply supercooled binary solution that resists crystallization. The diffusion coefficient in this mixture is 10^7 times smaller than that room temperature solution. Hence, a 1 cm thick sample would require over a million years to mix! Furthermore, this supercooled solution is “ideal” and the desorption from this solution is perfectly described by a kinetic model based on Raoult’s Law. The lifetime of the supercooled liquid is limited by the thermodynamic drive to form the lower free energy crystalline phase. By making the films thicker we can extend the time the system spends in the metastable region. This enables us to “watch” the metastable liquid phase separate into the equilibrium components dictated by the binary liquid-solid phase diagram. Attendant with precipitation of crystalline methanol the films undergo a dewetting transition. Future studies will explore the binary solutions where one of the components is water.

Wetting and Non-Wetting Adsorption of Water on Surfaces In collaboration with Greg Kimmel and Nikolay Petrik we have investigated the growth of crystalline ice (CI) and ASW films on Pt(111) and Pd(111) using rare gas physisorption. It is well-known that the water monolayer wets both of these metals and it was widely-believed that these substrates were good templates for the epitaxial growth of crystalline ice films. Our studies confirm that the water monolayer wets both substrates at all temperatures investigated (20-155 K) and that ASW films deposited below ~ 125 K also wet the water monolayer. Surprisingly, crystalline ice films grown at higher temperatures ($T > 135$ K) do not wet the water monolayer! Furthermore, the wetting ASW films dewet exposing the underlying water monolayer as they transform to CI upon heating. These findings demonstrate that the water monolayer on both Pt(111) and Pd(111) is *hydrophobic* with respect to the growth of CI.

The structure of the water monolayer on these metals is key to understanding the observed *hydrophobicity*. For both Pt(111) and Pd(111) recent experiments and theory indicate that all water molecules in the first monolayer interact significantly with the metal substrate. The water molecules form a nearly-planar, hexagonal array with each molecule hydrogen-bonded to three other water molecules in the array. In this array half the water molecules bind to the underlying metal through the oxygen lone pair and the other half have a hydrogen atom point toward the metal. Therefore, each water molecule in the monolayer forms four bonds, leaving no dangling OH groups or lone pair electrons protruding into the vacuum. Since this fully-coordinated water monolayer has no additional attachment points it is *hydrophobic* to additional water growth. Ongoing studies are exploring water adsorption on C(0001) and FeO(111) surfaces. On both these substrates ASW grows approximately layer-by-layer but crystalline ice growth exhibits non-wetting behavior. Future experiments will employ FTIR to understand the detailed nature of the water-substrate interface on Pt(111), Pd(111), Cu(111), FeO(111), and C(0001).

Synthesis, Characterization, and Reactivity of Nanoporous Thin Films Highly nanoporous materials can have useful applications in a variety of areas including catalysis and chemical sensors. The fundamental interaction of gases and fluids with these nanoporous films will determine the performance characteristics of such devices. Understanding these interactions is therefore essential for the rational design and synthesis of materials for particular applications. We have previously shown that morphology of vapor deposited ASW films is strongly dependent on the incident growth angle. A simple physical mechanism, ballistic deposition, can be used to understand the dependence of morphology on the growth angle. The basic premise of ballistic deposition is that molecules incident from the gas phase stick at the first site they encounter at the surface of the solid without subsequent diffusion. Ballistic deposition at or near normal incidence results in rough surfaces due to the stochastic nature of the deposition process. At grazing incidence, deposition can not occur in regions behind high points on the surface due to simple shadowing, resulting in the formation of columnar, porous materials. Previously, we developed a reactive variant of this technique, reactive ballistic deposition (RBD), to grow compositionally and structurally tailored nanoporous MgO films with extremely high porosities and surface areas.

Recently we have synthesized nanoporous, high-surface area films of TiO₂ by RBD of titanium metal in an oxygen ambient. These films consist of arrays of highly oriented, predominantly independent, columnar filaments tethered to the underlying substrate. Auger electron spectroscopy (AES) is used to investigate the stoichiometric dependence of the films on growth conditions (surface temperature and partial pressure of oxygen). Scanning and transmission electron microscopies show that the films consist of arrays of separated filaments. The surface area and the distribution of binding site energies of the films are measured as functions of growth temperature, deposition angle, and annealing conditions using temperature programmed desorption (TPD) of N₂. TiO₂ films deposited at 50 K at 70 degrees from substrate normal display the greatest specific surface area of ~100 m²/g. In addition, the films retain greater than 70% of their original surface area after annealing to 600 K. The combination of high surface area and thermal stability suggests that these films could serve as supports for applications in heterogeneous catalysis.

Nanoporous Pd films were also synthesized using ballistic deposition techniques. The surface area of Pd films was found to depend dramatically on the Pd dosing angle and annealing temperature. Pd films grown at 22 K with a 85° deposition angle exhibit the highest surface area of 120 m²/g. Ex situ SEM imaging reveals that these films consist of a tilted array of nanocrystalline filaments. The annealing studies show that the films densify upon annealing and lose approximately 50% of their surface area by 300 K and are almost completely dense by 500 K. Pd deposition at elevated temperatures (<300 K) produces denser Pd films compared to those grown at 22 K.

The interaction of gases and fluids with these nanoscale films forms the basis for a variety of the useful applications of porous materials. For example, the rates of uptake, sequestration, reaction, and release of gases in these materials often determines their performance characteristics in devices such as catalysts and chemical sensors. The adsorption and desorption kinetics of N₂ on porous ASW films were studied using molecular beam techniques, temperature programmed desorption (TPD), and reflection-absorption infrared spectroscopy (RAIRS). The ASW films were grown on Pt(111) at 23 K by ballistic deposition from a collimated H₂O beam at various incident angles to control the film porosity. The experimental results show that the N₂ condensation coefficient is essentially unity until near saturation, independent of the ASW film thickness indicating that N₂ transport within the porous films is rapid. The TPD results show that the desorption of a fixed dose of N₂ shifts to higher temperature with ASW film thickness. Kinetic analysis of the TPD spectra shows that a film thickness rescaling of the coverage dependent activation energy curve results in a single master curve. Simulation of the TPD spectra using this master curve results in a quantitative fit to the experiments over a wide range of ASW thicknesses (up to 1000 layers, ~0.5 μm). The success of the rescaling model indicates that N₂ transport within the porous film is rapid enough to maintain a uniform distribution throughout the film on a time scale faster than desorption.

Future studies will focus on examining the chemical reactivity of nanoporous films. Specifically, the catalytic activity of nanoporous TiO₂ and Pd films will be studied and compared to baseline reactivity studies on single crystal TiO₂(110) and Pd(111).

References to Publications of DOE sponsored Research (CY 2004- present)

1. "Adsorption, desorption, and clustering of H₂O on Pt(111)", J. L. Daschbach, B. M. Peden, R. S. Smith and B. D. Kay, *Journal of Chemical Physics*, **120**, 1516, (2004).
2. "Helium diffusion through H₂O and D₂O amorphous ice: Observation of a lattice inverse isotope effect", J. L. Daschbach, G. K. Schenter, P. Ayotte, R. S. Smith and B. D. Kay, *Physical Review Letters*, **92**, 198306, (2004).
3. "Reactive growth of nanoscale MgO films by Mg atom deposition onto O₂ multilayers", J. Kim, Z. Dohnalek, J. M. White and B. D. Kay, *Journal of Physical Chemistry B*, **108**, 11666, (2004).
4. "Role of water in electron-initiated processes and radical chemistry: Issues and scientific advances", B. C. Garrett, et al. *Chemical Reviews*, **105**, 355, (2005).

5. "Influence of surface morphology on D₂ desorption kinetics from amorphous solid water", L. Hornekaer, A. Baurichter, V. V. Petrunin, A. C. Luntz, B. D. Kay and A. Al-Halabi, *Journal of Chemical Physics*, **122**, 124701, (2005).
6. "n-Alkanes on MgO(100). I. Coverage-dependent desorption kinetics of n-butane", S. L. Tait, Z. Dohnalek, C. T. Campbell and B. D. Kay, *Journal of Chemical Physics*, **122**, 164707, (2005).
7. "n-Alkanes on MgO(100). II. Chain length dependence of kinetic desorption parameters for small n-alkanes", S. L. Tait, Z. Dohnalek, C. T. Campbell and B. D. Kay, *Journal of Chemical Physics*, **122**, 164708, (2005).
8. "Structural characterization of nanoporous Pd films grown via ballistic deposition", J. Kim, Z. Dohnalek and B. D. Kay, *Surface Science*, **586**, 137, (2005).
9. "Adsorption and Desorption of HCl on Pt(111)", JL Daschbach, J Kim, P Ayotte, RS Smith and BD Kay, *Journal of Physical Chemistry B*, **109**, 15506, (2005).
10. "Water Adsorption, Desorption and Clustering on FeO(111)", J. L. Daschbach, Z. Dohnálek, S-R. Liu, R. S. Smith, and B. D. Kay, *Journal of Physical Chemistry B* **109**, 10362, (2005).
11. "Methane Adsorption and Dissociation and Oxygen Adsorption and Reaction with CO on Pd Nanoparticles on MgO(100) and on Pd(111)", S. L. Tait, Z. Dohnálek, C. T. Campbell, B. D. Kay," *Surface Science* **591**, 90, (2005).
12. "Crystalline Ice Growth on Pt(111): Observation of a Hydrophobic Water Monolayer", G. A. Kimmel, N. G. Petrik, Z. Dohnálek, and B. D. Kay, *Physical Review Letters* **95**, 166102, (2005).
13. "What Determines the Sticking Probability of Water Molecules on Ice?", E.R. Batista, P. Ayotte, A. Bilic, B.D. Kay, and H. Jonsson, *Physical Review Letters* **95**, 223201, (2005).
14. "Cryogenic CO₂ Formation on Oxidized Gold Clusters Synthesized via Reactive Layer Assisted Deposition", J. Kim, Z. Dohnálek, and B. D. Kay, *Journal of The American Chemical Society Communication*, **127**, 14592, (2005).
15. "The Effect of Incident Collision Energy on the Phase and Crystallization Kinetics of Vapor Deposited Water Films", R. S. Smith, T. Zubkov, and B. D. Kay, *Journal of Chemical Physics*, **124**, 114710, (2006)
16. "Layer-by-layer Growth of Thin Amorphous Solid Water Films on Pt(111) and Pd(111)", G. A. Kimmel, N. G. Petrik, Z. Dohnálek, and B. D. Kay, *Journal of Chemical Physics*, **125**, 044713, (2006)
17. "Growth of Epitaxial Thin Pd(111) Films on Pt(111) and Oxygen Terminated FeO(111) Surfaces", Z. Dohnálek, J. Kim, and B. D. Kay, , *Surface Science* **600**, 3461 (2006).
18. "Physisorption of N₂, O₂, and CO on Fully-oxidized TiO₂(110)", Z. Dohnálek, J. Kim, O. A. Bondarchuk, J. M. White and B. D. Kay, *Journal of Physical Chemistry B*, **110**, 6229, (2006)
19. "Crystalline ice growth on Pt(111) and Pd(111): Non-wetting growth on a hydrophobic water monolayer", A. Kimmel, N. G. Petrik, Z. Dohnálek, and B. D. Kay, *Journal of Chemical Physics*, **126**, 114702, (2007).
20. "Reactive Ballistic Deposition of Porous TiO₂ Films: Growth and Characterization", D. W. Flaherty, Z. Dohnálek, A. Dohnálková, B. W. Arey, D. E. McCready, N. Ponnusamy, C. B. Mullins, and B. D. Kay, *Journal of Physical Chemistry C* **111**, 4765, (2007).
21. "Adsorption, Desorption and Diffusion of Nitrogen in a Model Nanoporous Material: I.: Surface Limited Desorption Kinetics in Amorphous Solid Water", T. Zubkov, R. S. Smith, T.R. Engstrom, and B. D. Kay, *Journal of Chemical Physics*, accepted for publication 2007).
22. "Adsorption, Desorption and Diffusion of Nitrogen in a Model Nanoporous Material: II.: Diffusion Limited Kinetics in Amorphous Solid Water", T. Zubkov, R. S. Smith, T.R. Engstrom, and B. D. Kay, *Journal of Chemical Physics*, accepted for publication 2007).

Understanding the Electron-water Interaction at the Molecular Level: Integrating Theory and Experiment in the Cluster Regime: DE-FG02-06ER15800

Program Manager: Dr. Gregory Fiechtner

K. D. Jordan (jordan@pitt.edu), Dept. of Chemistry, University of Pittsburgh, Pittsburgh, PA 15260
and M. A. Johnson (mark.johnson@yale.edu), Dept. of Chemistry, Yale University, New Haven, CT 06520

I. Overview

Our program exploits size-selected clusters as model systems through which to express molecular-level aspects of radiation chemistry. As such, these studies involve synthesis and characterization of neat water clusters in all charge states in addition to mixed complexes involving anionic and cationic solute ions as well as neutrals. The signature of our approach is that we focus on generating relatively complex systems (containing up to 20 molecules or so) close to their minimum energy structures, which we then characterize using a combination of theory and experiment. Most recent activity has been directed toward understanding the correlation between the vibrational band patterns observed in the 600 – 4400 cm^{-1} range and the electron binding energies of cluster anions determined through photoelectron spectroscopy. The vibrational spectra are taken in a linear action mode which facilitates theoretical analysis. In effect, we extend the mature tools refined in the study of polyatomic molecular photophysics to a more complex regime where H-bonded networks respond cooperatively to accommodate a solute. In our first four years under DOE support, we have concentrated our effort on understanding how an excess electron is attached to water clusters in order to define how different binding motifs are manifested in their spectral signatures. We are now extending this work to include the nascent cationic species present in the early stages of radiation damage as well as the speciation of reactive transients created in radiolysis such as the hydrated oxygen anion, O^- .

II. Summary of results

IIA. Local binding motifs and electron binding energies of water cluster anions

There has been much recent activity in the literature regarding the physical origin of the various classes of electron binding energies that have been reported for the negatively charged water cluster anions, $(\text{H}_2\text{O})_n^-$. These classes divide into three widely-spaced groups as indicated in the top graph in Fig. 1, and are denoted I, II and III in decreasing order of vertical electron detachment energy (VDE). One rationalization for this behavior, advanced by the Neumark group and supported by Coe and Bowen, is that these differ according to whether the electron is accommodated on the surface (II and III) or the interior of the cluster (I), a conjecture that has been challenged by Rossky on the basis of theoretical simulations. In earlier work, we have already established the importance of a local binding motif at play in the strongly bound, type I clusters, in which a *single* water molecule, attached to the network in a double H-bond acceptor arrangement, mediates the interaction with the excess electron.(4,7) In fact, the vibrational spectra of the small ($n = 3-6$) clusters are dominated by the displacements of this special water molecule, and it yields a unique spectral feature in the bending region

that is well displaced from those of the growing neutral network involving water molecules removed from the binding site.

The next challenge in our analysis of the cluster structures through vibrational spectroscopy involved adapting a photochemical population modulation scheme to isolate the vibrational signatures of the clusters belonging to classes I and II. This was accomplished for clusters in the size range $n = 6-8$, where the bending spectra of the type I and II forms are compared in the lower panel (B) of Fig. 1.(13,14) Most importantly, none of the lower binding type II forms display the telltale feature indicating electron binding to the AA water molecule, while all of the type I forms do possess this feature. Thus, in the size range where the type I and II forms are becoming increasingly differentiated into their asymptotic classes, they clearly display distinct *local* binding motifs. While not ruling out the surface/internal hypothesis for their behavior at larger sizes, the vibrational spectra raise the alternative scenario that they differ by their local electron binding motifs in the overall context of surface states.

Theoretical analysis of the bending spectra of the type II forms has been carried out and indicates that these more weakly bound forms attach the excess electron primarily to a single H-atom associated with a water molecule in an AAD H-bonding environment. This H-atom then accounts for the dominant transition in the bending vibrational spectrum.

We have recently completed a detailed experimental/theoretical study of the heptamer anion which has shown that there are at least two isomers in the type I class observed experimentally, which interconvert as one varies the number of attached Ar atoms.(14) In addition, we discovered a new class for this species which has an appreciably larger VDE than that observed previously. An interesting conclusion from this study is that the overall VDE is surprisingly strongly correlated with the net electric dipole moment of the associated neutral water network, independent of local motif. Another particularly important result of this analysis is that the cluster anions observed in free jet experiments are likely not the most stable forms, as there are lower energy isomers that are calculated to occur with structures more like those of the neutral clusters.

IIB. Temperature control of the bare clusters

One of the key uncertainties in the first generation of cluster ion experiments is that the internal energies and/or temperatures of the ion ensembles are not well

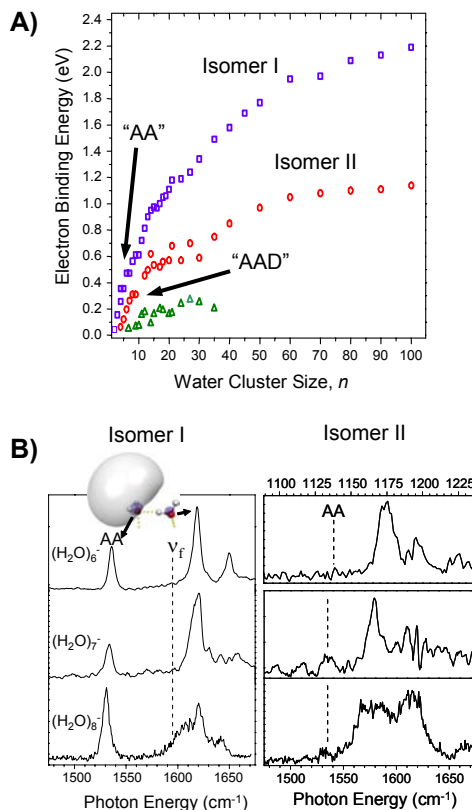


Fig. 1. (A) Vertical detachment energies (VDEs) of the $(\text{H}_2\text{O})_n^-$ clusters obtained from photoelectron spectroscopy, and (B) the vibrational spectra of the type I and II isomers of the $n = 6-8$ clusters selectively recorded through two-laser photochemical population labeling. Note that the characteristic feature indicating electron binding in the AA motif is missing in the type II forms.

characterized. Thus, the rare-gas “tagging” experiments are thought to quench the clusters close to their vibrational zero-point structures, but it is difficult to follow how the structures change as the internal energy is systematically increased. In the past year, we have made substantial strides in improving this situation by engaging a collaborative effort with Neumark at Berkeley and the Meijer group in Berlin, where we carried out similar vibrational spectroscopic studies as those performed at Yale, but with the use of a temperature controlled ion trap. This involved interfacing our ion source to a 22-pole radiofrequency trap cooled to 20 K. The first experiments explored the evolution of the characteristic “AA” transition in the HOH intramolecular bending region as a function of cluster size from $n = 15-50$.(1,12)

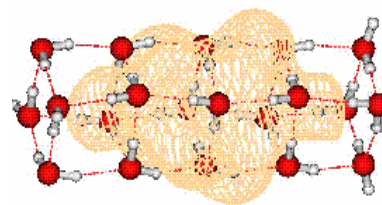


Fig. 2. Example of a cluster for which binding of the excess electron is dominated by polarization and dispersion

IIC. Application of the Drude model to probe new electron binding motifs in larger, three dimensional networks

Interpretation of the spectral patterns displayed by the $(\text{H}_2\text{O})_n^-$ isomers in the context of structures has been accomplished through a combination of model potential and traditional electronic structure calculations. Specifically, Monte Carlo simulations using the Drude model, developed in the Pittsburgh group, have been used to characterize the structural motifs present as a function of temperature, and the vibrational spectra of low-energy isomers thus identified have been calculated using *ab initio* methods. This strategy has proven especially valuable for identifying the observed anions of the water heptamer, $(\text{H}_2\text{O})_7^-$. The Drude model calculations have also revealed the existence of a new binding motif, illustrated in Fig. 2, in which the excess electron is bound primarily by the dispersion/polarization contribution (as opposed to the long range electric dipole moment evident in the observed structures like that of the tetramer). These studies have also discovered that the $(\text{H}_2\text{O})_6^-$ and $(\text{H}_2\text{O})_7^-$ clusters should have several isomers that weakly bind the excess electron and yet are more stable than the observed AA species.(10,11)

III. Future plans

From the experimental perspective, the scope of our DOE-supported activities has increased dramatically in the past year as we have completed construction of a new apparatus dedicated to this project. Not only does this enable us to carry out measurements without the delays caused by instrument sharing (typically with projects funded by NSF and AFOSR), but we have also built the DOE apparatus with unique

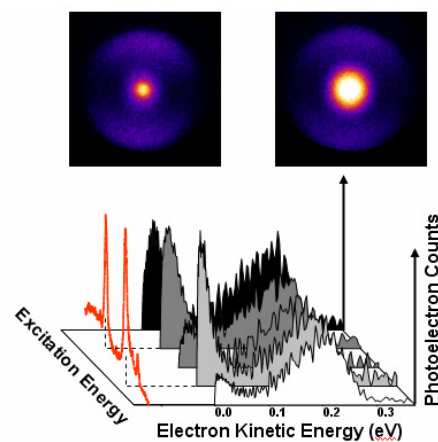


Fig. 3. Top: photoelectron images corresponding to (left) direct and (right) vibrationally mediated photodetachment. Bottom: Dispersed photoelectron spectra obtained by BASEX [Rev. Sci. Instr. 73, 2634 (2002).] reconstruction of images obtained as a laser is scanned through the OH stretch vibrational resonances.

capabilities that expand the range of cluster properties that can be studied. Most important among these is the implementation of photoelectron imaging to measure the energy and angular distributions of ejected electrons. We have already interfaced this with our infrared laser spectrometers to efficiently disperse detached electrons arising from excitation of vibrational resonances, as illustrated in Fig. 3. Our next objective for this combined IR/photoelectron scheme is to locate barriers for interconversion between the various binding energy classes by following the evolution of particular isomers injected with a precisely determined internal energy content through excitation of specific vibrational resonances. Parallel theoretical studies will be crucial to unravel the high expected data yield from this next generation of cluster anion experiments.

IV. References for papers published under DOE support

1. **“Infrared spectroscopy of water cluster anions, $(\text{H}_2\text{O})_{n=3-24}^-$ in the HOH bending region: Persistence of the double H-bond acceptor (AA) water molecule in the excess electron binding site of the class I isomers,”** J. R. Roscioli, N. I. Hammer and M. A. Johnson, *J. Phys. Chem. A*, **110**, 517-7520, 2006.
2. **“Vibrational predissociation spectroscopy of the $(\text{H}_2\text{O})_{6-21}^-$ clusters in the OH stretching region: Evolution of the excess electron-binding signature into the intermediate cluster size regime,”** N. I. Hammer, J. R. Roscioli, J. C. Bopp, J. M. Headrick and M. A. Johnson, *J. Chem. Phys.*, **123**, 244311, 2005.
3. **“Infrared spectrum and structural assignment of the water trimer anion,”** N. I. Hammer, J. R. Roscioli, M. A. Johnson, E. M. Myshakin and K. D. Jordan, *J. Phys. Chem. A*, **109**, 11526-11530, 2005.
4. **“Identification of two distinct electron binding motifs in the anionic water clusters: A vibrational spectroscopic study of the $(\text{H}_2\text{O})_6^-$ isomers,”** N. I. Hammer, J. R. Roscioli and M. A. Johnson, *J. Phys. Chem. A*, **109**, 7896-7901, 2005.
5. **“An infrared investigation of the $(\text{CO}_2)_n^-$ clusters: Core ion switching from both the ion and solvent perspectives,”** J.-W. Shin, N. I. Hammer, M. A. Johnson, H. Schneider, A. Glob and J. M. Weber, *J. Phys. Chem. A*, **109**, 3146-3152, 2005.
6. **“Role of water in electron-initiated processes and radical chemistry: Issues and scientific advances,”** Bruce C. Garrett *et al.*, *Chem. Rev.*, **105**, 355-390, 2005.
7. **“How do small water clusters bind an excess electron?”** N. I. Hammer, J.-W. Shin, J. M. Headrick, E. G. Diken, J. R. Roscioli, G. H. Weddle and M. A. Johnson, *Science*, **306**, 675-679, 2004.
8. **“Infrared signature of structures associated with the $\text{H}^+ \cdot (\text{H}_2\text{O})_n$, $n = 6-27$, clusters,”** J.-W. Shin, N. I. Hammer, E. G. Diken, M. A. Johnson, R. S. Walters, T. D. Jaeger, M. A. Duncan, R. A. Christie and K. D. Jordan, *Science*, **304**, 1137-1140, 2004.
9. **“The vibrational spectrum of the neutral $(\text{H}_2\text{O})_6$ precursor to the “magic” $(\text{H}_2\text{O})_6^-$ cluster anion by argon-mediated, population-modulated electron attachment spectroscopy,”** E. G. Diken, W. H. Robertson and M. A. Johnson, *J. Phys. Chem. A*, **108**, 64-68, 2004.
10. **“Electron Binding Motifs of $(\text{H}_2\text{O})_n^-$ Clusters,”** T. Sommerfeld and K. D. Jordan, *J. Am. Chem. Soc.*, **128**, 5828-5833, 2006.
11. **“Low-lying isomers and finite temperature behavior of $(\text{H}_2\text{O})_6^-$,”** T. Sommerfeld, S. D. Gardner, A. DeFusco, and K. D. Jordan, *J. Chem. Phys.*, **125**, 174309 (2006).
12. **“Infrared multiple photon dissociation of the hydrated electron clusters $(\text{H}_2\text{O})_{15-50}^-$,”** K. R. Asmis, G. Santambrogio, J. Zhou, E. Garand, J. Headrick, D. Goebbert, M. A. Johnson, D. M. Neumark, *J. Chem. Phys.*, **126**, 191105 (2007).
13. **“Isomer-specific spectroscopy of the $(\text{H}_2\text{O})_8^-$ cluster anion in the intramolecular bending region by selective photodepletion of the more weakly electron binding species (isomer II),”** J. R. Roscioli and M. A. Johnson, *J. Chem. Phys.*, **126**, 024307, 2007.
14. **“Exploring the correlation between network structure and electron binding energy in the $(\text{H}_2\text{O})_7^-$ cluster through isomer photoselected vibrational predissociation spectroscopy and ab initio calculations: Addressing complexity beyond types I-III,”** J. R. Roscioli, N. I. Hammer, M. A. Johnson, K. Diri and K. D. Jordan, *J. Chem. Phys.*, submitted.

Dynamics of Electrons at Interfaces on Ultrafast Timescales

Charles B. Harris, P.I.
Chemical Sciences Division, Lawrence Berkeley National Lab
1 Cyclotron Road, Mail Stop Latimer, Berkeley, CA 94720
CBHarris@lbl.gov

Program Scope

This is a comprehensive program to study the properties of electrons at molecule/metal interfaces on the femtosecond timescale and the nanometer lengthscale. We examine a broad variety of systems (examples include atomic adsorbates, polymer oligomers, and model solvents) and phenomena (electron solvation and localization, the band structure of interfaces, and the electronic coupling of adsorbates to a metal substrate) with both experiment and theory.

Our primary experimental technique is angle-resolved two-photon photoemission (2PPE). Briefly, a femtosecond laser pulse excites electrons from the valence band of a Ag(111) substrate to the interface with an adsorbed molecular film (typically 1–3 monolayers thick). Some delay time later, Δt , a second laser pulse photoemits the electron, sending it to a time-of-flight detector. From the kinetic energy of the electron and the photon energy of the probe pulse, we can deduce the binding energy of the electronic state. The wavelength dependence of the photoemission spectrum tells whether the state is initially occupied, unoccupied, or a final state resonance.

This technique also gives us access to a wealth of information about the electron's dynamics. The kinetics of population decay and dynamical energy shifts (two-dimensional electron solvation) are determined with < 35 meV energy resolution and ~ 100 fs time resolution. An additional experimental degree of freedom is the angle between the surface normal and the detector. Only electrons with a specific amount of momentum parallel to the surface will reach the detector. The energy versus parallel momentum (the dispersion) gives the effective mass of the electron, m^* . For localized electrons ($m^* \gg 1$) the amplitude of the signal versus parallel momentum can give an estimate of the spatial extent of localization in two dimensions.

Two-photon photoemission accesses both electronic states of the molecular film, such as the highest occupied molecular orbital (HOMO) and the lowest unoccupied molecular orbital (LUMO), as well as states intrinsic to the surface. Image-potential states (IPS) are an important example of the latter. The IPS electrons are bound a few angstroms from the metal surface, making them sensitive probes of the electronic structure and dynamics of monolayer adsorbate films. Any changes in IPS energies directly reflect the behavior of the thin film itself. Additionally, interactions with surface disorder or with the dynamic motions of adsorbates can localize the electron in the plane of the surface.

Recent Progress

Morphology-dependent Photo-conductivity of Organic Semiconductors : Photoconductivity in organic semiconductors has garnered considerable research attention in the search for sustainable energy sources. In particular, the factors for consideration in optimizing these devices, which include the efficiency of photo-generation and the carrier dynamics at an interface, merit a close investigation of the physical chemistry at the interface. Using 2PPE, we have probed the dynamics of charge carriers at the interface of Ag(111) and PTCDA, a widely-studied planar aromatic hydrocarbon. By varying the morphology of the surface, we have quantitatively examined the role of crystallinity or structural disorder in affecting the carrier dynamics and electronic structure at an interface. High substrate temperatures (> 400 K) cause the growth of a wetting layer with islands, and the exposed wetting layer inhibited the evolution of the vacuum level and valence band to bulk PTCDA values. In the layer-by-layer growth of low substrate temperatures, we observe the

transition of molecular state energies from monolayer to bulk values. Effective masses of the conduction band and the $n = 1$ image potential state varied from $2.1 m_e$ and $1.4 m_e$, resp., in disordered PTCDA layers to $0.5 m_e$ and $1.1 m_e$ in the most crystalline layers. Decay constants were obtained for electrons excited into the conduction band and into image potential states at different layer thicknesses and morphologies. Decay constants for the LUMO in crystalline systems were mediated by electron transfer back to the surface and were on the order of 100 fs, whereas layer-by-layer amorphous growth resulted in exponential decays with time constants of picoseconds present in films thicker than ~ 7 monolayers.

Thiophene : Another series of promising candidates for organic devices are thiophene-based oligomers and polymers. Via angle-resolved 2PPE, we are investigating the unoccupied states and their effective masses of the monomer thiophene unit at the Ag(111) interface. We have discovered a change in electronic structure based on a temperature-dependent phase transition of the surface monolayer, which is relevant to understanding the optimization of thiophene electronic behavior. In addition, we are able to collect LEED data and therefore structural information about the two phases, which enables us to correlate the electronic structure with changes in the crystallinity. Further work is underway to determine the unit cell and to identify all the electronic structure present in 2PPE data. Future work will scale the thiophene systems to longer oligomer units, to map the trends in electronic and interfacial structure in the transition from oligomer to polymer.

DMSO : In electrochemically relevant systems, interfacial capacitance affects electrochemical signal collection and heterogeneous charge transfer. At noble metal electrodes, dimethyl sulfoxide (DMSO), a common electrochemical solvent, exhibits uncharacteristically low interfacial capacitance of $7\text{--}10 \mu\text{F}/\text{cm}^2$ over a 1.5 V range which includes the potential of zero charge. This stands in contrast to similar, polar, high-dielectric constant electrochemical solvents, e.g., $50 \mu\text{F}/\text{cm}^2$ for acetonitrile under identical experimental conditions. Si and Gewirth have proposed that hindered rotation of the DMSO dipole at the surface lowers its interfacial capacitance and reduces the response of interfacial DMSO to changes in potential[5]. We directly tested this hypothesis with 2PPE by modelling the injected electron as a planar charge outside a capacitive layer. We measured a much weaker solvation response in a monolayer than multilayer coverages, which we attribute to hindered dipole rotation in the monolayer. The solvation responses are then interpreted as a comparison of the dielectric response of the monolayer with those of various multilayer coverages.

Mg : In addition to studying organic molecules adsorbed to the surface, we are extending our technique to study the evolution of the IPS in bimetallic systems. Previous work in this area has been performed by Osgood et al.[2] studying the IPS as a function of both Ag and Ni adsorbing onto Pt(111). All three of these metals have a bandgap in the surface normal direction which prevents IPS electrons from entering the metal on the time scale of 10–30 fs. Our study seeks to investigate the evolution of the IPS as the surface band gap is eroded. Magnesium is a bivalent hexagonal metal with the unique property of having its surface band gap occur 1.6 eV below the Fermi level and no experimentally observed image potential state. Experimental results indicate that by ~ 4 ML of Mg on the Ag(111) surface, the image potential state has broadened so significantly in energy (presumably due to decreasing lifetimes) that it is no longer spectroscopically visible. Further experiments and electronic structure calculations are underway to determine how the IPS can be extinguished by a metallic layer with a thickness much smaller than the mean free path length of an electron. We are also seeking to determine in the sub 4 ML regime whether the electron resides within the magnesium overlayer or outside the layer in the vacuum.

Continuing and Future work

Titanyl Phthalocyanine : Phthalocyanines have recently drawn attention as thermally stable metalated-organic semiconductors with n-type conductivity under vacuum conditions. Interchanging metal centers on

phthalocyanine derivatives affects the conductivity, spin properties, and dipole moments of phthalocyanines. In addition, the electron donating/withdrawing properties of different ligand substituents on phthalocyanine derivatives have been shown both to shift the valence band levels and to control the majority carrier type of phthalocyanine derivatives. The electron donating/withdrawing groups alter the charge density in the π -conjugated backbone, which has been qualitatively modeled as a localized charge acting as a majority charge carrier via a hopping mechanism. We are beginning experiments to probe the localization of both injected electrons and excitons at the TiOPc/Ag(111) interface using a combination of angle resolved 2PPE and quantum chemical calculations. We plan to study the localized mobile charge picture by probing the localization of electrons at the interface. We will also be able to study interband relaxation through the several closely spaced states collectively known as the Q-band using 2PPE. Later studies will focus on the role of metal centers at the metal/metalated organic interface.

MgO : In conjunction with our current investigation of the Mg/Ag(111) interface, we propose to study the MgO/Ag(111) surface using 2PPE in combination with LEED. Interest in the MgO(111) surface has developed recently due to its properties of catalytic activity as well as its highly polar nature. The MgO(111) surface should be an ionic surface terminated by either anionic oxygens or cationic magnesiums. As a result of the high surface energy associated with a plane of charges, the (111) surface has only been proposed to be the ground state for nanoparticles or in ultrathin films stabilized by charge transfer from a metal. Previous studies have disagreed on the nature of the interface. Kiguchi et al., using RHEED and Auger spectroscopy, have proposed that the interfacial ground state structure is the MgO(111)/Ag(111) surface[4], while theoretical results predict a graphene-like hexagonal structure[1]. Using LEED, we should be able to experimentally distinguish between the two surfaces, and using 2PPE we will be able to directly characterize the electronic structure of this unique surface.

Ionic Liquids : Room-temperature ionic liquids (RTIL's) are a relatively new class of potentially useful compounds for synthesis and electrochemistry. An array of physical investigations is stimulated by these highly unusual solutions composed completely of ions. The solvation behavior of RTIL's has been studied by multiple groups in bulk solution, and controversy remains over the nature of solvation at ultrafast timescales[3, 6]. Energy relaxation of the image potential state in RTIL ultrathin films is currently being investigated to elucidate solvation behavior. The unique opportunity to study interfacial dynamics of a solid/liquid interface with UHV techniques provides additional motivation.

References

- [1] J. Goniakowski, C. Noguera, and L. Giordano. "Using polarity for engineering oxide nanostructures: Structural phase diagram in free and supported MgO(111) ultrathin films." *Physical Review Letters*, 93(215702) (2004).
- [2] S. Smadici, D. Mocuta, and J. R. M. Osgood. "Lateral motion of image-state electrons for metal adsorbate regions on stepped metal substrates." *Physical Review B*, 69(035415), 1 (2004).
- [3] H. Cang, J. Li, and M. D. Fayer. "Orientational dynamics of the ionic organic liquid 1-ethyl-3-methylimidazolium nitrate." *Journal of Chemical Physics*, 119, 13017 (2003).
- [4] M. Kiguchi, S. Entani, K. Saiki, T. Goto, and A. Koma. "Atomic and electronic structure of an unreconstructed polar MgO(111) thin film on Ag(111)." *Physical Review B*, 68(115402) (2003).
- [5] S. K. Si and A. A. Gewirth. "Solvent organization above metal surfaces: Ordering of DMSO on Au." *Journal of Physical Chemistry B*, 104, 10775 (2000).
- [6] S. Arzhantsev, H. Jin, N. Ito, and M. Maroncelli. "Observing the complete solvation response of DCS in imidazolium ionic liquids, from the femtosecond to nanosecond regimes." *Chemical Physics Letters*, 417, 4–6, 524 (2006).

Articles supported by DOE funding 2004–2007

- [1] E. A. Glascoe, M. F. Kling, J. E. Shanoski, J. R. A. DiStasio, C. K. Payne, B. V. Mork, T. D. Tilley, and C. B. Harris. “Photoinduced beta-hydrogen elimination and radical formation with $\text{CpW}(\text{CO})_3(\text{CH}_2\text{CH}_3)$: Ultrafast IR and DFT studies.” *Organometallics*, **26**, 1424 (2007). Funded by *NSF* using *DOE* equipment.
- [2] E. A. Glascoe, K. R. Sawyer, J. E. Shanoski, and C. B. Harris. “The influence of the metal spin state in the iron-catalyzed alkene isomerization reaction studied with ultrafast infrared spectroscopy.” *J. Phys. Chem. C.*, **111**, 8789 (2007). Funded by *NSF* using *DOE* equipment.
- [3] J. F. Cahoon, M. F. Kling, K. R. Sawyer, H. Frei, and C. B. Harris. “19-electron intermediates in the ligand substitution of $\text{CpW}(\text{CO})_3$ with a Lewis base.” *J. Am. Chem. Soc.*, **128**, 3152 (2006). Funded by *NSF* using *DOE* equipment.
- [4] E. A. Glascoe, M. F. Kling, J. E. Shanoski, and C. B. Harris. “Nature and role of bridged carbonyl intermediates in the ultrafast photoinduced rearrangement of $\text{Ru}_3(\text{CO})_{12}$.” *Organometallics*, **25**(775) (2006). Funded by *NSF* using *DOE* equipment.
- [5] J. E. Shanoski, E. A. Glascoe, and C. B. Harris. “Ligand rearrangement reactions of $\text{Cr}(\text{CO})_6$ in alcohol solutions: Experiment and theory.” *J. Phys. Chem. B.*, **110**(996) (2006). Funded by *NSF* using *DOE* equipment.
- [6] S. Shipman, S. Garrett-Roe, P. Szymanski, A. Yang, M. Strader, and C. B. Harris. “Determination of band curvatures by angle-resolved two-photon photoemission in thin films of C_{60} on $\text{Ag}(111)$.” *J. Phys. Chem. B*, **110**, 10002 (2006).
- [7] J. F. Cahoon, M. F. Kling, S. Schmatz, and C. B. Harris. “19-electron intermediates and cage-effects in the photochemical disproportionation of $[\text{CpW}-(\text{CO})_3]_2$ with Lewis bases.” *J. Am. Chem. Soc.*, **127**(12555) (2005). Funded by *NSF* using *DOE* equipment.
- [8] S. Garrett-Roe, S. T. Shipman, P. Szymanski, M. L. Strader, A. Yang, and C. B. Harris. “Ultrafast electron dynamics at metal interfaces: Intraband relaxation of image state electrons as friction.” *J. Phys. Chem. B*, **109**, 20370 (2005).
- [9] J. E. Shanoski, C. K. Payne, M. F. Kling, E. A. Glascoe, and C. B. Harris. “Ultrafast infrared mechanistic studies of the interaction of 1-hexyne with group 6 hexacarbonyl complexes.” *Organometallics*, **24**(1852) (2005). Funded by *NSF* using *DOE* equipment.
- [10] P. T. Snee, J. E. Shanoski, , and C. B. Harris. “Mechanism of ligand exchange studied using transition path sampling.” *J. Am. Chem. Soc.*, **127**(1286) (2005). Funded by *NSF* using *DOE* equipment.
- [11] P. Szymanski, S. Garrett-Roe, and C. B. Harris. “Time- and angle-resolved two-photon photoemission studies of electron localization and solvation at interfaces.” *Prog. Surf. Sci.*, **78**, 1 (2005).
- [12] I. Bezel, K. J. Gaffney, S. Garrett-Roe, S. H. Liu, A. D. Miller, P. Szymanski, and C. B. Harris. “Measurement and dynamics of the spatial distribution of an electron localized at a metal–dielectric interface.” *J. Chem. Phys.*, **120**, 845 (2004).
- [13] M. F. Kling, J. F. Cahoon, E. A. Glascoe, J. E. Shanoski, and C. B. Harris. “The role of odd-electron intermediates and in-cage electron transfer in ultrafast photochemical disproportionation reactions in Lewis bases.” **126**(11414) (2004). Funded by *NSF* using *DOE* equipment.

Chemical Kinetics and Dynamics at Interfaces

Non-Thermal Reactions at Surfaces and Interfaces

Greg A. Kimmel (PI) and Nikolay G. Petrik

Fundamental Science Directorate

Pacific Northwest National Laboratory

P.O. Box 999, Mail Stop K8-88

Richland, WA 99352

gregory.kimmel@pnl.gov

Program Scope

The objectives of this program are to investigate 1) the non-thermal reactions at surfaces and interfaces, and 2) the structure of thin adsorbate films and how this influences the thermal and non-thermal chemistry. The fundamental mechanisms of radiation damage to molecules in the condensed phase are of considerable interest to a number of scientific fields ranging from radiation biology to astrophysics. In nuclear reactor design, waste processing, radiation therapy, and many other situations, the non-thermal reactions in aqueous systems are of particular interest. Since the interaction of high-energy radiation (gamma-rays, alpha particles, etc.) with water produces copious amounts of low-energy secondary electrons, the subsequent reactions of these low-energy electrons are particularly important. The general mechanisms of electron-driven processes in homogeneous, dilute aqueous systems have been characterized in research over the last several decades. More recently, the structure of condensed water and its interactions with electrons, photons, and ions have been extensively studied and a variety of non-thermal reaction mechanisms identified. However, the complexity of the electron-driven processes, which occur over multiple length and time scales, has made it difficult to develop a detailed molecular-level understanding of the relevant physical and chemical processes.

We are focusing on low-energy, electron-stimulated reactions in thin water films. Our approach is to use a molecular beam dosing system to create precisely controlled thin films of amorphous solid water (ASW) and crystalline ice (CI). Using isotopically layered films of D₂O, H₂¹⁶O and H₂¹⁸O allows us to explore the spatial relationship between where the incident electrons deposit energy and where the electron-stimulated reactions subsequently occur within the films. Furthermore, working with thin films allows us to explore the role of the substrate in the various electron-stimulated reactions.

Recent Progress:

Hydrogen bonding, H/D exchange and molecular mobility in thin water films on TiO₂(110)

The interaction of water with TiO₂ has technological implications for a variety of areas ranging from photocatalysis to self-cleaning surfaces. Scientifically, water on rutile TiO₂(110) is widely considered to be an important “benchmark” system for metal oxides. Thus, the interactions of water with TiO₂(110) for coverages, θ , of 1 monolayer (ML) and less have been extensively studied. However, understanding the water structure for $\theta > 1$ ML is important since the corrugated structure of TiO₂(110) and the strong binding of the first water ML are both likely to influence the structural transition to bulk water further from the surface, and thus the chemistry of aqueous/TiO₂(110) interfaces.

We have used the electron-stimulated desorption (ESD) of water from films of D₂O, H₂¹⁶O and H₂¹⁸O to investigate hydrogen bonding, H/D exchange and molecular mixing between water adsorbed in the first monolayer (H₂O_{Ti}, see Fig. 1) and water in the second monolayer (H₂O_{BBO}) on TiO₂(110) for $\theta \leq 2$ ML. By depositing H₂O_{Ti} at 190 K using one water isotope and H₂O_{BBO} at ≤ 70 K using a different isotope, films with no appreciable mixing isotopes between layers can be prepared. When H₂O_{BBO} is deposited at $T > 70$ K, partial or complete mixing with H₂O_{Ti} occurs depending on the temperature and time. H/D exchange between H₂O_{Ti} and H₂O_{BBO} occurs at ~ 15 K lower temperatures than H₂¹⁶O/H₂¹⁸O exchange. Isothermal experiments demonstrate that the mixing occurs with a distribution of activation energies centered on 0.29 ± 0.07 eV (0.26 ± 0.07 eV) for H₂¹⁶O/H₂¹⁸O (H/D) exchange. Thus in contrast

to MD simulations, the results show that $\text{H}_2\text{O}_{\text{Ti}}$ rapidly exchanges with $\text{H}_2\text{O}_{\text{BBO}}$ at temperatures well below 300 K. The results also demonstrate that $\text{H}_2\text{O}_{\text{BBO}}$ is hydrogen bonded to $\text{H}_2\text{O}_{\text{Ti}}$. Since the lateral distance (0.325 nm) for atop adsorption at these sites is too large for hydrogen bonding, one (or both) of the adsorbates must be displaced laterally toward the other in agreement with theoretical predictions.

Figure 1 shows the H_2^{18}O ESD yields versus time for several H_2^{18}O - H_2^{16}O films with $\theta = 2$ ML. The surface was first exposed to 6.5×10^{14} molecules/ cm^2 of either H_2^{16}O or H_2^{18}O at 190 K (where the thermal $\text{H}_2\text{O}_{\text{BBO}}$ desorption rate is large) to produce a saturation coverage of $\text{H}_2\text{O}_{\text{Ti}}$ without any $\text{H}_2\text{O}_{\text{BBO}}$. Next, 1 ML was deposited at either 50 K or 150 K using the other water isotope, and the films were irradiated with electrons at 50 K. For $\text{H}_2^{18}\text{O}_{\text{BBO}}$ deposited at 50 K, the H_2^{18}O ESD yield was initially high and then decreased with increasing time (Fig. 1, black line). For $\text{H}_2^{16}\text{O}_{\text{BBO}}$ deposited at 50 K, the H_2^{18}O ESD was initially small, but increased with time (Fig. 1, blue line). For $\text{H}_2^{18}\text{O}_{\text{BBO}}$ or $\text{H}_2^{16}\text{O}_{\text{BBO}}$ deposited at 150 K, the ESD yields were almost independent of the ordering of the isotopes and intermediate in magnitude (Fig. 1, green and red lines).

The results in Fig. 1 show that the H_2^{18}O ESD yield is sensitive to the order in which the H_2^{18}O and H_2^{16}O are deposited, and depends on the $\text{H}_2\text{O}_{\text{BBO}}$ deposition temperature. The changes in the ESD yields versus time in Fig. 1 are due to electron-stimulated processes in the water films. However, the results in Fig. 1 also show that the *initial* ESD yields can be used to probe the water structure *prior* to irradiation. The substantial difference in the ESD yield when the $\text{H}_2\text{O}_{\text{BBO}}$ was deposited at 50 K arises for three reasons: First for isotopically pure water films, the ESD yield for $\theta = 2$ ML is 4.5 times greater than for $\theta = 1$ ML. Second, for $1 < \theta \leq 2$ ML energy transfer from $\text{H}_2\text{O}_{\text{Ti}}$ to $\text{H}_2\text{O}_{\text{BBO}}$ also enhances the $\text{H}_2\text{O}_{\text{BBO}}$ ESD signal. Third, there is little or no molecular exchange between water in the first and second layers at 50 K. In contrast, substantial mixing occurs at 150 K and the ESD yield is nearly independent of the order in which the isotopes were deposited.

Figure 2 shows the initial integrated water ESD yields from isotopically labeled films using combinations of H_2^{16}O , H_2^{18}O and D_2^{16}O versus the $\text{H}_2\text{O}_{\text{BBO}}$ deposition temperature, T_{dep} . For H_2^{18}O - H_2^{16}O films with $\theta = 2$ ML, the H_2^{18}O ESD yield is small (large) for $T_{\text{dep}} < 90$ K when H_2^{16}O (H_2^{18}O) is deposited second, and monotonically increases (decreases) at higher temperatures (Fig. 2, circles). For these experiments, the midpoint of the transition from unmixed to mixed is at 112 ± 3 K.

For D_2O - H_2O films with $\theta = 2$ ML, the D_2O ESD yields versus T_{dep} (Fig. 2, triangles) are similar to the H_2O^{16} - H_2^{18}O films, except the H/D exchange occurs at lower temperature (midpoint = 95 ± 2 K). We also measured the D_2^{18}O ESD from D_2^{16}O - H_2^{18}O films (Fig. 2, squares) which permits measurement of H/D and molecular exchange in the same experiment. For $T_{\text{dep}} \leq 70$ K, very little mixing occurs and the D_2^{18}O ESD yield is small for both $\text{H}_2^{18}\text{O}_{\text{Ti}}$ - $\text{D}_2^{16}\text{O}_{\text{BBO}}$ (Fig. 2, solid squares), and $\text{D}_2^{16}\text{O}_{\text{Ti}}$ - $\text{H}_2^{18}\text{O}_{\text{BBO}}$ (Fig. 2, open

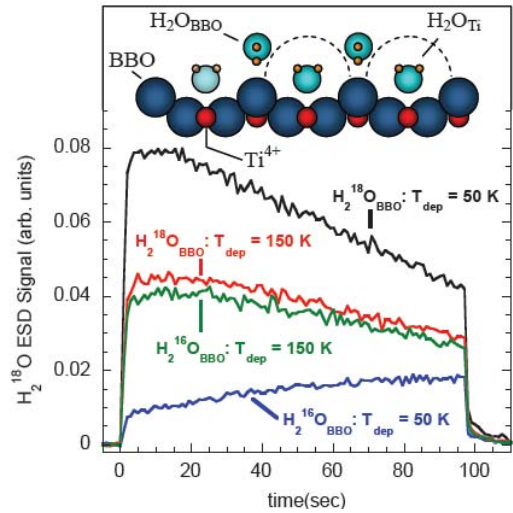


Fig. 1. H_2^{18}O ESD versus time from 2 ML water films of H_2^{16}O and H_2^{18}O on $\text{TiO}_2(110)$. Films deposited at 150 K are mixed, while films deposited at 50 K are “layered”.

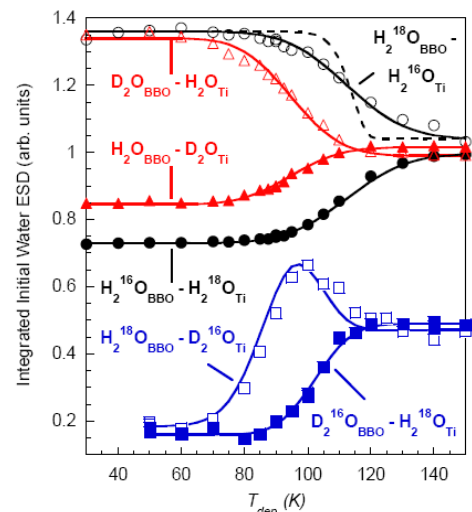


Fig. 2. Water ESD versus the temperature at which the second layer was deposited.

squares). For $70\text{ K} < T_{dep} < 90\text{ K}$, H/D exchange is significant while molecular mixing is slow. Therefore when H_2^{18}O is deposited second, H/D exchange leads to the formation D_2^{18}O in the second layer and the signal increases (Fig. 2, open squares). Above 90 K, molecular exchange turns on and the concentration of ^{18}O in the second layer *decreases*, leading to a *maximum* in the D_2^{18}O ESD yield at 100 K. In contrast when D_2^{16}O is deposited second, H/D exchange does not lead to an appreciable increase in the D_2^{18}O ESD signal for $T_{dep} < 90\text{ K}$ because those molecules are formed in the first layer where the ESD yield is low (Fig. 2, solid squares). Above 90 K, molecular exchange increases the ^{18}O (and D_2^{18}O) concentration in the second layer causing the D_2^{18}O ESD yield to increase. The observed H/D exchange (Fig. 2) indicates *water adsorbed on the Ti^{4+} rows is hydrogen-bonded to water adsorbed “on” the BBO rows.*

Wetting and Non-Wetting Adsorption of Water on Surfaces

In collaboration with Bruce D. Kay and Zdenek Dohnálek we have investigated the growth of crystalline ice (CI) and ASW films on Pt(111) and Pd(111) using rare gas physisorption. It is well-known that the water monolayer wets both of these metals and it was widely-believed that these substrates were good templates for the epitaxial growth of crystalline ice films. Our studies confirm that the water monolayer wets both substrates at all temperatures investigated (20-155 K) and that ASW films deposited below $\sim 125\text{ K}$ also wet the water monolayer. Surprisingly, crystalline ice films grown at higher temperatures ($T > 135\text{ K}$) do not wet the water monolayer! Furthermore, the wetting ASW films dewet exposing the underlying water monolayer as they transform to CI upon heating. These findings demonstrate that the water monolayer on both Pt(111) and Pd(111) is *hydrophobic* with respect to the growth of CI.

The structure of the water monolayer on these metals is key to understanding the observed *hydrophobicity*. For both Pt(111) and Pd(111) recent experiments and theory indicate that all water molecules in the first monolayer interact significantly with the metal substrate. The water molecules form a nearly-planar, hexagonal array with each molecule hydrogen-bonded to three other water molecules in the array. In this array half the water molecules bind to the underlying metal through the oxygen lone pair and the other half have a hydrogen atom point toward the metal. Therefore, each water molecule in the monolayer forms four bonds, leaving no dangling OH groups or lone pair electrons protruding into the vacuum. Since this fully-coordinated water monolayer has no additional attachment points it is *hydrophobic* to additional water growth. Ongoing studies are exploring water adsorption on C(0001) and FeO(111) surfaces. On both these substrates ASW grows approximately layer-by-layer but crystalline ice growth exhibits non-wetting behavior. Future experiments will employ FTIR to understand the detailed nature of the water-substrate interface on Pt(111), Pd(111), Cu(111), FeO(111), and C(0001).

Future Directions:

Important questions remain concerning the factors that determine the structure of thin water films on various substrates. We plan to investigate the structure of thin water films on non-metal surfaces, such as oxides, and on metals where the first layer of water does not wet the substrate. For the non-thermal reactions in water films, we will use FTIR spectroscopy to characterize the electron-stimulated reaction products and precursors. The mechanisms of the non-thermal precursor migration through ASW films need to be further explored. We will also investigate the non-thermal reactions at lower electron energies (i.e. closer to the ionization threshold for water). Finally, we plan to investigate the lifetimes of excited states in ASW and CI using pump-probe fluorescence measurements.

References to publications of DOE sponsored research (FY 2004 – present)

1. Nikolay G. Petrik and Greg A. Kimmel, “Electron-stimulated reactions in thin D_2O films on Pt(111) mediated by electron trapping,” *J. Chem. Phys.* **121**, 3727 (2004).
2. Nikolay G. Petrik and Greg A. Kimmel, “Electron-stimulated production of molecular hydrogen at the interfaces of amorphous solid water films on Pt(111),” *J. Chem. Phys.* **121**, 3736 (2004).

3. Nikolay G. Petrik and Greg A. Kimmel, "Electron-stimulated sputtering of thin amorphous solid water films on Pt(111)," *J. Chem. Phys.* **123**, 054702 (2005).
4. Bruce C. Garrett, et al., "Role of Water in Electron-Initiated Processes and Radical Chemistry: Issues and Scientific Advances," *Chem. Rev.* **105**, 355 (2005).
5. Greg A. Kimmel, Nikolay G. Petrik, Zdenek Dohnálek and Bruce D. Kay, "Crystalline ice growth on Pt(111): Observation of a hydrophobic water monolayer," *Phys. Rev. Lett.* **95** (2005) 166102.
6. Nikolay G. Petrik, Alexander Kavetsky and Greg A. Kimmel, "Electron-Stimulated Production of Molecular Oxygen in Amorphous Solid Water," *J. Phys. Chem. B.* **110**, 2723 (2006).
7. Greg A. Kimmel, Nikolay G. Petrik, Zdenek Dohnálek and Bruce D. Kay, "Layer-by-layer growth of thin amorphous solid water films on Pt(111) and Pd(111)," *J. Chem. Phys.* **125**, 044713 (2006).
8. Nikolay G. Petrik, Alexander Kavetsky and Greg A. Kimmel, "Electron-stimulated production of molecular oxygen in amorphous solid water on Pt(111): Precursor transport through the hydrogen bonding network," *J. Chem. Phys.* **125**, 124702 (2006).
9. Greg A. Kimmel, Nikolay G. Petrik, Zdenek Dohnálek and Bruce D. Kay, "Crystalline ice growth on Pt(111) and Pd(111): Non-wetting growth on a hydrophobic water monolayer," *J. Chem. Phys.* **126**, 114702 (2007).
10. Christopher D. Lane, Nikolay G. Petrik, Thomas M. Orlando, and Greg A. Kimmel, "Electron-stimulated oxidation of thin water films adsorbed on TiO₂(110)," *J. Phys. Chem. C.* **accepted** (2007).

THEORY OF THE REACTION DYNAMICS OF SMALL MOLECULES ON METAL SURFACES

Bret E. Jackson

Department of Chemistry
701 LGRT
University of Massachusetts
Amherst, MA 01003
jackson@chem.umass.edu

Program Scope

Our objective is to develop realistic theoretical models for molecule-metal interactions important in catalysis and other surface processes. The dissociative adsorption of molecules on metals, Eley-Rideal and Langmuir-Hinshelwood reactions, recombinative desorption and sticking on surfaces are all of interest. To help elucidate the UHV-molecular beam experiments that study these processes, we examine how they depend upon the nature of the molecule-metal interaction, and experimental variables such as substrate temperature, beam energy, angle of impact, and the internal states of the molecules. Electronic structure methods based on Density Functional Theory (DFT) are used to compute the molecule-metal potential energy surfaces. Both time-dependent quantum scattering techniques and quasi-classical methods are used to examine the reaction dynamics. Some effort is directed towards developing improved quantum scattering methods that can adequately describe reactions on surfaces, as well as include the effects of temperature (lattice vibration) in quantum dynamical studies.

Recent Progress

We continued our studies of H-graphite reactions, which play an important role in the formation of molecular Hydrogen on graphitic dust grains in interstellar space, as well as in the etching of the graphite walls of fusion reactors. In earlier work, using DFT-based electronic structure methods, we demonstrated that an H atom could chemisorb onto a graphite terrace carbon, with the bonding C atom puckering out of the surface plane by several tenths of an Å. We computed the potential energy surface for the Eley-Rideal (ER) reaction of an incident H atom with this chemisorbed H atom, and suggested that the reaction cross sections should be very large – on the order of 10 \AA^2 . Motivated by our studies, the group of Küppers (Bayreuth) showed experimentally that H could indeed chemisorb, and that the lattice did pucker. Küppers and co-workers then measured the cross sections for the $\text{H(g)} + \text{D/graphite}$ ER reaction to form HD(g) , and again, theory and experiment were in excellent agreement. We demonstrated that the H_2 formed in these ER reactions should be very highly excited, vibrationally. It has been suggested that vibrationally excited H_2 might be responsible for some of the unique chemistry that occurs in interstellar clouds.

More recently, both our efforts and the efforts of the experimental groups have been focused on graphite edges. Real graphite surfaces are rough in the sense that a sizable fraction of the exposed carbon atoms can be on the edges of graphite planes, as opposed to the terraces. We have performed DFT calculations to examine how molecular and atomic hydrogen reacts with edge carbons. We found that the hydrogenation of an edge carbon by H proceeded with no barrier, and that the barrier for addition of a second H to the edge carbons was small [1]. We have examined how molecular hydrogen can chemisorb onto edges, and have found two low

energy pathways where H_2 dissociatively adsorbs over one or two edge carbons, resulting in a doubly-hydrogenated edge carbon, or two neighboring singly-hydrogenated edge carbons, respectively [1]. These studies are also relevant to a sizable body of work examining molecular hydrogen adsorption in and on nano-crystalline graphite. The doubly-hydrogenated structure gives rise to a peak that has been observed (but not explained) in the radial distribution functions extracted from neutron scattering studies of graphitic nano-structures exposed to H_2 . We have demonstrated that the vapor pressure of H_2 in equilibrium with these hydrogenated structures is too small to be useful for hydrogen storage, due to the strength of the bonds.

The Küppers group measured the sticking probabilities of D on the graphite terrace and found it to be large, roughly 0.4. Given the significant lattice distortion required for chemisorption, this is surprising. We used DFT to map out the H-graphite interaction as a function of the position of the bonding carbon, and found a barrier to chemisorption of about 0.2 eV, in excellent agreement with recent experiments. A potential energy surface for trapping and sticking was constructed, and a low-dimensional collinear quantum study of the trapping process was implemented [3]. We found that the bonding carbon reconstructs in about 50 fs. Our results suggested that sticking proceeds via a trapping resonance, which relaxes by dissipating energy into the substrate over a ps or so. More recently we computed the full three-dimensional potential, and used classical mechanics to compute the sticking cross sections [5], which are on the order of 0.1 \AA^2 at energies not too far above the barrier. However, when averaged over the experimental incident energy distribution, the computed sticking probabilities for D were only around 0.08. The proposed mechanism involving a trapping resonance was confirmed. While an improved model that included a fully dynamical graphite lattice did not significantly increase the sticking, we have since come to understand the discrepancy between experiment and theory. Using DFT, we have found that the graphite lattice can undergo extensive reconstruction when additional H atoms are chemisorbed in the vicinity of an adsorbed H. The binding energies, and the barriers to chemisorption, can vary dramatically from site to site. Our work suggests that while the initial (true zero coverage) sticking may indeed be small, the addition of subsequent H atoms, in specific locations relative to the initial adsorbates, may happen with a large probability. This has now been confirmed by two sets of experiments. The Küppers group has now measured sticking down to (true) zero coverage, finding probabilities of around 0.1. They observe that sticking increases as coverage increases. This group and another have also observed pair formation, via STM, where H atoms are observed to cluster together on the surface, due to these preferred binding sites.

In an earlier study of H atom recombination on Ni(100), we allowed the lattice atoms to move, which required that we construct a potential energy surface based upon the instantaneous positions of the lattice atoms and the adsorbates. We avoided the usual problems associated with pairwise potentials by using a potential based upon ideas from embedded atom and effective medium theory, but instead of using the isolated atom electron densities, we fit the one and two-body terms to reproduce the results of our DFT calculations. More recently we have used the part of this potential describing the Ni-Ni interactions to study the sputtering of Ni surfaces by Ar beams, in order to further test the utility of these potentials [2]. We find that this form for the potential very accurately describes the energy required to severely distort the lattice or to remove one or more Ni atoms from the lattice. Agreement of sputtering yields and threshold energies with experiments is greatly improved over earlier models.

We concluded our studies of the $H(g) + Cl/Au(111)$ reaction, which have been motivated primarily by two detailed experimental studies of this system. These experiments observe strong H atom trapping and a thermal Langmuir-Hinshelwood channel for HCl formation, as well as ER and hot atom (HA) channels. One of our findings is that the ER reaction cross section is much

larger than for $H(g) + H/\text{metal}$ reactions, roughly $1 - 2 \text{ \AA}^2$. This is due to a steering mechanism, and arises from the relatively large distance of the adsorbed Cl above the metal. The incoming H atom is strongly attracted to both the Cl and the metal, but it encounters the layer of adsorbed Cl atoms first, and steers towards them. Thus there is no competition between ER reaction and trapping of the H atom onto the surface. There are also some interesting variations of ER reactivity with the Cl vibrational state, and an exchange pathway is observed (for the first time), in which the H remains bound while the Cl desorbs. Quasi-classical trajectories were used to study this reaction for the case of large Cl coverages, and with dissipation of the trapped hot atoms' energy into the lattice [4]. The ER and HA reaction pathways for HCl formation are a bit more complicated than for molecular Hydrogen formation. We find that HA reactions dominate the formation of HCl. We also find that there must be significant energy loss into the substrate excitations, perhaps into electron hole pair excitations, from either the trapping hot H atoms, or the excited product HCl, in order to agree with experiment.

For much of the past two years we have explored the dissociative adsorption of methane on metals. A problem that is not well understood is how methane reactivity varies with the temperature of the metal, and why the nature of this variation differs from metal to metal. To examine this we have used DFT to compute the barriers and explore the potential energy surfaces for methane dissociation on several metal surfaces. We have also examined how these barriers change due to lattice vibration and distortion. Starting with the Ni(111) surface, we found that at the transition state for dissociation, the Ni atom over which the molecule dissociates would prefer to pucker out of the surface by 0.23 \AA . Put another way, when this Ni atom vibrates in and out of the plane of the surface, the barrier to dissociation over this Ni atom increases and decreases, respectively. This should lead to a strong variation in the reactivity with temperature. In addition, it is not clear that a metal atom would have time to move or relax during a reactive collision. To explore these issues, high dimensional quantum scattering calculations were implemented, which allowed for the motion of several key methane degrees of freedom, as well as the metal lattice atom over which the reaction occurs. It was found that the lattice has time to at least partially relax (pucker) during the reaction, even at collision energies of an eV or so. The net result is that the reactivity was significantly larger than for the static lattice case. We compared our results with the surface oscillator model, used for many years to explain the effects of thermal lattice motion on dissociative adsorption. For this model, the lattice recoils into the surface during the collision, leading to a lower reactivity. We clearly demonstrated that when lattice relaxation in the presence of an adsorbate is possible, the physics is very different from what has long been assumed [6].

This model was also used to elucidate recent experiments of the Utz group (Tufts), who examined CD_3H dissociation on Ni(111). They were able to significantly enhance reactivity by laser exciting the C-H stretch of the molecule. Generally, the reactivity of the laser-excited molecules are compared with the "laser off" reactivity, and an open question has been to what extent vibrationally excited molecules contribute to this "laser off" reactivity. We were able to show that vibrationally excited molecules can significantly contribute to the laser off reactivity, particularly at lower incident energies where the ground vibrational state is "below the barrier".

We have also used DFT to explore the transition states for methane dissociation on Ni(100) and Pt(111). We find that there are similar forces for lattice relaxation and puckering on the metal atom over which the molecule dissociates. In order to examine how lattice mass might effect the dynamics of surface relaxation and methane reactivity, we have replaced the lattice mass in our Ni(111) model with the mass of a Pt atom. We showed that the lattice puckering becomes much less likely, significantly lowering the reaction probability.

Future Plans

We are currently using DFT to construct potential energy surfaces for methane dissociation on Ni(111), Pt(111) and Pt(100) that explicitly includes the position of the metal atom. As noted, the forces causing the lattice to pucker during the reaction are similar for these systems, but the different lattice masses and other aspects of the potential energy surface may lead to very different dynamics. The dissociation probability as a function of incident energy, surface temperature, and molecular vibrational state will be computed using our 5 degree-of-freedom quantum model. We will then analyze the wealth of experimental data that exists for these systems. Specifically, we hope to understand the role played by lattice motion and relaxation in this important reaction. Standard models have suggested that thermal effects should be more significant on Ni than Pt, due to the smaller mass, but this is not what has been observed. Perhaps the lattice relaxation can explain this discrepancy. The most significant shortcoming of our quantum scattering model is that it only includes the most reactive pathway, over the atop site. We have formulated, and hope to implement, an approximate way to average over the less reactive sites. Eventually we hope to also examine methane dissociation on the step and defect sites of these Ni and Pt surfaces. It is likely that the magnitudes of the thermal fluctuations and any relaxations are larger at these defect sites than on the terraces.

References

- [1]. X. Sha and B. Jackson, "The Location of Adsorbed Hydrogen in Graphite Nanostructures," *J. Am. Chem. Soc.* 126, 13095-13099 (2004).
- [2]. Z. B. Guvenc, R. Hippler and B. Jackson, "Bombardment of Ni(100) surface with low-energy argons: molecular dynamics simulations, *Thin Solid Films* 474, 346-357 (2005).
- [3]. X. Sha, B. Jackson, D. Lemoine and B. Lepetit, "Quantum studies of H Atom Trapping on a graphite surface," *J. Chem. Phys.* 122, 014709, 1-8 (2005).
- [4]. J. Quattrucci and B. Jackson, "Quasi-classical study of Eley-Rideal and Hot Atom reactions of H atoms with Cl adsorbed on a Au(111) surface, *J. Chem. Phys.* 122, 074705, 1-13 (2005).
- [5]. J. Kerwin, X. Sha and B. Jackson, "Classical studies of H atom trapping on a graphite surface," *J. Phys. Chem. B* 110, 18811-18817 (2006).
- [6]. S. Nave and B. Jackson, "Methane dissociation on Ni(111): the role of lattice reconstruction," *Phys. Rev. Lett.* 98, 173003, 1-4 (2007).

Program Title: Theoretical Studies of Surface Science and Intermolecular Interactions

Principal Investigator: Mark S. Gordon, 201 Spedding Hall, Iowa Sate University and Ames Laboratory, Ames, IA 50011; mark@si.msg.chem.iastate.edu

Program Scope. Our research effort spans the study of a variety or problems in surface science using *ab initio* cluster and embedded cluster methods, the development and application of sophisticated model potentials for the investigation of intermolecular interactions, including solvent effects in ground and excited electronic states, and the development and implementation of methods related to the study of molecules containing heavy elements, and general studies of mechanisms in organometallic chemistry. Many of the surface science studies are in collaboration with Jim Evans.

Recent Progress. Several studies of the Si(100) surface and processes that occur on this surface have been studied. The reactions of acetylene on the Si(100) surface were investigated using MCSCF wavefunctions augmented by second order perturbation theory (MRMP2), within the SIMOMM embedded cluster method³. Similar combined kinetic Monte Carlo (KMC)/electronic structure theory studies of the etching of the Si(100) surface^{5,12} and the diffusion of group III metals on the Si(100) surface is ongoing^{13,14}. SIMOMM studies have also been carried out on the diamond surface^{4,11}.

Because MCSCF calculations are limited with regard to the size of the active space that can be included, extensive studies have been initiated on methods that are designed to significantly increase the sizes of systems that can be realistically treated with this method. Two studies have also been completed on the structures of Si_mO_n clusters¹⁰ and on the prediction of novel silicon-based nanowires²⁶. A related paper on the design of a new class of quantum dots has been submitted.

As part of a NERI grant (PI: Francine Battaglia), an extensive series of calculations has been initiated to study the chemical vapor deposition processes of SiC, starting from CH₃SiCl₃ (MTS). The overall mechanism involves more than 100 reactions whose overall reaction energetics and barrier heights and activation energies have been predicted with many body perturbation theory and coupled cluster theory^{24,25}. As part of this effort, it has been demonstrated that the new CR-CCSD(T)_L method is in almost perfect agreement with full configuration interaction (FCI) for breaking a wide variety of single bonds.

Development of the effective fragment potential (EFP) method has continued with the derivation and implementation of a new approach to electrostatic damping and the application to the benzene dimer²³, the derivation and implementation of analytic gradients for the most demanding terms in the potential^{19,20}, and the implementation of a scalable EFP algorithm⁶. The EFP method has recently been extended to open shell species. EFP applications have included a study of the aqueous solvation of F⁻ and Cl⁻.⁹

Several studies of non-adiabatic interactions, including spin-orbit coupling have been published^{1,2,16}, and several papers on advances in high quality electronic structure theory have been completed^{7,8,17,19}.

Future Plans. In order to significantly expand the sizes of clusters that can realistically be modeled with MCSCF wavefunctions, the ORMAS (Occupation restricted Multiple Active Spaces) method is being tested on clusters of increasing size and compared with the full CASSCF calculations. This study is nearing completion. An exhaustive study of the diffusion of one and Al atoms on the Si(100) surface will be completed and then extended to heavier group III elements. The etching of the Si(100) surface by O was studied previously. This system is being revisited, partially to explore the importance of using larger basis sets and better levels of theory, and partially to study the diffusion of O along the surface. The energetics and structural information obtained for these processes will then be incorporated into the kinetic Monte Carlo analyses performed by the Evans group. The SIMOMM method is being extended to more complex species, such as silica. A primary motivation for this is to model the catalysis of various reactions in silica-based MSM pores. An interface between SIMOMM and EFP will be developed, so that the liquid solid interface can be studied at reliable levels of theory.

The EFP method is currently being interfaced with both the CI singles and time-dependent density functional (TDDFT) methods, so that solvent-induced shifts in electronic spectra can be investigated. Improved methods for treating weak intermolecular interactions, such as dispersion, will be developed and implemented, and then applied to important problems. A preliminary molecular dynamics (MD) code for the EFP method and a combined *ab initio* EFP MD code has been implemented, and more robust algorithms are being developed. An extensive investigation of the water dipole moment enhancement in the liquid vs. gas is nearing completion. Several studies of the aqueous solvation of ions and electrolytes, including NO_3^- , Na^+ , OH^- , and NaOH are underway. This includes a systematic study of the solvated structures (internal vs. external ions) and the convergence of ionization potentials and electron affinities to their gas phase values. The EFP method will also be used in extensive investigations of atmospheric aerosols, including the structures and reactions clusters of H_2SO_4 , HNO_3 , and their ions with water molecules. The latter study is in collaboration with Theresa Windus (Iowa State) and Shawn Kathmann (PNNL) and is supported by a generous computer grant from PNNL.

Ruedenberg and Bytautas have developed the very excited CEEIS (Correlation Energy Extrapolation with Intrinsic Scaling) that facilitates the prediction of the exact wavefunction (full CI at the complete basis set limit) for small molecules. The complete potential energy curve for F_2 , including the full complement of vibrational energy levels, has been calculated using this method. Three papers have been submitted, and an additional one is in progress to elucidate the fundamental nature of the long-range interaction between two open shell atoms as they come together to form a bond.

Analytic gradients and Hessians for the Klobukowski model core potentials (MCP) have been derived and implemented into GAMESS. Combined with the correlation consistent

basis sets, this provides a powerful approach to study mechanisms of reactions in transition metal organometallic chemistry, in collaboration with the Ames Laboratory catalysis group, especially Andreja Bakac.

In collaboration with Francine Battaglai and Rodney Fox, the NERI project will continue with the incorporation of the thermodynamic and rate constant data discussed above into bulk kinetic models, such as ChemKin. This will provide important insights to our experimentalist colleagues at ORNL.

References to publications of DOE sponsored research, 2004-present.

- [1] *Spin-orbit coupling methods and applications to chemistry*, D.G. Federov, M.W. Schmidt, S. Koseki, M.S. Gordon, in *Adv. in Relativistic Molecular Theory*, Vol. 5, World Sci., Singapore, pp. 107-136, 2004.
- [2] *Dissociation Potential Curves of Low-Lying States in Transition Metals. II. Hydrides of Groups 3 & 5*, S. Koseki, Y. Ishihara, D.G. Fedorov, M.W. Schmidt, M.S. Gordon, *J. Phys. Chem.* **108**, 4707 (2004).
- [3] *Adsorption of Acetylene on Si(100)*, J.M. Rintelman, M.S. Gordon, *J. Phys. Chem.* **108**, 7820 (2004).
- [4] *Theoretical Studies of Growth Reactions on Diamond Surfaces*, P. Zapol, L. A. Curtiss, H. Tamura, and M. S. Gordon, in *Comp. Materials Chemistry*, L.A. Curtiss, M.S. Gordon, Eds., pp. 266-307 (2004).
- [5] *Atomistic Modeling of Morphological Evolution during Simultaneous Etching and Oxidation of Si(100)*, M. Albao, D.-J. Liu, C. H. Choi, M.S. Gordon, J.W. Evans, *Surf. Sci.* **555**, 51 (2004).*
- [6] *Fast Fragments: The Development of a Parallel Effective Fragment Potential Method*, H.M. Netzloff and M.S. Gordon, *J. Comp. Chem.*, **25**, 1926 (2004).
- [7] *Multi-Reference Second-Order Perturbation Theory: How Size Consistent is Almost Size Consistent?* J. M. Rintelman, I. Adamovic, S. Varganov, and M. S. Gordon, *J. Chem. Phys.*, **122**, 044105 (2005).
- [8] *Advances in Electronic Structure Theory: GAMESS a Decade Later* M. S. Gordon and M. W. Schmidt *Theory and Applications of Computational Chemistry*, Ch. 41, C. E. Dykstra, G. Frenking, K. S. Kim, G. E. Scuseria, Eds., Elsevier, 2005.
- [9] *Theoretical Study of the Solvation of Fluorine and Chlorine Anions by Water*, D. D. Kemp and M. S. Gordon, *J. Phys. Chem. A*, **109**, 7688 (2005) [13th most downloaded paper July-Sept. 2005].
- [10] *Potential Energy Surfaces of Si_mO_n Cluster Formation and Isomerization*, P. V. Avramov, I. Adamovic, K.-M. Ho, C. Z. Wang, W. C. Lu, and M. S. Gordon, *J. Phys. Chem. A*, **109**, 6294 (2005).
- [11] *Ab initio study of Nucleation on the Diamond(100) Surface during Chemical Vapor Deposition with Methyl and H Radicals*, H. Tamura and M. S. Gordon, *Chem. Phys. Lett*, **406**, 197 (2005).
- [12] *Competitive Etching and Oxidation of Vicinal Si(100) Surfaces*, M. A. Albao, D.-J. Liu, C. H. Choi, M.S. Gordon, and J.W. Evans, *MRS Proceedings*, **859E**, JJ3.6.1-6 (MRS Pittsburgh, 2005), edited by J. W. Evans, C. Orme, M. Asta, and Z. Zhang.*
- [13] *Monotonically Decreasing Size Distributions for One-dimensional Ga Rows on Si(100)*, M.A. Albao, M.M.R. Evans, J. Nogami, D. Zorn, M.S. Gordon, and J.W. Evans, *Phys. Rev. B*, **72**, 035426 (2005), 8pp. (Also listed in *Virtual J. Nanoscale Science and Technology*, 2005)

- [14] *Simultaneous Etching and Oxidation of Vicinal Si(100) Surfaces: Atomistic Lattice-Gas Modeling of Morphological Evolution*, M. A. Albao, D.-J. Liu, M.S. Gordon, and J.W. Evans, *Phys. Rev. B*, **72**, 195420 (2005), 12pp.*
- [15] *Theoretical Study of the Formation and Isomerization of Al₂H₂*, T. J. Dudley and M. S. Gordon, *Mol. Phys.*, **104**, 751 (2006)
- [16] *Dissociation Potential Curves of Low-Lying States in Transition Metal Hydrides. III. Hydrides of Groups 6 and 7*, S. Koseki, T. Matsushita, and M.S. Gordon, *J. Phys. Chem*, **A110**, 2560 (2006).
- [17] *Parallel Coupled Perturbed CASSCF Equations and Analytic CASSCF Second Derivatives*, T. J. Dudley, R. M. Olson, M. W. Schmidt and M. S. Gordon, *J. Comp. Chem.* **27**, 353 (2006).*
- [18] *Gradients of the Exchange-Repulsion Energy in the Effective Fragment Potential Method*, H. Li and M. S. Gordon, *Theor. Chem. Accts.*, **115**, 385 (2006).*
- [19] *Scalable Implementation Of Analytic Gradients For Second-Order Z-Averaged Perturbation Theory Using The Distributed Data Interface*, C.M. Aikens and M.S. Gordon, *J. Chem. Phys.*, **124**, 014107 (2006).*
- [20] *Gradients of the Polarization Energy in the Effective Fragment Potential Method*, H. Li, H.M Netzloff, and M.S. Gordon, *J. Chem. Phys.*, **125**, 194103 (2006).*
- [21] *Reinvestigation of SiC₃ with Multi-reference Perturbation Theory*, J. M. Rintelman, M. S. Gordon, G. D. Fletcher, and J. Ivanic, *J. Chem. Phys.*, **124**, 034303 (2006).
- [22] *Reply to Comment on monotonically decreasing size distributions for one-dimensional Ga rows on Si(100)*, M.A. Albao, M.M.R. Evans, J. Nogami, D. Zorn, M.S. Gordon, and J.W. Evans, *Phys. Rev. B*, **74**, 037402 (2006).
- [23] *Electrostatic Energy in the Effective Fragment Potential (EFP) Method. Theory and Application to Benzene Dimer*, L. Slipchenko and M.S. Gordon, *J. Comp. Chem.*, **28**, 276 (2007)
- [24] *Theoretical Study of the Pyrolysis of Methyltrichlorosilane in the Gas Phase. I. Thermodynamics*, Y. Ge, M.S. Gordon, F. Battaglia, and R.O. Fox, *J. Phys. Chem.*, **A111**, 1462 (2007).
- [25] *Theoretical Study of the Pyrolysis of Methyltrichlorosilane in the Gas Phase. II. Reaction Paths and Transition States*, Y. Ge, M.S. Gordon, F. Battaglia, and R.O. Fox, *J. Phys. Chem.*, **A111**, 1475 (2007).
- [26] *Multiterminal Nanowire Junctions of Silicon: A Theoretical Prediction of Atomic Structure and Electronic Properties*, P.A. Avramov, L.A. Chernozatonskii, P.B. Sorokin, and M.S. Gordon, *Nano Letters*, in press.
- [27] *Breaking Bonds with the Left Eigenstate Completely Renormalized Coupled Cluster Method*, Y. Ge, M.S. Gordon, and P. Piecuch, *J. Chem. Phys.*, in press.

*Work includes partial support from USDOE Computational Chemistry SciDAC program.

Radiation Effects at the Solid-Aqueous Interface

Dan Meisel and Daniel M. Chipman,

The Radiation Laboratory, University of Notre Dame
Notre Dame, IN 46556

dani@nd.edu; chipman.1@nd.edu;

Program Scope

The objective of our effort is to outline quantitatively the details of the processes that occur at the surface of solid particles, largely at the nano-size regime, suspended in aqueous solutions in response to a radiation stimulus. The impetus for these studies is the abundance of similar interfaces across the DOE complex. Particularly, we are interested in the application of the basic knowledge to three technical arenas:^(1,2) a) The effect of the interface on processes that affect performance of nuclear power generation and related issues such as waste management of fissile materials. b) Potential utilization of nanoparticles in biomedical diagnostics or therapy, and c) the use of nanoparticles as redox catalysts in water splitting reactions of solar conversion.

The program uses radiation and photochemical techniques to generate radicals in the aqueous phase, or charge carriers in the solid particles, and a variety of spectroscopies to follow their dynamics and evolution. Of particular interest is the possible exchange of energy and charge between the two phases. The impact of such processes on many applications cannot be exaggerated. For example, we have shown in the past that the presence of large concentrations silica particles on in water suspensions may enhance, rather than reduce, the yield of radiolytic water decomposition to H₂. Similarly, we discuss below potential application of metallic nanoparticles to target radiolytic damage to specific locations, e.g. the surface of the particle.

Recent Progress

1) *Insulators and Insulator-Metal Hybrids*: We have shown that radicals from the aqueous phase strongly adsorb on gold nanoparticles and determined the relative adsorption constants of few functional groups on the radical (amines, ketones ethers and direct binding via the nitrogen center of nitroxy radicals). Other radicals were shown to adsorb to the surface of oxides and their cross-sections on the surface were determined.⁽³⁾ Using this information we were able to determine the distance that reducing equivalents (electrons, radicals or excitons) can reach the interface before they are annihilated by recombination or are localized in deep traps.⁽⁴⁾ We found that this distance is independent of surface coverage and for silica particles is 15 nm. We have studied the effect of particle size on the efficiency of the catalytic conversion of single-electron reducing radical to H₂ by gold. We conclude that the major factor to determine the efficiency is the surface area and not an intrinsic size effect.⁽⁵⁾

Using synthetic methodologies that we and others developed in the past we studied the effect of “inert” supports on the hydrogen evolution reaction from water by silica-supported silver nanoparticles. Contrary to expectations the support may adversely affect the catalyst efficiency.⁽⁶⁾ As the dose increases and hydrogen accumulates the overpotential required for the hydrogen evolution on the metal also increase. As a result, the rate of H₂ generation decreases. Other pathways for radical reactions, such as radical-radical recombination at the support surface, become dominant and eventually completely overtake hydrogen evolution. In the absence of the support the metallic catalyst generates hydrogen at the same and higher doses with no observable deterioration. Strategies to overcome this disadvantage of the support can now be developed.

Metallic Nanoparticles: Little information is available on the fate of electron-hole pairs

generated by ionizing radiation in metals. They are universally expected to be very short-lived but recent reports in the literature suggest that the presence of electron donors at the interface can efficiently interfere with carrier's recombination. Thus, citrate can efficiently transfer electrons to silver particles that are excited at the plasmon band of the particle (Redmond P., et al., *J. Phys. Chem. C* **111**, 8942, 2007). We conclude from these studies firstly, that interfering with carriers' recombination may indeed be possible and secondly, the presence of foreign molecules at the particles surface may be detrimental even at the shortest times. Clean interface becomes essential if capture of the carriers by the target is desired. .

We were attracted to a recently proposed method to synthesize naked metallic particles (Evanoff, D., et al *J. Phys. Chem. B* **108**, 13948, 2004). The method relies on the reduction of silver oxide by H_2 , thus the product contains no component other than silver, water and their ions. We studied the mechanism of production of the metallic particles and the properties of the particles.⁽⁷⁾ Briefly, the particles are stabilized by hydroxide ions and thus their surface resembles a hydrophilic oxide surface. This provides for exceptional stability of the otherwise hydrophobic metallic interface. This stability allows synthesis of extremely high particles concentrations without inducing agglomeration. The synthesis is a combination of two steps, dissolution of Ag_2O and reduction of the Ag^+ ions. Control of their rates allows synthesis of controlled sizes (30-200 nm).

On the less attractive side, because of the low redox potential of the H^+/H_2 couple used in the reduction, a relatively high residual Ag^+ ions concentration remains in the solution. We developed radiolytic methods utilizing the much more negative redox potential of reducing radical to control this residual concentration. We are at present in satisfactory control of the synthesis.

Some of the experiments described in the Future Plans section require high sensitivity of detection of species at the metallic interface. Surface enhanced Raman spectroscopy seems to be the technique of choice, although the ultra high sensitivity down to the single molecule level is a distraction for us. We initiated a study on the SERS activity of the particles described above. Preliminary observations show SERS activity for all of them. Based on electron microscopy we believe that junctions of agglomerated particles are minimal, so the somewhat random, super sensitivity is eliminated. Using probe molecules (*p*-aminothiophenol) at the surface we study the effect of radiation and silver ions on the SERS spectra of the probe. The SERS signal intensity is found to increase with the increase of silver ion concentrations (Figure 1) but decrease with increasing dose under reducing conditions. In the latter experiment electrons are pumped from the

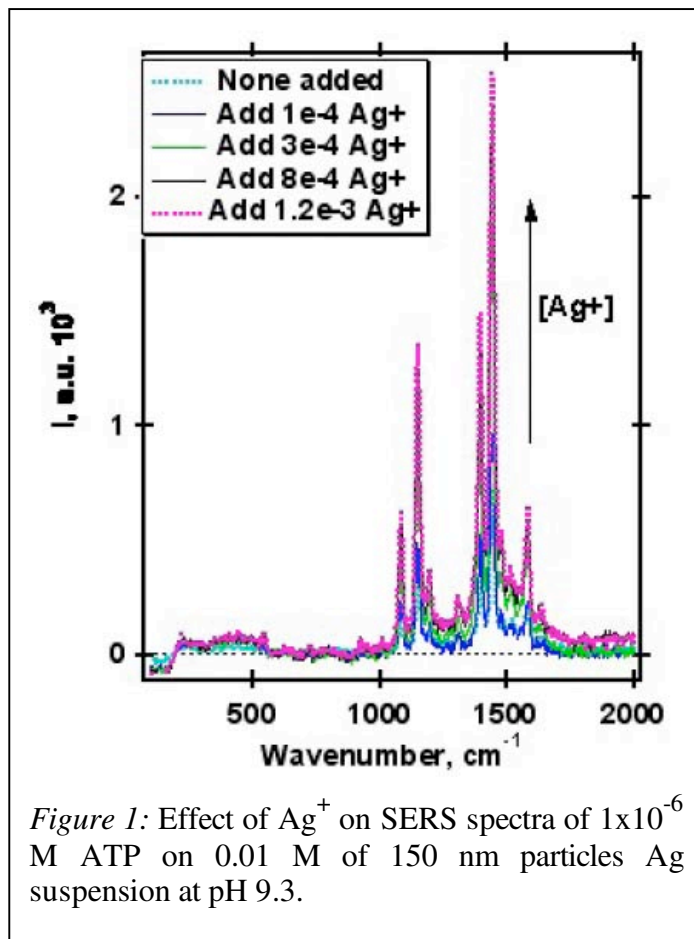


Figure 1: Effect of Ag^+ on SERS spectra of 1×10^{-6} M ATP on 0.01 M of 150 nm particles Ag suspension at pH 9.3.

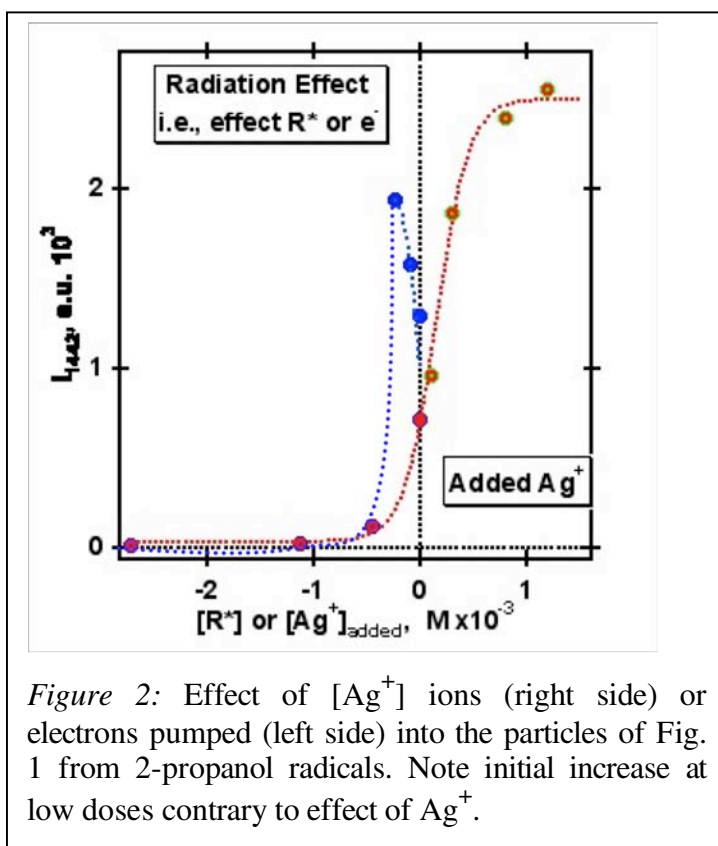


Figure 2: Effect of $[Ag^+]$ ions (right side) or electrons pumped (left side) into the particles of Fig. 1 from 2-propanol radicals. Note initial increase at low doses contrary to effect of Ag^+ .

reducing radicals into the particle, initially reducing residual silver ions and then raising the negative potential on the particle. The former process leads to increase in the SERS signal. When this precondition process is complete the signal decreases (Figure 2). We attribute the correlation of the SERS intensity with $[Ag^+]$ and dose to their effect on the Fermi level of the particle. However, reduction of the silver ions in the radiolytic environment is not equivalent to externally controlling their concentration. We will speculate on this difference in our presentation.

Future Plans

We will pursue our studies of radiolytic effects in size controlled silver particles. In the short term we will add a theoretical component to predict the effect of electrical field on the intensity of the various vibrational bands in the SERS spectra. In parallel we will extend our experimental studies to include

in-situ measurements of the SERS variations during irradiation. A time-resolved surface Raman spectrometer will then follow.

Our main interest is to determine yields of interfacial products from absorption of the energy by the solid particles. No report on escape of charge carriers from metallic systems has appeared so far. Our own preliminary experiments in comparing hydrogen yields from γ radiolysis to those from x-ray irradiation (at Argonne's APS, in collaboration with Prof. B. Bunker - Physics, Notre Dame) of concentrated solutions of metallic silver particles indicate that the yield does not change by tuning the energy around the silver K edge, even though the absorption of energy changes from predominantly the silver to the water phase. We will extend these experiments and will attempt to identify radiolysis product at the particle surface. These experiments require the high specificity and sensitivity of the SERS experiments. Once the principle is successfully demonstrated we will turn to time-domain experiments.

Publications Sponsored by this DOE Program, 2004-2007

1. Dan Meisel, "Radiation Chemistry in the Real World: Nanoparticles in Aqueous Suspensions", Proceedings of the International Atomic Energy Agency Workshop on "Advances in Radiation Chemistry," IAEA Press, Vienna, ISSN 1011-4289, ISBN 92-0-112504-6, pp. 5-14 (2004).
2. Dan Meisel, "Radiation Effects on Nanoparticles", Proceedings of the International Atomic Energy Agency Panel on "Emerging Applications of Radiation in Nanotechnology," IAEA Press, Vienna, ISSN 1011-4289, ISBN 92-0-100605-5, pp. 130-141 (2005).

3. "Kinetic and Thermodynamic Aspects of Adsorption on Silica Nanoparticles. A Pulse Radiolysis Study," Bratoljub H. Milosavljevic and Dan Meisel, *J. Phys. Chem. B*, *108*, 1827-30 (2004).
4. "Yields and Migration Distances of Reducing Equivalents in the Radiolysis of Silica Nanoparticles," Bratoljub H. Milosavljevic, Simon M. Pimblott and Dan Meisel, *J. Phys. Chem. B* *108*, 6996-7001, (2004).
5. "Radiolytic Yields in Aqueous Suspensions of Gold Particles," G. Merga, B. H. Milosavljevic, D. Meisel, *J. Phys. Chem. B* *110*, 5403-8 (2006).
6. "Effect of Silica-Supported Silver Nanoparticles on Dihydrogen Yields from Irradiated Aqueous Solutions," T. Zidki, H. Cohen, D. Meyerstein and Dan Meisel, *J. Phys. Chem. C* *111*, 10461-6 (2007).
7. "Redox Catalysis on "Naked" Silver Nanoparticles," Getahun Merga, Robert Wilson, Geoffrey Lynn, Bratoljub H. Milosavljevic, and Dan Meisel, *J. Phys. Chem. C* *111*, 12220-6 (2007).
8. "Bimetallic Pt-Ag and Pd-Ag Nanoparticles," D. Lahiri, B. A. Bunker, B. Mishra, Z. Zhang, D. Meisel, C. M. Doudna, M. F. Bertino, F. D. Blum, A. T. Tokuhira, S. Chattopadhyay, T. Shibata, J. Terry, *J. App. Phys.* *97*, 094304-12 (2005).
9. "The Role of Water in Electron-Initiated Processes and Radical Chemistry: Issues and Scientific Advances," Bruce C. Garrett, et al., *Chem. Rev.* *105*, 355-90, (2005).
10. "Synthesis and Composition Analysis of Microsilica Encapsulated Acetyl-Acetonato-Carbonyl-Triphenylphosphine-Rhodium Catalyst," Q. Dai, D. Menzies, Q. Wang, A. E. Ostafin, S. N. Brown, D. Meisel, E. J. Maginn, *Nanotech.* *5*, 677-82 (2006).
11. "Reactions of Radicals with Hydrolyzed Bismuth(III) Ions: A Pulse Radiolysis Study," R. Benoit, M-L. Saboungi, M. Tréguer-Delapierre, B. H. Milosavljevic, D. Meisel, , *J. Phys. Chem. A*, Accepted for Publication (2007).

Center for Radiation Chemistry Research: Excited States of Benzoquinone Radical Anion, New Ultrafast Single-Shot Detection at LEAF, and Non-Exponential Charge Capture.

Principle Investigators: Andrew R. Cook, John R. Miller

Chemistry Department, Brookhaven National Laboratory
 Bldg. 555, Upton NY 11973
acook@bnl.gov

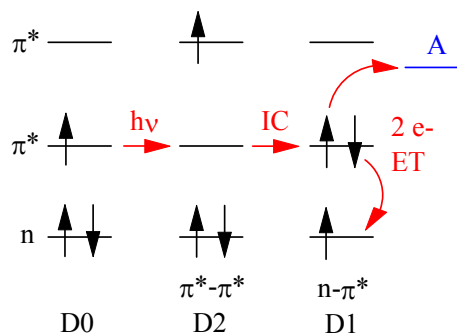
Program Scope:

This program examines charged and radical species in solution and develops tools to create and probe such species. Principal among these tools is the Laser Electron Accelerator Facility (LEAF) at Brookhaven that produces 7 ps electron pulses and associated detection systems. Pulse radiolysis is often the most convenient and sometimes the only method to rapidly produce and study isolated radical species. Presented are recent results in understanding the novel two electron lowest excited state in quinone radical anions, an exciting new picosecond time-domain detection technique which has already made possible new studies in our lab and which will open the door to additional new avenues of research at LEAF, and work to understand charge capture by large linear conjugated molecules which will lead to examination of charge transport along such molecules in solution. Additional efforts in our lab are separately described in summaries by Sergei Lymar, Jim Wishart, and John Miller.

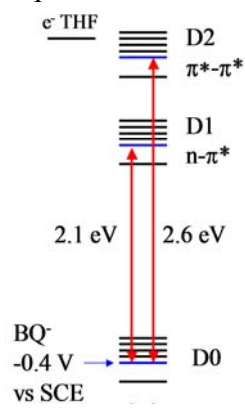
Recent Progress:

1. Excited States of Benzoquinone Radical Anion

One facet of this program focuses on identifying of radical anions and cations whose excited states could be useful for driving electron transfer reactions. The lowest excited state of *p*-benzoquinone radical anion ($BQ^{\bullet-}$) was of particular interest due to its large excited state energy and exceptionally long lifetime of 60 ns. However, previous bimolecular experiments showed no evidence for electron transfer where reactions with other solutes were energetically favorable. While this may simply be due to rapid back transfer of electrons in the encounter complex, the other fascinating possibility is that $BQ^{\bullet-}$ is somehow electron-transfer inert, unable to participate in rapid electron-transfer reactions. A source for such possible inhibitions are the 2-electron processes that occur in $BQ^{\bullet-}$ shown in the figure to the right. Photoexcitation of the ground D0 state at 460 nm of the allowed π^* - π^* transition forms the second excited doublet state, D2, which rapidly relaxes to the optically forbidden n - π^* D1 state through an orbital change of 2 electrons. Electron transfer either out of or into the D1 state will also require a 2-electron change. If electron transfer to/from D1 is inhibited, then it is likely that electron capture directly into the D1 state would be similarly inhibited, since it would require the same 2-electron change.



It was to test this second hypothesis that current experiments were focused. Electron capture in solvents like tetrahydrofuran and isooctane rapidly and preferentially forms excited states of $BQ^{\bullet-}$, which is expected since the energy of the solvated electron is estimated to be ~ 260 mV higher than the D2 state where no special 2-electron changes are needed. The situation changes however as alkyl-groups are added to BQ making the reduction potential more negative, as can be seen in the scheme to the left. The blue lines are the energies of the $BQ^{\bullet-}$ states, while the black lines are those of the substituted quinones assuming the excited state energies remain unchanged. Electron capture rates in THF have been measured and compared with literature rates. It is clear from this comparison that electron capture into the upper, D2, state is the best fit to the data. In fact, even for a quinone such as duroquinone where capture into the D2 state is estimated to be uphill by 80 mV, the D2 state is still preferred over the energetically more favorable D1 state. This large inhibition for electron capture into the lowest excited state is due to the 2-electron changes required, and is most likely what was responsible for the lack of observed bimolecular electron transfer in earlier experiments.



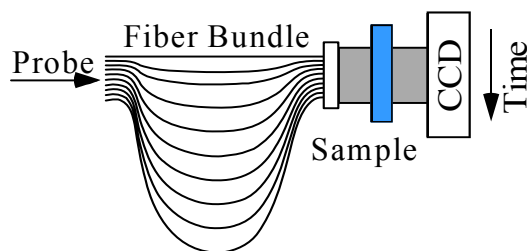
states of $BQ^{\bullet-}$, which is expected since the energy of the solvated electron is estimated to be ~ 260 mV higher than the D2 state where no special 2-electron changes are needed. The situation changes however as alkyl-groups are added to BQ making the reduction potential more negative, as can be seen in the scheme to the left. The blue lines are the energies of the $BQ^{\bullet-}$ states, while the black lines are those of the substituted quinones assuming the excited state energies remain unchanged. Electron capture rates in THF have been measured and compared with literature rates. It is clear from this comparison that electron capture into the upper, D2, state is the best fit to the data. In fact, even for a quinone such as duroquinone where capture into the D2 state is estimated to be uphill by 80 mV, the D2 state is still preferred over the energetically more favorable D1 state. This large

inhibition for electron capture into the lowest excited state is due to the 2-electron changes required, and is most likely what was responsible for the lack of observed bimolecular electron transfer in earlier experiments. Preliminary measurements of electron attachment rates using time-resolved microwave conductivity in collaboration with Richard Holroyd are likely consistent with this picture. In these experiments, rather than changing the energies of the quinone excited states by substitution, the energy of the solvated electron was shifted by either solvent mixtures of tetramethylsilane (TMS) and isooctane, or by increasing pressure in TMS. It is thought that the slow, $\sim 4 \times 10^{10} \text{ s}^{-1}$, electron attachment rate observed in TMS at atmospheric pressure is due to the energy of the solvated electron being below the D2 state. When isooctane is added or the pressure is increased, the energy, or V_0 , of the solvated electron increases making the gap to D2 state smaller or even downhill to D2. This is accompanied by a 2-3 order increase in electron attachment rate, supporting the notion that capture by the D1 state is strongly inhibited.

2. New Ultrafast Single-shot Detection at LEAF

While pulse radiolysis brings special benefits to investigation of electron transfer, its application to intramolecular electron transfer is usually limited to times longer than 0.1 ns. This limitation occurs because valuable donor-spacer-acceptor molecules cannot be subjected to the thousands of pulses needed to collect transients with the pulse-probe system. To bring these experiments to such molecules and also to examine viscous or solid samples such as ionic liquids that cannot be flowed, a novel ultrafast single-shot (UFSS) transient absorption detection system has been developed. This method also eliminates certain types of noise, greatly reduces data-collection times compared to classical delay line sampling techniques, and minimizes waste.

This new experimental technique uses a prototype bundle of 100 fibers of different length shown schematically to the right, with an average of 15 ps of delay fiber-to-fiber providing a data over a time window of 1.5 ns in a single laser shot. A 100 fs laser probe pulse is directed into the end of the bundle, an imaged successively in the sample, where it is collinearly overlapped with either (or both) an

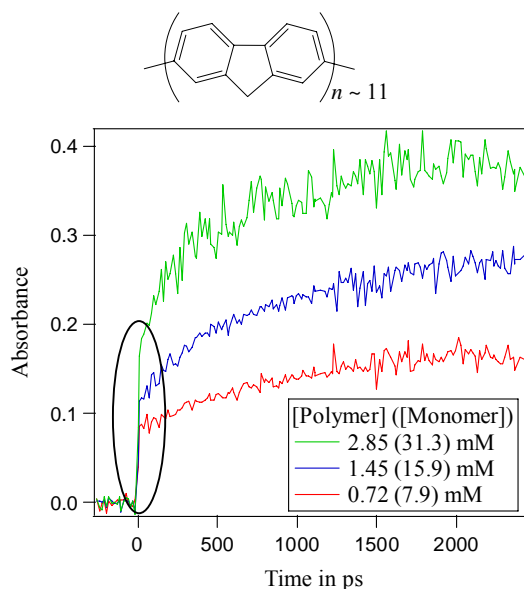


electron pulse or laser excitation pulse, and onto a signal CCD camera. A reference camera is also used. Each image collected thus contains 100 different spots, each of which has information at a different time relative to the electron pulse. The measured risetime of the system is 1.6 ps at 800 nm, which was shown to be improvable to 0.5 ps with fiber chirp precompensation. Data collected with this system show a rise time limited by the 5-10 ps electron pulse width, with a noise level near 1 mOD with averaging of 10-25 shots. Similar data collected with standard variably delayed electron pulse-laser probe spectroscopy requires $10^3 - 10^4$ shots! Probes with different colors have been accomplished with an OPA and simple refocusing. This new detection system has tremendous potential to enable new science in our lab, and the first application is described below.

3. Non-Exponential Charge Capture and Transport in Molecular Wires

It is well known that diffusion-controlled reactions of transiently produced species are characterized by transient terms in the Smoluchowski equation at early times. While typically unobserved for small molecules, such effects become important for long, relatively immobile molecules, providing a unique opportunity to probe such transient terms in the diffusion equation since their timescale can extend well into the nanosecond regime. These effects are known to depend on shape of the molecules, and are the subject of a recent theory by Traytak. Relevant not only to such basic physical chemistry questions, understanding and modeling these complicated kinetics and the corresponding yields of charges captured is important to work in our group involving charge motion in conjugated polymers. Good knowledge of charge capture kinetics is important to this project in order to separate them from charge transfer processes that may occur on comparable timescales in similar extended molecules with additional electron or hole sinks attached to their ends.

Polyfluorene molecules with an average of 11 fluorene units or 92 Å in length were studied using the new fiber-UFSS experiment described above. The figure to the right shows charge capture kinetics for three different concentrations of polymer in THF at 580 nm where the anion of the molecule absorbs strongly. Such data with 10 ps time resolution would not have been collectable with standard sampling pulse-probe techniques due to limited quantities of sample. There are 2 main features of this data. First is the large rise that occurs within the time resolution of the experiment. About 20 % of this step is due to absorption of solvated electrons. Using scavengers, it was possible to show that part of the step was due to rapidly formed excited states, but significant parts were identified to be due to wire anions and cations formed on timescales faster than diffusion. Given the very low concentration of molecules, capture of highly mobile presolvated or “dry” electrons cannot account for this component. Rather, it seems likely that due to the large volume of these molecules a sufficient number of electrons and holes are formed within a reaction distance, R_{ij} , of the wires and react before diffusion occurs



and before they can be scavenged. The second main feature of this data is the slower rise, which can be modeled together with the solvated electron disappearance after accounting for the fast rise. This component contains the diffusional part of electron capture. As expected, the kinetics are not adequately modeled by a single exponential capture rate, but were well described by two exponentials used as an approximation to the full Smoluchowski diffusion equation, where the reaction distance is an effective one described by the result of the 1-dimensional Traytak theory:

$k = 4\pi NR_{eff}D \left[1 + \frac{R_{eff}}{\sqrt{\pi Dt}} \right]$	$R_{eff} = \frac{nR_{ij}}{1 + \frac{2R_{ij}}{a} \ln n}$	R_{eff} – effective reaction distance D – diffusion coefficient a – distance between acceptors n – number of acceptors
---	---	---

Present efforts provide a sufficiently good description of the charge capture process to support future efforts in measuring charge transport in similar wires with endcaps. While the theory at this point can be used to largely qualitatively describe charge capture in the 11-unit polyfluorene, a far more quantitative test is the subject of current investigations. These efforts study electron attachment to both polyfluorene oligomers with lengths from 1 to 10 units, as well as polymer samples with average lengths from 20 to 133 units. These will also test the idea that experiments with fast electron pulses may provide information about how extended are the conformations of the conjugated polymers.

Future Plans:

- Confirmation of electron capture inhibition into the lowest excited state of BQ^{•*} will be sought with conductivity detected experiments using mixtures of ISO and TMS to smoothly vary V_0 around the π^* - π^* excited state of BQ[•]. Can the magnitude of the inhibition be determined?
- Significant noise reduction in fiber-UFSS experiments is expected to be possible and will be pursued. This will be combined with extended time range bundles and simplified wavelength tuning.
- Electron and hole capture will be studied in a variety of different length oligo-fluorenes and polythiophenes, and compared to the theory by Traytak to see if a consistent set of physically reasonable parameters can be determined. Can the model be used to accurately predict yields of ions and kinetics for arbitrary wire lengths?
- Apply the description of capture kinetics to systems with endcapped wires. Can we observe charge transfer rates to the ends of these molecules, and what factors effect them?

Recent DOE Supported Publications:

Faster Dissociation: Measured Rates and Computed Effects on Barriers in Aryl Halide Radical Anions, Takeda, N.; Poliakov, P. V.; Cook, A. R.; Miller, J. R. *J. Am. Chem. Soc.*, **2004**, *126*, 4301-4309.

The LEAF Picosecond Pulse Radiolysis Facility at Brookhaven National Laboratory, Wishart, J. F.; Cook, A. R.; Miller, J. R. *Rev. Sci. Inst.* **2004**, *75*, 4359-4366.

Optical Spectroscopy at the Spatial Limit

Wilson Ho

Department of Physics & Astronomy and Department of Chemistry
University of California, Irvine
Irvine, CA 92697-4575 USA

wilsonho@uci.edu

Program Scope:

This project is concerned with the experimental challenge of achieving sub-molecular spatial resolution in optical spectroscopy and photochemistry of a single molecule. These experiments would lead to an understanding of the inner machinery of single molecules that are not possible with other approaches. Results from these studies will provide the scientific basis for understanding the properties, processes, and phenomena in chemical and physical systems at the nanoscale. The experiments rely on the combination of the unique properties of lasers and scanning tunneling microscopes (STM).

Recent Progress:

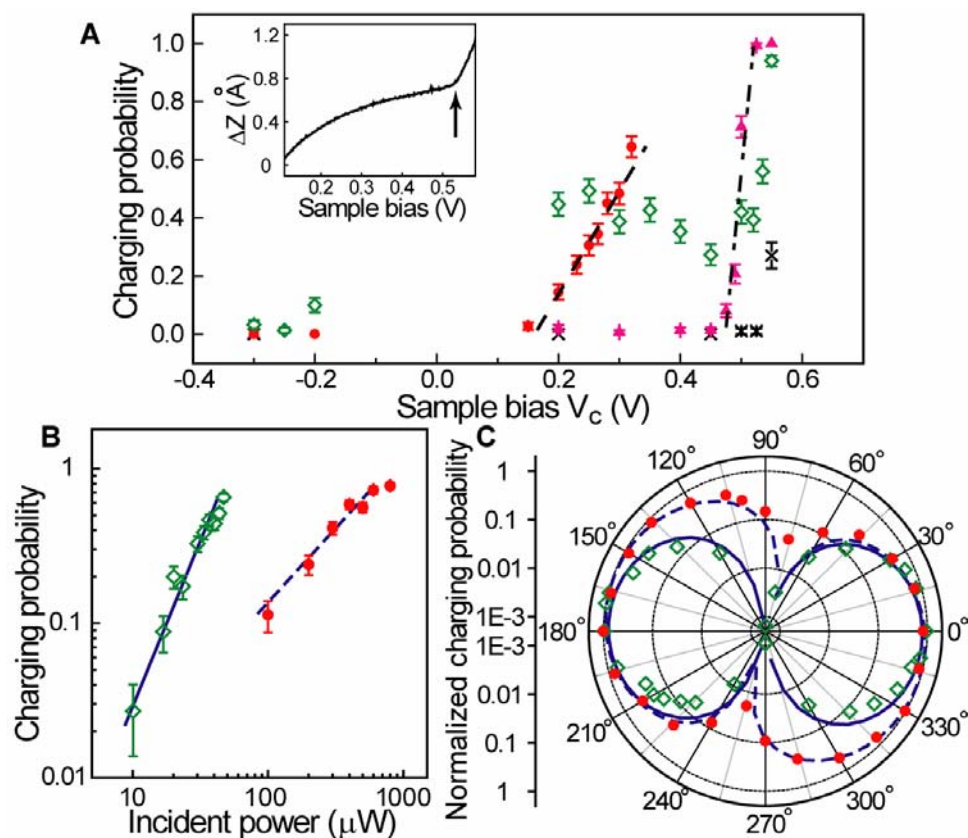
The study of optical phenomena at the atomic scale is expected to provide new understanding of molecules and their chemical dynamics. The combination of lasers with a scanning tunneling microscope (STM) provides new opportunities by tapping into the unique capabilities of both techniques: spectral and temporal information from lasers and ultrahigh spatial resolution in real space from the STM. One big problem, however, is the difficulty of delivering the electromagnetic energy from lasers with atomic precision and initiating the excitations of individual molecules on the surface one by one.

A series of experiments have been performed that couples lasers into a home-built ultrahigh-vacuum (UHV) STM operating at a base temperature of 9 K. The lasers (either CW or femtosecond pulsed lasers) were illuminated into the STM junction while the STM is in the tunneling regime, aiming to locally excite molecules on a surface. The coupling mechanism involves a two-step process of photo-induced hot electron tunneling, in which an electron is photoexcited to a higher level in the tip and then tunnels resonantly to a molecular state [2]. Therefore, light is coupled to the tunneling process. Because tunneling electrons are spatially confined within the atomic scale, this photo-induced hot electron tunneling mechanism also yields atomic-scale variation across a molecule adsorbed on a thin oxide surface. This variation follows the change in the interior structure of the electronic states inside the molecule.

The system that we used to demonstrate the rich phenomena that are possible with the combination of lasers with the STM is Mg-porphine adsorbed singly on a thin (~ 5 Å) Al_2O_3 film grown on NiAl(110) at 9 K. Voltage controlled conductance hysteresis and stepwise switching in a reversible manner were observed in a single Mg-porphine within a double-barrier junction defined by a scanning tunneling microscope (STM) at ~ 10 K [3]. In-situ visualization and

characterization of the junction using the STM revealed that the charge bistability of a single molecule on a polar alumina film is responsible for the conductance hysteresis and switching. Important parameters, such as molecular adsorption, are also discussed.

This single-molecule junction in the STM was irradiated with femtosecond laser pulses [4]. The photoexcited hot electrons in the STM tip resonantly tunnel into the excited states of the molecule, converting it from the neutral to the anion. This electron transfer rate depends quadratically on the incident laser power, suggesting a two-photon excitation process. This nonlinear optical process is further confirmed by the polarization measurement. Spatial dependence of the electron transfer rate exhibits atomic-scale variation.



(A) Charging probability as a function of sample bias under the irradiation of pulsed laser (center wavelength = 807 nm, pulse duration = ~ 70 fs, $P = 34 \mu\text{W}$, dark-green open diamonds), CW lasers ($\lambda = 800$ nm, $P = 146 \mu\text{W}$, magenta filled triangles; and $\lambda = 633$ nm, $P = 7.4 \mu\text{W}$, red filled circles), and without laser illumination (black crosses). The inset shows the tip height displacement ΔZ while ramping the sample bias V_b with the feedback on. (B) Charging probability is plotted as a function of incident power under illumination of pulsed laser ($\lambda = 807$ nm, dark-green open diamonds) and CW HeNe laser ($\lambda = 633$ nm, red filled circles). The dependences on the incident laser power were fitted to power law, $p \propto P^\gamma$, where $\gamma = 2.14 \pm 0.28$ (solid line) and $\gamma = 0.96 \pm 0.13$ (dash line) for pulsed laser and CW laser, respectively. (C) The normalized charging probability as the linear polarization of the laser rotates outside the UHV chamber. The data are normalized by dividing the charging probability by the laser power or square of the laser power and fitted by $\cos^2(\theta + \theta_0)$ (dash line) or $\cos^4(\theta + \theta_0)$ (solid line), depending on one-photon (red filled circles) or two-photon excitation (dark-green open diamonds).

The combination of a scanning tunneling microscope with optical excitation enabled the observation of photo-induced electron transfer through a single magnesium porphine molecule adsorbed on a thin oxide film grown on the NiAl(110) surface. The result of photo-induced electron transfer in the STM junction leads to the charging of molecule from the neutral to the anion. Individual charging events were recorded consecutively over a long period of time, typically one to two days [4]. Histogram analysis of the time trajectory revealed that the photo-induced charging of the molecule has no memory effect and the pathway of this process is through the tunneling of photoexcited hot electrons from the STM tip to the molecule. A simple theoretical model explains the dynamic process and identifies key parameters determining the rate of photo-induced electron transfer. Experiments requiring long time statistics are difficult by single molecule laser induced fluorescence due to irreversible changes in the molecule.

Future Plans:

This research will continue to push the limit of experimental technique in the coupling of a variety of lasers to a low temperature scanning tunneling microscope in ultrahigh vacuum and to explore the range of novel scientific problems that can be tackled with this new approach. The experiments are carried out on single crystal surfaces using surface science procedures under ultrahigh vacuum conditions in order to have well characterized systems optimized for fundamental understanding of spatially resolved single molecule chemistry. The optical detection has been augmented with an avalanche photodiode detector with appropriate bandpass filters to enable spatial imaging of fluorescence from different parts of a single molecule: fluorescence microscopy of the molecular interior with sub-Ångström spatial resolution. Such an experiment has not been carried out before and the results are expected to reflect beyond the molecular properties that could usually be extracted from fluorescence spectroscopy obtained with CCD-based spectrometer. Experiments using a photomultiplier and a Ti:sapphire femtosecond laser to detect second-harmonic generation from a single molecule on the surface and within the tunneling cavity are also planned. The goal is to determine the spatial resolution and chemical sensitivity of cavity enhanced nonlinear optical spectroscopy and microscopy.

References to Publications of DOE Sponsored Research (2003-present):

- [1] G.V. Nazin, X.H. Qiu, and W. Ho, "Charging and Interaction of Individual Impurities in a Monolayer Organic Crystal", *Phys. Rev. Lett.* **95**, 166103-1-4 (2005).
- [2] S.W. Wu, N. Ogawa, and W. Ho, "Atomic Scale Coupling of Photons to Single-Molecule Junction", *Science* **312**, 1362-1365 (2006).
- [3] S.W. Wu, N. Ogawa, G.V. Nazin, and W. Ho, "Conductance Hysteresis and Switching in Single-Molecule Junctions", *Phys. Rev. Lett.*, submitted (2007).
- [4] S.W. Wu and W. Ho, "Real-time Observation of Photo-induced Electron Transfer through a Single Molecule", *Proc. Nat. Acad. Sci.*, submitted (2007).

Progress Report for DE-FG02-00ER15072
Experimental and Theoretical Studies of the Functional Relationship between
Conformational Dynamics and Enzymatic Reactions

PI: Sunney Xie

Department of Chemistry and Chemical Biology, Harvard University

12 Oxford Street, Cambridge, MA 02138

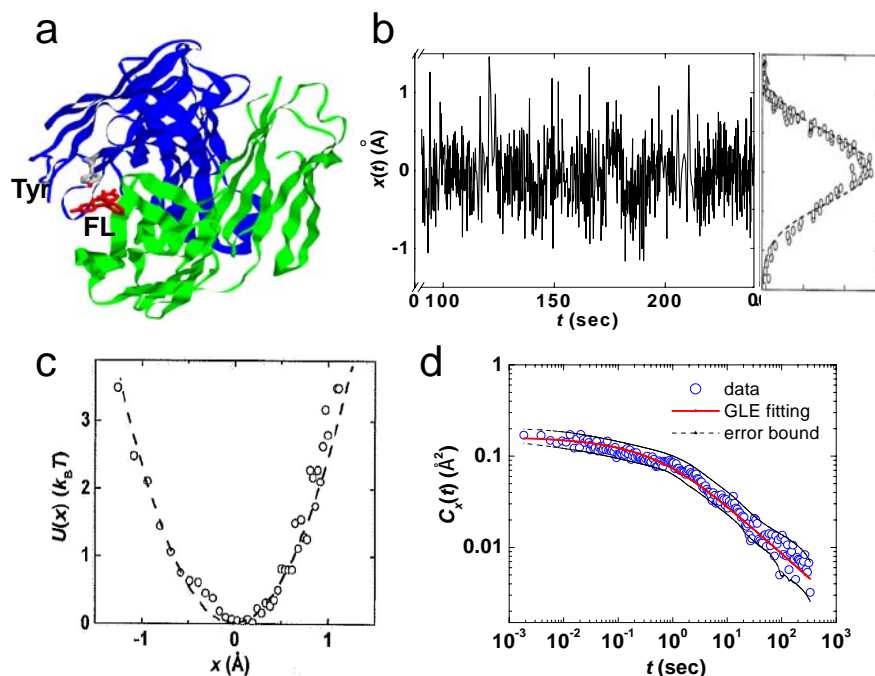
xie@chemistry.harvard.edu

Program Scope

Enzymes are nanometer-scale macromolecular machines designed and evolved by nature to carry out catalysis with high efficiency and selectivity. The quest for understanding how enzymes work has attracted more than a century of research. This project is aimed at a molecular-level understanding of enzymatic catalysis from a chemical physics perspective. We tackle this problem with both experimental and theoretical studies. Experimentally, we rely on single-molecule spectroscopy and enzymology to probe conformational motions and biochemical reactions of a single enzyme molecule in real time. The findings from the single molecule studies prompted us to develop a general theory to describe enzymatic catalyses in terms of nonequilibrium dynamics on a two-dimensional reaction free energy surface.

Recent Progress

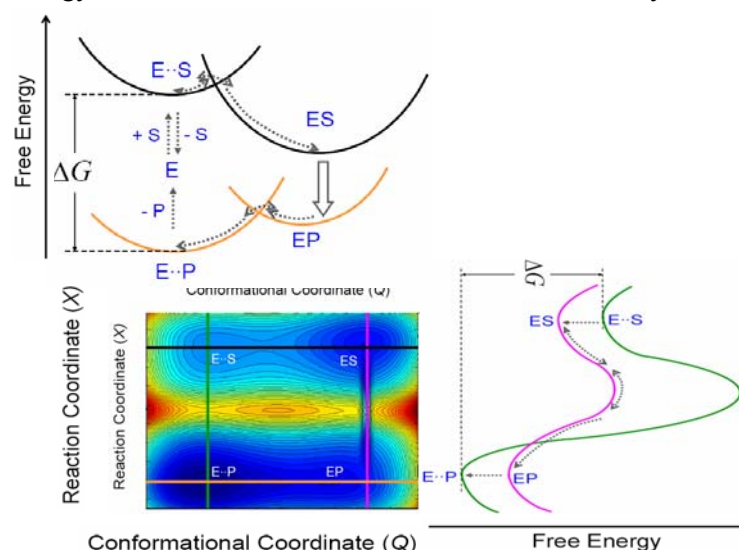
Nonequilibrium statistical mechanical theory of enzymatic cycles (Wei Min, graduate student, in collaboration with Professor Biman Bagchi, on sabbatical from the Indian Institute of Science)



The observation of protein conformational dynamics at biologically relevant timescales is crucial to the understanding of various protein functions. There are spontaneous (thermal) fluctuations and functionally important conformational motions induced by ligand binding and chemical reactions. Our

group initiated the use of electron transfer to study spontaneous conformational fluctuations in a single molecule on the angstrom-scale (Yang 2003, Min 2005). In a protein complex formed between fluorescein (FL) and monoclonal anti-fluorescein (anti-FL) (Fig. 1a), the distance between the donor (Tyrosine) and acceptor (FL), $x(t)$, is monitored as a function of time (Fig. 1b). Figure 1c shows the harmonic potential of mean force, $U(x) = -kT \ln P(x)$ from the Gaussian distribution of $x(t)$ (Fig. 1b). The rather slow dynamics in the one dimensional free energy surface was measured by the autocorrelation function of $x(t)$ (Fig. 1d), which is a multi-exponential decay spanning many decades of timescales (1ms-1s), reflecting a rugged energy landscape. This is a general phenomenon, also seen in MD simulations at pico to nanosecond timescales (Luo 2006). These conformational fluctuations result in fluctuations in the catalytic rate of single enzyme molecules (English et al, 2006).

Many functionally important conformational motions in an enzyme are nonequilibrium relaxations triggered by either substrate binding to the enzyme or the chemical reaction, each contributing to a fraction of the total free energy driving force for a substrate-to-product conversion. This free energy driving force is related to Haldane and Pauling's picture of "strain" - upon substrate binding, the free energy released is used to distort the substrate/enzyme complex in such a way as to facilitate the



subsequent reaction. To quantify this picture, we have developed a dynamic rate theory similar in spirit to Marcus electron transfer theory. In the upper left panel in Fig. 2, the 1D harmonic potentials of mean force are shown for E·S, ES, E·P, EP complexes as a function of the conformational coordinate Q. Upon tight binding of the substrate (from E·S to ES), the system relaxes downhill to a different equilibrium position from which the chemical reaction occurs.

The chemical reaction catalyzed by the enzyme has a reaction coordinate (Fig. 2 right panel), X, along which chemical bond breaking, or formation takes place. The chemical reaction is slaved by the slow rate-limiting motion of other atoms within the protein. Consequently, the barrier height along the reaction coordinate is dependent on Q.

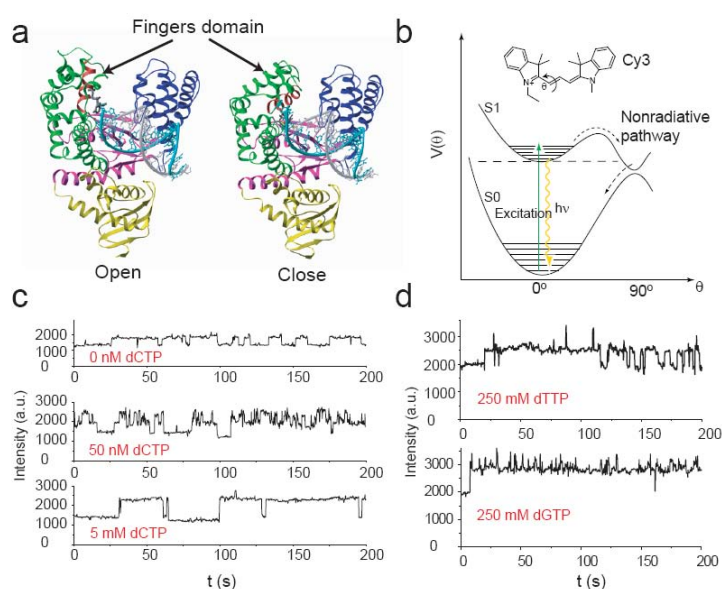
The bottom left panel in Fig. 2 shows the two dimensional free energy surface of an enzyme. The catalytic cycle is described as transitions from $E \cdot S \rightarrow ES \rightarrow E \cdot P \rightarrow EP$ of the four displaced harmonic surfaces in the XQ -space. The nonequilibrium relaxation upon substrate binding allows the enzyme to reach the well of ES at which the barrier for the chemical reaction in X is the smallest. This is the dynamic realization of the Pauling's well-known idea of transition state stabilization, which has often been presented only as a 1D picture as the right panel of Fig. 2.

This coarse-grained theory connects the protein conformational fluctuations that we measured in single molecule experiments with the thermodynamic driving force of the nonequilibrium enzymatic cycle (ΔG). Using this theory, we were able to account for the dispersed kinetics that we observed in single-molecule experiments (Min 2007a) and proves the validity of the Michaelis-Menten (MM)

equation under most conditions, and the deviation from the MM equation, i.e., the emergence of the positive and negative cooperativity (Min 2007b).

Single-molecule study of protein conformational change triggered by substrate binding (Dr. Guobin Luo, postdoctoral fellow, Dr. Mina Wang and Prof. William H. Konigsberg, collaborator at Yale Biochemistry)

To probe conformational change in the enzyme induced by substrate binding, we developed a new fluorescence assay for DNA polymerase, which replicates a single strand of DNA with extremely high fidelity with an error rate of 10^{-6} . The precise mechanism responsible for the base selectivity is an important and as yet unsolved problem. The crystal structure of DNA polymerase shows a hand-like structure (Fig. 3a). The binding of the substrate, dNTP, drives the closing of the fingers domain, which is a functionally important and large scale conformational change, followed by the chemical bond formation.



We take advantage of the environmental sensitivity of a Cy3 dye to monitor this functionally important conformational change in T7 DNA polymerase (T7 pol). The torsional motion of double bonds (Fig. 3b) in Cy3's excited state is responsible for the non-radiative relaxation of Cy3. Constraints of the torsional motion hinder the non-radiative decay pathway, giving a higher fluorescence quantum yield. This property makes Cy3 a valuable probe for detecting subtle conformational alterations.

Binding of T7 pol to an immobilized Cy3-labeled DNA duplex induces a $\sim 40\%$ intensity increase (top trace in Fig. 3b), allowing detection of the binding and dissociation kinetics of the T7 pol to the DNA duplex. An even higher intensity level of Cy3 appears when introducing a complementary substrate, dCTP, (middle trace Fig. 3c), to match the G base on the template. We attribute this highest intensity level to a new conformational state induced by substrate binding, reflecting the closing of the fingers domain. In contrast, when noncomplementary bases (dTTP or dGTP) were added, we observed fewer excursions to the highest level (Fig. 3d). We have determined that the rate constants of the conformational change induced by binding of complementary and noncomplementary substrates differ by a factor of 10^3 to 10^5 .

We reach the important conclusion that the observed conformational change is a very rapid step during DNA synthesis and allows efficient discrimination against the incorporation of non-complementary bases (Luo et al. 2007).

Future Plan

- We will continue to explore the relationship between conformational dynamics and the catalytic

reactivity and selectivity of enzymes. The predictions of our theory will be tested in a few enzymatic systems. In particular, the thermodynamic driving force dependence of the enzymatic activity will be investigated. Other single-molecule assays will be developed.

- We will study the molecular mechanism of allostery through single-molecule experiments.

Publications in 2004-2007 supported by DOE/BES

- (14) Min, Wei; Xie, X. Sunney; Bagchi, Biman "Enzyme Kinetics as a Non-Equilibrium Steady State Cycle on a Two Dimensional Reaction Free Energy Surface," *PNAS*, submitted (2007).
- (13) Min, Wei; Xie, X. Sunney; Bagchi, Biman "Two Dimensional Reaction Free Energy Surfaces of Catalytic Reaction: Effects of Protein Conformational Dynamics on Enzyme Catalysis," *J. Phys. Chem. B*, submitted (2007).
- (12) Luo, Guobin; Wang, Mina; Konigsberg, William H.; Xie, X. Sunney "Single-molecule and ensemble fluorescence assays for a functionally important conformational change in T7 DNA polymerase," *PNAS*, **104**, 12610-12615 (2007).
- (11) Min, Wei; Gopich, Irina V.; English, Brian P.; Kou, Sam C.; Xie, X. Sunney; Szabo, Attila "When Does the Michaelis-Menten Equation Hold for Fluctuating Enzymes?" *J. Phys. Chem. B*, **110**, 20093-7 (2006).
- (10) Luo, Guobin; Andricioaei, Ioan; Xie, X. Sunney; Karplus, Martin "Dynamic Distance Disorder in Proteins Is Caused by Trapping," *J. Phys. Chem. B*, **110**, 9363-9367 (2006).
- (9) Min, Wei; Xie, X. Sunney "Kramers Model with a Power-law Friction Kernel: Dispersed Kinetics and Dynamic Disorder of Biochemical Reactions," *Phys. Rev. E* **73**, 010902 (2006).
- (8) Min, Wei; Jiang, Liang; Yu, Ji; Kou, S.C.; Qian, Hong; Xie, X. Sunney "Nonequilibrium Steady State of a Nanometric Biochemical System: Determining the Thermodynamic Driving Force from Single Enzyme Turnover Time Traces," *Nano Lett.* **5**, 2373-2378 (2005).
- (7) Min, Wei; English, Brian P.; Luo, Guobin; Cherayil, Binny J.; Kou, S.C.; Xie, X. Sunney "Fluctuating Enzymes: Lessons from Single-Molecule Studies," *Acc. Chem. Res.* **38**, 923-931 (2005).
- (6) Debnath, Pallavi; Min, Wei; Xie, X. Sunney; Cherayil, Binny J. "Multiple Time Scale Dynamics of Distance Fluctuations in a Semiflexible Polymer: A One-dimensional Generalized Langevin Equation Treatment," *J. Chem. Phys.* **123**, 204903 (2005).
- (5) Krug II, John T.; Sánchez, Erik J. ; Xie, X. Sunney "Fluorescence Quenching in Tip-enhanced Nonlinear Optical Microscopy," *Appl. Phys. Lett.* **86**, 233102 (2005).
- (4) Kou, S.C.; Xie, X. Sunney; Liu, Jun S. "Bayesian Analysis of Single-molecule Experimental Data," *Appl. Statist.* **54**, 469 (2005).
- (3) Min, Wei; Luo, Guobin; Cherayil, Binny J.; Kou, S.C.; Xie, X. Sunney "Observation of a Power-Law Memory Kernel for Fluctuations within a Single Protein Molecule," *Phys. Rev. Lett.* **94**, 198302 (2005).
- (2) Kou, S.C.; Xie, X. Sunney "Generalized Langevin Equation with Fractional Gaussian Noise: Subdiffusion within a Single Protein Molecule," *Phys. Rev. Lett.* **93**, 18 (2004).
- (1) Cotlet, M.; Masuo, S.; Luo, G.B.; Hofkens, J.; Van der Auweraer, M.; Verhoeven, J.; Müllen, K.; Xie, X.S.; De Schryver, F. "Probing conformational dynamics in single donor-acceptor synthetic molecules by means of photoinduced reversible electron transfer," *Proc. Natl. Aca. Sci.* **101**, 14343 (2004).

Single-Molecule Dynamics in the Condensed Phase and at Interfaces

Time Resolved Single-Molecule Chemical Imaging Studies of Interfacial Electron Transfer

H. Peter Lu

Bowling Green State University
Department of Chemistry and Center for Photochemical Sciences
Bowling Green, OH 43403
hplu@bgsu.edu

Program Scope

Our research is focused on the use of single-molecule high spatial and temporal resolved techniques to understand molecular dynamics in condensed phase and at interfaces, especially, conformational dynamics associated with electron and energy transfer. Single-molecule approaches are unique for heterogeneous and complex systems because the static and dynamic inhomogeneities can be identified, characterized, and/or removed by studying one molecule at a time. Single-molecule spectroscopy reveals statistical distributions correlated with microscopic parameters and their fluctuations, which are often hidden in ensemble-averaged measurements. Single molecules (and molecular complexes) are observed in real time as they traverse a range of energy states, and the effect of this ever-changing "system configuration" on chemical reactions and other dynamical processes can be mapped. In this project, we focus on electron transfer reactions on solid surfaces (interfaces). An understanding of the fundamental interfacial ET processes will be important for developing efficient light harvesting systems for solar energy transformation and be broadly applicable to problems in interface chemistry and physics, and it is particularly powerful to study such heterogeneous systems by site-specific spectroscopy at single-molecule sensitivity and nanoscale specificity.

In our research, we have been integrating two complementary methodologies; single-molecule fluorescence spectroscopy and scanning probe microscopy (STM and AFM) to study interfacial electron transfer dynamics in solar energy conversion. We have been primarily focusing on studying electron transfer under ambient condition and electrolyte solution involving both single crystal and colloidal TiO₂ and related substrates. The molecular level understanding obtained from the fundamental interfacial electron transfer processes is significant and important for developing efficient light harvesting systems for solar cells and broadly applicable to problems in interface chemistry and surface physics, including redox reaction through bacterial cell surfaces and solar conversion in photosynthetic membranes.

Recent Progress and Future Plans

Correlated topographic and spectroscopic imaging of single-molecule interfacial electron transfer at TiO₂-electrolyte interfaces under solution. Interfacial electron transfer (ET) plays an important role in many chemical processes. For example, interfacial ET in TiO₂-based systems is critical to solar energy technology, catalysis, and waste water treatments. However, the microscopic mechanism of interfacial ET is not well understood with regard to atomic surface structure, molecular structure, bonding, orientation, and molecular motion. The complexity comes from both spatial and temporal inhomogeneities of the interfacial ET dynamics. We have applied single-molecule spectroscopy combined with AFM/STM imaging at room temperature under electrolyte solution to single-molecule studies of photo-sensitized interfacial ET processes in porphyrin-TiO₂ nanoparticle systems (Figure 1A and 1B). We have demonstrated STM imaging of single-molecule porphyrin derivative molecules under electrolyte solution

on an Au surface, and the redox states of the molecules can be controlled by a potential applied to the substrate surface (Figure 1C), and we have obtained both single-molecule fluorescence images and topographic images (Figure 1C and 2A) from porphyrin derivative molecules (Figure 1D).

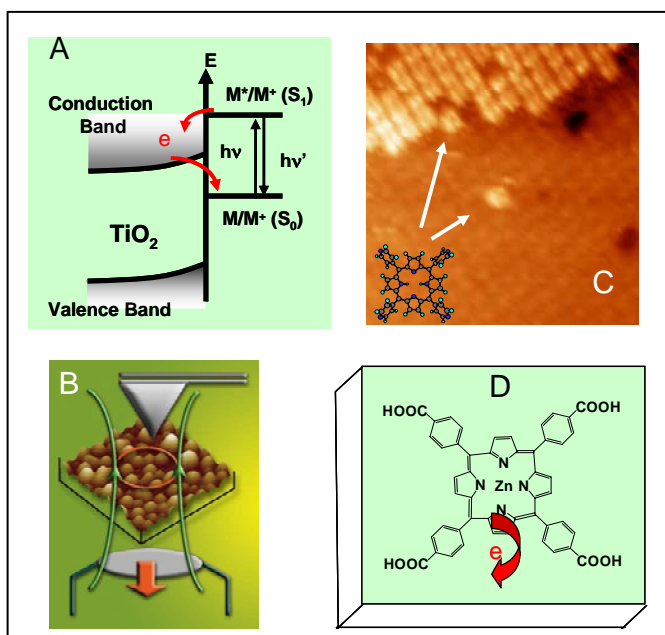


Figure 1. Correlated single-molecule spectroscopy imaging and scanning probe microscopy imaging of porphyrin/TiO₂ interfacial electron transfer dynamics under ambient conditions. **(A)** Schematic description of the interfacial electron transfer dynamics involved with both forward and backward electron transfers: Forward electron transfer from the excited state of the porphyrin derivative molecules to the conduction band or energetically-accessible surface states of TiO₂ single-crystals and nanoparticles; and backward electron transfer from TiO₂ to surface adsorbed porphyrin derivative molecule cations. **(B)** Correlated AFM/STM single-molecule imaging and single-molecule fluorescence imaging microscopy. The AFM/STM microscope and single-

molecule fluorescence imaging microscope are coupled in an over-and-under configuration for imaging the same nanoscale local sample area with single-molecule topographic and spectroscopic sensitivity, respectively. The STM imaging can also identify the redox state of the single-molecules. The features on the image are TiO₂ nanoparticles (~12±4 nm). **(C)** STM imaging (150 Å X 150 Å) of single-molecule porphyrin derivative molecules on an Au surface at a potential of 0.09 V_{SCE} and under 100 mM H₂SO₄ solution. **(D)** Molecular structure of the porphyrin derivative molecules that involve interfacial electron transfer on TiO₂ surfaces.

To decipher the underlying mechanism of the interfacial electron transfer dynamics, our on-going study of porphyrin interfacial electron transfer on single crystal TiO₂ surfaces will be continued by combining single-molecule fluorescence spectroscopy, AFM, and STM imaging. Our study will focus on understanding the interfacial electron transfer dynamics at specific crystal sites (kinks, planes, lattices, and corners) with high-spatially and temporally resolved topographic/spectroscopic characterization at individual molecule basis. In the future, we will further investigate single-molecule electronic coupling, electron transfer driving force, and back electron transfer dynamics in order to characterize the molecular-level origins of the inhomogeneous and complex interfacial electron transfer dynamics in the solar energy conversion system. Our experimental measurements will focus on electron transfer involving individual molecules, dimers, and small clusters of adsorbed molecules, on TiO₂ surfaces, under ambient conditions. AFM metal-tip and STM imaging will be performed on identical sites to extract dynamical data at a molecular spatial resolution. Using this approach, correlated information on the adsorption-site structure, molecular orientation, electronic structure, and single-molecule interfacial electron transfer dynamics will be obtained for the forward and backward electron transfer reactions.

Probing and analyzing single-molecule interfacial electron transfer dynamics. We have probed and characterized photo-induced single-molecule interfacial electron transfer processes in porphyrin-TiO₂ nanoparticle (NP) systems, using time-correlated single photon counting coupled with scanning confocal

fluorescence microscopy (Figure 2A). Fluorescence intensity trajectories of individual dye molecules adsorbed on TiO₂ NP surface showed fluorescence fluctuations and blinking, with time constants distributed from milliseconds to seconds (Figure 2B). We have also recorded the photon stamping single-molecule fluorescence trajectories to probe single photon arrival times and the photon delay times between photon to photon. We identified that the photons were all emitted from the S₁ → S₀ radiative transition when there is no electron transfer occurred, and the lag time between photon to photon is related to the back electron transfer time. We attributed the fluorescence fluctuations to the interfacial ET reaction rate fluctuations in competing with the nanosecond excited-state relaxation of the dye molecules, associating redox reactivity intermittency with the fluctuations of molecule-TiO₂ electronic and vibronic coupling. Intermittent interfacial ET dynamics of individual molecules, beyond the conventional kinetic scope, could be a characteristic of the surface chemical reactions strongly involved with and regulated by molecule-surface interactions. The fluorescence fluctuation dynamics were found to be inhomogeneous from molecule to molecule and from time to time, showing significant static and dynamic disorders in the interfacial ET reaction dynamics. The intermittent interfacial reaction dynamics that likely occur among single molecules in other interfacial and surface chemical processes can typically be observed by single-molecule studies, but not by conventional ensemble-averaged experiments. For the first time, we have observed that the back ET reactivity shows a strong memory effect, i.e., high reactivity likely follows high reactivity, and low reactivity follows low reactivity (Figure 2C and 2D). The origin of the memory effect is attributed to the electronic coupling fluctuation associated with molecular thermal motions. To decipher the underlying mechanism of the intermittent interfacial electron transfer dynamics, we plan to study porphyrin interfacial electron transfer on single crystal TiO₂ surfaces by using ps and sub-ps pump-probe ultrafast single-molecule spectroscopy. Our study will focus on understanding the interfacial electron transfer dynamics at specific crystal sites (kinks, planes, lattices, and corners) with high-spatially and temporally resolved topographic/spectroscopic characterization at individual molecule basis.

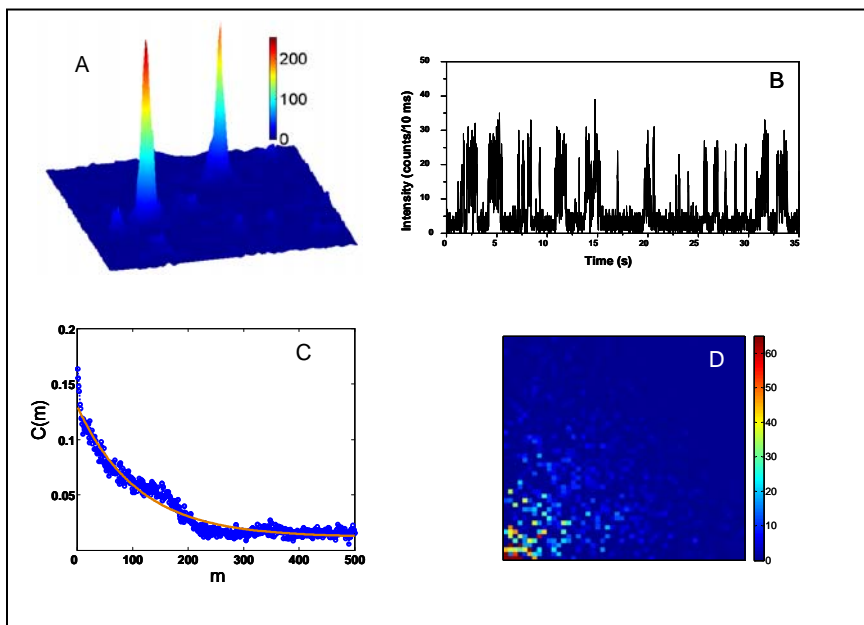


Figure 2: Single-molecule imaging and spectroscopy studies of interfacial electron transfer dynamics. **(A)** Single molecule porphyrin fluorescence image (10 μm X 10 μm) on a TiO₂ nanoparticle covered glass surface. The peaks are from the fluorescence photon counting of individual porphyrin molecules. **(B)** Single-molecule fluorescence intensity time trajectory. The fluctuating intensity reflects the intermittent electron transfer

activity: when the electron transfer activity is high, the fluorescence intensity is low; and vice versa. **(C)** Autocorrelation function of photon-pair time during high interfacial electron transfer activity period. The index number of consecutive pair times is “m.” The decay time of $\tau_m=150$ indicates that there is a memory time between the electron transfer active periods, i.e., a longer ET active time likely follows a longer ET active time, and a shorter ET active time likely follows a shorter ET active time. The memory effect exponentially decays to zero at a decay index of 150 consecutive ET active times. **(D)** A 2D plot of

consecutive photon-pair times ($t_{\text{pair-time}(i)}$ vs $t_{\text{pair-time}(i+1)}$) shows a memory effect evidenced by the higher population of data points along the diagonal region.

We will further develop our new approach that combines complementary techniques: single-molecule time-resolved fluorescence spectroscopy and scanning tunneling microscopy imaging to analyze the spatially and temporally complex interfacial ET dynamics. Our experimental measurements will focus on electron transfer involving individual molecules, dimers, and small clusters of adsorbed molecules, on TiO_2 surfaces, under ambient conditions. The adsorbed molecules will be selected porphyrin and perylene derivatives. The substrates will consist of single-crystal and thin film rutile and anatase. AFM metal-tip and STM imaging will be performed on identical sites to extract dynamical data at a molecular spatial resolution. Using this approach, correlated information on the adsorption-site structure, molecular orientation, electronic structure, and single-molecule interfacial electron transfer dynamics will be obtained for the forward and backward electron transfer reactions.

Revealing fluctuating solar energy conversion process in native photosynthetic membrane under ambient condition. The mechanism by which light is converted into chemical energy in a natural photosynthetic system has drawn considerable research interest. Using single-molecule fluorescence spectroscopy and AFM microscopic imaging, we have observed: (1) light harvesting complex proteins form short linear assemblies (aggregates) in native photosynthetic membranes, and (2) the inter-molecular protein fluorescence resonant energy transfers (FRET) amongst light harvesting proteins I and II (LH1 and LH2) in bacterial photosynthetic membranes is intermittent or highly fluctuating. The LH2 protein aggregation is typically 5 ± 2 proteins per aggregate. Our results suggest that the light harvesting complex proteins typically ($\sim 70\% \pm 10\%$ of the population) exist as linear aggregates in the photosynthetic membranes. Using two-channel FRET photon-counting detection and a novel two-dimension cross-correlation function amplitude mapping analysis, we revealed fluorescence intensity and spectral fluctuations of donor (LH2) and acceptor (LH1) fluorescence involving FRET. Our results suggest that there are dynamic coupled and non-coupled states of the light-harvesting protein assemblies in photosynthetic membranes. The light-harvesting complex assembly under ambient conditions and under water involves dynamic inter-molecular structural fluctuations that subsequently disturb the degree of energy transfer coupling between proteins in the membrane. Such intrinsic and dynamic heterogeneity of the native photosynthetic membranes, often emerged under the overall thermally-induced spectral fluctuations and not observable in an ensemble-averaged measurement, likely plays a critical role in regulating the light harvesting efficiency of the photosynthetic membranes. Single-molecule fluorescence lifetime measurement and correlated AFM/STM characterization will be applied to identify the optical coupling of the linear aggregation. The outcome of this study will likely have a high impact and will significantly enhance our knowledge about how the solar energy is harvested and converted in nature.

Publications of DOE sponsored research (FY2004-2007)

1. Duohai Pan, Dehong Hu, Ruchuan Liu, Xiaohua Zeng, Samuel Kaplan, H. Peter Lu, "Fluctuating Two-State Light Harvesting in a Photosynthetic Membrane," *J. Phys. Chem. C*, **111**, 8948-8956 (2007).
2. Qiang Lu, H. Peter Lu, and Jin Wang, "Exploring the Mechanism of Flexible Biomolecular Recognition with Single Molecule Dynamics," *Phys. Rev. Lett.* **98**, 128105 (2007).
3. V. Biju, D. Pan, Yuri A. Gorby, Jim Fredrickson, J. Mclean, D. Saffarini and H. Peter Lu, "Correlated Spectroscopic and Topographic Characterization of Nanoscale Domains and Their Distributions of a Redox Protein on Bacterial Cell Surfaces," *Langmuir* **23**, 1333-1338 (2007).

4. Ruchuan Liu, Dehong Hu, Xin Tan, and H. Peter Lu, "Revealing Two-State Protein-Protein Interactions of Calmodulin by Single-Molecule Spectroscopy," *J. Am. Chem. Soc.* **128**, 10034-10042 (2006).
5. Jin Wang, Qiang Lu, and H. Peter Lu, "Single-Molecule Dynamics Reveals Cooperative Binding-Folding in Protein Recognition," *PLoS Computational Biology*, **2**, 842-852 (2006).
6. Dehong Hu and H. Peter Lu, "Single molecule electron transfer process of ruthenium complexes," *Proc. SPIE* Vol. **6092**, 609207 (2006).
7. T. Zhang, S. N. Danthi, J. Xie, D. Hu, H. P. Lu, and K. Li, "Live cell imaging of the endocytosis and the intracellular trafficking of multifunctional lipid nanoparticles," *Proc. SPIE* Vol. **6095**, 60950D (2006).
8. Duohai Pan, Nick Klymyshyn, Dehong Hu, and H. Peter Lu, "Tip-enhanced near-field Raman spectroscopy probing single dye-sensitized TiO₂ nanoparticles," *Appl. Phys. Lett.*, **88**, 093121(2006).
9. Duohai Pan, Dehong Hu, and H. Peter Lu, "Probing Inhomogeneous Vibrational Reorganization Energy Barriers of Interfacial Electron Transfer," *J. Phys. Chem. B*, **109**, 16390-16395 (2005).
10. Dehong Hu and H. Peter Lu, "Single-Molecule Triplet-State Photon Antibunching at Room Temperature," *J. Phys. Chem. B*, **109**, 9861-9864 (2005).
11. H. Peter Lu, invited review article, "Probing Single-Molecule Protein Conformational Dynamics," *Acc. Chem. Res.* **38**, 557-565 (2005).
12. H. Peter Lu, "Single-Molecule Study of Protein-Protein and Protein-DNA Interaction Dynamics," an invited book chapter in *Protein-Ligand Interactions*, edited by Uli Nienhaus, The Humana Press Inc., 2005.
13. H. Peter Lu, invited review article, "Site-Specific Raman Spectroscopy and Chemical Dynamics of Nanoscale Interstitial Systems," *J. Physics: Condensed Matter*, **17**, R333-R355 (2005).
14. V. Biju, Miodrag Micic, Dehong Hu, and H. Peter Lu, "Intermittent Single-Molecule Interfacial Electron Transfer Dynamics," *J. Am. Chem. Soc.* **126**, 9374-9381 (2004).
15. Xin Tan, Dehong Hu, Thomas C. Squier, and H. Peter Lu, "Probing Nanosecond Protein Motions of Calmodulin by Single-Molecule Fluorescence Anisotropy," *Applied Phys. Lett.*, **85**, 2420-2422 (2004).
16. Miodrag Micic, Dehong Hu, Greg Newton, Margie Romine, H. Peter Lu, "Correlated Atomic Force Microscopy and Fluorescence Lifetime Imaging of Live Bacterial Cells," *Surface and Colloid B*, **34**, 205-212 (2004).
17. H. Peter Lu, invited review, "Single-molecule spectroscopy studies of conformational change dynamics in enzymatic reactions," a special issue of *Curr Pharm Biotech* (The way down from single genes, and proteins to single molecules.), **5**, 261-269 (2004).
18. Dehong Hu, H. Peter Lu, "Single Molecule Implanting of T4 Lysozyme on Bacterial Cell Surface: Towards Study Single Molecule Enzymatic Reaction in Living Cells," *Biophys. J.*, **87**, 656-661 (2004).
19. D. Hu, M. Micic, N. Klymyshyn, Y. D. Suh, H. Peter Lu, "Correlated topographic and spectroscopic imaging by combined atomic force microscopy and optical microscopy," *J. Luminescence*, **107**, 4-12 (2004).

20. G. Harms, G. Orr, H. Peter Lu, "Probing ion channel conformational dynamics using simultaneous single-molecule ultrafast spectroscopy and patch-clamp electric recording," *Appl. Phys. Lett.*, **84**, 1792-1794 (2004).
21. Xin Tan, Perihan Nalbant, Alexei Touthkine, Dehong Hu, Erich R. Vorpagel, Klaus M. Hahn, and H Peter Lu, "Single-Molecule Study of Protein-Protein Interaction Dynamics in a Cell Signaling System," *J. Phys. Chem. B.*, **108**, 737 (2004).
22. Miodrag Micic, Nicholas Klymyshyn, H. Peter Lu, "Finite Element Method Simulations of the Near-Field Enhancement at the vicinity of Fractal Rough Metallic Surfaces," *J. Phys. Chem. B.*, **108**, 2939 (2004).

Ab initio approach to interfacial processes in hydrogen bonded fluids

Christopher J. Mundy
Chemical and Materials Sciences Division
Pacific Northwest National Laboratory
902 Battelle Blvd, Mail Stop K1-83
Richland, WA 99352
chris.mundy@pnl.gov

Program Scope

The long-term objective of this research is to develop a fundamental understanding of processes, such as transport mechanisms and chemical transformations, at interfaces of hydrogen-bonded liquids. Liquid surfaces and interfaces play a central role in many chemical, physical, and biological processes. Many important processes occur at the interface between water and a hydrophobic liquid. Separation techniques are possible because of the hydrophobic/hydrophilic properties of liquid/liquid interfaces. Reactions that proceed at interfaces are also highly dependent on the interactions between the interfacial solvent and solute molecules. The interfacial structure and properties of molecules at interfaces are generally very different from those in the bulk liquid. Therefore, an understanding of the chemical and physical properties of these systems is dependent on an understanding of the interfacial molecular structure. The adsorption and distribution of ions at aqueous liquid interfaces are fundamental processes encountered in a wide range of physical systems. In particular, the manner in which solvent molecules solvate ions at the interface is relevant to problems in a variety of areas. Another major focus lies in the development of models of molecular interaction of water and ions that can be parameterized from high-level first principles electronic structure calculations and benchmarked by experimental measurements. These models will be used with appropriate simulation techniques for sampling statistical mechanical ensembles to obtain the desired properties.

Progress Report (2004-2007)

The progress report given by Christopher Mundy (marked with an asterisk) was work that was performed independently while he was at Lawrence Livermore National Laboratory until 2006. For completeness Mundy's work at LLNL is included because it demonstrates a clear relationship to BES funded previous and future work.

Characterization of aqueous liquid-vapor interface with DFT based interaction potentials*: We performed the first *ab initio* molecular dynamics calculation of the aqueous liquid-vapor interface giving a full elucidation of the electronic states and the concomitant reactivity.^{1,2} In order to make indirect contact with recent x-ray absorptions studies³, we computed the local hydrogen-bond populations at the interface and compared to results in the bulk. Our findings indicate the presence of the so-called "acceptor-only" moiety as well as an abundance of the well characterized "single-donor" species. Remarkably, the density functional theory (DFT) interaction potentials reproduced the surface expansion at the vicinity of the liquid-vapor interface that manifests itself in

lengthening of the average oxygen-oxygen that was measured in recent x-ray absorption experiments (XAS).⁴ A recent, detailed follow-up study directly compared DFT results to standard empirical potentials for water (including polarizable models). This study confirmed the DFT results of and enhanced population of the “acceptor-only” moiety in the vicinity of the liquid-vapor interface. It was found that the hydrogen-bond populations were independent of the interaction potential being used.⁵

Probing the statistical mechanics of *ab initio* interaction potentials with Gibb’s ensemble Monte Carlo*: The simulation of the liquid-vapor interface in the standard slab geometry (for example, see Mundy and Kuo²) will allow for the density in the center of the slab to equilibrate to the density prescribed by the underlying interaction potential. In the case of the DFT interaction potential, the density of bulk water at 300K and 1 atm was found to be significantly less than 1 g/cc. In fact, given the fact that DFT interaction potentials do not contain attractive forces due to dispersion, it is not clear that DFT is able to produce a stable liquid phase. Thus, in order to probe the statistical mechanics of DFT interaction potentials, new algorithms combining smart Monte Carlo moves with electronic structure calculations were developed. To this end, we performed the first *ab initio* Monte Carlo simulations providing benchmark calculations on the structure and thermodynamics of liquid water.⁶⁻⁸ *Our findings are consistent with those in the original interface study⁹ with a DFT interaction potential giving a density of liquid water at ambient conditions of roughly .9 g/cc.*

Development of DFT-based models of polarization*: Our previous attempt to construct a polarizable model based on the sound DFT methodology was applied to molten salts where polarization is known to be important.¹⁰ This first attempt was able to produce a working model of alkali-halide salts using an empirical potential fit to DFT runs, and polarizable parameters (e.g., basis functions, hardness, and electronegativity) fit to DFT linear-response calculations. Although the model was successful, the parameterization was cumbersome and a new approach had to be devised. To this end, we provided a pure DFT based model where the only input parameters were based on fits of the response basis functions, hardness, and electronegativity to simple atomic calculations. This model provided the same quality of results that were obtained from our original work where we fit to CPMD data using a simple parameterization scheme.¹¹

Future directions

Calculation of the surface potential for liquid-vapor interfaces. The electrostatic potential at the coexisting liquid-vapor phases is another sensitive probe of the structure of the fluid interface. Moreover, it is a quantity that cannot easily be measured and there is even some controversy as to the over-all sign of the surface potential from both theory and experiment.¹² The importance of understanding the origins and the sign of the surface potential has far reaching implications of understanding the free-energies of ion solvation and the hydrophobic interactions.^{13,14} In light of the new conventional wisdom emerging on the structure of ions at aqueous interfaces and interfacial structure of neat water and neat methanol interfaces, knowledge of the surface potential provides a piece of the fundamental chemical physics of hydrogen-bonded fluids. Although there have been many attempts to compute the surface potential using both fixed charge and polarizable

models yielding qualitative agreement between studies,¹⁵⁻¹⁹ it has been suggested that without the explicit treatment of electrons, the computed surface potential could yield a different relative sign.^{14,16-18} Our goal is to perform the calculation of the surface potential of methanol and water using DFT interaction potentials. These calculations will be used to further judge the accuracy and transferability of DFT applied to heterogeneous environments. Moreover, the degree to which the surface potential is non-monotonic in the vicinity of the interface will be examined without assumptions on the form of the electronic multipoles used to describe the electrostatic interactions. Using liquid-vapor interface trajectories of water and methanol obtained using DFT interaction potentials, we propose to compute the electrostatic potential resulting from the electron and core charges within DFT. It is this potential that will be averaged and integrated to obtain the electrostatic potential (and electric field) as a function of the interfacial coordinate. This methodology can be used in conjunction with configurations of ionic aqueous solutions to generate surface potentials of aqueous systems relevant to experiment in order to help resolve the discrepancies between experiment and theory.^{12,14}

Development of a intermolecular interactions based on a self-consistent treatment of polarization within a minimal basis set density functional theory (DFT): The ability to perform high-quality statistical mechanical analysis using interaction potentials based on first-principles is in its infancy. Although there are many well formulated statistical sampling methods in the literature that have been utilized with classical empirical interaction potentials, the treatment of charge transfer and bond breaking is imperative when investigating complex chemical reactions and structure that are present at the interfaces of hydrogen bonding fluids. In order to routinely perform large calculations on interfaces using first-principles interaction potentials, we will take full advantage of the existing framework for parallelization and fast electronic structure that is currently present in CP2K (www.cp2k.berlios.de). It is well known that minimal basis set DFT poorly describes hydrogen bonding and weak electrostatic complexes. However, the relative efficiency compared to the use of larger basis sets (*e.g.* double and triple zeta with polarization) in conjunction with state of the art diagonalization routines make minimal basis set methods attractive to study large condensed phase systems where charge transfer and chemistry can be dominant. In our proposed work, we will attempt to understand and improve the description of hydrogen bonding within a minimal basis set approach with the addition of a self-consistent polarization term that can be identified with the quadratic polarization self-energy of empirical models (*e.g.* linear response). This identification will allow us to make a direct comparison to polarizable empirical models and existing self-consistent tight-binding methods. By making a correspondence between DFT methods and empirical methods, we expect to be able to add extra polarization terms, capturing the diffuse nature of the electronic wave function in a self-consistent manner, and thus developing a “self-consistent polarization DFT” (SCP-DFT) theory. Furthermore, within this theoretical framework, a consistent expression for the dispersion energy that is based on second-order perturbation theory can be formulated. This is an extension of an approach that has already been applied to DFT and forms that basis of empirical generalizations of London dispersion^{20,21}.

- (1) Kuo, I. F. W.; Mundy, C. J. *Science* **2004**, *303*, 658-660.

- (2) Mundy, C. J.; Kuo, I. F. W. *Chemical Reviews* **2006**, *106*, 1282-1304.
- (3) Wilson, K. R.; Cavalleri, M.; Rude, B. S.; Schaller, R. D.; Nilsson, A.; Pettersson, L. G. M.; Goldman, N.; Catalano, T.; Bozek, J. D.; Saykally, R. J. *Journal of Physics-Condensed Matter* **2002**, *14*, L221-L226.
- (4) Wilson, K. R.; Schaller, R. D.; Co, D. T.; Saykally, R. J.; Rude, B. S.; Catalano, T.; Bozek, J. D. *Journal of Chemical Physics* **2002**, *117*, 7738.
- (5) Kuo, I. F. W.; Mundy, C. J.; Eggimann, B. L.; McGrath, M. J.; Siepmann, J. I.; Chen, B.; Viecelli, J.; Tobias, D. J. *Journal of Physical Chemistry B* **2006**, *110*, 3738-3746.
- (6) McGrath, M. J.; Siepmann, J. I.; Kuo, I. F. W.; Mundy, C. J.; VandeVondele, J.; Hutter, J.; Mohamed, F.; Krack, M. *Chemphyschem* **2005**, *6*, 1894-1901.
- (7) McGrath, M. J.; Siepmann, J. I.; Kuo, I. F. W.; Mundy, C. J.; VandeVondele, J.; Hutter, J.; Mohamed, F.; Krack, M. *Journal of Physical Chemistry A* **2006**, *110*, 640-646.
- (8) McGrath, M. J.; Siepmann, J. I.; Kuo, I. F. W.; Mundy, C. J.; VandeVondele, J.; Sprik, M.; Hutter, E.; Mohamed, F.; Krack, M.; Parrinello, M. *Computer Physics Communications* **2005**, *169*, 289-294.
- (9) Kuo, I. F. W.; Mundy, C. J.; McGrath, M. J.; Siepmann, J. I.; VandeVondele, J.; Sprik, M.; Hutter, J.; Chen, B.; Klein, M. L.; Mohamed, F.; Krack, M.; Parrinello, M. *Journal of Physical Chemistry B* **2004**, *108*, 12990-12998.
- (10) Tabacchi, G.; Mundy, C. J.; Hutter, J.; Parrinello, M. *Journal of Chemical Physics* **2002**, *117*, 1416-1433.
- (11) Tabacchi, G.; Hutter, J.; Mundy, C. J. *Journal of Chemical Physics* **2005**, *123*, 074108.
- (12) Parfenyuk, V. I. *Colloid Journal* **2002**, *64*, 588-595.
- (13) Pegram, L. M.; Record, M. T. *Proceedings of the National Academy of Sciences of the United States of America* **2006**, *103*, 14278-14281.
- (14) Beattie, J. K. *The Intrinsic Charge at the Hydrophobe/Water Interface*; Wiley-VCH Verlag GmbH & Co. KGaA: Weinheim, 2006.
- (15) Sokhan, V. P.; Tildesley, D. J. *Molecular Physics* **1997**, *92*, 625-640.
- (16) Pratt, L. R. *Journal of Physical Chemistry* **1992**, *96*, 25-33.
- (17) Wilson, M. A.; Pohorille, A.; Pratt, L. R. *Journal of Chemical Physics* **1988**, *88*, 3281-3285.
- (18) Wilson, M. A.; Pohorille, A.; Pratt, L. R. *Journal of Physical Chemistry* **1987**, *91*, 4873-4878.
- (19) Wick, C. D.; Dang, L. X.; Jungwirth, P. *Journal Of Chemical Physics* **2006**, *125*, 024706.
- (20) Misquitta, A. J.; Jeziorski, B.; Szalewicz, K. *Physical Review Letters* **2003**, *91*, 033201.
- (21) Misquitta, A. J.; Podeszwa, R.; Jeziorski, B.; Szalewicz, K. *Journal of Chemical Physics* **2005**, *123*, 214103.

Interfacial Oxidation of Complex Organic Molecules

G. Barney Ellison — (Grant DE-FG02-93ER14364)

We have fabricated a new experiment to study the oxidation of surfactants coating water droplets.¹ This instrument is designed to produce a stream of saline-water droplets that are coated with organics, to size-select them, and to inject them into an atmospheric flow tube where they will be dosed with OH radicals. The resulting oxidized particles will be analyzed with a mass spectrometer.

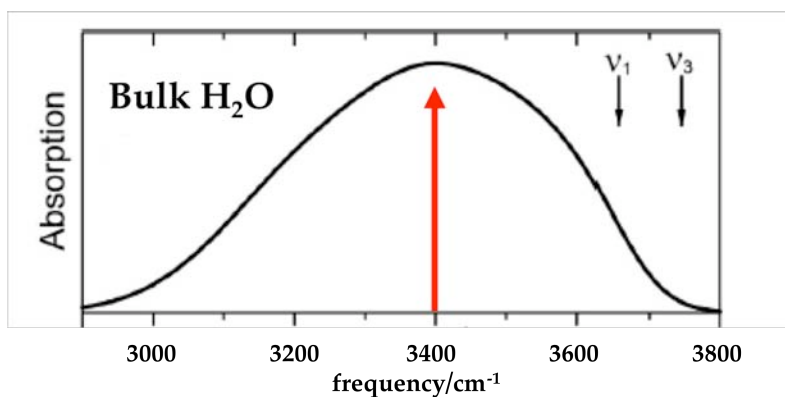
The instrument we have built is a novel mass spectrometer that can analyze a stream of μm -sized saline-water droplets that are coated with a film of surfactants.¹ These particles are entrained in a flow tube in a stream of dry air (20% O_2 /80% N_2) at 1 atm pressure. We plan to oxidize these surfactant-coated droplets with OH/ O_2 radicals. Micron-sized saline-water droplets are coated with the salt of an organic acid such as SDS or lauric acid, $\text{CH}_3(\text{CH}_2)_{10}\text{CO}_2^-\text{Na}^+$. We use an atomizer to produce a stream of particles that are dried and size-selected with a differential mobility analyzer (DMA). The DMA is selected to pass particles with $d_{\text{dry}} = 0.62 \text{ nm}$. The stream of monodisperse particles emerging from the DMA is re-humidified and the dried Na^+NO_3^- /surfactant particles will grow to $1 \mu\text{m}$ at 80% relative humidity (RH). Our device generates about 10^4 droplets cm^{-3} . The resulting saline-water droplets are entrained in a stream of air ($V_{\text{stream}} \cong 10 \text{ cm sec}^{-1}$) in a flow tube with the RH carefully regulated at 80%.

A $1 \mu\text{m}$ saline-water, organic aerosol contains roughly 10^{10} waters in the core and carries about 10^7 surfactant $\text{CH}_3(\text{CH}_2)_{10}\text{CO}_2^-$ ions at the droplet/atmosphere interface. The heat of vaporization of water is 40.7 kJ mol^{-1} so it takes roughly 1 nJ to vaporize a $1 \mu\text{m}$ aqueous droplet. The absorption spectrum of bulk water² is shown in the Fig. to the left. Because 3400 cm^{-1} is not resonant with any modes of a carboxylic acid, the droplet mass spectrometerⁱ

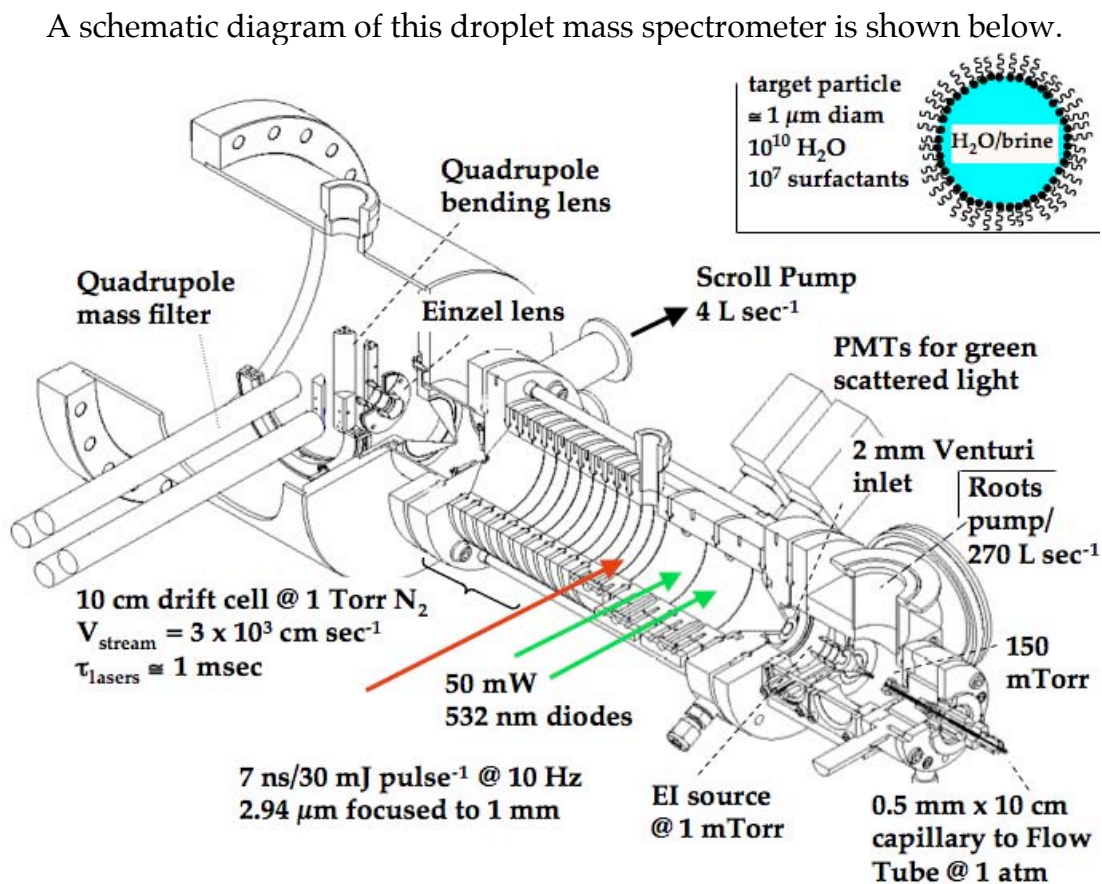
¹ Luis A. Cuadra-Rodriguez, Bradley A. Flowers, Donald E. David, Stephen E. Barlow, Alla Zelenyuk, and G. Barney Ellison, "Mass spectroscopy of saline-water droplets", J. Chem. Phys. (in preparation, 2007).

² W. H. Robertson & M. A. Johnson, Annu. Rev. Phys. Chem. **54**, 173 (2003).

uses an OPO IR source to dissociate these aqueous droplets. The LaserVision OPO is pumped by a YAG laser and delivers 30 mJ/7nsec of 2.94 μm (3400 cm^{-1}) radiation focused to a 1 mm spot. The imaginary part of the refractive index of water provides the absorption coefficient and a 1 μm droplet will absorb 18 nJ of the 10 mJ pulse. There are no organic vibrational modes that are resonant with the 3400 cm^{-1} radiation. The absorption coefficient of water, $\alpha(\text{H}_2\text{O}, 2.93 \mu\text{m})$, is measured to be 0.88 μm^{-1} so the penetration depth is roughly 1.1 μm . Consequently all of the 18 nJ will be absorbed by the saline-water core of the particle. The surfactant-coated droplet will completely dissociate and release the surfactant negative ions for analysis by a quadrupole mass filter.



A schematic diagram of this droplet mass spectrometer is shown below.



We have a major problem of the clustering of the surfactant anions to water. Extensive water-clustering of our target species will obscure the OH radical chemistry. We have built a drift region following the laser/aerosol dissociation region. The drift cell operates at about 100 Td and it will gently dissociate the $\text{RCO}_2^-(\text{water clusters})_n$. Photodissociation of a 1 μm droplet in the drift cell will release 10^7 ions and a gentle extraction lens (200 V cm^{-1}) will collect the resultant RCO_2^- ions into a quadrupole mass filter.

My student Luis Cuadra-Rodriguez continues to spend several months visiting EMSL at the Pacific Northwest National Laboratories where he works in Dr. A. Zelenyuk's laboratory. Some of the results from Cuadra-Rodriguez's visits to PNNL are described^{3 4} by two papers; other results were reported^{5 6 7 8} at several national meetings.

³ Alla Zelenyuk, Dan Imre, and Luis A. Cuadra-Rodriguez, "Evaporation of Water from Particles in the Aerodynamic Lens Inlet: An Experimental Study", *Anal. Chem.* **78**, 6942-6947 (2006).

⁴ Alla Zelenyuk, Dan Imre, Luis A. Cuadra-Rodriguez, and Barney Ellison, "Measurements and interpretation of the effect of a soluble organic surfactant on the density, shape and water uptake of hygroscopic particles", *J. Aerosol Sci.*, (2007). doi: [10.1016/j.jaerosci.2007.06.006](https://doi.org/10.1016/j.jaerosci.2007.06.006) (2007).

⁵ Cuadra-Rodriguez, L. A., Zelenyuk, A., Imre, D., and Ellison B. (2006). The Effect Of Organic Surfactants On The Properties Of Common Hygroscopic Particles: Effective Densities, Reactivity And Water Evaporation Of Surfactant Coated Particles, *Eos Trans. AGU*, 87(52), Fall Meet. Suppl., Abstract A33A-0951.

⁶ Zelenyuk, A., L. Cuadra-Rodriguez, D. Imre, S. Shimpi, and A. Warey. Comprehensive Characterization of Ultrafine Particulate Emission From 2007 Diesel Engines: PM Size Distribution, Loading And Individual Particle Size And Composition. *Eos Trans. AGU*, 87(52), Fall Meet. Suppl., Abstract A43A-0121.

⁷ Zelenyuk, A., D. Imre, L. Cuadra-Rodriguez, S. Shimpi, A. Warey. The Size And Composition Of Individual Ultrafine Diesel Emission Particulate From 2007 Diesel Engines With And Without After treatment. The 12th Annual Diesel Engine Emission Reduction (DEER) Conference, Detroit, MI, August 2006.

⁸ Zelenyuk, A., Imre, D., Cuadra-Rodriguez, L. A., and Ellison B. Measurements and Interpretation of the Effect of Soluble Organic Surfactants on the Density, Shape and Water Uptake of Hygroscopic Particles. The 26th Annual American Association for Aerosol Research (AAAR) Conference, September 24-28, 2007, Reno, NV.

Molecular Theory & Modeling

Development of Statistical Mechanical Techniques for Complex Condensed-Phase Systems

Gregory K. Schenter
Chemical & Materials Sciences Division
Pacific Northwest National Laboratory
902 Battelle Blvd.
Mail Stop K1-83
Richland, WA 99352
greg.schenter@pnl.gov

Program Scope

The long-term objective of this project is to advance the understanding of the relation between detailed descriptions of molecular interactions and the prediction and characterization of macroscopic collective properties. To do this, we seek to better understand the relation between the form and representation of intermolecular interaction potentials and simulation techniques required for statistical mechanical determination of properties of interest. Molecular simulation has the promise to provide insight and predictive capability of complex physical and chemical processes in condensed phases and interfaces. For example, the transport and reactivity of species in aqueous solutions, at designed surfaces, in clusters and in nanostructured materials play significant roles in a wide variety of problems important to the Department of Energy.

We start from the premise that a detailed understanding of the intermolecular interactions of a small collection of molecules, through appropriate modeling and statistical analysis, will enable us to understand the collective behavior and response of a macroscopic system, thus allowing us to predict and characterize thermodynamic, kinetic, material, and electrical properties. Our goal is to improve understanding at the molecular level in order to address increasingly more complex systems ranging from homogeneous bulk systems to multiple phase or inhomogeneous ones, to systems with external constraints or forces. Accomplishing this goal requires understanding and characterization of the limitations and uncertainties in the results, thereby improving confidence in the ability to predict behavior as systems become more complex.

Recent Progress

In our efforts to understand the balance between the complexity of molecular interaction and appropriate simulation techniques we have explored the quantum statistical mechanical treatment of nuclear degrees of freedom. Using the recently developed TTM2-F (2.1) flexible model for water that has been parameterized to reproduce the electronic Born-Oppenheimer energy surface determined from converged electronic structure calculations, quantum statistical path integral simulation techniques were employed to recover the radial distribution functions to be compared to experimental X-ray and neutron scattering measurements.¹² Quantitative agreement between simulation and measurement is seen for the peak position and width when quantum statistical mechanical sampling is taken into account. The heat of vaporization for this model of water predicts a value of 11.2 kcal/mol compared to the experimental measurement of 10.5 kcal/mol. This difference may be accounted for by improving the description of

intramolecular vibrational frequency shifts and has motivated the development of a next generation of water models to be used with quantum statistical mechanical simulation by Xantheas *et al.*

In a related effort, we considered the quantum statistical mechanical effects on the phase equilibria of water. Gibbs ensemble Monte Carlo coupled with Feynman path integration was employed using a TIP4P rigid model for water.⁹ Using the same molecular interaction, the quantum statistical mechanical simulation had lower liquid densities and higher vapor densities than the classical statistical mechanical simulation, resulting in a narrowing of the phase envelope. This corresponded to a 22K shift in the temperature of the system. (Figure 1)

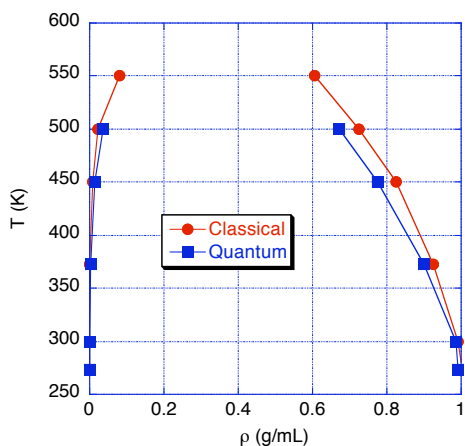


Figure 1a) Quantum phase equilibria of water.

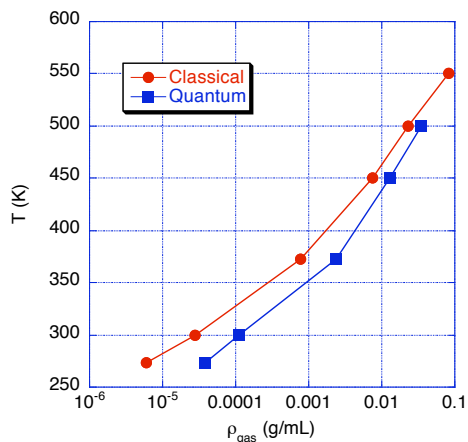


Figure 1b) Low density quantum phase equilibria of water.

In developing interaction potentials that can be used to describe ion-water interactions, we have recently focused on the relation between accurate *ab initio* electronic structure calculations of aqueous ion clusters, extended X-ray absorption fine structure (EXAFS) measurements and empirical potentials used in molecular simulation. A series of Ion-Water intermolecular potentials have been evaluated through comparison to EXAFS measurements. These include Ca^{2+} , Sr^{2+} ,^a K^+ ,⁷ and Cl^- .¹³ In all of these studies of the solvation of ions, the water-water interactions are described by the Dang-Chang rigid-body polarizable potential.^b In this work an ensemble of configurations is generated using the empirical potential and molecular dynamics simulation. From this ensemble, a series of electron multiple scattering calculations are performed using the FEFF8 code^c to generate a configuration averaged EXAFS spectra. The fine

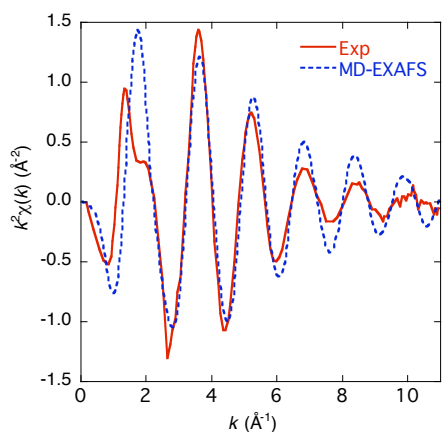


Figure 2a) $\text{Ca}^{2+}(\text{aq})$ EXAFS.

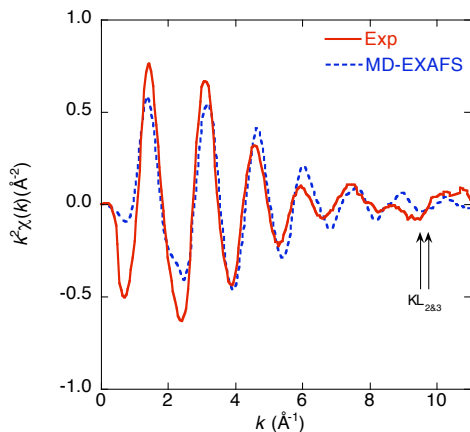


Figure 2b) $\text{K}^+(\text{aq})$ EXAFS.

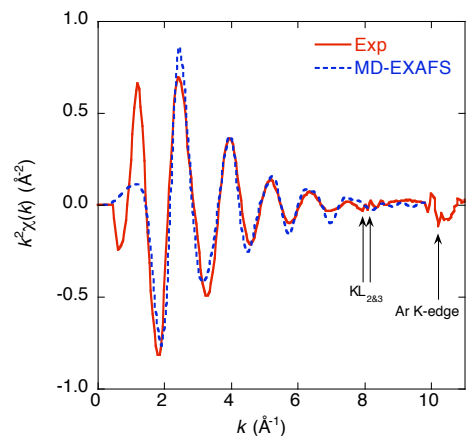


Figure 2c) $\text{Cl}^-(\text{aq})$ EXAFS.

structure $\chi = (\mu - \mu_0) / \Delta\mu_0$, where μ is the X-ray absorption, μ_0 is the background and $\Delta\mu_0$ is absorption edge jump. Quantitative agreement is recovered between experimental measurements (Exp) and ensemble averaged fine structure (MD-EXAFS) (See Figure 2).

Future Plans

In future studies we will consider the influence of molecular interaction between ion-pairs. Our challenge is to be able to account for changes in features in EXAFS measurement as a function of solute concentration. We have carried out some preliminary simulations of the

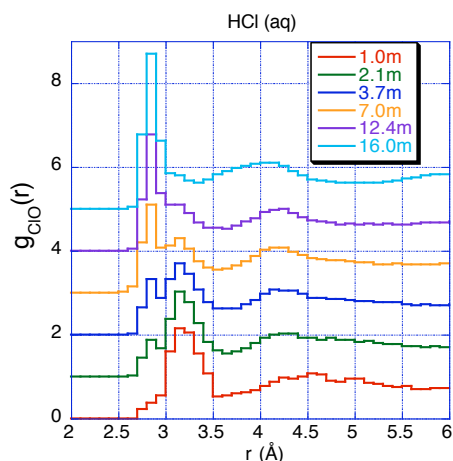


Figure 3a) Radial Distribution vs. concentration.

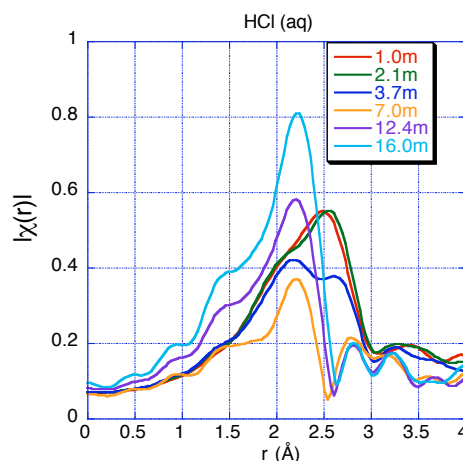


Figure 3b) Fourier transform of EXAFS.

concentration dependence of HCl using a rigid model of H_3O^+ . The goal is that EXAFS will allow us to better characterize H_3O^+ Cl^- ion pairing in aqueous solution. With this simplified model, we are able to see features in the radial distribution function as a function of concentration.

(Figure 3a) These features are reflected in the Fourier transform of the fine structure, $\chi(r)$. (Figure 3b) We will also study CaCl_2 and AgCl solutions as a function of concentration, building empirical potentials and developing a description of molecular interaction that is consistent with electronic structure calculations and experimental EXAFS measurements.

In an additional extension of our bulk EXAFS analysis, we will attempt to understand the influence of an interface on the observed ion solvation structure and how it manifests itself in an EXAFS measurement. It has been established that at an aqueous vapor-liquid interface the oxygen-oxygen distances expand. Initial analysis of ions at the vapor-liquid interface indicate that ion-oxygen distances contract. In future work we will investigate if these changes in the solvation structure can be observed from EXAFS measurements.

Collaborators on this project include C. D. Wick, S. M. Kathmann, C. J. Mundy, S. S. Xantheas, L. X. Dang, V.-A. Glezakou, J. Fulton, and Y. Chen. Battelle operates Pacific Northwest National Laboratory for the U. S. Department of Energy.

References

- L.X. Dang, G.K. Schenter, and J.L. Fulton, *J. Phys. Chem. B* **107**, 114119 (2003).
- L.X. Dang and T.M. Chang, *J. Chem. Phys.* **106**, 8149 (1997).
- J.J. Rehr, R. C. Albers, S.I. Zabinsky, *Phys. Rev. Lett.* **69**, 3397 (1992); M. Newville, B. Ravel, D. Haskel, J. J. Rehr, E. A. Stern, and Y. Yacoby, *Physica B*, **208-209**, 154 (1995); A. L. Ankudinov, C. Bouldin, J. J. Rehr, H. Sims, and H. Hung, *Phys Rev. B* **65**, 104107 (2002).

References to publications of DOE sponsored research (2004-present)

1. M. P. Hodges, R. J. Wheatley, G. K. Schenter, and A. H. Harvey, "Intermolecular potential and second virial coefficient of the water-hydrogen complex," *J. Chem. Phys.* **120**, 710 (2004).
2. S. M. Kathmann, G. K. Schenter, and B. C. Garrett, "Multicomponent dynamical nucleation theory and sensitivity analysis," *J. Chem. Phys.* **120**, 9133 (2004).
3. J. L. Daschbach, G. K. Schenter, P. Ayotte, R. S. Smith, and B. D. Kay, "Helium diffusion through H₂O and D₂O amorphous ice: Observation of a lattice inverse isotope effect," *Phys. Rev. Lett.* **92**, 198306 (2004).
4. S. M. Kathmann, G. K. Schenter, and B. C. Garrett, "Dynamical Nucleation Theory: Understanding the Role of Aqueous Contaminants," in Proceedings of the 16th International Conference on Nucleation and Atmospheric Aerosols, edited by M. Kulmala and M. Kasahara (Kyoto University Press, 2004), p. 243.
5. S. M. Kathmann, G. K. Schenter, and B. C. Garrett, "Ion-Induced Nucleation: The Importance of Chemistry," *Phys. Rev. Lett.* **94**, 116104 (2005).
6. B. C. Garrett, D. A. Dixon, et al "The Role of Water on Electron-Initiated Processes and Radical Chemistry: Issues and Scientific Advances," *Chem. Rev.* **105**, 355 (2005).
7. V. -A. Glezakou, Y. C. Chen, J. L. Fulton, G. K. Schenter and L. X. Dang "Electronic Structure, Statistical Mechanical Simulations, and EXAFS Spectroscopy of Aqueous Potassium" *Theoret. Chem. Acc.* **115**, 86 (2006).
8. T. D. Iordanov, G. K. Schenter, and B. C. Garrett, "Sensitivity Analysis of Thermodynamics Properties of Liquid Water: A General Approach to Improve Empirical Potentials," *J. Phys. Chem. A* **110**, 762 (2006).
9. C. D. Wick and G. K. Schenter, "Critical Comparison of Classical and Quantum Mechanical Treatments of the Phase Equilibria of Water," *J. Chem. Phys.* **124**, 114505 (2006).
10. B. C. Garrett, G. K. Schenter, and A. Morita, "Molecular Simulations of the Transport of Molecules across the Liquid/Vapor Interface of Water," *Chem. Rev.* **106**, 1355 (2006).
11. S. Du, J. S. Francisco, G. K. Schenter, T. D. Iordanov, B. C. Garrett, M. Dupuis, and J. Li, "The OH radical – H₂O molecular interaction potential," *J. Chem. Phys.* **124**, 224318 (2006).
12. G. S. Fanourgakis, G. K. Schenter, and S. S. Xantheas, "A Quantitative Account of Quantum Effects in Liquid Water," *J. Chem. Phys.* **125**, 141102 (2006).
13. L. X. Dang, G. K. Schenter, V. A. Glezakou and J. L. Fulton, "Molecular simulation analysis and X-ray absorption measurement of Ca²⁺, K⁺ and Cl⁻ ions in solution," *Journal of Physical Chemistry B* **110**, 23644 (2006).
14. S. M. Kathmann, G. K. Schenter and B. C. Garrett, "Comment on "Quantum nature of the sign preference in ion-induced nucleation"," *Phys. Rev. Lett.* **98**, 109603 (2007).
15. S. Kathmann, G. Schenter and B. Garrett, "The critical role of anharmonicity in aqueous ionic clusters relevant to nucleation," *J. Phys. Chem. C* **111**, 4977 (2007).
16. S. Y. Du, J. S. Francisco, G. K. Schenter and B. C. Garrett, "Ab initio and analytical intermolecular potential for ClO-H₂O," *J. Chem. Phys.* **126**, 114304 (2007).
17. M. Valiev, B. C. Garrett, M.-K. Tsai, K. Kowalski, S. M. Kathmann, G. K. Schenter, and M. Dupuis, "Hybrid approach for free energy calculations with high-level methods: Application to the S_N2 reaction of CHCl₃ and OH⁻ in water," *J. Chem. Phys.* **127**, 051102 (2007).

Research Summaries
(by PI)

Model Catalysis by Size-Selected Cluster Deposition

Scott Anderson, Chemistry Department, University of Utah, 315 S. 1400 E. Rm. 2020, Salt Lake City, UT 84112. anderson@chem.utah.edu

Program scope: We are interested in understanding the effects of cluster size on physical and chemical properties of planar model catalysts prepared to depositing size-selected cluster ions on well defined substrates in ultra-high vacuum. Tools available include a variety of pulsed and temperature-programmed mass spectrometric techniques, x-ray photoelectron spectroscopy (XPS), Auger electron spectroscopy (AES), ion scattering (ISS), and infrared reflection absorption spectroscopy (IRAS). The goal is produce model catalysts that are well characterized, and where properties such as metal loading, substrate defect density, and metal cluster size can be varied independently, allowing us new insights into these very complex systems.

Recent Progress

During the past year, the focus of our DOE supported work has been on the gold/TiO₂ system, specifically on CO oxidation catalysis and adsorption behavior of water and its effects gold sintering behavior. We have also begun to examine supported gold clusters using a type of single-electron tunneling spectroscopy, in collaboration with Clayton Williams in the U. of Utah Physics Department.

1. Instrument upgrades

To facilitate the microscopy experiments we designed a new sample holder system that allows us to exchange sample in vacuum, between our instrument's load/lock chamber and a UHV transfer chamber, which also interfaces to the microscope. The new sample holder has facilities for e-beam heating of the samples, and better and faster cooling. The latter is really not needed for the microscopy work per se, however, it allow us to do surface science experiments on the same samples used in the microscopy.

2. Au_n/TiO₂.

In past work, we found that Au_n deposited on vacuum-annealed TiO₂ did not sinter significantly on the time scale of our experiments. Later STM experiments agreed with the exception of Au atoms, where they observed substantial sintering under nominally identical conditions. Our speculation was that some contaminant was affecting the other groups' results by binding to vacancy sites present on the vacuum-annealed surface, thereby preventing them from binding Au. We thought that the fast time scale of our experiments might explain why our experiments suffered from this problem less than the STM experiments. Recent work by the Besenbacher and Hammer groups¹ pointed to water as the likely culprit, and since this is an important issue in our use of ISS for morphological probing, we felt the need to get a definitive answer.

We used temperature-programmed desorption (TPD) to monitor water dissociation, recombination, and desorption on TiO₂ and Au/TiO₂, and ion-scattering spectroscopy (ISS) to look at morphology changes in the gold induced by water adsorption either before or after gold deposition. One of the instrumentation problems was instabilities and poor time resolution (related to pumping speed) with the TPD mass spectrometer, resulting in mediocre signal/noise and broadened TPD peaks. In the end we had to repeat most of the experiments with the repaired mass spectrometer in order to have a complete set of data under consistent conditions. This work is completed and a paper has been submitted to J. Phys. Chem.

To summarize: water adsorption/desorption behavior was studied for clean, vacuum-annealed TiO₂(110) and for the same TiO₂ sample with 0.05 ML-equivalent of Au deposited as Au⁺. H₂¹⁸O was used so that we could examine molecular vs. dissociative chemisorption, and in the latter case measure the extent of oxygen isotope scrambling. There are three main water desorption features, consistent with previous studies of water TPD from rutile TiO₂(110).^{2,3} A peak centered at ~250 K is assigned to water desorbing from five-coordinate Ti ("5cTi") sites. A 164 K peak is assigned as water desorbing from two-coordinate O²⁻ ("2cO" = bridging oxygen) sites. Both of these sites are present in the perfect, stoichiometric surface, and one water molecule in each site constitutes complete monolayer coverage. The integrated intensity of the 5cTi and 2cO desorption features are nearly identical, as expected because

each TiO_2 unit cell has one of each site. If sufficient water is deposited, there is also a peak at ~ 150 K attributed to water adsorbed in multilayer (mostly 2nd layer) sites. For most experiments, the water dose ($\sim 6 \text{ L} = \sim 5 \text{ H}_2^{18}\text{O}/\text{unit cell}$) was chosen such that the 5cTi and 2cO sites are saturated, and there is significant water adsorbed into the multilayer. The presence of the multilayer peak is important in the data analysis because it is safe to assume that these water molecules desorb intact without $^{18}\text{O}/^{16}\text{O}$ exchange, and therefore the mass spectrum of this desorption feature provides an internal standard for estimating background from cracking/exchange in the mass spectrometer. If sufficient water is adsorbed, we also observe the amorphous-to-crystalline phase transition in the multilayer, as described by Kay and co-workers.⁴ For all the main desorption features discussed above, there is no isotope scrambling, implying that water in these sites is bound molecularly.

In analogous experiment done on TiO_2 with 0.05 ML-equivalent of Au deposited as Au^+ (the "Au/ TiO_2 " sample), there is one Au atom for every $\text{TiO}_2 \sim 8$ unit cells, thus we might expect to see a peak for water desorption from Au sites with intensity $\sim 13\%$ of that for the 5cTi or 2cO sites, along with a concomitant decrease in the 5cTi or 2cO desorption features. No distinct peak is observed for water/Au sites, and the 5cTi and 2cO peak intensities are unchanged, suggesting that desorption from Au sites on Au/ TiO_2 is buried under one of the peaks for water desorbing from the TiO_2 surface. There is no significant effect of Au on either the multilayer or 2cO peaks, however, close inspection shows that the peak for water at 5cTi sites is shifted slightly to higher temperature for the Au/ TiO_2 , compared to Au-free TiO_2 . Such a shift would occur if water binds to Au on TiO_2 slightly more strongly than to the 5cTi sites, resulting in a composite desorption feature shifted to higher temperature. Alternatively, it is possible that the presence of Au ($\sim 0.13 \text{ Au}/\text{unit cell}$) strengthens water binding to nearby 5cTi sites, resulting in a shift, and that water desorption from Au, itself, occurs at lower temperatures. As with clean TiO_2 , none of these desorption features leads to significant isotope scrambling, indicating that they correspond to molecular chemisorption.

In addition to the main desorption features, both TiO_2 and Au/ TiO_2 samples have a weak, broad feature between 420 and 550 K where significant isotope scrambling is observed. In previous work on TiO_2 , this feature was assigned to recombinative desorption of water dissociatively chemisorbed at oxygen vacancy sites.^{3,5,6} The combined ($\text{H}_2^{18}\text{O} + \text{H}_2^{16}\text{O}$) intensity of this recombinative desorption component is $\sim 6\%$ of the intensity of the 5cTi component for the clean, gold-free TiO_2 sample. Assuming, following previous authors^{3,6}, that this component corresponds to water dissociatively adsorbed at defects, primarily oxygen vacancies, then the results suggest that $\sim 6\%$ of unit cells have a vacancy, mostly among the bridging oxygen sites. This vacancy density is similar to what has been estimated by other researchers based on STM⁷ and TPD⁸, and consistent with the density we estimate from XPS.

For the Au/ TiO_2 sample, there is clearly considerably less recombinative desorption in the temperature range from 400 - 550 K compared to TiO_2 ($\sim 3\%$ oxygen vacancy density for Au/ TiO_2 , comparing with $\sim 6\%$ for TiO_2). As noted above, recombinative desorption is attributed to water dissociated at oxygen vacancy sites, and the vacancy density on both samples should be identical, because they are prepared identically prior to Au deposition. The difference in recombinative desorption signal suggests, therefore, that Au partially blocks the dissociative chemisorption pathway, presumably by binding at the oxygen vacancy sites. Recombinative desorption is accompanied by significant but incomplete $^{18}\text{O}/^{16}\text{O}$ isotope exchange, with nearly equal signals for $\text{H}_2^{18}\text{O}^+$ and $\text{H}_2^{16}\text{O}^+$.

We also used ISS to examine the effects on Au binding and diffusion, of water adsorption, both before and after deposition of Au. In both cases, the ISS Au/substrate ratios indicate that substantial sintering occurs at room temperature if water is allowed to hydroxylate the vacancy sites. This is true even if Au is bound into vacancy sites prior to water exposure.

Single electron tunneling

The goal of these experiments is two fold. Having images, even if they show only the density of clusters on the surface, with no atomic resolution, would provide us with an independent check of whether or not the clusters remain intact, for comparison with ISS. In addition, having some electronic

structure information (potentials where tunneling transitions occur, band gaps, charging energies), would be helpful in understanding the catalytic mechanisms. For example, in Au/TiO₂, there has been considerable debate about the charge state of the gold, and how this relates to activity. XPS can reveal charge state, in principle, but the interpretation is complicated by large final state effects.

The microscope allows STM and tunneling spectroscopy to be done on insulating samples, which is perfect for supported catalyst applications. It works by tunneling a single electron back and forth between sample and tip with an AC tunnel bias, rather than tunneling a DC current through the tip-sample junction. The operation mode is referred to as dynamic tunneling force microscopy (DTFM), and is similar to an atomic force microscopy technique known as dynamic force microscopy (DFM), where the tip is oscillated near, but not touching the surface, and the van der Waals force is measured as a change in the tip resonance frequency. In DTFM, the tip is biased, and as the tip approaches the surface, an electron can tunnel to or from a state on the surface to the metallic tip. Tunneling is detected by measuring the small changes in tip-sample force that occur when a single electron tunnels. Tunneling occurs only when there is a state on the surface that is energetically accessible at the bias voltage applied, so essentially, DTFM generates a map of electronic states on the surface. Small clusters are expected to have both filled and empty states near the Fermi level, and thus should be detectable this way.

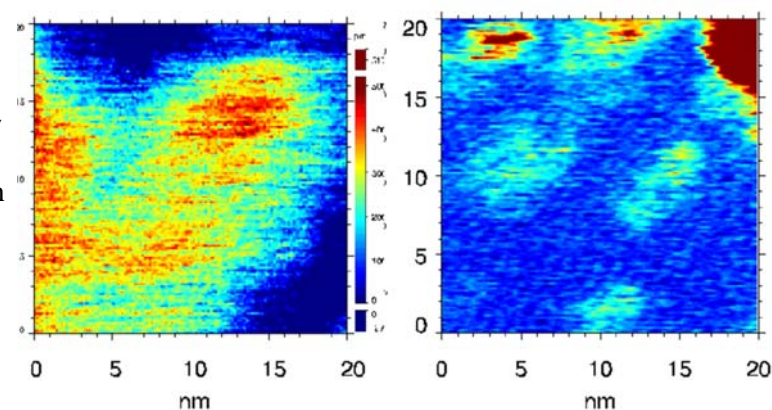
In our initial experiments, we prepared samples of gold on HfSiO_x, and transferred them to the microscope in a UHV transfer system. The image shown below is of small gold clusters, but note that the size of the clusters is not certain because in these initial experiments the samples were stored in the microscope, heated to desorb adventitious adsorbates, so sintering is likely. Nonetheless, the results are encouraging. The left image shows an AFM scan of the surface, showing relatively smooth topology (The clusters are too small to see in AFM on a thick, and therefore rough oxide film). The right image is a DTFM scan of the same area on the surface. Note the presence of six features in the DTFM image that are not present in AFM. This implies that there are regions where there are states on the surface not related to topology, and in scans of gold-free substrates, these feature were not seen. Furthermore, the density of features is just what we would expect from the amount of gold deposited, within the uncertainty of the size determination.

We tentatively conclude that these are DTFM images of gold clusters on the surface. The next step is to deposit size-selected clusters and repeat. Now that we have found the right conditions to locate small clusters with DTFM, we should be able image the surface fast enough to detect the nascent clusters, without much sintering.

Future Plans

One of the major findings in our previous DOE-sponsored research

⁹ was that small gold clusters on reduced TiO₂ (i.e., TiO₂ with ~6% missing oxygen defects, prepared by vacuum annealing) showed strongly size-dependent activity for CO oxidation. It was necessary to expose the samples to large O₂ exposures to activate them. One interesting question was what form the reactive oxygen was in, and how it was bound to the gold. Recent ab initio work by Hammer and co-workers¹⁰ investigated binding of gold (Au₇ – the most active cluster in our work) to the TiO₂ surface, with the surface in several different states. On the reduced surface, they found large activation barriers to the CO oxidation cycle, and this was also found to be true on a stoichiometric TiO₂ surface. Their finding was that the reactive form of Au₇/TiO₂ had an over-oxidized TiO₂ support, with O adatoms bound to the surface, and gold clusters bound to them. The O adatoms withdraw electron density from the gold, and that leads (in the calculations) to a nearly barrierless CO oxidation catalytic cycle. Our experiment was



somewhat different from the calculations. They added Au₇ to the over-oxidized surface, whereas we deposited Au_n on the reduced surface, and then exposed to a large flux of O₂. Nonetheless, their calculations raise the interesting possibility that what is happening in our experiment is that gold is catalyzing O₂ dissociation, and thus *producing* the over-oxidized surface. Our current experiments are aimed at testing this hypothesis. We have shown¹¹ that by annealing TiO₂ at somewhat lower-than-normal temperatures in O₂, it is possible to generate TiO₂ with substantial excess oxygen in the surface layer. It is also possible to get a smaller excess oxygen concentration by simply exposing vacuum-annealed TiO₂ to large doses of O₂ at room temperature.

Citations

- ¹ S. Wendt, R. Schaub, J. Matthiesen, E. K. Vestergaard, E. Wahlstrom, M. D. Rasmussen, P. Thostrup, L. M. Molina, E. Lægsgaard, I. Stensgaard, B. Hammer, and F. Besenbacher, *Surf. Sci.* **598**, 226–245 (2005).
- ² M. A. Henderson, *Surf. Sci.* **355**, 151 (1996).
- ³ M. A. Henderson, *Langmuir* **12** (21), 5093 (1996).
- ⁴ R. S. Smith, C. Huang, E. K. L. Wong, and B. D. Kay, *Surf. Sci.* **367** (1), L13 (1996).
- ⁵ M. B. Hugenschmidt, L. Gamble, and C. T. Campbell, *Surf. Sci.* **302**, 329 (1994).
- ⁶ R. Schaub, P. Thostrup, N. Lopez, E. Lægsgaard, I. Stensgaard, J. K. Nørskov, and F. Besenbacher, *Phys. Rev. Lett.* **87**, 266104 (2001).
- ⁷ U. Diebold, J. Lehman, T. Mahmoud, M. Kuhn, G. Leonardelli, W. Hebenstreit, M. Schmid, and P. Varga, *Surf. Sci.* **411**, 137 (1998).
- ⁸ W. S. Epling, C. H. F. Peden, M. A. Henderson, and U. Diebold, *Surf. Sci.* **412/413**, 333 (1998).
- ⁹ S. Lee, C. Fan, T. Wu, and S. L. Anderson, *J. Am. Chem. Soc.* **126** (18), 5682 (2004).
- ¹⁰ D. Matthey, J. G. Wang, S. Wendt, J. Matthiesen, R. Schaub, E. Lægsgaard, B. Hammer, and F. Besenbacher, *Science* **315**, 1692 (2007).
- ¹¹ M. Aizawa, S. Lee, and S. L. Anderson, *J. Chem. Phys.* **117**, 5001 (2002).

DOE-Funded Publications Since 2003

- "Deposition dynamics and chemical properties of size-selected Ir clusters on TiO₂", Masato Aizawa, Sungsik Lee, and Scott L. Anderson, *Surf. Sci.* 542 (2003) 253-75
- "CO oxidation on Au_n/TiO₂ catalysts produced by size-selected cluster deposition" Sungsik Lee, Chaoyang Fan, Tianpin Wu, and Scott L. Anderson, *JACS* (comm) 126 (2004) 5682-3.
- "Agglomeration, Support Effects, and CO Adsorption on Au/TiO₂ (110) Prepared by Ion Beam Deposition" Sungsik Lee, Chaoyang Fan, Tianpin Wu, and Scott L. Anderson, *Surf. Sci.* 578 (2005) 5-19
- "Agglomeration, Sputtering, and Carbon Monoxide Adsorption Behavior for Au/Al₂O₃ Prepared by Au_n⁺ Deposition on Al₂O₃/NiAl(110)", Sungsik Lee, Chaoyang Fan, Tianpin Wu, and Scott L. Anderson, *J. Phys. Chem. B* 109 (2005) 11340-11347
- "Cluster size effects on CO oxidation activity, adsorbate affinity, and temporal behavior of model Au_n/TiO₂ catalysts", Sungsik Lee, Chaoyang Fan, Tianpin Wu, and Scott L. Anderson, *J. Chem. Phys.* 123 (2005) 124710 13 pages.
- "Water on rutile TiO₂(110) and Au/TiO₂(110): Effects on Au mobility and the isotope exchange reaction", Tianpin Wu, William E. Kaden and Scott L. Anderson, *J. Phys. Chem C* (submitted).

“Investigating atoms to aerosols with vacuum ultraviolet radiation”

Musahid Ahmed, Kevin R. Wilson and Stephen R. Leone
Chemical Dynamics Beamline
MS 6R-2100, 1 Cyclotron road
Lawrence Berkeley National Laboratory
University of California, Berkeley, CA 94720
mahmed@lbl.gov

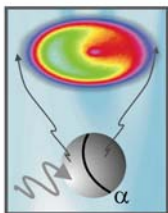
The Chemical Dynamics Beamline at the Advanced Light Source (ALS), is a synchrotron user facility dedicated to state-of-the-art investigations in combustion dynamics, aerosol chemistry, nanoparticle physics, biomolecule energetics, spectroscopy, kinetics, and chemical dynamics processes using tunable vacuum ultraviolet light for excitation or detection. The broad goals of the Chemical Dynamics Beamline are to perform high quality investigations in chemical physics and dynamics utilizing vacuum ultraviolet (VUV) light, while providing the user community with efficient access to the synchrotron and its sophisticated equipment, and at the same time fulfilling the missions and interests of the Department of Energy.

Aerosol Chemistry - Ambient aerosols are known to play a significant role in a variety of atmospheric processes such as direct and indirect effects on radiative forcing. Chemical composition can be an important factor in determining the magnitude of these effects (optical density, hygroscopicity, etc.). However, a major fraction (80 – 90%) of organic aerosols can not be resolved on a molecular level. Recent identification of high mass oligomeric species as a major component in laboratory and ambient organic aerosols has received much attention due to the possibility that these species may account for much of the unknown organic mass in ambient aerosols. Although, a few mechanisms have been proposed, the origin and formation processes of these compounds remain largely unknown. Using VUV photoionization aerosol mass spectrometry we provide strong evidence for a previously unidentified mechanism of rapid oligomer formation, via OH radical initiated oxidation of organic aerosols. This process appears capable of converting a sizable fraction of an organic particle to higher mass oligomers within only a day of exposure to OH radicals at typical atmospheric concentrations. Furthermore, we have found that rapid volatilization, followed by oligomerization, is also important for specific reaction systems (i.e. n-alkane particles), and can lead to the loss of a large fraction (> 60%) of the particle within a day of exposure to atmospheric OH. We propose that such a rapid processing (oligomerization and volatilization) is possible due to a radical chain reaction which quickly propagates throughout the entire particle and is only initiated by the surface OH reaction.

In addition to the oligomerization of primary particles, we have also found that OH radicals lead to the efficient generation of secondary organic aerosols (SOA). Using a coated flow tube reactor, rapid SOA formation is observed when an organic film (such as stearic acid) is exposed to OH radicals. In addition to films, we have also observed that OH oxidation of submicron organic particles also leads to similar SOA formation. These results suggest an entirely new, and very efficient, formation mechanism of SOA via OH radical oxidation of organic surfaces. Analysis of these SOA particles, via VUV photoionization mass spectrometry, suggests that they are chemically complex and perhaps oligomeric in nature. We suggest a potential mechanism for this process in which gas phase products, such as semi-volatile aldehydes and carboxylic acids, evolve from the oxidation of the organic films. Subsequent reactions of these volatile products with OH in the gas phase results in efficient SOA formation. This mechanism is supported by the observation that OH radical reactions with gas phase hexanal and nonanal leads to strong SOA formation. These results provide a direct link between volatile organic compounds produced by particle oxidation and SOA formation.

In other experiments, we have investigated the chemistry of particle surfaces coated in PAHs. The reaction between gas phase ozone and solid anthracene deposited at the surface of sodium chloride particles is studied by measuring both the particle size and chemical composition using a scanning mobility particle sizer (SMPS) and a VUV aerosol mass spectrometer. Experiments varying ozone concentration and anthracene coating thickness have been recorded to better understand the surface chemistry of semi-volatile PAHs.

Nanoparticle Physics- Velocity-map imaging (VELMI) photoelectron spectroscopy combined with synchrotron radiation allows simultaneous measurement of angular and kinetic energy release from ionization events. Detailed investigations were conducted on NaCl, KI, Au, and SiO₂ nanoparticles (50–500nm). The kinetic energy release suggests that these ultra-fine particles exhibit, as expected for this size range, bulk-like electronic properties. However, a dramatic size-dependent asymmetry in the angular distributions of photoelectrons was observed for insulating nanoparticles. Simply, photoelectrons are preferentially emitted from the side of the particle illuminated by the photon beam. While these particles are too large to exhibit quantum size effects, their dimensions are on the order of the photon penetration depth and electron inelastic mean free path. To obtain a more rigorous quantitative explanation for these size dependent effects, we have initiated a collaboration with George Schatz (Northwestern). Schatz and coworkers have computed the internal electric field distribution explicitly using Mie theory in an effort to better understand the underlying physics of this interesting particle size-dependent asymmetry.



quantitative explanation for these size dependent effects, we have initiated a collaboration with George Schatz (Northwestern). Schatz and coworkers have computed the internal electric field distribution explicitly using Mie theory in an effort to better understand the underlying physics of this interesting particle size-dependent asymmetry.

Hydrogen bonded Clusters and microhydration of DNA bases - The photoionization dynamics of water clusters is a window into understanding the properties of water from the gas phase to bulk. Tunable vacuum ultraviolet (VUV) photoionization studies of water clusters are performed using 10 - 14 eV synchrotron radiation and analyzed by reflectron time-of-flight (TOF) mass spectrometry. The appearance energies of a series of protonated water clusters are determined from the photoionization threshold for clusters composed of up to 79 molecules. These appearance energies represent an upper limit of the adiabatic ionization energy of the corresponding parent neutral water cluster in the supersonic molecular beam. The experimental results show a sharp drop in the appearance energy for the small neutral water clusters (from 12.62 ± 0.05 eV to 10.94 ± 0.06 eV, for (H₂O) and (H₂O)₄, respectively), followed by a gradual decrease for clusters up to (H₂O)₂₃ converging to a value of 10.6 eV (± 0.2 eV). The dissociation energy to remove a water molecule from the corresponding neutral water cluster is derived through thermodynamic cycles utilizing the dissociation energies of protonated water clusters reported previously in the literature.

Using the same apparatus we performed a photoionization study of the micro-hydration of the four naturally occurring DNA bases. Gas phase clusters of water with DNA bases (Guanine (G), Cytosine (C), Adenine (A) and Thymine (T)) are generated via thermal vaporization of the bases and expansion of the resultant vapor in a continuous supersonic jet expansion of water seeded in Ar. The resulting clusters are investigated by single photon ionization with tunable vacuum-ultraviolet (VUV) synchrotron radiation and mass analyzed using reflectron mass spectrometry. Photoionization efficiency curves (PIE) are recorded for the DNA bases and the following water (W) clusters – G, GW_n (n=1-3); C, CW_n (n=1-3); A, AW_n (n=1,2); T, TW_n (n=1-3). Appearance energies (AE) are derived from the onset of these PIE curves. The AE's of the DNA bases decrease slightly with addition of water molecules (up to 3) but do not converge to values found for photo-induced electron removal from DNA bases in solution.

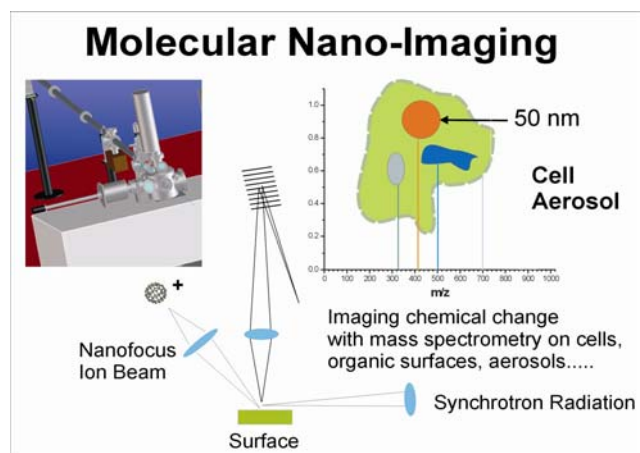
Cluster photoionization studies- Small carbon clusters (C_n, n=2-15) (M. Duncan, Georgia) are produced in a molecular beam by pulsed laser vaporization and studied with vacuum ultraviolet (VUV) photoionization mass spectrometry. Mass spectra at various ionization energies reveal the relative abundances of the neutral carbon clusters produced. By far the most abundant species is C₃. Ionization threshold spectra are recorded for the clusters up to 15 atoms in size. To interpret the ionization thresholds for different cluster sizes, new *ab initio* calculations are carried out on the clusters for n=4-10. (F. Schaefer, Georgia) A focal point extrapolation method is applied to both neutral and cation species to determine adiabatic and vertical ionization potentials. The comparison of computed and measured ionization potentials makes it possible to investigate the isomeric structures of the neutral clusters produced in this experiment. The measurements are inconclusive for the n=4-6 species because of unquenched excited electronic states. However, the data

provide evidence for the prominence of linear structures for the $n=7,9,11$ etc. species and the presence of cyclic C_{10} .

Hydrogen-deficient hydrocarbon radicals (C_3H) are generated in situ via laser ablation of graphite and seeding the ablated species in acetylene gas, which acts as a carrier and reactant simultaneously. By recording photoionization efficiency curves (PIE) and simulating the experimental spectrum with computed Franck-Condon (FC) factors, we can reproduce the general pattern of the PIE curve of $m/z=37$. We recover ionization energies of 9.15 eV and 9.76 eV for the linear and cyclic isomers, respectively. Our combined experimental (R. Kaiser, Hawaii) and theoretical (J. Bowman, Emory) studies provide an unprecedented, versatile pathway to investigate the ionization energies of even more complex hydrocarbon radicals in situ, which are difficult to prepare by classical synthesis, in future experiments.

The ablation apparatus is being modified to incorporate better cooling for clusters. In addition, an aerodynamic lens system will be installed in this apparatus to focus nanoparticles in the 3-20 nm regime. This will allow access to size dependent processes – quantum confinement, catalysis – hitherto not possible with our aerosol apparatus. In parallel, efforts to perform mass analysed threshold ionization (MATI) using quasi cw synchrotron radiation proved successful. Rydberg states of atoms and molecules (Ar, N_2 , O_2) were prepared outside the ion extraction region of the TOFMS, and subsequently field ionized when they arrived in the ion extraction region and a pulsed field applied. Coupling this technique to the medium resolution monochromator at the beamline will allow for vibrational selection of the resulting cation and structural elucidation when coupled to electronic structure calculations.

Molecular nano-imaging- A truly integrative tool for visualizing chemical change on surfaces would be to generate chemical specificity at the molecular level coupled with spatial resolution down to the nanoscale. A major effort in this direction is being developed in our group to probe chemical modifications of inter and intra cellular dynamics of various cells and organic aerosols. The basic principle is to build upon the exciting advances in secondary ion mass spectrometry (SIMS) microscopy by adding enhanced molecular specificity, which is essential to probe more complex aspects of biological systems. As the spatial resolution is increased, the number of detected ions decreases dramatically. Furthermore, ion signals measured by the energetic desorption method fluctuate dramatically due to the competition of different ionization mechanisms, which



can be strongly influenced by surface properties and substrate effects. The efficiency of producing molecular ions is also low due to extensive fragmentation. Neutral molecules produced by ion sputtering are typically 3 to 6 orders of magnitude greater than secondary ion yields. Consequently, post-ionization of desorbed neutrals can improve the sensitivity over traditional SIMS. Sub-micron resolution has been achieved with post-ionization; the theoretical lateral limit of static SIMS is about 5-10 nm while depth profiling can be performed at the monolayer level. Single photon ionization (SPI), where absorption to intermediate levels is not required, shows much promise as an efficient method of ionizing fragile molecules. Tunable vacuum ultraviolet (VUV) photoionization has been shown to be a selective, yet universal technique in elucidating molecular specific information from gas phase studies of the building blocks of life. Imaging by chemical species mass, by detecting the parent ion mass intact, is unique in microscopy in that labeling is not required due to the high molecular specificity of the mass spectrometry method.

An apparatus (**TOF.SIMS 5-100**) purchased from IONTOF will be installed at the Chemical Dynamics Beamline in November 2007. The apparatus includes a sophisticated cryo-cooled sample holder with provision for nano manipulation using vacuum compatible stages. The apparatus has the full

functionality of a conventional SIMS machine. This includes electron detectors to image samples via secondary electron emission or VUV photoemission. This capability is essential for locating the position of the primary ion beam and synchrotron and is commonly used to image topological features in a sample. An optical microscope is included in the experimental suite. The apparatus design is flexible to accommodate laser desorption and MALDI experiments. The machine draws heavily on the proven design concepts of the field exemplified by the IONTOF apparatus, including a sample preparation chamber for introducing biological specimens into vacuum. To complement the beamline work, a dedicated laser laboratory is being customized at the ALS. This laboratory affords a space where instrument and protocol development may be performed utilizing high repetition rate UV lasers on a desorption apparatus equipped with a reflectron mass spectrometer.

References (DOE funded research 2005-present):

1. M.J. Northway, J.T. Jayne, D.W. Toohey, M.R. Canagaratna, A. Trimborn, K-I. Akiyama, A. Shimono, J.L. Jimenez, P.F. DeCarlo, K.R. Wilson, and D.R. Worsnop. "Demonstration of a VUV lamp photoionization source for improved organic speciation in an aerosol mass spectrometer." *Aerosol Science & Technology* (In press)
2. L. Belau, K. R. Wilson, S. R. Leone and M. Ahmed, "Vacuum Ultraviolet (VUV) photoionization of small water clusters." *J. Phys. Chem. A*. (In press)
3. L. Belau, S. E. Wheeler, B. W. Ticknor, M. Ahmed, S. R. Leone, W. D. Allen, H. F. Schaefer III, and M. A. Duncan, "Ionization Thresholds of Small Carbon Clusters: Tunable VUV Experiments and Theory." *J. Am. Chem. Soc.* **129**, 10229 (2007)
4. K. R. Wilson, S. Zou, J. Shu, E. Rühl, S. R. Leone, G. C. Schatz and M. Ahmed, "Size-Dependent Angular Distributions of Low Energy Photoelectrons emitted from NaCl Nanoparticles." *Nano Letters* **7**, 2014 (2007)
5. L. Belau, K. R. Wilson, S. R. Leone, and M. Ahmed, "Vacuum-Ultraviolet photoionization studies of the micro-hydration of DNA bases (Guanine, Cytosine, Adenine and Thymine)." *J. Phys. Chem. A*. **111**, 7562 (2007)
6. R. I. Kaiser, L. Belau, S. R. Leone, M. Ahmed, Y. Wang, B. J. Braams, and J. M. Bowman, "A combined experimental and computational study on the ionization energies of the cyclic and linear C₃H isomers." *ChemPhysChem* **8**, 1236 (2007)
7. M. Ahmed, "Photoionization of desorbed neutrals from surfaces." *Encyclopedia of Mass Spectrometry, Vol. 6, Elsevier* (2007).
8. E. Gloaguen, E. R. Mysak, S. R. Leone, M. Ahmed, and K. R. Wilson, "Investigating the chemical composition of mixed organic-inorganic particles by "soft" VUV photoionization: the reaction of ozone with anthracene on sodium chloride particles." *Int. J. Mass Spectrom.* **258**, 74 (2006).
9. J. Shu, K. R. Wilson, M. Ahmed, and S. R. Leone, "Coupling a versatile aerosol apparatus to a synchrotron: vacuum ultraviolet light scattering, photoelectron imaging, and fragment free mass spectrometry." *Rev. Sci. Instrum.* **77**, 043106 (2006)
10. K. R. Wilson, L. Belau, C. Nicolas, M. Jimenez-Cruz, S. R. Leone, and M. Ahmed, "Direct determination of the ionization energy of histidine with VUV synchrotron radiation." *Int. J. Mass Spectrom.* **249-250**, 155, (2006)
11. K. R. Wilson, D. S. Peterka, M. Jimenez-Cruz, S.R. Leone, and M. Ahmed. "VUV Photoelectron Imaging of Biological Nanoparticles – Ionization energy determination of nano-phase glycine and phenylalanine-glycine-glycine." *Phys. Chem. Chem. Phys.* **8**, 1884 (2006).
12. K. R. Wilson, M. Jimenez-Cruz, C. Nicolas, L. Belau, S. R. Leone, and M. Ahmed, "Thermal Vaporization of Biological Nanoparticles: Fragment-Free VUV Photoionization Mass Spectra of Tryptophan, Phenylalanine-Glycine-Glycine and β -Carotene." *J. Phys. Chem. A* **110**, 2106 (2006)
13. J. Shu, K. R. Wilson, M. Ahmed, S. R. Leone, C. E. Graf, and E. Rühl, "Elastic light scattering from nanoparticles by monochromatic vacuum-ultraviolet radiation." *J. Chem. Phys.* **124**, 034707 (2006)
14. C. Nicolas, J. Shu, D. S. Peterka, M. Hochlaf, L. Poisson, S. R. Leone, and M. Ahmed, "Vacuum ultraviolet photoionization of C₃." *J. Am. Chem. Soc.* **128**, 220 (2006)
15. R. B. Metz, C. Nicolas, M. Ahmed, and S. R. Leone, "Direct determination of the ionization energies of FeO and CuO with VUV radiation." *J. Chem. Phys.* **123**, 114313 (2005).
16. J. Shu, K. R. Wilson, A. N. Arrowsmith, M. Ahmed, and S. R. Leone, "Light scattering of ultrafine silica particles by VUV synchrotron radiation." *Nano Lett.* **6**, 1009 (2005)
17. E. R. Mysak, K. R. Wilson, M. Jimenez-Cruz, M. Ahmed, and T. Baer. "Synchrotron Radiation Based Aerosol Time-of-Flight Mass Spectrometry for Organic Constituents" *Anal. Chem.* **77**, 5953 (2005)

THERMOCHEMISTRY AND REACTIVITY OF TRANSITION METAL CLUSTERS AND THEIR OXIDES

P. B. Armentrout

315 S. 1400 E. Rm 2020, Department of Chemistry, University of Utah,
Salt Lake City, UT 84112; armentrout@chem.utah.edu

Program Scope

The objectives of this project are to obtain quantitative information regarding the thermodynamic properties of transition metal clusters, their binding energies to various ligands, and their reactivities. This is achieved using a metal cluster guided ion beam tandem mass spectrometer (GIBMS) to measure absolute cross sections as a function of kinetic energy for reactions of size-specific transition metal cluster ions with simple molecules. Analysis of the kinetic energy dependent cross sections reveals quantitative thermodynamic information as well as kinetic and dynamic information regarding the reactions under study.

Since 2004, our DOE sponsored work has included studies of the kinetic energy dependences of the size-specific chemistry of Co_n^+ ($n = 2 - 16$) cluster ions reacting with D_2 ,¹ of Co_n^+ ($n = 2 - 20$) reacting with O_2 ,² of Fe_n^+ ($n = 1 - 19$) cluster ions reacting with N_2 ,³ and of Ni_n^+ ($n = 2 - 16$) with methane (CD_4).⁴ Data has been obtained for reactions of Co_n^+ ($n = 2 - 16$) cluster ions reacting with N_2 and CD_4 ,^{5,6} and these results are presently being written up. These works can be directly compared with our previous studies of the $\text{Fe}_n^+ + \text{N}_2$ and $\text{Fe}_n^+ + \text{Ni}_n^+ + \text{CD}_4$ systems.^{4,7} As such, these systems are designed to allow us to examine the periodic trends in the thermochemistry and reaction mechanisms for activation of dinitrogen and methane.

An invited review of our recent work that emphasizes the relationship to bulk phase properties is presently being considered for publication.⁸ The latter point is illustrated in Figure 1 for the example of cobalt clusters bound to hydrogen and oxygen where it is clear that bulk phase bond dissociation energies (BDEs) are approached for modest-sized clusters. Comparable behavior has been observed for V, Cr, Fe, and Ni clusters bound to D and O atoms.

Recent Progress

Reactions of Clusters with D_2 . We have now studied V_n^+ ($n = 2 - 13$),⁹ Cr_n^+ ($n = 2 - 14$),¹⁰ Fe_n^+ ($n = 2 - 15$),¹¹ Co_n^+ ($n = 2 - 16$),¹ and Ni_n^+ ($n = 2 - 16$)¹² cluster ions reacting with D_2 . For all four metal systems, the only products observed are M_nD^+ and M_nD_2^+ . The failure to observe M_mD^+ and M_mD_2^+ products where $m < n$ indicates that the M_nD^+ and M_nD_2^+ products dissociate exclusively by D and D_2 loss, consistent with the thermochemistry derived in this work.

In the Co system, all clusters that form Co_nD_2^+ , $n = 4, 5, \geq 9$, do so in barrierless exothermic processes except for $n = 9$. Comparison of the thermal rates of reaction for cobalt clusters finds that they approach the collision limit for large clusters ($n \geq 11$) and parallel but are somewhat faster than the rates observed for neutral cobalt clusters.

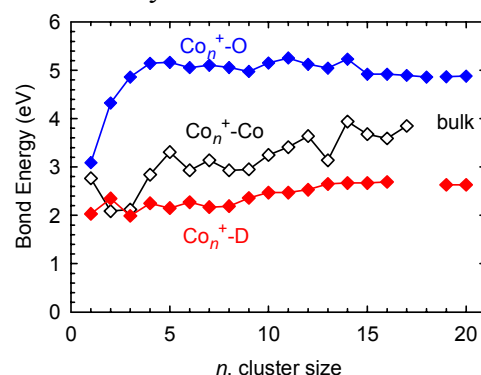


Figure 1. BDEs of D, Co, and O to Co_n^+ as a function of cluster size. Lines labeled bulk indicate the BDEs of H and O atoms to Co films.

Using methods developed over the past decade,¹³ we analyze the kinetic energy dependence of the endothermic cross sections in order to determine threshold energies for these processes, which can then be directly related to $D_0(M_n^+-D)$. The BDEs obtained are shown in Figure 1. For smaller clusters, variations in the BDEs must be related to the geometric and electronic structures of the metal cluster ions. Values for larger clusters can be compared to values for H atom binding to bulk cobalt surfaces, between 2.60 and 2.65 eV.¹⁴ Figure 1 shows that the largest Co_n^+-D BDEs ($n \geq 13$) equal the bulk phase value. Similar correspondences were observed in the Cr, V, Fe, and Ni systems even though the limiting values vary with the metal, which shows that the cluster bonds accurately track the variations in the bulk phase thermochemistry of different metals. Such correspondences with such small cluster sizes are somewhat surprising, but can be understood by the local nature of chemical bonding.

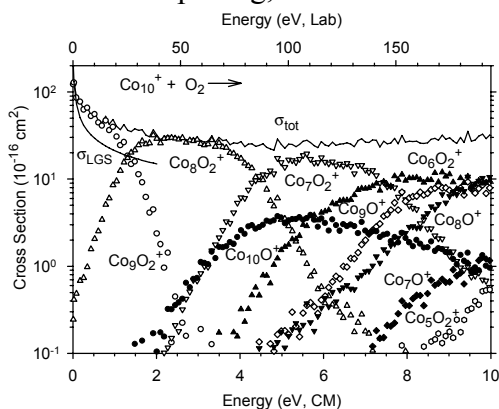


Figure 2. Reaction of Co_{10}^+ with O_2 . Dioxide (open symbols) and monoxide (closed symbols) product ions are shown.

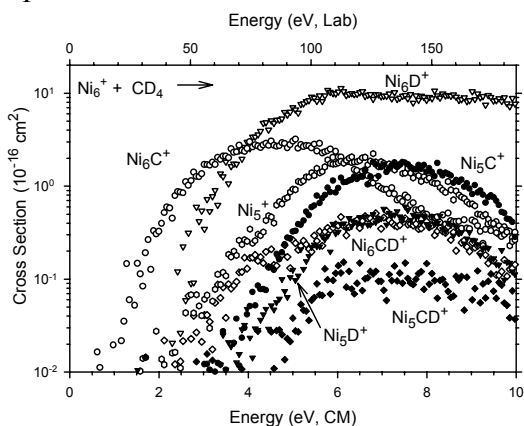


Figure 3. Reaction of Ni_6^+ with CD_4 with primary (open symbols) and secondary (closed symbols) products.

whereas for nickel, double dehydrogenation is efficient enough that the $Ni_nCD_2^+$ species is not observed except for the smallest and largest clusters. These results are qualitatively consistent with observations that carbide formation is an activated process for reactions of hydrocarbons on Fe, Co, and Ni surfaces.

Reactions of Clusters with O_2 . Studies of the kinetic energy dependences of the V_n^+ ($n = 2 - 17$),¹⁵ Cr_n^+ ($n = 2 - 18$),¹⁶ Fe_n^+ ($n = 2 - 18$),¹⁷ Co_n^+ ($n = 2 - 20$),² and Ni_n^+ ($n = 2 - 18$)^{Error! Bookmark not defined.} cluster ions reacting with O_2 have been completed. The reactions of metal cluster cations with O_2 yield a large number of products, e.g., the results of Figure 2 are representative of clusters larger than Co_5^+ . The magnitudes of the total reaction cross sections at thermal energies are comparable to the collision cross section, indicating that the reactions are efficient and exothermic. Cluster dioxide ions are the dominant products at low energies for all metals. This work shows that metal-oxygen bonds are stronger than metal-metal bonds for all five metals, hence, primary products dissociate by sequential metal atom loss to form smaller cluster dioxide ions. Oxygen atom loss to form cluster monoxide ions, M_nO^+ , is much less efficient. Analysis of the kinetic energy dependence is used to provide both $D_0(M_n^+-O)$ and $D_0(M_n^+-2O)$. As shown in Figure 1, the metal cluster oxygen BDEs measured in our work compare favorably to those for bulk phase surfaces.

Reactions of Clusters with CD_4 . We have studied the kinetic energy dependences of reactions of Fe_n^+ ($n = 2 - 16$)⁷ and Ni_n^+ ($n = 2 - 16$)⁴ with CD_4 , and that for Co_n^+ ($n = 2 - 16$) is undergoing final analysis.⁶ Figure 3 shows results typical of most clusters. All observed reactions are endothermic. The lowest energy process for iron and cobalt clusters is dehydrogenation,

Thresholds for the various primary and secondary reactions are analyzed and BDEs for cluster bonds to C, CD, and CD₂ are determined. Importantly, the accuracy of these BDEs can be assessed because there are usually two independent routes to measure BDEs for each cluster to D, C, CD, and CD₂, e.g., $D_0(\text{Ni}_6^+-\text{D})$ can be measured in the primary reaction of Ni_6^+ or the secondary reaction of Ni_7^+ . Values obtained from the primary and secondary processes are in good agreement for D (which also agree with the results from D₂ studies), C, and CD. For the CD₂ ligand, BDEs obtained from primary reactions are generally low compared to those from secondary reactions, which demonstrates that the initial dehydrogenation reactions have barriers in excess of the endothermicity. For larger clusters, this barrier appears to correspond to the initial dissociative chemisorption step.

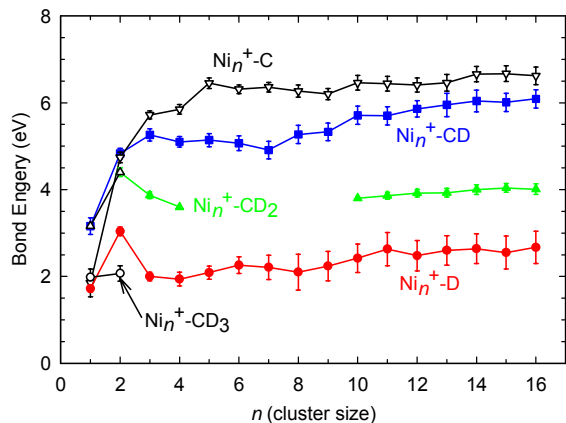


Figure 4. BDEs of D, C, CD, CD₂, and CD₃ to Ni_n^+ vs. cluster size.

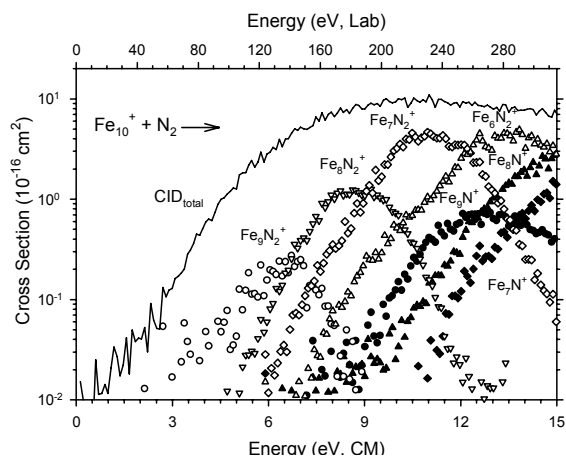


Figure 5. Reaction of Fe_{10}^+ with N_2 showing cross sections for dinitride (open symbols), mononitride (closed symbols), and the total CID products (solid line).

largest clusters. Fe_n^+-N and Fe_n^+-2N bond energies as a function of cluster size are derived from threshold analysis of the kinetic-energy dependences of the endothermic reactions. These experimental values are somewhat smaller than bulk phase values, although this is potentially because the activation barriers for N_2 activation have been underestimated in the surface work, as previously suggested by Benziger.¹⁸

Figure 4 shows the final BDEs determined in the nickel study,⁴ which vary for small clusters but rapidly reach a relatively constant value at larger cluster sizes. The magnitudes of these bonds are consistent with simple bond order considerations, namely, D (and CD₃) form one covalent bond, CD₂ forms two, and CD and C form three. Given the results of Figure 1, it seems reasonable that our experimental BDEs for larger clusters should provide reasonable estimates for heats of adsorption to surfaces. As little experimental information is available for *molecular* species binding to surfaces, the thermochemistry derived here for clusters bound to C, CD, and CD₂ provides some of the first experimental thermodynamic information on such molecular species.

Reactions of Clusters with N_2 . Our studies of the reactions of N_2 with Fe_n^+ ($n = 1 - 19$)³ and Co_n^+ ($n = 1 - 18$), which is undergoing final analysis,⁵ are designed to provide insight into the rate-limiting step in the Haber process, which uses a promoted iron catalyst to manufacture ammonia from N_2 and H_2 at high pressures and temperatures. Despite the very strong N_2 bond energy of 9.76 eV, activation of this molecule on iron and cobalt cluster cations is observed, as illustrated in Figure 5. Both Fe_mN_2^+ and Fe_mN^+ product ions, where $m \leq n$, are observed and the former can be identified as a dinitride species. An energetic barrier for N_2 activation of about 0.48 eV is obtained for the

Future Plans

We have also initiated studies of oxygenated iron clusters, Fe_nO_m^+ , which might mimic the chemistry of metal oxide surfaces. A broad range of stoichiometries have been produced although larger clusters tend to form clusters containing nearly equal numbers of iron and oxygen atoms. Initially, our studies are focusing on characterizing the thermodynamic stabilities of these clusters by examining their dissociation behavior in collisions with Xe. Some 30 different iron oxide cluster cations (with $n = 1 - 10$) have been examined, including FeO_x^+ ($x = 1 - 5$), Fe_2O_x^+ ($x = 1 - 6$), Fe_3O_x^+ ($x = 2 - 4, 8$), Fe_4O_x^+ ($x = 1 - 6$), Fe_5O_x^+ ($x = 4 - 6$), Fe_6O_x^+ ($x = 5 - 8$), Fe_7O_x^+ ($x = 6 - 8$), Fe_8O_x^+ ($x = 7 - 9$), Fe_9O_x^+ ($x = 8 - 10$), and $\text{Fe}_{10}\text{O}_x^+$ ($x = 9 - 11$). The kinetic energy dependent collision-induced dissociation cross sections are being analyzed to obtain both oxygen and iron bond energies for these clusters. We then intend to examine the possibility that specific oxidation states of the iron clusters might induce efficient oxidation of species like methane.

Publications resulting from DOE sponsored research in 2004 – present (1 – 6, 8) and References

1. F. Liu and P. B. Armentrout, *J. Chem. Phys.* **122**, 194320-1-12 (2005).
2. F. Liu, F.-X. Li, P. B. Armentrout, *J. Chem. Phys.* **123**, 064304-1-15 (2005).
3. L. Tan, F. Liu, P. B. Armentrout, *J. Chem. Phys.* **124**, 084302-1-14 (2006).
4. F. Liu, X.-G. Zhang, R. Liyanage, and P. B. Armentrout, *J. Chem. Phys.* **121**, 10976 (2004).
5. F. Liu, L. Tan, and P. B. Armentrout, work in progress.
6. Liu, F.; Armentrout, P. B. work in progress.
7. R. Liyanage, X.-G. Zhang, and P. B. Armentrout, *J. Chem. Phys.* **115**, 9747 (2001).
8. P. B. Armentrout; W. C. Castleman and P. Jena, editors; submitted for publication.
9. R. Liyanage, J. Conceição, and P. B. Armentrout, *P. B. J. Chem. Phys.* **116**, 936 (2002).
10. J. Conceição, R. Liyanage, and P. B. Armentrout, *Chem. Phys.* **262**, 115 (2000).
11. J. Conceição, S. K. Loh, L. Lian, and P. B. Armentrout, *J. Chem. Phys.* **104**, 3976 (1996).
12. F. Liu, R. Liyanage, and P. B. Armentrout, *J. Chem. Phys.* **117**, 132 (2002).
13. P. B. Armentrout, *Advances in Gas Phase Ion Chemistry*, Vol. 1; N. G. Adams and L. M. Babcock, Eds.; JAI: Greenwich, 1992; pp. 83-119.
14. K. Christmann, *Surf. Sci. Report*, **9**, 1 (1988). M. E. Bridge, C. M. Comrie, and R. M. Lambert, *J. Catal.* **58**, 28 (1979). K. H. Ernst, E. Schwarz, and K. Christmann, *J. Chem. Phys.* **101**, 5388 (1994).
15. J. Xu, M. T. Rodgers, J. B. Griffin, and P. B. Armentrout, *J. Chem. Phys.* **108**, 9339 (1998).
16. J. B. Griffin and P. B. Armentrout, *J. Chem. Phys.* **108**, 8062 (1998).
17. J. B. Griffin and P. B. Armentrout, *J. Chem. Phys.* **106**, 4448 (1997).
18. J. B. Benziger, in *Metal-Surface Reaction Energetics*, edited by E. Shustorovich (VCH, New York, 1991), pp. 53–107.

“Electronic Structure of Transition Metal Clusters, and Actinide Complexes, and Their Reactivities” October 2007

K. Balasubramanian

Dept of Mathematics, computer science and physics, California State University East Bay, Hayward CA; Chemistry and Material Science Directorate, Lawrence Livermore National Laboratory, University of California, Livermore, California 94550; Glenn T. Seaborg Center, Lawrence Berkeley National Laboratory, Berkeley, California 94720;

kris.bala@csueastbay.edu

Program Scope

Our efforts during 2006-2007 were focused on: computing spectroscopic properties of transition metal carbides and computational modeling of actinide complexes pertinent to environmental management of high-level nuclear wastes. All of our studies were motivated by experimental works on gas-phase spectroscopy of transition metal compounds and actinide complexes in solution. Our computational actinide chemistry was carried out concurrently with ongoing experimental studies by Professor Heino Nitsche and coworkers at LBNL. Such studies of actinide complexes are also important to understanding of the complexes found in geochemical and biochemical environment and are thus critical to management of high-level nuclear wastes. We have computed the geometrical and electronic properties such as ionization potentials, electron affinities, spectroscopic properties, potential energy curves, and binding energies of transition metal species. Especially third and second row transition metal clusters transition metal carbides have been considered. Actinide complexes such as uranyl, neptunyl, and plutonyl complexes have been studied in aqueous solution. These studies are made with relativistic complete active space multi-configuration self-consistent-field (CASSCF) followed by large-scale CI computations and relativistic CI (RCI) computations up to 60 million configurations. We have also employed PCM models to study actinide complexes in aqueous solution not only for the computation of spectroscopic properties and geometries but also thermodynamic properties such as Gibbs free energies.

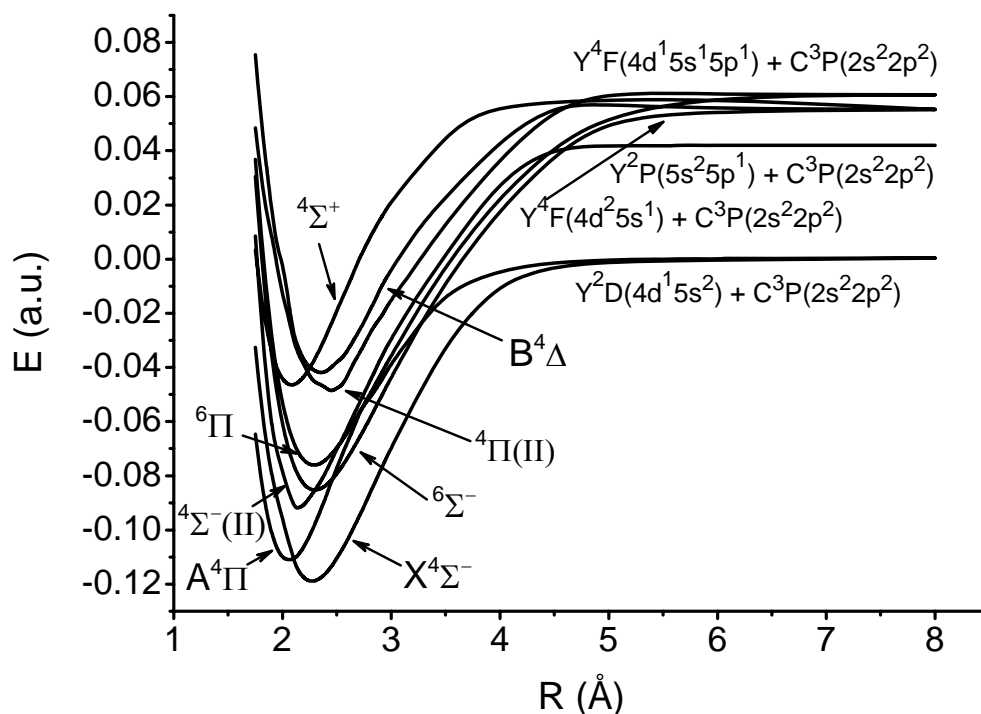
Recent Progress

Results of our computational studies and comparison with experiment have been described extensively in publications¹⁻¹⁸, which contain further details such as tables and figures. We have provided here the major highlights, in each of the categories.

Spectroscopic Properties of Transition Metal Species.

Spectroscopic constants and potential energy curves of a number of second-row transition metal carbides, especially NbC⁴, ZrC¹² and YC¹⁷. In addition in collaboration with surface science experimentalists, we have studied the reaction of H₂ molecules on actinide metal surfaces^{9,11,15}. All of these studies are challenging due to the open-shell nature of the metal resulting in a number of low-lying electronic states for this molecule. We have carried out state-of-the-art complete active space multi-configuration self-consistent field followed by multireference configuration interaction methods in conjunction with relativistic effects. Our computed potential energy curves for a few low-lying electronic states are shown in Fig 1, while more curves can be found in Ref. 17. Our computations support the assignment of the observed spectra to a B⁴Δ (Ω=7/2) ← A⁴Π (Ω=5/2) transition with a reinterpretation that the A⁴Π state is appreciably populated under the experimental conditions as it is less than 2000 cm⁻¹ of the X⁴Σ⁻

ground state, and the previously suggested $^4\Pi$ ground state is reassigned to the first low-lying excited state of YC . The potential energy curves of the YC^+ confirm a previous prediction by Prof. Armentrout and coworkers that the ground state of YC^+ is formed through a second pathway at higher energies. The calculated ionization energy of YC is 6.00 eV while the adiabatic electron affinity is 0.95 eV at the MRSDCI level. Our computed ionization energy of YC and dissociation energy of YC^+ confirm the revised experimental estimates provided by Armentrout and coworkers although direct experimental measurements yielded results with greater errors due to uncertainty in collisional cross sections for YC^+ formation.



We have studied the reaction of H_2 molecule on actinide metal interfaces in collaboration with ongoing experimental studies on these species. Our computations have revealed several fascinating trends for transition metal sites on actinide materials as catalytic sites for the hydrogen reactions. More details are in refs. 9, 11, and 15..

Electronic Structure of Actinide Complexes.

We have carried out collaborative on actinide complexes with Prof. Heino Nitsche's group at Berkeley... The hydrolysis reactions of curium (III), uranium, neptunyl and plutonyl complexes have received considerable attention due to their geochemical and biochemical importance but the results of free energies in solution and the mechanism of deprotonation have been topic of considerable uncertainty. We have computed the geometries, IR spectra and thermodynamic properties of such complexes in both gas phase and aqueous solution. We have shown in Fig 2 and 3 select optimized geometries of neptunyl and Cm(III) complexes. Further details on such actinide complexes can be found in refs. 3, 5, 7, 14, and 18. Extensive *ab initio* computations have been carried out to study the equilibrium structure, infrared spectra, and bonding characteristics of a variety of hydrated $NpO_2(CO_3)_m^{q-}$ complexes by considering the solvent as a polarizable dielectric continuum as well as the corresponding anhydrate complexes in the gas-phase. The computed structural parameters and vibrational results at the MP2 level in aqueous solution are in good agreement with Clark et al.'s experiments and provide realistic pictures of the neptunyl complexes in an aqueous environment. Our computed hydration energies

reveal that the complex with water molecules directly bound to it yields the best results. Our analysis of the nature of the bonding of neptunyl complexes provides insight into the nature of 6d and 5f-bonding in actinide complexes .

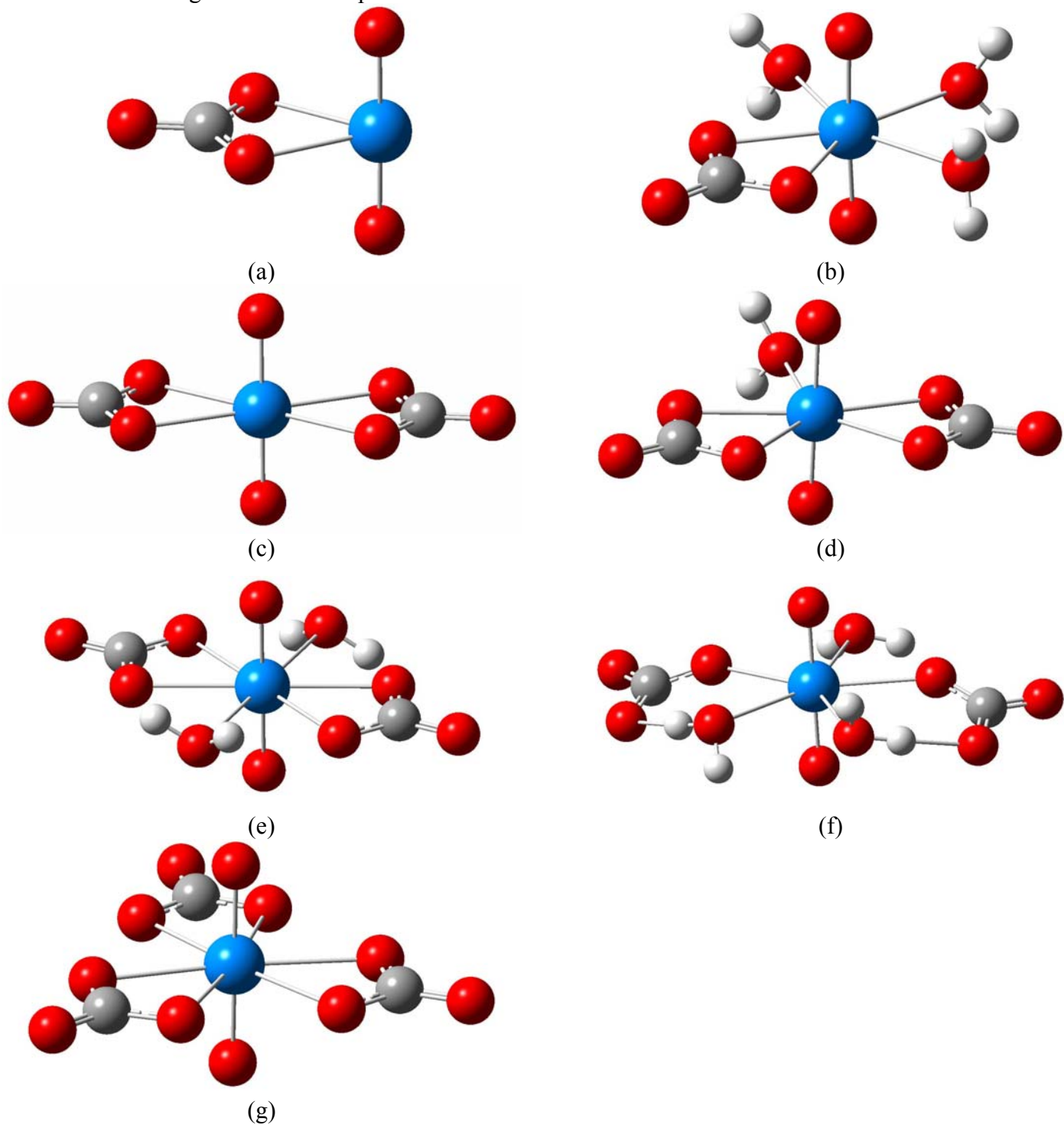
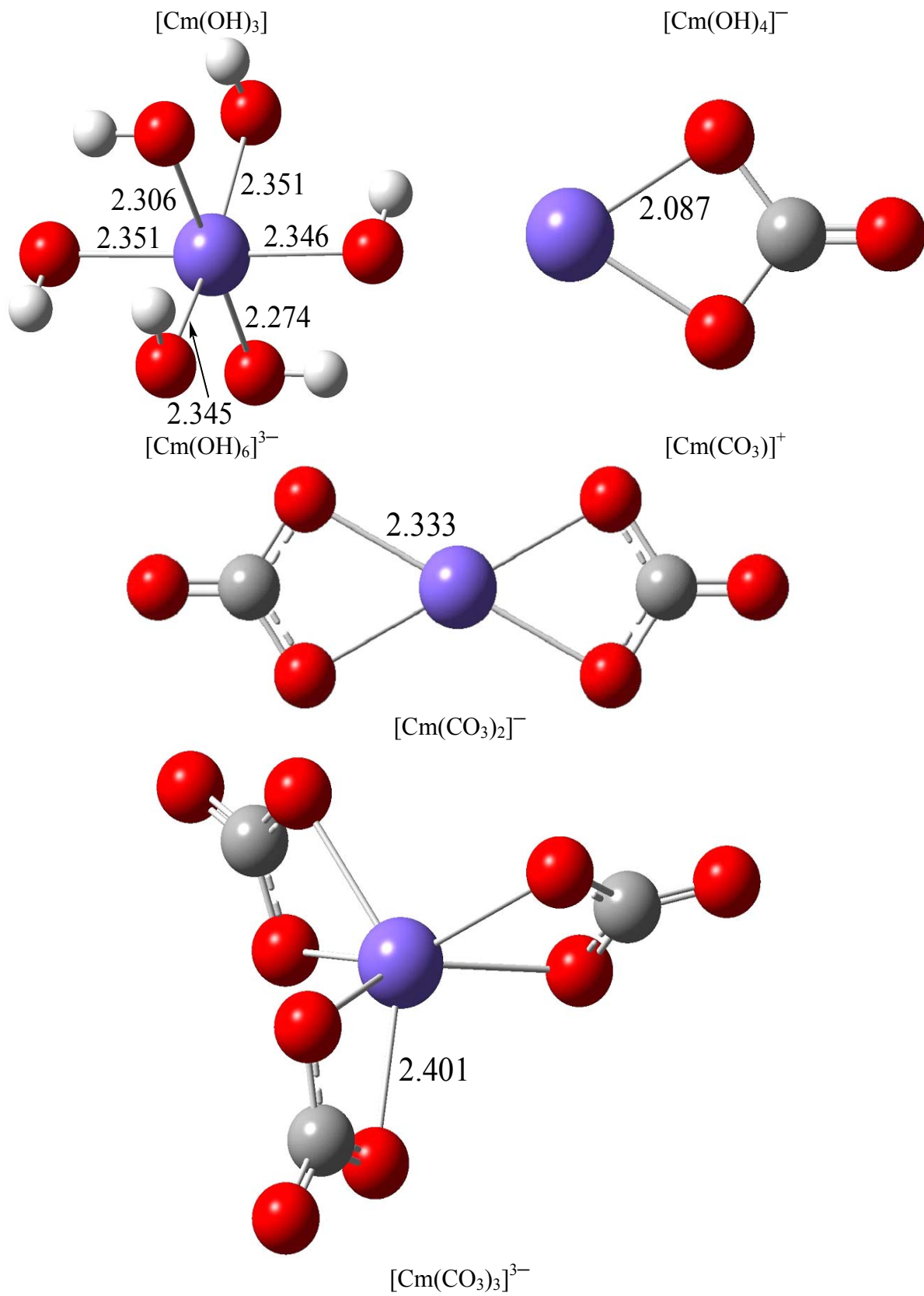


Fig. 2 Optimized Geometries of $[\text{NpO}_2(\text{CO}_3)_n(\text{H}_2\text{O})_m]^{q+}$ in aqueous solution



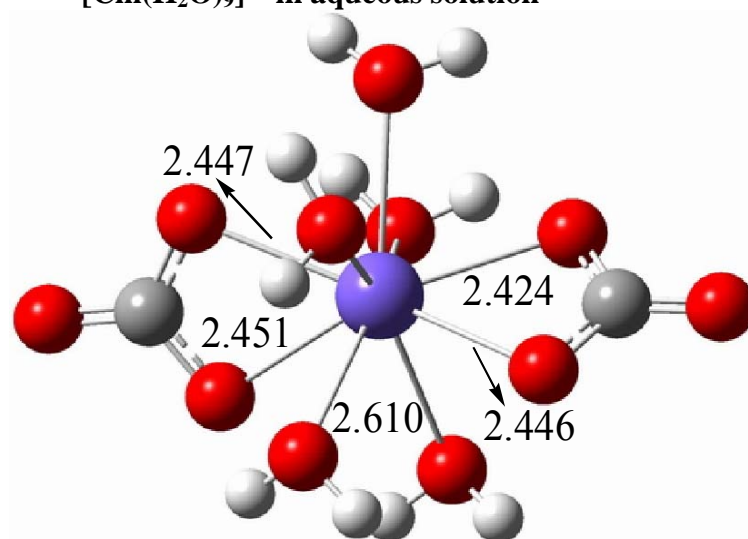
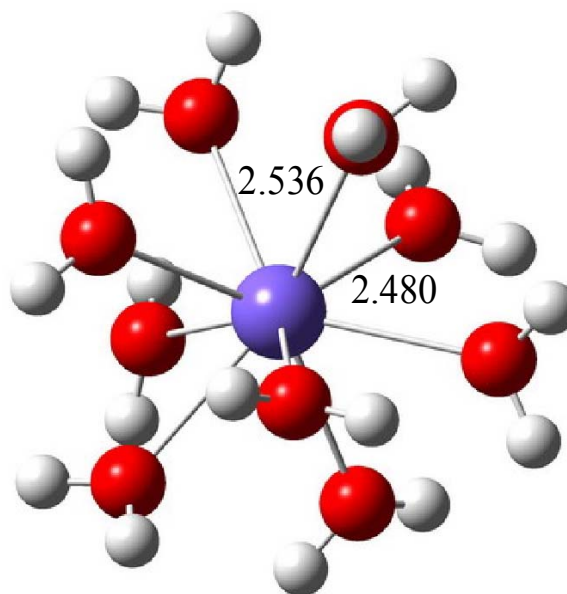
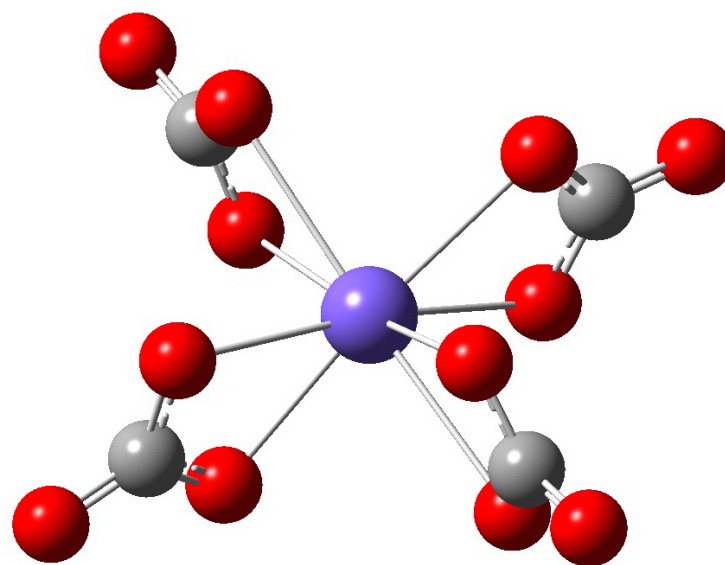


Fig 3 Optimized geometries of Curium (III) complexes in the gas phase and in aqueous solution.

Future Plan

We are studying Am(III) and Cm(III) complexes of experimental importance in collaboration with Prof Nitsche. Likewise a variety of plutonyl complexes are being studied both in gas phase and solution. There are mind boggling questions concerning the nature of these species and the role of 5f versus 6d orbitals in bonding and how relativistic effects influence the structures of these species. There are many challenges as we attempt to study these species. Both relativistic effects including spin-orbit effects and electron correlation effects must be considered accurately. We have also been investigation actinide complexes of environmental importance and their salvation phenomena. We have been looking at methods to consider aqueous actinide complexes.

References to Publications of DOE-sponsored work in 205-2007

1. Balasubramanian, K., Relativistic Effects in the Chemistry of very Heavy and super heavy Molecules. *Lecture Series on Computer & Chemical sciences* **2005**, 4, 759-764. [\[PDF\]](#)
2. Balasubramanian, K., Computational and Mathematical Approaches to Fullerenes and Proteomes. *Lecture Series on Computer & Chemical science* **2005**, 4, 765-767. [\[PDF\]](#)
3. Majumdar, D.; Balasubramanian, K., Theoretical studies on the electronic structures of $\text{UO}_2(\text{CO}_3)_2^{2-}$ and its metal salts: $\text{M}_2\text{UO}_2(\text{CO}_3)_2$ ($\text{M} = \text{Li}^+$, and Na^+). *Molecular Physics* **2005**, 103, (6-8), 931-938. [\[PDF\]](#)
4. Denis, P. A.; Balasubramanian, K., Theoretical characterization of the low-lying electronic states of NbC. *Journal of Chemical Physics* **2005**, 123, (5), 9. [\[PDF\]](#)
5. Cao, Z. J.; Balasubramanian, K., Theoretical studies of $\text{UO}_2^{2+}(\text{H}_2\text{O})_n$, $\text{NpO}_2^{2+}(\text{H}_2\text{O})_n$, and $\text{PuO}_2^{2+}(\text{H}_2\text{O})_n$ complexes ($n=4-6$) in aqueous solution and gas phase. *Journal of Chemical Physics* **2005**, 123, (11), 12. [\[PDF\]](#)
6. Balasubramanian, K., Electronic and spectroscopic properties of transition metal and main group clusters and compounds. *Abstracts of Papers of the American Chemical Society* **2005**, 230, U2871-U2871. [\[PDF\]](#)
7. Balasubramanian, K., In *Relativity and Chemical Bonding: Chemistry of heavy to superheavy Elements*, Proceedings of the 20th DUBROVNIK INTERNATIONAL COURSE & CONFERENCE MATH / CHEM / COMP 2005, Dubrovnik, June 20, 2005; Ante Graovac, A.; Pokri, B., Vickic-Topic, D., Eds. Dubrovnik, 2005. [\[PDF\]](#)
8. Balasubramanian, K., Mathematical Basis of Periodicity in Atomic and Molecular Spectroscopy. In *Mathematics of the Periodic Table*, Rouvray, D. H., R. B. King, Ed. Nova Science Publishers: New York, 2006; pp 189-216. [\[PDF\]](#)
9. Balasubramanian, K., T. E. Felter, Tom Anklam, T. W. Trelenberg, William McLean II, Atomistic Level Relativistic Quantum Modeling of Plutonium Hydriding. In *Plutonium Science-Futures Conference*, Pacific Grove CA, 2006. [\[PDF\]](#)

10. Balasubramanian, K., Relativistic Quantum Computations of Clusters. In *Proceedings of the 46th Sanibel Symposium*, St. Simons, GA, 2006. [\[PDF\]](#)
11. Balasubramanian, K., Bryan Balazs and William McLean Relativistic Quantum Modeling of Uranium Hydriding-Trends in Impurities and actinide complexes. *Chemtracts* **2006**, 19, 66-77. [\[PDF\]](#)
12. Denis, P. A.; Balasubramanian, K., Multireference configuration interaction study of the electronic states of ZrC. *Journal of Chemical Physics* **2006**, 124, (17), 8. [\[PDF\]](#)
13. Denis, P. A.; Balasubramanian, K., Electronic states and potential energy curves of molybdenum carbide and its ions. *Journal of Chemical Physics* **2006**, 125, (2), 9. [\[PDF\]](#)
14. Balasubramanian, K.; Cao, Z. J., Fluxional motions and internal rotational barriers of water molecules bound to UO_2^{2+} , NpO_2^+ , and PuO_2^{2+} . *Chemical Physics Letters* **2007**, 433, (4-6), 259-263. [\[PDF\]](#)
15. Balasubramanian, K.; Felter, T. E.; Anklam, T.; Trelenberg, T. W.; McLean II, W., Atomistic level relativistic quantum modelling of plutonium hydrogen reaction. *Journal of Alloys and Compounds* **2007**, In Press, Corrected Proof. [\[PDF\]](#)
16. Balasubramanian, K., In *Computational Modeling of Actinide Complexes*, AAAS and the Northwest Regional ACS Conference on Chemistry of Advanced Nuclear Systems, Boise, ID, June 16-21, 2007. [\[PDF\]](#)
17. Suo, B.; Balasubramanian, K., Spectroscopic constants and potential energy curves of yttrium carbide (YC). *Journal of Chemical Physics* **2007**, In Press. [\[PDF\]](#)
18. Cao, Z., Balasubramanian, K., "Theoretical Studies on Structures of Neptunyl Carbonates: $\text{NpO}_2(\text{CO}_3)_m(\text{H}_2\text{O})_n^{q-}$ ($m=1-3$, $n=0-3$) in Aqueous Solution", *Inorganic Chemistry*, 2007, in Review

Influence of medium on radical reactions

David M. Bartels, John Bentley and Daniel M. Chipman
Notre Dame Radiation Laboratory, Notre Dame, IN 46556
e-mail: bartels.5@nd.edu; Bentley.1@nd.edu ; chipman.1@nd.edu

Program definition

This project pursues the use of radiolysis as a tool in the investigation of solvent effects in chemical reactions, particularly the free radicals derived from solvent which are copiously generated in the radiolysis excitation process. Most recently we have focused on radical reactions in high-temperature water, and some of these results are described below. The project has now evolved toward the particular study of solvent effects on reaction rates in supercritical (sc-)fluids where the fluid density becomes a primary variable. One proposed thrust will be the study of solvated electrons under these conditions. Others will focus on small radicals in supercritical water and CO₂. A theoretical component has also recently been joined with this project, which will be directed to support the analysis and interpretation of experimental results.

An anthropomorphic way to think about near-critical phenomena, is that the fluid is trying to decide whether it is a liquid or a gas. The cohesive forces between molecules that tend to form a liquid are just being balanced by the thermal entropic forces that cause vaporization. The result, on a microscopic scale, is the highly dynamic formation and dissipation of clusters and larger aggregates. The fluid is extremely heterogeneous on the microscopic scale. A solute in a supercritical fluid can be classified as either attractive or repulsive, depending on the potential between the solute and solvent. If the solute-solvent potential is more attractive than the solvent-solvent potential, the solute will tend to form the nucleus of a cluster. When the solute-solvent potential is repulsive, one might expect the solute to remain in a void in the fluid as the solvent molecules cluster together. Extremely large partial molal volumes are known for hydrophobic molecules in near-critical water, indicating an effective phase separation. Such variations in local density around the solute will have implications for various spectroscopies and for reaction rates.

The ultimate goal of our study is the development of a predictive capability for free radical reaction rates, even in the complex microheterogeneous critical regime. Our immediate goal is to determine representative free radical reaction rates in sc-fluid and develop an understanding of the important variables to guide development and use of predictive tools. Electron beam radiolysis of water (and other fluids) is an excellent experimental tool with which to address these questions. The primary free radicals generated by radiolysis of water, (e⁻)_{aq}, OH, and H, are respectively ionic, dipolar, and hydrophobic in nature. Their recombination and scavenging reactions can be expected to highlight the effects of clustering (i.e. local density enhancements) and solvent microheterogeneity both in terms of relative diffusion and in terms of static or dynamic solvent effects on the reaction rates. We already have transient absorption data for several of these species that highlights interesting and unexpected reaction rate behavior. A major thrust of the next several years will be to push time-resolved EPR detection of H atoms in sc-water. The Chemically Induced Dynamic Electron Polarization (CIDEP) generated in H atom recombination reactions provides another unique probe of the cage dynamics and potential of mean force. How different will be the potential of mean force between H atoms and between (e⁻)_{aq} and H? How easily will H atoms penetrate into water clusters?

Recent Progress

Data analysis was completed on pulse radiolysis/transient absorption data collected on alkaline water saturated with H_2 at high pressure. The primary reactions are as follows:



All radicals are converted to the easily detected solvated electron. Rates for reactions 1 and 2 were determined in previous studies over the 100-350°C temperature range of interest here. At low radiation dose the decay is purely second order from reaction (3). At very high dose, H atoms are present for a microsecond or so, and a large fraction of electrons decay via reaction (4). Both second order reaction rates can be extracted from the data, which is collected as a function of radiation dose and $[OH^-]$.

In Figure 1 we plot the rate constants determined for reaction 4. Analysis of these rate constants using the Smoluchowski equation indicates that the reaction distance is very large (13 angstrom) at room temperature, and decreases up to about 200°C.

We believe this is consistent with a long-range electron transfer of the electron from the solvent potential well onto the H atom. The super-arrhenius behavior seen at higher temperature in figure 1 can only be explained by much higher than anticipated diffusion rate of the hydrated electron. The rate constant for reaction (3), which is diffusion limited up to 150°C, drops quickly at higher temperatures. By 250°C, it is slower than room temperature. We now believe the mechanism for this reaction involves a proton transfer from water, which is stimulated by the near proximity of two solvated electrons (reaction distance on the order of 10 angstroms up to 150°C). This produces a hydrogen atom in close proximity to a solvated electron, and reaction (4) follows immediately with unit probability.

Why is there a large red shift in the absorption spectrum of solvated electrons as temperature is increased? This very old question was apparently answered by a recent simulation study which showed that solvent density, rather than temperature is the important variable. However, earlier work in our laboratory showed that in supercritical water, as the density is changed over a factor of six at constant temperature, the spectrum barely changes. Apparently the bulk density is only critical when the free volume available to the electron is small enough. To test this further, we recorded solvated electron spectra in supercooled water. This allows us to compare spectra at the same bulk density but with different temperatures, thanks to the water density maximum at 4°C. We found a continuous blue shift of the spectrum in supercooled water, just as in normal water above 0°C. There is clearly a separate effect of

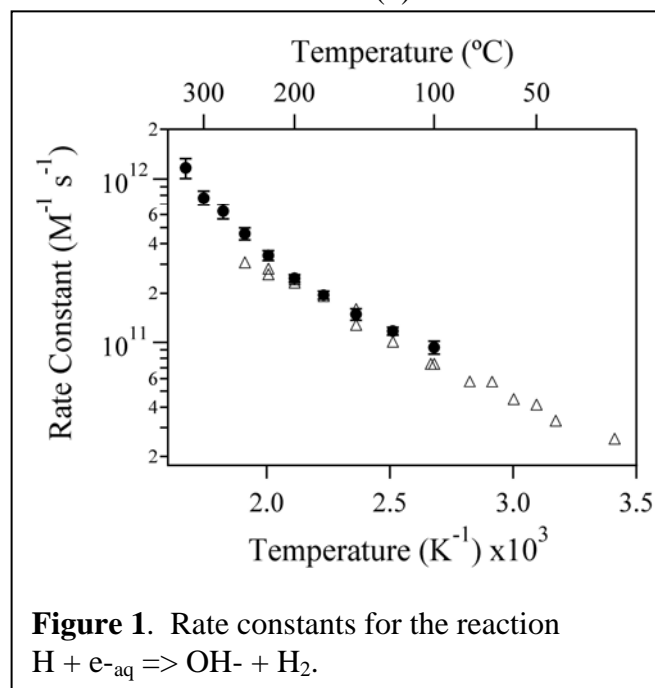


Figure 1. Rate constants for the reaction $H + e^-_{aq} \Rightarrow OH^- + H_2$.

temperature as well as density (pressure) on the solvated electron spectrum. While the popular pseudopotential models for the solvated electron omit many-electron effects by design, EPR and Raman data both indicate significant coupling of the unpaired electron to the water molecules in the hydration shell. These molecules are in turn connected to the H – bond network of the water as clearly demonstrated by the Raman data. We presume it is this direct and indirect coupling of the electrons to the solvent which is ultimately responsible for the additional temperature effect on the spectrum. In this case it would seem that a many-electron ab initio MD approach will be necessary to successfully model the solvated electron spectrum vs. temperature.

Work has been initiated to understand the detailed mechanisms of the key radiolytic reactions $\text{H} + \text{OH} \Rightarrow \text{H}_2\text{O}$ and $\text{H} + \text{O}_2 \Rightarrow \text{HO}_2$ in aqueous solution, using electronic structure methods. Bulk dielectric effects are found to produce some quantitative but no qualitative changes in the gas phase potential energy surfaces. However, calculations in small water clusters indicate that inclusion of explicit water molecules can significantly alter the mechanisms. In addition to acting as spectators, some individual water molecules can be intimately involved as chemical participants through undergoing partial or even full fragmentation during the course of the reactions. These findings will be used to design and guide molecular dynamics methods suitable for studying the reaction mechanisms.

Future Plans

Immediate plans are to continue the optical transient absorption measurements of OH radical and hydrated electron reaction rates. Calculations are in progress to characterize the nature of the OH absorption at 250nm in water, with a view toward understanding why this absorption seems to disappear in supercritical water. A most important target for experimental measurement is the reaction $\text{H}_2 + \text{OH}$ in supercritical water. Mechanisms of prototypical radiolytic reactions in aqueous solution such as $\text{H} + \text{OH} \rightarrow \text{H}_2\text{O}$, $\text{H}_2 + \text{OH} \rightarrow \text{H} + \text{H}_2\text{O}$, $\text{H}_2 + \text{O}^- \rightarrow \text{H} + \text{OH}^-$, $\text{OH} + \text{OH} \rightarrow \text{H}_2\text{O}_2$ and $\text{OH} + \text{OH}^- \rightarrow \text{O}^- + \text{H}_2\text{O}$, as well as the OH/O⁻ equilibrium, will be characterized by ab initio methods as initial steps toward the ultimate goal of understanding their unusual temperature dependences. Work on understanding of solvated electron reaction rates is to be continued by measuring reaction rates in supercritical alcohols for comparison with unusual behavior in supercritical water.

A major new effort will involve direct EPR measurements of free radicals in supercritical water. The primary target of this experiment is the hydrogen atom. The hydrogen atom is the prototypical free radical, and its reactions in condensed phase are naturally a subject of great theoretical interest. Moreover, extensive isotope effect information can be generated by comparison of D atom and muonium atom reactions. H (and D) atoms are readily generated in acidic water by electron beam radiolysis. Time-resolved EPR is found to be a convenient and specific technique for H atom detection. The large hyperfine coupling of H or D atoms make their signals unambiguous. Virtually always, time-resolved H atom signals are found to be polarized by Chemically Induced Dynamic Electron Polarization (CIDEP) in the radical recombination reactions. The latter phenomenon can give information on potential of mean force and diffusional dynamics in the encounter pairs.

Publications, 2005-2007

Bonin, J.; Janik, I.; Janik, D.; Bartels, D. M. (2007). *J. Phys. Chem. A* 111(10): 1869-1878. Reaction of the Hydroxyl Radical with Phenol up to Supercritical Conditions.

Du, Y.; Price, E.; Bartels, D. M. (2007). *Chem. Phys. Lett.* 438: 234-237. Solvated electron spectrum in supercooled water and ice.

Janik, I.; Bartels, D. M.; Jonah, C. D. (2007). *J. Phys. Chem. A* 111: 1835-1843. Hydroxyl Radical Self-Recombination Reaction and Absorption Spectrum in Water up to 350°C.

Janik, I.; Marin, T.; Jonah, C. D.; Bartels, D. M. (2007). *J. Phys. Chem. A* 111(1): 79-88. Reaction of O₂ with the Hydrogen Atom in Water up to 350°C.

Marin, T. W.; Takahashi, K.; Jonah, C. D.; Chemerisov, S.; Bartels, D. M. (accepted). *J. Phys. Chem. A*. Recombination of the Hydrated Electron at High Temperature and Pressure in Hydrogenated Alkaline Water.

Marin T.W.; Takahashi K.; Bartels D.M. (2006). *J. Chem. Phys.* 125, 104314. Temperature and density dependence of the light and heavy water ultraviolet absorption edge.

Chipman D.M. (2006). *J. Chem. Phys.* 124, 224111/1-10. New formulation and implementation for volume polarization in dielectric continuum theory.

Chipman D.M.; Chen F. (2006). *J. Chem. Phys.* 124, 144507/1-5. Cation electric field is related to hydration energy.

Shao Y.; Molnar L.F.; Jung Y.; Kussmann J.; Ochsenfeld C.; Brown S.T.; Gilbert A.T.B.; Slipchenko L.V.; Levchenko S. V.; O'Neill D. P.; DiStasio Jr. R.A.; Lochan R. C.; Wang T.; Beran G.J.O.; Besley N.A.; Herbert J.M.; Lin C.Y.; Van Voorhis T.; Chien S.H.; Sodt A.; Steele R. P.; Rassolov V.A.; Maslen P.E.; Korambath P.P.; Adamson R.D.; Austin B.; Baker J.; Byrd E.F.C.; Dachselt H.; Doerksen R.J.; Dreuw A.; Dunietz B.D.; Dutoi A.D.; Furlani T.R.; Gwaltney S.R.; Heyden A.; Hirata S.; Hsu C.-P.; Kedziora G.; Khalliulin R.Z.; Klunzinger P.; Lee A.M.; Lee M.S.; Liang W.Z.; Lotan I.; Nair N.; Peters B.; Proynov E.I.; Pieniazek P.A.; Rhee Y.M.; Ritchie J.; Rosta E.; Sherrill C.D.; Simmonett A.C.; Subotnik J.E.; Woodcock III H.E.; Zhang W.; Bell A.T.; Chakraborty A.K.; Chipman D.M.; Keil F.J.; Warshel A.; Hehre W.J.; Schaefer III H.F.; Kong J.; Krylov A.I.; Gil P.M.W.; Head-Gordon M. (2006). *Phys. Chem. Chem. Phys.* 8, 3172-3191. Advances in methods and algorithms in a modern quantum chemistry program package.

Bartels D.M.; Takahashi K.; Cline J.A.; Marin T.W.; Jonah C.D. (2005). *J. Phys. Chem. A* 109, 1299-307. Pulse radiolysis of supercritical water III. Spectrum and thermodynamics of the hydrated electron.

Chipman D.M.; Bentley J. (2005). *J. Phys. Chem. A* 109, 7418-28. Structures and energetics of hydrated oxygen anion clusters.

Garrett B.C.; Dixon D.A.; Camaioni D.M.; Chipman D.M.; Johnson M.A.; Jonah C.D.; Kimmel G.A.; Miller J.H.; Rescigno T.N.; Rossky P.J.; Xantheas S.S.; Colson S.D.; Laufer A.H.; Ray D.; Barbara P.F.; Bartels D.M.; Becker K.H.; Bowen H.; Bradforth S.E.; Carmichael I.; Coe J.V.; Corrales L.R.; Cowin J.P.; Dupuis M.; Eisenthal K.B.; Franz J.A.; Gutowski M.S.; Jordan K.D.; Kay B.D.; LaVerne J.A.; Lymar S.V.; Madey T.E.; McCurdy C.W.; Meisel D.; Mukamel S.; Nilsson A.R.; Orlando T.M.; Petrik N.G.; Pimblott S.M.; Rustad J.R.; Schenter G.K.; Singer S.J.; Tokmakoff A.; Wang L.S.; Wittig C.; Zwier T.S. (2005). *Chem. Rev.* 105, 355-89. Role of water in electron-initiated processes and radical chemistry: Issues and scientific advances

Marin T.W.; Jonah C.D.; Bartels D.M. (2005). *J. Phys. Chem. A*, 109, 1843-8. Reaction of hydrogen atoms with hydroxide ions in high-temperature and pressure water.

Mezyk S.P.; Bartels D.M. (2005). *J. Phys. Chem. A* 109, 11823-7. Rate constant and activation energy measurement for the reaction of atomic hydrogen with thiocyanate and azide in aqueous solution.

ELECTRON-DRIVEN PROCESSES IN CONDENSED PHASES

PRINCIPAL INVESTIGATORS

I Carmichael (*carmichael.1@nd.edu*), DM Bartels, DM Chipman, JA LaVerne
Notre Dame Radiation Laboratory, University of Notre Dame, Notre Dame, IN 46556

SCOPE

Fundamental physicochemical processes in water radiolysis are probed in an experimental program measuring spur kinetics of key radiolytic transients at elevated temperatures and pressures using a novel laser-based detection system with interpretation supported by computer simulations. Related experimental and computational studies focus on the electronic excitation of liquid water, important aqueous radiolytic species, and the significance and mechanism of dissociative electron attachment in the liquid. Radiolytic decay channels in nonaqueous media are investigated, both experimentally, with product analysis under γ and heavy-ion irradiation and transient identification under pulse radiolysis, and theoretically, via kinetic track modeling and electronic structure calculations.

PROGRESS AND PLANS

Experimental measurements of molecular hydrogen including the use of isotopic techniques are combined with track model calculations to determine H atom yields in the radiolysis of water. The production of H atoms in the radiolysis of water is relatively small and usually inferred by indirect methods, but is important for fundamental considerations. H atoms are formed by the decay of excited states of water at the sub-picosecond time scale and by hydrated electron reactions during the diffusion-kinetic evolution of the particle track up to microseconds. The competition between H atom loss by combination reactions and its formation by reactions of the hydrated electron makes prediction of the H atom kinetics very difficult. Total molecular hydrogen production in neat water and in formate solutions is being used to infer H atom yields, while the isotopic distribution of molecular hydrogen measured using deuterated formate as a scavenger gives more direct information on the yield of H atoms in particle tracks. Techniques have been developed and experiments have been performed with γ -radiolysis, 5 MeV proton radiolysis, and 5 MeV helium ion radiolysis. Total hydrogen measurements with γ -radiolysis match well with previous results on similar systems. Monte Carlo track model calculations are used to analyze the measured experimental yields and to elucidate the underlying H atom kinetics in the radiolysis of water.

H atom yields strongly depend on the kinetics of the hydrated electron. A significant amount of H atoms is formed in intratrack processes due to reactions of the hydrated electron with hydrated protons. Different solutes will be used with a wide range of concentration to elucidate the dependence of hydrogen atom yields on the hydrated electron scavenging capacity. These endeavors will be aided by Monte Carlo track model calculations, which can isolate the contributions of individual reactions. The validity of estimating H atom yield from measurements of molecular hydrogen with and without added solutes will be determined by comparison with the isotopic scavenging experiments. In the latter case, H atoms should be determined directly by measurements of HD in experiments with deuterated solutes such as formate, methanol, and 2 propanol. Heavy ion experiments will be performed to elucidate the effects of higher order reactions at high linear energy transfer, LET.

A laser-based detection system has been installed at our electron linear accelerator to allow both visible and deep UV measurement of spur kinetics during high-temperature water radiolysis. Preliminary experiments have begun. These time-resolved measurements will complement product yield studies performed here and elsewhere.

Previous experimental and theoretical works have suggested that dissociative electron attachment (DEA) processes are important in the radiolysis of ice and liquid water, but details are poorly understood. To help elucidate the matter, we have utilized multireference configuration interaction methods to computationally characterize the lowest energy Feshbach resonance state of water dimer anion. The potential energy surface in the analogous state of water monomer anion is known to be repulsive, so that electron attachment leads directly to dissociation of H^- . In contrast, we find for the dimer that an energetic barrier is encountered as the hydrogen-bonded OH moiety is stretched from its equilibrium position toward the hydrogen bond acceptor. The migrating hydrogen can thereby be held near the Franck-Condon region in a quasibound vibrational state for a time long compared to the OH vibrational period. This behavior is found both for the case of an icelike dimer structure and for a substantial majority of liquidlike dimer structures. These findings raise the possibility that hydrogen bonding may allow for a localized molecule-centered anionic entity to exist in condensed water phases that is metastable both to electron detachment and to bond dissociation, and which may live long enough to be considered as a species affecting DEA processes in water radiolysis.

Another target for theoretical understanding is the deep UV absorption spectrum of liquid water, which changes enormously from that of the water monomer. Experimentally, we wish to measure the absorption spectrum as a function of density in supercritical water to track this change. A high-temperature cell has been designed for vacuum UV measurements of the absorption spectrum in supercritical water. Because of the high water density, a very short path is required together with a very large dynamic range. Photon counting experiments are planned for the coming year at the synchrotron light source at the University of Wisconsin.

The radiation of liquid organics has focused on simple cyclic compounds such as cyclohexane, benzene, and pyridine because of the relatively small number of products formed. The radiation chemical yields of the main products produced in liquid pyridine radiolysis (molecular hydrogen and dipyridyl) have been examined as a function of LET with protons, helium ions, and carbon ions of a few to 30 MeV and compared to γ -radiolysis. Anthracene and biphenyl scavenging techniques have been used to clarify the role of the triplet excited state. An increase in triplet scavenger concentration leads to a decrease in pyridine triplet excited state with a concurrent decrease in dipyridyl, but formation of the latter does not primarily involve pyridyl radicals expected to be produced in the decomposition of the triplet excited state. A decrease in the yield of dipyridyl and an increase in molecular hydrogen are observed with increasing track average LET. The dipyridyl yield with 10 MeV carbon ions is 0.20 molecules/100 eV, which is only 16% of that of observed with γ -rays. The low yield of dipyridyl with carbon ions is attributed to intratrack triplet-triplet (T-T) annihilation processes due to the increase in local triplet excited state concentrations with increasing LET. An increasing yield of molecular hydrogen with increasing LET is probably due to an increase in the formation and subsequent decay of singlet excited states produced by the T-T annihilation.

A pulse radiolysis study of the formation and decay of triplet excited state in liquid pyridine has been carried out using quenching techniques. The pyridine triplet is observed in the absorption

band at $\lambda = 310$ nm, which has a first-order decay with a lifetime of 72 ns. The yield of pyridine triplet is estimated to be 1.3 molecules/100 eV by the Stern-Volmer plot for the quenching of pyridine triplet using anthracene, naphthalene, and biphenyl. Dipyridyl is the predominant single condensed phase product in the γ -radiolysis of liquid pyridine with a yield of 1.25 molecules/100 eV matching well with the pyridine triplet yields. The rate coefficient for the pyridine triplet scavenging by oxygen is estimated to be $1.8 \times 10^9 \text{ M}^{-1} \text{ s}^{-1}$. Oxygen is a relatively good scavenger of the pyridine triplet and of its precursor, whereas nitrous oxide is a poor scavenger of the precursor of pyridine triplet. Pyridyl-pyridine (dimer) radicals produced in the pulse radiolysis of neat liquid pyridine are detected at $\lambda = 390$ nm, which is assigned by iodine scavenging studies; as a tentative mechanism for the formation of dimer radical, an ion-molecule reaction of the radical cation with parent pyridine is proposed. Support for these spectral assignments and reaction mechanisms is offered by the results of extensive computational chemistry calculations employing Density Functional Theory.

The major decomposition mode of the cyclic organic liquids is the breaking of the C – H bond to give appropriate radical species. H atom yields are obviously important in determining the initial molecular decomposition and in product formation. Scavenging techniques to determine H atoms yields will employ iodine with the formation of HI and deuterated solutes with the formation of HD. H atom yields will be coupled with measurements of the triplet excited states, which are thought to be the main precursors. No addition product due to H atoms has been positively identified and gel permeation chromatography techniques will be used to search for possible polymer formation following H atom addition reactions to the parent compound. Monte Carlo track model calculations are not commonly applied to organic liquids because of the lack of experimental cross-section data and difficulty in accurately predicting the effects of long range forces on the kinetics. The latter problem seems to have been overcome recently and Monte Carlo track model calculations are currently being developed for hydrocarbon liquids

BES supported publications (2005-2007)

Chipman D.M. *J. Chem. Phys.* **2007**, (*accepted*). Dissociative electron attachment to the hydrogen-bond OH in water dimer through the lowest anionic Feshbach resonance.

Du Y.; Price E.; Bartels D.M. *Chem. Phys. Lett.* **2007**, *438*, 234-7. Solvated electron spectrum in supercooled water and ice.

Enomoto K.; LaVerne J.A.; Araos M.S. *J. Phys. Chem. A* **2007**, *111*, 9-15. Heavy ion radiolysis of liquid pyridine.

Janik I.; Bartels D.M.; Jonah C.D. *J. Phys. Chem. A* **2007**, *111*, 1835-43. Hydroxyl radical self-recombination reaction and absorption spectrum in water up to 350 °C.

LaVerne J.A.; Enomoto K.; Araos M.S. *Radiat. Phys. Chem.* **2007**, *76*, 1272-4. Radical yields in the radiolysis of cyclic compounds.

Pimblott S.M.; LaVerne J.A. *Radiat. Phys. Chem.* **2007**, *76*, 1244-7. Production of low energy electrons by ionizing radiation.

Chipman D. *J. Chem. Phys.* **2006**, *124*, 224111/1-10. New formulation and implementation for volume polarization in dielectric continuum theory.

Chipman D.M. *J. Chem. Phys.* **2006**, *124*, 044305/1-9. Stretching of hydrogen-bonded OH in the lowest singlet excited electronic state of water dimer.

Chipman D.M.; Chen F. *J. Chem. Phys.* **2006**, *124*, 144507/1-5. Cation electric field is related to hydration energy.

Enomoto K.; LaVerne J.A.; Pimblott S.M. *J. Phys. Chem. A* **2006**, *110*, 4124-30. Products of the triplet excited state produced in the radiolysis of liquid benzene.

Enomoto K.; LaVerne J.A.; Seki S.; Tagawa S. *J. Phys. Chem. A* **2006**, *110*, 9874-9. Formation and decay of the triplet excited state of pyridine.

Filipiak P.; Camaioni D.M.; Fessenden R.W.; Carmichael I.; Hug G.L. *J. Phys. Chem. A* **2006**, *110*, 11046-52. Reactions of 1-hydroxy-1-methylethyl radicals with NO₂⁻: Time-resolved electron spin resonance.

Maiti N.C.; Zhu Y.P.; Carmichael I.; Serianni A.S.; Anderson V.E. *J. Org. Chem.* **2006**, *71*, 2878-80. ¹J_{CH} correlates with alcohol hydrogen bond strength.

Marin T.W.; Takahashi K.; Bartels D.M. *J. Chem. Phys.* **2006**, *125*, 104314/1-11. Temperature and density dependence of the light and heavy water ultraviolet absorption edge.

Päch M.; Macrae R.M.; Carmichael I. *J. Am. Chem. Soc.* **2006**, *128*, 6111-25. Hydrogen and deuterium atoms in octasilsesquioxanes: Experimental and computational studies.

Stevens F.; Carmichael I.; Callens F.; Waroquier M. *J. Phys. Chem. A* **2006**, *110*, 4846-53. Density functional investigation of high-spin XY (X = Cr, Mo, W and Y = C,N,O) molecules.

Stevens F.; Van Speybroeck V.; Carmichael I.; Callens F.; Waroquier M. *Chem. Phys. Lett.* **2006**, *421*, 281-6. The Rh-ligand bond: RhX (X = C, N, O, F, P and C) molecules.

Thomas S.L.; Carmichael I. *Physica B* **2006**, *374-375*, 290-4. Hyperfine interactions in muonium-containing radicals.

Bartels D.M.; Takahashi K.; Cline J.A.; Marin T.W.; Jonah C.D. *J. Phys. Chem. A* **2005**, *109*, 1299-307. Pulse radiolysis of supercritical water III. Spectrum and thermodynamics of the hydrated electron.

Chipman D.M. *J. Chem. Phys.* **2005**, *122*, 044111/1-10. Excited electronic states of small water clusters.

Chipman D.M.; Bentley J. *J. Phys. Chem. A* **2005**, *109*, 7418-28. Structures and energetics of hydrated oxygen anion clusters.

Garrett B.C. et al. *Chem. Rev.* **2005**, *105*, 355-89. Role of water in electron-initiated processes and radical chemistry: Issues and scientific advances.

Hiroki A.; LaVerne J.A. *J. Phys. Chem. B* **2005**, *109*, 3364-70. Decomposition of hydrogen peroxide at water - ceramic oxide interfaces.

LaVerne J.A. *J. Phys. Chem. B* **2005**, *109*, 5395-7. H₂ Formation in the radiolysis of liquid water with zirconia.

LaVerne J.A.; Carmichael I.; Araos M.S. *J. Phys. Chem. A* **2005**, *109*, 461-5. Radical production in the radiolysis of liquid pyridine.

LaVerne J.A.; Stefanic I.; Pimblott S.M. *J. Phys. Chem. A* **2005**, *109*, 9393-401. Hydrated electron yields in the heavy ion radiolysis of water.

LaVerne J.A.; Stefanic I.; Pimblott S.M. *J. Japan. Soc. Rad. Chem.* **2005**, *79*, 9-12. Hydrated electron yields in the proton radiolysis of water.

Mahoney J.M.; Stucker K.A.; Jiang H.; Carmichael I.; Brinkmann N.R.; Beatty A.M.; Noll B.; Smith B.D. *J. Am. Chem. Soc.* **2005**, *127*, 2922-8. Molecular recognition of trigonal oxyanions using a ditopic salt receptor: Evidence for anisotropic shielding surface around nitrate anion.

Wenska G.; Taras-Goslinska K.; Skalski B.; Hug G.L.; Carmichael I.; Marciniak B. *J. Org. Chem.* **2005**, *70*, 982-8. Generation of thiyl radicals by the photolysis of 5-iodo-4-thiouridine.

Wisniowski P.; Bobrowski K.; Filipiak P.; Carmichael I.; Hug G.L. *Res. Chem. Intermed.* **2005**, *31*, 633-41. Reactions of hydrogen atoms with α -(alkylthio)carbonyl compounds. Time-resolved ESR detection and DFT calculations.

An Exploration of Catalytic Chemistry on Au/Ni(111)
Professor S. T. Ceyer
Department of Chemistry
Massachusetts Institute of Technology, Cambridge, MA 02139
stceyer@mit.edu

Project Scope

This project explores the breadth of catalytic chemistry that can be effected on a Au/Ni(111) surface alloy. A Au/Ni(111) surface alloy is a Ni(111) surface on which 10-30% of the Ni atoms are replaced at random positions by Au atoms. That is, the vapor deposition of a small amount of Au onto Ni single crystals does not result in an epitaxial Au overlayer or the condensation of the Au into droplets. Instead, it results in a strongly bound surface alloy. Gold atoms at coverages less than 0.3 ML replace Ni atoms on a Ni(111) surface, even though Au is immiscible in bulk Ni. The two dimensional structure of the clean Ni surface is preserved. This alloy is found to stabilize an adsorbed peroxy-like O₂ species that is shown to be the critical reactant in the low temperature catalytic oxidation of CO and that is suspected to be the critical reactant in other oxidation reactions. These investigations may reveal a new, practically important catalyst for catalytic converters and for the production of some widely used chemicals.

Recent Progress

We discovered that the Au/Ni(111) surface alloy, with Au coverages up to 0.3 ML, efficiently catalyzes the oxidation of CO at 70 K. Saturation coverage of molecular O₂ is adsorbed on the 0.24 ML Au/Ni surface alloy at 77 K. The dominant feature, at 865 cm⁻¹, of the vibrational spectrum of the oxygen layer, as measured by high resolution electron energy loss spectroscopy, is assigned to the vibration of the O=O bond of molecular oxygen adsorbed on the alloy with its bond axis largely parallel to the surface. Molecular oxygen so adsorbed is characterized as a peroxy (O₂⁻²) or superoxy (O₂⁻¹) species. Shoulders at about 950 cm⁻¹ and 790 cm⁻¹ indicate the presence of both peroxy or superoxy species at multiple sites.

The feature at 865 cm⁻¹ and its shoulders disappear after heating this layer to 150 K while two features at 580 and 435 cm⁻¹, attributed to atomically adsorbed O, grow in. The feature at 580 cm⁻¹ is the same frequency as observed for O atoms bound to Ni(111) while a lower frequency feature, at 435 cm⁻¹, is attributed to O atoms bound to Ni atoms that are adjacent to the Au atoms. Note that there is no evidence for atomically bound O at 77 K. Therefore, O₂ adsorption on the Au/Ni(111) surface alloy at 77 K is solely molecular. In contrast, O₂ dissociatively adsorbs on Ni(111) at 8 K, while it adsorbs neither molecularly nor dissociatively on Au(111) at or above 100 K.

When a beam of thermal energy CO is directed at the O₂ covered Au/Ni(111) surface alloy held at 70 K, gas phase CO₂ is immediately produced. A control experiment demonstrates that no CO₂ is produced when the CO beam impinges on the crystal mount. Clearly, CO reacts with molecularly adsorbed O₂ on this alloy at 70 K.

After exposure of the O₂-covered surface alloy at 70 K to CO, two C=O stretch vibrational modes are observed at 2170 and 2110 cm⁻¹, along with the Au/Ni-CO stretch mode at 435 cm⁻¹. The O=O mode at 865 cm⁻¹ is much reduced in intensity, while the shoulder at 790 cm⁻¹ has maintained its intensity. The decrease in intensity of the 865 cm⁻¹ feature is interpreted to mean that some of the molecularly adsorbed O₂ has reacted with CO to form gas phase CO₂. The product remaining from this reaction is an O atom adsorbed to Au, as evidenced by the appearance of a new feature at 660 cm⁻¹. The molecularly adsorbed O₂ that gives rise to the feature at 790 cm⁻¹ does not react with CO.

This alloy surface covered with CO and some adsorbed O₂ is heated at 2 K/s while the partial pressures at masses 44 and 28 are monitored. Rapid production and desorption of CO₂ is clearly observed between 105-120 K, along with CO desorption. Production of CO₂ in this temperature range occurs at the same temperature at which O₂ dissociates. This observation suggests that CO₂ formation occurs between a CO and a "hot" O atom that has not yet equilibrated with the surface after bond dissociation. From 120 K to about 250 K, CO₂ is slowly produced by reaction of the adsorbed O atoms represented by 660 cm⁻¹ mode and by the adsorbed O atoms that did not react immediately as a hot O atom upon O₂ dissociation. No O₂ is observed to desorb.

These results demonstrate that Au/Ni(111) catalyzes the oxidation of CO at low temperature. Clearly, substitution of a small number of Ni atoms on the Ni(111) surface by Au atoms has dramatically changed the Ni chemistry. The oxidation of CO on Ni has never been observed under UHV laboratory conditions, presumably because both the oxygen atom and CO are too strongly bound, and hence the barrier to their reaction is too large. Introduction of gold into the Ni lattice serves to weaken the bonds between oxygen and CO so as to allow the reaction to proceed. These results also imply that nanosize Au clusters are not a necessary requirement for low temperature CO oxidation in general. Rather, interaction of the Au atoms around the perimeter of the Au nanocluster with the transition metal of the oxide support likely provides the active sites that stabilize the adsorption of molecular O₂ that is necessary for the oxidation of CO.

Current Status

We temporarily ceased experimentation in order to move our apparatus into a newly renovated laboratory. Despite attempts to minimize downtime, we were not able to operate the machine until recently, because of a series of unfinished electrical and

mechanical items tied to the space renovation. In the meantime, we redesigned and fabricated our Au atom source and our pumping manifold so that we have a more reliable setup. On the bright side, MIT has invested nearly 2 million dollars into the renovation of our lab. There is now adequate cooling, ventilation for pump exhaust, a mechanical pump room for isolation of the mechanical pumps, a hood for working with chemicals, gas cabinets to house our toxic gases and about 1000 sq ft more room to work. It is an amazing transformation of laboratory space that has not been renovated in 35 years.

We have been working to bring the vacuum chamber and equipment up to its operating condition prior to the move. We have achieved ultrahigh vacuum conditions in our main chamber, have obtained signal from our high resolution electron energy loss spectrometer and calibrated our new Au source. The new Au source allows us to have exquisite control over the Au coverage, down to less than a hundredth of a monolayer. We remeasured the adsorbed O₂ vibrational spectra at smaller increments of Au coverage. To our surprise, we discovered at least three more O₂ binding sites as identified by three new vibrational frequencies of the adsorbed peroxo (O₂⁻²) or superoxo (O₂⁻¹) species. We are presently making detailed measurements of the intensities of the six adsorbed O₂ vibrational stretch frequencies as a function of Au coverage. These high resolution vibrational spectra will serve as important benchmarks for the continued development of density functional theory for adsorbates on surfaces.

Future Plans

A major thrust of this project is to explore the range of reactivity of the O₂ species molecularly adsorbed on the Au/Ni(111) surface alloy. The hypothesis is that our newly observed molecular O₂ adsorbate is the crucial reactant in two oxidation reactions to be studied: the direct synthesis of H₂O₂ from H₂ and O₂ and the epoxidation of propylene to form propylene oxide. In addition, it is planned to investigate whether the Au/Ni surface alloy is also active for the reduction of NO by CO. It is possible that a molecularly adsorbed NO species with a bond order approaching one is the active species in the NO reduction reaction at low temperature on the Au/Ni(111) surface alloy.

Publication

Catalyzed CO Oxidation at 70 K on an Extended Au/Ni Surface Alloy
D. L. Lahr and S. T. Ceyer, *J. Am. Chem. Soc.* **128**, 1800 (2006)

Ph.D. Thesis

Molecular Oxygen Adsorbates at a Au/Ni(111) Surface Alloy and Their Role in Catalytic CO Oxidation at 70 – 250 K. D. L. Lahr - June, 2006 – MIT

Patent Application

U.S. Pat. Apl. Ser. No.: 11/335,865. S. T. Ceyer and D. L. Lahr

Chemical Kinetics and Dynamics at Interfaces

Solvation/Fluidity on the Nanoscale, and in the Environment

James P. Cowin, Fundamental Sciences Division
Pacific Northwest National Laboratory
P.O. Box 999, Mail Stop K8-88, Richland, Washington 99352
jp.cowin@pnl.gov

Program Scope

Interfaces have a unique chemistry, unlike that of any bulk phase. This is true even for liquid interfaces, where one might have (incorrectly) pre-supposed that a liquid's lack of rigidity might strongly suppress perturbations due to the interface. Ice interfaces also tend to have adherent liquid brine films in nature, and even pure ice has surface regions with sufficient disorder (for a monolayer or two) to resemble liquids. This program explores interfacial effects including changes in fluidity and transport, and solvation. The knowledge gained relates to reactions and transport across two-phase systems (like microemulsions), electrochemical systems, and where a fluid is present in molecular-scale amounts... such as in cell membranes, enzymes and ion channels, or at environmental interfaces at normal humidities, such as the surfaces of atmospheric or soil particles. We explore these systems via re-creating liquid-liquid interfaces using molecular beam epitaxy, and use of a molecular soft landing ion source. We also explore fundamental properties of bulk ice, that relate to such issues as proton transport, amorphous ice properties, and even the effect of ice in formation of planets.

Recent Progress (2005-2007)

Mapping the Oil-Water Interface's Solvation Potential [1] (**Richard C. Bell, Kai Wu, Martin J. Iedema, Gregory K. Schenter, James P. Cowin**)

Any ion that traverses the junction of water and low dielectric constant materials (air, oil, cell membranes, proteins, etc.) will experience a solvation energy that varies strongly according to its location with respect to the interface. Recently much progress has been made in understanding these interfaces, largely through recent advances in computational methods. This study adds important new measurements to the field. Directly measured is the solvation potential for Cs^+ as they approach the oil-water interface ("oil" = 3-methylpentane), from 0.4 to 4 nm away. The oil-water interfaces with pre-placed ions are created at 40K using molecular beam epitaxy and a soft-landing ion beam. The solvation potential slope was determined at each distance by balancing it against an increasing electrostatic potential made by increasing the number of imbedded ions at that distance, and monitoring the resulting ion motion.

Figure 1 shows what a solvation chemical potential (in heavy solid and dashed black lines) might look like, for a single ion approaching a 30\AA or 7.1 monolayer (ML) film of water (shaded blue), immersed in 3-methylpentane (3MP) (yellow). To the far left (not shown) is a metallic substrate. In a previous work [2], we estimated the well depth of the solvation potential versus the thickness of the water film, using the measured temperature at which ions escape that potential while the temperature was slowly ramped upward. Those well depths were in fair agreement with expectations and with a Born potential. In this study we map this solvation potential in detail, eliminating many limitations of those earlier experiments [2]. When ions are placed several monolayers away from the oil water interface, as on the left of Figure 1, the ions alter the solvation potential by adding to it an electric potential that the ions collectively produce, as shown by the dashed curves on the left side of Figure 1. For very few ions, the potential is unchanged from the heavy black curve. Then as long as the ions are several kT below the top of the well, they will all be trapped in the potential, migrating to the right to reach the water layer. But for increasing number of ions, the net potential begins to bend down, eventually reaching (and exceeding) zero slope at the initial ion position. When the number of ions is sufficient to bend the potential to locally have zero slope, this should profoundly alter the

ion motion. Simulations show that there should be a maximum amount of charge that can be trapped, and this corresponds closely to that charge needed to bend the solvation potential to have zero slope. What this implies is that the maximum amount of trapped charge/voltage is a direct measure of the slope of the solvation potential at that distance.

As predicted, experimentally we found for small numbers of ions, nearly all the ions are trapped, while for increasing numbers of ions, the amount trapped reaches an asymptotic limit. The voltage this produces, divided by the distance to the Pt (100 ML= 42 nm) gives the slope of the solvation potential at that distance away from the oil-water interface. Experiments were done for ions placed from 1 to 10 ML away from the water layer, and for water layers ranging from 2 to 30 ML thick. One initially surprising result was the determined slope of the solvation potential was independent of the water film thickness. This data produced the slope of the solvation potential for 1 to 10 ML from the oil water interface. This was fitted to an interpolating function, and integrated to give the experimentally determined solvation potential. This is shown as the thick black dotted line to the right of 0 nm in Figure 1, over the range of 1 to 10 ML (0.42 to 4.2 nm). This is compared to the potential from the Born model with a 5Å radii, and water dielectric constant of 5 (blue curve). The water thickness for the blue curve is 4.3ML, not the thicker 7.1ML water film indicated by the blue shaded region. The Born model parameters give a well depth consistent with the temperature observed for the final escape of the ions (>95K). The potential seems to have a different shape than the Born model, which was initially surprising, especially at the larger distances. But if a “k-dependent” dielectric constant was the proper picture, then the Born model with a fixed ϵ_2 should not give the solvation potential shape. At large distances the shape might be better given using the Born model with a large ϵ_2 value. Shown in Figure 1 are the Born calculations for a water dielectric constant of 100. The calculated curves are nearly identical at distances greater or equal to 1ML (0.42nm) from the water films’ right edge, consistent with the observation that the solvation potential slope at these distances does not change with water film thickness. The potential to the right of the water for a dielectric constant of 100 matches fairly well the shape of the experimentally determined potential better, but not its “offset”. The experiment only measured the slopes of the potential. Thus we can offset the original (dashed) curve by -0.035 eV, to yield the solid heavy black curve. This closely follows the $\epsilon_2=100$ Born model for all but the shortest distances.).

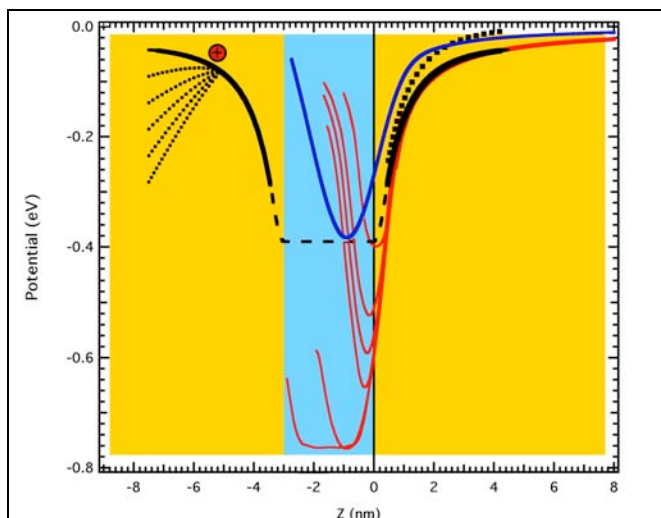


Figure 1 The blue shaded region shows 3 nm (7.1 ML of water), within a 3-methylpentane film (yellow). The solvation chemical potential for a single ion approaching the water film is shown as the heavy black solid and dashed line.. The dashed curves at the left show the net potential that arises from the collective field of ions placed 5 ML (2.1 nm) from the left side of the water film, so as to add 2, 4, 6, 8 $\times 10^7$ V/m E-fields. The red curves are Born calculations for 5Å = r_b , $\epsilon_1=1.9$, $\epsilon_2=100$, and water films 0.15, 0.3, 0.45, 0.6, 1.8, and 3.0 nm (7.1 ML) thick. Blue curve is Born model for a 1.8 nm water film with $\epsilon_2=5$. The heavy dashed curve at the right is the "raw" integrated potential derivative (without the -0.035 eV offset).

The measurement of the solvation potential at the oil water interface over the distances of 1 to 10 ML of intervening 3MP is unique, to our knowledge, in its directness and its bridging of molecular to semi-macroscopic distances. It is somewhat remarkable that a single measurement approach works so well over this transitional region. And while the numerical results, being in general accord with expectations, are not directly surprising, it is reassuring that concepts used to fit single ion solvation energies, or the capacitance of 1 of 2 ML of water at electrode surface "double layers" can be applied to a broader range of phenomena.

Dissociation of Water on Pt(111), Buried Under Ice [3] (Yigal Lilach, Martin J. Iedema, James P. Cowin)

Adsorbed water, well studied on metallic surfaces, is largely thought to not dissociate on Pt(111). As illustrated in Figure 2, as long as ΔH_{ads} is several kT 's smaller than the activation energy required for dissociation E_a , the molecules will desorb rather than dissociate. How could one manipulate this, to induce water to dissociate on Pt? Either by: 1) Increasing the kinetic barrier to desorption till it is bigger than E_a (i.e. the bricks in Figure 2) (this keeps the molecules on the surface at temperatures above their "usual" desorption temperature) 2) Changing in the energy levels of the reactants or products. We showed that growing thick layers of ice on Pt(111) does both, and leads to extensive dissociation in the first layer of water. Careful, 3-step temperature programmed desorption (TPD) and work function measurements show that water dissociates on Pt(111) for T as low as 151K [3][4].

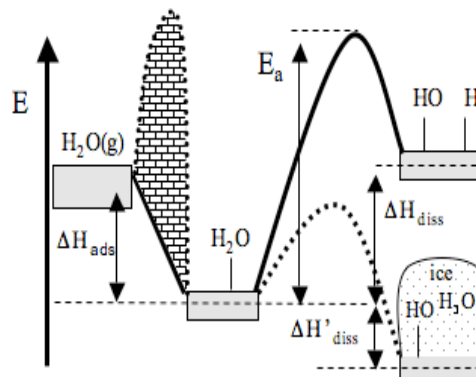


Figure 2: First monolayer water dissociation energies diagram. Adding ice on top of the first ML blocks its desorption kinetics (i.e. the brick wall). The dissociation kinetic barrier E_a and ΔH_{diss} are both shown as preventing dissociation until altered by the ice layers (lower right).

Proton Segregation at Ice Interfaces [4] (Yigal Lilach, Martin J. Iedema, James P. Cowin)

Hydronium segregates to the surface of H_2O (D_2O) ice films grown on Pt(111) above 151K (158K). This is observed as a voltage that develops across the films, utilizing work function measurements. Figure 3 shows $-\Delta\Phi$ for 3500 ML D_2O ice films, grown via the tube doser at T_{growth} between 140-178K at about 400 ML/s. After growth, the gas-source is removed, and the temperature dropped to about 80 K. Then as the films are slowly heated (0.2K/sec) changes in $-\Delta\Phi$ of the sample are measured. The drop in $-\Delta\Phi$ above 200 K happens when the multilayer water desorbs, and the clean Pt is recovered. For $T_{\text{growth}} > 155$ K: the films abruptly form with a positive voltage. This positive initial voltage gets much larger as T_{growth} increases, reaching around 8V. The H_2O films have a slightly lower threshold temperature, 153K.

The coverage dependence of film voltages show that it is initially linear with coverage, then it reaches a saturation value at a coverage of several thousands of monolayers. This, and other evidence indicate that this voltage originates from charges on top of and within the ice films, that originally came from the Pt-ice interface. We found that a simple model fits the data well. Hydronium from the dissociation of water at the Pt-ice interface, at an concentration had a small probability ($\sim 1\%$) of being found at the ice-vacuum interface, in some sort of equilibrium, for the very first part of the ice growth, say up to about 30 ML. As the films get thicker, these hydroniums (~ 0.01 ML) at the ice-vacuum interface become trapped there, in a local minimum. As the film grows, most of these ions will stay on top of the ice film. But a small fraction ($\approx .02\%$) are lost for each new monolayer of ice, to become trapped in the bulk ice. Since $\Delta G = -RT \ln K_{\text{equil}}$, the free energy for the charge segregation to the vacuum ice interface, compared to being stranded in the bulk ice was estimated. With some additional assumptions we extracted the free energy of moving a hydronium from the Pt-ice interface to the ice-vacuum interface.

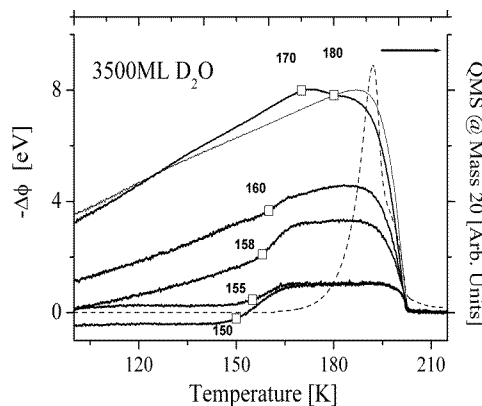


Figure 3: $-\Delta\Phi$ after adsorbing 3500 ML of D_2O on Pt(111) at the indicated temperature, cooling the sample to 80K and then reheating at a constant rate of 0.2K/sec. The QMS desorption signal is indicated as a dashed line.

Future Plans

We recently added FTIR, to probe the surface and bulk species in our films. We have already added low energy secondary ion mass spectrometry (15 to 150 eV Cs ions). Together these will tell us a great deal about the identity and location of ions on and within the films. It will also answer many questions we have about the nature of the dissociated water created for the thick ice films. We will be able to understand the solvation effects on ion dissociation and transport much better, because of these new measurements. We also hope to better understand in bulk ice the motion of hydronium and L and D defects.

We are working to expand our studies of liquids, and accordingly have proposed to the Mid-scale Instrumentation Program of BES a new instrument, as a joint submission with the principle investigator of James Cowin, and co-P.I.'s of Greg Kimmel, Kevin Rosso, and Mike Henderson, all of PNNL:

In-Situ/Liquid TOF-SIMS for Environmental Interfaces. Chemistry of liquid interfaces is extremely important in environmental and industrial processes but is poorly understood. Liquid layers coat nearly all real-world systems from the oceans to atmospheric particles, and include surface "brines" that coat rocks and soils, and ice, selective membranes for energy storage and production, important industrial catalysts, and even us. New tools are needed to study these inherently inhomogeneous systems, under realistic conditions of humidity and in the presence of trace and reactive gases. We propose an In-Situ/Liquids Time-of-Flight Secondary Ion Mass Spectrometer (ISL-TOFSIMS) system, that will for the first time allow a comprehensive molecular-specific understanding of chemistry at liquid and liquid/solid interfaces. Major recent developments in TOFSIMS (cluster beams) and novel micro-scale chemistry methods make this revolutionary advance possible and timely. The proposed system can measure molecular and ion concentrations, microsecond reaction kinetics with high spatial resolution (120 nm laterally, 1 nm vertically) and 3D mapping capability, and has a unique "in operation" sensitivity calibration. These features will enable exploring pressing issues in interface-specific photochemistry, surface segregation and transport at liquid, brine, ice and mineral surfaces, and transport across aqueous-based membranes and adherent films, all under relevant gaseous conditions.

References (Papers under BES support from 2004-present, in **Bold**)

- [1] R. C. Bell, Kai Wu, M. J. Iedema, G. K. Schenter, J. P. Cowin Mapping the Oil-Water Interface's Solvation Potential [submitted to *Science*, Sept. 2007]
- [2] K. Wu, M.J. Iedema, J.P. Cowin, "Ion Penetration of the Oil-Water Interface", *Science* 286 (1999) 2482
- [3] Y Lilach, MJ Iedema, JP Cowin, "Dissociation of Water on Pt(111), Buried Under Ice", ***Phys. Rev. Lett.* 98 (2006) 016105**
- [4] Y. Lilach, M.J. Iedema, J.P. Cowin, "Proton Segregation on a Growing Ice Interface Accepted *J. Phys. Chem.* (2007)

- Garrett BC, et al. "Role of water in electron-initiated processes and radical chemistry: Issues and scientific advances", *Chem. Rev.* 105: 355-389 (2005)
- Wang, HF, RC Bell, MJ Iedema, AA Tsekouras, JP Cowin, "Sticky Ice Grains Aid Planet Formation", *Astrophys. J.* 620, 1027 (2005).
- Lilach, Y. MJ Iedema, JP Cowin, "Reply to Comment on 'Dissociation of Water on Pt(111), Buried Under Ice'", ***Phys. Rev. Lett.* 99, 109602 (2007)**
- Bell RC, K. Wu, MJ Iedema, JP Cowin, "Hydronium ion motion in nanometer 3-methyl-pentane films" ***J. Chem. Phys.* 127 024704 (2007)**

Primary Processes of Radiation Chemistry: Solvent Mediated Charge Transfer Chemistry via Time-Resolved X-ray Spectroscopy

Robert A. Crowell,¹ James Wishart,¹ Eric Landahl,² and Don Arms²

¹Chemistry Department, Brookhaven National Laboratory, P.O. Box 5000, Upton NY, 11973; crowell@bnl.gov

²Advanced Photon Source, Argonne National Laboratory, 9700 S. Cass Ave., Argonne, IL 60439

Scope

One of the most fundamental events caused by ionizing radiation is charge separation that results in the formation of reactive ionic and radical species. In aqueous systems, the extent of charge separation and recombination is strongly influenced by water structure and dynamics. An understanding of solvent structure and dynamics is essential in order to help gain a complete understanding of chemical reactivity in liquids. The fundamental aspects of solvent mediated charge transfer processes are not unique to radiation chemistry, but also play a critical role in such DOE related areas as solar energy conversion and the advancement of energy storage technology. One of the main methodological problems in studying solvation is the lack of direct *structural* information about the solvent degrees of freedom that is obtained from traditional pump-probe techniques.

In this project we apply methods of transient x-ray absorption spectroscopy that have been recently developed Sector 7 of the Advanced Photon Source at Argonne National Laboratory. We are currently pursuing time-resolved X-ray absorption (XAS) studies of charge-transfer-to-solvent (CTTS) reactions involving photoexcited inorganic anions in aqueous media (these may be viewed as photoionization reactions involving a negatively charged species). The objective is to study the solvation of residual radicals and follow the separation dynamics of the contact pairs comprised of such radicals and e^-_{aq} that are caged by the solvent.

Recent Progress

We have been studying the photoinduced electron detachment from aqueous bromide. The choice of this anion is dictated by (i) the convenience of XAS detection in the fluorescence mode and relatively large absorption cross-section at the K edge (11.4 keV), (ii) the large absorptivity of bromide at 200 nm with a near-unity photodetachment yield. We have previously studied photodetachment from bromide using ultrafast transient absorption spectroscopy and found that the charge separation proceeds (as is the case for other halide and pseudohalide anions) through the formation of a close ($Br^- \cdot e^-_{aq}$) pair with a life time of 20 ps.

Details about the hydration of halogen atoms are not well known, but XAS is uniquely suited for probing the interaction of the atom with its aqueous environment. The hydration of halogen atoms (X^0) is very different from the hydration of negatively charged halide anions (X^-). Whereas the anion forms strong hydrogen bonds with several water molecules in the first solvent shell, hydrophobic effects dominate the solvation of neutral halogen atoms. There is also evidence that halogen atoms interact directly with a single solvent molecule, leading to an ultraviolet charge transfer (CT) absorption band. The CT absorption promotes an electron from the water molecule onto the halogen atom.

Fig. 1(a) compares the static spectrum of the bromide solution with the transient spectrum at 1 ns delay. The conversion of a fraction of Br^- anions to neutral Br^0 atoms by the 200 nm ionizing laser pulse is evident from the resonant $1s-4p$ transition below the bromine K-edge. Subtracting the static spectrum of Br^- from the transient spectra at delays of 1 and 154 ns gives the difference

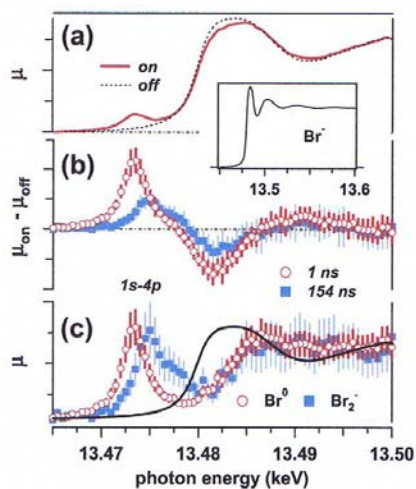


Figure 1 Laser-on and laser-off x-ray absorption spectra from aqueous Br^- , at various time delays.

spectra in Fig. 1(b). The spectrum is different at the two delay times because nearly half of the Br^0 atoms at 1 ns react with excess Br^- to form Br_2^- by 154 ns, while most of the other Br^0 atoms recombine with the hydrated electron. Other than Br^- , the predominant species at 1 ns and 154 ns are Br^0 and Br_2^- , respectively. The resonant transition in Br_2^- is 1.6 eV higher in energy than the transition in Br^0 , where the difference is largely due to splitting of the bonding (σ_g) and antibonding (σ_u^*) molecular orbitals relative to the atomic 4p orbital. Excitation of Br^0 promotes a 1s electron into the 4p vacancy produced by detaching an electron from Br^- , whereas the resonant transition for the Br_2^- anion excites an electron to the σ_u^* antibonding orbital. The optical transition energies for $\sigma_g-\sigma_u^*$ and $\sigma_g-\sigma_u^*$ excitation are 1.7 and 3.4 eV, respectively, confirming that the 1.6 eV shift of the resonant band comes predominantly from the splitting of the molecular orbitals rather than a shift of the relative 1s orbital energy from Br^0 to Br_2^- .

The 1.6 eV spectral shift of the resonant band allows us to observe the reaction kinetics. The reaction kinetics were measured at 13.473 and 13.476 keV. Predominantly Br^0 atoms absorb at the lower energy, therefore the decay of the absorbance indicates the loss of Br^0 atoms as they recombine with hydrated electrons and react with Br^- . Although Br^0 also contributes to the 13.476 keV absorption at short delay times, that signal increases on the timescale of the Br^0 decay due to production of Br_2^- . The kinetics give accurate estimates of the product concentrations and thus allow us to reconstruct the spectra of the transient species by subtracting the contribution from Br^- . These spectra are shown in Fig. 1(c), along with the spectrum of Br^- . The K edge absorption energy is ~ 5 eV higher for the transient species than for bromide. The higher energy for Br^0 reflects the electrostatic attraction of the outgoing electron to the positively charged core. A similar shift of ~ 5 eV for the absorption edge of Br_2^- is somewhat surprising given the negative charge of the diatomic anion and likely reflects solvent screening and delocalization of the valence electron.

The large reduction in the modulation depth for the Br^0 atom relative to the Br^- anion is perhaps the most intriguing feature of the recovered x-ray absorption spectrum. A Monte Carlo (MC) simulation of the solvent structure provides helpful insight to understand the difference in the x-ray absorption fine structure (XAFS) above the K edge. For Br^- , the narrow peak at 3.2 Å is due to strong hydrogen bonding ($\text{Br}^- \cdots \text{H}-\text{OH}$) between the anion and ~ 6 water molecules in the first solvent shell. The RDF for the Br^0 atom lacks this feature because the hydrophobic atom interacts weakly with the solvent. Instead, the atom occupies a nearly spherical cavity formed by 10-12 water molecules that are hydrogen bonded to other water molecules in the first and second solvent shells. The only distinctive feature in this RDF is a shoulder at 3 Å that corresponds to a weak $\text{Br}^0 \cdots \text{OH}_2$ adduct involving a single water molecule. For other water molecules, the Br^0 -O distances are significantly longer, ~ 3.7 Å.

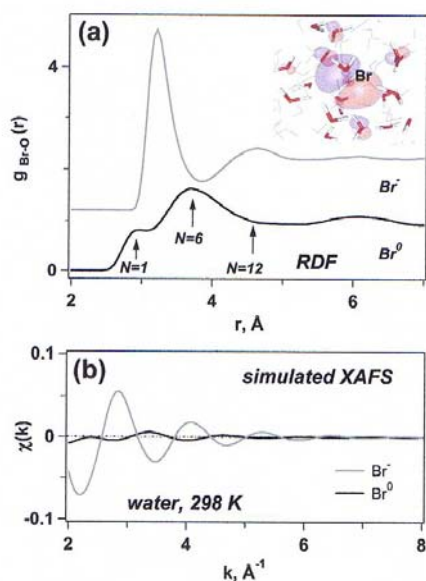


Figure 2. (a) Calculated Br-O RDF for hydrated Br^- and Br^0 . Oxygen coordination numbers N are indicated by arrows. (b) The simulated XAFS spectra for hydrated Br^- and Br^0 .

For further insight, we simulate the XAFS spectra of Br^- and Br^0 [Fig. 2(b)] using the program FEFF8 and nuclear configurations of water molecules with $r(\text{Br}-\text{O}) < 8 \text{ \AA}$ from the MC ensemble. The highly organized hydrogen bonding structure of hydrated Br^- gives deep oscillations in the static spectrum, but the magnitude of the oscillations is ~ 10 times smaller for hydrated Br^0 atoms. Although the calculation pertains to higher x-ray energies than the present experiment covers, the modulation is clearly much weaker in the reconstructed spectrum of Br^0 than in the Br^- spectrum. The contribution from the $\text{Br}^0 \cdots \text{OH}_2$ complex is small compared with the contributions from the other 10-12 O atoms in the first solvent shell and therefore does not give a strong XAFS signal.

Future Directions

Future work will focus measurement of the full EXAFS at nanosecond delay times to study the role of water in the $\text{Br}^- + \text{Br} \rightarrow \text{Br}_2^-$ reaction. While it is presently impossible to study rapid solvation reactions that involve small-scale solvent motions (the current pulse duration at the APS is 90 ps), such an opportunity might present itself when APS is upgraded (so that the pulse duration will be a few

picoseconds, this upgrade is scheduled for Fall of 2008). Analogous work will be carried out with bromine containing ionic liquids. It will be possible to temporally resolve the solvation dynamics in these viscous systems. As it comes online future studies will be carried at NSLS II. Our program of introducing X-ray absorption and diffraction methods in radiation chemistry will take advantage of the new sources of short-pulse X-ray radiation that are gradually becoming available.

DOE Publications 2004-present

1. C. G. Elles, R. A. Crowell, I. A. Shkrob, S. E. Bradforth "Excited state dynamics of liquid water: Insight from the dissociation reaction following two-photon excitation," *J. Chem. Phys.* 126, 164503 (2007)
2. M. Ave et al, "Measurement of the pressure dependence of air fluorescence emission induced by electrons," *Astrophys.*, 28, 41 (2007).
3. B. Shen, Y. Li, K. Nemeth, H. Shang, R. Soliday, R. A. Crowell, E. Frank, W. Gropp and J. Cary "Triggering wave breaking in a laser plasma bubble by a nanowire," *Phys. Plasma.* 14, 053115 (2007).
4. D. A. Oulianov, R. A. Crowell, D. J. Gosztola, I. A. Shkrob, O. J. Korovyanko, R. C. Rey-de-Castro, "Ultrafast pulse radiolysis using a terawatt laser wakefield accelerator," *J. Appl. Phys.* 101, 053102 (2007).
5. Y. Li and R. A. Crowell, "Shortening of a laser pulse with a self-modulated phase at the focus of a lens," *Opt. Lett.* 32, 93 (2007).

6. I. A. Shkrob, M. C. Sauer, Jr., R. Lian, R. A. Crowell, D. M. Bartels and S. E. Bradforth "Quantum yields and recombination dynamics in electron photodetachment from aqueous anions III. The effect of ionic strength on picosecond dynamics, quantum yields and the escape fraction of hydrated electrons in anion CTTS systems," *J. Phys. Chem. A*, 110, 9071 (2006).
7. C. G. Elles, A. E. Jailaubekov, R. A. Crowell, S. E. Bradforth, "Excitation energy dependence of the mechanism for two-photon ionization of liquid H₂O and D₂O from 8.3 eV to 12.4 eV," *J. Chem. Phys.* 125, 044515 (2006)
8. D. A. Oulianov, R. A. Crowell, D. J. Gosztola, and Y. Li "Ultrafast time-resolved x-ray absorption spectroscopy of solvent-solute transient structures," *Nucl. Instr. and Meth. in Phys. Res. B*. 241, 82 (2005)
9. R. A. Crowell, I. A. Shkrob, D. A. Oulianov, O. Korovyanko, D. J. Gosztola, Y. Li and R. Rey-Castro, "Motivation and development of ultrafast laser based accelerator techniques for chemical physics research," *Nucl. Instr. and Meth. in Phys. Res. B* , 241, 9 (2005).
10. M. C. Sauer Jr., I. A. Shkrob, R. Lian, R. A. Crowell, D. M. Bartels, X. Chen, D. Suffren, and S. E. Bradforth, "Electron photo-detachment from aqueous anions. II. Ionic strength effect on geminate recombination dynamics and quantum yield for hydrated electron," *J. Phys. Chem. A*. 108, 10414 (2004).
11. R. Lian, R. A. Crowell, and I. A. Shkrob "Solvation of electrons generated by two 200nm photon ionization of liquid H₂O and D₂O," *J. Phys. Chem. A*. 109, 1510 (2005).
12. R. Lian, R. A. Crowell, I. A. Shkrob, D. M. Bartels, D. A. Oulianov, and D. J. Gosztola, "Recombination of Geminate (OH:e⁻) Pairs in Concentrated Alkaline Solutions: Lack of Evidence for Hydroxyl Radical Deprotonation," *Chem. Phys. Lett.* 389, 379 (2004).
13. M. C. Sauer Jr., I. A. Shkrob, and R. A. Crowell "Electron Photodetachment from Aqueous Anions. I. Quantum Yields for Generation of Hydrated Electron by 193 and 248nm Laser Photoexcitation of Sundry Inorganic Anions," *J. Phys. Chem A*, 108, 5490 (2004).
14. R. A. Crowell, R. Lian, I. A. Shkrob, J. Qian, D. A. Oulianov, and S. Pommeret, "Light-induced temperature jump causes power-dependent ultrafast kinetics of electrons generated in multiphoton ionization of liquid water," *J. Phys. Chem. A* 108, 9105 (2004).
15. R. Lian, D. A. Oulianov, I. A. Shkrob and R. A. Crowell, "Geminate recombination of electrons generated by above the gap (12.4eV) photoionization of liquid water," *Chem. Phys. Lett.*, 398, 102.
16. R. Lian, R. A. Crowell, I. A. Shkrob, D. M. Bartels, X. Chen, and S. E. Bradforth, "Ultrafast Dynamics for the Electron Photodetachment of Aqueous Hydroxide," *J. Chem. Phys.* 120, 11712 (2004).
17. I. A. Shkrob, D. A. Oulianov, R. A. Crowell, and S. Pommeret "Frequency Domain single-shot (FDSS) ultrafast transient absorption spectroscopy" *J. Appl. Phys.* 96, 25 (2004).
18. R. A. Crowell, R. Lian, D. A. Oulianov, and I. A. Shkrob "Geminate recombination of the hydroxyl radicals generated from the 200nm photodissociation of hydrogen peroxide," *Chem. Phys. Lett.* 383, 481 (2004).
19. R. A. Crowell, D. J. Gosztola, I. A. Shkrob, D. Oulianov, C. D. Jonah, and T. Rajh "Ultrafast Processes in Radiation Chemistry," *Radiat. Phys. Chem.* 70, 501 (2004)
20. L. Zhao, R. Lian, I. A. Shkrob, R. A. Crowell, S. Pommeret, E. L. Chronister, A. D. Liu, and A. D. Trifunac,, "Ultrafast studies on the photophysics of matrix-isolated radical cations of polycyclic aromatic hydrocarbons," *J. Phys. Chem. A* 108, 25 (2004).

Computational Studies of liquid interfaces

Liem X. Dang

Chemical and Materials Sciences Division

Pacific Northwest National Laboratory

902 Battelle Blvd., Mail Stop K1-83

Richland, WA 99352

liem.dang@pnl.gov

Background and Significance

Molecular processes at interfaces of hydrogen-bonded liquids are of fundamental importance in a number of areas. For example, transport and chemical reactivity at liquid interfaces play crucial roles in a wide variety of problems important to the U.S. Department of Energy (DOE). Past practices at DOE production sites resulted in the discharge of chemical and radioactive material and extensive contamination of soils and ground water at these sites. A fundamental need in understanding the fate and transport of environmental contaminants is a detailed understanding of the factors that control the partitioning of ions and molecules between carrier solvents, minerals, and groundwater as well as the concomitant chemistry. Partitioning is dependent on interfacial structures, transport, and chemical reactivity. Underlying chemical and physical processes that govern transport across and chemical reactions at interfaces is the manner in which water molecules solvate ions. In addition, the structure and stability of large molecules and membranes are strongly dependent on the distribution of ions and counter-ions. The interface, including the adsorption and distribution of solute molecules such as hydroxyl or ozone and ions at interfaces, is a fundamental process encountered in a wide range of chemical, environmental, and biological systems.

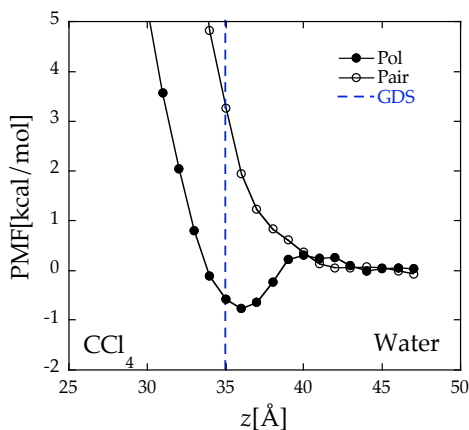
Progress Report

Hydroxyl radical transfer rate from interface to bulk by transition path sampling.

The transition path sampling technique was used to investigate the mechanism determining the rate of transfer of the hydroxyl radical from the water interface to the bulk and analyze its transition state. Polarizable potentials were used to model the interactions between the hydroxyl radical and the Dang-Chang water force field. To calculate the rate, a total of 37,250 trajectories 4 ps in length, connecting states where the hydroxyl radical was at the interface with cases when it is in the bulk, were performed. We report the accurate classical rate from transition path sampling of $k_{CI} = 0.004 \pm 0.0005 \text{ ps}^{-1}$ and a rate computed by classical transition state theory along a PMF of $k_{TST} = 0.015 \text{ ps}^{-1}$. The ratio k_{CI}/k_{TST} corresponds to a transmission coefficient of 0.27, compared to a value of 0.15 ± 0.05 for the transfer of a model solute across a model liquid-liquid interface, showing good agreement between two methods. *It was found that while an interfacial hydroxyl radical was most likely to have its hydrogen pointing towards the water bulk, cases where its hydrogen pointed away were more likely to result in a transfer into the bulk.*

Computed PMF for transferring a polarizable iodide anion across the H₂O/CCl₄ liquid-liquid interface.

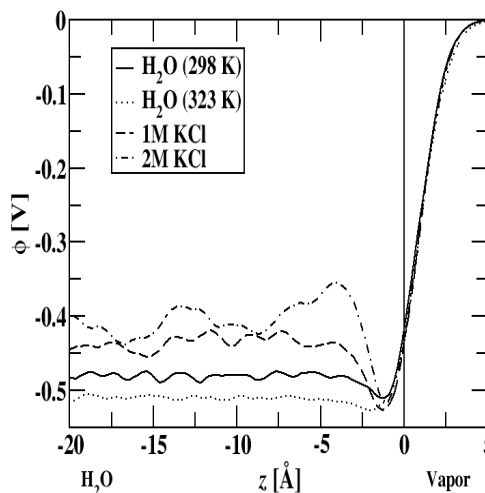
Accurately describing the PMF for ion transport across the liquid/liquid interface can be very challenging. In addition to the technical aspects, potential models that describe the interactions among the species are also very important. We studied the transfer process by calculating the PMF for transferring a polarizable iodide anion across the H₂O/CCl₄ liquid-liquid interface. Upon examining the PMF, we observed the computed free energy undergoes major changes as the polarizable iodide anion approach the Gibbs dividing surface (GDS). The PMF exhibits a well-defined minimum near the GDS, with a well depth of approximately -0.75 kcal/mol, is indicative of the stability of the surface aqueous state of the polarizable iodide anion. In addition, we have also carried out a similar study using non-polarizable models for iodide, water and CCl₄ (label as Pair) and we observed that there is no free energy minimum near the interface. This characteristic is similar to that found in a corresponding study water vapor/liquid interface. *The results obtained in this study demonstrate the importance incorporating polarization effects in simulation studies and provides the foundation of our future proposed research on ion transport across more complicated liquid/liquid interfaces such dichloroethane or nitrobenzene.*



Computed PMFs for transferring an iodide anion across water/CCl₄ liquid-liquid interface.

Simulated surface potentials at the vapor-water interface for the KCl aqueous electrolyte solution.

We recently completed a study of the surface potential of ionic aqueous solutions. The surface potential is defined as the difference in electrical potential between a neutral aqueous liquid and its coexisting vapor phase. The direct experimental determination of the surface potential remains an open question. For instance, the surface potential across the interface between a vapor and neat water is a point of contention, with surface potential measurements not always agreeing on sign. The total electric potential as a function of position for all systems studied is given. *The value obtained in the current study for water (-480 mV) is consistent with that of a previous study of the surface potential of the Dang-Chang water, and the most recent values calculated for the non-polarizable TIP4P and SPC/E water models.*

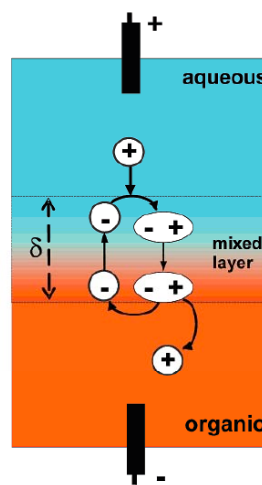


The total electric potential as a function of distance from the interface.

Proposed Work

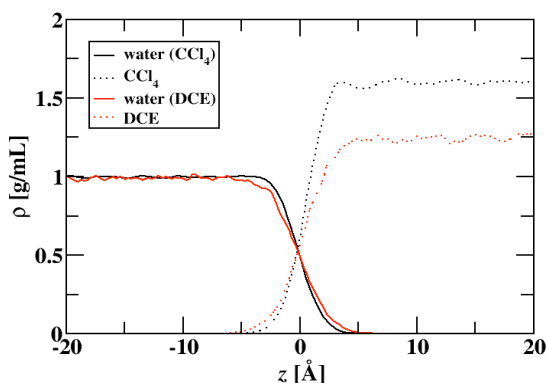
Computational studies of ions at the water-dichloroethane interface and the mechanism of transport ions across the liquid-liquid interfaces.

The transfer mechanism of ions from water to organic phases is, in most cases, energetically unfavorable. This property is of particular importance in many technological and biological systems. For example, in separation systems, the differences in energetics and kinetics of transfer across the liquid-liquid interface determine the efficiency of the extraction of a particular ionic species. Living cell membranes, whose interior can be compared to hexadecane, inhibit ion crossing, thus enabling selective transport through pores and ion channels. In the absence of a facilitating agent, ion-transfer reactions are assumed to be “simple,” one-step processes. In the past, experiments carried out at the nanometer-sized interfaces between water and neat organic solvents showed that the generally accepted one-step mechanism cannot explain important features of transfer processes for a wide class of ions including metal cations, protons, and hydrophilic anions. Results obtained from these studies have led to a proposed new mechanism of ion transfer involving transient interfacial ion pairing and shuttling of a hydrophilic ion across the mixed-solvent layer.

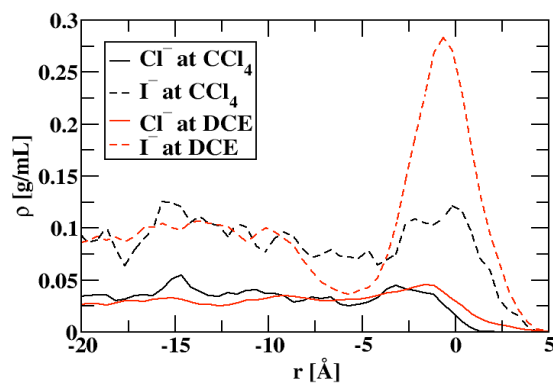


A proposed mechanism of ion transfer involving transient interfacial ion pairing and shuttling of a hydrophilic ion across the mixed-solvent layer.

We have begun a study on the ion distributions at the interface between water and dichloroethane (DCE). This study required the parameterization of a new polarizable DCE model. The model was parameterized to reproduce the DCE liquid density, dielectric constant, and heat of vaporization, and had reasonable agreement with experiment for the trans-to-gauche ratio for the Cl-C-C-Cl dihedral in liquid DCE. The resulting model was used to perform molecular dynamics calculations for a system with water and DCE in slab geometry. The simulation was box elongated in the z direction, and two water-DCE interfaces formed along the xy plane. The calculated interfacial tension for this system was 30 ± 5 dyn/cm, which compares reasonably well with the experimental value of 24 dyn/cm. In addition, a hyperbolic fit to the water densities was performed, giving an interfacial thickness of 4.84 \AA for water-DCE, being much larger than CCl_4 -water or the air-water interfacial thicknesses of 3.55 \AA and 3.64 \AA , respectively. The density profiles comparing the water-DCE and CCl_4 -water systems, showing that water-DCE is more diffuse, which is in agreement with previous experimental and computational studies. The main focus of this study was to understand the effect of DCE on interfacial anion distributions at the water interface. Simulations were performed for 1M NaCl and 1M NaI water-DCE solutions. The chloride and iodide density profiles in the CCl_4 -water and DCE-water systems are computed. It should be noted that interfacial iodide concentration is somewhat higher at the air-water interface



The density profiles comparing the water-DCE and CCl₄-water systems.

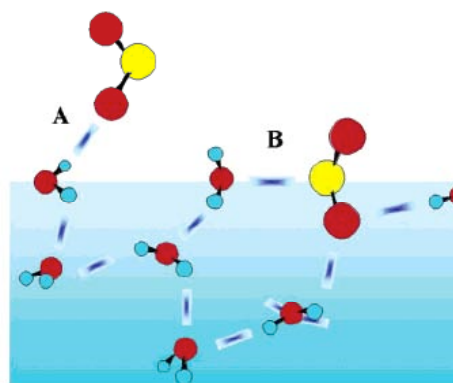


The computed chloride and iodide density profiles in the CCl₄-water and DCE-water

when compared with the CCl₄-water interface, and chloride concentration is the same at both interfaces.

The results here show that chloride concentration is shifted away from the DCE phase when compared to CCl₄, and that iodide concentration has very little to no enhancement at the DCE-water interface unlike all other aqueous interfaces that have been reliably investigated. Snapshots of the 1M NaI-water-DCE system taken during dynamics simulations show the diffuse nature of the DCE-water interface, which likely plays an important role in why iodide concentration is not enhanced there. We are carrying out PMF calculations for transferring ions across the water/DCE liquid/liquid interface to characterizing the mechanism of ion transfer processes. We also plan to examine the role of counter ions (i.e., ion-pairing) on the transferring processes. Our results will be compared to the new proposed shuttling mechanism on the ion transfer process. We are expecting that the PMF for the water/DCE interface will also be challenging and interesting.

Simulation studies of ions and solutes at the vapor-liquid interface. In recent years, it has become clear that the air-water interface plays a more significant role in gas adsorption and reaction kinetics of many atmospheric processes than had previously anticipated. Recently, surface complexes have been invoked to explain the initial step in a number of surface reaction mechanisms, including the reaction of gas phase SO₂ with water. Understanding SO₂ interaction at aqueous surfaces is essential because of the central role of sulfur in many atmospheric aerosols. Richmond and co-workers carried out an experimental study on the solvation of the SO₂ molecules at the vapor-liquid interface using vibrational sum frequency spectroscopy. Among other results discussed in this work, their work demonstrated the presence of a weak SO₂:H₂O complex at the water surface prior to reaction and dissolution. Richmond et al. proposed a structure of the complex SO₂-air-water



A proposed structure of the complex SO₂/air/water interface.

interface. The focus of our work on solvation of the solute at the vapor-liquid interface aligns with previous work on the hydroxyl solvation at the water vapor-liquid interface. We begin this work by developing a polarizable model for the SO₂:H₂O complex. To our knowledge, no such potential model has been described in the literature. We will make use of *ab initio* quantum chemical calculations on the SO₂:H₂O complex, and we will use this information as well as the observed data to construct the potential model. We will carry out the PMF calculations and also molecular dynamics simulations on the solvation of SO₂ molecules to characterize the distribution and solvation property of the SO₂ molecules at the water surface and to compare to the result reported by Richmond et al.

References to publications of DOE sponsored research (2004-present)

1. M. Roeselova, J. S. Vieceli, L. X. Dang, B. C. Garrett and D. J. Tobias “Hydroxyl radical at the air-water interface” *Journal of American Chemical Society* **126**, 16308 (2004).
2. T.-M. Chang and L. X. Dang “Liquid/Vapor Interface of Methanol-Water Mixtures: A Molecular Dynamics Study” *Journal of Physical Chemistry B* **109**, 5759 (2005).
3. M. M., T. Frigato, L. Levering, H. C. Allen, D. J. Tobias, L. X. Dang, and P. Jungwirth “A unified molecular picture of the surfaces of aqueous acid, base, and salt solutions” *Journal of Physical Chemistry B* **109**, 7617 (2005). **Featured on Journal Cover**
4. Hofft O, A Borodin, U Kahnert, V Kempter, LX Dang, and P Jungwirth, “Surface segregation of dissolved salt ions.” *J. Phys. Chem. B* **110**, 11971-11976 (2006).
5. Wick CD and LX Dang, “Distribution, structure, and dynamics of cesium and iodide ions at the H₂O-CCl₄ and H₂O-vapor interfaces.” *J. Phys. Chem. B* **110**, 6824-6831 (2006).
6. Wick CD and LX Dang, “Distribution, structure, and dynamics of cesium and iodide ions at the H₂O-CCl₄ and H₂O-vapor interfaces.” *J. Phys. Chem. B* **110**, 6824-6831 (2006).
7. Wick CD, LX Dang, and P Jungwirth, “Simulated surface potentials at the vapor-water interface for the KCl aqueous electrolyte solution.” *J. Chem. Phys.* **125**, 024706 (2006)
8. Chang TM and LX Dang, “Recent advances in molecular simulations of ion solvation at liquid interfaces.” *Chem. Rev.* **106**, 1305-1322 (2006).
9. Thomas JL, Roeselova M, Dang LX, et al.”Molecular dynamics simulations of the solution-air interface of aqueous sodium nitrate” *J. Phys. Chem A* **111** (16): 3091-3098 APR 26 2007.
10. Wick C, Dang LX “Molecular mechanism of transporting a polarizable iodide anion across the water-CCl₄ liquid/liquid interface” *J. Chem. Phys* **126** (13): Art. No. 134702 APR 7 2007.
11. Wick C, Dang LX “Hydroxyl radical transfer between interface and bulk from transition path sampling” *Chemical Physics Letters* **444**, 66-70, 2007.

Molecular Theory & Modeling
Electronic Structure and Reactivity Studies in Aqueous Phase Chemistry

Michel Dupuis
Chemical Sciences Division
Pacific Northwest National Laboratory
902 Battelle Blvd.
Mail Stop K1-83
Richland, WA 99352
michel.dupuis@pnl.gov

Summary.[#] We are interested in the theoretical characterization of molecular properties and reactivity of molecular systems in clusters and in the condensed phase. A primary motivation centers around the initial molecular processes that follow the primary energy deposition in radiolysis of water as observed in various applied technologies. We aim to characterize: i) the mechanisms and dynamics of the intrinsic reactions; ii) the effects of medium on the dynamics; iii) the mechanism of energy transfer within the solute and into the solvent. Much of our work is done with *direct ab initio molecular dynamics* (MD) calculations. The same methodology combined with quasi-classical initial conditions is a powerful approach to calculating vibrational spectra of clusters with accurate account of anharmonicities and mode coupling. These effects are known to be particularly large in strongly interacting ion-water clusters. We continue to carry out such calculations for several ion-water clusters for which high resolution experimental data that are becoming available.

Signature OH Absorption Spectrum from Cluster Models of Solvation: a solvent-to-solute charge transfer state (*Dupuis with Tsai, Kowalski, Valiev, PNNL*)

Motivation: Water radiolysis remains extensively studied because reactions of radicals created by water radiolysis are of importance in nuclear reactors, storage of trans-uranic and high-level mixed wastes, biological effects of radiation therapy, and industrial materials processes. The primary product of water radiolysis is the OH radical. There remain uncertainties and discrepancies about the assignment of the signature absorption band of the OH radical in aqueous solution and in super-critical water. The most recent measurements by Janik et al. show a weak absorption band around 310 nm (4.00 eV) for temperatures above 300 °C in supercritical conditions. This absorption is not observed at room temperature and is assigned to the ${}^2\Sigma^+ \leftarrow {}^2\Pi$ transition of a "free" OH radical. The absorption intensity is stronger in the range of 320 nm (3.88 eV) to 230 nm (5.39 eV). The absorption intensity at 230 nm decreases with increasing temperature 30 °C to 350 °C. These authors describe this 230 nm absorption band as a charge transfer transition from the solvent water molecules to the OH moiety that is modulated by the hydrogen bond network of the environment. In contrast Nielsen *et al.* describe the transition near 230 nm as essentially a ${}^2\Sigma^+ \leftarrow {}^2\Pi$ transition in the OH moiety that is perturbed by various situations of hydrogen bonding of the radical with the solvent.

Approach: We carried out extensive *ab initio* electronic structure calculations on the 'free' OH radical and on hydrated clusters of selected sizes $\text{OH}(\text{H}_2\text{O})_n$ ($n = 1-7, 16$), as mimics of aqueous solvation using the time-dependent DFT approach supported by EOM-CCSD(T) calculations on the smaller clusters. We analyzed the variations in vertical excitation energies as a function of the degree of hydration and characterized the absorption bands of the OH radical in these hydrated environments.

Results: The third excitation in all the clusters $\text{OH}(\text{H}_2\text{O})_n$ ($n = 1-7, 16$) was found to involve a solvent-to-solute charge transfer transition, in the region of 250 nm (calculated), close to the region of experimental observation of 230 nm. Of particular interest was the low energy $n=16$ cluster that was found to have a large solvent-to-solute transition oscillator strength. The donor and acceptor orbitals in that excitation were found to have favorable near coaxial alignment. Orbital alignment and solvent-solute oxygen-oxygen distances were shown to be important factors affecting the intensity of the solvent-to-solute charge transfer excitation absorption. Although dynamics, temperature, and pressure were not explicitly accounted for in the present investigation, nevertheless the series of clusters allowed us to infer on the observed temperature dependence of the transition in the 230nm region. The temperature effects were indirectly addressed by varying the size of $\text{OH}(\text{H}_2\text{O})_n$ clusters. The larger clusters studied here depicted a fully solvated OH radical that is relevant to low temperature conditions, with one structure exhibiting a large oscillator strength for the solvent-to-solute transition due to favorable structure and orbital features. (In other structures and with unfavorable orbital alignment the oscillator strength for such a transition is small.) The smaller clusters that are likely to be relevant at high temperature in supercritical conditions all display small oscillator strengths. These findings are consistent with the experimentally observed attenuation of the OH signature absorption transition at higher temperature. Finally we noted that the third transition energy increased with decreasing cluster size. Accordingly the calculations suggested that the maximum of the absorption peak in the region of 230nm shifts to the blue with increasing temperature.

References to publications of DOE Chemical Physics sponsored research (2005-present)

1. M. Aida and **M. Dupuis**, “Fundamental Absorption Frequency from Quasi-classical Direct ab initio Molecular Dynamics: Diatomic Molecule”, Chem. Phys. Lett. 401, 170 (2005).
2. B. C. Garrett, D. A. Dixon, D. M. Camaioni, D. M. Chipman, M. A. Johnson, C. D. Jonah, G. A. Kimmel, J. H. Miller, T. N. Rescigno, P. J. Rossky, S. S. Xantheas, St. D. Colson, A. H. Laufer, D. Ray, P. F. Barbara, D. M. Bartels, K. H. Becker, K. H. Bowen, Jr., S. E. Bradforth, I. Carmichael, J. V. Coe, L. R. Corrales, J. P. Cowin, **M. Dupuis**, K. B. Eisenthal, J. A. Franz, M. S. Gutowski, K. D. Jordan, B. D. Kay, J. A. LaVerne, S. V. Lymar, T. E. Madey, C. W. McCurdy, D. Meisel, S. Mukamel, A. R. Nilsson, T. M. Orlando, N. G. Petrik, S. M. Pimblott, J. R. Rustad, G. K. Schenter, S. J. Singer, A. Tokmakoff, L. S. Wang, C. Wittig, and T. S. Zwier, “The Role of Water on Electron-Initiated Processes and Radical Chemistry: Issues and Scientific Advances“, Chem. Rev. 105, 355 (2005).
3. J.D. Watts and **M. Dupuis**, “A Coupled-Cluster Analysis of the Photoelectron Spectrum of FeCl_3 ”, Molec. Phys. 103, 2223 (2005).
4. S. Hirata, M. Valiev, **M. Dupuis**, S.S. Xantheas, S. Sugiki, and H. Sekino, “Fast electron correlation methods for molecular clusters in the ground and excited states”. Molec. Phys. 103 2255 (2005).
5. M.Aida and **M. Dupuis**, “Fundamental Absorption Frequency from Quasi-classical Direct ab initio Molecular Dynamics: Diatomic Molecule”, Chem. Phys. Lett. 401, 170 (2005).
6. J.D. Watts and **M. Dupuis**, “A Coupled-Cluster Analysis of the Photoelectron Spectrum of FeCl_3^- “, Molec. Phys. 103, 2223 (2005).
7. M. Kolaski, H.M. Lee, C. Pak, **M. Dupuis**, and K.S. Kim, “Ab Initio Molecular Dynamics Simulations of an Excited State of $\text{X}(\text{H}_2\text{O})_3$ ($\text{X}=\text{Cl}, \text{I}$) Complex”, J. Phys. Chem. A 109, 9419 (2005).
8. S. Du and J.S. Francisco, G.K. Schenter, T.D. Iordanov, B.C. Garrett, **M. Dupuis**, and J. Li, “The OH Radical-H₂O Molecular Interaction Potential”, J. Chem. Phys. 124, 224318 (2006).

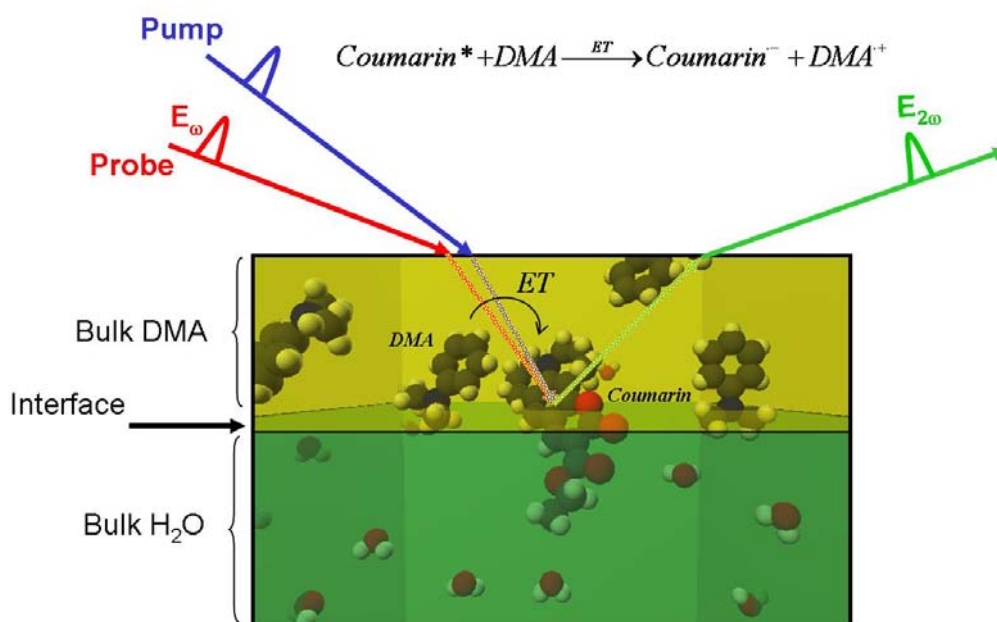
9. A. Furuhashi, **M. Dupuis**, and K. Hirao, "Reactions associated with ionization in water: a direct ab initio dynamics study of ionization in $(\text{H}_2\text{O})_{17}$ ", J. Chem. Phys. 124, 164310 (2006).
10. M. Valiev, B.C. Garrett, M.K. Tsai, K. Kowalski, S. M. Kathman, G. K. Schenter, and **M. Dupuis**, "Hybrid Coupled Cluster Approach for Free Energy Calculations: Application to the Reaction of CHCl_3 and OH^- in water", J. Chem. Phys. 127, 051102 (2007).
11. B. Gonovska, D. M. Camaioni, and **M. Dupuis**, "Reaction pathways and excited states in $\text{H}_2\text{O}_2 + \text{OH}^- \rightarrow \text{HO}_2 + \text{H}_2\text{O}$: a New ab initio Investigation", J. Chem. Phys. 127, 084389 (2007).
12. M.K. Tsai, K. Kowalski, M. Valiev, **M. Dupuis**, "Signature OH Absorption Spectrum from Cluster Models of Solvation: A Solvent-to-Solute Charge Transfer State", J. Phys. Chem. A 000, 0000 (2007).
13. Furuhashi, **M. Dupuis**, and K. Hirao, "Kinetic energy partitioning for the analysis of ab initio dynamics: Application to ionization dynamics in water tetramers $(\text{H}_2\text{O})_4^{++}$ ", submitted to Phys.Chem.Chem.Phys. (2007).

This research was performed in part using the Molecular Science Computing Facility in the William R. Wiley Environmental Molecular Sciences Laboratory (EMSL) at the Pacific Northwest National Laboratory (PNNL). The EMSL is funded by DOE's Office of Biological and Environmental Research. PNNL is operated by Battelle for DOE.

Photochemistry at Interfaces
 Kenneth B. Eisenthal
 Department of Chemistry
 Columbia University
 New York, NY 10027
 kbe1@columbia.edu

Electron Transfer Dynamics

Electron transfer and acid-base reactions are the most important classes of reactions in bulk and interfacial chemistry. We have shown that femtosecond second harmonic generation (SHG) can be used to measure the dynamics of electron transfer from a donor molecule, which in these experiments is *N,N'*-dimethylaniline, to various excited state coumarin acceptor molecules at a liquid/liquid (*N,N'*-dimethylaniline/aqueous) interface. These studies are the first direct measurements of ultrafast electron transfer at liquid interfaces.



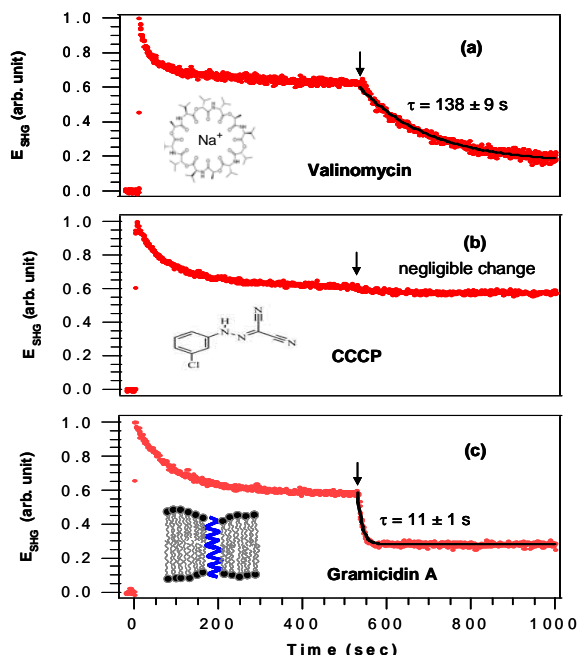
The activation free energy in electron transfer theory depends linearly on the redox potentials of the donor and acceptor molecules. To investigate this dependence of the dynamics we have initiated experiments on coumarin C152, which has a reduction potential that is less negative by 0.11 eV than C314, which we have also investigated. The less negative reduction potential, keeping the donor the same, increases the electron transfer rate because the “electron affinity” of the acceptor molecule has increased. We find that the forward electron transfer from the ground state donor, *N,N'*-dimethylaniline to photoexcited C152 is 3.2 ± 0.5 ps, which is significantly faster than the C314 transfer time of 14 ± 2 ps at the same interface. In order to test interfacial electron treatments the only significant parameter in the theory we need an estimate of is the reorganization energy. To achieve this objective we have initiated a collaboration with Prof. Ilan Benjamin, who will calculate the reorganization energy for the systems that we have investigated. Compared with electron transfer studies of C314 and C152 in bulk DMA we find that electron transfer is somewhat faster for C314 at the DMA/aqueous

interface than in the bulk, 25 ps (0.7) and 3.4 ps (0.3), but slower for C152 at the interface than in the bulk DMA, 0.44 ps (0.77) and 2.5 ps (0.23). Based on redox potentials and the lower polarity estimated from SHG measurements of their interfacial spectra, we would expect both coumarins to be faster at the interface. However we do not know the reorganization energies, which clearly are crucial factors. The Benjamin calculations could explain these opposite findings.

In these interfacial electron transfer experiments we have succeeded in using different measurements to probe not only the forward electron transfer but the back electron transfer, which generates the ground state donor and the ground state acceptor molecules. Bulk studies of both the forward and the back electron transfer dynamics are not available for coumarins in DMA. One method that we have used measures the decay time of the $\text{DMA}^{\cdot+}$ radical cation to ground state DMA, $\text{C314}^{\cdot} + \text{DMA}^{\cdot+} \rightarrow \text{C314} + \text{DMA}$, which is the true back electron transfer time. The other method is indirect, based on the increase in the ground state C314 population as the reaction occurs, $\text{C314}^{\cdot} + \text{DMA}^{\cdot+} \rightarrow \text{C314} + \text{DMA}$. The donor cation decay time, yields the back electron transfer time of 163 ± 4 ps, whereas the return of C314^{\cdot} to ground state C314 is 183 ± 5 ps. The apparently slower recovery time of C314 is attributed to the relative orientation of the $\text{DMA}^{\cdot+} - \text{C314}^{\cdot}$ pair that is required for back electron transfer to occur. As a consequence the newly formed C314 molecules are not likely to be in their equilibrium orientational distribution. Thus they undergo orientational motions to achieve orientational equilibrium, which increases the observed C314 recovery time.

Transport of Organic Ions Across Nanoparticle Membrane Interface

Transmembrane movement of ions across the enormous range of membrane structures are important processes in science and technology. We have shown that SHG can be used to measure in real time the transport of an organic cation, malachite green (MG), across the phospholipid(DOPG) bilayer of a 110 ± 5 nm liposome in aqueous solution. The principal idea of the method is that on rapidly mixing, ~ 1 s, a solution containing liposomes with a solution containing MG, there is a rapid rise, ~ 1 s, in the SHG signal as MG adsorbs to the outer layer of the liposome, which then decreases in time as MG crosses into the inner compartment of the liposome and adsorbs to the inner layer of the liposome. By symmetry the MG that adsorbs to the inner layer have the opposite orientation to those adsorbed to the outer layer. Because the thickness of the bilayer, ~ 5 nm, is much less than the SHG coherence length, the incident light induced second order polarizations for MG in the outer vs. inner layers have opposite signs and therefore cancel. This cancellation reduces the SHG signal as MG crosses the bilayer and adsorbs to the inner layer. Although the MG concentration gradient from outside to inside the liposome drives MG across the membrane, there is a buildup of positive charge inside the liposome as this occurs, which opposes the further transport of MG to the inner compartment. It is this creation of a positively charged “barrier” that we attribute the observation that the SHG signal does not decay to a value determined by the ratio of the inner to outer surface, ~ 0.15 areas, but rather to a value of 0.59 ± 0.03 . We have shown in some earlier experiments that introducing the ionophore valinomycin Val, that can carry Na^+ across a phospholipid bilayer prevents the formation of an electrostatic “barrier” by a process in which as MG crosses into the inner compartment, a Na^+ ion is transported out of the liposome balancing the flow of charge. Experiments in the presence of the ionophore were found to yield a decay of the SHG signal to a value of 0.15 ± 0.02 , which is in good agreement with the predicted value.



protons across a phospholipid membrane, in contrast to valinomycin that transports alkali ions but not protons. We have found that the CCCP ionophore has a very small effect, on the SHG signal indicating that there is an insufficient population of protons inside the liposome to cross to the outside as the MG crosses to the inner compartment. We were unable to use pH indicators to measure the inside pH because of photochemical processes for the indicators used. To probe a different mechanism for transporting small ions across membranes we have used a polypeptide, gramicidin A, gA, which forms a channel across the bilayer enabling small cations to cross. In contrast to the ionophore

We have extended these studies to include an ionophore, CCCP, that transports only Val we observed a much faster decay in the SHG signal 11 ± 1 s using gA versus 138 ± 9 s using Val. However the SHG does not decay to a value close to 0.15, but rather levels off well above at 0.25 ± 0.03 , indicating that the maximum population of MG inside is not achieved. The different behavior of gA is attributed to the fact that protons as well as sodium ions can cross via the gA channel whereas for Val sodium ions but not protons can be carried across the bilayer. As a consequence the passage of protons via the gA channel does not relieve the buildup of positive charge inside the liposome. It then follows that MG does not reach its maximum inner population and the SHG signal remains high. The final steady state value of the MG inner population is determined by the balance of the concentration gradients of MG, sodium ions, and protons. Experiments at different outer pH values and sodium concentrations will be performed to test the proposed explanation of the different transport properties of these three antibiotics.

Acid – Base Chemistry at a Polymer Microparticle Interface

A significant manifestation of the unique properties of liquid interfaces is the change in chemical equilibria relative to bulk liquids. In our current research we use SHG to measure the pK_a of $0.91 \mu\text{m}$ polystyrenecarboxyl spheres in aqueous solution. We refer to the method that we use as the $\chi^{(3)}$ method because it is the third order polarization $P_{2\omega} = \chi^{(2)}E_{\omega}E_{\omega} + \chi^{(3)}E_{\omega}E_{\omega}E_{\text{static}}$ that is sensitive to the surface charge due to the electric field E_{static} that it creates. The surface charge is determined by the population of the charged species, acid or base, in these experiments it is the anionic carboxylate moiety, which in turn depends on the interfacial chemical equilibrium, pK_a . Because the electric field due to the surface charge extends into the bulk water, polarizing the bulk water molecules, we integrate the contributions to SHG from infinity to zero, which yields the electrostatic potential at the particle surface, Φ . From measurements of the SHG signal as a function of bulk electrolyte concentration we obtain the electrostatic potential at the particle/aqueous interface. We then measure the SHG signal as a function of bulk pH. The interfacial pH is assumed to be related to the bulk pH by the

Boltzmann factor, which is obtained from our measurement of the surface potential, $\exp(-e\Phi/kT)$. We find that the interfacial carboxyl group of the polymer particle is 3-4 times less acidic than carboxylic acids of similar structure in bulk water. The decrease in acidity is due to the repulsive interactions of the carboxylate groups, which shifts the pK_a to the neutral carboxyl form.

Future Plans

We have set up a sum frequency generation laser system that enables us to probe ultrafast excited electronic state dynamics, e.g. energy relaxation, chemical reactions, and interfacial solvent and solute motions. In preliminary experiments we have pumped organic molecules to an excited electronic state and measured interfacial molecular rotational motions of a SFG active vibrational chromophore. We plan to probe different vibrational chromophores in a given molecule so that we can obtain the change in the absolute orientation of the molecule with time. We have completed the first step in selecting an organic molecule and measuring its absolute orientation at the air/aqueous interface using the SFG method that we have developed.

Publications

Absolute orientation of molecules at interfaces" Y. Rao, M. Comstock and K. B. Eisenthal, *Journal of Physical Chemistry B*, **110**,4,1727-1732 (2006).

Molecular rotation at negatively charged surfactant/aqueous interfaces" K. T. Nguyen, X. M. Shang and K. B. Eisenthal, *Journal of Physical Chemistry B*, **110**,40,19788-19792 (2006).

Ultrafast excited-state electron transfer at an organic liquid/aqueous interface" E. A. McArthur and K. B. Eisenthal, *Journal of the American Chemical Society*, **128**,4,1068-1069 (2006).

"Second harmonic spectroscopy of aqueous nano- and microparticle interfaces" K. B. Eisenthal, *Chemical Reviews*, **106**,4,1462-1477 (2006).

Antibiotic assisted molecular ion transport across a membrane in real time" J. Liu, X. M. Shang, R. Pompano and K. B. Eisenthal, *Faraday Discussions*, **129**,291-299 (2005).

"Role of water in electron-initiated processes and radical chemistry: Issues and scientific advances" B. C. Garrett, et al, *Chemical Reviews*, **105**,1,355-389 (2005).

Electrostatic surface charge at aqueous/ α -Al₂O₃ single-crystal interfaces as probed by optical second-harmonic generation" J. P. Fitts, X. M. Shang, G. W. Flynn, T. F. Heinz and K. B. Eisenthal, *Journal of Physical Chemistry B*, **109**,16,7981-7986 (2005).

Second-harmonic generation and theoretical studies of protonation at the water/ α -TiO₂ (110) interface" J. P. Fitts, M. L. Machesky, D. J. Wesolowski, X. M. Shang, J. D. Kubicki, G. W. Flynn, T. F. Heinz and K. B. Eisenthal, *Chemical Physics Letters*, **411**,4-6,399-403 (2005).

Femtosecond aqueous solvation at a positively charged surfactant/water interface" A. V. Benderskii, J. Henzie, S. Basu, X. M. Shang and K. B. Eisenthal, *Journal of Physical Chemistry B*, **108**,37,14017-14024 (2004).

The Proton Pump in Bacteriorhodopsin, the other Photosynthetic System in Nature

Mostafa A. El-Sayed

School of Chemistry and Biochemistry, Georgia Institute of Technology 770 State Street, Atlanta Georgia 30332-0400.

email: melsayed@gatech.edu

Halophile bacteria like *Halobacterium halobium* are equipped with a light-energy transducing membrane called purple membrane. Such membrane contains a single protein: bacteriorhodopsin (bR), capable of absorbing light and converting it to an electrochemical gradient with surprising efficiency; gradient that is then used by the bacteria for ATP synthesis and other vital functions. The protein folds in seven helices (named A to G) arranged in an arc-like structure. Retinal is covalently bound to one of the helices through a base Schiff to Lys216. Upon light absorption the Retinal Schiff Base (RSB) goes through several metastable intermediates with various lifetimes ranging from hundreds of femtoseconds to the microsecond timescale.

BR is the most studied proton pump biological system. A great amount of work is carried in its function. In this study, the effect of plasmonic field on the rate of the different steps in its photocycle is being examined. The effect on the primary step following femtosecond excitation are obtained and discussed

Recent progress:

Trials to introduce Gold nanoparticle in bR

The introduction of Au-NPs on the bR was system attempted by using different strategies.

The first attempt was based on recent reports in the literatures of Au-NPs being synthesized biologically inside living cells such as bacteria¹⁻³ and human cell⁴. The same type of strategy was used to induce the formation of Au-NPs on the surface of *Halobacterium halobium* (strain S9), by adding H₂AuCl₄ in known concentrations to the growth medium. Concentrations around 1 mM in H₂AuCl₄ were used and the bacteria were left to grow in the presence of Au(III) ions for few days, after which TEM images of the bacteria were taken. They revealed the presence of Au-NPs of various sizes, from 10 to 250 nm, both on the bacteria surface and in the medium, having irregular shapes.

After bR is purified from the bacteria according to the standard procedure⁵; NPs are not present anymore on it. The procedure involving bacteria lysis followed by repeated washes and centrifugations, completely removed the NPs from the bR.

A second approach consisted of the addition of H₂AuCl₄ in concentration around 1 mM to the already purified bR patches in water solution.

After few minutes from the addition of the Gold (III) chloride trihydrate the bR solutions goes from deep purple to dark yellow. Linear spectra of the solutions show that the Retinal Base Schiff (RBS) band has disappeared which is a clear sign of a bleached purple membrane. The formation of Au-NPs on the bleach protein was observed both by dark field microscope and TEM. Their size range is again broad, since they are formed under uncontrolled condition. The samples obtained are of no use since the heart of the system, the RBS, is missing.

The third approach consisted on adding Au and Ag-NPs, citrate capped, to a solution of bR in a buffer. After addition of the NPs, the dark field microscope reveals that NPs are gathering around the bR patches, covering their surfaces. This approach has been considered the more

successful since it allows control of the NPs size used, and with no chemicals added, it has virtually no impact on bR.

Effect of the plasmon field on the Protein Raman

Raman spectroscopy and lately SERS from plasmonic nanoparticles and nanorods in particular has been extremely useful in providing information from biological systems like cells^{6, 7}.

Raman spectra of bR and bR with Au and Ag-NPs at 785nm are taken. When NPs are present in the sample the retinal base Schiff spectrum normally obtained at this wavelength is replaced by a different set of peaks.

Below the normalized spectrum of bR with Ag-NPs citrate capped (red) and the spectrum of just Ag-NPs (gray) are reported.

The blue arrows on fig. 1 indicate peaks that belong to the bR system.

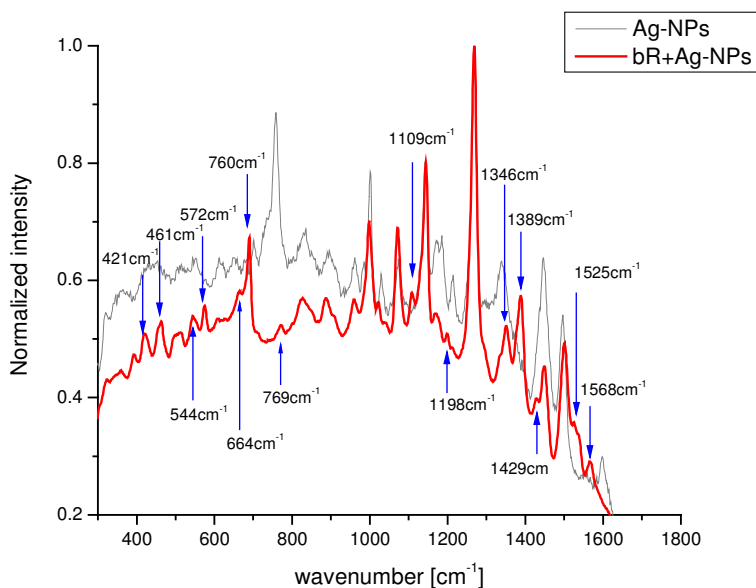


Fig1: Raman spectra at 785nm of Ag-NPs citrate capped and bR with Ag-NPs citrate capped

The possibility of studying protein at wavelength in the near IR, without using damaging UV excitation wavelength as was done in the past^{8, 9} could open the possibility of study bR photocycle from the protein stand point by time resolved Raman spectroscopy.

Effect of the plasmon field on bR primary step¹⁰

The prevailing model for describing the evolution of the RBS out of the Frank-Condon region after absorption of a photon is based on pump-probe experiments with subpicosecond resolution^{11, 12}. It is believed that a relaxation time of ≈ 100 fs takes place from the Frank Condon to the I_{460} state. Time-resolved Raman confirmed that no actual rotation is taking place during this time along the $C_{13}=C_{14}$ bond, but instead that the double bond distance changes¹³.

The complete twisting is believed to happen while going from the I_{460} to J_{625} intermediates¹⁴ although in the literature there are papers questioning this point as well¹⁵.

Even though the dynamic details of the first light-induced event in bR have not yet been defined completely, the lifetime of I_{460} was confirmed to be around 500 fs¹¹.

In this study fs time resolved pump-probe experiment was designed to measure I_{460} decay time when bR is in presence of 40 nm Au-NPs citrate capped. The excitation wavelength of 560 nm, used for all the samples, exciting both the retinal and the Au-NPs surface plasmon while the white light probe is set at 490 nm.

By exciting the NPs surface plasmon, the collective oscillation of the conduction electrons generates a strong spatial field distribution that reaches steady state few femtosecond after excitation¹⁶. The dynamic the electron-phonon coupling was measured for the 40 nm Au-NPs synthesized and it was found to be 1.8 ps.

As reported on table 1 I_{460} lifetime increases when NPs are present, not only that, as the NPs concentration increases so is their effect on I_{460} lifetime.

Sample	40 nm Au-NPs conc./ 10^{-9} Mol	I_{460} Decay lifetime / fs
bR	-	470
Solution A	0.16	515
Solution B	1.6	720
Solution C	2.4	800

Table 1: I_{460} lifetime for bR and bR in presence of 40 nm Au-NPs citrate capped at different concentration in phosphate solution (50 mM) at pH 7.0.

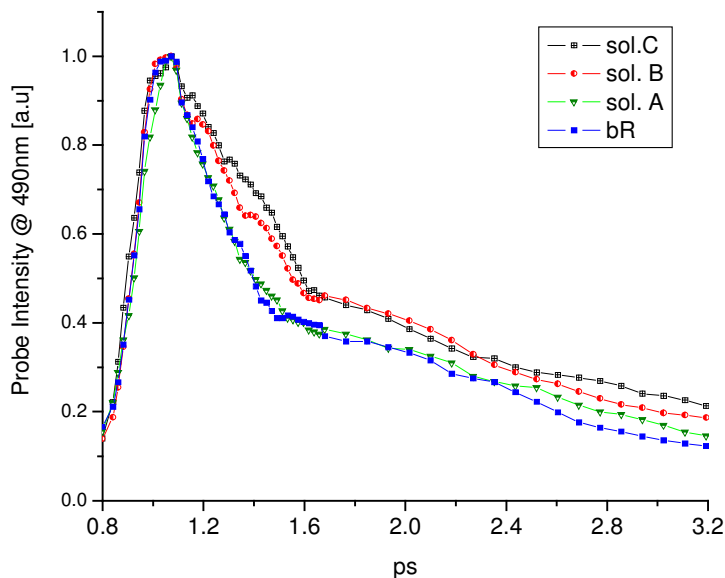


Fig.2: Time resolve fs pump-probe of bR and bR with different concentration of Au-NPs (40 nm diameter citrate capped). As the gold nanoparticles increases, the excited state of the bR retinal increases.

It is important to realize that the photon-photon relaxation time in gold nanospheres is one hundred picosecond¹⁶. This and the fact that the repetition rate of the laser system is 500 Hz eliminates the possibility that the observed change in the dynamic is a result of thermal effects resulting from the phonon-phonon relaxation within the nanoparticles, leaving the field generated upon plasmon excitation as the only cause for such observed change in excited state lifetime. In order to understand the origin of such differences in the I_{460} decay time the dynamic of what happens as the retinal system is rapidly excited within the protein cavity has to be considered.

An aspect where theoretical calculations and experiments agree upon is the large charge redistribution in RBS following the absorption of light. Theoretical prediction for the Schiff base

system immediately after excitation is close to a neutral amino group with a positively charged polyene chain¹⁷. The charge is rearranged and goes from the amino group to the polyene chain. This charge-unbalanced system should induce polarization on the protein cavity around it in the presence of an oscillating plasmonic electric field. As a result, the retinal electronic system is going to have a different potential energy surface than the unperturbed system. This should affect the rate, of its dynamic within its protein pocket, as shown by the experimental data on fig. 2. As more and more NPs accumulate on bR surface, getting close to one another and adding up their fields, the effect is ultimately amplified as table 1 shows.

Future plan

The other main process in bR proton pump is the rise and decay of M₄₁₂ intermediate in which the proton is released and recombined. This will be studied in presence of NPs and as function of their concentrations in details.

1. Mukherjee, P., Senapati, S., Mandal, D., Ahmad, A., Islam Khan, M., Kumar, R., Sastry, M., *ChemBioChem* **2002**, 5, 461-463.
2. Sastry, M., Ahmad, A., Islam Khan, M., Kumar, R., *Curr. Sci.* **2003**, 85, 162-170.
3. Ahmad, A., Senapati, S., Islam Khan, M., Kumar, R., Ramani, R., Srinivas, V., Sastry, M., *Nanotechnology* **2003**, 14, 824-828.
4. Anshup, V., J. S., Subramaniam, C., Kumar, R. R., Priya, S., Santhosh, T., Kumar, R., Omkumar, R V., John, A., Pradeep, T., *Langmuir* **2005**, 21, 11562-11567.
5. Oesterhelt, D., Stoeckenius, W., *Methods in enzymology* **1974**, 31, 667-678.
6. Manfait, M., Morjani, H., Nabiev, I., *J. Cell. Pharmacol.* **1992**, 3, 120.
7. Morjani, H., Riou, J. F., Nabiev, I., Lavelle, F., Manfait, M., *Cancer Res.* **1993**, 53, 4784.
8. Harada, I., Yamagishi, T., Uchida, K., Takeuchi, H., *J. Am. Chem. Soc.* **1990**, 112, (6), 2443-2445.
9. Hashimoto, S., Sasaki, M., Takeuchi, H., Needleman, R., Lanyi, K. J., *Biochemistry* **2002**, 41, (20), 6495-6503.
10. Biesso, A., Wei, Q., El-Sayed, M. A., *Biophys. J.* **2007** ASAP
11. Mathies, A. R., Brito Cruz, H. C., Pollard, T. W., Shank, V. C., *Science* **1988**, 240, 777-779.
12. Dobler, J. Z., W., Kaiser, K., Oesterhelt, D., *Chem. Phys. Lett.* **1988**, 144, 215-220.
13. Song, L., El-Sayed, A. M., *J. Am. Chem. Soc.* **1998**, 120, 8889-8890.
14. Zhong, Q., Ruhman, S., Ottolenghi, M., *J. Am. Chem. Soc.* **1996**, 118, 12828-12829.
15. Atkinson, H. G., Ujj, L., Zhou, Y., *J. Phys. Chem. A* **2000**, 104, 4130-4139.
16. Link, S., El-Sayed A. M., *Int. Rev. Phys. Chem.* **2000**, 19, 409-453.
17. Salem, L., Bruckmann, P., *Nature* **1975**, 258, 526-528.

Statistical Mechanical and Multiscale Modeling of Surface Reaction Processes

Jim Evans (PI) and Da-Jiang Liu
Ames Laboratory – USDOE and Department of Mathematics,
Iowa State University, Ames, IA 50011
evans@ameslab.gov

PROGRAM SCOPE:

A major component of the Chemical Physics Program at Ames Laboratory focuses on the modeling of **heterogeneous catalysis and other complex reaction phenomena** (mainly at surfaces). This effort integrates *electronic structure analysis, non-equilibrium statistical mechanics, and multi-scale modeling*. The *electronic structure* component includes DFT-VASP analysis of chemisorption and reaction energetics on metal surfaces, as well as application of QM/MM methods (in collaboration with M.S. Gordon) to treat adsorption and reaction phenomena on semiconductor surfaces. The *non-equilibrium statistical mechanics and multi-scale modeling studies* of surface phenomena include Kinetic Monte Carlo (KMC) simulation of atomistic models, coarse-grained, and heterogeneous multiscale formulations. One aspect of this effort relates to heterogeneous catalysis on metal surfaces, where we consider both reactions on extended single crystal surfaces (including connecting atomistic to mesoscale behavior) as well as nanoscale catalyst systems (exploring the role of fluctuations). Another aspect focuses on reaction processes on semiconductor surfaces (including etching and oxidation). In addition, we are exploring cooperative behavior in statistical mechanical models for general reaction processes which exhibit non-equilibrium phase transitions and critical phenomena.

RECENT PROGRESS:

HETEROGENEOUS CATALYSIS ON METAL SURFACES

(i) Multi-site lattice-gas modeling of CO-oxidation on metal(100) surfaces. A basic goal for theoretical surface science since the early 1980's has been to develop realistic atomistic models for key catalytic reactions on metal surfaces. For low-pressure conditions, a challenge is that behavior is impacted by high mobility and delicate ordering of reactant adspecies. We have successfully developed realistic multi-site lattice-gas models and efficient KMC simulation algorithms to describe CO-oxidation on unreconstructed metal(100) surfaces [1-3,12,20]. Essential ingredients include: multiple adsorption sites with distinct binding; accurate adspecies interactions which control ordering in the mixed adlayer; rapid surface mobility of CO and lower mobility of O; realistic description of adsorption-desorption and LH reaction kinetics. Energetic parameters are determined with guidance from DFT analysis, but refined to describe key aspects of experimental observations for constituent single-adspecies systems. Recent work focused on CO+O/Rh(100) where DFT fails to predict relative binding energies for CO at various sites. We described ordering and TPD for the constituent adspecies, and TPR kinetics for CO-oxidation.

(iii) Analysis of catalytic reactions for higher pressures and smaller (nanoscale) systems: To begin to explore reaction behavior “closing the pressure gap”, the above realistic atomistic models are applied to analyze CO-oxidation behavior for higher pressures, but still below the threshold for oxide formation. For such pressures (or for lower temperatures), we find reactant phase separation which can produce atomically sharp reaction fronts. To also “close the materials

gap” by considering nanoscale reaction systems, the models are used to explore fluctuation-dominated CO-oxidation behavior on nanofacets. Previously, we have characterized fluctuation-induced transitions in such bistable nanosystems using simplified lattice-gas models, and also characterized non-equilibrium critical phenomena near cusp points in the bifurcation diagram. For higher pressures or lower temperatures, we find non-mean-field-type fluctuation-induced transitions associated with reactant phase separation [15,16]. Studies of CO-oxidation on metal Field Emitter Tips provide a powerful tool for in-situ real-time investigation of such effects.

OTHER COMPLEX SURFACE AND MESOPOROUS REACTION SYSTEMS

(i) Polymerization reactions in mesoporous silica systems. Our broad goal is to develop models for catalysis in mesoporous systems. Initially, we are focusing on the kinetics of polymerization of PPB within mesoporous silica (MCM-41) which has been functionalized with internal catalytic sites. We have adopted a stochastic atomistic lattice-gas modeling strategy accounting for anomalous diffusive transport of reactant monomers to a distribution of catalytic sites within the pore. Model output yields the resulting polymerization kinetics, the extent of product polymer extrusion, product chain length distribution and spatial distribution.

(ii) Morphological evolution during etching and oxidation of vicinal Si(100). Exposure of vicinal Si(100) to oxygen at $\sim 600^\circ\text{C}$ produces step recession due to etching [$\text{Si} + \text{O}(\text{ads}) \rightarrow \text{SiO}(\text{gas}) + \text{vacancy}$] in competition with surface oxide formation [$\text{Si} + 2\text{O}(\text{ads}) \rightarrow \text{SiO}_2$]. Oxide islands mask etching of the underlying Si and pin receding steps [8,10]. Previous atomistic modeling recovered the observed dramatic bending of meandering S_B steps around pinning sites, and the snap-off of stiffer S_A steps. It also described mixed-mode etch pit nucleation and step flow on alternating terraces. However, model reliability was inhibited by limited characterization of oxide nucleation. New STM studies provide further insight into this process, which can be tested with QM/MM analysis from the Gordon group, and which is being incorporated into a refined model. Work continues on implementing phase-field modeling of surface morphologies coupled with appropriate reaction kinetics – providing a powerful and versatile modeling tool.

FUNDAMENTAL PHENOMENA IN FAR-FROM-EQUILIBRIUM REACTION SYSTEMS

Other general statistical mechanical studies of non-linear reaction systems focus on non-equilibrium phase transitions and associated metastability and criticality phenomena. The goal is to advance understanding of these phenomena to a level comparable to that for equilibrium systems. The significance of such problems was highlighted in the preliminary report of the *BESAC Science Grand Challenges* subcommittee under the heading *Cardinal Principles of Behavior beyond Equilibrium*. We have thus analyzed a statistical mechanical version of Schloegl’s second model for autocatalysis (aka. the quadratic contact process) revealing a discontinuous non-equilibrium transition between reactive and extinct states displaying metastability. In dramatic contrast to equilibrium systems, we find a remarkable “generic two-phase coexistence” for a finite range of control parameter! We explain this feature in terms of dependence of equistability on the orientation of the interface between the coexisting phases. We also analyze unusual features of non-equilibrium reaction kinetics (including nucleation rates and Arvami behavior in the metastable regime), associated spatio-temporal behavior, and develop approximate analytic tools to elucidate behavior. We are extending these analyses to consideration of idealized ZGB-type surface reaction models, which although too simplest to describe standard low-pressure reaction behavior, may provide a valuable paradigm for higher pressure low-mobility fluctuation-dominated reactions.

FUTURE PLANS:

HETEROGENEOUS CATALYSIS ON METAL SURFACES

(i) Chemisorbed adlayer structure and dynamics (probed by STM) and the role of steps in reactions (probed by LEEM). We plan to explore surface phenomena related to ordering and dynamics in chemisorbed layers on metal surfaces probed by in-situ STM: self-organized S complexes on Ag (Thiel - Ames Lab), and the dynamics of CO clusters in CO + H on Pd (Salmeron - LBL). We will also explore the role of steps in reactions, particularly involving NO dissociation. Our goal here is to develop models which couple reaction kinetics to step dynamics, and which allow description of behavior observed with in-situ LEEM as planned by Imbihl.

(ii) CO-oxidation and NO-reduction reactions on metal surfaces of Rh, Pd, etc. We will develop further realistic atomistic models for catalytic reactions on various extended single-crystal metal (111) and (100) surfaces. In addition, such models will be applied to elucidate reaction behavior in nanoscale systems (e.g., on the nanofacets of FET's and supported clusters). Efforts will begin to explore higher-pressure catalysis and associated oxide formation processes. Our models will incorporate input from electronic structure studies, and we will analyze reaction behavior primarily utilizing KMC simulation.

(iii) Heterogeneous Coupled Lattice-Gas (HCLG) multiscale modeling of pattern formation in surface reactions. We will continue to develop multiscale algorithms as part of our HCLG approach (including implementation of parallel KMC simulation and efficient algorithms for on-the-fly analysis of chemical diffusion). Most other heterogeneous multiscale methods assume local equilibration, a feature which is often not satisfied in surface reaction systems with long-range ordering of the adlayer. We will pursue development of reliable "lifting procedures" generating micro- from macro-states facilitating efficient treatment of such systems.

OTHER COMPLEX SURFACE AND MESOPOROUS REACTION SYSTEMS

Our modeling of etching, oxidation, and other reactions on vicinal Si(100) will focus on development of coarse-grained phase-field type formulations describing evolution of surface morphology. This latter approach is versatile, allowing efficient integration of various models for the surface chemistry with a computationally efficient framework to describe complex surface morphologies. DFT and QM/MM will be applied to provide precise and detailed information on key energetics as input to such modeling. Processes of interest will include etching and CVD.

We will pursue investigations of the stochastic atomistic model for polymerization kinetics in mesoporous systems, implementing refinements to integrate new experimental observations (e.g., polymer diffusivity from NMR-PFG studies). Further effort will focus on the "extrusion regime" of particular interest for experiments. We aim to model entropic or other driving forces for extrusion, the distribution of catalytic sites, and control of reactant input (including chiral selectivity) via gatekeepers which could induce diffusion offsets for different reactants.

FUNDAMENTAL PHENOMENA IN FAR-FROM-EQUILIBRIUM REACTION SYSTEMS

Analysis will continue of non-equilibrium phase transitions in a variety of statistical mechanical reaction models. Issues of metastability and nucleation, and well as critical phenomena, are of fundamental interest for these non-equilibrium systems where the standard thermodynamic framework (e.g., involving a free energy) cannot be applied. The ramifications of anomalous behavior such as "generic two-phase coexistence" will be explored.

PUBLICATIONS SUPPORTED BY USDOE FOR 2004-PRESENT: (*partial SciDAC support)

- [1] *Lattice-Gas Modeling of CO Adlayers on Pd(100)*, D.-J. Liu, J. Chem. Phys. **121**, 4352 (2004), 6pp.
- [2] *Lattice-Gas Modeling of the Formation and Ordering of Oxygen Adlayers on Pd(100)*, D.-J. Liu, J.W. Evans, Surface Science **563**, 13-26 (2004).
- [3] *From Atomic Scale Reactant Ordering to Mesoscale Reaction Front Propagation: CO Oxidation on Pd(100)*, D.-J. Liu, J.W. Evans, Phys. Rev. B **70**, 193408 (2004), 4pp.
- [4] *Crossover between Mean-Field and Ising Critical Behavior in a Lattice-Gas Reaction-Diffusion Model*, D.-J. Liu, N. Pavlenko, J.W. Evans, J. Stat. Phys., **114**, 101-114 (2004).
- [5] *Atomistic Modeling of Morphological Evolution during Simultaneous Etching and Oxidation of Si(100)*, M. Albao, D.-J. Liu, C. H. Choi, M.S. Gordon, J.W. Evans, Surf. Sci. **555**, 51-67 (2004).*
- [6] *Connecting-the-Length-Scales from Atomistic Ordering to Mesoscale Spatial Patterns in Surface Reactions: HCLG Algorithm*, D.-J. Liu, J.W. Evans, SIAM Multiscale Model. **4**, 424-446 (2005)*
- [7] *Kinetic Monte Carlo Simulation of Non-Equilibrium Lattice-Gas Models...*, J.W. Evans, Handbook Materials Modeling A, S. Yip, Ed. (Springer, Berlin, 2005), Ch.5.12.*
- [8] *Competitive Etching and Oxidation of Vicinal Si(100) Surfaces*, M.A. Albao, D.-J. Liu, C.H. Choi, M.S. Gordon, J.W. Evans, MRS Proc. **859E**, JJ3.6 (2005), 6pp.*
- [9] *Monotonically Decreasing Size Distributions for One-Dimensional Ga Rows on Si(100)*, M.A. Albao, M.M.R Evans, J. Nogami, D. Zorn, M.S. Gordon, J.W. Evans, Phys. Rev. B **71**, 071523 (2005), 8pp.*
- [10] *Simultaneous Etching and Oxidation of Vicinal Si(100) Surfaces: ...Modeling of Morphological Evolution*, M.A. Albao, D.-J. Liu, M.S. Gordon, J.W. Evans, Phys. Rev. B. **72**, 195420 (2005), 12pp.
- [11] *Morphological Evolution during Epitaxial Thin Film Growth: Formation of 2D Islands and 3D Mounds*, J.W. Evans, P.A. Thiel, M.C. Bartelt, Surface Science Reports, **61**, 1-128 (2006).
- [12] *Atomistic Lattice-Gas Modeling of CO-oxidation on Pd(100): Temperature-Programmed Spectroscopy & Steady-State Behavior*, D.-J. Liu, J.W. Evans, J. Chem. Phys. **124**, 154705 (2006), 13pp.
- [13] *Reply to Comment: Monotonically Decreasing Size Distributions for Ga Rows on Si(100)*, M.A. Albao, M. Evans, J. Nogami, D. Zorn, M.S. Gordon, J.W. Evans, Phys. Rev. B **74**, 037402 (2006), 3pp.*
- [14] *Chemical Diffusion in Mixed CO+O Adlayers and Reaction Front Propagation in CO-oxidation on Pd(100)*, D.-J. Liu, J.W. Evans, J. Chem. Phys. **125**, 054709 (2006), 8pp.*
- [15] *Fronts and Fluctuations in a Tailored Model for CO-oxidation on Unreconstructed Metal(100) Surfaces*, D.-J. Liu, J.W. Evans, J. Phys.: Cond. Matt., **19**, 065129 (2007).
- [16] *Chemical Diffusion in Mixed CO+O Adlayers and Reaction Front Propagation in CO-oxidation on Pd(100) Fluctuations and Patterns in Nanoscale Surface Reaction Systems: Influence of Reactant Phase Separation during CO-oxidation*, D.-J. Liu, J.W. Evans, Phys. Rev. B **75**, 073401 (2007), 4pp.*
- [17] *Quadratic Contact Process: Phase Separation with Interface-Orientation-Dependent Equistability*, D.-J. Liu, X. Guo, J.W. Evans, Phys. Rev. Lett., **98**, 050601 (2007), 4pp.
- [18] *Generic Two-Phase Coexistence, Relaxation, Kinetics, and Interface Propagation in the Quadratic Contact Process: Simulation Studies*, X. Guo, D.-J. Liu, J.W. Evans, Phys. Rev. E., **75**, 061129 (2007).
- [19] *Generic Two-Phase Coexistence, Relaxation, Kinetics, and Interface Propagation in the Quadratic Contact Process: Analytic Studies*, X. Guo, J.W. Evans, D.-J. Liu, Physica A, in press (2007).
- [20] *CO-oxidation on Rh(100): Multi-site Atomistic LG Modeling*, D.-J. Liu, J. Phys. Chem. C (2007).

Chemical Kinetics and Dynamics at Interfaces
Fundamentals of Solvation under Extreme Conditions

John L. Fulton
Chemical Sciences Division
Pacific Northwest National Laboratory
902 Battelle Blvd.
Mail Stop K1-83
Richland, WA 99352
john.fulton@pnl.gov

Program Scope

The primary objective of this project is to describe, on a molecular level, the solvent/solute structure and dynamics in fluids such as water under extremely non-ideal conditions. The scope of studies includes solute–solvent interactions, clustering, ion-pair formation, and hydrogen bonding occurring under extremes of temperature, concentration and pH. The effort entails the use of spectroscopic techniques such as x-ray absorption fine structure (XAFS) spectroscopy, coupled with theoretical methods such as molecular dynamics (MD-XAFS), and electronic structure calculations in order to test and refine structural models of these systems. In total, these methods allow for a comprehensive assessment of solvation and the chemical state of an ion or solute under any condition. The research is answering major scientific questions in areas related to energy-efficient separations, hydrogen storage (thermochemical water splitting) and sustainable nuclear energy (aqueous ion chemistry and corrosion). This program provides the structural information that is the scientific basis for the chemical thermodynamic data and models in these systems under non-ideal conditions.

Recent Progress

When a transition metal ion forms a contact ion pair with a halide ion in water the resultant bond often involves a certain degree of covalency. This association profoundly changes the coordination structure about the hydrated ion. Under ambient conditions, the predominant species is usually the fully hydrated ion but at extreme temperature or high halide concentrations the contact ion pair is generated. From XAFS measurements of these species we have found that conventional molecular dynamics simulations and standard thermodynamic models often fail to accurately predict the ion pair structure. Increasingly we find that electronic structure calculations for small clusters and, more importantly, ab initio molecular dynamics simulations provide an accurate prediction of structure. A vivid example of this is shown in Figure 1 where the unusual structure of the CuCl_2^- contact ion pair in water is presented. XAFS measurements clearly show a complete absence of hydrating waters about Cu^{1+} . Further, this mostly bare Cu^{1+} ion binds two Cl^- in a collinear arrangement. As shown in Fig. 1, classical molecular dynamics simulations and the best available thermodynamic models (Born model) completely fail to capture the major features of the structure. On the other hand, recent ab initio molecular dynamics simulations provide a remarkably accurate representation of the structure including (i) the Cu-Cl coordination number, (ii) the Cu-Cl bond length and (iii) the absence of hydrating waters about the Cu.

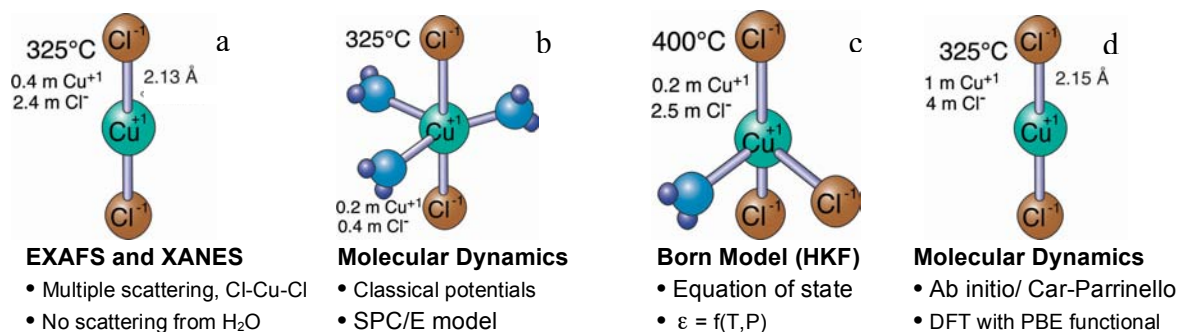


Figure 1. Contrasting XAFS measurements of the Cu⁺/Cl⁻ contact ion pair structure with recent results from simulations and thermodynamic models. a. XAFS measurements from diamond window cell at 325°C,^{1,2} b. classical molecular dynamics simulation,^{1,2} c. Born model equation of state,³ d. Car-Parrinello molecular dynamics simulations.⁴

To follow up on these new and interesting findings we have made measurements of the Ag⁺/Cl⁻ contact ion pair. These XAFS measurements are shedding light on the mechanism that leads to a complete loss of hydrating waters about the cation. This is the first time that the full molecular structure of AgCl₂⁻ has been determined in water. We have found that the structure of AgCl₂⁻ is nearly identical to that of CuCl₂⁻ including the loss of hydrating waters about the cation. Cu(I) ([Ar] 3d¹⁰) and Ag(I) ([Kr] 4d¹⁰) have very similar electronic structures although their coordination structures are often different. Crystalline Ag(I) compounds often exhibit linear twofold coordination that has in part been attributed to hybridization of the 4d_{z²} and 5s orbitals. Electronic structure calculations of a Cl-Ag-Cl cluster show a large amount of charge transfer between the Cu and the Cl, reducing the local electrostatic charge on Ag from +1 to about +0.26. Hence we have shown that Ag⁺ loses waters-of-hydration upon formation of the AgCl₂⁻ ion pair due to reduced ionic charge on Ag via covalent bonding with Cl. Future studies will explore ab initio molecular dynamics simulations of the contact ion pair.

Future Plans

Long established views of hydration and ion pairing are being challenged in a series of XAFS studies. These XAFS structural results will be tested and refined using electronic structure calculations of small cluster and ab initio molecular simulations techniques. Along these lines we are planning a series of low-energy studies at the Cl K-edge and the Ag L₃ edge. The Cl K-edge spectra probe the local coordination structure about Cl⁻ from the extended x-ray absorption region. Equally important is the near-edge spectral region containing the 1s → np transition providing a direct measure of the covalency of cation-Cl bond. Several systems are currently under investigation:

Chloride/Hydronium Interaction. Experimental measurements of the structure of hydronium ion (H₃O⁺) in water are scarce. A recent, concerted effort, using neutron diffraction (NDIS) returned limited results.⁵ In this case, the various pair distribution functions could not be fully resolved, mandating reliance on Monte Carlo interpretation with only partially satisfactory results. For instance, the measured Cl-H₃O distance from NDIS is significantly

different than the distance predicted from DFT molecular dynamics simulations.⁶ The DFT simulation shows that the Cl-O distance for hydronium is about 0.2 Å shorter than that for a hydrating water molecule. We have recently developed methods for making XAFS transmission measurements of aqueous at these low x-ray energies. Preliminary data shows a shortening of the Cl-O distance (from H₃O⁺) that is approximately equal to the theoretical value. Thus this study will provide the first direct measure of the Cl⁻/H₃O⁺ distance and provide an excellent comparison to ab initio molecular dynamics studies of the same system.

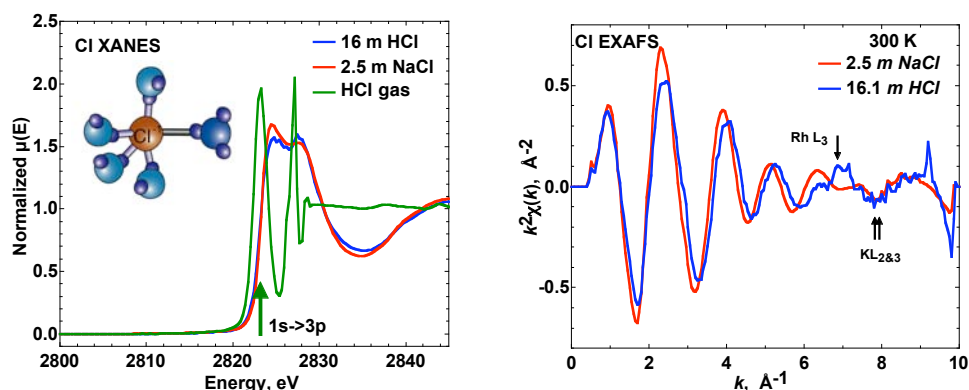


Figure 2. XAFS spectra of Cl⁻ in aqueous systems probing the electronic state of the ion pair interaction and the coordination structure.

Silver Ion Hydration. The conventional view of hydrated Ag⁺ is that four water molecules form a purely tetrahedral structure about the ion. This result is based upon NDIS and XAFS studies from nearly two decades ago. Recent electronic structure calculations for small clusters and ab initio molecular dynamics simulations show that the structure can be better described as trigonal bipyramidal or distorted octahedral. In the K-edge spectrum of aqueous Ag⁺, we discovered the existence of a strong multiple scattering (MS) peak at twice the Ag-O distance. Multiple scattering can originate from either the collinear O-Ag-O paths (octahedral structure) or from the double return Ag-O scattering path (tetrahedral structure) making it impossible to clearly differentiate the two structures. We discovered that by evaluating both the K- and L₃-edge EXAFS spectra, it is possible to differentiate the two structures. In the L₃-edge spectra, the double-return, multiple scattering path is 180° phase shifted with respect to the collinear paths (due to initial state excitation from s vs p orbital). Hence by simultaneous fitting both spectra, we will be able to clearly identify the hydration symmetry. These Ag studies should completely rewrite our understanding of Ag⁺ hydration bringing experimental studies inline with recent theory.

Hydration of Iodide and Ion Pairing with Hydronium. Finally we are beginning to explore aqueous iodide as I⁻/H₃O⁺ and I₂⁻ and I⁻ in concentrated HI/H₂SO₄ solutions at elevated temperature. Very little is known about the I⁻ coordination chemistry under these conditions. These extremely nonideal conditions are used in the sulfur-iodide thermochemical route to water splitting for H₂ generation

Collaborators on this project include G.K Schenter, S. M. Kathmann, C. J. Mundy, L. X. Dang, V.-A. Glezakou, and Y. Chen. Battelle operates Pacific Northwest National Laboratory for the U. S. Department of Energy.

Cited References

1. Fulton, J. L., Hoffmann, M. M., Darab, J. G., Palmer, B. J., Stern, E. A., **J. Phys. Chem. A**, 104, 11651-11663, (2000)
2. J. L. Fulton, M. M. Hoffmann, and J. G. Darab, **Chemical Physics Letters**, 330, 300-308, (2000)
3. Liu and McPhail, **Chemical Geology**, 221, 21, (2005)
4. Sherman, **Geochimica et Cosmo. Acta**, 71, 714, (2007)
5. Botti, A.; Bruni, F.; Ricci, M. A.; Soper, A. K. **Journal of Chemical Physics** 125, Art. No. 014508 (2006).
6. Heuft, J. M.; Meijer, E. **J. Physical Chemistry Chemical Physics** 8, 3116. (2006).

References to publications of DOE sponsored research (2004-present)

1. J. L. Fulton Y. Chen, S. M. Heald, and M. Balasubramanian, "High-pressure, high temperature XAFS transmission cell for the study of aqueous ions with low absorption-edge energies", **Rev. Sci. Instruments.**, 75(12), 5228-5231, (2004).
2. J. L. Fulton, D. W. Matson, K. H. Pecher, J. E. Ammonette, J. C. Linehan, "Iron-based and Iron Oxide Nanoparticle Synthesis from the Rapid Expansion of Carbon Dioxide Solutions" **Journal of Nanoscience and Nanotechnology**, 6, 562-567 (2006).
3. Y. Chen, J. L. Fulton, J. C. Linehan, T. Autrey, "In-situ XAFS and NMR Study of Rhodium Catalyst Structure during Dehydrocoupling of Dimethylamine Borane. " **J. Am. Chem. Soc.**, 127, 3254-3255, (2005)
4. Y. Chen, J. L. Fulton, W. Partenheimer. The structure of the homogeneous oxidation catalyst, Mn(II)- (Br⁻¹)_x, in supercritical water: An x-ray absorption fine structure study. **J. Am. Chem. Soc.** 127, 14085-14093, (2005).
5. V. Glezakou, Y. Chen, J. L. Fulton, G. K. Schenter and L. X. Dang. Electronic structure, statistical mechanical simulations, and EXAFS spectroscopy of aqueous potassium. **Theor. Chem. Acc.** 115, 86-99, (2006)
6. Y. Chen, J. L. Fulton, W. Partenheimer. A XANES and XAFS Study of Hydration and Ion Pairing in Ambient Aqueous MnBr₂ Solutions. **J. Solution Chem.** 34(9) **2005**, 993-1007.
7. J. L. Fulton, J. C. Linehan, T. Autrey, M. Balasubramanian, Y. Chen, and N. K. Szymczak. When is a Nanoparticle a Cluster? An Operando EXAFS Study of Amine Borane Dehydrocoupling by Rh₄₋₆ Clusters. **J. Am. Chem. Soc.**, (2007), in press.
8. "Calcium Ion Hydration and Ion Pairing in Supercritical Water", J. L. Fulton Y. Chen, S. M. Heald, and M. Balasubramanian, **J. Chem. Phys.**, 125(9), Art. No. 094507, (2006).
9. "Molecular simulation analysis and X-ray absorption measurement of Ca²⁺, K⁺ and Cl⁻ ions in solution", Liem X. Dang, Gregory K. Schenter, Vassiliki-Alexandra Glezakou and John L. Fulton, **J. Phys. Chem. B**, 110(47), 23644, (2006)

Molecular Theory & Modeling

Reactions of Ions and Radicals in Aqueous Systems

Bruce C. Garrett
Chemical & Materials Sciences Division
Pacific Northwest National Laboratory
902 Battelle Blvd.
Mail Stop K9-90
Richland, WA 99352
bruce.garrett@pnl.gov

The long-term objective of this project is to understand the factors that control the chemical reactivity of atomic and molecular species in aqueous environments. Chemical reactions in condensed phase environments play crucial roles in a wide variety of problems important to the Department of Energy (DOE), (e.g., corrosion in nuclear reactors promoted by reactive radical species such as OH, release of hydrogen from hydrogen storage materials, catalysis for efficient energy use, and contaminant degradation in the environment by natural and remedial processes). The need in all of these areas is to control chemical reactions to eliminate unwanted reactions and/or to produce desired products. The control of reactivity in these complex systems demands knowledge of the factors that control the chemical reactions and requires understanding how these factors can be manipulated to affect the reaction rates. The goals of this research are the development of theoretical methods for describing reactions in condensed phases (primary aqueous liquids) and their application to prototypical systems to develop fundamental knowledge need to solve problems of interest to DOE.

A recent focus of our work is the development of a hybrid approach for free energy calculations that utilizes high-level electronic structure methods such as coupled cluster (CC) theory. The use of accurate electronic structure methods in calculations of reaction energetics for condensed phase reactions is often impractical because of the need to sample over a large number of degrees of freedom. To circumvent this problem, we use an approach that is similar in spirit to the layered electronic structure methods of Morokuma and coworkers, which constructs a sequence of multiple representations of the reactive region allowing the bulk of statistical averaging to be shifted toward less expensive descriptions of the energetics.

We begin by separating the condensed phase system into a reactive part (denoted the solute), which is treated quantum mechanically, and the rest of the system (denoted the solvent), which is treated by a classical molecular mechanics (MM) model. Three different descriptions of the solute are employed – CC, density functional theory (DFT) and electrostatic potential (ESP). In the ESP, the QM atoms are represented by effective ESP charges such that the electrostatic potential outside the solute region is the same as that produced from the full electron density $\rho(\mathbf{r})$. We use a thermodynamic cycle as depicted in the figure to take advantage of the state function property of the potential of mean force (PMF), W . The free energy, or PMF, for going from a point in the configuration space of the solute, \mathbf{r}_A , to a second point, \mathbf{r}_B , is given by

$$\Delta W_{AB} = \left(\Delta W_{AA}^{cc \rightarrow dft} - \Delta W_{BB}^{cc \rightarrow dft} \right) + \left(\Delta W_{AA}^{dft \rightarrow esp} - \Delta W_{BB}^{dft \rightarrow esp} \right) + \Delta W_{AB}^{esp}$$

The first and second terms represent free energy difference for changing the description of the *fixed* solute region from the CC to DFT representations and from DFT to classical ESP representations, respectively. The third term represents the free energy difference for changing

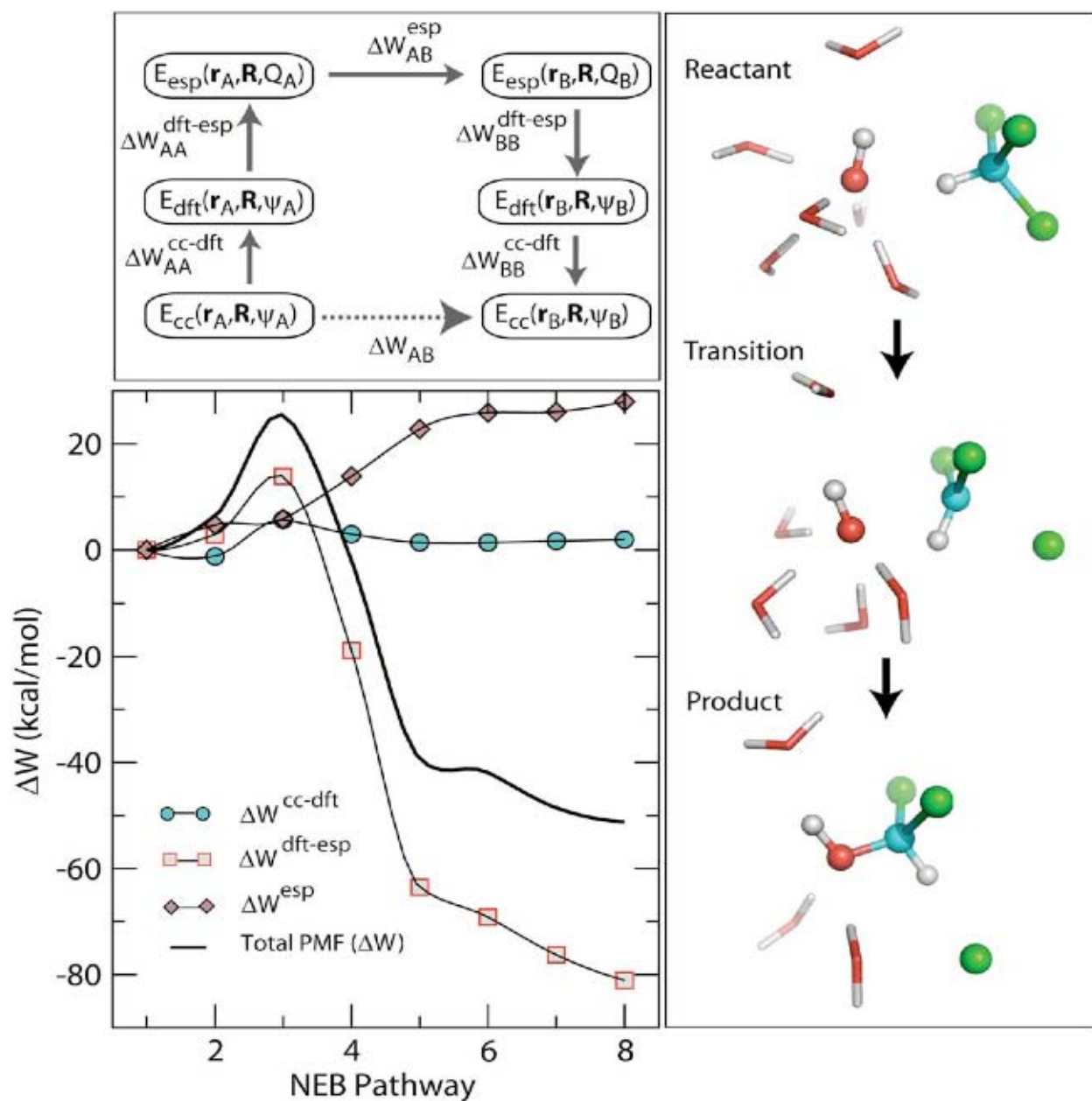


Figure: Thermodynamic cycle for free energy calculations (top left); free energy profile (bottom left) and reactant, transition, and product states (right) for the reaction $\text{OH} + \text{CHCl}_3 \rightarrow \text{CHCl}_2\text{OH} + \text{Cl}^-$.

solute configuration from \mathbf{r}_A to \mathbf{r}_B within the classical ESP/MM description. The benefit of using an intermediate DFT description is that the ground state DFT electron density should be fairly close to the nearly exact density generated by CC theory. The electron density is the sole coupling parameter between the solute electronic degrees of freedom and the solvent, therefore, the potential of mean force for the change from CC to DFT can be approximated by a simple total energy difference. The potential of mean force calculated with the electrostatic potential, $\Delta W_{AB}^{\text{esp}}$, involves only classical molecular mechanics terms, which allows sampling to be performed over ensembles that are sufficiently large to converge the averages. Evaluation of

$\Delta W_{AA}^{dft \rightarrow esp}$ uses a resampling strategy in which a small number of solvent configurations from the ESP/MM simulation are used to evaluate the average.

This approach was applied to the S_N2 reaction of CHCl_3 and OH^- in aqueous solution. The DFT calculations used the B3LYP exchange correlation functional with the 6-31+G* basis set, and the CC description was based on the locally renormalized variant of CC theory with single, double, and perturbative triple excitations (LR-CCSD(T)) with the aug-cc-pVDZ basis set. The solute was embedded in a 30 Å cubic box of 888 SPC/E water molecules representing the MM region. A zero-temperature minimum energy path was calculated for the total system at the DFT/MM level of theory using the nudged elastic band method. The free energy profile, including contributions from the different terms, is shown in the figure. Overall we find that the CC/MM approach gives a free energy reaction barrier of 29.3 kcal/mol and an overall reaction free energy of -46.7 kcal/mol. We note that DFT/MM treatment of the same process underestimates the reaction barrier (24.6 kcal/mol) but agrees well on the reaction free energy (-47 kcal/mol).

Another focus of our research in the past few years has been on understanding the factors controlling radical reactions in aqueous systems. An important factor is the effect of the open-shell nature of the radical on the solvation structure around the radical, since solvation and solvent reorganization can play an important role in chemical reactivity. Towards this end, we studied OH radical interactions with water to understand how the unpaired orbital in OH can affect the interaction energy. We employed CCSD(T)/aug-c-pVTZ calculations to decompose the binding energies of the $\text{OH}\cdot(\text{H}_2\text{O})_n$ ($n=2, 3$) complexes into their many-body contributions. We performed the energy decomposition with the scheme introduced by Hankins et al. [J. Chem. Phys. **53**, 4544 (1970)] and applied by Xantheas [J. Chem. Phys. **100**, 7523 (1994)] to water clusters. Geometries for the clusters were chosen to be the same as for the water clusters studied by Xantheas, with one of the hydrogen atoms removed from one of the water molecules. We find that the 3-body contributions to total binding energies of these clusters are comparable to those seen for the water clusters. With basis set superposition error included, the 3-body contribution is about 17% in the $\text{OH}\cdot(\text{H}_2\text{O})_2$ cluster and about 24% in the $\text{OH}\cdot(\text{H}_2\text{O})_3$ cluster. The 4-body contribution is only 2% for the $\text{OH}\cdot(\text{H}_2\text{O})_3$ cluster, which is very similar to the value for the $(\text{H}_2\text{O})_4$ cluster. We are using these results to assess the accuracy of the newly developed hydroxide-water interaction potential where the water part is described by the Thole-type model (TTM) for larger OH – water clusters.

Collaborators on this project include M. Valiev, M.-K. Tsai, G. K. Schenter, M. Dupuis, T. Iordanov, S. S. Xantheas, J. Li, S. Du, and J. Francisco. Some of the work was performed using the Molecular Science Computing Facility in the Environmental Molecular Sciences Laboratory, a national scientific user facility sponsored by the Department of Energy's Office of Biological and Environmental Research and located at Pacific Northwest National Laboratory (PNNL). Battelle operates PNNL for DOE.

References to publications of DOE sponsored research (2005-present)

1. B. C. Garrett, D. A. Dixon, D. M. Camaioni, D. M. Chipman, M. A. Johnson, C. D. Jonah, G. A. Kimmel, J. H. Miller, T. N. Rescigno, P. J. Rossky, S. S. Xantheas, S. D. Colson, A. H. Laufer, D. Ray, P. F. Barbara, D. M. Bartels, K. H. Becker, H. Bowen, S. E. Bradforth, I. Carmichael, J. V. Coe, L. R. Corrales, J. P. Cowin, M. Dupuis, K. B. Eisenthal, J. A. Franz, M. S. Gutowski, K. D. Jordan, B. D. Kay, J. A. LaVerne, S. V. Lymar, T. E. Madey, C. W. McCurdy, D. Meisel, S. Mukamel, A. R. Nilsson, T. M.

- Orlando, N. G. Petrik, S. M. Pimblott, J. R. Rustad, G. K. Schenter, S. J. Singer, A. Tokmakoff, L. S. Wang, C. Wittig, and T. S. Zwier, "Role of Water in Electron-Initiated Processes and Radical Chemistry: Issues and Scientific Advances," *Chemical Reviews* **105**, 355-389 (2005).
2. S. M. Kathmann, G. K. Schenter, and B. C. Garrett, "Ion-induced Nucleation: The Importance of Chemistry," *Physical Review Letters* **94**, 116104 (2005).
 3. B. C. Garrett and D. G. Truhlar, "Variational Transition State Theory," in Theory and Applications of Computational Chemistry: The First 40 Years, edited by C. E. Dykstra, G. Frenking, K. S. Kim, and G. E. Scuseria (Elsevier, Amsterdam, 2005), p. 67-87.
 4. T. D. Iordanov, G. K. Schenter, and B. C. Garrett, "Sensitivity analysis of thermodynamic properties of liquid water: A general approach to improve empirical potentials," *Journal of Physical Chemistry A* **110**, 762-771 (2006).
 5. L. X. Dang, T. M. Chang, M. Roeselova, B. C. Garrett, and D. J. Tobias, "On NO_3^- - H_2O Interactions in Aqueous Solutions and at Interfaces," *Journal of Chemical Physics* **124** (2006).
 6. B. C. Garrett, G. K. Schenter, and A. Morita, "Molecular Simulations of the Transport of Molecules Across the Liquid/Vapor Interface of Water," *Chemical Reviews* **106**, 1355-1374 (2006).
 7. S. Du, J. S. Francisco, G. K. Schenter, T. D. Iordanov, B. C. Garrett, M. Dupuis, and J. Li, "The OH Radical - H_2O Molecular Interaction Potential," *Journal of Chemical Physics* **124**, 224318 (2006).
 8. D. G. Truhlar and B. C. Garrett, "Variational Transition State Theory in the Treatment of Hydrogen Transfer Reactions," in Handbook of Hydrogen Transfer, edited by H. H. Limbach, J. T. Hynes, J. Klinman, and R. L. Schowen (Wiley-VCH, New York, 2007), Vol. 2, pp. 833-875.
 9. A. Fernandez-Ramos, B. A. Ellingson, B. C. Garrett, and D. G. Truhlar, "Variational Transition State Theory with Multidimensional Tunneling," in Reviews in Computational Chemistry, edited by K. B. Lipkowitz, Cundari, T. R., and D. B. Boyd (John Wiley & Sons, Hoboken, 2007), Vol. 23, pp. 125-232.
 10. S. Y. Du, J. S. Francisco, G. K. Schenter, and B. C. Garrett, "Ab initio and Analytical Intermolecular Potential for $\text{ClO}-\text{H}_2\text{O}$," *Journal of Chemical Physics* **126**, 114304 (2007).
 11. S. Kathmann, G. Schenter, and B. Garrett, "The Critical Role of Anharmonicity in Aqueous Ionic Clusters Relevant to Nucleation," *Journal of Physical Chemistry C* **111**, 4977-4983 (2007).
 12. S. M. Kathmann, G. K. Schenter, and B. C. Garrett, "Comment on "Quantum Nature of the Sign Preference in Ion-Induced Nucleation","" *Physical Review Letters* **98**, 109603 (2007).
 13. M. Valiev, B. C. Garrett, M.-K. Tsai, K. Kowalski, S. M. Kathmann, G. K. Schenter, and M. Dupuis, "Hybrid Approach for Free Energy Calculations with High-Level Methods: Application to the $\text{S}_{\text{N}}2$ Reaction of CHCl_3 and OH^- in Water," *Journal of Chemical Physics* **127**, 051102 (2007).
 14. S. M. Kathmann, G. K. Schenter, and B. C. Garrett, "The Impact of Molecular Interactions in Atmospheric Radiative Forcing," in Advances in Quantum Chemistry: Applications of Theoretical Methods to Atmospheric Science, edited by M. E. Goodsite and M. S. Johnson (Elsevier, Oxford, in press).

Ion Solvation in Nonuniform Aqueous Environments

Principal Investigator

Phillip L. Geissler

Faculty Scientist, Chemical Sciences, Physical Biosciences & Materials Sciences Divisions

Mailing address of PI:

Lawrence Berkeley National Laboratory

1 Cyclotron Road

Mailstop: HILDEBRAND

Berkeley, CA, 94720

Email: geissler@cchem.berkeley.edu

Research in this program applies computational and theoretical tools to determine structural and dynamical features of aqueous salt solutions. It focuses specifically on heterogeneous environments, such as liquid-substrate interfaces and crystalline lattices, that figure prominently in the chemistry of energy conversion. In these situations conventional pictures of ion solvation, though quite accurate for predicting bulk behavior, appear to fail dramatically, e.g., for predicting the spatial distribution of ions near interfaces. We develop, simulate, and analyze reduced models to clarify the chemical physics underlying these anomalies. We also scrutinize the statistical mechanics of intramolecular vibrations in nonuniform aqueous systems, in order to draw concrete connections between spectroscopic observables and evolving intermolecular structure. Together with experimental collaborators we aim to make infrared and Raman spectroscopy a quantitative tool for probing molecular arrangements in these solutions.

Our research efforts over the past year have primarily focused on developing a prototype computational model for understanding the spatial arrangements of ions near an interface between liquid water and vapor. Others have shown that detailed empirical models of liquid water predict accumulation of polarizable anions (e.g., iodide) such an interface. By contrast, physical intuition developed for ion solvation in bulk polar solvents suggests that ions should be unambiguously repelled from the interface. We aim to determine whether this unexpected behavior is unique to aqueous solutions, in which case its explanations likely lie in the specific mechanics of hydrogen bonding. Alternatively, ion “adsorption” to a liquid-vapor interface could result from a more generic interplay between dielectric response and molecular granularity at the edge of a liquid. Theoretical tools that usefully apply to these two scenarios are distinct in many ways, and discriminating between them is an important first step. To this end we are performing molecular dynamics simulations of a Stockmayer liquid, which caricatures a polar solvent as a collection of spheres engaging in both van der Waals and dipolar interactions. We have chosen the parameters of this model to reproduce the surface tension and dielectric constant of liquid water.

We calculate the density profile of a single ion relative to a liquid slab’s center of mass using importance sampling. Specifically, we apply a series of bias potentials that

confine the ion to a thin cross-section of the slab, and reconstruct its complete spatial distribution using weighted histogram analysis. Preliminary results indicate no (or very weak) adsorption for non-polarizable ions comparable in size to solvent molecules. In the near future we will systematically vary the ion's size and polarizability and consider a slightly elaborated solvent model that breaks charge symmetry and includes molecular polarizability.

We have also continued previous efforts to build a quantitative framework for interpreting Raman spectra of liquid water and salt solutions. Specifically, we have shown that electric field statistics of the liquid mirror vibrational line shapes measured in experiment very closely, even in the tails of thermal distributions. This correspondence holds both for the pure liquid (more specifically, an isotopic mixture of dilute HOD in D_2O) and for alkali halide solutions (even at high ionic strength). Line shape predictions depend primarily on a single adjustable parameter (whose value is the same in all cases), which serves as an effective molecular dipole converting the liquid's fluctuating electric field into an instantaneous vibrational frequency. This parameter appears to accurately encode effects of solvent dynamics and quantization, both neglected entirely in our treatment. Fig. 1 illustrates the accuracy we have achieved in predicting Raman spectra. How solvent dynamics contribute only a renormalization of the effective molecular dipole is not at all obvious, and lies in contrast to calculations based on dynamical formulae. Resolving this issue is the final step in establishing an accurate predictive theory of Raman spectroscopy for aqueous solutions. To do so we plan: (1) to decompose spectra computed from dynamical schemes according to trajectories' initial frequencies, in order to isolate specific fast modes of relaxation that currently distort predicted line shapes; (2) to calculate the full quantum dynamics of an excited vibration in a classical bath, rather than invoke idealizations of solvent-solute and radiation-solute coupling that may not be appropriate for aqueous systems; and (3) to incorporate non-radiative dissipation of vibrational energy into the solvent using ring polymer molecular dynamics.

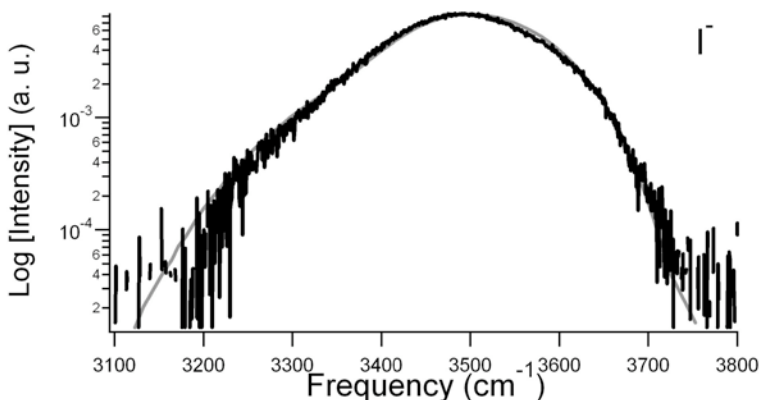


Figure 1. Calculated (smooth grey line) and measured (dark line) Raman spectra for an aqueous solution of KI. Solvent comprised D_2O and, in much smaller proportion, HOD molecules. Note the logarithmic scale, highlighting close agreement well below peak intensity.

COMPUTATIONAL NANOPHOTONICS: MODELING OPTICAL INTERACTIONS AND TRANSPORT IN TAILORED NANOSYSTEM ARCHITECTURES

Stephen K. Gray (gray@tcg.anl.gov),¹ Julius Jellinek (jellinek@anl.gov),¹
George C. Schatz (schatz@chem.northwestern.edu),² Mark A. Ratner
(ratner@chem.northwestern.edu),² Mark I. Stockman (mstockman@gsu.edu),³ Koblar A. Jackson
(jackson@phy.cmich.edu),⁴ Serdar Ogut (ogut@uic.edu)⁵

¹Chemistry Division, Argonne National Laboratory, Argonne, IL 60439; ²Department of Chemistry, Northwestern University, Evanston, IL 60208; ³Department of Physics and Astronomy, Georgia State University, Atlanta, GA 30303; ⁴Department of Physics, Central Michigan University, Mt. Pleasant, MI 48859; ⁵Department of Physics, University of Illinois at Chicago, Chicago, IL 60607

PROGRAM SCOPE

Computational methods are used to study light interactions with nanosystems. Metallic nanostructures are of particular interest owing to the useful properties of surface plasmons. Microscopic studies of electronic, structural and optical properties, and continuum-level electrodynamic studies are involved. A goal is to learn how to confine and manipulate electromagnetic energy on the nanoscale. A wide range of methods is needed, and another goal is to develop a suite of nanophotonics simulation tools. We also work with applied mathematicians and computer scientists in developing algorithms and software with high-performance capabilities.

At a microscopic level, we must understand the mechanisms underlying the assembly of atoms into clusters and clusters into larger systems. Understanding these mechanisms and the parameters they depend on is essential for designing cluster-based architectures with desired nanophotonics properties. Atomic-level mechanisms are ultimately defined by interatomic interactions. Accurate, efficient descriptions of these interactions are sought in order to uncover correct mechanisms. This work also provides optical information, e.g. static and dynamic polarizabilities, for the estimation of size-dependent dielectric properties relevant to our electrodynamic work.

The electromagnetic fields that result when light interacts with nanostructures are predicted with computational electrodynamic methods. We seek to develop and apply theory and computational methods that enable a quantitative description of metallic nanostructures and, from this, understanding of the physical phenomena that are taking place.

RECENT PROGRESS

Microscopic Studies of Electronic, Structural and Optical Properties: We continued our work on the development of accurate, computationally efficient many-body potentials for metals, which are crucial for predictive large-scale dynamical simulations of nanoassembly relevant to nanophotonics. In collaboration with M. J. Lopez (University of Valladolid, Spain), we developed further the conceptual foundation of our fitting procedure (the minimal maximum error fitting scheme) by introducing an error analysis for linearly dependent physical characteristics. This analysis allows for *an a priori* selection of a set of linearly independent fitting properties that lead to the most accurate potential. The new approach is universal in that it is applicable to any element. In addition to Ni, Ag, Au, and Al, considered earlier, we developed new potentials for Cu and Pt. To make these potentials more adequate for the nanoscale regime, properties of both the bulk and the diatomic of the elements were included in the fitting set. The current work

focuses on the analysis of structural and dynamical properties of Cu and Pt particles of different sizes.

We extended our earlier density functional theory (DFT) studies of structural and electronic properties of neutral Cu [22] and Ag [23] clusters to their anionic and cationic counterparts. For each cluster size, we identified a number of low-energy isomers. Analysis shows that the changes in the shapes of the most stable isomers can be correlated with and explained in terms of electron shell filling as defined by the jellium model. Work is in progress on computation of the spectra of electron binding energies of the anionic Cu_n^- and Ag_n^- . We use different schemes, including our own, to convert the nonphysical DFT Kohn-Sham eigenenergies into electron binding energies (a byproduct of this study will be a critical evaluation of the different procedures). As measured photoelectron spectra are available for Cu_n^- and Ag_n^- , comparison of the measured and computed results will be used to verify the validity of the structural forms predicted by the computations and/or to identify those structures that actually were generated in the experiments.

We continued the development and application of our methodology for partitioning the total dipole moment and polarizability of finite systems into site-specific contributions, which are then further divided into the so-called dipole and charge transfer parts [29,45]. We illustrated the power of this methodology as a tool of analysis of the site-, size-, shape- and structure-specific features in the response properties of Si clusters [29,45] and applied it recently to Na clusters [46]. Similarly to the case of Si, Na atoms on the periphery exhibit much stronger responses to an external electric field than the interior atoms. The cumulative fraction of the charge transfer components in the total polarizability increases with the cluster size. The anisotropy of the polarizability correlates with the shape anisotropy of the clusters as gauged by their principal moments of inertia. Interestingly, it is the charge transfer component of the polarizability that is almost exclusively responsible for its anisotropy.

In the past year we generalized our scheme to heterogeneous systems. This has been achieved through replacing the Voronoi cell based apportionment of the total charge density to individual atoms by the so-called stockholder partitioning methodology (the two give very similar results for homogeneous systems). Work is in progress on application of the new scheme to Si_nH_m and C_nH_m clusters. The issues under investigation are the effects of the type, number, and location of the heteroatoms (in this case, H) on the response properties of nanosystems (in this case, Si_n and C_n), and the use of heteroatoms as a means of changing and tuning the dielectric and, consequently, optical properties of nanosystems.

We also continued our DFT-based studies of dielectric and optical properties of metal [6,26,27,47,48] and semiconductor [5,28] particles. In particular, we extended our earlier explorations of these properties in Ag_n , $n=2-8$, [6] and Au_n , $n=1-3$, [27] to Ag and Au clusters of larger sizes. Through exhaustive search we identified eight low-energy isomers of Ag_{11} (all of them lie within ~ 0.3 eV of each other) and characterized their static polarizabilities and optical absorption spectra [47]. Measured spectra are available for Ag_{11} embedded in argon matrices grown at 10 K and 28 K and in a Ne matrix grown at 6 K, and the three display different absorption peaks. This indicates the importance of the embedding environment. Through a careful analysis we have shown that it is the most stable structure of Ag_{11} whose fingerprints can be identified in all three measured spectra. Our analysis also points to the more important role of the d electrons in optical transitions in Ag_{11} than in Ag_n clusters of smaller sizes. Work is in progress on extending these studies to different isomeric forms of Ag_n , $n=10$ and 12-20.

The work on Au_n clusters focused on the most stable structures for $n=2-14$ and 20. Our main findings include the following: 1) Below $n=14$ the polarizability shows an overall increase with

the cluster size modulated by odd-even oscillations; 2) The polarizability of Au₁₄ is noticeably lower, which correlates with the 2D-to-3D transition in the preferred structure at n=14; 3) The *d* electrons are involved in the optical transitions to a substantially larger degree than in similar size Ag clusters; 4) The computed optical spectra are in very good agreement with the available experimental results. Work is also in progress on extending our earlier investigations of the structural/electronic [1] and dielectric [26] properties of hollow cage vs space-filling conformations of Au_n, n=32, 38, 44, 50, 56, to their optical properties.

In another extension [48] we used DFT to examine the anionic Mn₁₃ and Co₁₃ clusters encapsulated in an icosahedral Au₂₀ cage and to analyze the effects of the “gold coating” on their structural, electronic, and magnetic characteristics. One of the interesting findings is that whereas the gold coating substantially enhances the magnetic moment of Mn₁₃⁻, it attenuates it for Co₁₃⁻. A question we intend to answer in the future is: Is this difference also reflected in the dielectric and optical properties of the two systems? Regarding semiconductor particles, work is in progress on electronic and optical characteristics of spherical Si shells. Other work in progress includes studies of silver-doped quartz surfaces and methodological issues related to the GW-Bethe-Salpeter formalism for description of optical properties. The latter subject involves collaboration with J. R. Chelikowsky’s group (University of Texas, Austin).

Electrodynamics Studies: Central themes of our computational electrodynamics work are close collaboration with experimental groups and a drive to quantitatively predict and understand light interactions in systems relevant to chemical sensing, nanoscale energy concentration and control, and other exciting possibilities.

We studied the light transmission through nanoholes in silver and gold films, which are potential sensors. Extensive studies with the finite-difference time-domain (FDTD) method revealed the dependence of transmission on hole size, shape, film thickness, and the effect of circular rings around the holes [32, 52]. We did a collaborative study with Rowlen (Univ. of Colorado) on surface enhanced Raman scattering near holes. In collaborative work with the experimental groups of Rogers and Nuzzo (Univ. of Illinois), we used large-scale FDTD calculations to understand the origins of the large refractive index sensitivities found in periodic nanowell systems [38].

Our studies of light scattering by particles continues to be active [30,31,35, 37]. This year, for example, we collaborated with S. Leone and others at LBL to study photoelectron emission by NaCl nanoparticles. We collaborated with Bumm (Univ. of Oklahoma) to model near-field optical microscopy experiments for silver nanoprisms. We studied how metal nanoparticles respond to fluorescence from nearby molecules, pointing to interesting scattering effects when plasmons are excited [39]. The introduction of a nonlinear medium between metal nanowires was studied, and a novel optical limiting effect was predicted [37].

We have developed a time-dependent DFT approach to calculating the excited states of metal particles, and of molecules interacting with metal particles. Very recent calculations have revealed the connection between the quantum and continuum electrodynamics extinction spectra of small silver clusters for the first time.

We are continuing our study of the electrodynamic forces acting on metallic nanoparticles interacting with strong radiation fields [39]. Most recently we have adapted the discrete dipole approximation to the calculation of these forces. Of particular interest in recent work was the enhancement in forces due to plasmon excitation, and the dependence of the forces on particle size.

Computational theory for tailoring nanoplasmonic systems to concentrate and control optical energy at the nanoscale was also a focus [40-44,53-53]. We developed a Green's function approach to describe the coherent control of the mechanical rotation of octupolar metal nanosystems (nanotriangles and nano-tetrahedra). This rotation occurs due to the interference of the fields at the second-harmonic (SH) frequency and the SH polarization. In Ref. [53] we developed a two-dimensional Wentzel-Kramers-Brillouin (WKB) approximation to describe the spatio-temporal coherent control of the adiabatic energy concentration at the nanoscale. This allows one to build a reliable and accurate enough initial approximation for numerical computations in this multi-scale, three-dimensional electrodynamic problem that poses significant computational challenges. Significant progress in solving the problem of coherent control of the optical energy distribution at the nanoscale has been achieved. Using the time-reversal approach in Green's function theory, we were able to build shaped waveforms that drive a nanosystem in such a way that the optical excitation converges at a given nano-spot at a required instance of time.

FUTURE PLANS

The work on more accurate semiempirical potentials will include new metals and will be extended to bimetallic systems as well as metal particle-support interactions. We will use the new potentials to carry out large-scale dynamical simulations of cluster-based nanoassembly on supports. The goal is to understand and characterize the mechanism governing the assembly processes as a function of the cluster material and size and the material, morphology, and temperature of the support. Such an understanding is the prerequisite of rational design and eventual assembly of nanoarchitectures with desired characteristics, including photonic. An integral part of the studies will be exploration of the important issue of thermal stability of the assembled nanosystems.

We will continue our DFT studies of structural, electronic, and optical properties of metal and semiconductor clusters. The issues that will be covered include size-, material-, and structure-specificity. Of particular interest is the degree of versatility of the different properties in isomeric forms that are energetically very close but have very different geometric structures (e.g., hollow cages *vs* space-filling conformations). Another important issue is combining the size effects with the composition effects to change the dielectric and optical characteristics of nanosystems and even tune them to the desired specifications. We will study this issue through adding dopants to clusters of different sizes and considering a cluster of one material endohedrally encapsulated in a cluster of another material. Yet another factor is the role of the charge state. It may have a direct effect on the dielectric and optical properties and an indirect one, which may arise because of the fact that a change in the charge of a small nanosystem may cause a change in its preferred geometric structure.

We will continue to develop and apply our new methodology for analysis of the site-specificity and dipole *vs* charge transfer character of the dipole moments and polarizabilities of finite systems. We will use it to enhance our atomic-level understanding of the evolution of these properties with the size and/or structure/shape of systems of interest to nanophotonics. We will explore the connection between the details of the response features of these systems and the specificity of their optical properties. In another application, we will use the methodology to establish classes of similarity of nanosystems of different materials as defined by the details of their response behavior. We will also utilize it to formulate a new analysis of the degree of metallicity, which will be used to explore and understand the intricate phenomenon of size-induced transition to a metallic state. Among the issues that will be examined is the possible correlation between the degree of metallicity and the optical properties. The methodological work

will also include further analysis and adaptation of the GW-Bethe-Salpeter approach. The exploration on silver doped quartz surfaces will be continued as well.

Our ultimate aim is a fundamental, comprehensive understanding of the finite-size specificity of the structural, thermal, electronic, and optical properties of nanosystems and the couplings between these properties, all considered as a function of system size and composition. This understanding will lead to physical models for efficient evaluation of photonic characteristics over a broad size range and establishment of connection with the electrodynamics of the bulk limit.

Regarding our electrodynamics simulations, we will collaborate with Odom (Northwestern) to determine the influence of the index of refraction of a fluid that is on one side of the film on the transmission of light through a hole array/metal film structure. Of particular interest are conditions where surface plasmon polariton (SPP) excitation on one side of the film can be coupled to Wood's anomaly (WA) excitation on the other side, as this combines the narrow lineshape of the WA with strong surface dielectric sensitivity of the SPP. As an extension of our particle-based Kerr work, we will study how introducing a nonlinear Kerr medium within the holes of a hole array will influence transmission. We studied the effect of a Kerr nonlinear medium in the transmission of light through a hole array structure. We will also work with Van Duyne to model his measurements of extinction and SERS spectra of silver nanoparticle clusters for which transmission electron microscope (TEM) images are also measured. The TEM measurements provide exciting opportunities to connect the atomic scale structure (and defects) in the nanoparticles with their optical properties. Also, the TEM measurements, in conjunction with SERS measurements and theory will tell us what are the unique hot spots that give rise to single-molecule SERS.

We are developing an interface between classical electrodynamics and quantum chemistry so that we can study the coupling of molecules to enhanced electromagnetic fields on metal particle surfaces. Our electronic structure studies of plasmon excitation effects will be extended to studies of SERS and surface enhanced hyperRaman scattering.

Concerning our work on optical concentration and control on the nanoscale, in the coming year we plan to: (i) Develop an adaptive grid computational scheme to solve the problem of a self-similar nanolens, (ii) Numerically investigate spatio-temporal coherent control at the nanoscale, and (iii) Numerically investigate temporal-polarization coherent control at the nanoscale.

PUBLICATIONS OF DOE SPONSORED RESEARCH (2005-2007)

1. Hollow cages versus space-filling structures for medium-Sized gold clusters: The spherical aromaticity of the Au₅₀ cage, J. Wang, J. Jellinek, J. Zhao, Z. Chen, R. B. King and P. v. R. Schleyer, *J. Phys. Chem. A* **109**, 9265-9269 (2005).
2. Stuffed fullerene structures for medium-sized silicon clusters, J. Zhao, J. Wang, J. Jellinek, S. Yoo, and X. C. Zeng, *Eur. Phys. J. D* **34**, 35-37 (2005).
3. First-principles investigations of the polarizability of small and intermediate-sized Cu clusters, M. Yang and K. Jackson, *J. Chem. Phys.* **122**, 184317 (2005).
4. Statistical evaluation of the big bang search algorithm, K.A. Jackson, M. Horoi, I. Chaudhuri, Th. Frauenheim, and A. A. Shvartsburg, *Comp. Mater. Sci.* **35**, 232-237 (2005).
5. Shape, polarizability and metallicity in Si clusters, K. A. Jackson, I. Chaudhuri, M. Yang, and Th. Frauenheim, *Phys. Rev. A* **71**, 033205 (1-6) (2005).
6. Size dependence of static polarizabilities and optical absorption spectra of Ag_n (n = 2 – 8) clusters from first principles, J. C. Idrobo, S. Ogut, and J. Jellinek, *Phys. Rev. B* **72**, 085445 (1-8) (2005).
7. Observation of the quadrupole plasmon mode for a colloidal solution of gold nanoprisms, J. E. Millstone, S. Park, K. L. Shuford, L. Qin, G. C. Schatz and C. A. Mirkin, *J. Am. Chem. Soc.* **127**, 5312-5313 (2005).

8. Multipolar Excitation in Triangular Nanoprisms, K. L. Shuford, M. A. Ratner and G. C. Schatz, *J. Chem. Phys.* **123**, 114713 (1-9) (2005).
9. Surface plasmon generation and light transmission by isolated nanoholes and arrays of nanoholes in thin metal films, S.-H. Chang, S. K. Gray and G. C. Schatz, *Optics Express* **13**, 3150-3165 (2005).
10. Electrodynamics simulations of surface plasmon behavior in metallic nanostructures, S. K. Gray, T.-W. Lee, S.-H. Chang and G. C. Schatz, *Proc. SPIE Int. Soc. Opt. Eng.* **5927**, 96 (2005).
11. Surface plasmon standing waves in large-area subwavelength hole arrays, E.-S. Kwak, J. Henzie, S.-H. Chang, S. K. Gray, G. C. Schatz, and T. W. Odom, *Nano Lett.*, **5**, 1963-1967 (2005).
12. Near-field photochemical imaging of noble metal nanostructures, C. Hubert, A. Remyantsev, G. Lerondel, J. Grand, S. Kostcheev, L. Billot, A. Vial, R. Bachelot, P. Royer, S.-H. Chang, S. K. Gray, G. P. Wiederrecht, and G. C. Schatz, *Nano Lett.* **5**, 615-619 (2005).
13. Controlled spatiotemporal excitation of metal nanoparticles with chirped optical pulses, T.-W. Lee and S. K. Gray, *Phys. Rev. B*, **71**, 035423 (1-9) (2005).
14. Regenerated surface plasmon polaritons, T.-W. Lee and S. K. Gray, *Appl. Phys. Lett.* **86**, 141105 (1-3) (2005).
15. Subwavelength light bending by metal slits, T. W. Lee and S. K. Gray, *Optics Express*, **13**, 9652-9659 (2005).
16. Surface plasmon amplification by stimulated emission in nanolenses, K. Li, Xiangting Li, M. I. Stockman, and D. J. Bergman, *Phys. Rev. B* **71**, 115409 (1-4) (2005).
17. Enhanced second harmonic generation in a self-similar chain of metal nanospheres, K. Li, M. I. Stockman, and D. J. Bergman, *Phys. Rev. B* **72**, 153401(1-4) (2005).
18. Giant fluctuations of second harmonic generation on nanostructured surfaces, M. I. Stockman, *Chem. Phys.* (invited paper) **318**, 156-162 (2005).
19. Nanolocalized nonlinear electron photoemission under coherent control, M. I. Stockman and P. Hewageegana, *Nano Lett.* **5**, 2325-2329 (2005).
20. Hole-assisted energy deposition in dielectrics and clusters in the multiphoton regime, L. N. Gaier, M. Lein, M. I. Stockman, G. L. Yudin, P. B. Corkum, M. Y. Ivanov, and P. L. Knight, *J. Mod. Optics* **52**, 1019-1030 (2005).
21. Imperfect perfect lens, I. A. Larkin and M. I. Stockman, *Nano Lett.* **5**, 339-343 (2005).
22. Structure and shape variations in intermediate size copper clusters, M. L. Yang, K. A. Jackson, C. Koehler, T. Frauenheim, and J. Jellinek, *J. Chem. Phys.* **124**, 024308 (1-6) (2006).
23. First-principles study of intermediate size silver clusters: Shape evolution and its impact on cluster properties, M. Yang, K. A. Jackson, and J. Jellinek, *J. Chem. Phys.* **125**, 144308 (1-6) (2006).
24. Structural evolution of anionic silicon clusters Si_N ($20 \leq N \leq 45$), J. Bai, L.-F. Cui, J. Wang, S. Yoo, X. Li, J. Jellinek, C. Koehler, T. Frauenheim, L.-S. Wang, and X. C. Zeng, *J. Phys. Chem. A* **110**, 908-912 (2006).
25. Density-functional study of small and medium-sized As_n clusters up to $n = 28$, J. Zhao, X. Zhou, X. Chen, J. Wang, and J. Jellinek, *Phys. Rev. B* **73**, 115418 (1-10) (2006).
26. Dipole polarizabilities of medium-sized gold clusters, J. Wang, M. Yang, J. Jellinek, and G. Wang, *Phys. Rev. A* **74**, 023202 (1-5) (2006).
27. Structural, electronic, and optical properties of noble metal clusters from first principles, S. Ogut, J. C. Idrobo, J. Jellinek, and J. Wang, *J. Clust. Sci.*, **17**, 609-626 (2006).
28. First principles absorption spectra of medium-sized Si clusters: Time-dependent local density approximation versus predictions from Mie theory, J. C. Idrobo, M. Yang, K. A. Jackson and S. Ogut, *Phys. Rev. B*, **74**, 153410 (1-4) (2006).
29. Site-specific polarizabilities: Probing the atomic response of silicon clusters to an external electric field, K. Jackson, M. Yang, and J. Jellinek, in *Lecture Series in Computer and Computational Sciences*, Vol. 6, G. Maroulis and T. Simos, Eds., Brill, Leiden, 2006, pp. 165-176.
30. Multiple plasmon resonances in gold nanorods, E. K. Payne, K. L. Shuford, S. Park, G. C. Schatz and C. A. Mirkin, *J. Phys. Chem. B* **110**, 2150-2154 (2006).
31. Manipulating the optical properties of pyramidal nanoparticle arrays, J. Henzie, K. L. Shuford, E.-S. Kwak, G. C. Schatz and T. W. Odom, *J. Phys. Chem. B* **110**, 14028-14031 (2006).
32. Finite-difference time-domain studies of light transmission through nanohole structures, K. L. Shuford, Mark A. Ratner, S. K. Gray and G. C. Schatz, *Appl. Phys. B* **84**, 11-18 (2006).

33. Apertureless scanning near-field optical microscopy: a comparison between homodyne and heterodyne approaches, L. Gomez, R. Bachelot, A. Bouhelier, G. P. Wiederrecht, S.-H. Chang, S. K. Gray, G. Lerondel, F. Hua, S. Jeon, J. A. Rogers, M. E. Castro, S. Blaize, I. Stephanon, and P. Royer, *J. Opt. Soc. Am. B* **23**, 823-833 (2006).
34. Error signal artifact in apertureless scanning near-field optical microscopy, L. Billot, M. Lamy de la Chapelle, D. Barchiesi, S.-H. Chang, S. K. Gray, J.A. Rogers, A. Bouhelier, P.-M. Adam, J.-L. Bijeon, G. P. Wiederrecht, R. Bachelot, and P. Royer, *Appl. Phys. Lett.* **89**, 023105 (1-3) (2006).
35. A computational study of the interaction of light with silver nanowires of different eccentricity, J. M. Oliva and S. K. Gray, *Chem. Phys. Lett.* **427**, 383-389 (2006).
36. Fourier spectral simulations and Gegenbauer reconstructions for electromagnetic waves in the presence of a metal nanoparticle, M. S. Min, T.-W. Lee, P. F. Fischer, and S. K. Gray, *J. Comp. Phys.* **213**, 730-747 (2006).
37. Ultrafast pulse excitation of a metallic nanosystem containing a Kerr nonlinear material, X. Wang, G. C. Schatz, and S. K. Gray, *Phys. Rev. B*, **74**, 195439 (1-5)(2006).
38. Quantitative multispectral biosensing and 1D imaging using quasi-3D plasmonic crystals, M. E. Stewart, N. H. Mack, V. Malyarchuk, J. A. N. T. Soares, T.-W. Lee, S. K. Gray, R. G. Nuzzo, and J. A. Rogers, *Proc. Nat. Acad. Sci. (USA)* **103**, 17143-17148 (2006).
39. Geometry dependent features of optically induced forces between silver nanoparticles, V. Wong and M. A. Ratner, *J. Phys. Chem. B* **110**, 19243-19253 (2006).
40. Generation of traveling surface plasmon waves by free-electron impact, M. V. Bashevov, F. Jonsson, A. V. Krasavin, N. I. Zheludev, Y. Chen, and M. I. Stockman, *Nano Lett.* **6**, 1113-1115 (2006).
41. Slow Propagation, Anomalous Absorption, and Total External Reflection of Surface Plasmon Polaritons in Nanolayer Systems, M. I. Stockman, *Nano Lett.* **6**, 2604-2608 (2006).
42. M. Stockman, in *Topics in Applied Physics*, edited by K. Kneipp, M. Moskovits and H. Kneipp, *Electromagnetic Theory of SERS* (Springer Verlag, 2006), p. 47-66.
43. Reply to Comment On Self-Similar Chain of Metal Nanospheres as an Efficient Nanolens, K. Li, M. I. Stockman, and D. J. Bergman, *Phys. Rev. Lett.* **97**, 079702 (2006).
44. Octupolar Metal Nanoparticles as Optically Driven, Coherently Controlled Nanorotors, M. I. Stockman, K. Li, S. Brasselet, and J. Zyss, *Chem. Phys. Lett.* **433**, 130-135 (2006).
45. Site-specific analysis of dielectric properties of finite systems, K. A. Jackson, M. Yang, and J. Jellinek, *J. Phys. Chem. C* (in press).
46. Site-specific analysis of response properties of sodium clusters, K. A. Jackson, M. Yang, and J. Jellinek, in *Atomic cluster collisions: Structure and dynamics*, A. V. Solov'yov, Ed., Imperial College Press, London (in press).
47. First-Principles Isomer-Specific Absorption Spectra of Ag₁₁, J. C. Idrobo, S. Ogut, K. Nemeth, J. Jellinek, and R. Ferrando, *Phys. Rev. B* **75**, 233411(1-4) (2007).
48. Gold-coated transition metal anion [Mn₁₃@Au₂₀] with ultrahigh magnetic moment, J. Wang, J. Bai, J. Jellinek, and X. C. Zeng, *J. Am. Chem. Soc.* **129**, 4110-4111 (2007). (Communication).
49. Heterodyne apertureless near-field scanning optical microscopy on periodic gold nanowells, J. F. Hall, G. P. Wiederrecht, S. K. Gray, S.-H. Chang, S. Jeon, J. A. Rogers, R. Bachelot, and P. Royer, *Opt. Express* **15**, 4098-4105 (2007).
50. Computational study of fluorescence scattering by silver nanoparticles, M. H. Chowdhury, S. K. Gray, J. Pond, C. D. Geddes, K. Aslan, and J. R. Lakowicz, *J. Opt. Soc. Am. B* **24**, 2259-2267 (2007).
51. Multigrid FDTD with Chombo, Z. Meglicki, S. K. Gray, and B. Norris, *Comp. Phys. Comm.* **176**, 109-120 (2007).
52. Electric field enhancement and light transmission in cylindrical nanoholes, K. L. Shuford, M. A. Ratner, S. K. Gray, and G. C. Schatz, *J. Comp. Theor. Nanoscience* **4**, 1-8 (2007).
53. Toward Full Spatio-Temporal Control on the Nanoscale, M. Durach, A. Rusina, K. Nelson, and M. I. Stockman, *Nano Lett.* **7**, (DOI:10.1021/nl071718g, 5 pages) (2007).
54. Criterion for Negative Refraction with Low Optical Losses from a Fundamental Principle of Causality M. I. Stockman, *Phys. Rev. Lett.* **98**, 177404 (1-4) (2007).
55. Attosecond Nanoplasmonic Field Microscope, M. I. Stockman, M. F. Kling, U. Kleineberg, and F. Krausz, *Nature Photonics* **1**, 539-544 (2007).

Acknowledgment: Work at Argonne National Laboratory was supported by the U.S. Department of Energy, Office of Basic Energy Sciences, Division of Chemical Sciences, Geosciences, and Biosciences under DOE Contract No. DE-AC02-06CH11357.

Catalysis at Metal Surfaces Studied by Non-Equilibrium and STM Methods

Ian Harrison

Department of Chemistry, University of Virginia

Charlottesville, VA 22904-4319

harrison@virginia.edu

This research program aims to employ non-equilibrium techniques to investigate the nature of the transition states for activated dissociative chemisorption of small molecules on catalytic metal surfaces. Two separate approaches/ideas are under investigation. In the first, we posit that dissociative chemisorption reactions on metal surfaces are primarily surface mediated electron transfer reactions for many hard-to-activate small molecules. Accordingly, the lowest lying affinity levels of these adsorbates, which are accessible by surface photochemistry and scanning tunneling microscopy (STM), will play a key electronic structure role in determining barrier heights for dissociative chemisorption. Electron transfer excitation into these adsorbate affinity levels followed by image potential acceleration towards the surface and rapid quenching may leave the adsorbate in the “transition state region” of the ground state potential relevant to thermal catalysis from where desorption and/or dissociation may ultimately occur. Using a low temperature scanning tunneling microscope (STM) we have been investigating the thermal, electron, & photon induced chemistry of CH_3Br ,¹ CO_2 , and CH_4 on Pt(111).² In our second approach towards probing surface transition states, we dose hot gas-phase molecules on to a cold surface and measure dissociative sticking coefficients macroscopically^{3,4} via Auger electron spectroscopy (AES) or microscopically by imaging chemisorbed fragments via low T_s STM. A local hot spot, microcanonical unimolecular rate theory (MURT) model of gas-surface reactivity^{5,6,7} can be used to extract transition state characteristics for dissociative chemisorption. The MURT model has proven useful for understanding, analyzing, and simulating the dynamics of activated dissociative chemisorption for systems ranging in size from H_2 on Cu(111),⁸ to C_2H_6 on Pt(111),⁴ even at quantum state resolved levels of detail.⁸⁻¹⁰ An important long-range goal of our research is to microscopically characterize the different transition states for dissociative chemisorption occurring at metal terrace sites as compared to step sites – a goal of long-standing interest to the catalysis and electronic structure theory communities.¹¹

Activated dissociative chemisorption of methane is believed to be rate limiting in the steam reforming of natural gas on Ni catalysts,¹² the process that yields the industrial supply of H_2 and synthesis gas. MURT simulations of thermal dissociative sticking coefficients, S_T , for CH_4 on low index single crystal metal surfaces, based on prior extraction of transition state parameters from analysis of supersonic molecular beam experiments, are several orders of magnitude higher than apparent S_T values derived from turnover rates for CH_4 reforming on supported nanocatalysts.¹³ It is likely that most of the surface atoms on the nanocatalysts become poisoned or tempered by a build-up of graphitic carbon under the high working temperatures and pressures of catalysis such that their *macroscopically* averaged reactivity does not accurately characterize the microscopic reactivity at their most active sites. We are currently working towards using low T_s STM in conjunction with heated effusive molecular beam measurements to *microscopically* characterize the transition states for CH_4 dissociation on terraces and at step edges on a Pt(111) surface. A new low energy electron microscope (LEEM) at Virginia may afford a complementary insitu means to characterize the high T_s growth of graphitic C from CH_4 .

DOE Publications since 2004:

T.C. Schwendemann, I. Samanta, T. Kunstmann, and I. Harrison, "CH₃Br Structures on Pt(111): Kinetically Controlled Self-Assembly of Dipolar and Weakly Adsorbed Molecules," *J. Phys. Chem. C* **111**, 13137-13148 (2007).

References:

- 1 T.C. Schwendemann, I. Samanta, T. Kunstmann, and I. Harrison, "CH₃Br Structures on Pt(111): Kinetically Controlled Self-Assembly of Dipolar and Weakly Adsorbed Molecules," *J. Phys. Chem. C* **111**, 13137-13148 (2007).
- 2 T.C. Schwendemann, *Atomic Scale Investigations of the Thermal and Electron Induced Chemistry of Small Molecules on Pt(111) as Revealed by Scanning Tunneling Microscopy*. (Ph.D. Thesis, University of Virginia, Charlottesville, December 9, 2005).
- 3 K. M. DeWitt, L. Valadez, H. L. Abbott, K. W. Kolasinski, and I. Harrison, "Using effusive molecular beams and microcanonical unimolecular rate theory to characterize CH₄ dissociation on Pt(111)," *J. Phys. Chem. B* **110**, 6705-6713 (2006).
- 4 K. M. DeWitt, L. Valadez, H. L. Abbott, K. W. Kolasinski, and I. Harrison, "Effusive molecular beam study of C₂H₆ dissociation on Pt(111)," *J. Phys. Chem. B* **110**, 6714-6720 (2006).
- 5 A. Bukoski, D. Blumling, and I. Harrison, "Microcanonical unimolecular rate theory at surfaces. I. Dissociative chemisorption of methane on Pt(111)," *J. Chem. Phys.* **118**, 843-871 (2003).
- 6 H. L. Abbott, A. Bukoski, and I. Harrison, "Microcanonical unimolecular rate theory at surfaces. II. Vibrational state resolved dissociative chemisorption of methane on Ni(100)," *J. Chem. Phys.* **121**, 3792-3810 (2004).
- 7 A. Bukoski, H. L. Abbott, and I. Harrison, "Microcanonical unimolecular rate theory at surfaces. III. Thermal dissociative chemisorption of methane on Pt(111) and detailed balance," *J. Chem. Phys.* **123**, 094707 (2005).
- 8 H.L. Abbott and I. Harrison, "Microcanonical Transition State Theory for Activated Gas-Surface Reaction Dynamics: Application to H₂/Cu(111) with Rotation as a Spectator," *J. Phys. Chem. A* **111**, in press (2007); <http://dx.doi.org/10.1021/jp074038a>
- 9 H. L. Abbott and I. Harrison, "Activated dissociation of CO₂ on Rh(111) and CO oxidation dynamics," *J. Phys. Chem. C* **111**, 13137-13148 (2007).
- 10 H. L. Abbott, A. Bukoski, D. F. Kavulak, and I. Harrison, "Dissociative chemisorption of methane on Ni(100): Threshold energy from CH₄ (2ν₃) eigenstate-resolved sticking measurements," *J. Chem. Phys.* **119**, 6407-6410 (2003).
- 11 F. Abild-Pedersen, O. Lytken, J. Engbaek, G. Nielsen, I. Chorkendorff, and J. K. Nørskov, "Methane activation on Ni(111): Effects of poisons and step defects," *Surf. Sci.* **590**, 127 (2005).
- 12 J. M. Wei and E. Iglesia, "Isotopic and kinetic assessment of the mechanism of reactions of CH₄ with CO₂ or H₂O to form synthesis gas and carbon on nickel catalysts," *J. Catal.* **224**, 370-383 (2004).
- 13 H. L. Abbott and I. Harrison, "Methane Dissociative Chemisorption on Ru(0001) and Comparison to Metal Nanocatalysts," to be submitted (2007).

Fluctuations in Macromolecules Studied Using Time-Resolved, Multi-spectral Single Molecule Imaging

Carl Hayden
Sandia National Laboratories
P. O. Box 969, MS 9055
Livermore, CA 94551-0969
cchayde@sandia.gov

Haw Yang
Department of Chemistry
University of California at Berkeley
Berkeley, CA
hawyang@uclink.berkeley.edu

Program Scope

The goal of this research program is to study local chemical environments and their fluctuations in macromolecules using single molecule methods. We focus on methods that provide simultaneous, correlated measurements of both the spectrum and temporal decay of fluorescence from probe fluorophores in single macromolecules. An important component of this work is the development of new data analysis methods to extract the maximum information about the macromolecule fluctuations from the experimental record of photons.

In bulk samples the averaging of many fluctuations makes the system essentially time independent and hence the fluorescence properties can usually be measured sequentially. In contrast, to determine the time-dependent behavior of a fluorophore within a single macromolecule the relevant fluorescence properties must be measured simultaneously, with the sensitivity to detect single fluorophores. In many cases multiple fluorescence properties will fluctuate at the same time, thus the ability to interpret the result will be enhanced by measurements that reveal correlations between multiple fluorescence properties.

Recent Progress:

Fluorescence resonance energy transfer (FRET) in single quantum dot-dye hybrids.

Fluorescence based probes can be used to sense many properties such as pH, ion concentration and ligand binding in complex chemical and biological systems. FRET between donor and acceptor fluorophores is a sensitive detection mechanism for these probes if the separation between the fluorophores can be designed to depend on the quantity of interest. As donor fluorophores, semiconductor quantum dots (QDs) offer significant advantages over fluorescent dyes including, superior photostability, broad absorption, and narrow, size-tunable emission. Thus, QD-organic dye hybrids are becoming popular for FRET-based sensing¹⁻⁴ and they also show promise for fundamental studies of macromolecule conformational changes. For most purposes multiple acceptors are bound to a single QD hub that serves as the sole energy donor. A major obstacle to single-particle measurements with these QD-multiple-acceptor systems is that the FRET signal must be distinguished from acceptor dye photo-bleaching events, flickering emission caused by the QD donor blinking, and direct excitation of the acceptors. By measuring changes of multiple spectral parameters synchronized through emission intensity jumps, we are developing methods to identify events with high confidence even in these noisy situations.

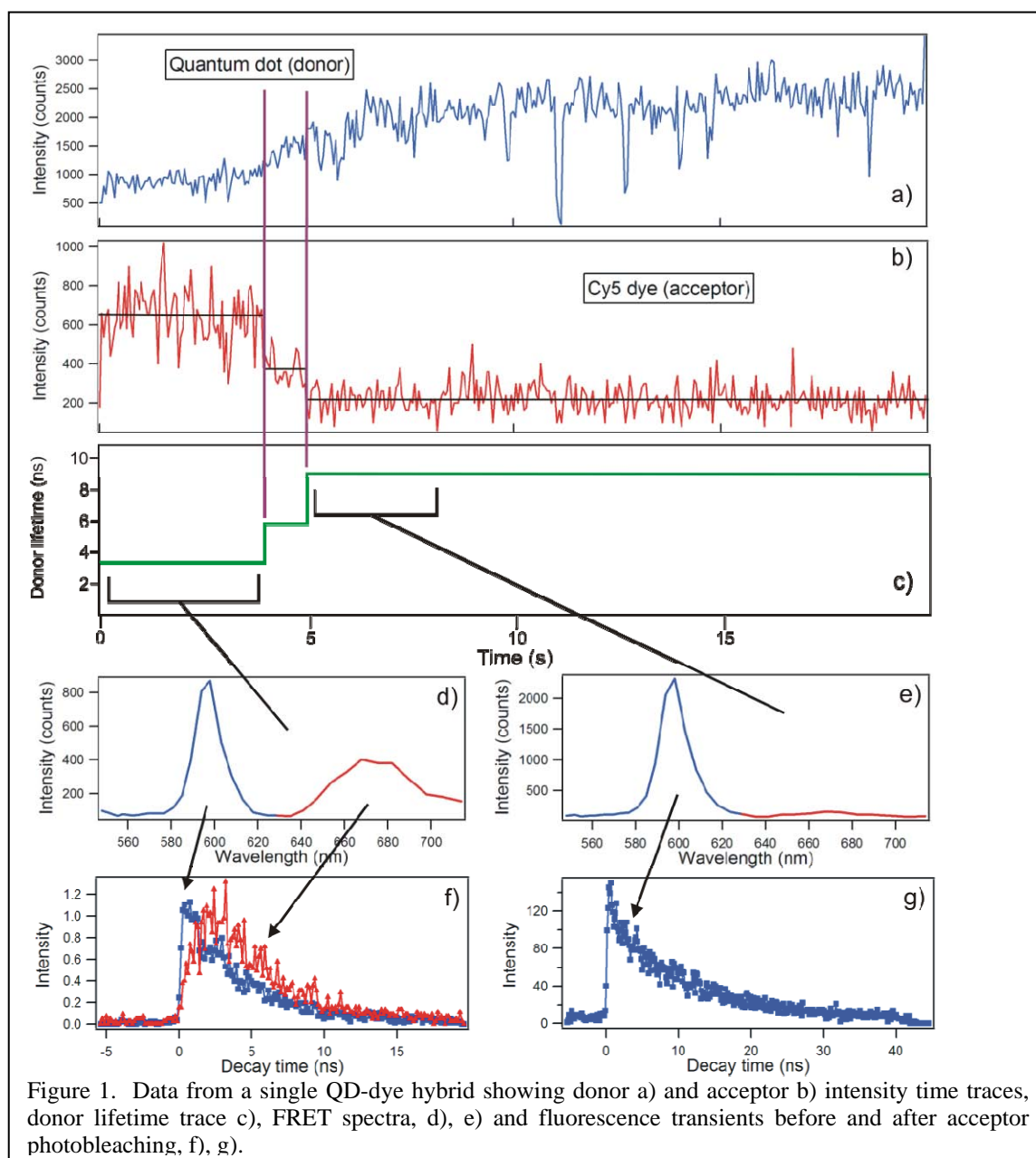


Figure 1. Data from a single QD-dye hybrid showing donor a) and acceptor b) intensity time traces, donor lifetime trace c), FRET spectra, d), e) and fluorescence transients before and after acceptor photobleaching, f), g).

We assemble QD-dye hybrids from biotin conjugated, 605nm QDs, bound to streptavidin labeled with Cy5 dye. Our time-resolved, multi-spectral microscope⁵ measures the wavelength, emission delay relative to excitation (excited-state lifetime), and chronological time (intensity) for each fluorescence photon detected from individual hybrid particles. The initially excited QD donor emission at ~605nm is readily distinguished from the acceptor dye emission around 675nm in the spectrally resolved data.

Typical data from a single hybrid are shown in Figure 1. In this example dye photobleaching is the event to be detected. The acceptor intensity traces are analyzed using a changepoint method.⁶ This model-free statistical analysis quantitatively determines the emission intensity changes identifying stepwise decreases (vertical lines) in the acceptor emission due to individual dye photobleaching. This assignment is confirmed by synchronized increases in the donor lifetime, Fig. 1c, due to reduced acceptor quenching. The emission spectrum, Fig. 1d shows initial strong FRET, but after ~5 seconds the FRET and hence red emission disappears due to

photobleaching of the acceptor dyes (Fig. 1e). The time evolution of the QD and dye spectral components, Fig.1f,g directly illustrates the energy transfer process. Before dye photobleaching, the donor lifetime is quenched due to energy transfer to the acceptor. The acceptor emission exhibits a slower rise because it is excited by energy transfer from the donor. In addition, the decay of the acceptor emission is prolonged from its ~ 1.4 ns intrinsic lifetime to match the donor lifetime, because energy transfer can occur throughout the longer donor lifetime (Fig. 1f). The form of the acceptor emission transient demonstrates that the acceptor emission is from FRET and not direct acceptor excitation. Once the dyes photobleach the QD lifetime increases as it is no longer quenched (Fig.1g). The results of this work provide a robust approach for using QD-dye hybrids in single particle applications.

Conformational dynamics of maltose binding protein (MBP)

We are investigating the conformational dynamics of MBP from *E.Coli* using single molecule FRET. From crystallographic and NMR evidence the two lobes of the protein close in response to maltose binding resulting in a large ($\sim 30^\circ$) hinge motion between the two lobes.⁷ There is debate whether the protein in solution is always open without ligand and always closed with ligand, or samples an ensemble of conformations including both open and closed states.⁸ To distinguish these two possibilities we have performed single molecule experiments measuring the time dependent distance changes between the two lobes of the protein in the absence and presence of maltose.

A mutant protein was constructed with two cysteine residues (K34C and D207C) to enable selective attachment of fluorescent dyes (Alexa Fluor 555 and Alexa Fluor 647). A C-terminal His₆-tag was also added to the protein to allow immobilization of the protein with a His₆ antibody.⁹ Single-molecule experiments were performed on a confocal microscope, at U. C. Berkeley, that registers individual photon arrival times in two wavelength channels.¹⁰ Intensity vs. time traces were converted to distance vs. time profiles with the maximum information method¹¹ and probability

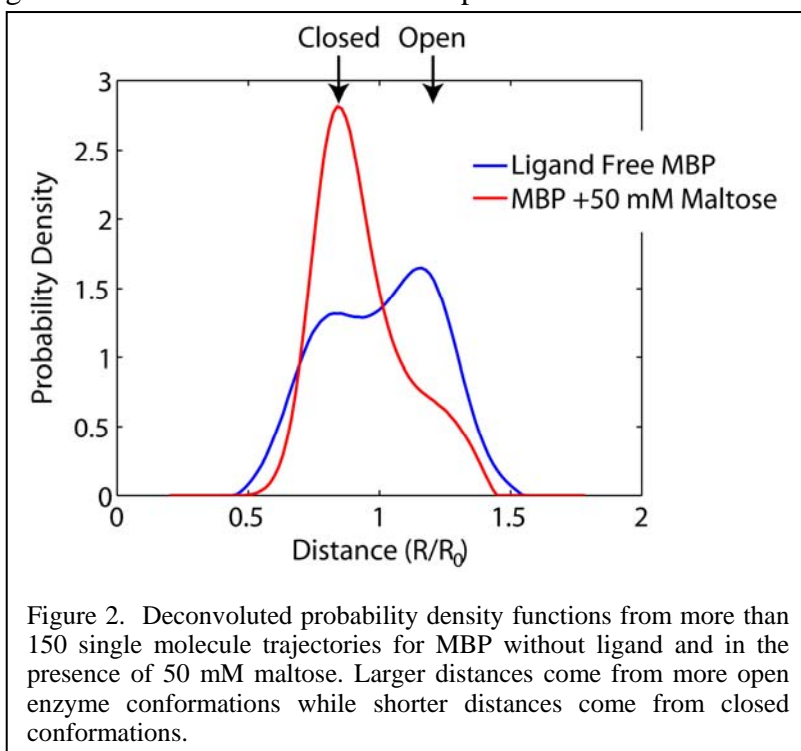


Figure 2. Deconvoluted probability density functions from more than 150 single molecule trajectories for MBP without ligand and in the presence of 50 mM maltose. Larger distances come from more open enzyme conformations while shorter distances come from closed conformations.

distributions for the separation of the two dyes were constructed using the maximum entropy method,¹⁰ which allows unbiased deconvolution of the noise from the distributions. Figure 2 shows deconvoluted probability density functions for MBP in the presence and absence of 50 mM maltose. From these distributions it is evident that the protein is capable of sampling an open and a closed conformation, supporting the idea that the conformation of MBP in solution is an ensemble of inter-converting states. Further investigation revealed that the shape of the distribution is dependent on the time resolution at which the data analysis is performed, with the

two states becoming less well resolved at the slower time resolutions. These observations demonstrate that the protein is at a dynamic equilibrium between open and closed states on the millisecond timescale.

Future Plans:

Quantum dot-dye hybrids.

We are continuing studies of QD-dye hybrids. Our investigations will focus on using smaller, noncommercial quantum dots to increase the FRET efficiency per attached dye. We will investigate QD's where proteins can be conjugated more closely to the QD core. If the FRET efficiency with a single dye can be significantly improved the QD-dye hybrids will be attractive for studying conformational fluctuations of macromolecules immobilized on them.

Studies of small ligand binding proteins.

Our work on maltose binding protein is ongoing. FRET studies of this protein will continue. In addition, several single fluorophore indicators of binding in maltose protein are known. We will compare our FRET based measurements of opening and closing rates to those obtained with single fluorophore probes. The single fluorophore approach has the potential for better temporal resolution because the measurements are not subject to rapid photobleaching of the acceptor dye.

We are also working on studies of the biotin binding protein streptavidin. This protein strongly interacts with several fluorophores when they are bound to it via linkers to biotin. Streptavidin has four deep hydrophobic pockets where biotin is bound so this protein provides a opportunity to study the details of how fluorophores interact with specific protein chemical environments.

References:

1. Goldman, E. R.; Medintz, I. L.; Whitley, J. L.; Hayhurst, A.; Clapp, A. R.; Uyeda, H. T.; Deschamps, J. R.; Lassman, M. E.; Mattoussi, H. *J. Am. Chem. Soc.* **2005**, *127*, 6744.
2. Zhang, C. Y.; Yeh, H. C.; Kuroki, M. T.; Wang, T. H. *Nat. Mater.* **2005**, *4*, 826.
3. Medintz, I. L.; Clapp, A. R.; Mattoussi, H.; Goldman, E. R.; Fisher, B.; Mauro, J. M. *Nat. Mater.* **2003**, *2*, 630.
4. Snee, P. T.; Somers, R. C.; Nair, G.; Zimmer, J. P.; Bawendi, M. G.; Nocera, D. G. *J. Am. Chem. Soc.* **2006**, *128*, 13320.
5. Luong, A.K.; Gradinaru, C.C.; Chandler, D.W.; and Hayden, C.C. *J. Phys. Chem. B*, **2005**, *109*, 15691.
6. Watkins, L. P.; Yang, H. *J. Phys. Chem. B* **2005**, *109*, 617.
7. Dippel, R.; Boos, W. *Journal of Bacteriology* **2005**, *187*, 8322.
8. Doring, K.; Surrey, T.; Nollert, P.; Jahnig, F. *European Journal of Biochemistry* **1999**, *266*, 477.
9. Pal, P.; Lesoine, J.F.; Lieb, M.A.; Novotny, L.; Knauf, P.A. *Biophys. J.* **2005**, *89*, L11.
10. Watkins, L.P.; Chang, H.Y.; Yang, H. *J. Phys. Chem. A* **2006**, *110*, 5191.
11. Watkins, L.P.; Yang, H. *Biophys. J.* **2004**, *86*, 4015.

DOE sponsored publications, 2007

1. C. S. Xu, H. Kim, H. Yang and C. C. Hayden, "Multiparameter Fluorescence Spectroscopy of Single Quantum Dot-Dye FRET Hybrids," *J. Am. Chem. Soc.*, **129**, 11008 -11009, 2007.
2. C. S. Xu, H. Kim, C. C. Hayden and H. Yang, "Joint Statistical Analysis of Multi-Channel Time Series from Single Quantum Dot-(Cy5)_n Constructs," *J. Phys. Chem.*, *submitted*.

ELECTRONIC STRUCTURE AND OPTICAL RESPONSE OF NANOSTRUCTURES

Martin Head-Gordon (mhg@cchem.berkeley.edu)¹,
Steven G. Louie (sglouie@berkeley.edu)²,
Lin-Wang Wang (lwwang@lbl.gov)³,
Emily A. Carter (eac@princeton.edu)⁴,
James R. Chelikowsky (jrc@ices.utexas.edu)⁵,

¹*Department of Chemistry, University of California, and Chemical Sciences Division, Lawrence Berkeley National Laboratory, Berkeley, CA 94720;* ²*Department of Physics, University of California, and Materials Sciences Division, Lawrence Berkeley National Laboratory, Berkeley, CA 94720;* ³*Computational Research Division, Lawrence Berkeley National Laboratory, Berkeley, CA 94720;* ⁴*Department of Mechanical & Aerospace Engineering, Princeton University, Princeton, NJ 08544;* ⁵*Departments of Physics and Chemical Engineering, Institute for Computational Engineering and Sciences, University of Texas, Austin, TX 78712*

1. Scope of Project.

There has been much progress in the synthesis, characterization and theoretical studies of various nanostructures such as nanotubes, nanocrystals, atomic wires, organic and biological nanostructures, and molecular junctions. However, there remain immense challenges to obtain a basic understanding of the properties of these structures and their interactions with external probes to realize their potential for applications. Some exciting frontiers in nanoscience include molecular electronics, nanoscale opto-electronic devices, nanomechanics (nanomotors), light harvesting and emitting nanostructures. The ground and electronic excited properties of the nanostructures and how they are coupled to the external stimulations/probes are crucial issues.

Since nanostructures are neither at the molecular nor the bulk limits, the calculations of their electronic and optical properties are subject to severe computational bottlenecks. The present program therefore focuses on the electronic structure theory and modeling of nanostructures, including their electronic excited-state and optical properties, with applications to topics of current interest. We are attacking the rate-determining steps in these approaches in collaboration with a team of applied mathematicians, led by Juan Meza, Head of LBNL's High Performance Computing Research Department.

2. Summary of Recent Progress.

As this is a large multi-investigator program, space precludes us summarizing all projects that are underway. Below, we highlight a selection of recent accomplishments. See also Jim Chelikowsky's separate abstract for additional detail and references on work led by his group on new large-scale methods for electronic excitations in nanostructures and associated applications.

Embedding methods for metallic systems: Kondo effect for Co on Cu and chemisorption of CO on transition metals. [12,13] We have been developing an embedded correlated wavefunction methodology for the study of localized features (e.g. point defects, adsorbates) in solids. For metals, the highly delocalized conduction electrons require us to combine a high-level, ab initio wavefunction treatment for the localized region of interest, with a lower-level density functional

theory (DFT) model for the periodic background. Recent technical developments have focused on eliminating previous difficulties associated with the treatment of core electrons.

Over the past year, we have extended our first ab initio description of the Co on Cu(111) Kondo state to examine Co on the (100) surface of Cu. The detailed lineshape of the experimentally observed Kondo resonance is markedly different for Co on the (111) and (100) surfaces of Cu. Our embedded wavefunction approach finds that the Co d-electron configuration and symmetries differ when adsorbed on the (111) and (100) surfaces, which provides an explanation for the striking difference seen in the Kondo lineshapes.

We are also using the ECI theory to characterize chemisorption of CO on transition metal surfaces, where it is known that DFT frequently fails to provide even a qualitatively correct description, predicting the wrong site preference. By applying our embedded wavefunction method, we have shown that for, e.g., CO on Cu(111), the correct site preference is obtained and the binding energy is in good agreement with experiment, due to correlated wavefunction description of the metal-CO π -backbonding.

Excitons in metallic carbon nanotubes. [1,3,14] Continuing previous efforts on elucidating the optical spectroscopy of carbon nanotubes, employing our accurate first-principles GW-BSE approach, we investigated the existence of bound exciton states in metallic single-walled carbon nanotubes (SWCNTs) [1]. Such states had been predicted by our group previously for nanotubes of small diameter. In the current work, we considered metallic nanotubes of experimentally observable diameters -- the armchair (10,10) and zig-zag (12,0) SWCNTs. Both tubes exhibit exciton binding energies of ~ 50 meV associated with each van Hove singularity in the non-interacting joint density of states. We also provided experimentally verifiable indications of the existence of such bound states by analysis of the spectral lineshapes.

Optimal Brillouin zone sampling for computationally efficient spectroscopy. We have refined and implemented a technique for performing efficient sampling of electronic structure throughout the Brillouin zone (BZ), by constructing a numerically-optimal basis spanning the Bloch-periodic component of electronic states throughout the BZ. This technique has been tested on metals, insulators, and semiconductors, as well as large supercells appropriate for nanostructures. With this approach, one constructs a Hamiltonian in the small optimal basis which parameterized with respect to \mathbf{k} in the BZ. We have extended the approach to excited state properties, and it is now being applied successfully to the excited state properties of carbon nanotubes.

Self-consistent ab initio transport calculations using planewave pseudopotential Hamiltonian. [9] Following our previous development of a new algorithm to calculate the scattering states using planewave pseudopotential Hamiltonian, we have now worked out the formalism and finished the code implementation for charge density and potential self-consistency under this approach. The self-consistent iteration converges well using a potential mixing scheme. We found an interesting phenomenon for localized states with eigen-energy between the left and right Fermi energies. The occupation status of such state has a significant influence on transport properties. We also find a prolonged influence of the central molecule on the charge of the electrode near the molecule, especially for small electrodes. We expect wide applications of our now finished transport package to molecular electronics.

Screened exchange density functional calculations for d-states and algorithm developments for density functional theory (DFT) calculations. [8,10,19,20] Due to the difference of LDA pseudopotential, d-state wavefunctions and the all electron wavefunctions, the exchange interaction calculated with the pseudo-wavefunction becomes different from the correct all electron results. To solve this problem, we have developed and implemented an approach based on using atomic wavefunction projection to restore the original all electron exchange interaction. Working with our math colleagues in this project, we have developed a new algorithm (direct constrained minimization, DCM, that minimizes within a space only three times the number of states) for the update of the wavefunction. As a further step, we have deployed the trust region algorithm on top of the DCM algorithm. The result is a fast and robust algorithm for self-consistent DFT calculations.

Scaled opposite spin electron correlation for ground and excited states. [4,15,16,17,18] Earlier in this grant, we developed possibly the simplest useful many body method, based on scaling the opposite spin second order many body correlation energy. It is both computationally less expensive, and more accurate than standard second order perturbation theory. This year we have made two important extensions of this framework. First, we have developed and implemented the analytical gradient for the ground state. Second, we have extended the theory to treat electronic excitations in nanomaterials, with results that exceed time-dependent density functional theory in accuracy and reliability, while being inexpensive enough for routine applications to large systems (over 100 atoms).

Local coupled cluster theory with smooth potential energy surfaces. [7,21] To make accurate infinite order many body methods feasible for nanoscale systems requires a partitioning that treats weak correlations by lowest order perturbation theory, and strong correlations to infinite order. Previous attempts to do this have shown promising computational speedups, but have failed to give potential energy surfaces that are smooth with respect to nuclear displacements. We have designed the first partitioning that yields mathematically smooth potential energy surfaces, by modifying the matrix elements describing electron correlation with a “bump function” that takes them to zero smoothly and rapidly. We have extended the bumping procedure to also bump integrals for larger speedups, and we have worked on developing bump function arguments that ensure “chemical” as well as mathematical smoothness in the resulting potential energy surfaces (defined as not generating false stationary points or inflection points).

3. Summary of Research Plans.

- Development of new computational optimizations for the GW-BSE methodology.
- Apply all-electron embedding to study the Kondo resonance of Co on Ag surfaces, and Rh on Cu(111) where no Kondo effect is seen.
- Formulation of quasi-degenerate opposite spin correlation model for electronic excitations.
- Study carbon nanotubes of different diameters and chiralities, and wide bandgap BN nanotubes for which we expect even more dominant excitonic effects.
- Algorithmic improvements and forces for the smooth local coupled cluster method.
- Joint development of new eigensolvers for electronic structure calculations.
- Explore phonon-electron coupling for inelastic transport phenomena

4. Partial list of publications from DOE Sponsored Work, 2006-present.

- [1] S.B. Cronin, Y. Yin, A. Walsh, R.B. Capaz, A. Stolyarov, P. Tangney, M. L. Cohen, S.G. Louie, et al, "Temperature dependence of the optical transition energies of carbon nanotubes: the role of electron-phonon coupling and thermal expansion," *Phys. Rev. Lett.* **96**, 127403 (2006)
- [2] C.H. Park, C.D. Spataru, and S.G. Louie, "Excitons and many-electron effects in the optical response of single-walled boron nitride carbon nanotubes," *Phys. Rev. Lett.* **96**, 126105 (2006).
- [3] E.B. Barros, R.B. Capaz, A. Jorio, G.G. Samsonidze, A.G. Souza Filho, S. Ismail-Beigi, C.D. Spataru, S.G. Louie, G. Dresselhaus, M.S. Dresselhaus, "Selection rules for one- and two-photon absorption by excitons in carbon nanotubes," *Phys. Rev. B* **73**, 241406(R) (2006).
- [4] Y. Jung and M. Head-Gordon, "A fast correlated electronic structure method for computing interaction energies of large van der Waals complexes applied to the fullerene-porphyrin dimer", *Phys. Chem. Chem. Phys.* **8**, 2831-2840 (2006).
- [5] Y.M. Rhee, R.A. DiStasio Jr., R.C. Lochan, and M. Head-Gordon, "Analytical gradient of restricted second order Møller-Plesset correlation energy with the resolution of the identity approximation, applied to the TCNE dimer anion complex", *Chem. Phys. Lett.* **426**, 197-203 (2006).
- [6] R. Steele, R.A. Distasio Jr., Y. Shao, J. Kong & M. Head-Gordon, "Dual basis second order Møller-Plesset theory: a reduced cost reference for correlation calculations", *J. Chem. Phys.* **125**, 074108 (2006).
- [7] J.E. Subotnik, A. Sodt, and M. Head-Gordon, "A near linear-scaling smooth local coupled cluster algorithm for electronic structure", *J. Chem. Phys.* **125**, 074108 (2006)
- [8] B. Lee, L.W. Wang, "Electronic structure of zinc-blende $\text{Al}_x\text{Ga}_{1-x}\text{N}$: screened-exchange study", *Phys. Rev. B* **73**, 153309 (2006).
- [9] A. Garcia-Lekue, L.W. Wang, "Elastic quantum transport calculations for molecular nanodevices using plane waves", *Phys. Rev. B* **74**, 245404 (2006).
- [10] C. Yang, J. Meza, L.W. Wang, "A constrained optimization algorithm for total energy minimization in electronic structure calculation", *J. Comp. Phys.* **217**, 709 (2006).
- [11] A.Sodt, J.E. Subotnik, and M. Head-Gordon, "Linear scaling density fitting", *J. Chem. Phys.* **125**, 194109 (2006) (9 pages).
- [12] P. Huang and E. A. Carter, Self-consistent embedding theory for locally correlated configuration interaction wave functions in condensed matter *J. Chem. Phys.* **125**, 084102 (2006).
- [13] P. Huang and E. A. Carter, Local electronic structure around a single Kondo impurity *Nano Lett.* **6**, 1146 (2006)
- [14] J. Deslippe, C. D. Spataru, D. Prendergast, and S. G. Louie, "Bound excitons in metallic single-walled carbon nanotubes" *Nano Letters* **7**, 1626 (2007).
- [15] R.C. Lochan, Y. Shao, and M. Head-Gordon, "Quartic scaling analytical gradient of scaled opposite spin second order Møller-Plesset Perturbation theory", *J. Chem. Theory Comput.* **3**, 988-1003 (2007).
- [16], Y. Jung, Y. Shao, and M. Head-Gordon, "Fast evaluation of scaled opposite spin second order Møller-Plesset correlation energies using auxiliary basis expansions and exploiting sparsity", *J. Comput. Chem.* **28**, 1953-1964 (2007).
- [17] R. Lochan, M. Head-Gordon, "Orbital-optimized opposite-spin 2nd order correlation: an economical method to improve the description of open-shell molecules", *J. Chem. Phys.* **126**, 164101 (2007)
- [18] Y.M. Rhee, M. Head-Gordon, "Scaled 2nd order perturbation corrections to configuration interaction singles: efficient and reliable excitation energy methods", *J. Phys. Chem. A* **111**, 5314-5326 (2007).
- [19] B. Lee, L.W. Wang, C. D. Sparatus, S. G. Louie, "Nonlocal exchange-correlation in screened exchange density functional methods", *Phys. Rev. B* (in press).
- [20] C. Yang, L.W. Wang, J. Meza, "The use of trust region in Kohn-Sham total energy minimization", *J. Comp. Phys.* (in press).
- [21] J.E. Subotnik, A. Sodt and M. Head-Gordon, "Localized orbital theory and ammonia triborane", *Phys. Chem. Chem. Phys.* (in press, 2007).
- [22] J. Schrier, B. Lee, L.W. Wang, "Mechanical and electronic structure properties of compressed CdSe tetrapod nanocrystals", *J. Nanosci. Nanotech.* (in press).

Influence of Co-Solvents and Temperature on Nanoscale Self-Assembly of Biomaterials

Teresa Head-Gordon
Department of Bioengineering, UC Berkeley
Physical Biosciences Division, Lawrence Berkeley National Laboratory
TLHead-Gordon@lbl.gov

Program Scope

Synthesis of tailor-made biomaterials requires a detailed understanding of the effect of solvent on structure, stability, and dynamics. How these physical quantities develop during self-assembly will be affected by the nature of the solvent, as evidenced by the fact that biopolymers such as proteins can be denatured or stabilized by various additives. Non-aqueous solvents such as guanadinium hydrochloride and urea are used to denature proteins [1]. Additions of trifluoro-ethanol or methanol can lead to specific stabilization of certain structural motifs, [2] whereas other organic solvents such as acetone, formamide, and DMSO are known to destabilize protein native states. The formulation of effective co-solvents is important in biopharmaceutical production of peptide and proteins to improve their long-term storage and delivery [3]. In principle, molecular switches can be created by control over protein function and reactivity through their solvent environment; such a possibility was recently demonstrated by embedding hemoglobin in a glassy solid of low water content trehalose solutions to reduce the protein conformational transitions and thereby turn off function [4]. Clearly, solvent interactions mediate the thermodynamics and kinetics of protein conformations that in turn influence their self-assembly and co-assembly properties. Understanding solvent environmental influences may lead to the ability to exploit not only differences in monomer composition but solvent composition, to create polymers, both biological and non-biological, with desired properties.

Recent Progress

Dielectric Relaxation of Aqueous Solutions of Hydrophobic and Hydrophilic Peptides [5]. We report on molecular dynamics simulations of the frequency-dependent dielectric relaxation spectra at room temperature for aqueous solutions of a model of the hydrophilic backbone, N-acetyl-glycine-methylamide (NAGMA), and a model of a hydrophobic side chain, N-acetyl-leucine-methylamide (NALMA). We find that only the NALMA peptide exhibits all of the anomalous dielectric response exhibited by aqueous protein solutions: a dielectric increment over bulk water, an imaginary part of the frequency-dependent dielectric that is bimodal at high concentration, a real part of the frequency-dependent dielectric of the high concentration peptide solution that drops precipitously and below the value for the low concentration, and two δ -relaxations at the picosecond and nanosecond timescales. We find that the anomalous dielectric properties of the high concentration NALMA solution arises due to an abrupt slowing of all peptide and water self- and cross-relaxations upon change of amino acid chemistry, which emerges as a second δ -relaxation (~ 1 ns) well-separated in time from the first δ -relaxation (~ 25 ps). We suggest that the molecular origin of the dielectric relaxation anomalies is due to frustration in the water network that in turn does not allow the NALMA solute molecules to reorient on the picosecond timescale of bulk water motions. This explanation is consistent with the idea of “slaving” of residue side chain motions to protein surface water, and furthermore suggests that the anomalous dynamics observed from a number of spectroscopies arises at the interface of hydrophobic

and hydrophilic domains on the protein surface.

Single-Particle and Collective Hydration Dynamics for Hydrophobic and Hydrophilic Peptides [6]. We have conducted extensive molecular dynamics simulations to study the single-particle and collective dynamics of water in solutions of N-acetyl-glycine-methylamide (NAGMA), a model hydrophilic protein backbone, and N-acetyl-leucine-methylamide (NALMA), a model (amphiphilic) hydrophobic peptide, as a function of peptide concentration. Various analytical models commonly used in the analysis of incoherent quasi-elastic neutron scattering (QENS), are tested against the translational and rotational intermediate scattering function, the mean square displacement of the water molecule center of mass, and fits to the second-order rotational correlation function of water evaluated directly from the simulation data. We find that while the agreement between the model free analysis and analytical QENS models is quantitatively poor, the qualitative feature of dynamical heterogeneity due to caging is captured well by all approaches. The center of mass collective and single particle intermediate scattering functions of water calculated for these peptide solutions show that the crossover from collective to single particle-dominated motions occurs at a higher value of Q for high concentration solutions relative to low concentration because of the greater restriction in movement of water molecules due to confinement. Finally we have shown that at the same level of confinement of the two peptides, the aqueous amphiphilic amino acid solution shows the strongest deviation between single particle and collective dynamics relative to the hydrophilic amino acid, indicating that chemical heterogeneity induces even greater spatial heterogeneity in the water dynamics.

Hydrophobic Solvation at Large Lengthscales in Modified Water Model [7]. The solvation of large hydrophobic solutes, modeled as repulsive and attractive Gay-Berne ellipsoids, is characterized in several modified water liquids using the SPC/E model as the reference water fluid. We find that small amounts of attraction between the Gay-Berne particle and any model fluid results in wetting of the hydrophobic surface. However significant differences are found among the modified and SPC/E water models and the distances in which they dewet the hydrophobic surface of repulsive Gay-Berne particles. We find that the dewetting trends for repulsive Gay-Berne particles correlate with the measured liquid-vapor surface tensions, and widths of the interfaces they form, of the various model liquids. This is related to changes in the network structure in the liquids.

Publications of work described last year [8-13]. See CPIMS abstract (2005-2006).

Future Plans

Models suggest that denaturants and non-denaturants interact differently with the water structure that results in stabilizing or destabilizing the folded state of the protein. Chaotropes (protein destabilizers) such as DMSO are thought to be weakly hydrated, and a molecular model proposes that as a result these chaotropes are then “pushed” onto the protein surface by stronger water-water hydrogen bonds, thereby dewetting the protein surface and promoting denaturation. Weak hydration of these co-solvents also implies greater solubilization of hydrophobic groups that could also help stabilize the unfolded state. In molecular terms, protein stabilizers (kosmotropes) such as glycerol or trehalose are thought to have a complex interaction with water so that they are excluded from the first solvation shell of the protein, resulting in hydration forces that oppose protein denaturation and therefore stabilize the folded form of the protein. However it is also observed that while osmolytes such as sugars may function as cryoprotectants, they can also exhibit a more complicated role as a destabilizing agent under conditions that may depend on the protein, on the water content, on temperature, or some combination of all variables. Presently we don’t know whether co-solvents promote (or decrease) protein stabilization through selective hydration of certain amino acid side chains, or how specific water and co-solvent interactions might change as a function of temperature and therefore allow predictive tuning of solvent conditions for self-assembly.

In order to probe the molecular origins of the water-protein and interactions with different chaotrope and kosmotrope co-solvents, we propose to study the structure and dynamics of the water near a single amino acid peptide with and without the co-solvent included. Recent (elastic) neutron scattering work performed at ISIS, shows a clear difference in the water-NALMA interactions and water-water interaction when DMSO co-solvent is added compared to glycerol. The hydrogen bond between the carbonyl group of NALMA and water disappears when DMSO cosolvent is added but is still present when glycerol is present. This shows that neither the water-NALMA direct correlation nor the water-water distribution is affected by the presence of a kosmotrope but both are disrupted when a chaotrope is added [14].

In future experiments and simulation, we will characterize the temperature dependence of the water. To this end, we choose two very well-characterized model peptides: a prototypical hydrophobic amino acid, N-acetyl-leucine-methylamide (NALMA) and hydrophilic amino acid N-acetyl-glycine-methylamide (NAGMA). The study of water dynamics around the NALMA and NAGMA peptide as a function of temperature and without co-solvent was performed at NIST on the DCS and HFBS spectrometer and published in [9]. That recent QENS study combining both DCS and HFBS instruments (two time resolutions) allowed a clean separation of two observable translational components. The first translational motion corresponds to a relaxation process of the bound surface water, the second non-Arrhenius translational component is a dynamical signature of the α -relaxation of more fluid water [9]. This clear separation was also observed by molecular dynamics and the slow motion was observed close to the hydrophilic region of the amphiphilic amino acid [15]. These well-characterized water- amino acid systems will therefore be used as a benchmark to study the effect of a kosmotrope and chaotrope co-solvents on the dynamics of water as a function of temperature. In order to clearly characterize the effect of a kosmotrope and chaotrope cosolvents on the water dynamics at the surface of the hydrophilic and hydrophobic model peptides (NALMA and NAGMA) we will use the combination of two experiments with different resolutions (using DCS and HFBS), supported by simulations and empirical polarizable force field models that show promise in quantitative descriptions of structure and dynamics for these systems [15].

References

1. C. N. Pace (1986). *Meth. Enzym.* 131, 266; G. I. Makhatadze (1999). *J. Phys. Chem. B*, 103, 4781.
3. M. Buck (1998). *Quarterly Reviews of Biophysics* 31, 297.
4. L. N. Bell (1997). *Biotechnology Progress* 13, 342.
5. D. S. Gottfried (1996). *J. Phys. Chem.* 100, 12034.
6. R. K. Murakra and T. Head-Gordon (2007). Dielectric relaxation of aqueous solutions of hydrophobic and hydrophilic peptides. *JPC-B*, *accepted*.
7. R. K. Murakra and T. Head-Gordon (2007). Single particle and collective hydration dynamics of hydrophobic and hydrophilic peptides. *J. Chem. Phys.* 126, 215101-215109.
8. R. M. Lynden-Bell and T. Head-Gordon (2007). *In preparation*.
9. M. E. Johnson, T. Head-Gordon, A. A. Louis (2007). Representability problems for coarse-grained water models. *J. Chem. Phys.* 126, 144509-144519.
10. C. Malardier-Jugroot and T. Head-Gordon (2007). Separable cooperative and localized translational motions of confined water. *Phys. Chem. Chem. Phys.* 9, 1962-1971.
11. T. Head-Gordon and S. Rick (2007). Consequences of chain networks on thermodynamic, dielectric and structural properties for liquid water. *Phys. Chem. Chem. Phys.* 8, 83-91.
12. R. M. Lynden-Bell and T. Head-Gordon (2007). Solvation in modified water models: toward understanding hydrophobic solvation. *Mol. Phys.* 104, 3593-3605.
13. T. Head-Gordon & M. E. Johnson (2006). Tetrahedral structure or chains for liquid water? *Proc. Natl. Acad. Sci.* 103, 7973-7977.

14. C. Malardier-Jugroot, M. Johnson, T. Head-Gordon (2007). Work in progress.
15. C. Malardier-Jugroot, M. Johnson, R.K. Murarka, T. Head-Gordon (2007). Work in progress.

Chemical Kinetics and Dynamics at Interfaces

Laser induced reactions in solids and at surfaces

Wayne P. Hess (PI), Kenneth M. Beck, and Alan G. Joly

Chemical and Materials Sciences Division
Pacific Northwest National Laboratory
P.O. Box 999, Mail Stop K8-88,
Richland, WA 99352, USA
wayne.hess@pnl.gov

Additional collaborators include A L Shluger, P V Sushko, J T Dickinson, K Tanimura, G Xiong, P Perozzo, and M Henyk

Program Scope

The chemistry and physics of electronically excited solids and surfaces is relevant to the fields of photocatalysis, radiation chemistry, and solar energy conversion. Irradiation of solid surfaces by UV, or higher energy photons, produces energetic species such as core holes and free electrons, that relax to form electron-hole pairs, excitons, and other transient species capable of driving surface and bulk reactions. These less energetic secondary products induce the transformations commonly regarded as radiation damage. The interaction between light and nanoscale oxide materials is fundamentally important in catalysis, microelectronics, sensor technology, and materials processing. Photo-stimulated desorption, of atoms or molecules, provides a direct window into these important processes and is particularly indicative of electronic excited state dynamics. Excited state chemistry in solids is inherently complex and greater understanding is gained using a combined experiment/theory approach. We therefore collaborate with leading solid-state theorists who use *ab initio* calculations to model results from our laser desorption and photoemission experiments.

Approach:

We measure velocities and state distributions of desorbed atoms or molecules from ionic crystals using resonance enhanced multiphoton ionization and time-of-flight mass spectrometry. Photon energies are chosen to excite specific surface structural features that lead to particular desorption reactions. The photon energy selective approach takes advantage of energetic differences between surface and bulk exciton states and probes the surface exciton directly. Application of this approach to controlling the yield and state distributions of desorbed species requires detailed knowledge of the atomic structure, optical properties, and electronic structure. To date we have thoroughly demonstrated surface-selective excitation and reaction on alkali halides. However, the technological applications of alkali halides are limited compared to oxide materials. Oxides serve as dielectrics in microelectronics and form the basis for exotic semi- and super-conducting materials. Although the electronic structure of oxides differs considerably from alkali halides, it now appears possible to generalize the exciton model for laser surface reactions to these interesting new materials. Our recent studies have explored nanostructured samples grown by chemical vapor deposition or thin films grown by reactive ballistic deposition (RBD). We have demonstrated that desorbed products states can be selected by careful choice of laser wavelength, pulse duration, and delay between laser pulses. Recently, we have applied the technique of

photoemission electron microscopy (PEEM) to these efforts. In particular, we are developing a combined PEEM: two photon photoemission approach to probe spatially resolved electronic state dynamics in nanostructured materials. Our experiments are designed specifically to test hypothetical models and theoretical predictions resulting from the calculations.

Recent Progress

We have induced selective solid-state chemistry using tunable femtosecond and nanosecond lasers by exciting wide-gap materials under surface science conditions. For MgO and CaO the energies required to generate bulk excitons are 7.7 and 6.8 eV, respectively. Our calculations indicate that it is possible to excite the surface over the bulk of ionic oxide crystals to induce controllable bulk or surface specific reactions. We have confirmed that surface excitons can be directly excited in both CVD and RBD MgO thin films and RBD films of CaO and that bulk excitons may be specifically excited in both materials. Therefore, site-selective excitation is possible for low-coordinated surface sites of oxide materials.

In the particular case of CaO RBD-grown films, we have recently recorded the O-atom desorption yield as a function of photon energy. For the excitation energy range from 3.7 to 5.4 eV, there is a stepwise increase with excitation energy. An associated optical emission spectrum reveals one asymmetric curve, which suggests that more than one excitation process contributes to the emission yield consistent with our yield results. The optical absorption spectrum can be decomposed into two constituents at 4.2 and 4.7 eV which corresponds to the steps in the atomic yield. Additional theoretical modeling and experiments are required to achieve a more complete mechanistic understanding of these processes.

Future Directions

We ask the question “Can an oxide surface exciton or a combination of a surface exciton and a trapped hole lead to controllable atomic desorption and hence specific surface modification?” If exciton-based desorption can be generalized from alkali halides to oxides then selective excitation of specific surface sites could lead to controllable surface modification, on an atomic scale, for a general class of important materials. The O-atom KE distribution is clearly hyperthermal indicating that a surface exciton mechanism is likely responsible for the observed atomic desorption and that surface excitons may indeed combine with trapped surface holes.

Our excitation techniques are site specific as it is possible to selectively excite terrace, step, or corner surface sites. Therefore, we have explored various sample preparation techniques that produce high concentrations of low-coordinated surface sites such as 4-coordinated steps and 3-coordinated corner or kink sites. In particular, we have employed reactive ballistic deposition (a technique developed in Bruce Kay’s lab) to grow very high surface area MgO thin films. These films have been thoroughly characterized using XPS, SEM, TEM, and XRD techniques. Similarly, we have also studied laser desorption of MgO nano-powders grown by a chemical vapor deposition technique. The nano-powders show cubic structure and edge lengths ranging between 3 and 10 nm (through TEM analysis). Both sample types provide unique insight into site-selective exciton-based desorption processes and are the focus of ongoing work. We plan to grow and study several other oxide surfaces in the near term including CaO, BaO, ZrO₂, and TiO₂.

While exciton-based desorption is plausible for MgO and CaO, we note that the higher valence may require a “hole plus exciton” mechanism. The details of this mechanism need to be delineated and confirmed by demonstrating laser control of the various desorption processes. We have recently observed hyperthermal neutral Mg-atom desorption. This is quite a novel result as Mg-atom desorption requires that two electron transfer to a corner site Mg^{2+} ion in a very short time and then desorb prior to relaxation. The hyperthermal distribution indicates that the exciton model is extendable now to metal atom desorption processes – a previously unknown mechanism. Future plans include femtosecond pulse-pair photo-emission electron microscopy to probe dynamics of oxide nanostructures on surfaces. We are also presently developing capabilities to perform energy-resolved TPPE using a hemispherical analyzer XPS instrument. In combination we expect these two techniques will provide the first *spatially-resolved* electronic state dynamics of nanostructured oxide materials.

References to publications of DOE BES sponsored research (2004 to present)

1. “Determination of surface exciton energies by velocity resolved atomic desorption.” WP Hess, AG Joly, KM Beck, PV Sushko, and AL Shluger, Surf. Sci. **564**, 62 (2004).
2. “Laser control of product electronic state: desorption from alkali halides.” KM Beck, AG Joly, N Dupuis, P Perozzo, W Hess, P Sushko, and A Shluger, J. Chem. Phys. **120**, 2456 (2004).
3. “The origin of temperature-dependent yield of Frenkel-pairs generated by valence excitation in NaCl.” K Tanimura and WP Hess, Phys. Rev. B, **69**, 155102 (2004).
4. “Interaction of wide band gap single crystals with 248 nm excimer laser irradiation: laser induced near-surface absorption in single crystal NaCl.” K H Nwe, SC Langford, WP Hess, and JT Dickinson, J. Appl. Phys. **97**, 043501 (2005).
5. “Interaction of wide band gap single crystals with 248 nm excimer laser irradiation: The effect of water vapor and temperature on laser desorption of neutral atoms from sodium chloride.” KH Nwe, SC Langford, WP Hess, and JT Dickinson, J. Appl. Phys. **97**, 043502 (2005).
6. “A mechanism of photo-induced desorption of oxygen atoms from MgO nano-crystals.” PE Trevisanutto, PV Sushko, AL Shluger, KM Beck, M Henyk, A.G. Joly, and W.P. Hess. Surf. Sci. **593**, 210 (2005).
- 7) “Laser control of desorption through selective surface excitation.” WP Hess, AG Joly, KM Beck, M Henyk, PV Sushko, PE Trevisanutto, and AL Shluger, J. Phys. Chem. **109**, (2005).
- 8) “Surface electronic properties and site-specific laser desorption processes of highly structured nanoporous MgO thin films.” M Henyk, KM Beck, MH Engelhard, AG Joly, WP Hess, and JT Dickinson, Surf. Sci. **593**, 242 (2005).
- 9) “Introduction to Photoelectron Emission Microscopy: Principles and Applications.” G Xiong, AG Joly, WP Hess, M Cai, and JT Dickinson, J. Chin. Elec. Microsc. Soc. **25**, 16 (2006).
- 10) “Carrier Dynamics in $\alpha\text{-Fe}_2\text{O}_3$ Thin-films and Single Crystals Probed by Femtosecond Transient Absorption and Reflectivity.” AG Joly, JR Williams, SA Chambers, G Xiong, WP Hess, and DM Laman, J. Appl. Phys. **99**, 1 (2006).

- 11) "In-situ photoemission electron microscopy study of thermally-induced martensitic transformation in CuZnAl shape memory alloy." G Xiong, AG Joly, KM Beck, WP Hess, M Cai, SC Langford, and JT Dickinson, *Appl. Phys. Lett.* **88**, 091910 (2006).
- 12) "Site-specific laser modification of MgO nano-clusters: Towards atomic scale surface structuring." KM Beck, M Henryk, C Wang, PE Trevisanutto, PV Sushko, WP Hess, and AL Shluger, *Phys. Rev. B* **74**, 045404 (2006).
- 13) "Two-hole localization mechanism for electronic bond rupture of surface atoms by laser-induced valence excitation of semiconductors." K Tanimura, E Inami, J Kanasaki, and WP Hess *Phys. Rev. B* **74**, 035337 (2006).
- 14) "Excited carrier dynamics of α -Cr₂O₃/ α -Fe₂O₃ core-shell nanostructures." G Xiong, AG Joly, WP Hess, G Holtom, CM Wang, DE McCready, and KM Beck, *J. Phys Chem. B* **110**, 16937 (2006).
- 15) "Probing electron transfer dynamics at MgO surfaces by Mg-atom desorption." A.G. Joly, M Henryk, KM Beck, PE Trevisanutto, PV Sushko, WP Hess, and AL Shluger, *J. Phys. Chem. B Lett.* **110**, 18093 (2006).
- 16) "Laser-induced oxygen vacancy formation and diffusion on TiO₂ (110) surfaces probed by photoemission electron microscopy." G Xiong, AG Joly, KM Beck, WP Hess, *Phys. Stat. Sol. (c)* **3**, 3598 (2006).
- 17) "Study of martensitic phase transformation in a NiTiCu thin film shape memory alloy using photoelectron emission microscopy." M Cai, SC Langford, JT Dickinson, MJ Wu, WM Huang, G Xiong, TC Droubay, AG Joly, KM Beck, and WP Hess, *Adv. Funct. Mater.* **17**, 161 (2007).
- 18) "An *In-situ* Study of the Martensitic Transformation in Shape Memory Alloys using Photoemission Electron Microscopy," M Cai, SC Langford, JT Dickinson, G Xiong, TC Droubay, AG Joly, KM Beck and WP Hess, *J. Nuc. Mater.* **361**, 306 (2007).
- 19) "Study of copper diffusion through a ruthenium thin film by photoemission electron microscopy." W. Wei, S. L. Parker, Y.-M. Sun, and J. M. White, G Xiong, AG Joly, KM Beck, and WP Hess, *Appl. Phys. Lett.* **90**, 111906 (2007).
- 20) "Synthesis and photoexcited charge carrier dynamics of β -FeOOH nanorods." AG Joly, G Xiong, C Wang, DE McCready, KM Beck, and WP Hess, *Appl. Phys. Lett.* **90**, 103504 (2007).
- 21) "Photoemission electron microscopy of TiO₂ anatase films embedded with rutile nanocrystals." G Xiong, R Shao, TC Droubay, AG Joly, KM Beck, SA Chambers, and WP Hess, *Adv. Funct. Mater.* **17**, 2133 (2007).
- 22) "Proceedings of the Eighth International Conference on Laser Ablation (COLA 05)." WP Hess, PR Herman, D Bäuerle, and H Koinuma, Editors, *Journal of Physics: Conference Series*, Vol. **59**, pages 1 -729 (2007).

Probing catalytic activity in defect sites in transition metal oxides and sulfides using cluster models: A combined experimental and theoretical approach

Caroline Chick Jarrold and Krishnan Raghavachari

Indiana University, Department of Chemistry, 800 East Kirkwood Ave.
Bloomington, IN 47405

cjarrold@indiana.edu, kraghava@indiana.edu

I. Program Scope

It is difficult to overstate the importance of continued research on catalytic systems: Improving the efficiency of globally important catalytically driven processes could vastly reduce energy consumption. Further, the sharp increase in fossil fuel consumption in China and India coupled with dramatic deterioration of air quality underscores the need for both cleaner fuels and alternative fuel sources. The broad goal of this project is to identify the critical electronic and structural features in metal oxide- and sulfide-based catalysts that govern their catalytic activity. This project provides a systematic, multi-prong approach to determining the chemical and physical properties of metal *suboxide* and *subsulfide* clusters to model sites which have been demonstrated in numerous bulk and computational studies to be the locus of catalytic activity. The ultimate goal of the program is to improve environmental and economic conditions directly related to metal oxide- and metal sulfide-based heterogeneous catalytic processes. Optimization of the catalytic applications targeted in this project can lead to reduced energy consumption in common catalytically-driven synthetic processes, viable alternative fuel sources, and improved desulfurization of existing fossil fuels.

Transition metal oxides and sulfides are important in a wide range of catalytic applications. While bulk properties of these materials are well characterized, catalytically active sites are believed to be on surface defects or edges. The strategy of this project is to determine the defect structures that exhibit the essential balance between structural stability and electronic activity necessary to be simultaneously robust and catalytically active. Metal oxide and sulfide systems that are under-coordinated relative to the bulk are electron-rich defect sites with the added benefit of being sterically less hindered. Therefore, cluster models of these systems are the focus of this project. An important point for consideration is the coupling between adjacent metal centers in disparate oxidation states. This type of chemical tension is exploited in many biological systems, though the systems proposed for study herein have distinctly industrial applications. Specifically, $\text{Mo}_x\text{O}_{y<3x}$, $\text{Mo}_x\text{S}_{y<2x}$, $\text{W}_x\text{O}_{y<3x}$ and $\text{W}_x\text{S}_{y<2x}$ clusters will be studied. The suboxides and subsulfides are of particular interest because they model oxygen and sulfur vacancies in the bulk. As bonding in predominantly ionic materials is localized, extending what is learnt from small cluster systems can be more rationally scaled to particulate systems and supported metal catalysts.

Both experimental and computational approaches being taken in this project. Experimentally, the bare metal oxide and sulfide clusters will be produced using the laser

ablation/pulsed molecular beam cluster source, then probed using mass spectrometry to survey which clusters are particularly stable. Mass isolated cluster anions will then be spectroscopically interrogated using anion photoelectron (PE) spectroscopy and resonant two-photon detachment spectroscopy to map out the electronic structures of the neutral and anionic clusters, respectively. Mass-specific reactivity studies will be carried out along with spectroscopic investigation of the resulting complexes to characterize the bonding in these systems. Finally, we wish to explore the energetics associated with catalyst activity and regeneration: The impact of electronic excitation of the complexes will be studied using resonant two-color experiments in which the effect of electronic excitation on structural rearrangement or photodissociation of the complex will be determined. Density functional theory (DFT) calculations will be carried out in parallel with all the experimental studies, which will be critical in making structural assignments for the clusters and the complexes they form. Calculations will also be used to predict full-cycle catalytic processes on the clusters. In the spirit of keeping the studies relevant to applied systems, M_xO_y clusters will be reacted with hydrocarbons (important process: dehydrogenation and aromatization),¹ W_xO_y clusters with water (photoelectrochemical decomposition of water)² and both chalcogenides with organosulfur molecules (hydrodesulfurization).³

II. Recent Progress

The studies described below build largely on our previous work on metal atom,^{4,5,6} metal cluster^{7,8} and metal oxide cluster reactivity.^{9,10,11,12,13} In anticipation of the start of the award, calculations on the reactions between Mo_xO_y anionic and neutral clusters toward methane have been ongoing. In previous experiments, cluster fragmentation followed by oxidative addition of methane was inferred from the product distribution observed when mixed $Mo_xO_y^-$ clusters were exposed to CH_4 , though calculations showed that the oxidative addition of a single methane to a cluster such as $Mo_2O_4^-$ was highly endothermic. However, calculations have also shown that participation of multiple methane molecules in the reaction has the effect of lowering the endothermicity.

Experimentally, modifications to the existing dual mass spectrometer- anion photoelectron spectrometer described in detail in the literature¹⁴ are being made to incorporate a mass filter between the cluster source and reaction cell. A small device with modest resolution on the order of 100 $m/\Delta m$ is required since we wish only to separate a particular oxide from the adjacent species (e.g., to isolate $Mo_4O_7^-$ from $Mo_4O_6^-$ and $Mo_4O_8^-$, $m/\Delta m$ of 30 is required). The rectilinear ion trap (RIT) developed by Cooks and coworkers¹⁵ appears to be well suited to the task in that the resolution is adequate, and the number densities required for subsequent PE spectroscopic studies can be accommodated. Additionally, a simple miniaturized Wien velocity filter is being built for separation of the lightest clusters.

III. Future Plans

The highest priority of the experimental component of this project is to complete, install, and optimize operation of the ion trap. Ambiguity surrounding the identity of the

reactants leading to specific products observed in mass spectra of the reaction products has been the primary weakness in the approach used. Mass-specific reactivity studies will then be carried out on a number of systems involving the molybdenum and tungsten oxides and sulfides. The electronic and physical structures of clusters and their complexes resulting from exposure to methane, ethane, methanol, CO (+ H₂), water, and thiophene will be measured using anion photoelectron spectroscopy. Resonant two-photon detachment studies will map the electronic structure of the anionic clusters and complexes, which is important because metal oxides and sulfides tend to accumulate negative charge in solution. Further, numerous complexes have shown evidence of photodissociation. We will perform experiments to identify the charge and nature of the dissociative state because of the obvious relevance to catalyst regeneration.

The goal of theoretical efforts is to provide a conceptual and physical framework for the identification, design, and optimization of target group VI oxide and sulfide systems to catalyze specific chemical reactions of interest (e.g., hydrocarbon activation, water dissociation, hydrodesulfurization, etc.). Theory will be used in conjunction with the photoelectron spectroscopic work to understand the electronic structure and chemical reactivity of Mo_xO_y and W_xO_y clusters. This will provide a molecular level understanding of such clusters as models for defects at oxide surfaces that can participate in catalytic chemistry. Theoretical investigations will be extended to analogous larger cluster models as well to investigate additional chemical reactions at identified cluster systems that may not be easily studied experimentally.

IV. References to publications of DOE sponsored research that have appeared in 2004–present or that have been accepted for publication

Not yet applicable.

References

¹ For example: “Methane dehydroaromatization under nonoxidative conditions over Mo/HZSM-5 catalysts: Identification and preparation of the Mo active species,” H. M. Liu, X.H. Bao, Y. D. Xu, *J. Catal.* **239**, 441–450 (2006); “Catalytic conversion of methane to benzene over Mo/ZSM-5,” D. Wang, J. Lunsford, M. Rosynek, *Topics in Catal.* **3–4**, 289-297 (1996); “Control of reactivity in C-H bond breaking reactions in oxide catalysts: Methanol oxidation on supported molybdenum oxide,” S. Oyama, R. Radhakrishnan, M. Seman, J. Kondo, K. Domen, and K. Asakura, *J. Phys. Chem. B* **107**, 1845-52 (2003).

² For example: “Photoelectrochemical Cells,” M. Grätzel, *Nature* **414**, 338-344 (2001); “Photoelectrochemical properties of nanostructured tungsten trioxide films,” C. Santato, M. Ulmann, J. Augustynski, *J. Phys. Chem. B* **105** 936-940 (2001).

³ For example: “A refinement on the notion of type I and II (Co)MoS phases in hydrotreating catalysts,” E.J.M. Hensen, V.H.J. de Beer, J.A.R. van Veen, and R.A.A. van Santen, *Catal. Lett.* **84**, 59-67 (2002); S. Crisol, J.-F Paul, C. Schovsbo, E. Veilly, E. Payen, “DFT study of thiophene adsorption on molybdenum sulfide, *J. Catal.* **239**, 145-153 (2006).

- ⁴ “A comparison of stable carbonyls formed in the gas-phase reaction between precious metal atomic anions and methanol or methoxy radicals: Anion photoelectron spectroscopy and density functional theory calculations on HNiCO^- , PdCO^- and PtCO^- ,” B. Chatterjee, F. A. Akin, C. C. Jarrold and K. Raghavachari, *J. Chem. Phys.* **119**,10591 (2003).
- ⁵ “The electronic structure of PdC_2H and PdC_2HN determined by anion photoelectron spectroscopy,” V. D. Moravec and C. C. Jarrold, *J. Chem. Phys.* **112**, 792-8 (2000).
- ⁶ “Comparison of nickel-group metal cyanides and acetylides and their anions using anion photoelectron spectroscopy and density functional theory calculations,” B. Chatterjee, F. A. Akin, C. C. Jarrold, and K. Raghavachari, *J. Phys. Chem. A*, 109, 6880-6 (2005).
- ⁷ “Anion photoelectron spectroscopy of small tin clusters,” V. D. Moravec, S. A. Klopčič and C. C. Jarrold, *J. Chem. Phys.* **110**, 5079-88 (1999).
- ⁸ “Study of tin- and tin cluster-cyano complexes using anion photoelectron spectroscopy and density functional theory calculations,” V. D. Moravec and C. C. Jarrold, *J. Chem. Phys.* **113**, 1035-45 (2000).
- ⁹ “Separating contributions from multiple structural isomers in anion photoelectron spectra: Al_3O_3^- beam hole-burning,” F. A. Akin, C. C. Jarrold, *J. Chem. Phys.* **118**, 1773-1778 (2003).
- ¹⁰ “Addition of water and methanol to Al_3O_3^- studied by mass spectrometry and anion photoelectron spectroscopy,” F. A. Akin and C. C. Jarrold, *J. Chem. Phys.* **118**, 5841-5851 (2003).
- ¹¹ “Addition of water to Al_5O_4^- determined by anion photoelectron spectroscopy and quantum chemical calculations,” U. Das, K. Raghavachari, and C. C. Jarrold, *J. Chem. Phys.* **122**, 014313-1 - 8(2005).
- ¹² “Reactivity of Al_3O_3^- toward water studied by density functional theory,” F. A. Akin, C. C. Jarrold, *J. Chem. Phys.* **120**, 8698- 8706 (2004).
- ¹³ “Structures of Mo_2O_y^- and Mo_2O_y via anion photoelectron spectroscopy and DFT calculations”, B. L. Yoder, J. T. Maze, K. Raghavachari and C. C. Jarrold, *J. Chem. Phys.* **122**, 094313 (2005).
- ¹⁴ “Reactivity of small Mo_xO_y^- clusters toward methane and ethane,” Richard B. Wyrwas, Bruce L. Yoder, Joshua T. Maze, and Caroline Chick Jarrold, *J. Phys. Chem. A* **110**, 2157-2165 (2006); “Separating contributions from multiple structural isomers in anion photoelectron spectra: Al_3O_3^- beam hole burning,” F. A. Akin and Caroline Chick Jarrold, *Journal of Chemical Physics*, **118**, 1773-1778 (2003).
- ¹⁵ Z. Ouyang, Z.; Wu, G.; Song, Y.; Li, H.; Plass, W.R.; Cooks, R.G., Rectilinear Ion Trap: Concepts, Calculations, and Analytical Performance of a New Mass Analyzer, *Anal. Chem.* **76**, 4595-4605 (2004).

Molecular Theory & Modeling

Nucleation: From Vapor Phase Clusters to Crystals in Solution

Shawn M. Kathmann
Chemical and Material Sciences Division
Pacific Northwest National Laboratory
902 Battelle Blvd.
Mail Stop K1-83
Richland, WA 99352
shawn.kathmann@pnl.gov

Program Scope

The objective of this work is to develop a understanding of the chemical physics governing nucleation in both the vapor and in solution. The thermodynamics and kinetics of the embryos of the nucleating phase are important because they have a strong dependence on size, shape and composition and differ significantly from bulk or isolated molecules. The technological need in these areas is to control chemical transformations to produce specific atomic or molecular products without generating undesired byproducts, or nanoparticles with specific properties.

Compared to gas-phase chemical transformation, which in most cases can be viewed as isolated encounters of two reactant species, the proximity of condensing solvent atoms or molecules can profoundly alter reaction kinetics and thermodynamics. Computing reaction barriers and understanding condensed phase mechanisms is much more complicated than those in the gas phase because the reactants are surrounded by solvent molecules and the configurations, energy flow, and electronic structure of the entire statistical assembly must be considered.

Recent Progress

Water Cluster Activation Energies and Potentials of Mean Force

Modern transition state theory can be viewed in terms of the local equilibrium rate at which the system crosses a dividing surface in phase space. Alternatively, this rate can be expressed in terms of a rate over a barrier in the potential of mean force (PMF) along the relevant reaction coordinate. The activation energy, and hence the rate, is typically thought to arise solely from the barrier along the PMF. However, when the reaction coordinate is not separable from the remaining degrees of freedom in the system, one must include this non-separability in the reactant state free energy, which will contribute to the magnitude of the activation energy. Stated another way, the activation energy calculated in the present work has two contributions: (1) from the PMF barrier, and (2) from the free energy due to motion of the reactant states along the reaction coordinate.

We start by writing the DNT evaporation rate constant, α , in the traditional transition state theory form: $\alpha \equiv e^{-\beta W} / \beta h Q^R$, where h is Planck's constant, and the PMF, $W = W(r_{\text{cut}})$. In what follows, the transition state value of the reaction coordinate located at the top of the PMF barrier for a given i -cluster will be denoted by r_{cut}^\ddagger , and the minima in the PMF denoted by $r_{\text{cut}}^{\text{min}}$. In order to obtain an expression for the activation energy in terms of (1) the PMF barrier and (2) the contribution arising from reaction coordinate non-separability, we start with the Arrhenius rate expression, $\alpha = \tilde{A} e^{-\beta E_a}$, where \tilde{A} is a pre-exponential factor and E_a is the activation

energy. The activation energy is defined $E_a \equiv -\partial \ln \alpha / \partial \beta$.

Substituting and simplifying yields

$E_a = \Delta W - A_{\xi}^R$, where $\Delta W = W^{\ddagger} - W^{\min}$, is the PMF barrier evaluated at $r_{\text{cut}}^{\ddagger}$ and r_{cut}^{\min} , respectively. A_{ξ}^R is the i -cluster Helmholtz free energy including *only that motion of the molecules along the reaction coordinate* ξ . The resulting activation energies E_a are plotted for comparison in Figure 1. The limiting behavior of the computed activation energies E_a should approach the negative of the bulk

enthalpy of vaporization; $\Delta H_{\text{vap}}^{\text{expt.}} = -9.9$ kcal/mol. The Arrhenius collision prefactors, \tilde{A} , increase from 10^{13}s^{-1} for $i = 2$ up to 10^{16}s^{-1} for $i = 10$. The VTST prefactor $k_B T / h \sim 10^{13} \text{s}^{-1}$ at ambient conditions, indicating that the larger Arrhenius prefactors are characteristic of “loose” transition states. Our calculations have shown that the free energy due to motion along r_{cut} can be a substantial fraction of the activation energy E_a .

EXAFS of Classical and Quantum Ag^+ in Water

Crystallization is one of the most challenging problems in chemical physics. Salts having large solubilities require higher salt concentrations to crystallize than salts with lower solubilities. Nucleation is inherently a rare event and trying to observe it directly via molecular simulation at realistic conditions is computationally intractable at realistic conditions – the majority of time being spent searching irrelevant regions of the solution configuration space. Nucleation of salt from concentrated solution presents several challenges not present in the dilute limit typically encountered in molecular simulations. Charge transfer effects are important in dictating the difference between salts of AgCl versus NaCl . To this end, we calculate EXAFS signals from both a classical (SPC/E) and quantum (DFT) description of an Ag^+ ion in water.

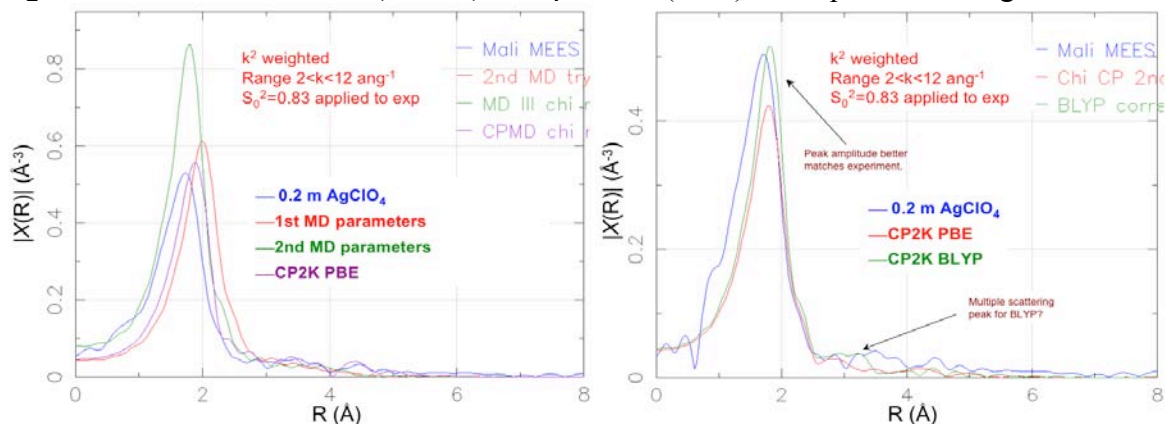


Figure 2. (Left) EXAFS spectra of two classical parameterizations compared to CP2K PBE and experiment. (Right) EXAFS spectra of two CP2K functionals (PBE and BLYP) compared with experiment (Thanks to John Fulton).

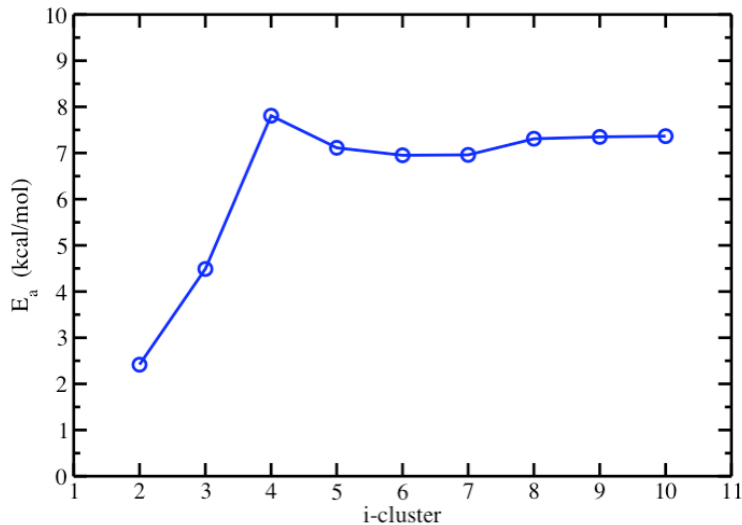


Figure 1. E_a for water monomer evaporation using the D-C model.

Future Plans

Charge Transfer in Solution

Recent electronic structure calculations have shown that charge transfer is important in aqueous solutions of AgCl. Figure 3 shows gas-phase calculations of the difference in charge transfer between NaCl and AgCl. Figure 4 shows the significant difference between the CP2K PBE gas-phase and condensed-phase charges on the Ag⁺ and Cl⁻ as a function of distance between the ions.

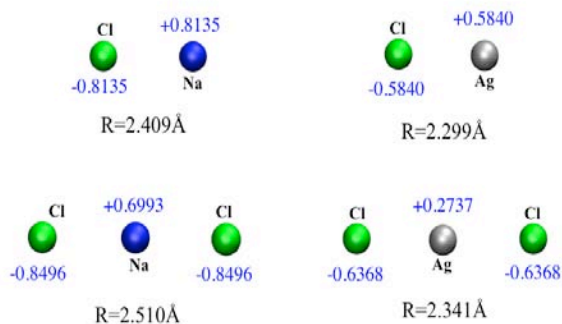


Figure 3. Comparison of NaCl (left) and AgCl (right) charge transfer: QCISD/aug-cc-pvtz-pp

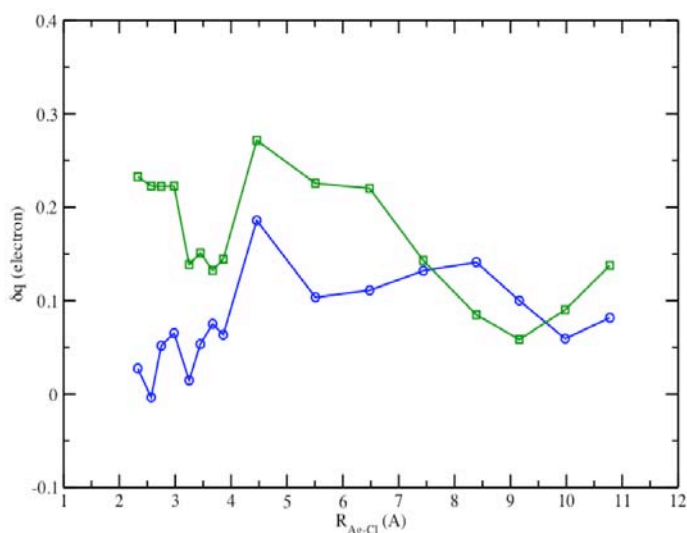


Figure 4. Difference in charge as a function of the distance between Ag⁺ and Cl⁻ in aqueous solution.

the population of electronic states in the band gap and calculate excited state energies to see if they are consistent with visible light. Figure 5 shows the clustering of Na⁺ and Cl⁻ ions in solution and some gas-phase fragments of NaCl crystals that are being explored with TDDFT to calculate excited state energies and oscillator strengths both with and without Ag⁺ trace impurities – experimental observation indicates that when Ag⁺ is present the crystalloluminescence is enhanced.

Crystalloluminescence

It has been known since the 1700's that the crystallization of certain substances from solution is accompanied by the emission of light - *crystalloluminescence*. But, in aqueous solution the ionic electronic states are lowered relative to the radical states. It is found that at the early stage of crystal nucleation a burst of some 10⁵ photons in the range of 390 to 570 nm is emitted. Could the light be coming from defect states? We will monitor the electronic DOS for different types of defects to explore

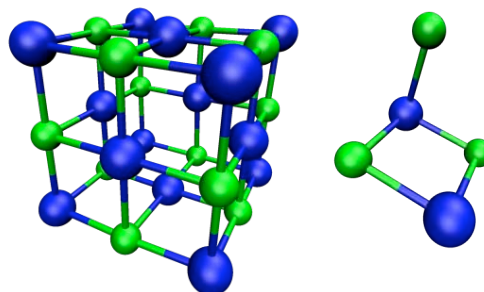
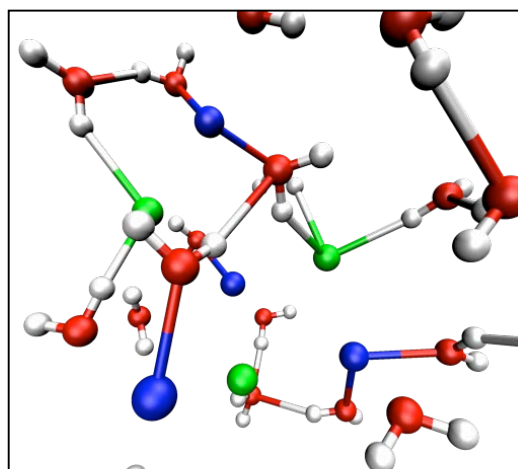


Figure 5. (Top) Na⁺ and Cl⁻ ions crystallizing out of solution. (Left) An F-center defect in NaCl. (Right) A small cluster of NaCl.

Publications of DOE Sponsored Research (2004-present)

1. Multi-Component Dynamical Nucleation Theory And Sensitivity Analysis, S.M. Kathmann, G.K. Schenter, and B.C. Garrett, *J. Chem. Phys.*, **120**, 9133 (2004).
2. Ion-Induced Nucleation: The Importance of Chemistry, S.M. Kathmann, G.K. Schenter, and B.C. Garrett, *Physical Review Letters*, **94**, 116104 (2005).
3. **Invited Article:** Understanding the Chemical Physics of Nucleation, S.M. Kathmann, A New Perspectives Issue: *Theoretical Chemistry Accounts*, **116**, 169-182, (2006).
4. The Use of Processor Groups in Molecular Dynamics Simulations to Sample Free Energy States, Bruce J. Palmer, Shawn M. Kathmann, Manoj Krishnan, Vinod Tipparaju, and Jarek Nieplocha, *Journal of Chemical Theory and Computation*, **3**, 583 (2006).
5. The Critical Role of Anharmonicity in the Aqueous Ionic Clusters Relevant to Nucleation, Shawn M. Kathmann, Gregory K. Schenter, and Bruce C. Garrett, *Journal of Physical Chemistry B*, **111**, 4977 (2007).
6. Comment on “Quantum Nature of the Sign Preference in Ion-Induced Nucleation”, Shawn M. Kathmann, Gregory K. Schenter, and Bruce C. Garrett, *Physical Review Letters*, **98**, 109603 (2007).
7. Activation Energies and Potentials of Mean Force for Water Cluster Evaporation, Shawn M. Kathmann, Bruce J. Palmer, Gregory K. Schenter, and Bruce C. Garrett, *Journal of Chemical Physics*, submitted (2007).
8. **Invited Article:** The Impact of Molecular Interactions on Atmospheric Aerosol Radiative Forcing, Shawn M. Kathmann, Gregory K. Schenter, and Bruce C. Garrett, *Advances in Quantum Chemistry: Applications of Theoretical Methods to Atmospheric Sciences*, **Accepted** (2007).
9. **Invited Article:** “Water, The Wellspring of Life”, Chris J. Mundy, Shawn M. Kathmann, Gregory K. Schenter, *Natural History*, **Accepted** (2007).

Radiation Effects in Heterogeneous Systems and at Interfaces

Jay A. LaVerne, Dan Meisel, Ian Carmichael, Daniel M. Chipman,

Radiation Laboratory, University of Notre Dame, Notre Dame, IN 46556

laverne.1@nd.edu; meisel.1@nd.edu; carmichael.1@nd.edu; chipman.1@nd.edu;

Program Scope

Radiation chemistry techniques are used to probe the influence of solid interfaces on the decomposition of water and aqueous solutions. Experimental examination of systems ranging from aqueous dispersions of nanoparticles to hydroxide monolayers are coupled with model calculations on the stability of transient and interfacial species to give a complete description of the radiolytic processes. Interfaces provide the opportunity for the transfer of energy and charge between two phases and are relevant to many practical technological problems of importance to the Department of Energy. Heterogeneous systems are frequently encountered in the management of nuclear materials and nuclear waste, and in nuclear power plant infrastructure. The development of new materials are intended to give the ability to localize radiation damage.

One part of the experimental thrust is to examine the influence of ceramic oxide interfaces on the stable products in the radiolysis of water. Aqueous suspensions or slurries are used to determine the effect of different oxide interfaces on the radiolytic production or destruction of H_2 and H_2O_2 . Variations in surface-bound species such as hydroxides and other oxides are being examined using FTIR and Raman reflection techniques. The focus is to identify and quantify the species escaping from the interface as well as those absorbed on it following radiolysis. An important contribution to this program includes the atomistic level characterization of the interface, which greatly aids in identification of the decomposition mechanism.

A second experimental component of this program is to determine the fate of charge carriers, generated by ionizing radiation, in multi-phase systems, e.g., aqueous suspensions of solid nanoparticles. Particularly important is the distance that the carriers can migrate to the interface and thereby affect the chemical processes that occur in the either one of the two phases. The exchange of carriers across the interface is in competition with recombination and trapping processes within the parent phase and therefore is expected to dependent not only on the material but on also on the processing and history of the composite. Both wide-band semiconductors or insulators and metallic systems are of interest in this study. Wet colloidal - chemistry strategies are used to prepare the heterogeneous system on the nanometer scale, and both steady state, as well as time domain radiation chemistry techniques are utilized to determine the dynamics of the carriers.

Recent Progress

Modifications to water – zirconia nanoparticle interfaces induced by γ -irradiation have been examined using diffuse reflection infrared Fourier transform (DRIFT), Raman scattering, and electron paramagnetic resonance (EPR) techniques. Spectroscopy with *in situ* heating was used to probe variations in the dissociatively bound chemisorbed water on the zirconia nanoparticles following evaporation of the physisorbed water. DRIFT spectra show that the bridged Zr – OH – Zr species decreases relative to the terminal Zr – OH species upon irradiation.

No variation is observed with Raman scattering, indicating that the zirconia morphology is unchanged. EPR measurements suggest the possible formation of the superoxide ion, presumably by modification of the surface OH groups. Trapped electrons and interstitial H atoms are also observed by EPR.

Under typical ambient conditions there are about 2 layers of physisorbed water on the surface of nanometer sized ZrO_2 particles and at least one layer of dissociated chemisorbed water. This overlayer of physisorbed water can readily be observed as a broad peak at 3435 cm^{-1} in the DRIFT spectrum. Examination of the water – ZrO_2 interface was possible by increasing the sample temperature. Much of the physisorbed water is eliminated on heating to 473 K resulting in the appearance of the chemisorbed OH bands. A band at 3696 cm^{-1} assigned to the $\nu(\text{OH})$ bridged $\text{Zr} - \text{OH} - \text{Zr}$ group shifts down by 44 cm^{-1} and decreases in intensity when the temperature was raised to 703 K. An additional band appears at 3733 cm^{-1} and is assigned to $\nu(\text{OH})$ of the terminal $\text{Zr} - \text{OH}$ group. The $\text{Zr} - \text{OH}$ and $\text{Zr} - \text{OH} - \text{Zr}$ bands after γ -radiolysis show different peak intensities, especially at 3733 cm^{-1} , indicating the participation of these surface groups in the irradiation process.

Preliminary steps have been taken to gain insight into these surface processes. *Ab initio* density functional theory was used to investigate the stable and metastable states of adsorbed molecular water on the $\alpha\text{-Al}_2\text{O}_3$ (0001) surface as a function of coverage ranging from dry, through partially hydroxylated, to fully hydrated. At no coverage is the water binding great enough to overcome the energetic preference for water to dissociatively adsorb. However the calculations also reveal thermodynamically stable arrangements combining both partially dissociated and molecularly-intact layers. Spectroscopic signatures have been developed for the various predicted species

The effect of seemingly inert support (silica particles) for silver nanoparticles on the fate of the primary species in the radiolysis of aqueous suspensions was studied. The support may lead to a relatively rapid deterioration of the activity of the particle, which otherwise can persistently operate as a redox catalyst in converting single-electron transfer radicals to molecular hydrogen. As the hydrogen evolution reaction progresses and hydrogen accumulates, the Fermi level of the particles rises, which in turn leads to a reduced rate of electron transfer from the reducing radicals to the metallic particle. However, this redox reaction competes with radical-radical recombination reactions, presumably catalyzed at the surface of the support, which become dominant at high doses. Strategies to minimize these adverse effects of the support can be offered once the underlying mechanism is available.

Irradiation with relatively low-energy x-rays (tens of keV) is a promising approach to direct the radiation damage to a selected region within the target. Because of the selectivity of the absorption of energy in this energy range, primarily by the photoionization process, high-Z element, e.g. metals, absorb significantly more energy than common organic- and bio-molecules. However, for the damage to reach the target molecule the charge carriers need to arrive at the metallic surface. Preliminary experiments have measured aqueous yields (H_2 , for example) in suspensions of high concentrations of metallic particles. These yields are measured at Argonne's APS (in collaboration with Prof. B. Bunker) as a function of x-ray energy and compared with yields from high-energy (MeV range) γ -irradiation at Notre Dame. Preliminary results with particles of $\sim 30\text{ nm}$ size indicate efficient yield of energy transfer to the interface. These particles require the synthetic methodology outlined below.

Synthetic methods for the production of metallic nanoparticles in aqueous suspension in the absence of any organic or inorganic foreign substance have been developed. These methods

are based on reduction of the corresponding oxide with molecular hydrogen. Thus only the metal at its various oxidation states (dominated by the metallic state, of course) and water or its ions are present in the system. In the case of silver, the mechanism of production of the particles has been outlined and the particles, their surface potential, point of zero charge, and composition of the suspensions have been determined. The performance of these catalysts in the hydrogen evolution reaction has been tested. Because the production reaction utilizes a relatively low reduction-potential reductant (H^+/H_2 couple), the presence of parent metallic ions at the end of the reaction cannot be prevented. Some of the initial reduction equivalents that are produced by the radiation are therefore utilized to complete the reduction of the ions and to build high enough over-potential that can sustain hydrogen evolution. The extent of this required “preconditioning” of the particles has been measured and methods to minimize it have been developed for silver suspensions.

Future Plans

Observation of the processes occurring in the radiolysis of water – ceramic oxide interfaces under ambient conditions is obscured by the presence of the overlayer of physisorbed water. Furthermore, reflectance optical methods for the examination of powder surfaces are difficult to quantify because of surface irregularities. A device is currently under construction that will allow for the *in situ* irradiation and observation of powder samples. The device will initially be designed to measure DRIFT spectra, but other capabilities will be added as the program progresses. Optical variations of the ceramic oxide surfaces will be coupled with stable product formation and theoretical predictions of interfacial species in order to elucidate the radiation induced reactions at interfaces.

Minimum energy paths linking the various locally-stable structures for water absorption onto the α - Al_2O_3 (0001) surface will be elucidated and kinetically accessible transformations characterized. Calculations will be extended to encompass more relevant ceramic oxides such as zirconia.

Low-energy x-rays may be able to direct radiation damage to a selected region within the target because of the selectivity of the absorption of energy. Future experiments will measure aqueous yields such as H_2 in suspensions of high concentrations of metallic particles using the APS at Argonne (in collaboration with Prof. B. Bunker). Variation of x-ray energy will tune for the selective absorption of energy by the high Z elements of metallic particles as compared to the surrounding water or organic compounds. The results will be compared with yields from high-energy γ -irradiation at Notre Dame.

Synthetic methods have been developed for the production of metallic nanoparticles in aqueous suspension in the absence of any organic or inorganic foreign substance. Preliminary experiments on the effectiveness of these particles in enhancing Raman activity have begun. The particles at various stages of their preparation all show intense Surface Enhanced Raman Scattering, SERS, of probe molecules at sub-micromolar concentration levels. At these concentrations little radiation-induced damage to the probe is detected (or expected) and the probe only reports on the state of the particles. The effect of particle size, radiation dose, concentrations of electrolyte and pH on the probe-SERS intensity, relative line intensities, and band position will be examined. These studies will be extended to allow time-resolved determination of the evolution of the particles during hydrogen evolution redox catalysis.

Publications Sponsored by this DOE Program, 2004-2007

- R. Benoit, M-L. Saboungi, M. Tréguer-Delapierre, B. H. Milosavljevic, D. Meisel (2007) "Reactions of Radicals with Hydrolyzed Bismuth (III) Ions: A Pulse Radiolysis Study," **J. Phys. Chem. A**, accepted.
- V. A. Ranea, W. F. Schneider and I. Carmichael (2007) Molecular water absorption on the α -Al₂O₃(0001) surface. A DFT investigation." **Surf. Sci.** accepted.
- Getahun Merga, Robert Wilson, Geoffrey Lynn, Bratoljub H. Milosavljevic, and Dan Meisel (2007) "Redox Catalysis on "Naked" Silver Nanoparticles," **J. Phys. Chem. C** *111*, 12220-6.
- T. Zidki, H. Cohen, D. Meyerstein and Dan Meisel (2007) "Effect of Silica-Supported Silver Nanoparticles on Dihydrogen Yields from Irradiated Aqueous Solutions," **J. Phys. Chem. C** *111*, 10461-6.
- G. Merga, B. H. Milosavljevic, and D. Meisel (2006) "Radiolytic Yields in Aqueous Suspensions of Gold Particles," **J. Phys. Chem. B** *110*, 5403-8.
- Q. Dai, D. Menzies, Q. Wang, A. E. Ostafin, S. N. Brown, D. Meisel, and E. J. Maginn (2006) "Synthesis and Composition Analysis of Microsilica Encapsulated Acetyl-Acetonato-Carbonyl-Triphenylphosphine-Rhodium Catalyst," **Nanotech.** *5*, 677-82.
- F. Stevens, I. Carmichael, F. Callens, M. Waroquier (2006) "Density functional investigation of high-spin XY (X = Cr, Mo, W and Y = C,N,O) molecules" **J. Phys. Chem. A** *110*, 4846-53..
- F. Stevens, V. Van Speybroeck, I. Carmichael, F. Callens, M. Waroquier (2006) "The Rh-ligand bond: RhX (X = C, N, O, F, P and Cl) molecules" **Chem. Phys. Lett.** *421*, 281-6..
- D. Lahiri, B. A. Bunker, B. Mishra, Z. Zhang, D. Meisel, C. M. Doudna, M. F. Bertino, F. D. Blum, A. T. Tokuhira, S. Chattopadhyay, T. Shibata, and J. Terry (2005) "Bimetallic Pt-Ag and Pd-Ag Nanoparticles," **J. App. Phys.** *97*, 094304-12.
- Jay A. LaVerne (2005) "H₂ Formation from the Radiolysis of Liquid Water with Zirconia", **J. Phys. Chem. B** *109*, 5395-5397.
- A. Hiroki and Jay A. LaVerne (2005) "Decomposition of Hydrogen Peroxide at Water-Ceramic Oxide Interfaces", **J. Phys. Chem. B** *109*, 3364-3370.
- Bruce C. Garrett, et al. (2005) "The Role of Water in Electron-Initiated Processes and Radical Chemistry: Issues and Scientific Advances," **Chem. Rev.** *105*, 355-90.
- Dan Meisel (2005) "Radiation Effects on Nanoparticles", Proceedings of the International Atomic Energy Agency Panel on "Emerging Applications of Radiation in Nanotechnology, "IAEA Press, Vienna, ISSN 1011-4289, ISBN 92-0-100605-5, pp. 130-141.
- Bratoljub H. Milosavljevic, and Dan Meisel (2004) "Kinetic and Thermodynamic Aspects of Adsorption on Silica Nanoparticles. A Pulse Radiolysis Study" **J. Phys. Chem. B** *108*, 1827-30.
- Bratoljub H. Milosavljevic, Simon M. Pimblott and Dan Meisel (2004) "Yields and Migration Distances of Reducing Equivalents in the Radiolysis of Silica Nanoparticles" **J. Phys. Chem. B** *108*, 6996-7001.
- Dan Meisel (2004) "Radiation Chemistry in the Real World: Nanoparticles in Aqueous Suspensions", in "Proceedings of the International Atomic Energy Agency Workshop on "Advances in Radiation Chemistry", IAEA Press, Vienna, ISSN 1011-4289, ISBN 92-0-112504-6, pp. 5-14.
- Jay A. LaVerne (2004) in: Proceedings of the International Atomic Energy Agency Workshop on "Advances in Radiation Chemistry of Polymers", IAEA Press, Vienna, p. 15-20.

Solution Reactivity of Nitrogen Oxides, Oxoacids, and Oxoanions

Sergei V. Lymar

Chemistry Department, Brookhaven National Laboratory, Upton, NY 11973-5000

e-mail: lymar@bnl.gov

Program Scope

This program investigates the physical chemistry of (primarily inorganic) nitrogen-oxygen compounds that are involved in environmental problems and are also central to the radiation-induced reactions that occur during nuclear fuel processing and within radioactive nuclear waste. Equally important and diverse are the biological roles of nitrogen oxides, their oxoacids, and anions.

Inorganic nitrogen forms a large number of metastable compounds whose thermodynamic properties and reactivity are not sufficiently understood, especially for the nitrogen in low positive oxidation states, the subject of the greatest current interest. Despite a large body of research, there is no consensus concerning the fundamental properties of this species. This is an area where there is a clear need for accurate elucidation of the prospective reactions in terms of their rates and mechanisms. On the experimental side, this program applies the radiation chemistry techniques (primarily pulse radiolysis) and, to a lesser extent, other kinetic methods (flash photolysis, stopped flow).

Progress

The nearest redox neighbors of NO and the simplest nitrogen(+1) species are nitroxyl (H-N=O) and its conjugate NO⁻ anion. Although numerous reactions of nitroxyl have been proposed, important aspects of the nitroxyl aqueous chemistry have been misunderstood and little quantitative information exists on the reactivity of nitroxyl and its adducts. Among the latter, prominent are the so-called NONOates, the compounds of the general structure X[N(O)NO]⁻, where X is a strongly nucleophilic group, such as aminyl (R₂N) or oxyl (O⁻).¹

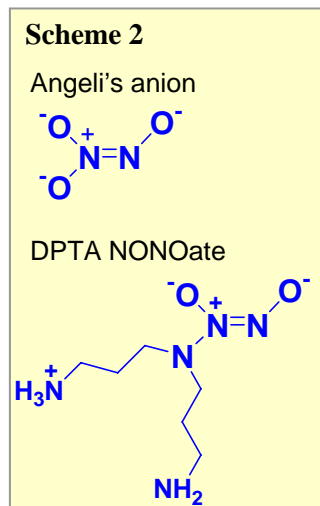
Recently, we²⁻⁵ have suggested a reevaluation of the molecular and thermodynamic properties of nitroxyl by concluding that: (i) NO⁻ has a triplet ground state, whereas the ground state of HNO is a singlet, and (ii) ¹HNO is a much weaker acid, pK_a(¹HNO/³NO⁻) ≈ 11.4, than it was widely accepted previously (pK_a of 4.7^{6,7}). In nearly all reported cases invoking nitroxyl as an intermediate, the rate-determining step was its generation, which allows little insight into properties and reactivity. In contrast, we have used pulse radiolysis to rapidly generate the nitroxyl species and to investigate their reactivity.

One-electron reduction of aqueous NO by the hydrated electrons and hydrogen atoms has been investigated by pulse radiolysis.⁵ Both the hydrated electron and the hydrogen atom reduce NO to yield the ground state triplet ³NO⁻ and singlet ¹HNO, respectively, which further react with NO to produce the N₂O₂⁻ radical, albeit with the very different specific rates, k(³NO⁻ + NO) = (3.0 ± 0.8) × 10⁹ and k(¹HNO + NO) = (5.8 ± 0.2) × 10⁶ M⁻¹ s⁻¹ (Scheme 1). These reactions occur much more rapidly than the spin-forbidden acid-base equilibration of ³NO⁻ and ¹HNO under all experimentally accessible conditions. As a result and contrary to the previously accepted reaction mechanism,^{6,7} the spin prohibition gives rise to two reaction pathways well separated in time, but leading to the same intermediates and products. The N₂O₂⁻ radical extremely rapidly acquires another NO, k(N₂O₂⁻ + NO) = (5.4 ± 1.4) × 10⁹ M⁻¹ s⁻¹, producing the

closed-shell N_3O_3^- anion, which unimolecularly decays to the final $\text{N}_2\text{O} + \text{NO}_2^-$ products with $\sim 300 \text{ s}^{-1}$ rate constant.

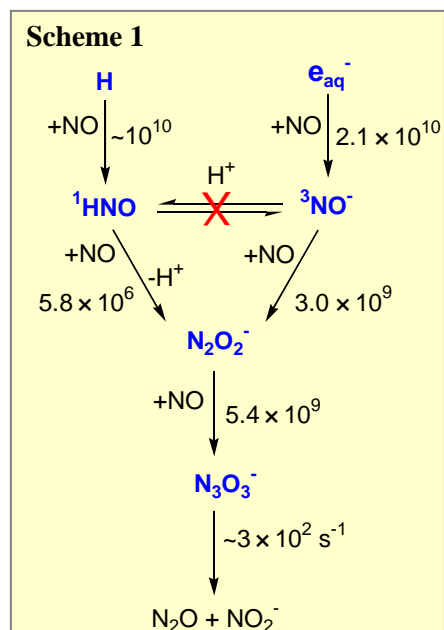
Contrary to the previous belief, N_2O_2^- is stable with respect to NO elimination and so is N_3O_3^- . The optical spectra of all intermediates have also been re-evaluated. The only intermediate whose spectrum can be cleanly observed in the pulse radiolysis experiments is the N_3O_3^- anion ($\lambda_{\text{max}} = 380 \text{ nm}$, $\epsilon_{\text{max}} = 3.76 \times 10^3 \text{ M}^{-1} \text{ cm}^{-1}$). The spectra previously assigned to the NO^- anion and to the N_2O_2^- radical are due, in fact, to a mixture of species (mainly N_2O_2^- and N_3O_3^-) and to the N_3O_3^- anion, respectively. Spectral and kinetic evidence suggests that the same reactions occur when $^3\text{NO}^-$ and ^1HNO are generated by photolysis of the monoprotonated anion of Angeli's anion, HN_2O_3^- , in NO-containing solutions.

Photoinduced release of nitroxyl and nitric oxide from NONOates has been investigated⁸ by laser kinetic spectroscopy in a comparative



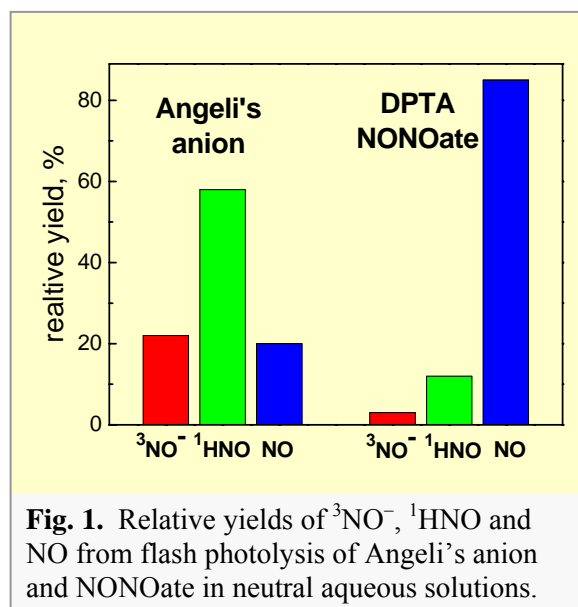
study of diazen-1-ium-1,2,2-triolate (Angeli's anion) and (Z)-1-[N-(3-aminopropyl)-N-(3-aminopropyl)amino]diazen-1-ium-1,2-diolate (DPTA NONOate, Scheme 2). The $[\text{N}(\text{O})\text{NO}]^-$ group is photosensitive, decomposing upon illumination in its characteristic mid-UV absorption band.

In neutral aqueous solutions, a 266 nm photolysis of these NONOates generates a unique spectrum of primary products including the triplet $^3\text{NO}^-$ and singlet ^1HNO nitroxyl species, and NO (Fig. 1). Formation of these products has been revealed and quantitatively assayed by analyzing a complex set of their cross-reactions leading to the formation of colored intermediates, the N_2O_2^- radical and N_3O_3^- anion. The experimental design employed takes advantage of the extremely slow spin-forbidden protic equilibration between $^3\text{NO}^-$ and ^1HNO and the vast difference in their reactivity toward NO. To account for the kinetic data, a novel combination reaction, $^3\text{NO}^- + ^1\text{HNO}$, is introduced and its rate constant of $6.6 \times 10^9 \text{ M}^{-1} \text{ s}^{-1}$ is measured by competition with the reduction of methylviologen by $^3\text{NO}^-$. The latter reaction occurring with $2.1 \times 10^9 \text{ M}^{-1} \text{ s}^{-1}$ rate constant and leading to the stable, colored methylviologen radical cation is useful for detection of $^3\text{NO}^-$. The distributions of the primary photolysis products (Angeli's anion: 22% $^3\text{NO}^-$, 58% ^1HNO , and 20%



Angeli's anion) and (Z)-1-[N-(3-aminopropyl)-N-(3-aminopropyl)amino]diazen-1-ium-1,2-diolate (DPTA NONOate, Scheme 2). The $[\text{N}(\text{O})\text{NO}]^-$ group is photosensitive, decomposing upon illumination in its characteristic mid-UV absorption band.

In neutral aqueous solutions, a 266 nm photolysis of these NONOates generates a unique spectrum of primary products including the triplet $^3\text{NO}^-$ and singlet ^1HNO nitroxyl species, and NO (Fig. 1). Formation of these products has been revealed and quantitatively assayed by analyzing a complex set of their cross-reactions leading to the formation of colored intermediates, the N_2O_2^- radical and



NO; DPTA NONOate: 3% $^3\text{NO}^-$, 12% ^1HNO , and 85% NO) show that neither diazeniumdiolate is a highly selective photochemical generator of nitroxyl species or nitric oxide, although the selectivity of DPTA NONOate for NO generation is clearly greater.

Future Plans

The reactions of $^3\text{NO}^-$ with O_2 and $^1\text{HNO}/^3\text{NO}^-$ with NO remain the only two nitroxyl reactions measured directly despite the expectations of the rich chemistry for nitroxyl, which is simultaneously a Lewis acid and base, a hydrogen atom donor, and a redox agent. This chemistry will be explored along with the properties and reactivity of the most consequential adducts of nitroxyl.

Pathways and energetics of NO reduction will be investigated with the purposes to develop new methods of generating nitroxyl and to establish its thermochemistry. With respect to the former, reduction of NO by the CO_2^- radical is of interest. All present estimates for the reduction potentials for NO and $\text{p}K_a$ for HNO involve significant assumptions spreading a range of ~ 0.1 V and ~ 4 $\text{p}K_a$ units; we will attempt determination of nitroxyl thermochemistry by measuring its redox equilibria.

Spin-forbidden bond breaking/making reactions involving nitroxyl will be investigated. The first is protonation of $^3\text{NO}^-$ by Brønsted acids; reactions of this type could appreciably modulate nitroxyl reactivity in buffered environments. The second spin-forbidden reaction of interest is the addition of $^3\text{O}_2$ to ^1HNO , which could directly lead to peroxynitrite, ONOO^- , and is potentially very significant because it replaces mildly reducing HNO by strongly oxidizing ONOO^- .

Properties and reactivity of nitroxyl adducts with NO and NO_2^- will be investigated. We have found that the NO adduct, the hyponitrite radical (N_2O_2^-), is rapidly formed from $^1\text{HNO}/^3\text{NO}^-$ in NO-containing environments⁵ and should be both strongly oxidizing and moderately reducing.⁴ However, nothing is known about N_2O_2^- reactivity and the most important prospective reactions will be explored.

Thermal decomposition of trioxodinitrate ($\text{N}_2\text{O}_3^{2-}$) is the most widely used source of nitroxyl. Redox potentials for $\text{N}_2\text{O}_3^{2-}$ are unknown, but we expect it to be readily oxidizable. It therefore will be of interest to investigate the one-electron oxidation mechanism and possible formation and properties of the N_2O_3^- radical, which has been implicated in various reactions. One-electron reduction of $\text{HN}_2\text{O}_3/\text{N}_2\text{O}_3^{2-}$ that may provide a convenient alternative pathway to the hyponitrite radical will also be explored.

Collaborators on this project include V. Shafirovich (NYU) and N. Shaikh (BNL); past contribution from G. A. Poskrebshev is acknowledged. Other pulse radiolysis work involving solvent protonation of aryl radical anions has been done in collaboration with J. Miller.⁹

References (DOE sponsored publications in 2004-present are marked with asterisk)

- (1) Hrabie, J. A.; Keefer, L. K. *Chem. Rev.* **2002**, *102*, 1135-1154.
- (2) Shafirovich, V.; Lyman, S. V. *Proc. Natl. Acad. Sci. USA* **2002**, *99*, 7340-7345.
- (3) Shafirovich, V.; Lyman, S. V. *J. Am. Chem. Soc.* **2003**, *125*, 6547-6552.
- (4*) Poskrebshev, G. A.; Shafirovich, V.; Lyman, S. V. "Hyponitrite Radical, A Stable Adduct of Nitric Oxide and Nitroxyl," *J. Am. Chem. Soc.* **2004**, *126*, 891-899.

- (5*) Lymar, S. V.; Shafirovich, V.; Poskrebyshv, G. A. "One-Electron Reduction of Aqueous Nitric Oxide: A Mechanistic Revision," *Inorg. Chem.* **2005**, *44*, 5212-5221.
- (6) Grätzel, M.; Taniguchi, S.; Henglein, A. *Ber. Bunsen-Ges. Phys. Chem.* **1970**, *74*, 1003-1010.
- (7) Seddon, W. A.; Fletcher, J. W.; Sopchyshyn, F. C. *Can. J. Chem.* **1973**, *51*, 1123-1130.
- (8*) Lymar, S. V.; Shafirovich, V. "Photoinduced Release of Nitroxyl and Nitric Oxide from Diazeniumdiolates," *J. Phys. Chem. B* **2007**, *111*, 6861-6867.
- (9*) Funston, A. M.; Lymar, S. V.; Saunders-Price, B.; Czapski, G.; Miller, J. R. "Rate and Driving Force for Protonation of Aryl Radical Anions in Ethanol," *J. Phys. Chem. B* **2007**, *111*, 6895-6902.
- (10*) Garrett, B. C.; Dixon, D. A.; Camaioni, et al. "Role of Water in Electron-Initiated Processes and Radical Chemistry: Issues and Scientific Advances," *Chem. Rev.* **2005**, *105*, 355-390.

Spectroscopy of Organometallic Radicals

Michael D. Morse

Department of Chemistry

University of Utah

315 S. 1400 East, Room 2020

Salt Lake City, UT 84112-0850

morse@chem.utah.edu

I. Program Scope:

In this project, we seek to obtain fundamental physical information about unsaturated, highly reactive organometallic radicals containing open *d* subshell transition metal atoms. Gas phase electronic spectroscopy of jet-cooled transition metal molecules is used to obtain fundamental information about ground and excited electronic states of such species as the transition metal carbides and organometallic radicals such as CrC₂H, CrCH₃, and NiCH₃. High resolution infrared spectroscopy is applied to the unsaturated transition metal carbonyls, MCO, M(CO)₂, M(CO)₃, *etc.*

II. Recent Progress:

A. Optical spectroscopy of RuC, CrC₂H, CrCH₃, NiCH₃, YF, and OsC

During 2004-2007, we have used resonant two-photon ionization (R2PI) and dispersed fluorescence (DF) spectroscopic methods to investigate the transition metal carbides, RuC¹ and OsC;⁶ the polyatomic transition metal radicals CrC₂H, CrCH₃, and NiCH₃;² and have discovered and analyzed a spin-forbidden band system in YF.⁵ Our work on RuC characterized several excited states of the molecule,¹ making it one of the best understood of all the transition metal carbides. More recently, we have obtained and analyzed high quality spectra of OsC,⁶ which allow us to make comparisons between the isovalent molecules FeC, RuC, and OsC, all of which have been studied in our laboratories. Considering only the valence *nd* and (*n*+1)*s* orbitals of the metals and the 2*s*, 2*p* orbitals of carbon, the valence orbitals of the MC molecules are the low-lying 1σ, 2σ, and 1π orbitals, the non-bonding 1δ and 3σ orbitals, and the antibonding 2π and 4σ orbitals. Among the FeC, RuC, and OsC molecules, the 1σ, 2σ, and 1π orbitals are all filled, and the 4 remaining electrons are distributed between the non-bonding 1δ and 3σ orbitals. A molecular orbital diagram appropriate for these molecules is provided in Figure 1 below. Our work has shown that the ground states of these species are 1δ³ 3σ¹ for FeC and OsC, but 1δ⁴, 1Σ⁺ for RuC. Figure 2 below displays a rotationally resolved spectrum of ¹⁹²Os¹²C, demonstrating that the molecule possesses a ³Δ₃ ground term. In addition to determining the ground state, our recent work on OsC shows that the first excited state of this molecule is the 1δ² 3σ², ³Σ⁻ (Ω = 0⁺) term,⁶ which lies very high in energy in RuC. The observation of a low-energy 1δ² 3σ², ³Σ⁻ state in OsC demonstrates the relativistic stabilization of the 3σ orbital, which is shown by our hyperfine measurements to be primarily Os 6*s* in character.

In other work, we have published the vibrationally resolved R2PI and DF spectra of CrC₂H, CrCH₃, and NiCH₃.² These molecules are among the most complicated open *d*-subshell molecules yet known for which gas phase optical spectra have been obtained. The vibronically resolved spectra that have been recorded for CrC₂H and NiCH₃ have allowed metal-carbon

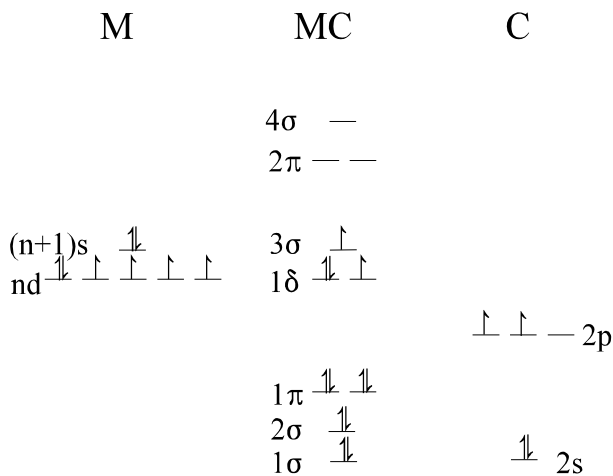


Figure 1. Molecular orbital diagram for the transition metal carbides FeC, RuC, and OsC.

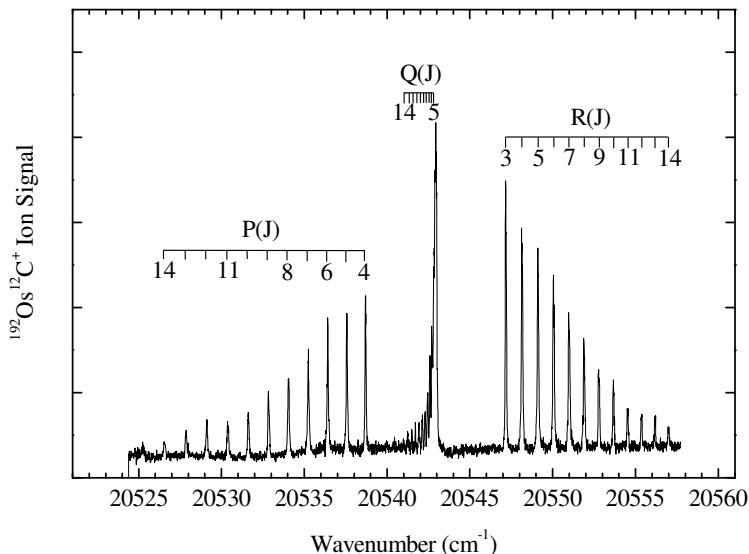


Figure 2. Rotationally resolved spectrum of the [20.6] $\Omega' = 3 \leftarrow X^3\Delta_3$ 0-0 band of $^{192}\text{Os}^{12}\text{C}$.

vibrational frequencies and anharmonicities to be measured for these species in their excited states. For NiCH_3 , values of ω_e and $\omega_e x_e$ were also obtained for the ground state. For CrCH_3 and CrC_2H , values of $\Delta G_{1/2}$ for the Cr-C stretching vibration were also obtained for the ground state. Rotationally resolved scans over all three molecules have been accomplished, but these have not yet yielded to analysis. The NiCH_3 scans show obvious perturbations, since the different vibrational levels of the upper state and the scans over the ^{58}Ni and ^{60}Ni isotopomers are all very different in appearance. In contrast, the rotationally resolved spectra of CrC_2H and CrCH_3 are a forest of lines. In the case of the $^6\Sigma^+ \leftarrow X^6\Sigma^+$ transition of CrC_2H (which has 54 rotational branches), we have been able to identify lines that belong to the P_1 , R_1 , R_2 , R_5 , R_{31} , R_{35} , R_{42} , and R_{62} branches. We are now experimenting with different numberings of these lines, and expect that we will be able to analyze and fit the spectrum.

During the collection of data on CrC_2H , we also recorded the spectrum of the minor isotopomer of chromium hydride, $^{50}\text{Cr}^1\text{H}$. We measured the excited state lifetime of this species, which is currently of considerable interest in astrophysics. This paper has now been published in the *Astrophysical Journal*.³

During a study of the YCo diatomic metal molecule (funded by the NSF), we noticed transitions occurring at the mass of YF .⁵ The YF molecules are formed by accident by the reaction of atomic yttrium with Teflon tape residue that remains in the instrument after it was used many years ago. A quick scan of the published spectroscopy of YF showed that some of the bands that were observed in this extremely well-studied molecule had not been previously observed. Accordingly, we expanded our investigation to include a study of these features, which fall within the framework of the DOE project. The new bands were found to belong to the spin-forbidden $c^3\Sigma_1^+ \leftarrow X^1\Sigma^+$ band system. Our investigation provided a linkage between the singlet and triplet manifolds of YF , along with a detailed analysis of the spin-orbit interactions

within the states arising from the $Y^+ (^1,^3D) + F^- (^1S)$ states of the separated ions. The analysis showed that the $c^3\Sigma_1^+$ state is contaminated with approximately 2% $B^1\Pi$ character, and this spin-orbit mixing causes the $c^3\Sigma_1^+ \leftarrow X^1\Sigma^+$ band system to gain sufficient intensity to be observed.

B. Infrared Spectroscopy of unsaturated transition metal carbonyls

We have developed a slit-jet discharge source diode laser spectrometer for high-resolution investigations of unsaturated transition metal carbonyls, and have used it to record a spectrum of the monoligated molecule NiCO. This species provides a model for the interaction between CO molecules and a Ni surface. The fitted constants from our study provide band origins of 2010.692 89(34) and 2010.645 28(23) cm^{-1} for $^{58}\text{NiCO}$ and $^{60}\text{NiCO}$, respectively. Rotational constants and bond lengths determined from the spectra are consistent with values reported from the millimeter wave spectroscopic study that was published in 2004.

While collecting the NiCO spectrum, we also observed the spectrum of a molecule that depleted when the discharge was turned on. This was surprising, since the parent molecule, $\text{Ni}(\text{CO})_4$ has no known transitions in this region. After some investigation, the spectrum was determined to arise from the isotopically substituted species, $\text{Ni}(\text{CO})_3(^{13}\text{CO})$ and $\text{Ni}(\text{CO})_3(\text{C}^{18}\text{O})$, which constitute only 4.3 % and 0.8 % of the molecules in the sample, respectively. From the measured rotational constants, $B''(\text{Ni}(\text{CO})_3(^{13}\text{CO})) = 0.034736(2) \text{ cm}^{-1}$ and $B''(\text{Ni}(\text{CO})_3(\text{C}^{18}\text{O})) = 0.033764(4) \text{ cm}^{-1}$, the Ni-C and C-O bond lengths were determined to be $r_0(\text{Ni-C}) = 1.839(7) \text{ \AA}$ and $r_0(\text{C-O}) = 1.121(10) \text{ \AA}$.

III. Future Plans

A. R2PI and DF spectroscopy of transition metal carbides and radicals

Projects for the upcoming year include: (1) Assignment of the rotational lines in the ${}^6\Sigma^+ \leftarrow X^6\Sigma^+$ band system of CrCCH and fitting of the spectrum to extract the spectroscopic constants; (2) Analysis of the rotationally resolved spectrum of TiC, using dispersed fluorescence from single rovibronic levels to identify the lines; (3) Resolution of the rotational structure and analysis of a red band system of MoC; (4) Attempts to record and analyze the spectra of several transition metal cyanides (or isocyanides) will be made. Species to be investigated will include CuCN, AgCN, AuCN, ScNC, and YNC (these latter two molecules are thought to be isocyanides, while the former are expected to be cyanides). When the spectrum of CrCCH has been successfully analyzed, we will attempt to record the spectrum of the isovalent molecule, CrCN.

B. IR spectroscopy of unsaturated transition metal carbonyls

We have been having difficulty finding spectra of other unsaturated transition metal carbonyls beyond FeCO, $\text{Fe}(\text{CO})_2$, and NiCO. We have searched for spectra of CrCO, $\text{Cr}(\text{CO})_2$, $\text{Ni}(\text{CO})_2$, and $\text{Fe}(\text{CO})_3$ without success. Attempts to modify the nozzle to allow the metal atom and CO to recombine more readily have been made, again without success. To gain greater control over the fragmentation process, in the hope of being able to detect spectra of species with additional CO ligands, we are now moving to a photolysis source. It is our hope that by controlling the wavelength of the photolysis, we will be able to control the loss of CO atoms so that species such as $\text{Fe}(\text{CO})_3$, $\text{Ni}(\text{CO})_2$, and $\text{Ni}(\text{CO})_3$ may be investigated.

C. Photodissociation spectroscopy of cold, trapped ions

During my 2005 sabbatical leave working with John Maier at the University of Basel, I was very impressed with the capabilities of his newly-constructed mass-selected ion trap photodissociation spectrometer, which produces spectra of cryo-cooled gas phase ions with unprecedented signal-to-noise ratios. I have decided to build a similar device here at the University of Utah, for the study of unsaturated transition metal cation species (among other species). This project is a major part of my renewal proposal, and I have already begun collecting the equipment needed to construct the instrument. The instrument will eventually be able to use either a laser-ablation, an electrospray, or an electric discharge ion source. The ions will be mass selected using a quadrupole mass filter and trapped in a 22-pole radio frequency ion trap that contains a low pressure of helium (about 0.4 mTorr). The trap will be connected to a cryostat, allowing it to be cooled to about 5 K, and this low temperature will be transferred to the trapped ions by collisions with helium. The trapped ions will then be subjected to pulsed dye laser radiation, leading to photofragmentation when the dye laser is resonant with a transition that leads to 1- or 2-photon fragmentation. The ions will then be released from the trap into a second quadrupole mass filter, tuned to transmit the expected fragment ions, which are then detected using a Daly detector. The fragment ion intensity, as a function of the wavenumber of the dye laser, then provides the spectrum of the trapped ion.

To facilitate building the new instrument, I have recently acquired a used Sciex API III triple quadrupole mass spectrometer, which provides a significant fraction of the required equipment. In addition to the two required quadrupole mass filters, this instrument also has an electrospray ion source and vacuum pumps that will be very useful in putting together our trapped ion photodissociation spectrometer.

IV. Publications from DOE Sponsored Research 2004-present:

1. N. F. Lindholm, D. A. Hales, L. A. Ober and M. D. Morse, "Optical spectroscopy of RuC: 18 000 - 24 000 cm⁻¹," J. Chem. Phys. **121**, 6855-60 (2004).
2. D. J. Brugh, R. S. DaBell and M. D. Morse, "Vibronic spectroscopy of unsaturated transition metal complexes: CrC₂H, CrCH₃, and NiCH₃," J. Chem. Phys. **121**, 12379-85 (2004).
3. S. Shin, D. J. Brugh, and M. D. Morse, "Radiative lifetime of the v=0,1 levels of the A⁶Σ⁺ state of CrH," Astrophys. J. **619**, 407-11, (2004).
4. Alonzo Martinez and Michael D. Morse, "Infrared Diode Laser Spectroscopy of Jet-Cooled NiCO, Ni(CO)₃(¹³CO), and Ni(CO)₃(C¹⁸O)," J. Chem. Phys. **124**, 124316/1 - 124316/8 (2006).
5. Ramya Nagarajan and Michael D. Morse, "Spin-forbidden c³Σ₁⁺ ← X¹Σ⁺ band system of YF," J. Chem. Phys. **126**, 144309/1-6 (2007).
6. Olha Krechkivska and Michael D. Morse, "Resonant two-photon ionization spectroscopy of jet-cooled OsC," J. Chem. Phys. (accepted for publication).

LASER DYNAMIC STUDIES OF PHOTOREACTIONS ON NANOSTRUCTURED SURFACES

Richard Osgood,

Center for Integrated Science and Engineering, Columbia University, New York, NY 10027, Osgood@columbia.edu

Program Scope or Definition:

Freestanding “nanoobjects,” such as colloidal quantum dots and nanoclusters, are of interest because of their practical applications, such as light emitters, solar collectors, and catalysts, and because of their interesting fundamental material properties such as their size-dependent electronic structure and excitation energies. Because of the rapid growth of the material-preparation methods for nanoscience, a large number of new techniques have been developed for the growth and probing of such nanoobjects. *Despite these advances there have been relatively few attempts to probe and understand photochemical dynamics on the surfaces of these nanomaterials.* From the viewpoint of surface dynamics we anticipate that the reactions on these nanoscale objects will pose new scientific questions. For example, on large-scale single-crystal surfaces the dominant photoreaction channel is determined by the subtle balance between excited-state quenching and dissociation; how is this balance changed on surfaces of nanoobjects of varying sizes due to reduced density of states and the nature of elementary excitations, e.g. plasmons?

Thus we are undertaking studies of *photoreaction* dynamics on these nanoscale surfaces. Initially we will develop methods to prepare and characterize metal-oxide nanoparticles, taking into account our recent work on measuring photodynamics on single-crystal, metal-oxide surfaces as well as key nano-oxide research done in other universities and National Labs, e.g. PNNL, BNL, and ANL. Our research will address molecular fragmentation-dynamics measurements on two types of freestanding nanoobjects: a) *in-situ* grown metal-oxide nanoparticles and b) *in-situ*-grown noble-metal particles. *Specifically the research goal of our program is to extend our understanding of the photodynamics of molecular adsorbates on surfaces of in-situ-formed metal-oxide-semiconductor nanoparticles and plasmonically active metallic nanoparticles.* Our experiments will use low-energy nanosecond UV pulses to fragment adsorbed-molecules on the particles; these fragments will be detected using TOF mass spectroscopy in our UHV chamber.

Recent Progress:

In-Situ Synthesis and Synthesis Chemistry of Nanoscale-Oxide Particles for UHV Surface Dynamics Experiments: We have made considerable progress in synthesizing and characterizing oxide nanocrystals in our UHV STM system. We have adopted *in situ* nanoparticle-preparation methods for our research, since the most common method of preparation of nanocrystals, colloidal growth, does not easily lend itself to the preparation of a pristine surface following synthesis.

Our approach to synthesis uses *in-situ* UHV growth by reactive-layer growth (RLAD). We have focused on RLAD for synthesis rather than other methods because of the quality of the nanocrystals and the fact they have reasonably narrow size dispersion. In RLAD, a physisorbed multilayer of one reactant is first deposited on a substrate, typically at cryogenic temperatures, *viz* $\sim 110\text{K}$, and the second reactant (metal atoms) is then physical vapor deposited onto this layer. In this case the metal atoms react with the

loosely bound molecular multilayers at relatively low temperatures, perhaps even near their ice temperature. Further raising the substrate temperature causes any unreacted, adsorbed molecules and volatile reaction products to desorb from the substrate surface; the final product compound is then left on the surface as an ensemble of nanoparticles.

Our initial work on synthesis characterized the chemical, structural and electronic properties of these oxide nanoparticles using XPS, STM and STS in collaboration with Jan Hrbek at Brookhaven National Laboratory. We have now begun to examine in more detail the surface synthesis chemistry of these objects in preparation for dynamical studies. This study has used the STM facility at Columbia and has focused on understanding the factors controlling the crystallinity of the particles, including annealing temperature and surface-coverage of reactants. These more recent studies (see Fig. 1) have

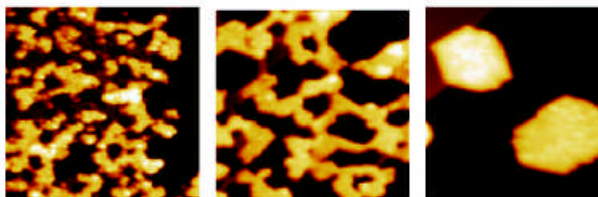


Fig 1: STM images showing the evolution of micro-structure of TiO_2 nanocrystals as a function of annealing temperature. All images are of the same length scale and each picture shows a region 25nm by 25nm.

shown clearly that temperatures of $>800\text{K}$ are needed to fully aggregate the initial nano-clusters so as to form fully single-crystal TiO_2 particles, which are typically $\sim 5\text{nm}$ in size; see Fig. 2. The crystallinity of these particles has been examined by our Group. The re-

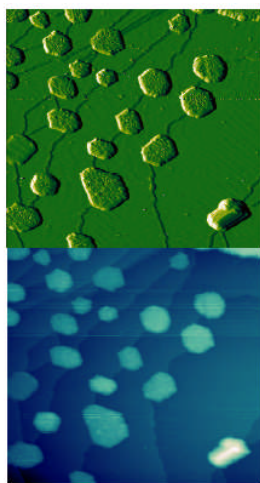


Fig: 2: TiO_2 nanoparticles annealed to 920K. The top image shows the result of differentiation of the data in the bottom image. Islands are 5-15 nm in dimensions.

sults show that after being fully formed and annealed at 800 K the majority of the titania nanocrystals have hexagonal shape with edges oriented along the close-packed directions on Au(111). Note that in most cases the nanocrystals are flat and only 2 lattice constants (0.6 nm) in height. Under certain preparation conditions, different structural phases form; these phases vary with annealing temperature and reactant coverage. In addition, we have found that there is a second chemical phase that is present under conditions of excess surface-adsorbed water and are currently exploring the origin of this phase. This degree of control over the composition and structure of the nanoparticle will be of much use in our TOF photofragment studies. Each of the different nanocrystal types will offer different photoreaction sites and dynamics. In addition, we have recently seen evidence that our nanoparticles can be oriented by our Au(111) substrate surface. With such an oriented particle array, it is possible for the resulting fragments to have a coherent angular distribution for angle-resolved TOF.

We have examined reaction of methanol on our TiO_2 nanoparticles and found evidence that their reactivity is much greater than that of a single-crystal substrate, a result in agreement with measurements by Friend and Madix Groups, Harvard using nanoparticles made by dry oxidation of Ti islands. We note that a crucial aspect of experiments to measure thermal and photoreactions is the ability to distinguish reactions on the nanoparticles from reactions on the background single crystal substrate. We have demonstrated a TPD capability on a preliminary basis for thermal re-

actions, and anticipate on the basis of relative flux that the same conditions should apply in the case of photoinitiated fragmentation. However from a more general viewpoint, accomplishing TPD on low-density surface concentrations of nanoparticles with high S/N ratio is challenging, particular in the spatially constrained environment of our STM and with the small sample size typical in such an instrument. Thus, a major preparation effort in the last ½ year has been to develop the compact instrumentation for quadrupole studies of a narrow field of view on an UHV-prepared surface. This effort makes use of an earlier design of this apparatus developed by the White Group at BNL. We have now assembled this apparatus at Columbia and are currently undertaking preliminary measurements on our TiO₂ particles.

Photofragmentation on Metal-Oxide Nanoparticles: The central focus of our research is to investigate photoreaction dynamics involving adsorbate molecules on these metal-oxide nanoparticle surfaces using our excimer-laser/tunable dye-laser TOF system at Columbia. The fundamental thrust of these experiments is to examine reaction mechanism, site, and yield via examination of the fragment energy and desorption angle and thus address issues such as how adsorbate photoreactions proceed on a nanoscale particle in comparison to that on a single-crystal sample. Work using this technique on oxide surfaces has already been applied in our lab to a set of different single-crystal iron-oxide surfaces as well as in an extensive series of prior experiments by the Stair/Weitz Group and Petek Group on single-crystal oxide surfaces.

This experimental work relies on the particles being formed *in situ* in our time-of-flight system using synthesis conditions, which are identical to those developed using our STM system. During this last year we have installed and tested additional instrumentation for this *in situ* synthesis of TiO₂ nanoparticles on our TOF system, such as thermal evaporator, load-lock, etc. With this *in situ* system we have begun to examine the formation of nanocrystal TiO₂ for time of flight measurements. Because of the multistep nature of the synthesis process, it is desirable, from the viewpoint of high data rate, that sample surfaces can be cleaned rapidly *in situ*, rather than requiring a new synthesis step after each reactive run. Our recent work both via STM (collaboration with the Flynn Group) and via TPD in our laboratory have shown that in metal-oxide systems adsorbate products, including chemisorbed halogen species, can be removed via high-temperature “annealing.” Our preliminary experiments on our TiO₂ nanoparticles show that reaction products can also be removed in this case via suitable annealing.

Plasmonically Enhanced Reactions on UHV-Deposited Metal Nanoparticles: Photochemistry on metallic nanoparticles is also an area of growing interest because catalyzed reactions can be derived from near-field enhancement of an incident optical beam due to local-plasmon excitation or if mounted on a dielectric substrate due to surface waves and their scattering. While interest in this area has grown rapidly, the original work was reported by the author of this report using UV reactions on Cd nanoparticles; at this point a dynamics study in this area is needed. Recently, several groups have described new methods for preparing metallic nanoclusters *in situ* in a UHV environment, such as buffer-layer-assisted-growth (BLAG), which yields clusters as small as ~5 Å for noble metals. Both noble metal and Cd are known to exhibit size- and shape-dependent-plasmonic effects in the presence of either visible or UV light, respectively, and we are currently planning a synthesis route for these particles. The optical fields for single particles or clusters of these particles are enhanced by resonant plasmonic effects driven by the behavior of the metal dielectric constant. For single

the behavior of the metal dielectric constant. For single particles, these effects can be estimated via the static-field approximation and a realistic dielectric constant. For more complicated geometries or clusters of particles, methods such as finite difference-time-domain computation can be used, an approach which we have employed and done research on in many recent plasmonic studies in our group. We have recently developed additional computational tools for these calculations and in fact have recently examined nonlinear optical effects in surface-plasmon scattering (see Ref. 14 below).

Future Plans:

Our current plans are to complete our study of the chemistry for forming nanocrystals using RLAD so as to understand the conditions for obtaining monodisperse and/or monophase nanocrystals. Continued work will be carried out on the formation of other nanocrystal types including doped varieties and ... We will also begin studies of non-angle resolved TOF measurements using our current nanoparticle TiO₂ preparation methods. Our goal is to compare TOF velocity signatures on a well defined single-crystal sample with those obtained on nanoparticle surfaces.

Recent DOE-Sponsored Publications:

1. K. Adib, G.G. Totir, J.P. Fitts, T. Miller, G.W. Flynn, S.A. Joyce and R.M. Osgood, Jr., "Chemistry of CCl₄ on Fe₃O₄(111)-(2x2) Surfaces in the Presence of Adsorbed D₂O." *Surf. Sci.* **537**, 191 (2003).
2. Z. Zhu, A. Srivastava, and R.M. Osgood, Jr., "Reactions of Organosulfur Compounds with Si(100)," *J. Phys. Chem.* **B 107**, 13939 (2003).
3. A. Srivastava and R.M. Osgood, Jr., "State-Resolved Dynamics of 248 nm Methyl-Iodide Fragmentation on GaAs(110)." *J. Chem. Phys.* **119**, 10298 (2003).
4. K.T. Rim, J.P. Fitts, T. Muller, K. Adib, N. Camillone III, R.M. Osgood, Jr., S.A. Joyce and G.W. Flynn, "CCl₄ Chemistry on the Reduced Selvege of a α -Fe₂O₃(0001) Surface: A Scanning Tunneling Microscopy Study." *Surf. Sci.* **541**, 59 (2003).
5. K.T. Rim, T. Muller, J.P. Fitts, K. Adib, N. Camillone III, R.M. Osgood, Jr., E.R. Batista, R.A. Friesner, B.J. Berne, S.A. Joyce, and G.W. Flynn, "An STM Study of Competitive Surface Reactions in the Dissociative Chemisorption of CCl₄ on Iron Oxide Surfaces," *Surf. Sci.* **524**, 113 (2003).
6. R.M. Osgood, Jr., "Making it Stick - with a Flash!" *Perspective Comments.* *Perspective in Surf. Sci.* **573**, 147 (2004)
7. G. G. Totir, Y. Le and R. M. Osgood, Jr., "Photoinduced-Reaction Dynamics of Halogenated Alkanes on Iron-Oxide Surfaces: CH₃I on Fe₃O₄ (111)-(2x2)," *J. Phys. Chem.* **B 109**, 8452 (2005).
8. Z. Zhu, T. Andelman, M. Yin, T-L. Chen, S.N. Ehrlich, S.P. O'Brien, R.M. Osgood, Jr., "Synchrotron X-ray Scattering of ZnO Nanorods: Periodic Ordering and Lattice Size," *J. Mater. Res.* **21**, 1033 (2005).
9. Z. M. Zhu, T. Chen, Y. Gu, J. Warren and R. M. Osgood, Jr., "Zinc-Oxide Nanowires Grown by Vapor-Phase Transport Using Selected Metal Catalysts: A Comparative Study," *Chem. Mats.* **17**, 4227 (2005).
10. Z. Song, J. Hrbek, R.M. Osgood, Jr., "Formation of TiO₂ Nanoparticles by Reactive-Layer-Assisted Deposition and Characterization by XPS and STM," *Nano. Letts.* **5**, 1357(2005).
11. G.Y. Le, G.G. Totir, G.W. Flynn, and R.M. Osgood, Jr., "Chloromethane Surface Chemistry on Fe₃O₄(111)-(2x2): A Thermal Desorption Spectroscopy Comparison of CCl₄, CBr₂Cl₂, and CH₂Cl₂." *Surf. Sci.* **600**, 665 (2006).
12. N. Camillone III, T.R. Pak, K. Adib, R.M. Osgood, Jr., "Tuning Molecule-Surface Interactions with Sub-Nanometer-Thick Covalently-Bound Organic Monolayers." *J. Phys. Chem* **B 110**, 11334 (2006).
13. R.M. Osgood, Jr., "Photoreaction Dynamics of Molecular Adsorbates on Semiconductor and Oxide Surfaces." *Chem. Rev.* **106**, 4379 (2006).
14. L. Cao, N.-C. Panoiu, and R.M. Osgood, Jr., "Surface Second-Harmonic Generation from Surface Plasmon Waves Scattered by Metallic Nanostructures." *Phys. Rev.* **B 75**, 205401 (2007).

Optical manipulation of ultrafast electron and nuclear motion on metal surfaces

Hrvoje Petek (petek@pitt.edu)
 Department of Physics and Astronomy
 University of Pittsburgh
 Pittsburgh, PA 15269

Since the pioneering work of Langmuir, alkali atom overlayers on metal surfaces have been central to development of theories of chemisorption.^{1,2} Our research goal is to study dynamics of alkali atoms on noble metal surfaces in response to excitation by a near UV light. The surface desorption dynamics are initiated by the photoinduced charge transfer from the metal substrate to the chemisorbed alkali atoms. Transforming the ionized alkali atoms in the ground state into a neutral excited state turns on the repulsive forces initiating the alkali atom photodesorption.³ To be able to interpret the dynamical studies, it is important to characterize the electronic structure of chemisorbed alkali atoms. Our activities have focused on: 1) the experimental measurement and theoretical calculation of the unoccupied electronic structure of alkali atoms; 2) the lifetimes of the first excited s- resonance of alkali atoms; 3) the characterization of higher energy p_x and p_y symmetry resonances; 4) coherent phonon excitation of alkali atom overlayers on Cu surfaces; 5) formation of C_{60} quantum wires and quantum wells; and 6) exploration of the alkali atom-like unoccupied states of C_{60} on Cu surfaces.

The universal electronic structure of alkali atoms on noble metals. Last year we reported on two-photon photoemission (2PP) spectroscopy of Li – Cs on Cu(111) and Ag(111) surfaces. We found period independent energy of 1.8 – 2.0 eV below the vacuum level for the lowest ns -resonance of alkali atoms on noble metal surfaces. This year we developed a simple theory that explains how the intrinsic electronic structures of the bare surface and of isolated atoms define the electronic structure of their interface.⁴ Theoretical modeling attributes the common interfacial electronic structure, which surprisingly is independent of the periodic trends in the atomic size and ionization potential, to the Coulomb interaction among the ns electron, the alkali ionic core, and the conduction band electrons of the substrate.

We determined the chemisorption structures of alkali

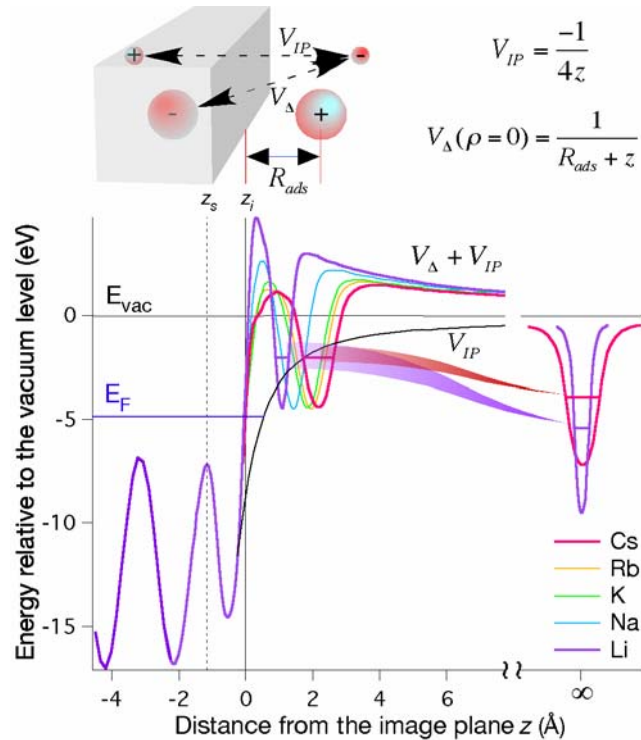


Figure 1. The potentials of the Cu(111) surface and free alkali atoms, and the effective potentials for the chemisorbed system. The period independent electronic structure is explained by the image charge interaction.

atoms on Cu(111) and Ag(111) surface by DFT slab calculations for various alkali atom coverages. At the calculated equilibrium distance from the surface, the excitation laser light induces charge transfer from the metal substrate to the chemisorbed alkali ion, to produce the neutral alkali atom in its lowest electronic state. To calculate the energies of the electronic resonances of the atom-surface system, we solved the Schrödinger equation at the chemisorption distance using an electronic wave packet propagation method. The resulting *ns*-resonance energies, in good agreement with experiment, are essentially independent of the alkali atom period.

From these calculations we conclude that the *ns* resonance energy is given by the attractive interaction of the *ns* electron with its own image charge and the repulsive interaction with the image charge of the ionic core. The net destabilization of the *ns* electron as the adsorption distance R_{ads} in atomic units is $\Delta E = +1/4R_{ads}$. The period independent *ns* electron binding energy $E_b = \Delta E - I$ implies that there is nearly exact compensation between image charge interaction ΔE and free atom ionization potential I at R_{ads} . This compensation is related to Pauli exclusion: the size of the ionic core determines how strongly an alkali ion core can bind the *ns* electron as well as how close it chemisorbs to a metal surface.

Surface femtochemistry of alkali atoms on noble metals. We have performed interferometric two-pulse correlation measurements of two 2PP near the alkali atom resonance for all alkali atoms on Cu(111) and Ag(111) surface, except for Rb/Ag(111), for which the measurements will be completed within this year. The measurements probe the alkali atom resonance relaxation mainly by elastic reverse charge transfer to the substrate, as well as energy stabilization of the resonance due to the desorptive motion of alkali atoms from the surface. In the past, we have investigate the nuclear wave packet motion induced by charge transfer excitation of Cs atoms on Cu(111).³ Other chemisorption systems appeared to have shorter lifetimes, making such measurements difficult.

By investigating the *ns* resonance decay dynamics over a broader energy range, however, we found that the decay of the Cs resonance on Ag(111) is even slower than for Cu(111). The resonance energy decreases from 2.5 eV at zero delay by ~ 0.4 eV in ~ 180 fs. The rapid energy stabilization may be a consequence of the heavier mass of Ag atoms than Cu, which allows more efficient recoil of Cs atoms from the surface. This observation suggests that the desorption dynamics of Cs from Au(111) surface may be even more efficient.

Alkali atom p_x and p_y symmetry resonances. Until now there has only been discussion of the *ns* resonance of alkali atoms on noble metals (strictly speaking the observed resonance is the anti-bonding hybridization of s and p_z orbitals). By performing

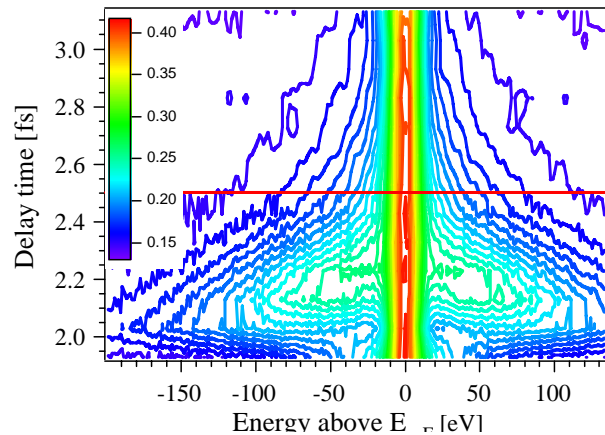


Figure 2. A contour plot of the Cs *ns* resonance population decay constructed from two-pulse correlation measurements taken in 0.1 eV increments. The red line indicates the *ns* resonance energy at zero delay.

angle dependent 2PP measurements at higher (>0.05 ML) alkali atom coverages we found a new resonance 0.4 eV above the ns resonance that has antisymmetric character with respect to the surface normal as expected for the p_x and p_y orbitals of alkali atoms. We observed these new states for K and Cs on both Cu(111) and Ag(111) surfaces (Fig. 3), but not for Na/Ag(111). Their appearance for K and larger alkali atoms suggests that these orbitals may be stabilized by hybridization with the appropriate symmetry d orbitals, which are at significantly higher energy for Na than for K and Cs. This new spectroscopic feature provides important new information on the unoccupied electronic structure of alkali atoms. The existence of p_x and p_y states has been predicted by our collaborators led by Prof. Pedro Echenique at Donostia International Physics Center, where Petek is spending his sabbatical. The theoretical analysis is in progress.⁵

Related to Fig. 3, we have developed a simple model that can explain the $k_{||}$ (angular) 2PP intensity distribution, such as for the sp -band of Ag. This is an important step in developing a quantitative model for describing the excitation of alkali atoms and in general adsorbates on metal surfaces.⁶ This research was performed by Dr. Aimo Winkelmann, a visitor from the Max Planck Institute for Microstructure Physics.

Coherent phonon excitation of alkali atom overlayers. We investigated the coherent phonon excitation in Na/Cu(111) chemisorption system at ~ 1 ML coverage. At low coverage, the charge transfer excitation to the ns alkali atom resonance induces the wave packet dynamics such as observed in Fig. 2. We investigated the coherent phonon excitation at the Na-Cu interface by ultrafast surfaces second harmonic generation measurements with a tunable excitation source of Prof. Y. Matsumoto at the Institute for Molecular Science in Japan. Contrary to our expectation, the action spectrum for the coherent phonon excitation reproduces the threshold for d- to sp -band excitation in Cu, rather than with surface excitations. We conclude that the coherent interface motion is driven by charge density fluctuations induced by the bulk interband excitation.⁷

C₆₀ quantum wires. We have initiated a related research program on the STM (STS) investigation on the unoccupied electronic structure of adsorbates on metal surfaces. In collaboration with Prof. John Yates, we have employed z -V spectroscopy as a general method to extend spectroscopic measurements of adsorbates up to the vacuum level.⁸ We have performed measurements on C₆F₆ and C₆₀ on Cu and Au surfaces. The electronic structure of the anion state of C₆F₆ can be described on all surfaces by the model developed for alkali atoms.⁹

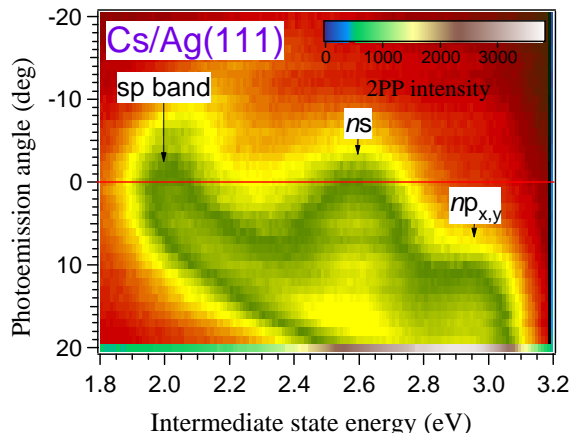


Figure 3. A 3D plot of *angle resolved 2PP* showing the Cs atom resonances and the dispersing two-photon transition between the upper and lower sp band.

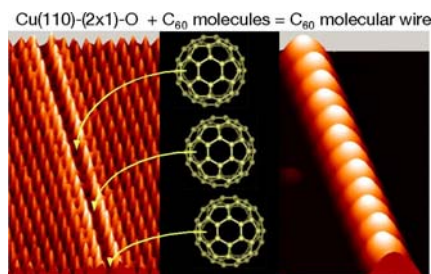


Figure 4. Self-assembly of a C₆₀ wire on the Cu(110) (2x1)-O template.

We have also developed a general way to self-assemble molecular wires by exploiting unusual oxidation properties of the Cu(110) surfaces. By adjusting O₂ dosing conditions, we have been able to make atomically perfect, >100 nm long, one Cu atom wide troughs of bare Cu bounded by regions of Cu(110) (2x1)-O domains. The chemical nanopatterning forms templates for single molecule wide wires of molecules such as C₆₀, which have preference for adsorption in the bare metal troughs.¹⁰ Fig. 4 shows the Cu(110) (2x1)-O template and the resulting C₆₀ wire. In such a manner, wires exceeding lengths of tens of nanometers can be grown.

Free-electron like properties of C₆₀ assemblies.

We have investigated the spatially and energy resolved DOS of single C₆₀ molecules, C₆₀ wires, and quantum wells. With bias voltages below 3.5 V the images resolve the topmost π -symmetry orbitals of LUMO+1 and LUMO+2 states. Above 3.5 V, we observe diffuse orbitals where the entire C₆₀ molecule appears as an s, p, or d symmetry atomic orbital. DFT calculations using a plane wave basis find a new type of electronic state of C₆₀ molecules where electrons are bound by a central potential in orbitals that resemble s, p, and d orbitals of atoms rather than to individual C atoms. We dub these new molecular states, the superatom states. We find that superatom states of C₆₀ dimers hybridize into σ and π orbitals resembling the H₂⁺ molecule. For larger assemblies, the superatom states hybridize into free-electron like bands (Fig. 5). We conclude that the superatom states are a general feature of hollow molecules and nanotubes.¹¹

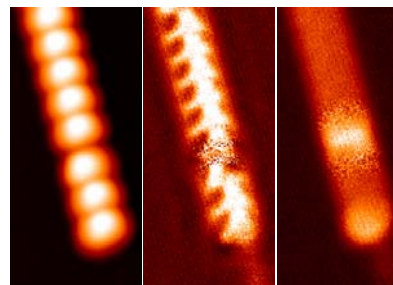


Figure 5. The topography of a C₆₀ wire (left), the dI/dV image of its LUMO+2 (center), and the dI/dV image of its s-symmetry orbital derived superatom state.

Other results. Dr. Jin Zhao of Petek's group received the M. T. Thomas Award for excellence in postdoctoral research for her computations (alkali atom electronic structure, etc) done at the computing facilities at EMSL.

Other results. Dr. Jin Zhao of Petek's group received the M. T. Thomas Award for excellence in postdoctoral research for her computations (alkali atom electronic structure, etc) done at the computing facilities at EMSL.

Future research. We will be extending the studies of alkali atom electronic structure and dynamics to TiO₂ and graphite surfaces. The superatom states represent a novel way to tailor the electronic structure of hollow molecules. We are will explore the stabilization of surperatom states by endohedral doping.

References (*results of the current DOE support)

- ¹ H. Petek, H. Nagano, M. J. Weida, et al., J. Phys. Chem. B **105**, 6767 (2001).
- ² H. Petek and S. Ogawa, Annu. Rev. Phys. Chem. **53**, 507 (2002).
- ³ H. Petek, H. Nagano, M. J. Weida, et al., Science **288**, 1402 (2000).
- ⁴ *J. Zhao, N. Pontius, A. Winklemann, et al., PNAS (submitted).
- ⁵ *A. Borisov, V. Sametoglu, J. Zhao, et al., (in preparation).
- ⁶ *A. Winklemann, V. Sametoglu, N. Pontius, et al., Phys. Rev. B (in press).
- ⁷ *M. Fuyuki, K. Watanabe, D. Ino, et al., Phys. Rev. B **76**, 115427 (2007).
- ⁸ *D. B. Dougherty, P. Maksymovych, J. Lee, et al., Phys. Rev. B (in press).
- ⁹ *D. B. Dougherty, M. Feng, J. Zhao, et al., Nature Materials (in preparation).
- ¹⁰ *M. Feng, J. Lee, J. Zhao, et al., J. Am. Chem. Soc. (in press).
- ¹¹ *M. Feng, J. Zhao, and H. Petek, Nature (submitted).

X-ray Spectroscopy of Volatile Liquids and their Surfaces

Richard J. Saykally
Department of Chemistry
University of California
Berkeley, CA 94720-1460
saykally@berkeley.edu
and
Chemical Sciences Division
Lawrence Berkeley National Laboratory

Program Scope or Definition

The goal of this project is to explore and develop novel methodologies for probing the nature of volatile liquids and solutions and their surfaces, employing combinations of liquid microjet technology, with synchrotron X-ray and Raman spectroscopies.

Recent Progress

Utilizing the intense monochromatic soft X-Rays available at the LBNL Advanced Light Source (ALS), and employing liquid microjets for convenient temperature and composition control, we have extended our systematic investigation of the local solvation environments of simple inorganic cations and anions to tri- and tetravalent species. Earlier studies have established that monovalent cations have a very small effect on the local electronic structure, whereas simple anions are strongly perturbative[5]. Moreover, these anions exhibit markedly ion-specific perturbations, while the monovalent cations all produce the same effects. Divalent cations[12] exhibit ion-specific perturbations, however, and we attribute these (as well as the ion-specific anion perturbations) to a combination of electric field effects on and charge transfer with the first solvent shell molecules, as deduced via comparisons with density functional theory calculations. While the analysis of new XAS data for the higher charged ions is still ongoing, these trends of increasing charge transfer with ion charge are evidenced. We have carried out a similar study of the hydration of the hydroxide ion, finding support for recent predictions of a hyper-coordinated first solvation shell, wherein the ion accepts four H-bonds but donates none[16]. Also, we previously identified a strong blue-shift in the k-edge spectrum of the hydronium ion, relative to that of water, probably due to the tighter electron binding[11].

We have found that Raman spectroscopy of liquid microjets provides a useful complement to our XAS studies. Building on our recent investigation of the temperature-dependent Raman spectrum of water, wherein we found that a histogram of the electric field distribution along the OH bonds computed from a Monte Carlo simulation accurately represents the observed spectra[8], we have proceeded to study ionic solutions by this combined experimental/theoretical approach as a means of ascertaining the local environments around aqueous ions. We again find that the E-field histograms faithfully reproduce the T-dependent Raman spectra, and make it possible to deduce a detailed new molecular picture of how simple ions are solvated in water[18].

Liquid microjet technology affords the opportunity to study the details of water evaporation, free from the obfuscating effects of condensation that have plagued previous studies. Studying small (diameter < 5 μm) jets with Raman thermometry, we find compelling evidence for the existence of a significant energetic barrier to evaporation, in contrast to most current models[10,14]. Similar studies of heavy water are ongoing, indicating a similar evaporation coefficient, and thus an energetic barrier similar to that of normal water. A transition state model developed for this process provides a plausible mechanism for evaporation in which variations in libration and translational frequencies account for the observed isotope effects[15].

Using liquid microjets to avoid the problem of radiation damage to fragile solutes, we have measured the pH-dependent NEXAFS spectra of several amino acids, including glycine, proline, lysine, and the dipeptide diglycine[4,9]. We find that the nitrogen terminus of primary amino acids is sterically shielded at high pH, and exists in an “acceptor-only” state, wherein neither amine proton is involved in hydrogen bonding to the surrounding solvent. The diglycine study characterized a similar behavior in this first study of the peptide bond hydration. This work has been extended to examine the hydration of several nucleotide bases and related molecules. We have also exploited the sensitivity of XAS to ionic perturbations of the empty orbitals of carboxylates to support the prediction that sodium interacts more strongly than potassium with protein carboxylate groups[19], offered as an explanation for the much higher intracellular concentration of sodium existing in cells.

We have recently addressed the long standing controversy over whether continuum or a multi-component (“intact” or “broken bond,” etc.) models best describe the hydrogen bond interactions in liquid water. The temperature dependence of water’s Raman spectrum has long been considered to be among the strongest evidence for a multi-component distribution. However, we have shown, using a combined experimental and theoretical approach, that many of the features of the Raman spectrum considered to be hallmarks of a multi-state system, including the asymmetric band profile, the isosbestic (temperature invariant) point, and van’t Hoff behavior, actually result from a continuous distribution[5]. This work complements our study of the structure of pure liquids by X-ray absorption spectroscopy that has been ongoing. We have published a joint theory/experiment study of liquid methanol that characterized the nature of H-bonded domains[6,7].

We have examined the high electrical charging of liquid water microjets that can be effected by metal nozzles, proposing a mechanism based on selective adsorption of hydroxide to the metal surface and subsequent electrokinetic charge separation, and we have demonstrated the use of this “protonic charging” for a novel method of hydrogen generation[17].

Future Plans

1. Complete the XAS study of ionic perturbation of local water structure, such that the entire Hofmeister series is ultimately addressed. We seek a comprehensive picture of the effects of both cations and anions on the local structure of water. Raman spectroscopy measurements will also be performed on these systems, the data from which provide complementary insights and aid in the theoretical modeling. We will further develop the use of E-field distributions from simulations to interpret the spectra.

2. Extend our XAS studies of local hydration to important free radical species, generated in liquid water microjets by excimer laser photolysis.
3. Extend our studies of amino acid hydration vs. pH to include all natural amino acids. Use the same approach to study hydration of the peptide bonds in small polypeptides, nucleotide bases, nucleosides, and nucleotides.
4. Measure NEXAFS spectra for pure liquid water, alcohols, and hydrocarbons, seeking to achieve deep supercooling via controlled evaporation. In conjunction with theoretical modeling, we will seek a coherent description of the liquid structure and bonding in these systems.
5. We will continue to explore and compare ion and electron detection of NEXAFS spectra, seeking to reproduce earlier measurements of surface phenomena obtained with ion detection. Thus far, we have not been able to reproduce the original measurements with our newly-designed X-ray spectrometer.
6. We plan to continue our exploration of the evaporation of liquid water by Raman thermometry and mass spectrometry, seeking to ascertain the effects of salts on the evaporation process.

References (DOE supported papers 2004-present) – 19 Total

1. K.R. Wilson, B.S. Rude, J. Smith, C.D. Cappa, D.T. Co, R.D. Schaller, M. Larsson, T. Catalano, and R.J. Saykally, "Investigation of volatile liquid surfaces by synchrotron x-ray spectroscopy of liquid microjets," *Review of Scientific Instruments* **75**, 725-736 (2004). LBNL-56347
2. C.D. Cappa, K.R. Wilson, B.M. Messer, R.J. Saykally, and R.C. Cohen, "Optical cavity resonances in water micro-droplets: Implications for shortwave cloud forcing," *Geophysical Research Letters* **31**, L10205 (2004). LBNL-56357
3. J.D. Smith, C.D. Cappa, K.R. Wilson, B.M. Messer, R.C. Cohen, and R.J. Saykally, "Energetics of Hydrogen Bond Network Rearrangements in Liquid Water," *Science* **306**, 851-853 (2004). LBNL-56349
4. B.M. Messer, C.D. Cappa, J.D. Smith, K.R. Wilson, M.K. Gilles, R.C. Cohen, and R.J. Saykally, "pH Dependence of the Electronic Structure of Glycine," *J. Phys. Chem. B* **109**, 5375-5382 (2005). LBNL-56348 *Cover Article.
5. C.D. Cappa, J.D. Smith, K.R. Wilson, B.M. Messer, M.K. Gilles, R.C. Cohen, and R.J. Saykally, "Effects of Alkali Metal Halide Salts on the Hydrogen Bond Network of Liquid Water," *J. Phys. Chem. B* **109**, 7046-7052 (2005). LBNL-56812 *Cover Article.
6. J.D. Smith, C.D. Cappa, B.M. Messer, R.C. Cohen and R.J. Saykally, Response to Comment on "Energetics of Hydrogen Bond Network Rearrangements in Liquid Water," *Science* **308**, 793b (2005). LBNL-57117
7. K.R. Wilson, M. Cavalleri, B.S. Rude, R.D. Schaller, T. Catalano, A. Nilsson, L.G.M. Pettersson, and R.J. Saykally, "X-ray Absorption Spectroscopy of Liquid Methanol

- Microjets: Bulk Electronic Structure and Hydrogen Bonding Network,” *J. Phys. Chem. B* **109**, 10194-10203 (2005). LBNL-56350 *Cover Article.
8. J.D. Smith, C.D. Cappa, K.R. Wilson, R.C. Cohen, P.L. Geissler, and R.J. Saykally, “Unified description of temperature-dependent hydrogen-bond rearrangements in liquid water,” *PNAS* **102**, 14171-14174 (2005). LBNL-58789
 9. B.M. Messer, C.D. Cappa, J.D. Smith, W.S. Drisdell, C.P. Schwartz, R.C. Cohen, R.J. Saykally, “Local Hydration Environments of Amino Acids and Dipeptides Studied by X-ray Spectroscopy of Liquid Microjets,” *J. Phys. Chem. B* **109**, 21640-21646 (2005). LBNL-59184
 10. C.D. Cappa, W. Drisdell, J.D. Smith, R.J. Saykally, and R.C. Cohen, “Isotope Fractionation of Water During Evaporation Without Condensation,” *J. Phys. Chem. B* **109**, 24391-24400 (2005). LBNL-59505
 11. C.D. Cappa, J.D. Smith, B.M. Messer, R.C. Cohen, and R.J. Saykally, “The Electronic Structure of the Hydrated Proton: A Comparative X-ray Absorption Study of Aqueous HCl and NaCl Solutions,” *J. Phys. Chem. B* **110**, 1166-1171 (2006). LBNL-59504
 12. C.D. Cappa, J.D. Smith, B.M. Messer, R.C. Cohen, and R.J. Saykally, “Effects of Cations on the Hydrogen Bond Network of Liquid Water: New Results from X-ray Absorption Spectroscopy of Liquid Microjets,” *J. Phys. Chem. B* **110**, 5301-5309 (2006). LBNL-59955
 13. J.D. Smith, C.D. Cappa, B.M. Messer, W.S. Drisdell, R.C. Cohen, and R.J. Saykally, “Probing the Local Structure of Liquid Water by X-ray Absorption Spectroscopy,” *J. Phys. Chem. B* **110**, 20038-20045 (2006). LBNL-61736
 14. J.D. Smith, C.D. Cappa, W.S. Drisdell, R.C. Cohen, and R.J. Saykally, “Raman Thermometry Measurements of Free Evaporation from Liquid Water Droplets,” *JACS* **128**, 12892-12898 (2006). LBNL-61735
 15. C.D. Cappa, J.D. Smith, W.S. Drisdell, R.J. Saykally, and R.C. Cohen, “Interpreting the H/D Isotope Fractionation of Liquid Water During Evaporation Without Condensation,” *J. Phys. Chem. C* **111**, 7011-7020 (2007). LBNL-62751
 16. C.D. Cappa, J.D. Smith, B.M. Messer, R.C. Cohen, and R.J. Saykally, “Nature of the Aqueous Hydroxide Ion Probed by X-ray Absorption Spectroscopy,” *J. Phys. Chem. A* **111**, 4776-4785 (2007). LBNL-62752 *Cover Article.
 17. A.M. Duffin and R.J. Saykally, “Electrokinetic Hydrogen Generation from Liquid Water Microjets,” *J. Phys. Chem. C* **111**, 12031-12037 (2007).
 18. J.D. Smith, R.J. Saykally, and P.L. Geissler, “The Effects of Dissolved Halide Anions on Hydrogen Bonding in Liquid Water,” *JACS* (submitted 2007).
 19. J.S. Uejio, C.P. Schwartz, A.M. Duffin, W.S. Drisdell, and R. J. Saykally, “Selective Binding of Alkali Cations with Carboxylate in Aqueous Solution Confirmed by X Ray Absorption Spectroscopy,” *Chem. Phys. Lett.* (submitted 2007).

Computational Nanophotonics: Model Optical Interactions and Transport in Tailored Nanosystem Architectures

DOE Grant DE-FG02-03ER15486

PI: Mark Stockman

**Department of Physics and Astronomy, Georgia State University, Atlanta, GA
30303**

E-mail: mstockman@gsu.edu, URL: <http://www.phy-astr.gsu.edu/stockman>

Report for the Period of 9/2006 – 9/2007

Program Scope

The program is directed toward development of new computational approaches to photoprocesses in nanostructures whose geometry and composition are tailored to obtain desirable optical responses. The emphasis of this specific program is on the development of computational methods and prediction and computational theory of new phenomena of optical energy transfer and transformation on the extreme nanoscale (down to a few nanometers).

1 Recent Progress

1.1 Coherent Control of Ultrafast Energy Localization at Nanoscale [1, 2]

Our research has significantly focused on problem of controlling localization of the energy of ultrafast (femtosecond) optical excitation on the nanoscale. We have proposed and theoretically developed a general approach to solving this fundamental problem [3-9]. It is difficult to overestimate possible applications of this effect, including nano-chip computing, nanomodification (nanolithography), and ultrafast nano-sensing. A major obstacle in using these ideas of the coherent control at the nanoscale has been the absence of efficient numerical methods to compute the waveform of the excitation pulses required to localize the optical energy at a given nanosite at a required time. Recently we have developed such a method based on the idea of the time reversal [1, 2]. Numerically, this method requires the computation of the retarded dyadic Green's functions for the system. It is sufficiently efficient with respect to the CPU time, very stable but requires very large RAM memory (in the tens to hundred Gigabyte range).

Following our pioneering work, there has recently been an explosion of activity on both theoretical [10-13] and experimental [14-18] investigations of the ultrafast coherent control on the nanoscale. This field will rapidly grow into one of the most important in the nanoscience with application to the nanoscale computations, sensing, spectroscopy, etc. It will require our increased attention to stay at the forefront. We are currently investigating this new time-reversal approach to include the polarization of the excitation pulses.

1.2 Spatio-Temporal Coherent Control at Nanoscale [19]

We have developed a new approach to dynamically control the nanoscale distribution of optical energy [19]. This approach amalgamates three principles: adiabatic compression [20], spatial coherent control (optical aperture synthesis) [21-23], and the temporal coherent control at the nanoscale [1-4, 6, 8]. An example of the system that can be used for the spatio-temporal control, we consider a plasmon-polaritonic tapered waveguide, in particular, a silver wedge whose maximum thickness is in a 30-nm range, and the minimum thickness is on order of a few (2-3) nanometers. There are nanoparticles (or nano-indentations) situated at the thick edge, on which we will focus the output a spatio-temporal modulator. These nanoparticles will couple the incident radiation to the surface plasmon polaritons (SPPs) propagating in the plane of the wedge toward its thick edge. This is illustrated in Fig. 1(a) where the coupling nanoparticles are shown by circles and the rays of the SPPs are indicated by lines. The phases of the excitation waves focused at the individual particles define the

curvature of the SPP wave front in the plane shown by concave curves. These wavefronts are adjusted by the phase modulation in such a way that these SPP rays converge at a nanofocus at the thin edge of the wedge [Fig. 1 (a) and (b)]. To have the pulses of the SPP coming along each ray to coincide at the nanofocus and produce there an ultrashort (a few fs) pulse of the local fields, each of the excitation pulses should be modulated in time as shown in Fig. 1(c).

The problem of the adiabatic concentration is extremely complicated numerically: it includes the three spatial coordinates and time. There are large ratios of the maximum to minimum scales present in each dimension. Its full numerical solution at this time using, e.g., finite difference time-domain method would be too complex. Therefore as the first step in solving this problem and to obtain a reasonable initial field, we have employed a WKB approximation, which is expected to work well precisely for these conditions of the large maximum/minimum scale ratios. This is how the solution shown in Fig.1 has been obtained [19]. In the future, we will aim to obtain a full numerical solution using the large scale computations.

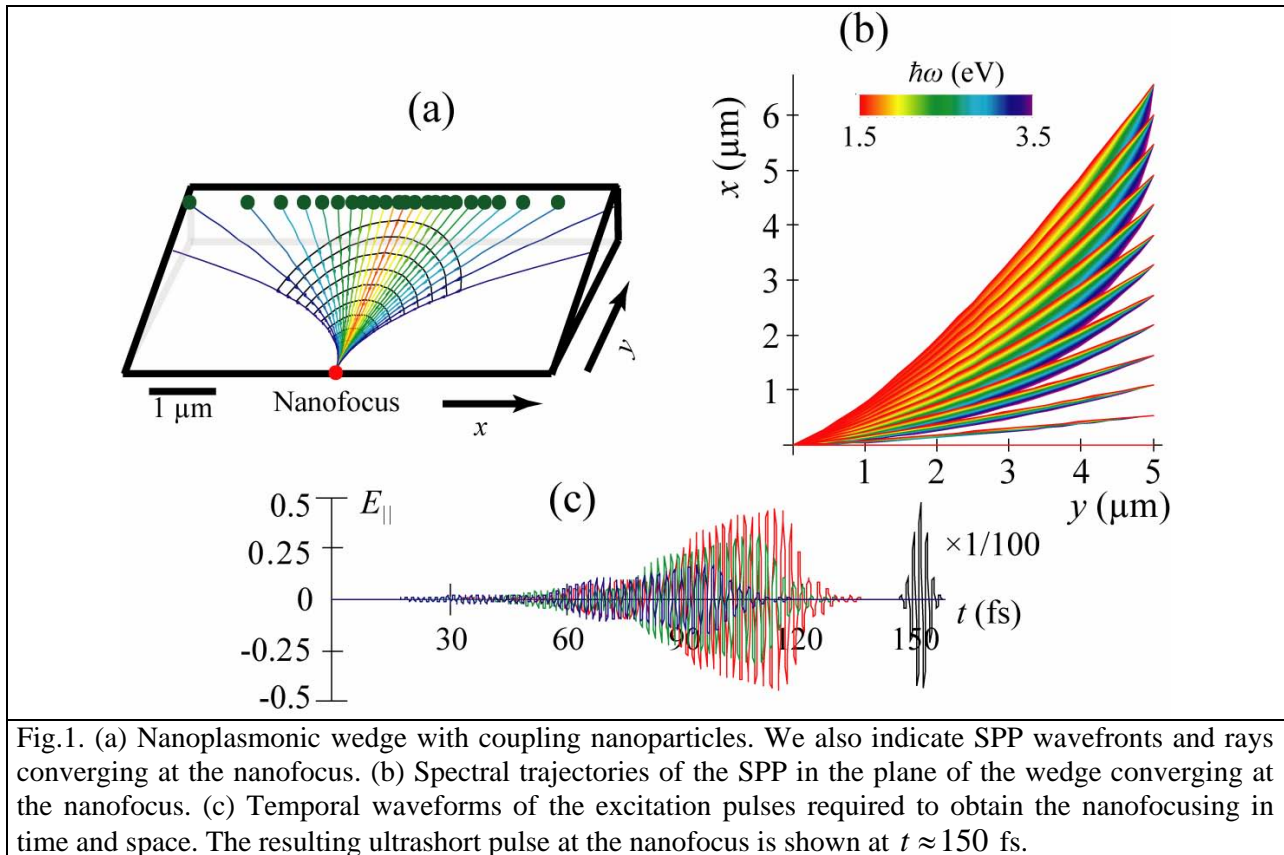


Fig.1. (a) Nanoplasmonic wedge with coupling nanoparticles. We also indicate SPP wavefronts and rays converging at the nanofocus. (b) Spectral trajectories of the SPP in the plane of the wedge converging at the nanofocus. (c) Temporal waveforms of the excitation pulses required to obtain the nanofocusing in time and space. The resulting ultrashort pulse at the nanofocus is shown at $t \approx 150$ fs.

1.3 SERS in Nanolenses [24]

As an efficient nanolens, we have proposed a self-similar linear chain of several metal nanospheres with progressively decreasing sizes and separations [25]. The proposed system can be used for nano-optical detection, Raman characterization, nonlinear spectroscopy, nano-manipulation of single molecules or nanoparticles, and other applications. We have also computationally found the enhancement coefficient of the Surface Enhanced Raman Scattering (SERS) and have shown that it is considerably different from commonly used fourth power of the field enhancement [24].

1.4 Computational Studies of SERS [24, 26]

We have revisited theory of one of the most important phenomena in nanoplasmonics, Surface Enhanced Raman Scattering [24, 26]. This theory shows that the predicted levels of enhancement in the red spectral region are still several orders of magnitude less than the enhancement factors $\sim 10^{13} - 10^{14}$ observed experimentally. The difference may be due to the effects not taken into account by the theory: self-similar enhancement [25] or chemical enhancement [27]. We are planning further computational studies of SERS in

systems with adiabatic compression that we have introduced earlier [20]. Note that recently the adiabatic compression effect that we predicted has been observed in two independent experiments [28, 29]. We trust that we can find a way to make SERS radiation much more intense by the better coupling between the far- and near-field zones that the adiabatic compression effect provides. This will provide unmatched sensitivity to SERS based methods of monitoring and detection of chemical and biological substances (threats).

1.5 Excitation of Surface Plasmon Polaritons (SPPs) by Free Electron Impact [30]

We have provided theoretical support and interpretation for the experimental investigation of the SPP generation by free-electron impact. This effect can be used as a basis of a novel method to visualize eigenmodes of plasmonic nanosystem by exciting them with an electron microscope beam.

2 Publications Resulting from the Grant

The major articles published by our group during this Report (2006-2007) period, which obtained the major support from this grant are indicated by bold typeface at the corresponding headings above. Overall, during the period of 2006-2007 we have published Refs. [1, 2, 19, 24, 30-37].

3 Directions for Future Work

We intend to concentrate on numerical methods for ultrafast processes on nanoscale. Special emphasis will be made on coherent control where we intend to use the time-reversal method. We intend to add polarization, which will double the number of the field degrees of freedom available to control the nanosystems. Another focus point will be many-multipole full-electrodynamic computational theory of the spatio-temporal coherent control.

References

1. X. Li and M. I. Stockman, *Time-Reversal Coherent Control in Nanoplasmonics*, arXiv:0705.0553 (2007).
2. X. Li and M. I. Stockman, *Coherent Control by Time-Reversal in Nanoplasmonics*, Phys. Rev. Lett. (Submitted) (2007).
3. M. I. Stockman, S. V. Faleev, and D. J. Bergman, *Coherent Control of Femtosecond Energy Localization in Nanosystems*, Phys. Rev. Lett. **88**, 67402-1-4 (2002).
4. M. I. Stockman, S. V. Faleev, and D. J. Bergman, *Coherently Controlled Femtosecond Energy Localization on Nanoscale*, Appl. Phys. B **74**, S63-S67 (2002).
5. M. I. Stockman, S. V. Faleev, and D. J. Bergman, *Coherently-Controlled Femtosecond Energy Localization on Nanoscale*, Appl. Phys. B **74**, 63-67 (2002).
6. M. I. Stockman, D. J. Bergman, and T. Kobayashi, in Proceedings of SPIE: Plasmonics: Metallic Nanostructures and Their Optical Properties, edited by N. J. Halas, *Coherent Control of Ultrafast Nanoscale Localization of Optical Excitation Energy* (SPIE, San Diego, California, 2003), Vol. 5221, p. 182-196.
7. M. I. Stockman, S. V. Faleev, and D. J. Bergman, in Ultrafast Phenomena XIII, *Coherently-Controlled Femtosecond Energy Localization on Nanoscale* (Springer, Berlin, Heidelberg, New York, 2003).
8. M. I. Stockman, D. J. Bergman, and T. Kobayashi, *Coherent Control of Nanoscale Localization of Ultrafast Optical Excitation in Nanosystems*, Phys. Rev. B **69**, 054202-10 (2004).
9. M. I. Stockman and P. Hewageegana, *Nanocalibrated Nonlinear Electron Photoemission under Coherent Control*, Nano Lett. **5**, 2325-2329 (2005).
10. M. Sukharev and T. Seideman, *Phase and Polarization Control as a Route to Plasmonic Nanodevices*, Nano Lett. **6**, 715-719 (2006).
11. M. Sukharev and T. Seideman, *Coherent Control Approaches to Light Guidance in the Nanoscale*, J. Chem. Phys. **124**, 144707-1-8 (2006).
12. T. Brixner, F. J. G. d. Abajo, J. Schneider, C. Spindler, and W. Pfeiffer, *Ultrafast Adaptive Optical near-Field Control*, Physical Review B **73**, 125437 (2006).
13. T. Brixner, F. J. G. d. Abajo, J. Schneider, and W. Pfeiffer, *Nanoscope Ultrafast Space-Time-Resolved Spectroscopy*, Phys. Rev. Lett. **95**, 093901-1-4 (2005).
14. A. Kubo, K. Onda, H. Petek, Z. Sun, Y. S. Jung, and H. K. Kim, *Femtosecond Imaging of Surface Plasmon Dynamics in a Nanostructured Silver Film*, Nano Lett. **5**, 1123-1127 (2005).

15. A. Kubo, K. Onda, H. Petek, Z. Sun, Y. S. Jung, and H. K. Kim, in *Ultrafast Phenomena XIV*, edited by T. Kobayashi, T. Okada, T. Kobayashi, K. A. Nelson and S. D. Silvestri, *Imaging of Localized Silver Plasmon Dynamics with Sub-Fs Time and Nano-Meter Spatial Resolution* (Springer, Niigata, Japan, 2004), Vol. 79, p. 645-649.
16. P. v. d. Walle, L. Kuipers, and J. L. Herek, in *Ultrafast Phenomena XV, Coherent Control of Light in Metal Nanostructures* (Pacific Grove, California, 2006), p. Paper TuD3.
17. M. Bauer, D. Bayer, T. Brixner, F. J. G. d. Abajo, W. Pfeiffer, M. Rohmer, C. Spindler, and F. Steeb, in *Ultrafast Phenomena XV, Adaptive Control of Nanoscopic Photoelectron Emission* (Pacific Grove, California, 2006), p. Paper ThB3.
18. M. Aeschlimann, M. Bauer, D. Bayer, T. Brixner, F. J. G. d. Abajo, W. Pfeiffer, M. Rohmer, C. Spindler, and F. Steeb, *Adaptive Subwavelength Control of Nano-Optical Fields*, *Nature* **446**, 301-304 (2007).
19. M. Durach, A. Rusina, K. Nelson, and M. I. Stockman, *Toward Full Spatio-Temporal Control on the Nanoscale*, *Nano Lett.* **7**, (DOI:10.1021/nl071718g, 5 pages) (2007).
20. M. I. Stockman, *Nanofocusing of Optical Energy in Tapered Plasmonic Waveguides*, *Phys. Rev. Lett.* **93**, 137404-1-4 (2004).
21. M. M. Wefers and K. A. Nelson, *Ultrafast Optical Wave-Forms*, *Science* **262**, 1381-1382 (1993).
22. M. M. Wefers, K. A. Nelson, and A. M. Weiner, *Multidimensional Shaping of Ultrafast Optical Waveforms*, *Opt. Lett.* **21**, 746-748 (1996).
23. T. Feurer, J. C. Vaughan, and K. A. Nelson, *Spatiotemporal Coherent Control of Lattice Vibrational Waves*, *Science* **299**, 374-377 (2003).
24. K. Li, M. I. Stockman, and D. J. Bergman, *Li, Stockman, and Bergman Reply to Comment On "Self-Similar Chain of Metal Nanospheres as an Efficient Nanolens"*, *Phys. Rev. Lett.* **97**, 079702 (2006).
25. K. Li, M. I. Stockman, and D. J. Bergman, *Self-Similar Chain of Metal Nanospheres as an Efficient Nanolens*, *Phys. Rev. Lett.* **91**, 227402-1-4 (2003).
26. M. I. Stockman, in *Springer Series Topics in Applied Physics*, edited by K. Kneipp, M. Moskovits and H. Kneipp, *Surface Enhanced Raman Scattering – Physics and Applications* (Springer-Verlag, Heidelberg New York Tokyo, 2006).
27. J. Jiang, K. Bosnick, M. Maillard, and L. Brus, *Single Molecule Raman Spectroscopy at the Junctions of Large Ag Nanocrystals*, *J. Phys. Chem. B* **107**, 9964-9972 (2003).
28. E. Verhagen, L. Kuipers, and A. Polman, *Enhanced Nonlinear Optical Effects with a Tapered Plasmonic Waveguide*, *Nano Lett.* **7**, 334-337 (2007).
29. C. Ropers, C. C. Neacsu, T. Elsaesser, M. Albrecht, M. B. Raschke, and C. Lienau, *Grating-Coupling of Surface Plasmons onto Metallic Tips: A Nano-Confined Light Source*, *Nano Lett.* **7**, 2784-2788 (2007).
30. M. V. Bashevov, F. Jonsson, A. V. Krasavin, N. I. Zheludev, Y. Chen, and M. I. Stockman, *Generation of Traveling Surface Plasmon Waves by Free-Electron Impact*, *Nano Lett.* **6**, 1113-1115 (2006).
31. M. I. Stockman, *Slow Propagation, Anomalous Absorption, and Total External Reflection of Surface Plasmon Polaritons in Nanolayer Systems*, *Nano Lett.* **6**, 2604-2608 (2006).
32. M. Stockman, in *Topics in Applied Physics*, edited by K. Kneipp, M. Moskovits and H. Kneipp, *Electromagnetic Theory of SERS* (Springer Verlag, 2006), p. 47-66.
33. M. I. Stockman, K. Li, S. Brasselet, and J. Zyss, *Octupolar Metal Nanoparticles as Optically Driven, Coherently Controlled Nanorotors*, *Chem. Phys. Lett.* **433**, 130-135 (2006).
34. M. I. Stockman, *Criterion for Negative Refraction with Low Optical Losses from a Fundamental Principle of Causality*, *Phys. Rev. Lett.* **98**, 177404-1-4 (2007).
35. M. Durach, A. Rusina, K. Nelson, and M. I. Stockman, *Toward Full Spatio-Temporal Control on the Nanoscale*, arXiv:0705.0725 (2007).
36. M. I. Stockman and P. Hewageegana, *Absolute Phase Effect in Ultrafast Optical Responses of Metal Nanostructures*, *Appl. Phys. A* (In Print; Published on Line: DOI: 10.1007/s00339-007-4105-7) (2007).
37. M. I. Stockman, M. F. Kling, U. Kleineberg, and F. Krausz, *Attosecond Nanoplasmonic Field Microscope*, *Nature Photonics* **1**, 539-544 (2007).

Understanding Nanoscale Confinement Effects in Solvent-Driven Chemical Reactions

Ward H. Thompson

Department of Chemistry, University of Kansas, Lawrence, KS 66045

Email: *wthompson@ku.edu*

Program Scope

It is now possible to synthesize nanostructured porous materials with a tremendous variety of properties including sol-gels, zeolites, organic and inorganic supramolecular assemblies, reverse micelles, vesicles, and even proteins. The interest in these materials derives from their potential for carrying out useful chemistry (*e.g.*, as microporous and mesoporous catalysts with critical specificity, fuel cell electrodes and membranes, molecular sieves, and chemical sensors) and for understanding the chemistry in similar systems found in nature. Despite the advances in synthetic techniques, our understanding of chemistry in solvents confined in nanoscale cavities and pores is still relatively limited. Ultimately, one would like to design nanostructured materials adapted for specific chemical purposes, *e.g.*, catalysis or sensing, by controlling the cavity/pore size, geometry, and surface chemistry. To develop guidelines for this design, we must first understand how the characteristics of the confining framework affect the chemistry. Thus, the overarching question addressed by our work is *How does a chemical reaction occur differently in a nano-confined solvent than in a bulk solvent?*

Solvent-driven reactions, typically those involving charge transfer, should be most affected by confinement of the solvent. The limited number of solvent molecules, geometric constraints of the nanoscale confinement, and solvent-wall interactions can have dramatic effects on both the reaction energetics and dynamics. Our primary focus is on proton transfer and related processes. A fundamental understanding of such solvent-driven reactions in nano-confined solvents will impact many areas of chemistry and biology. The diversity among nanoscale cavities and pores (*e.g.*, in their size, shape, flexibility, and interactions with the solvent and/or reactants) makes it difficult to translate studies of one system into predictions for another. Thus, we are focusing on developing a unified understanding of reaction dynamics in the diverse set of confinement frameworks, including nanoscale pores of varying surface chemistry.

Recent Progress

Proton Transfer. We have investigated a number of properties of a model intramolecular phenol-amine proton transfer system in a CH₃Cl solvent confined in a smooth, hydrophobic spherical cavity. We have developed a valence bond description for the reaction complex based loosely on a widely applied model.¹ Monte Carlo and mixed quantum-classical (MQC) molecular dynamics (MD) simulations have previously been used to investigate complex position distributions, free energy curves, and proton transfer reaction dynamics.^{2,3}

Most recently we have calculated the infrared spectrum of this model proton transfer reaction complex in a nanoconfined solvent using MQC-MD.⁴ The reaction free energy was varied to explore cases with varying degrees of proton transfer. We found that both $0 \rightarrow 1$ and $0 \rightarrow 2$ vibrational transitions contribute to the infrared spectrum, due to configurations in which the excited vibrational state of the proton is delocalized, a process we labeled “attempted chemical exchange.” This attempted chemical exchange gives broad lineshapes for the IR spectra when proton transfer is possible; actual chemical exchange, *i.e.*, proton transfer, is too slow to lead to significant broadening. Moreover, the vibrational transition frequency is directly related to a collective solvent coordi-

nate, such that the distribution of frequencies is determined by the sampling of different solvent coordinate values. Finally, the frequency autocorrelation function, $\langle \delta\omega(0) \delta\omega(t) \rangle$, which is accessible in nonlinear IR experiments, has a long-time tail that appears to contain information about the proton transfer reaction rate constants. Understanding in detail what information vibrational spectroscopy provides about proton transfer reaction equilibria and dynamics is important for its use as a characterization tool in nanoconfined solvents where the proton transfer dynamics can be particularly diverse.³

Entropic Effects in Nanoconfined Solvents. While there have been some experimental measurements of charge transfer reactions in nanoconfined solvents, the changes in the relevant solvation dynamics are typically probed using time-dependent fluorescence (TDF) Stokes shift spectroscopy. In TDF experiments the fluorescence energy of a probe dye molecule is monitored as a function of time after excitation to follow the solvent reorganization in response to the change in dipole associated with promotion of the molecule from the ground to the excited electronic state. In nanoconfined solvents, TDF measurements generally find that the fluorescence energy decays on multiple time scales including ones that are significantly longer (often by 2-3 orders-of-magnitude) than those observed in the corresponding bulk liquid. Clearly such substantial modification of the solvation dynamics upon nanoscale confinement also affects how a chemical reaction occurs. We have recently completed a study of one of the key driving forces for these changes: entropy.⁵

Specifically, we have calculated the contributions of entropy and internal energy to the Helmholtz free energy of a model dye molecule dissolved in three nanoconfined solvents (CH_3I , CH_3CN , and CH_3OH) by Monte Carlo simulations. This follows up on our previous studies that revealed that the dye molecule position depends strongly on the electronic state⁶ and that this leads to a long-time component in the TDF signal due to solute diffusion after excitation.⁷ Our results indicate that entropic contributions are central in controlling the shape of the free energy surfaces of the ground and excited state solute. Electrostatic interactions, which can be straightforwardly seen in the internal energy, $\Delta U(d)$, are most favorable when the solute center-of-mass is between two solvent layers, with one atom of the diatomic dye model in each solvent layer. It is entropic considerations that minimize the free energy at positions where the solute center-of-mass is in the solvent layers, but the internal energy ultimately determines in which solvent layer the global free energy minimum is located. Moreover, it is rotational entropy that represents a significant component of the effect due to differences in orientational freedom in varying locations in the nanocavity.

Linear Response in Nanoconfined Solvents. Linear response (LR) theory is frequently applied to describe dynamics in liquids and has been widely successful. In particular, TDF is frequently simulated based on a linear-response approximation. Nanoconfined solvents represent an important and interesting test for these approaches given their complex dynamics. We tested two LR approximations – one based on ground state equilibrium dynamics, the other on excited state equilibrium dynamics – for TDF in nanoconfined solvents by comparing to nonequilibrium MD simulations.⁸ The calculations showed that, while the ground state and excited state LR results are dramatically different, the excited state approximation is quite accurate.

These results led us to investigate the underlying assumptions of the LR approximations. Specifically, in collaboration with Prof. Brian B. Laird at KU, we have shown that the excited state LR approximation gives the same result as assuming that the fluorescence energy gap exhibits Gaussian statistics.⁹ This means one does not need to rely on previous derivations that required either an equivalence between ground and excited state dynamics (clearly not observed in this case) or small deviations from the average energy gap (also not the case). Thus, this provides insight into the much discussed relationship between linear response and Gaussian statistics. In particular, subtle but important differences between the two approximations are illuminated that suggest the result

is likely more generally applicable than suggested by the usual linearization procedure. In addition, the assumption of Gaussian statistics directly points to straightforward checks of the validity of the approximation with essentially no additional computational effort. While these results have particular relevance to nanoconfined solvents, they are general and should add broadly to our understanding of LR-type approximations.

Smoluchowski Equation Description of Dynamics in Nanoconfined Solvents. A number of models have been proposed to describe the multi-exponential, long-time decay observed in time-dependent fluorescence studies of nanoconfined solvents. While molecular dynamics simulation provides a particularly appealing avenue for exploring these models, full nonequilibrium simulations can be quite time consuming. In nanoconfined solvents the effort is compounded by the heterogeneity of the system and the long-time dynamics, which together mean that many lengthy nonequilibrium trajectories are required. This provides an impetus for developing other ways of rapidly simulating the TDF dynamics, and ultimately reaction dynamics, for a large number of nanoconfined solvent systems. To that end, we have developed a Smoluchowski equation approach for the description of time-dependent fluorescence in solvents confined in spherical cavities and cylindrical pores.¹⁰

In addition to providing a rapid approach to simulating the time-dependent Stokes shift and solute diffusive motion, the Smoluchowski equation has a number of other advantages. Specifically, the entire time-dependent fluorescence spectrum is obtained as a function of time; this is typically not feasible in nonequilibrium MD simulations. The full time-dependent solute position distribution function is also calculated in the approach, allowing insight into the mechanism(s) of diffusion. Further, it is quite easy to change the geometry of the confining framework within the Smoluchowski equation, so that spherical, cylindrical, and slit pore geometries can be straightforwardly compared. The approach does require knowledge of the potential of mean force for the solute as a function of both the solute position and a collective solvent coordinate, but reasonably constructed model free energy surfaces are often sufficient. We have validated the Smoluchowski equation approach by comparison to MD simulation results¹⁰ for which at least part of the free energy surfaces are known accurately.⁵

Model Silica Pores. One of the most critical characteristics of confining frameworks is the surface chemical functionality. We have previously developed a method for generating roughly cylindrical pores in amorphous silica in which the surface functionality (*e.g.*, hydrophilicity/hydrophobicity) can be fully controlled.¹² We have previously used MD simulations of ethylene glycol confined in roughly cylindrical hydrophilic silica pores (radius ~ 12 Å) to test the frequently applied two-state model for nanoconfined liquids. Confined ethylene glycol has been experimentally observed to have a conformational equilibrium that is dependent on pore size in hydrophilic sol-gel pores.¹³ We found that the two-state model was not generally supported by our results.¹⁴ Rather, the molecular-level picture of the liquid near the interface in these confined environments changes significantly less dramatically than suggested by a two-state model. We are currently completing simulations of ethylene glycol in hydrophobic, $-\text{O}-\text{C}(\text{CH}_3)_3$ terminated, pores for which, interestingly, the conformational equilibrium does not depend on pore size.¹³ We are also beginning MQC-MD simulations of proton transfer reaction dynamics and hydrogen bond formation and breaking in these silica pores.

Future Plans

We are currently working on several extensions of this work. We are developing, based on *ab initio* calculations, new valence bond models for intra- and intermolecular proton transfer systems that are experimentally accessible. We are examining proton transfer reactions in the model silica

pores with varying surface chemistry described above; the infrared spectra of the proton transfer reaction complex in these environments will also be calculated. In order to compute the reaction rate constants we are developing reactive flux-type approaches for nonadiabatic reaction dynamics within a classical mapping formalism. This will allow the reaction rate constants to be efficiently and accurately calculated. Finally, we are developing Smoluchowski equation approaches to modeling proton transfer reaction dynamics in nanoconfined solvents that will make long time and length scales accessible.

References

- [1] H. Azzouz and D. Borgis, *J. Chem. Phys.* **98**, 7361-7375 (1993).
- [2] †S. Li and W.H. Thompson, *J. Phys. Chem. B* **109**, 4941-4946 (2005). “Proton Transfer in Nano-confined Polar Solvents. I. Free Energies and Solute Position ”
- [3] †W.H. Thompson, *J. Phys. Chem. B* **109**, 18201-18208 (2005). “Proton Transfer in Nano-confined Polar Solvents. II. Adiabatic Proton Transfer Dynamics”
- [4] †K.R. Mitchell-Koch and W.H. Thompson, *J. Phys. Chem. B* (submitted). “Infrared Spectroscopy of a Model Phenol-Amine Proton Transfer Complex in Nanoconfined CH₃Cl”
- [5] †K.R. Mitchell-Koch and W.H. Thompson, *J. Phys. Chem. C* **111**, 11991-12001 (2007). “How Important is Entropy in Determining the Position-Dependent Free Energy of a Solute in a Nanoconfined Solvent?”
- [6] W.H. Thompson, *J. Chem. Phys.* **117**, 6618-6628 (2002).
- [7] †W.H. Thompson, *J. Chem. Phys.* **120**, 8125-8133 (2004). “Simulations of Time-Dependent Fluorescence in Nano-Confined Solvents”
- [8] †B.B. Laird and W.H. Thompson, (in preparation). “Time-Dependent Fluorescence in Nanoconfined Solvents: Linear Response Approximations and Gaussian Statistics”
- [9] †B.B. Laird and W.H. Thompson, *J. Chem. Phys.*, **126**, 211104 (2007). “On the Connection between Gaussian Statistics and Excited-State Linear Response for Time-Dependent Fluorescence,”
- [10] †X. Feng and W.H. Thompson, *Journal of Physical Chemistry C*, (in press). “Smoluchowski Equation Description of Solute Diffusion Dynamics and Time-dependent Fluorescence in Nanoconfined Solvents”
- [11] †X. Feng and W.H. Thompson, (in preparation). “Time-dependent Fluorescence in Nanoconfined Solvents. A Smoluchowski Equation Model Study”
- [12] †T.S. Gulmen and W.H. Thompson, “Model Silica Pores with Controllable Surface Chemistry for Molecular Dynamics Simulations” in *Dynamics in Small Confining Systems VIII*, edited by J.T. Fourkas, P. Levitz, R. Overney, M. Urbakh (Mater. Res. Soc. Symp. Proc. **899E**, Warrendale, PA, 2005), 0899-N06-05.
- [13] R.-S. Luo and J. Jonas, *J. Raman. Spectrosc.* **32**, 975-978 (2001).
- [14] †T.S. Gulmen and W.H. Thompson, “Testing the Two-State Model of Nanoconfined Liquids: The Conformational Equilibrium of Ethylene Glycol in Amorphous Silica Pores,” *Langmuir* **22**, 10919-10923 (2006).

†DOE-sponsored publication.

The Role of Electronic Excitations on Chemical Reaction Dynamics at Metal, Semiconductor and Nanoparticle Surfaces

John C. Tully

Department of Chemistry, Yale University, 225 Prospect Street,

P. O. Box 208107, New Haven, CT, 06520-8107 USA

john.tully@yale.edu

Program Scope

Achieving enhanced control of the rates and molecular pathways of chemical reactions at the surfaces of metals, semiconductors and nanoparticles will have impact in many fields of science and engineering, including heterogeneous catalysis, photocatalysis, materials processing, corrosion, solar energy conversion and nanoscience. However, our current atomic-level understanding of chemical reactions at surfaces is incomplete and flawed. Conventional theories of chemical dynamics are based on the Born-Oppenheimer separation of electronic and nuclear motion. Even when describing dynamics at metal surfaces where it has long been recognized that the Born-Oppenheimer approximation is not valid, the conventional approach is still used, perhaps patched up by introducing friction to account for electron-hole pair excitations or curve crossings to account for electron transfer. There is growing experimental evidence that this is not adequate. We are examining the influence of electronic transitions on chemical reaction dynamics at metal and semiconductor surfaces. Our program includes the development of new theoretical and computational methods for nonadiabatic dynamics at surfaces, as well as the application of these methods to specific chemical systems of experimental attention. Our objective is not only to advance our ability to simulate experiments quantitatively, but also to construct the theoretical framework for understanding the underlying factors that govern molecular motion at surfaces and to aid in the conception of new experiments that most directly probe the critical issues.

Recent Progress

Our efforts over the last year have focused on two fronts. First, we have derived a hierarchy of computational procedures for simulating chemical processes at metal surfaces that properly incorporate nonadiabatic electronic transitions and electron transfer. Our theoretical framework goes beyond prior weak-coupling “electronic friction” models, and can be implemented in fully-quantum, semiclassical and pseudo-classical versions with corresponding tradeoffs between practicality and accuracy. Second, we have completed our construction of an *ab initio* based “diabatic” Hamiltonian describing the interaction of the nitric oxide molecule with the (111) surface of gold. This system has been shown in the Wodtke laboratory to exhibit striking nonadiabatic behavior inconsistent with the friction picture. Our diabatic Hamiltonian will serve as a testing ground for theories of nonadiabatic molecule-surface dynamics. We have carried out dynamics simulations in the adiabatic limit with this Hamiltonian as a benchmark, and are now gearing up for including nonadiabatic effects with both the electronic friction model and with various manifestations of our diabatic dynamics theory.

In the prior year of this project (2006) we developed a formulation of nonadiabatic dynamics at metal surfaces in which motion occurs on multiple “diabatic” electronic potential energy surfaces, i.e., surfaces with gradually changing electronic character. Our original formulation, published in Phys. Rev. (Ref. 2) is fully quantum mechanical and therefore impractical for many-atom systems. In the current year (2007), we developed more practical semiclassical and pseudo-classical versions of the theory. The motivation for these efforts derives from experiment. It has become increasingly clear that at metal surfaces nonadiabatic behavior is the rule rather than the exception. Electron-hole pair transitions, charge transfer and hot-electron-induced motion can be dominant pathways for energy flow. Recent experiments in the groups of Wodtke, Somorjai, MacFarland, Hasselbrink, and others have demonstrated that molecular vibrational energy, adsorption energy and reaction exothermicity can produce highly excited electrons, even resulting in electron emission. The widely accepted electronic friction theory of nonadiabatic dynamics at metal surfaces invokes multiple low-energy excitations, clearly inconsistent with the production of high kinetic energy electrons. In contrast to the friction model, our current approach does not assume weak coupling, and can be applied even to cases where a sudden electron jump between the molecule and the surface may occur. Our approach is based on adapting a prior model, developed to describe gas-phase electron-molecule scattering, to interactions of molecules with metal surfaces. The continuum of electronic states now arises from the metallic conduction band rather than from free electron states, but the formalism remains essentially the same (see Ref. 2). This theory allows the motion on each potential energy surface to be treated independently, a huge simplification. However, the motion is still quantum mechanical. Quantum evolution for systems with many degrees of freedom, even when confined to a single potential energy surface, is computationally prohibitive. An additional complication is that the potential energy surfaces in this case have complex-valued energies, the imaginary part related to the lifetime of the electronic state. In 2007 we developed semiclassical (accepted for publication in Phys. Rev. Lett.) and pseudo-classical (unpublished) procedures for evolving nuclear motion that are much more computationally tractable. First, we extended the semiclassical Gaussian wave packet approach developed by Heller to treat complex-valued Hamiltonians with off-diagonal couplings among many states, providing a practical procedure that is quite accurate, at least for short timescales. We discovered an enormous simplification in evolving nuclear motion on the continuum of charge-transfer potential energy surfaces (Ref. 3). Under the assumption that these surfaces are parallel, wave packets need to be propagated on only one representative surface. The motion on all of the others can be extracted simply by properly summing wave packets with phases appropriate for each specific continuum state. The method has direct applicability to electron transfer at metal and semiconductor surfaces, and we plan to extend it to apply to spin transitions in open-shell molecules, a controlling factor in many important chemical reactions at surfaces.

Very recently (unpublished) we have extended the semiclassical model to a classical-like limit. The resulting model invokes classical mechanical motion on each diabatic potential energy surface, with transitions among surfaces in the spirit of the surface hopping approach, but controlled by the imaginary part of the energy. Hopping among the myriad (infinite number) of potential energy surfaces exhibited by the interaction of molecular states with a metallic conduction band may appear daunting.

However, the “wide-band limit” that underlies our original formulation, Ref. 2, greatly reduces the number of “hops” between different diabatic electronic states. We expect this pseudo-classical implementation to become the workhorse for simulating nonadiabatic dynamics at metal surfaces.

In 2006 we completed an *ab initio* calculation of the potential energy surfaces and nonadiabatic couplings that govern the interaction of the NO molecule with the Au(111) surface. Our prior effort using finite gold clusters was not sufficiently accurate, so we applied the plane wave density functional code VASP. The resulting energies and molecular charges appear much more accurate and consistent. In 2007 we completed the next stage of the program, construction of a diabatic 2x2 Hamiltonian matrix from the *ab initio* results, required to examine dynamics beyond the adiabatic (ground state) approximation. The diagonal elements of the 2x2 matrix are the diabatic neutral and charged potential energy surfaces. These are coupled by an off-diagonal potential surface such that the resulting ground state becomes a mixture of charged and neutral configurations; i.e., the lower energy root of the 2x2 Hamiltonian matrix. In order to uniquely define the 2x2 symmetric matrix, we need three independent pieces of information at each nuclear configuration. Previously we computed only two, the ground state energy and the Löwdin or Bader charge on the NO molecule, which we assign to be the square of the coefficient of the ionic configuration in the ground state. We have now supplied the missing third piece of information by computing the shift in the *ab initio* ground state energy upon application of a small electric field. We have recently accomplished construction of a diabatic 2x2 Hamiltonian, with diagonal and off-diagonal elements fit to analytic expressions, that provides an accurate fit to the *ab initio* energies, charges and electric field induced shifts for all positions, orientations and internuclear separations of the NO molecule interacting with the gold surface. The diabatic Hamiltonian properly incorporates all major aspects of the interaction, including the image force and the electron transfer at extended N-O bond separations.

We have carried out the first stage of simulating NO-gold dynamics with the diabatic Hamiltonian, adiabatic dynamics. Our main interests are the importance and nature of nonadiabatic effects, of course, but we first need to understand adiabatic behavior. Our computed sticking probabilities are now in reasonably good accord with experiments of the Wodtke group, in contrast with our earlier attempts. We observe considerable vibrational energy transfer at low incident NO velocities, although nonadiabaticity will certainly be required to reproduce experiment. A somewhat counter-intuitive prediction has emerged, that the non-dissociative sticking probability for a highly vibrationally excited NO molecule can be larger than that for an unexcited molecule. It will be interesting to see if this behavior survives when nonadiabatic effects are properly accounted for.

Now that we have a relatively simple and reliable representation of the NO-Au(111) interaction in the form of a 2x2 diabatic Hamiltonian matrix, we are in position to explore nonadiabatic effects using both electronic friction and our diabatic approaches. For the latter, we will begin with the pseudo-classical version since this is simplest and should reveal the major mechanisms and pathways. If quantization of the NO vibration appears to have a significant effect, we then plan to implement the semiclassical wave-packet version. These results will be directly compared to experiment. In addition, the

diabatic Hamiltonian can serve as a platform for use by others to evaluate new methods and explore nonadiabatic dynamics in a realistic, complex and well-studied system.

Future Plans

The goals of our research program include both specific aspects of the NO-Au system and more general investigations of nonadiabatic behavior at surfaces. The next steps in the study are.

1. Complete the current benchmark adiabatic molecular dynamics simulations as required to subsequently assess the importance of nonadiabatic transitions.
2. Carry out “molecular dynamics with electronic friction” (Head-Gordon and Tully) simulations using the 2x2 diabatic Hamiltonian.
3. Expand the 2x2 matrix representation into an (n+1) by (n+1) representation to provide the bound-continuum interactions required for full treatment of nonadiabatic behavior.
4. Carry out pseudo-classical diabatic dynamics simulations as described above to introduce electronic excitations and electron transfer beyond the friction model.
5. Extend and apply the diabatic dynamics strategy beyond the wide band (Markov) approximation, as required to describe the double or multiple “on” and “off” electron hops that may control the NO-Au dynamics. *This may prove to be a significant challenge.*
6. Through analysis of the results of application of this hierarchy of theoretical methods, draw conclusions about the importance and nature of nonadiabatic electronic transitions both in the NO-Au system and more generally.
7. Develop improved *ab initio* methods for computing energies and widths of lifetime-broadened electronic states near metal and semiconductor surfaces, through extension of “constrained density functional theory”. These are the properties that determine the rate and extent of electron transfer as a molecule approaches the surface; i.e., that are required to construct a diabatic Hamiltonian.
8. Carry out *ab initio* calculations of energies, charge distributions and level widths as input to constructing valence-bond type Hamiltonians for a number of chemical systems, including the CO oxidation reaction on platinum. Somorjai and coworkers have recently demonstrated that hot-electrons are produced as this reaction unfolds.
9. Explore the dynamics of open shell species with metal surfaces. An example is the oxygen molecule where transitions between the ground state triplet and low-lying singlet states may occur without spin-orbit interactions via a two-electron exchange with the conduction band, with major implications to chemical reactivity.

References to Publications of DOE-Sponsored Research: 2006-2007

1. Neil Shenvi, Sharani Roy, Priya Parandekar and John C. Tully, “Vibrational relaxation of NO on Au(111) via electron-hole pair generation”, *J. Chem. Phys.* **125**, 154703, 2006.
2. Neil Shenvi, Hongzhi Cheng and John C. Tully, “Nonadiabatic dynamics near metal surfaces: Decoupling quantum equations of motion in the wide-band limit”, *Phys. Rev.* **A74**, 062902 (2006).
3. Hongzhi Cheng, Neil Shenvi and John C. Tully, “A semiclassical approach to nonadiabatic dynamics near metal surfaces”, *Phys. Rev. Lett.*, in press.

Chemical Kinetics and Dynamics at Interfaces

*Gas Phase Investigation of Condensed Phase Phenomena*¹

Lai-Sheng Wang (PI)

Department of Physics, Washington State University, 2710 University Drive, Richland, WA, 99354 and the Chemical & Materials Sciences Division, Pacific Northwest National Laboratory, P.O. Box 999, MS K8-88, Richland, WA 99352. E-mail: ls.wang@pnl.gov

Program Scope

The broad scope of this program is aimed at microscopic understanding of condensed phase phenomena using clusters as model systems. Our current focus is on the microsolvation of complex anions that are important in solution chemistry. The primary experimental technique is photoelectron spectroscopy of size-selected anions. Unique experimental techniques have been developed by coupling electrospray ionization with photoelectron spectroscopy, that allows complex anions, including multiply charged anions and solvated clusters, from solution samples to be investigated in the gas phase. Experimental studies are combined with ab initio calculations to:

- obtain a molecular-level understanding of the solvation of complex anions (both singly and multiply charged) important in condensed phases
- understand the molecular processes and initial steps of dissolution of salt molecules by polar solvents
- probe the structure and dynamics of solutions and air/solution interfaces

Complexes anions, in particular multiply charged anions, are ubiquitous in nature and often found in solutions and solids. However, few complex anions have been studied in the gas phase due to the difficulty in generating them and their intrinsic instability as a result of strong intramolecular Coulomb repulsion in the case of multiply charged anions. Microscopic information on the solvation and stabilization of these anions is important for the understanding of solution chemistry and properties of inorganic materials or atmospheric aerosols involving these species. Gas phase studies with controlled solvent numbers and molecular specificity are ideal to provide such microscopic information. We have developed a new experimental technique to investigate multiply charged anions and solvated species directly from solution samples and probe their electronic structures, intramolecular Coulomb repulsion, stability, and energetics using electrospray and PES. A central theme of this research program lies at obtaining a fundamental understanding of environmental materials and solution chemistry. These are important to waste storage, subsurface and atmospheric contaminant transport, and other primary DOE missions.

Recent Progress (2004-2007)

First Steps Towards Dissolution of NaSO₄⁻ by Water: Detailed knowledge of how polar molecules are dissolved in a solvent is essential to understanding the chemistry taking place in salt solutions and the fate and transport of environmental pollutants. Sulfate in particular is ubiquitous in drinking water, soils, and atmospheric aerosols. We have been interested in the microsolvation of the sulfate dianion (SO₄²⁻) and studied how this dianion is stabilized and solvated in hydrated clusters in the gas phase previously. In the current work, we aimed at understanding how a sulfate salt molecule is desolved and hydrated. Solvated clusters of sulfate in the form of NaSO₄⁻(H₂O)_n (*n* = 0 – 4) were generated using electrospray to simulate the first dissolution steps of sulfate salts in water. Photoelectron

¹ Collaborators on these projects include X. B. Wang.

spectroscopy and theoretical calculations indicated that the first three water molecules strongly interact with both Na^+ and SO_4^{2-} , forming a three-water solvation ring, which separates the cation from the anion (Fig. 1). Such contact ion pairs may exist in concentrated solution.

Microsolvation of the Dicyanamide Anion: $[\text{N}(\text{CN})_2^-](\text{H}_2\text{O})_n$ ($n = 0-12$): The dicyanamide anion $\text{N}(\text{CN})_2^-$ is a very stable anion in both solution and solids. Its transition metal salts have attracted recent attention because of their potential use as molecular magnets and multifunctional materials. In this work, we probe the electronic structure of $\text{N}(\text{CN})_2^-$ and its solvated clusters. Photoelectron spectra of $[\text{N}(\text{CN})_2^-](\text{H}_2\text{O})_n$ ($n = 0-12$) have been measured at room temperature and also at low temperature for $n = 0-4$. Vibrationally resolved photoelectron spectra are obtained for $\text{N}(\text{CN})_2^-$, allowing the electron affinity of the $\text{N}(\text{CN})_2$ radical to be determined accurately as 4.135 ± 0.010 eV. The electron binding energies and the spectral width of the hydrated clusters are observed to increase with the number of water molecules. The first five waters are observed to provide significant stabilization to the solute, whereas the stabilization becomes weaker for $n > 5$. The spectral width, which carries information about the solvent reorganization upon electron detachment in $[\text{N}(\text{CN})_2^-](\text{H}_2\text{O})_n$, levels off for $n > 6$. Theoretical calculations reveal several close-lying isomers for $n = 1$ and 2 due to the fact that the $\text{N}(\text{CN})_2^-$ anion possesses three almost equivalent hydration sites. In all the hydrated clusters, the most stable structures consist of a water cluster solvating one end of the $\text{N}(\text{CN})_2^-$ anion.

Observation of Weak C-H...O Hydrogen-Bonding by Unactivated Alkanes: Weak C-H...O hydrogen bonding has been recognized to play a major role in biological molecular structures and functions. Using the newly developed low-temperature PES apparatus we studied the C-H...O hydrogen bonding between unactivated alkanes and the carboxylate functional group. We observed that gaseous linear carboxylates, $\text{CH}_3(\text{CH}_2)_n\text{CO}_2^-$, assume folded structures at low temperatures due to weak C-H...O hydrogen bonding between the terminal CH_3 and CO_2^- groups for $n \geq 5$. Temperature-dependent studies showed that the folding transition depends on both the temperature and the aliphatic chain length. Theoretical calculations revealed that for $n = 3-8$, the folded conformations are more stable than the linear structures, but C-H...O hydrogen bonding only forms for species with $n \geq 5$ due to steric constraint in the smaller species. One C-H...O hydrogen bond is formed in the $n = 5$ and 6 species, whereas two C-H...O hydrogen bonds are formed for $n = 7$ and 8. Comparison of the photoelectron spectral shifts for the folded relative to the linear conformations yielded lower limits for the strength of the C-H...O hydrogen bonds in $\text{CH}_3(\text{CH}_2)_n\text{CO}_2^-$, ranging from 1.2 kcal/mol for $n = 5$ to 4.4 kcal/mol for $n = 8$.

Temperature-Dependent Photoelectron Spectroscopy of Methyl-Benzoate Anions and the Observation of Steric Effect in ortho-Methyl-Benzoate: Temperature-dependent photoelectron spectra of benzoate anion ($\text{C}_6\text{H}_5\text{CO}_2^-$) and its three methyl-substituted isomers (*o*-, *m*-, *p*- $\text{CH}_3\text{C}_6\text{H}_4\text{CO}_2^-$) have been obtained using a newly developed low-temperature PES apparatus that features an electrospray source and a cryogenically controlled ion trap. Detachment channels due to removing electrons from the carboxylate group and benzene ring π electrons were distinctly observed. Well-resolved vibrational structures were obtained in the lower binding energy region due to the OCO bending modes, except for *o*- $\text{CH}_3\text{C}_6\text{H}_4\text{CO}_2^-$, which yielded broad spectra even at the lowest ion trap temperature (18 K). Theoretical calculations revealed a large geometry change in the OCO angles between the anion and neutral ground states, consistent with the broad ground state bands observed for all species. A strong steric effect was observed between the carboxylate and the methyl group in *o*- $\text{CH}_3\text{C}_6\text{H}_4\text{CO}_2^-$, such that the $-\text{CO}_2^-$ group is pushed out of the plane of the benzene ring by $\sim 25^\circ$ and its internal rotational barrier is significantly reduced. The low rotational barrier in *o*- $\text{CH}_3\text{C}_6\text{H}_4\text{CO}_2^-$, which makes it very difficult to be cooled vibrationally, and the strong coupling between the OCO bending and CO_2 torsional modes yielded the broad PES spectra for this isomer. It is shown that there is *no* C-H...O hydrogen bond in *o*- $\text{CH}_3\text{C}_6\text{H}_4\text{CO}_2^-$ and the interaction between the carboxylate and methyl groups in this anion is found to be repulsive in nature.

Probing the Low-Barrier Hydrogen Bond in Hydrogen Maleate in the Gas Phase: Photoelectron spectra of maleic and fumaric acid monoanions (*cis*-/*trans*-HO₂CCH=CHCO₂⁻) were obtained at low temperatures to investigate the strength of the low-barrier hydrogen bond in hydrogen maleate. Vibrational structure was observed for *trans*-HO₂CCH=CHCO₂⁻ due to the OCO bending modes; however *cis*-HO₂CCH=CHCO₂⁻ yielded a broad and featureless spectrum. The electron binding energy of *cis*-HO₂CCH=CHCO₂⁻ is about 1 eV blue-shifted relative to *trans*-HCO₂CH=CHCO₂⁻ due to the formation of a strong intramolecular hydrogen bond in the *cis*-isomer. Theoretical calculations (CCSD(T)/aug-cc-pVTZ and B3LYP/aug-cc-pVTZ) were carried out to estimate the strength of the intramolecular hydrogen bond in *cis*-HO₂CCH=CHCO₂⁻. Combining experimental and theoretical calculations, the intramolecular hydrogen bond strength in hydrogen maleate is estimated to be 21.5 ± 2.0 kcal/mol.

Low-Temperature PES of Aliphatic Dicarboxylate Monoanions, HO₂C(CH₂)_nCO₂⁻ (n = 1 – 10): Hydrogen Bond Induced Cyclization and Strain Energies: Photoelectron spectra of singly-charged dicarboxylate anions HO₂C(CH₂)_nCO₂⁻ (n = 1 – 10) were obtained at two different temperatures (300 and 70 K). The electron binding energies of these species were observed to be much higher than the singly-charged monocarboxylate anions, suggesting the singly-charged dicarboxylate anions are cyclic due to strong intramolecular H-bonding between the terminal –CO₂H and –CO₂⁻ groups. The measured electron binding energies were observed to depend on the chain length, reflecting the different –CO₂H...⁻O₂C–H-bonding strength as a result of strain in the cyclic conformation. A minimum binding energy was found at n = 5, indicating that its intramolecular hydrogen bond is the weakest. At 70 K, all spectra are blue-shifted relative to the room temperature spectra with the maximum binding energy shift occurring at n = 5. These observations suggest that the cyclic conformation of HO₂C(CH₂)₅CO₂⁻ (a ten-membered ring) is the most strained among the ten anions. The present study shows that the –CO₂H...⁻O₂C– hydrogen bonding strength is different among the ten anions and it is very sensitive to the strain in the cyclic conformations.

Future Plans

The main thrust of our BES program will continue to focus on cluster model studies of condensed phase phenomena in the gas phase. The experimental capabilities developed provide us with opportunities to examine fundamental chemical physics issues in complex anion solvation and solution chemistry. While we continue our work on the molecular processes of solvation of complex anions, the following outline a few themes for the Chemical Physics Program for the immediate and near future.

Confirmation Change vs. Temperature: the Effect of Entropy: The low-temperature electrospray PES apparatus recently completed in our laboratory has significantly expanded our capability and flexibility to study solvated species in the gas phase. In the past couple of years, we have studied the effects of temperature and hydrogen bonding on the confirmations of a series of complex anions containing the carboxylate functional groups. In the near future, we plan to reexamine the microsolvation of dicarboxylate dianions, which has been investigated previously using our room temperature apparatus. We observed an interesting phenomenon of solvent-induced conformation change, that is, the linear dicarboxylate dianions become folded at certain solvent number due to strong cooperative water-water hydrogen bonding. Although the previous experiment was done at room temperature, the real temperature of the cluster was unknown. However, theoretical calculations indicate that the folding transition is not only dependent on the solvent number, but also on the cluster temperature due to the effect of entropy. In our new apparatus, the ion trap temperature can be controlled and varied from 17 to 400 K. Systematic studies of the folding conformation change as a function of temperature will be performed. For example, for the suberate anion with 6 CH₂ groups, our preliminary data suggest that at low temperatures the folding transition occurs at 14 water vs. 16 water at room temperature. Detailed temperature-dependent studies will be carried out to determine the thermodynamic stabilities of the different conformations and possibly the folding kinetics. Studies on different chain lengths will also be

performed. In particular, molecules with very long chains will be interesting because the entropic effect is expected to play a much stronger role, i.e., more dramatic temperature effect may be observed.

Probing the Initial Steps of Dissolution: Our initial studies on the hydrated clusters of the form, $\text{NaSO}_4^- (\text{H}_2\text{O})_n$, suggests that they may indeed yield valuable information about the dissolution of polar molecules. We will continue similar studies on larger cluster, as well as other divalent anions, which provide a convenient handle in the form of ion pairs, A^+B^{2-} and allow us to study them in the form of singly charged anions.

References to Publications of DOE Sponsored Research (FY 2004-2007)

1. "Solvent-Mediated Folding of A Doubly Charged Anion" (X. Yang, Y. J. Fu, X. B. Wang, P. Slavicek, M. Mucha, P. Jungwirth, and L. S. Wang), *J. Am. Chem. Soc.* **126**, 876-883 (2004).
2. "Solvation of the Azide Anion (N_3^-) in Water Clusters and Aqueous Interfaces: A Combined Investigation by Photoelectron Spectroscopy, Density Functional Calculations, and Molecular Dynamics Simulations" (X. Yang, B. Kiran, X. B. Wang, L. S. Wang, M. Mucha, and P. Jungwirth), *J. Phys. Chem. A* **108**, 7820-7826 (2004).
3. "Bulk vs. Interfacial Aqueous Solvation of Dicarboxylate Dianions" (B. Minofar, M. Mucha, P. Jungwirth, X. Yang, Y. J. Fu, X. B. Wang, and L. S. Wang), *J. Am. Chem. Soc.* **126**, 11691 (2004).
4. "Direct Experimental Observation of the Low Ionization Potentials of Guanine in Free Oligonucleotides Using Photoelectron Spectroscopy" (X. Yang, X. B. Wang, E. R. Vorpagel, and L. S. Wang), *Proc. Natl. Acad. Sci. (USA)* **101**, 17588-17592 (2004).
5. "The Role of Water on Electron-Initiated Processes and Radical Chemistry: Issues and Scientific Advances" (B. C. Garrett, *et al.*), *Chem. Rev.* **105**, 355-389 (2005).
6. "Interior and Interfacial Aqueous Solvation of Benzene Dicarboxylate Dianions and Their Methylated Analogues: A Combined Molecular Dynamics and Photoelectron Spectroscopy Study" (B. Minofar, L. Vrbka, M. Mucha, P. Jungwirth, X. Yang, X. B. Wang, F. J. Fu, and L. S. Wang), *J. Phys. Chem. A* **109**, 5042-5049 (2005).
7. "Observation of Weak C-H...O Hydrogen-Bonding by Unactivated Alkanes" (X. B. Wang, H. K. Woo, B. Kiran, and L. S. Wang), *Angew. Chem. Int. Ed.* **44**, 4968-4972 (2005).
8. "Vibrational Cooling in A Cold Ion Trap: Vibrationally Resolved Photoelectron Spectroscopy of Cold C_{60}^- Anions" (X. B. Wang, H. K. Woo, and L. S. Wang), *J. Chem. Phys.* **123**, 051106 (2005).
9. "Probing the Low-Barrier Hydrogen Bond in Hydrogen Maleate in the Gas Phase: A Photoelectron Spectroscopy and *Ab initio* Study" (H. K. Woo, X. B. Wang, L. S. Wang, and K. C. Lau), *J. Phys. Chem. A* **109**, 10633-10637 (2005).
10. "Temperatures Dependent Photoelectron Spectroscopy of Methyl-Benzoate Anions: Observation of Steric Effect in *Ortho*-Methyl-Benzoate" (H. K. Woo, X. B. Wang, B. Kiran, and L. S. Wang), *J. Phys. Chem. A* **109**, 11395-11400 (2005).
11. "Determination of the Electron Affinity of the Acetyloxyl Radical (CH_3COO) by Low Temperature Anion Photoelectron Spectroscopy and *ab initio* Calculations" (X. B. Wang, H. K. Woo, L. S. Wang, B. Minofar, and P. Jungwirth), *J. Phys. Chem. A* **110**, 5047-5050 (2006).
12. "Low-Temperature Photoelectron Spectroscopy of Aliphatic Dicarboxylate Monoanions, $\text{HO}_2\text{C}(\text{CH}_2)_n\text{CO}_2^-$ ($n = 1 - 10$): Hydrogen Bond Induced Cyclization and Strain Energies" (H. K. Woo, X. B. Wang, K. C. Lau, and L. S. Wang), *J. Phys. Chem. A* **110**, 7801-7805 (2006).
13. "First Steps Towards Dissolution of NaSO_4^- by Water" (X. B. Wang, H. K. Woo, B. Jagoda-Cwiklik, P. Jungwirth, and L. S. Wang), *Phys. Chem. Chem. Phys.* **8**, 4294-4296 (2006).
14. "Microsolvation of the Dicyanamide Anion: $[\text{N}(\text{CN})_2^-](\text{H}_2\text{O})_n$ ($n = 0-12$)" (B. Jagoda-Cwiklik, X. B. Wang, H. K. Woo, J. Yang, G. J. Wang, M. F. Zhou, P. Jungwirth, and L. S. Wang), *J. Phys. Chem. A* **111**, 7719-7725 (2007).

Surface Chemical Dynamics

M.G. White^a, N. Camillone III^a, and A.L. Harris^b

Brookhaven National Laboratory, Chemistry Department, Building 555, Upton, NY 11973
(mgwhite@bnl.gov, nicholas@bnl.gov, alexh@bnl.gov)

1. Program Scope

This program focuses on fundamental investigations of the dynamics, energetics and morphology-dependence of thermal and photoinduced reactions on bulk planar and nanoparticle surfaces that play key roles in energy-related catalysis and photocatalysis. Laser pump-probe methods are used to investigate the dynamics of interfacial charge and energy transfer that leads to adsorbate reaction and/or desorption on metal and metal oxide surfaces. State- and energy-resolved measurements of the gas-phase products resulting from thermal and photoinitiated reactions are used to infer the dynamics of product formation and desorption. Time-resolved correlation techniques are used to follow surface reactions in real time and infer the dynamics of adsorbate–substrate energy transfer and desorption. Planned extensions of this work include investigations of the size-dependence of photoinduced desorption and vibrational dynamics of small molecules on surfaces of supported metal nanoparticles. Complementary efforts use cluster ion beams for studying the structure, dynamics and reactivity of size-selected metal and metal compound nanoclusters in the gas-phase and deposited onto solid supports.

2. Recent Progress

Ultrafast Investigations of Desorption Dynamics. We have examined in detail the ultrafast dynamics of photoinduced desorption of O₂ and CO from Pd(111) and the photoinduced reaction of O and CO on Pd(111). Temporally well-defined excitation of the adsorbate–substrate complexes is achieved with ~ 100 fs, 780 nm-wavelength pulses, and the dynamics are probed through coverage, laser fluence and time-resolved correlation studies. This work has provided new insights into the dynamics of energy transfer involved in these diabatic surface processes.

Site-dependent desorption dynamics. Our coverage-dependent photodesorption studies of O₂/Pd(111) indicate that substrate–adsorbate energy transfer is more efficient for more strongly-bound O₂. Following adsorption at 90 K temperature-programmed desorption (TPD) studies indicate three molecular adsorption states, labeled α_1 , α_2 , and α_3 , in order of decreasing desorption activation energies.¹ By controlling the O₂ coverage we have been able to systematically probe the desorption dynamics corresponding to the three adsorption states. Two-pulse correlation (2PC) measurements show a strong increase in desorption probability with decreasing binding energy, however, the time response of the adsorbate–substrate complex is essentially coverage independent, indicating that the desorption is driven by the same electron-mediated mechanism. In order to fit the coverage-dependent 2PC measurements and fluence dependence measurements, two-temperature model (2TM) simulations of the substrate–adsorbate energy transfer require that the substrate electron–adsorbate coupling strength, η , decreases with decreasing adsorption energy, *i.e.*, $\eta_{\alpha_1} > \eta_{\alpha_2} > \eta_{\alpha_3}$. Thus, the more strongly-bound states are more efficiently excited by diabatic coupling in this system (Fig. 1).

Support for the pseudo-thermal model for photoinduced desorption. Femtosecond pulse photodesorption is commonly described as resulting from energy transfer from the substrate to the reaction coordinate (via friction or electronic transitions) leading to cleavage of the molecule–surface bond. The cleavage step is typically modeled by an Arrhenius expression as the crossing of an activation energy barrier presumed to be the same as that used to describe thermal desorption.² We have used a combination of thermal and laser-induced heating to independently control the equilibrium and nonequilibrium excitation during photodesorption of CO from a Pd(111). Measurements of the photoyield (Fig. 2), fluence dependence and 2PC response as a function of initial surface temperature (T_i) exhibit marked dependences in the 100–375 K range. These dependences can be understood in terms of the initial degree of vibrational excitation in the adsorbate–surface and substrate lattice modes. Increasing T_i decreases the energy needed to drive the adsorbate over the barrier and slows the cooling of the system, enhancing the photodesorption efficiency. We

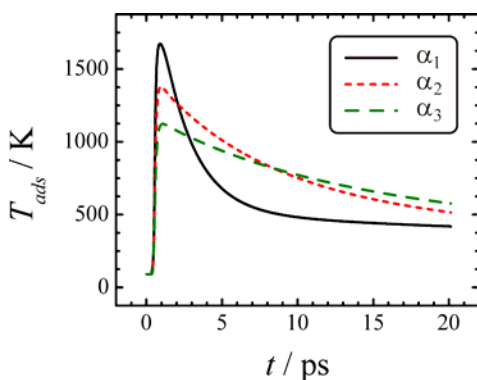


Figure 1. Adsorption-state-dependent adsorbate excitation predicted by two-temperature model simulations following excitation by laser pulses delivering a peak absorbed fluence of 4.6 mJ cm^{-2} .

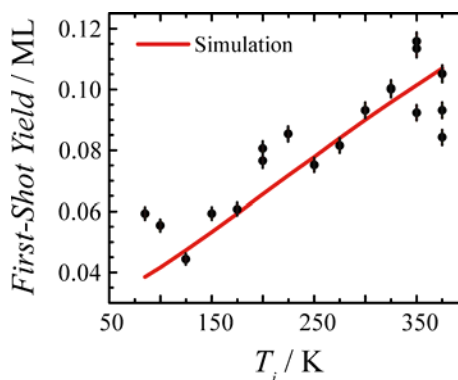


Figure 2. Femtosecond pulse photodesorption of 0.33 ML CO from Pd(111) as a function of initial temperature T_i . The line shows the result of two-temperature model simulations.

have developed a 2TM model that fits all available experimental data with a single parameter set and indicates that the desorption is driven by resonantly-enhanced electronic coupling. Systematic variation of the activation energy and prefactor for desorption indicates that the energy barrier to photodesorption is in good agreement with that found in thermal desorption experiments, supporting the simple Arrhenius description of the desorption step.

A snapshot of a surface chemical reaction. We have measured the photodesorption and photooxidation of CO in mixed monolayers of CO and atomic oxygen on Pd(111). Photoinduced oxidation is 5–10 times more efficient compared to that observed on Ru(001).³ The cause for the relatively high oxidation yield may be structural; STM indicates a mixed $p(2 \times 2)_{\text{O+CO}}$ structure wherein each O atom is surrounded by up to six CO molecules.⁴ Nevertheless, we find a strong preference for CO desorption that increases with increasing CO coverage (Fig. 3), consistent with a decrease in the CO desorption activation energy with increasing coverage as indicated by TPD studies. Thermal oxidation is markedly more efficient than femtosecond-pulse photooxidation, likely due to the fact that the slower thermal process allows time for diffusion and, therefore, a higher probability for reactions between species that were not nearest neighbors in the initial state. This implies that femtosecond photodesorption permits us to take a “snapshot” of the reaction efficiency of the initial monolayer that cannot be obtained by thermal excitation.

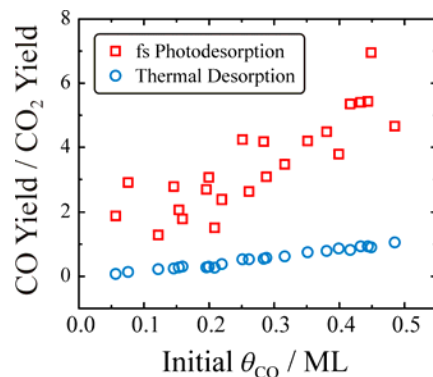


Figure 3. Coverage-dependence of the branching ratio for photodesorption vs. photooxidation of CO from CO+O/Pd(111).

Photoinduced Desorption and Reaction of O_2 on $\text{TiO}_2(110)$ Surfaces. We are currently investigating photoinduced reactions on single crystal $\text{TiO}_2(110)$ (rutile) surfaces with the goal of understanding the excitation and energy transfer processes important in photooxidation reactions. Adsorbed molecular oxygen is linked to the photooxidation activity of TiO_2 surfaces, however, fundamental questions remain as to the nature of the O_2 adsorption sites and the mechanism for desorption and/or reaction. Previous studies using UV-lamp excitation have shown that the photodesorption of O_2 from reduced $\text{TiO}_2(110)$ (rutile) surfaces exhibits multi-exponential decay rates which are both temperature and intensity dependent.⁵ The multi-component decay curves have been attributed to two different adsorbed O_2 species, $\alpha_1\text{-O}_2$ (“fast” decay) and $\alpha_2\text{-O}_2$ (“slow” decay), both of which are thought to be interconverted to a third state, $\beta\text{-O}_2$, by heating the $\text{O}_2/\text{TiO}_2(110)$ surface above 200 K. More recent studies account for the observed desorption rates by a fractal kinetics model involving one-dimensional networks of interconnected vacancy sites.⁵ In this work, we have used laser pump-probe techniques to measure the kinetic energy distributions of O_2 photodesorbed as a function of UV photoexcitation energy. The basic idea is that the presence of chemically-distinct surface-

bound O₂ species, *e.g.*, α -O₂ or β -O₂, should result in multiple O₂ desorption channels with different final state properties. The experiments make use of a one-photon ionization scheme for O₂ detection with very high sensitivity recently developed in our laboratory. Recent experiments show that the translational energy distributions of the photodesorbed O₂ molecules are trimodal, with characteristic energies of 0.35 eV, 0.1 eV and near zero energy, independent of UV photoexcitation energy (see Fig. 4). The multiple peaks in the translational energy distributions suggest the presence of different initial binding states of adsorbed oxygen, although the very “slow” channel may result from trapping-desorption of photoexcited species at the low surface temperature used in these measurements (100 K). The fact that the distributions are independent of photon energy is also consistent with an indirect photodesorption mechanism in which an adsorbed O₂⁻/O₂²⁻ species is neutralized by capturing a hole (h⁺) that was photogenerated in the titania substrate. Temperature-dependent measurements currently underway will probe the correlation between initial O₂ binding state, *e.g.*, α -O₂ or β -O₂, with final state distributions as well as the possibility of surface trapping.

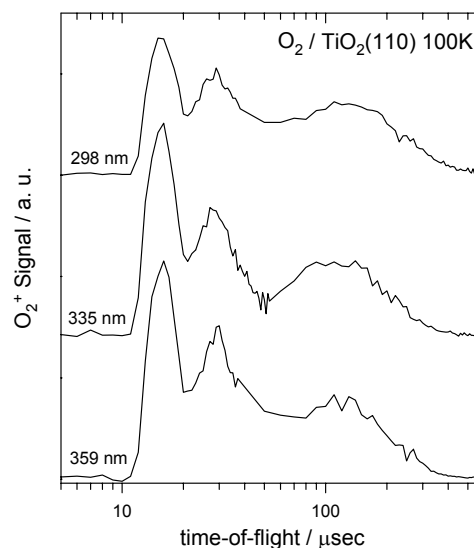


Figure 4. Time-of-flight distributions for O₂ photodesorbed by UV radiation of various wavelengths from a reduced TiO₂(110) surface at 100K. Note the log scale for the time-of-flight axis.

Structure and Reactivity of Transition Metal Compounds Clusters. We are using mass-selected cluster ion beams and surface science techniques to investigate the physical and chemical properties of transition metal compound clusters (*e.g.*, metal carbides, oxides and sulfides) deposited onto solid surfaces which are models for supported catalysts. In addition to providing precise knowledge of the cluster size (mass), stoichiometry and coverage, cluster beam deposition is particularly useful for investigations of small nanoclusters, 1–2 nm (< 200 atoms), where the geometric and electronic structure is evolving from molecular clusters to that of the extended solid (*e.g.*, semi-metal to metal transition). Our recent work has focused on investigations of the structure and reactivity of a number of molybdenum sulfide clusters, Mo_xS_y⁺ (x/y = 3/7, 4/6, 5/7, 6/8, 7/10, 8/12) in the gas-phase and deposited on a Au(111) substrate. Commercially, MoS₂ is widely used as a catalyst for hydrogenation (HYD), hydrodesulfurization (HDS), and hydrodenitrogenation (HDN), where it is dispersed as nanoparticles on a high surface area support.⁶ Based on the low S/Mo ratios and structures obtained from DFT calculations, the molybdenum sulfide nanoclusters studied here are all expected to have exposed Mo metal sites available for bonding and reaction. For both gas-phase and deposited clusters, experiments have shown that the adsorption/desorption of probe molecules such as CO or NH₃ are sensitive probes of the number and electronic character of the exposed Mo sites, which in turn reflect the structure and stability of the cluster. For example, the CO TPD peaks are narrow for clusters with symmetric cage-like structures, *i.e.*, Mo₄S₆ and Mo₆S₈, whereas those clusters predicted to have dangling S-atoms (Mo₃S₇, Mo₅S₇) exhibit broad CO TPD curves. It is likely that the Mo₃S₇ and Mo₅S₇ clusters undergo significant structural distortion and/or multiple binding configurations on the Au(111) substrate. In the case of the highly stable Mo₄S₆ “magic” cluster, we were unable to detect any NH₃ adsorption by TPD for the deposited cluster, whereas the gas-phase Mo₄S₆⁺ cluster was observed to bind both CO and NH₃, with calculated binding energies that are very similar.⁷ The TPD results were corroborated by DFT calculations performed by Dr. Ping Liu (BNL/Chemistry) that showed that charge redistribution between the Mo₄S₆ cluster and Au atoms at the surface results in a significantly weaker Mo-NH₃ interaction compared to Mo-CO. Current work involves the study of the thermal stability of the deposited clusters using ion scattering and Auger spectroscopy, as well investigations of the electronic structure using photoelectron spectroscopy (UPS and XPS).

3. Future Plans

Our planned work develops three interlinked themes: (i) the chemistry of supported nanoparticles and nanoclusters, (ii) the exploration of chemical dynamics on ultrafast timescales, and (iii) the photoinduced chemistry of molecular adsorbates. The investigations are motivated by the fundamental need to connect chemical reactivity to chemical dynamics in systems of relevance to catalytic processes — in particular metal and metal-compound nanoparticles and nanoclusters supported on oxide substrates. They are also motivated by fundamental questions of physical changes in the electronic and phonon structure of nanoparticles and their coupling to adsorbates and to the nonmetallic support that may alter dynamics associated with energy flow and reactive processes.

Ultrafast experiments investigating the dynamics of photoinduced desorption from nanoparticles will address development of a fundamental understanding of the changes in this simplest surface reaction (desorption) as the size of the metal substrate material is reduced from macroscopic (planar bulk surfaces) to the nanoscale. Size-dependent chemical dynamics will also be the focus of experiments using our new cluster beam source to prepare a range of supported, size-selected nanoclusters for structure and reactivity studies. The latter will be complemented by ultrafast two-photon photoemission experiments to investigate the electronic structure and dynamics of the nanoclusters and molecular resonances involved in chemistry at their surfaces. Future studies of photo-induced processes on titania surfaces will work to resolve open questions regarding the surface binding sites and photodesorption dynamics of molecular oxygen. We are also in the beginning stages of extending pump-probe methods to investigations of photooxidation of organic species, *e.g.*, acetone, and butanone, in which the translational energy distributions of gas-phase products will be used to infer the mechanism for surface reaction.

Literature Cited

1. X. Guo, A. Hoffman, J.T. Yates, Jr., *J. Chem. Phys.*, **90**, 5787 (1989).
2. L.M. Struck, L.J. Richter, S.A. Buntin, R.R. Cavanagh, J.C. Stephenson, *Phys. Rev. Lett.*, **77**, 4576 (1996).
3. M. Bonn, S. Funk, C. Hess, D.N. Denzler, C. Stampfl, M. Scheffler, M. Wolf, G. Ertl, *Science*, **285**, 1042 (1999).
4. J. Méndez, S.H. Kim, J. Cerdá, J. Wintterlin, G. Ertl, *Phys. Rev. B*, **71**, 085409 (2005).
5. T.L. Thompson, J.T. Yates, *J. Phys. Chem. B*, **110**, 7431 (2006).
6. H. Topsoe, B.S. Clausen, F.E. Massoth, *Hydrotreating Catalysis* (Springer, New York, 1996).
7. J.M. Lightstone, M.J. Patterson, M.G. White, *Chem. Phys. Lett.*, **413**, 429 (2005).

DOE-Sponsored Research Publications (2004–2007)

1. R.J. Beuhler and M.G. White, “State-resolved dynamics of oxygen atom recombination on polycrystalline Ag,” *J. Chem. Phys.*, **120**, 2445 (2004).
2. J.M. Lightstone, M.J. Patterson and M.G. White, “Reactivity of the $M_4S_6^+$ (M-Mo, W) cluster with CO and NH_3 in the gas-phase,” *Chem. Phys. Lett.*, **413**, 429 (2005).
3. P. Liu, J.M. Lightstone, M.J. Patterson, J.A. Rodriguez, J.T. Muckerman and M.G. White, “Gas-phase interaction of thiophene with the $Ti_8C_{12}^+$ and Ti_8C_{12} met-car clusters,” *J. Phys. Chem. B*, **110**, 7449 (2006).
4. J. M. Lightstone, M. J. Patterson, P. Liu, and M. G. White, “Gas-phase reactivity of the $Ti_8C_{12}^+$ Met-car with triatomic sulfur-containing molecules: CS_2 , SCO , and SO_2 ,” *J. Phys. Chem. A*, **110**, 3505 (2006).
5. N. Camillone III, T. Pak, K. Adib, K.A. Khan, and R.M. Osgood, Jr., “Tuning molecule-surface interactions with nanometer-thick covalently-bound organic overlayers,” *J. Phys. Chem. B*, **110**, 11334 (2006).
6. P. Szymanski, A.L. Harris, N. Camillone III, “Adsorption-state-dependent subpicosecond photoinduced desorption dynamics,” *J. Chem. Phys.*, **126**, 214709 (2007). (Note: Selected for the July 2007 issue of the *Virtual Journal of Ultrafast Science*.)
7. P. Szymanski, A.L. Harris, N. Camillone III, “Temperature-dependent electron-mediated coupling in subpicosecond photoinduced desorption,” *Surf. Sci.*, **601**, 3335 (2007).
8. P. Szymanski, A.L. Harris, N. Camillone III, “Temperature-dependent femtosecond photoinduced desorption in CO/Pd(111),” *J. Phys. Chem.*, **accepted** (2007).

^a Principal Investigator; ^b Contributing Investigator

Ionic Liquids: Radiation Chemistry, Solvation Dynamics and Reactivity Patterns

James F. Wishart

Chemistry Department, Brookhaven National Laboratory, Upton, NY 11973-5000

wishart@bnl.gov

Program Definition

Ionic liquids (ILs) are a rapidly expanding family of condensed-phase media with important applications in energy production, nuclear fuel and waste processing, improving the efficiency and safety of industrial chemical processes, and pollution prevention. ILs are generally nonvolatile, noncombustible, highly conductive, recyclable and capable of dissolving a wide variety of materials. They are finding new uses in chemical synthesis, catalysis, separations chemistry, electrochemistry and other areas. Ionic liquids have dramatically different properties compared to conventional molecular solvents, and they provide a new and unusual environment to test our theoretical understanding of charge transfer and other reactions. We are interested in how IL properties influence physical and dynamical processes that determine the stability and lifetimes of reactive intermediates and thereby affect the courses of chemical reactions and product distributions.

Successful use of ionic liquids in radiation-filled environments, where their safety advantages could be significant, requires an understanding of ionic liquid radiation chemistry. For example, characterizing the primary steps of IL radiolysis will reveal radiolytic degradation pathways and suggest ways to prevent them or mitigate their effects on the properties of the material. An understanding of ionic liquid radiation chemistry will also facilitate pulse radiolysis studies of general chemical reactivity in ILs, which will aid in the development of applications listed above. Very early in our radiolysis studies it became evident that slow solvation dynamics of the excess electron in ILs (which vary over a wide viscosity range) increases the importance of pre-solvated electron reactivity and consequently alters product distributions. Parallel studies of IL solvation phenomena using coumarin-153 dynamic Stokes shifts and polarization anisotropy decay rates are done to compare with electron solvation studies and to evaluate the influence of ILs on charge transport processes.

Methods. Picosecond pulse radiolysis studies at BNL's Laser-Electron Accelerator Facility (LEAF) are used to identify reactive species in ionic liquids and measure their solvation and reaction rates. We and our collaborators (R. Engel (Queens College, CUNY) and S. Lall-Ramnarine, (Queensborough CC, CUNY)) develop and characterize new ionic liquids specifically designed for our radiolysis and solvation dynamics studies. IL solvation and rotational dynamics are measured by TCSPC and fluorescence upconversion measurements in the laboratory of E. W. Castner at Rutgers Univ. Investigations of radical species in irradiated ILs are carried out at ANL by I. Shkrob and S. Chemerisov using EPR spectroscopy. Diffusion rates are obtained by PGSE NMR in S. Greenbaum's lab at Hunter College, CUNY and S. Chung's lab at William Patterson U. Professor Mark Kobrak of CUNY Brooklyn College performs molecular dynamics simulations of solvation processes. A collaboration with M. Dietz and coworkers at ANL is centered around the properties and radiolytic behavior of ionic liquids for nuclear separations. Collaborations with C. Reed (UC Riverside), D. Gabel (U. Bremen) and J. Davis (U. South Alabama) are aimed at characterizing the radiolytic and other properties of borated ionic liquids, which could be used to make fissile material separations processes inherently safe from criticality accidents.

Recent Progress

Pre-solvated electron reactivity and its relation to solvation dynamics in ILs. In the course of kinetic measurements on reactions of electrons with various scavengers it was found that relatively low scavenger concentrations substantially reduced the initial yield of solvated electrons. Direct scavenging of pre-solvated ("dry") electrons competes effectively with the slower electron solvation processes in ionic liquids. For example, a pyrene concentration of only 63 mM reduces the solvated electron yield to 37% of the scavenger-free value. This finding has major implications for processing of radioactive materials, where seemingly innocuous quantities of solutes may scavenge electrons very effectively. Conversely, dry electron scavenging facilitates the use of pulse radiolysis in electron transfer studies by providing a way to circumvent diffusion-limited precursor formation rates. Measurements of excess electron solvation processes and emission dynamics (Stokes shift and polarization

anisotropy decay) of solvatochromic coumarin-153 show that the reorganization dynamics of ionic liquids occur on much longer timescales (nanoseconds) than in conventional polar solvents (picoseconds). The slow solvation dynamics would also be expected to significantly alter transition state dynamics and provide a potential means to control product distribution.

To look at electron solvation with higher time resolution, we used low-viscosity pyrrolidinium salts and developed novel ionic liquids with even lower melting points and viscosities, based on ether-substituted pyrrolidinium cations. These liquids have RT viscosities low enough (65-95 cP) to flow through the picosecond pulse-probe transient absorption system at LEAF, which requires sample exchange to avoid cumulative radiation effects. Consequently, the electron solvation process was directly observed in three ILs by monitoring the decay of pre-solvated electrons at multiple wavelengths (to yield a solvated electron spectrum similar to the blue curve above). In *N*-methyl,*N*-butyl-pyrrolidinium NTf₂⁻ the electron solvation lifetime $\langle\tau_{\text{solv}}\rangle$ is 260 ps, while $\langle\tau_{\text{solv}}\rangle$ obtained from coumarin 153 Stokes shift measurements is 346 ps (see next section).

Even slower solvation processes were observed in pulse radiolysis studies of ionic liquids containing ether-, alcohol- and alkyl-functionalized quaternary ammonium dications $(\text{CH}_3)_2(\text{R})\text{N}^+(\text{CH}_2)_n\text{N}^+(\text{R})(\text{CH}_3)_2$ (NTf₂⁻)₂, where R = (CH₂)₃OH, (CH₂)₂OCH₂CH₃, or (CH₂)₃CH₃ and n = 3–8. Spectra on nanosecond timescales revealed that solvation of the excess electron is particularly slow in the case of the alcohol-derivatized ionic liquids. The blue shift of the electron spectrum to the customary 650 nm peak takes 25-40 nanoseconds at RT (viscosities ~4500-6800 cP). Comparison with the ~1 ns electron solvation time observed in similarly viscous 1,2,6-trihydroxyhexane (2500 cP) reveals the hindering effect of the ionic liquid lattice on hydroxypropyl side chain reorientation [1].

Solvation dynamics in ILs using fluorescent probes. The solvation and reorientational dynamics for a series of four ionic liquids were probed as functions of temperature (278-353 K) using coumarin 153 (C153). The ionic liquids are comprised of saturated organic cations (methyltributylammonium, hexyltributylammonium, methylbutylpyrrolidinium, and methyl(ethoxyethyl)pyrrolidinium) paired with a common anion, bis(trifluoromethylsulfonyl)imide. The observed solvation dynamics and fluorescence depolarization dynamics occur over a broad range of time scales that can only be adequately fit by functions including three or more exponential components. Stretched exponential distributions could not adequately fit our data. For both the solvation dynamics and the probe reorientational dynamics, the observed temperature dependences of the average relaxation times are well fit by Vogel-Tammann-Fulcher laws. To correlate the observed microscopic dynamics with macroscopic physical properties, temperature-dependent viscosities were also measured. Differential scanning calorimetry was used to study the thermodynamics of the phase transitions from the liquid to supercooled liquid to glassy states. For the two tetraalkylammonium liquids, the observed melting transitions occur near 300 K, so we are able to study the dynamics in a clearly supercooled regime. [10] (In collaboration with E. W. Castner, Rutgers University.)

EPR studies of radical species in ILs. Since our standard technique of transient optical detection cannot detect many important intermediates that lack strong absorption features, particularly hole-derived species, we have begun to use EPR to identify ionization products in ILs [11]. Radical intermediates were generated by radiolysis or photoionization of low-temperature ionic liquid glasses composed of ammonium, phosphonium, pyrrolidinium, and imidazolium cations and bis(triflyl)amide, dicyanamide, and bis(oxalato)borate anions. Large yields of terminal and penultimate C-centered radicals are observed in the aliphatic chains of the phosphonium, ammonium and pyrrolidinium cations, but not for imidazolium cation (where the ring is the predominant site of oxidation). This pattern is indicative of efficient deprotonation of a hole trapped on the parent cation (the radical dication) that competes with rapid electron transfer from a nearby anion. This charge transfer leads to the formation of stable N- or O-centered radicals; the dissociation of parent anions is a minor pathway. Production of •CF₃ from (CF₃SO₂)₂N⁻ evidently proceeds primarily through an excited state of the anion rather than via ionization.

Radiolysis of simulated IL-based nuclear extraction systems. Addition of 10-40 wt% of trialkylphosphate (a common agent for nuclear separations) has relatively little effect on the fragmentation of the ILs. The yield of the alkyl radical fragment generated by dissociative electron attachment to the trialkylphosphate is < 4% of the yield of the radical fragments derived from the IL solvent. The currently used hydrocarbon/tributylphosphate extraction systems involve a highly resistant, structurally simple solvent (like kerosene) that efficiently transfers charge and energy to the functional solute (tributylphosphate), resulting in the fragmentation of the latter and degradation of extraction efficiency. The results suggest a different paradigm for radiation protection: a solvent in which the

damage transfer is reversed. Such a solvent actively protects the functional solute in a sacrificial way, but overall radiolytic damage is still kept to a low level by the radiolytic properties of the solvent [11] (in collaboration with I. Shkrob and S. Chemerisov, ANL).

Radiolysis of borated ionic liquids. A group from Los Alamos calculated that processing plutonium in boron-containing ionic liquids could substantially reduce the risk of nuclear criticality accidents. Subsequently we investigated the radiation chemistry of ionic liquids prepared from carborane (CB^-) and bis(oxalato)borate (BOB^-) anions. Experiments in liquids derived from the $\text{CB}_{11}\text{H}_6\text{Br}_6^-$ and BOB^- anions and studies of the same anions diluted in NTf_2^- ionic liquids indicate the major radiation stability concern may be the reaction of the solvated electron with the CB and BOB anions, a problem that could be addressed by including imidazolium or pyridinium cations in the ionic liquid mixtures. By contrast, trialkylammonio borate anions ($[\text{R}_3\text{N}-\text{B}_{12}\text{H}_{11}]^-$) form low-melting salts with many cations but do not react with solvated electrons (with D. Gabel, Bremen, submitted).

Future Plans

Electron solvation and reactivity. Pre-solvated electron scavenging mechanisms will be explored by studying the competition between the electron solvation and attachment processes in ILs. Electron solvation dynamics in several families of low-viscosity ILs will be measured by pulse-probe radiolysis. Subsequently, scavengers will be added to measure the kinetics of pre-solvated electron capture. It is well known from work in molecular solvents that many scavengers, for example SeO_4^{2-} , have widely different reactivity profiles towards pre-solvated and solvated electrons. We have begun quantitative measurement of the scavenging profiles of benzophenone, SeO_4^{2-} , NO_3^- , and Cd^{2+} using the ultrafast single-shot detection system at LEAF, through which we hope to explain such conundrums mechanistically. C-153 solvation dynamics results will be compared with electron and benzophenone anion solvation measurements.

Charge transport in ionic liquids. ILs have proved to possess valuable characteristics for solar energy photoconversion systems such as the Grätzel cell. Pulse radiolysis and flash photolysis methods will be used to study how ionic liquids affect charge-transport reactions in bridged electron donor-acceptor systems. Focus areas will be the combined effects of ionic solvation and slow solvent relaxation on the energy landscape of charge transport, including specific counterion effects depending on the ionic liquid, and the influence of the lattice-like structure of ionic liquids on the distance dependence of electron transport reactions.

Non-classical diffusion in ionic liquids. Ionic liquids show unusual solute diffusion behavior on the basis of solute charge and size, which will be explored through reaction kinetics and high-pressure pulsed-gradient spin echo NMR studies of diffusion rates of charged and neutral species. This information is important for modeling geminate recombination kinetics to understand why radiolytic damage accumulates slower in ionic liquids than many other materials.

EXAFS studies of structure and reaction dynamics in ionic liquids. In collaboration with R. Crowell and coworkers, we will use Br EXAFS to study the structures of neat bromide ionic liquids and the effect of solutes, and we will use photoionization coupled with time-resolved EXAFS to probe the solvation dynamics of Br^0 atoms in ILs and the effect of the ionic liquid environment on the $\text{Br}^- + \text{Br}^0 \rightarrow \text{Br}_2^-$ reaction. The results can be applied to understanding related iodide systems of interest in solar photoconversion.

Publications on ionic liquids

1. *Effects of Functional Group Substitution on Electron Spectra and Solvation Dynamics in a Family of Ionic Liquids* J. F. Wishart, S. I. Lall-Ramnarine, R. Raju, A. Scumpia, S. Bellevue, R. Ragbir, and R. Engel *Radiat. Phys. Chem.* **72**, 99-104 (2005).
2. *Dynamics of Fast Reactions in Ionic Liquids* A. M. Funston and J. F. Wishart in "Ionic Liquids IIIA: Fundamentals, Progress, Challenges and Opportunities" Rogers, R. D. and Seddon, K. R., Eds.; *ACS Symp. Ser.* **901**, Ch. 8, American Chemical Society, Washington, DC, 2005. (ISBN 0-84123-893-6).
3. *Ultrafast Dynamics of Pyrrolidinium Cation Ionic Liquids* H. Shirota, A. M. Funston, J. F. Wishart, E. W. Castner, Jr. *J. Chem. Phys.* **122**, 184512 (2005), selected for the *Virtual Journal of Ultrafast Science* (6/05).
4. *Radiation Chemistry of Ionic Liquids* J. F. Wishart, A. M. Funston, and T. Szreder in "Molten Salts XIV, Proceedings of the 2004 Joint International Meeting of the Electrochemical Society, Honolulu, HI, 2004", R. A. Mantz, et al., Eds.; The Electrochemical Society, Pennington, NJ, 2006, pp. 802-813. (ISBN 1-56677-514-0)

5. *Tetraalkylphosphonium polyoxometalates: electroactive, "task-specific" ionic liquids* P. G. Rickert, M. R. Antonio, M. A. Firestone, K.-A. Kubatko, T. Szreder, J. F. Wishart, and M. L. Dietz *Dalton Trans.* **2006**, 529-531 (2006).
6. *The Physical Chemistry of Ionic Liquids (Editorial for Special Issue)* J. F. Wishart, and E. W. Castner, *J. Phys. Chem. B*, **111**, 4639-4640 (2007).
7. *Tetraalkylphosphonium Polyoxometalate Ionic Liquids: Novel, Organic-Inorganic Hybrid Materials*, P. G. Rickert, M. P. Antonio, M. A. Firestone, K.-A. Kubatko, T. Szreder, J. F. Wishart, and M. L. Dietz, *J. Phys. Chem. B*, **111**, 4685-4692 (2007).
8. *Intermolecular Interactions and Dynamics of Room Temperature Ionic Liquids that have Silyl- and Siloxy-Substituted Imidazolium Cations* H. Shirota, J. F. Wishart, and E. W. Castner, Jr., *J. Phys. Chem. B*, **111**, 4819-4829 (2007).
9. *Nuclear Magnetic Resonance Study of the Dynamics of Imidazolium Ionic Liquids with $-CH_2Si(CH_3)_3$ vs $-CH_2C(CH_3)_3$ Substituents* S. H. Chung, R. Lopato, S. G. Greenbaum, H. Shirota, E. W. Castner, Jr. and J. F. Wishart, *J. Phys. Chem. B*, **111**, 4885-4893 (2007).
10. *Fluorescence Probing of Temperature-Dependent Dynamics and Friction in Ionic Liquid Local Environments* A. M. Funston, T. A. Fadeeva, J. F. Wishart, and E. W. Castner, *J. Phys. Chem. B*, **111**, 4963-4977 (2007).
11. *The Initial Stages of Radiation Damage in Ionic Liquids and Ionic Liquid-Based Extraction Systems* I. A. Shkrob, S. D. Chemerisov, and J. F. Wishart, *J. Phys. Chem. B*, **111**, ASAP (2007). DOI: 10.1021/jp073619x
12. *Intermolecular Dynamics, Interactions and Solvation in Ionic Liquids* E. W. Castner, Jr., J. F. Wishart, and H. Shirota, *Acc. Chem. Res.* **40**, in press (2007).

Publications on other subjects

13. *Radiation Chemistry of Methyl-tert-Butyl Ether (MTBE) in Aqueous Solution* S. P. Mezyk, J. Jones, W. J. Cooper, T. Tobien, M. G. Nickelsen, J. W. Adams, K. E. O'Shea, D. M. Bartels, J. F. Wishart, P. M. Tornatore, K. S. Newman, K. Gregoire, and D. J. Weidman *Envir. Sci. Tech.*, **38**, 3994-4001 (2004).
14. *Long-Range Electron Transfer across Peptide Bridges: the Transition from Electron Superexchange to Hopping* R. Abdel Malak, Z. Gao, J. F. Wishart, and S. S. Isied, *J. Am. Chem. Soc.* **126**, 13888-13889 (2004).
15. *The LEAF Picosecond Pulse Radiolysis Facility at Brookhaven National Laboratory* J. F. Wishart, A. R. Cook, and J. R. Miller *Rev. Sci. Inst.* **75**, 4359-4366 (2004), selected for the *Virtual Journal of Ultrafast Science* (12/04).
16. *Search for the 3-body Photodisintegration of Be* D. E. Alburger, R. E. Chrien, R. J. Sutter, and J. F. Wishart, *Phys. Rev. C* **70**, 064611 (2004).
17. *Convergence of Spectroscopic and Kinetic Electron Transfer Parameters for Mixed-Valence Binuclear Dipyriddyamide Ruthenium Ammine Complexes* A. J. Distefano, J. F. Wishart, and S. S. Isied *Coord. Chem. Rev.*, **249**, 507-516 (2005).
18. *Radiolysis with RF Photoinjectors: Supercritical Xenon Chemistry* J. F. Wishart in "Femtosecond Beam Science" Uesaka, M., Ed.; Imperial College Press, London, 2005, pp. 351-356. (ISBN 1-86094-343-8).
19. *Reactivity of Acid Generators for Chemically Amplified Resists with Low-Energy Electrons* A. Nakano, T. Kozawa, S. Tagawa, T. Szreder, J. F. Wishart, T. Kai and T. Shimokawa *Jpn. J. Appl. Phys.*, **45**, L197-L200 (2006).
20. *Pulse radiolysis and steady-state analyses of the reaction between hydroethidine and superoxide and other oxidants* J. Zielonka, T. Sarna, J. E. Roberts, J. F. Wishart, B. Kalyanaraman, *Arch. Biochem. Biophys.*, **456**, 39-47 (2006).
21. *Conformational Analysis of the Electron Transfer Kinetics across Oligoproline Peptides Using N,N-dimethyl-1,4-benzenediamine Donors and Pyrene-1-sulfonyl Acceptors* J. B. Issa, A. S. Salameh, E. W. Castner, Jr., J. F. Wishart and S. S. Isied, *J. Phys. Chem. B*, **111**, 6878-6886 (2007).
22. *Tools for radiolysis studies*, J. F. Wishart in "Radiation chemistry: from basics to applications in material and life sciences" Spothem-Maurizot, M., Douki, T., Mostafavi, M., and Belloni, J., Eds.; L'Actualité Chimique Livres, Paris, Ch. 2, in press.

Title: Electronically non-adiabatic interactions in molecule metal-surface scattering: Can we trust the Born-Oppenheimer approximation in surface chemistry?

Principal Investigators: Alec M. Wodtke, Department of Chemistry and Biochemistry, University of California Santa Barbara, Santa Barbara, CA 93106 wodtke@chem.ucsb.edu and Daniel J. Auerbach, GRT-Inc. Santa Barbara CA. Auerbach@grt-inc.com

Program Scope and Definitions: When molecules with low levels of vibrational excitation collide with metal surfaces, vibrational coupling to electron-hole pairs is not found to be strong unless incidence energies are high. However, there is accumulating evidence that coupling of large amplitude molecular vibration to metallic-electron degrees-of-freedom can be much stronger even at the lowest accessible incidence energies. We pose the basic question: are electronically non-adiabatic couplings important to chemically relevant processes at surfaces? We have indirect evidence in at least one example that the dynamics and rates of chemical reactions at metal surfaces may be strongly influenced by electronically non-adiabatic coupling. This implies that theoretical approaches relying on the Born-Oppenheimer approximation may not accurately reflect the nature of transition-state traversal in reactions of catalytic importance. Developing a predictive understanding of surface reactivity beyond the Born-Oppenheimer approximation represents one of the most important challenges to current research in chemical dynamics. We have developed a new instrument optimized in several important respects to allow us to investigate a wider variety of molecule surface interactions, recognizing that most important evidence now comes from a very limited number of studied systems. In this instrument, sensitivities are extremely high and a first generation infrared source has been developed for overtone pumping of H-containing species, so that both stimulated emission pumping and overtone pumping are possible with this instrument.

Recent Progress: We have completed construction and commissioning of the new instrument and carried out a series of initial studies on the vibrational excitation of HCl on Au(111). This system exhibits much smaller vibrational excitation probabilities than any previously reported system, demonstrating the sensitivity of the new instrument and providing us an example of vibrational energy transfer where electronically non-adiabatic effects have been “switched off”, at least at low surface temperatures. As we increase the surface temperature we find a transition to a new energy transfer mechanism, which strongly resembles expectations for electron mediated energy transfer. We have also begun the first studies of vibrationally excited HCl($v=2$) prepared by overtone pumping. With our new instrument, we are able to excite the HCl molecules in a very small (1 mm or less) packet very close to the surface (within 5 mm). Then by performing REMPI detection of recoiling molecules at only a 15 mm distance, we may obtain very high resolution TOF information, reflecting the changes in velocity that accompany the scattering events. The figure below shows some of the first results in this direction, after the raw TOF data has been inverted to Flux vs. Translational energy. The upper panel shows that even for the vibrationally elastic channel, more than 60% of the incident translational energy is transferred to surface excitation. Comparison to purely mechanical systems like Ar/Pt with a similar mass ratio exhibit much less energy transfer. We believe

this data may be some of the first clear evidence for strong translational excitation of electron hole pairs. For vibrational relaxation (shown in the lower panel) the translational energy distribution is remarkably similar, suggesting that vibrational to translation energy transfer plays only a minor role here.

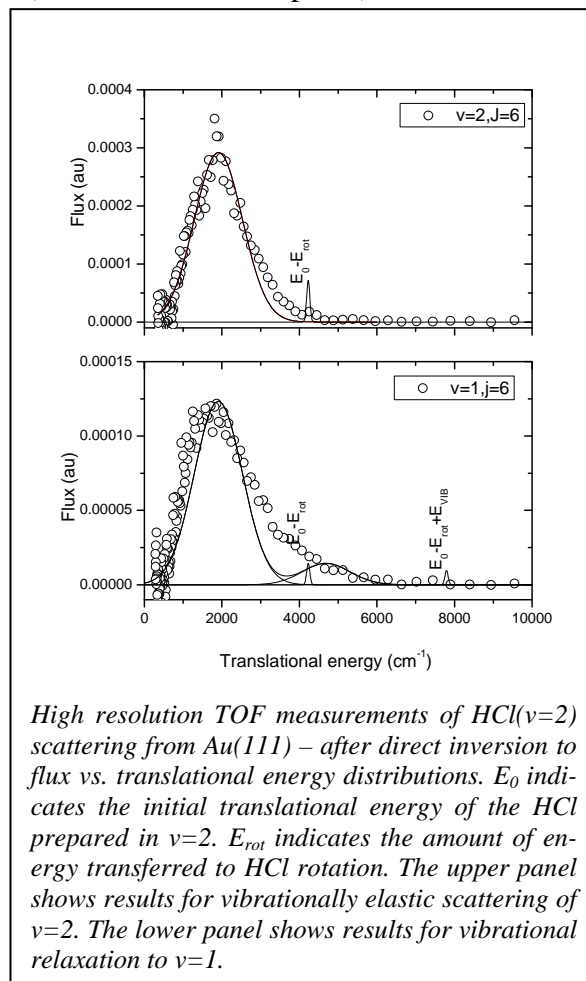
Future Plans: In the next year, comprehensive studies of the HCl($v=2$) scattering will be carried out, with full angle and velocity resolution. With simple improvements a new generation of PUMP/PUMP double overtone excitation experiments will also be possible.

Publications from this grant

1. *Direct translation-to-vibrational energy transfer of HCl on Gold: Measurement of absolute vibrational excitation probabilities*, Qin Ran, Daniel Matsiev, Daniel J. Auerbach, Alec M. Wodtke, Proceedings of the 16th International Workshop on Inelastic Ion-Surface Collisions; Nuclear Instruments and Methods in Physics Research, Section B: Beam Interactions with Materials and Atoms (NIMB) **258**(1) 1-6 (2007)
2. *Change of vibrational excitation mechanism in HCl/Au collisions with surface temperature: transition from electronically adiabatic to non-adiabatic behavior*, Q. Ran, D. Matsiev, D. J. Auerbach, A. M. Wodtke, Physical Review Letters **98**(23), 237601 (2007)
3. *An advanced molecule-surface scattering instrument for study of vibrational energy transfer in gas-solid collisions*, Qin Ran, Daniel Matsiev, Daniel J. Auerbach, Alec M. Wodtke (accepted in Rev. Sci. Instrum.)

List of public presentations of work related to this grant

1. Invited lecture. Symposium on Atomic, Cluster and Surface Physics (SASP), La Thuile (Aosta) Italy, Invited lecture. "Electronically non-adiabatic interactions in



- molecule metal-surface scattering: Can we trust the Born-Oppenheimer approximation in surface chemistry?”, February 1-6 2004
2. Invited Lecture, “State-specific surface scattering with laser prepared molecules”, Conference on the Dynamics of Molecular Collisions, Asilomar CA, July 10-15 2005.
 3. Invited Lecture, American Chemical Society Meeting, Symposium on “The Influence of Local Structure and Reagent Energy on Chemical Reactions at Solid Surfaces”, Electronically non-adiabatic interactions at the molecule metal interface, August 28- Sept. 1 2005
 4. Invited Lecture, European Conference on Surface Science, “Electronically non-adiabatic interactions at the molecule metal interface”, Sept. 3-9 2005
 5. Invited Lecture, Pacifichem, Honolulu, HI, Evidence for Photolytic Production of Cyclic-N₃, Dec. 9-14, Dec. 15-20 2005
 6. Keynote Lecture and UCSB Delegation Leader to ‘Israeli Chemical Society Annual Meeting’ Feb 27-28, 2006 Tel Aviv, The “Standard Model” of chemical reactivity: How well does it describe reactions at metallic interfaces?
 7. Invited Lecture, “Electronically non-adiabatic influences on chemistry at the gas-solid interface” Gordon Research Conference on Atomic and Molecular Interactions Colby-Sawyer College, July 9-14 2006.
 8. Invited Lecture, “Electronically non-adiabatic energy dissipation at surfaces”, International Workshop of the Collaborative Research Centre SFB 616 „Energy Dissipation at Surfaces“, Sept. 24th to Sept 28th at Schloß Eichholz in Wesseling, Germany.
 9. Invited Lecture, “Electronically non-adiabatic influences on chemistry at the gas-solid interface”, Joint SSRL-ALS Workshop On Ultrafast Dynamics On Surfaces And In Liquids. SSRL, October 11 2006.
 10. Invited Lecture, “Do we have a theory for reactions at metal interfaces?: The unsolved problem of electronic non-adiabaticity”, 7 November 2006, California Institute of Technology, Department of Chemistry, Chemical Physics Seminar

11. Invited Lecture, "Do we have a theory for reactions at metal interfaces?: The unsolved problem of electronic non-adiabaticity", XXII International Symposium on Molecular Beams, May 27-June 1 2007, Freiburg Germany.
12. Invited Lecture, "State-specific molecule-surface scattering", Gordon Conference on Gas-Surface Dynamics, August 12-17, 2007, Proctor Academy, Andover New Hampshire
13. Invited Lecture, "Inverse velocity dependence of vibrationally promoted electron emission from a metal surface", Elementary Reactive Processes at Surfaces; Donostia-San Sebastian, Spain, August 30-Sept. 1, 2007
14. Invited Lecture, "Inverse velocity dependence of vibrationally promoted electron emission from a metal surface", Institute of Atomic and Molecular Sciences, Taipei, Taiwan, Sept. 12, 2007
15. The Hong Kong Institute for Advanced Study UCSB International Centre for Materials Research workshop on Advanced Materials. Hong-Kong University of Science and Technology, September 12-15, 2007
16. Invited Lecture, "Inverse velocity dependence of vibrationally promoted electron emission from a metal surface", National Tsinghua University, Beijing, China, Sept. 14, 2007
17. Invited Lecture, "Electronic Excitations induced by molecule-surface interactions", Non-Adiabatic Dynamics at Surfaces, Oct. 22-25 2007, Schloß Reisenburg, Germany
18. Invited Lecture, "Electronic Excitations induced by molecule-surface interactions", Leiden University, Oct. 26, 2007, Leiden, the Netherlands
19. Invited Lecture, "Do we have a theory for reactions at metal interfaces?: The unsolved problem of electronic non-adiabaticity", 2007 Symposium on Chemical Physics, Nov 9-11 2007, University of Waterloo

Author Index

Ahmed, M.....	102	Johnson, M.....	46
Anderson, S.	98	Joly, A.	187
Armentrout, P.	106	Jordan, K.....	46
Arms, D.....	132	Kathmann, S.	195
Auerbach, D.....	247	Kay, B.....	42
Balasubramanian, K	110	Kimmel, G.....	54
Bartels, D.....	117,121	Landahl, E.....	132
Beck, K.....	187	LaVerne, J.	121,199
Bentley, J.....	117	Leone, S.	102
Booth, C.....	13	Liu, D-J.....	152
Camillone, N.	239	Louie, S.	179
Carmichael, I.....	121,199	Lu, H. P.....	81
Carter, E.....	179	Lymar, S.	203
Castleman, Jr., A.....	22	Meisel, D.	66,199
Ceyer, S.	125	Miller, J.	70
Chandler, D.	1	Morse, M.	207
Chelikowsky, J.	5,179	Mundy, C.....	87
Chipman, D.	66,117,121,199	Ogut, S.....	166
Cook, A. R.....	70	Osgood, R.	211
Cowin, J.....	128	Petek, H.	215
Crowell, R.	132	Petrik, N.....	54
Dang, L.....	136	Ratner, M.	166
Dohnalek, Z.....	42	Raghavachari, K.....	191
Duncan, M.....	26	Ray, A.....	14
Dupuis, M.....	141	Saykally, R.....	219
Eisenthal, K.	144	Schatz, G.	166
Ellison, G.	91	Schenter, G.	94
El-Sayed, M.....	148	Skanthakumar, S.....	16
Evans, J.....	152	Smith, R.	42
Fayer, M.	34	Soderholm, L.....	16
Fulton, J.	156	Steimle, T.....	18
Garrett, B.....	160	Stockman, M.....	166,223
Geissler, P.....	164	Thompson, W.	227
Gordon, M.....	62	Tokmakoff, A.	30
Gray, S.....	166	Tully, J.	231
Harris, C.	50	Wang, L-S.....	235
Harris, A.	239	Wang, L.-W.....	179
Harrison, I.....	173	White, M.....	239
Hayden, C.....	175	Wilson, K.	102
Head-Gordon, M.	179	Wilson, R.	16
Head-Gordon, T.....	183	Wishart, J.....	132,243
Heaven, M.....	17	Wodtke, A.....	247
Hess, W.	187	Xantheas, S.	38
Hirata, S.....	9	Xie, S.	77
Ho, W.	74	Yang, H.....	175
Jackson, B.....	68		
Jackson, K.	166		
Jarrold, C.	191		
Jellinek, J.....	166		

Participants

Ahmed, Musahid
Lawrence Berkeley National Laboratory
MS 6R-2100, 1 Cyclotron road
Berkeley, CA 94720
E-Mail: mahmed@lbl.gov
Phone:(510)486-6355

Anderson, Scott
University of Utah
Chemistry/315 S. 1400 E. Rm 2020
Salt Lake City, UT 84112
E-Mail: anderson@chem.utah.edu
Phone:(801)585-7289

Armentrout, Peter
University of Utah
Chemistry/315 S. 1400 E. Rm 2020
Salt Lake City, UT 84112
E-Mail: armentrout@chem.utah.edu
Phone:(801)581-7885

Balasubramanian, Krishnan
California State University East Bay & LLNL
Lawrence Livermore Lab L-268
Livermore, CA 94550
E-Mail: kris.bala@csueastbay.edu
Phone:(925)422-4984

Bartels, David
Notre Dame Radiation Laboratory
University of Notre Dame
Notre Dame, IN 46556
E-Mail: bartels.5@nd.edu
Phone:(574)361-5561

Camillone, Nicholas
Brookhaven National Laboratory
Chemistry Department, Building 555
Upton, NY 11973
E-Mail: nicholas@bnl.gov
Phone:(631)344-4412

Carmichael, Ian
Notre Dame Radiation Laboratory
University of Notre Dame
Notre Dame, IN 46556
E-Mail: carmichael.1@nd.edu
Phone:(574)631-4502

Carter, Emily
Princeton University
Department of Mechanical and Aerospace
Eng, EQUAD, Suite D404A
Princeton, NJ 08544
E-Mail: eac@princeton.edu
Phone:(609)258-5391

Casassa, Michael
DOE Basic Energy Sciences
SC22.1 DOE, 19901 Germantown Rd.
Germantown, MD 20874
E-Mail: michael.casassa@science.doe.gov
Phone:(301)903-0448

Castleman, Jr., A. Welford
Penn State University
104 Chemistry Building
University Park, PA 16802
E-Mail: awc@psu.edu
Phone:(814)865-7242

Ceyer, Sylvia
Massachusetts Institute of Technology
6-217 77 Mass Ave
Cambridge, MA 02139
E-Mail: stceyer@mit.edu
Phone:(617)253-4537

Chandler, David
University of California, Berkeley & Lawrence
Berkeley National Laboratory
Department of Chemistry,
Berkeley, CA 94720
E-Mail: chandler@cchem.berkeley.edu
Phone:(510)643-6821

Chelikowsky, James
University of Texas
1 University Station C0200
Austin, TX 78712
E-Mail: jrc@ices.utexas.edu
Phone:(512)232-9083

Chipman, Daniel
Notre Dame Radiation Laboratory
University of Notre Dame
Notre Dame, IN 46556
E-Mail: chipman.1@nd.edu
Phone:(574)631-5562

Participants

Cook, Andrew
Brookhaven National Laboratory
Bldg. 555 Chemistry
Upton, NY 11973
E-Mail: acook@bnl.gov
Phone:(631)344-4782

Booth, Corwin
Lawrence Berkeley National Laboratory
Chemical Sciences Division, MS 70A-1150
Berkeley, CA 94720
E-Mail: chbooth@lbl.gov
Phone:(510)486-6079

Cowin, James
Pacific Northwest National Laboratory
3335 Q Ave M/S K8-88
Richland, WA 99354
E-Mail: jp.cowin@pnl.gov
Phone:(509)376- 6330

Crowell, Robert
Brookhaven National Laboratory
Chemistry Department
Upton, NY 11973
E-Mail: rob_crowell@anl.gov
Phone:(631)655-3922

Dang, Liam
Pacific Northwest National Laboratory
PO Box 999, K1-83
Richland, WA 99352
E-Mail: liem.dang@pnl.gov
Phone:(509)375-2557

Duncan, Michael
University of Georgia
Department of Chemistry
Athens, GA 30602
E-Mail: maduncan@uga.edu
Phone:(706)542-1998

Dupuis, Michel
Pacific Northwest National Laboratory
PO Box 999, K1-83
Richland, WA 99352
E-Mail: michel.dupuis@pnl.gov
Phone:(509)375-2617

Eisenthal, Kenneth
Columbia University
3000 Broadway MC 3107
New York, NY 10027
E-Mail: kbe1@columbia.edu
Phone:(212)854-3175

Ellison, Barney
University of Colorado
Department of Chemistry and Biochemistry
Boulder, CO 80309
E-Mail: barney@jila.colorado.edu
Phone:(303)492-8603

El-Sayed, Mostafa
Georgia Tech
Department of Chemistry and Biochemistry
Atlanta, Ga 30332
E-Mail: melsayed@gatech.edu
Phone:(404)894-0292

Evans, James
Ames Laboratory - Iowa State University
315 Wilhelm Hall
Ames, Iowa 50011
E-Mail: evans@ameslab.gov
Phone:(515)294-1638

Fayer, Michael
Stanford University
Department of Chemistry
Stanford, CA 94305
E-Mail: fayer@stanford.edu
Phone:(650)723-4446

Fiechtner, Gregory
DOE/BES SC-22.1
19901 Germantown Road
Germantown, MD 20874
E-Mail: Gregory.Fiechtner@science.doe.gov
Phone:(301)903-5809

Fulton, John
Pacific Northwest National Laboratory
PO Box 999, P8-19
Richland, WA 99352
E-Mail: john.fulton@pnl.gov
Phone:(509)376-7011

Participants

Garrett, Bruce
Pacific Northwest National Laboratory
PO Box 999, MSIN K9-90
Richland, WA 99354
E-Mail: bruce.garrett@pnl.gov
Phone:(509)372-6344

Geissler, Phillip
University of California, Berkeley
Dept. of Chemistry
Berkeley, CA 94720
E-Mail: geissler@cchem.berkeley.edu
Phone:(510)642-8716

Gordon, Mark
Ames National Laboratory
201 Spedding Hall
Ames, IA 50011
E-Mail: mark@si.fi.ameslab.gov
Phone:(515)294-0452

Gray, Stephen
Argonne National Laboratory
Chemistry Division
Argonne, IL 60439
E-Mail: gray@tcg.anl.gov
Phone:(630)252-3594

Harris, Alex
Brookhaven National Laboratory
Chemistry Department, Building 555
Upton, NY 11973
E-Mail: alexh@bnl.gov
Phone:(631)344-4301

Harris, Charles
Lawrence Berkeley National Laboratory
Department of Chemistry
Berkeley, CA 94720
E-Mail: cbharris@berkeley.edu
Phone:(510)642-2814

Harrison, Ian
University of Virginia
Dept of Chemistry
Charlottesville, VA 22904
E-Mail: harrison@virginia.edu
Phone:(434)924-3639

Hayden, Carl
Sandia National Laboratories
P.O. Box 969, M/S 9055
Livermore, CA 94551
E-Mail: cchayde@sandia.gov
Phone:(925)294-2298

Head-Gordon, Martin
Lawrence Berkeley National Laboratory
Chemical Sciences Division
Berkeley, CA 94720
E-Mail: mhg@cchem.berkeley.edu
Phone:(510)642-5957

Heaven, Michael
Emory University
Department of Chemistry
Atlanta, GA 30322
E-Mail: heaven@euch4e.chem.emory.edu
Phone:(404)727-6617

Hess, Wayne
Pacific Northwest National Lab
902 Battelle Blvd
Richland, WA 99352
E-Mail: wayne.hess@pnl.gov
Phone:(509)376-9907

Hilderbrandt, Richard
DOE/BES SC-22.1
19901 Germantown Rd.
Germantown, MD 20874
E-Mail: Richard.Hilderbrandt@science.doe.gov
Phone:(301)903-0035

Hirata, So
University of Florida
Quantum Theory Project
Gainesville, FL 32611
E-Mail: hirata@qtp.ufl.edu
Phone:(352)392-6976

Ho, Wilson
University of California, Irvine
Departments of Physics and Chemistry
Irvine, CA 92697
E-Mail: wilsonho@uci.edu
Phone:(949)824-5234

Participants

Jackson, Bret
University of Massachusetts Amherst
Department of Chemistry, 701 LGRT
Amherst, MA 01003
E-Mail: jackson@chem.umass.edu
Phone:(413)545-2583

Jackson, Koblar
Central Michigan University
Physics Department
Mount Pleasant, MI 48858
E-Mail: jacks1ka@cmich.edu
Phone:(989)774-3321

Jarrold, Caroline
Indiana University
Department of Chemistry
800 East Kirkwood Avenue
Bloomington, IN 47405
E-Mail: cjarrold@indiana.edu
Phone:(812)856-1190

Jellinek, Julius
Argonne National Laboratory
9700 S. Cass Ave.
Argonne, IL 60439
E-Mail: jellinek@anl.gov
Phone:(630)252-3463

Johnson, Mark
Yale University
Department of Chemistry, P.O. Box 208107,
New Haven, CT 06520
E-Mail: mark.johnson@yale.edu
Phone:(203)432-5226

Jordan, Kenneth
University of Pittsburgh
Dept. of Chemistry
Pittsburgh, PA 15260
E-Mail: jordan@pitt.edu
Phone:(412)243-1455

Kathmann, Shawn
Pacific Northwest National Laboratory
PO Box 999, K1-83
Richland, WA 99352
E-Mail: Shawn.Kathmann@pnl.gov
Phone:(509)375-2870

Kay, Bruce
Pacific Northwest National Laboratory
MS K8-88 PO Box 999
Richland, WA 99352
E-Mail: bruce.kay@pnl.gov
Phone:(509)376-0028

Kimmel, Greg
Pacific Northwest National Lab
P.O. Box 999 K8-88
Richland, WA 99352
E-Mail: Gregory.kimmel@pnl.gov
Phone:(509)376-2501

Krause, Jeffrey
US Department of Energy
19901 Germantown Rd.
Germantown, MD 20874
E-Mail: jeff.krause@science.doe.gov
Phone:(301)903-5827

LaVerne, Jay
Notre Dame Radiation Laboratory
University of Notre Dame
Notre Dame, IN 46556
E-Mail: laverne.1@nd.edu
Phone:(574)631-5563

Lu, H. Peter
Bowling Green State University
021 Overman Hall
Bowling Green, OH 43402
E-Mail: hplu@bgsu.edu
Phone:(419)372-1840

Lymar, Sergei
Brookhaven National Laboratory
Chemistry Department, BLDG 555
Upton, NY 11973
E-Mail: lymar@bnl.gov
Phone:(631)344-4333

Marceau, Diane
DOE/BES SC-22.1
19901 Germantown Road
Germantown, MD 21702
E-Mail: diane.marceau@science.doe.gov
Phone:(301)903-0235

Participants

Meisel, Dan
Notre Dame Radiaton Laboratory
University of Notre Dame
Notre Dame, IN 46556
E-Mail: dani@nd.edu
Phone:(574)631-6163

Miller, John
DOE/BES SC-22.1
19901 Germantown Rd.
Germantown, MD 20874
E-Mail: john.miller@science.doe.gov
Phone:(301)903-5806

Miller, John
Brookhaven National Lab
555 Chemistry
Upton, NY 11973
E-Mail: jrmiller@bnl.gov
Phone:(631)344-4354

Morse, Michael
University of Utah
Department of Chemistry
Salt Lake City, UT 84112
E-Mail: morse@chem.utah.edu
Phone:(801)581-8319

Mundy, Christopher
Pacific Northwest National Laboratory
PO Box 999, K1-83
Richland, WA 99352
E-Mail: chris.mundy@pnl.gov
Phone:(509)375-2404

Ogut, Serdar
University of Illinois at Chicago
845 West Taylor Street (M/C 273)
Chicago, IL 60607
E-Mail: ogut@uic.edu
Phone:(312)413-2786

Osgood, Richard
Columbia University
500 West 120th St
New York, NY 10027
E-Mail: Osgood@columbia.edu
Phone:(212)854-4462

Petek, Hrvoje
University of Pittsburgh
3941 O'Hara St
Pittsburgh, PA 15260
E-Mail: petek@pitt.edu
Phone:(412)478-3933

Rahn, Larry
DOE/BES SC-22.1
19901 Germantown Road
Germantown, MD 20874
E-Mail: Larry.Rahn@science.doe.gov
Phone:(301)903-2508

Ray, Asok
University of Texas at Arlington
Department of Physics
Arlington, TX 76019
E-Mail: akr@uta.edu
Phone:(817)272-2503

Ray, Douglas
Pacific Northwest National Laboratory
902 Battelle Boulevard
Richland, WA 99352
E-Mail: doug.ray@pnl.gov
Phone:(509)375-2500

Saykally, Richard
University of California, Berkeley
Department of Chemistry, D31 Hildebrand Hall
Berkeley, CA 94720
E-Mail: saykally@berkeley.edu
Phone:(510)642-8269

Schatz, George
Northwestern University
2426 Central Park Ave.
Evanston, IL 60208
E-Mail: schatz@chem.northwestern.edu
Phone:(847)491-5657

Schenter, Gregory
Pacific Northwest National Laboratory
PO Box 999, K1-83
Richland, WA 99352
E-Mail: greg.schenter@pnl.gov
Phone:(509)375-4334

Participants

Soderholm, Lynda
Argonne National Laboratory
Chemistry Division, Bldg. 200 M163
Argonne, IL 60439
E-Mail: ls@anl.gov
Phone:(630)252-4364

Steimle, Timothy
Arizona State University
College of Liberal Arts & Sciences
Tempe, AZ 85287
E-Mail: tsteimle@asu.edu
Phone:(480)965-3265

Thompson, Ward
University of Kansas
Department of Chemistry
Lawrence, KS 66045
E-Mail: wthompson@ku.edu
Phone:(785)864-3980

Tokmakoff, Andrei
Massachusetts Institute of Technology
Room 6-225, 77 Mass Ave.
Cambridge, MA 02139
E-Mail: tokmakof@mit.edu
Phone:(617)253-4503

Tully, John
Yale University
Dept of Chemistry, P.O. Box 208107
New Haven, CT 06520
E-Mail: john.tully@yale.edu
Phone:(203)432-3934

Wang, Lai-Sheng
Washington State University & Pacific
Northwest National Lab
2710 University Drive
Richland, WA 99354
E-Mail: ls.wang@pnl.gov
Phone:(509)376-8709

White, Michael
Brookhaven National Laboratory
Chemistry Department
Upton, NY 11973
E-Mail: mgwhite@bnl.gov
Phone:(631)344-4345

William, Kirchhoff
US DOE SC-22.1, retired
19901 Germantown Road
Germantown, MD 20874
E-Mail: william.kirchhoff@att.net
Phone:(301)903-0235

Windus, Theresa
Ames National Laboratory
42 Spedding Hall
Ames, IA 50011
E-Mail: theresa@fi.ameslab.gov
Phone:(515)294-6134

Wishart, James
Brookhaven National Laboratory
Chemistry Department
Upton, NY 11973
E-Mail: wishart@bnl.gov
Phone:(631)344-4327

Xantheas, Sotiris
Pacific Northwest National Laboratory
PO Box 999, K1-83
Richland, WA 99352
E-Mail: sotiris.xantheas@pnl.gov
Phone:(509)375-3684

Xie, X. Sunney
Harvard University
12 Oxford Street
Cambridge, MA 02138
E-Mail: xie@chemistry.harvard.edu
Phone:(617)496-9925